frontiers | Research Topics

Mechanisms in duchenne muscular dystrophy pathophysiology and treatment

Edited by
Atsushi Asakura, Masatoshi Suzuki
and Katsumasa Goto

Published in
Frontiers in Physiology

ISSN 1664-8714
ISBN 978-2-8325-3380-2
DOI 10.3389/978-2-8325-3380-2

About Frontiers

Frontiers is more than just an open access publisher of scholarly articles: it is a pioneering approach to the world of academia, radically improving the way scholarly research is managed. The grand vision of Frontiers is a world where all people have an equal opportunity to seek, share and generate knowledge. Frontiers provides immediate and permanent online open access to all its publications, but this alone is not enough to realize our grand goals.

Frontiers journal series

The Frontiers journal series is a multi-tier and interdisciplinary set of open-access, online journals, promising a paradigm shift from the current review, selection and dissemination processes in academic publishing. All Frontiers journals are driven by researchers for researchers; therefore, they constitute a service to the scholarly community. At the same time, the *Frontiers journal series* operates on a revolutionary invention, the tiered publishing system, initially addressing specific communities of scholars, and gradually climbing up to broader public understanding, thus serving the interests of the lay society, too.

Dedication to quality

Each Frontiers article is a landmark of the highest quality, thanks to genuinely collaborative interactions between authors and review editors, who include some of the world's best academicians. Research must be certified by peers before entering a stream of knowledge that may eventually reach the public - and shape society; therefore, Frontiers only applies the most rigorous and unbiased reviews. Frontiers revolutionizes research publishing by freely delivering the most outstanding research, evaluated with no bias from both the academic and social point of view. By applying the most advanced information technologies, Frontiers is catapulting scholarly publishing into a new generation.

What are Frontiers Research Topics?

Frontiers Research Topics are very popular trademarks of the *Frontiers journals series*: they are collections of at least ten articles, all centered on a particular subject. With their unique mix of varied contributions from Original Research to Review Articles, Frontiers Research Topics unify the most influential researchers, the latest key findings and historical advances in a hot research area.

Find out more on how to host your own Frontiers Research Topic or contribute to one as an author by contacting the Frontiers editorial office: frontiersin.org/about/contact

Mechanisms in duchenne muscular dystrophy pathophysiology and treatment

Topic editors

Atsushi Asakura — University of Minnesota Twin Cities, United States
Masatoshi Suzuki — University of Wisconsin-Madison, United States
Katsumasa Goto — Toyohashi Sozo University, Japan

Citation

Asakura, A., Suzuki, M., Goto, K., eds. (2023). *Mechanisms in duchenne muscular dystrophy pathophysiology and treatment*. Lausanne: Frontiers Media SA.
doi: 10.3389/978-2-8325-3380-2

Table of contents

frontiers | Frontiers in Physiology

TYPE Review
PUBLISHED 27 September 2022
DOI 10.3389/fphys.2022.984373

OPEN ACCESS

EDITED BY
Norio Fukuda,
Jikei University School of Medicine, Japan

REVIEWED BY
Boel De Paepe,
Ghent University, Belgium
Tomasz Prószyński,
Łukasiewicz Research Network - PORT The Polish Center for Technology Development, Poland

*CORRESPONDENCE
Atsushi Asakura,
asakura@umn.edu

SPECIALTY SECTION
This article was submitted to Striated Muscle Physiology, a section of the journal Frontiers in Physiology

RECEIVED 01 July 2022
ACCEPTED 05 September 2022
PUBLISHED 27 September 2022

CITATION
Den Hartog L and Asakura A (2022), Implications of notch signaling in duchenne muscular dystrophy. *Front. Physiol.* 13:984373. doi: 10.3389/fphys.2022.984373

Implications of notch signaling in duchenne muscular dystrophy

Lily Den Hartog and Atsushi Asakura*

Department of Neurology, Stem Cell Institute, Paul and Sheila Wellstone Muscular Dystrophy Center, University of Minnesota Medical School, Minneapolis, MN, United States

This review focuses upon the implications of the Notch signaling pathway in muscular dystrophies, particularly Duchenne muscular dystrophy (DMD): a pervasive and catastrophic condition concerned with skeletal muscle degeneration. Prior work has defined the pathogenesis of DMD, and several therapeutic approaches have been undertaken in order to regenerate skeletal muscle tissue and ameliorate the phenotype. There is presently no cure for DMD, but a promising avenue for novel therapies is inducing muscle regeneration via satellite cells (muscle stem cells). One specific target using this approach is the Notch signaling pathway. The canonical Notch signaling pathway has been well-characterized and it ultimately governs cell fate decision, cell proliferation, and induction of differentiation. Additionally, inhibition of the Notch signaling pathway has been directly implicated in the deficits seen with muscular dystrophies. Here, we explore the connection between the Notch signaling pathway and DMD, as well as how Notch signaling may be targeted to improve the muscle degeneration seen in muscular dystrophies.

KEYWORDS

notch, muscular dystrophy, muscle regeneration, satellite cell, muscle stem cell

Introduction

Muscular dystrophies are a group of inherited disorders that involve progressive muscle weakness and degeneration of skeletal muscle (Lovering et al., 2005). Duchenne muscular dystrophy (DMD) is one of the most severe forms of inherited muscular dystrophy, proving to be lethal in 100% of cases, and is also the most prevalent, with an incidence of one per 5,136 male births (Crisafulli et al., 2020; Yao et al., 2021). This qualifies it as one of the most widespread recessive disorders among the human population (Mah, 2016). Becker muscular dystrophy (BMD) is also prevalent, but somewhat less common and less severe (Duan et al., 2021). Since there is currently no cure for DMD, it is crucial that further research be done in order to identify and optimize potential treatments and therapies (Guiraud et al., 2015).

DMD is caused by mutations of the *dystrophin/DMD* gene, which is located at the Xp21 locus on the X chromosome (Venugopal and Pavlakis, 2022). Because DMD is an X-linked disorder, it almost exclusively affects males, with females acting as asymptomatic carriers (Crisafulli et al., 2020). The *dystrophin* gene is the largest known human gene, containing 79 exons and spanning >2,200 kb (Gao and McNally, 2015). Secondary to its

large size is its complex mutational spectrum; it has a high spontaneous mutation rate and there are >7,000 known mutations of the gene, with 1/3 of DMD cases resulting from sporadic mutations (Mah, 2016; Venugopal and Pavlakis, 2022). In current research, mutation rate is the probability that a unit length of DNA will mutate over time. Thus, the *dystrophin* gene has a high mutation rate, in part due to its huge gene size (Balin and Cascalho, 2010).

Deletion mutations account for 60%–70% of DMD cases, and point mutations and exonic duplications are also common (Gao and McNally, 2015; Duan et al., 2021). *Dystrophin* codes for the protein dystrophin, whose production can be limited and even eliminated by *dystrophin* mutation (Duan et al., 2021; Yao et al., 2021). Out-of-frame *dystrophin* mutations or premature stop-codon mutations typically lead to complete loss of the dystrophin protein and are more severe, while in-frame mutations that lead to the synthesis of a partially functional truncated protein produce milder forms of muscular dystrophy, such as BMD (Mah, 2016; Duan et al., 2021).

Dystrophin is located at the sarcolemma (cell membrane) of skeletal muscle cells and cardiomyocytes, interacting with a group of peripheral membrane and transmembrane proteins to form the dystrophin-associated glycoprotein complex (DGC) (Jiang et al., 2014). In healthy muscle, the DGC provides structural stability to skeletal and heart muscle, participates in transmembrane signaling, and plays a role in the vasomotor response to physical activity (Mah, 2016). In dystrophic muscle, however, loss of dystrophin diminishes the DGC, leading to weakness of the cytoskeleton, sarcolemmal lesions, and increased membrane fluidity (Wilschut et al., 2012; Venugopal and Pavlakis, 2022). This causes abnormal calcium influx and inflammation, which has catastrophic ramifications including the altered composition of structural glycoproteins in the extracellular matrix, activation of proteases and proinflammatory cytokines, ischemic injury, oxidative and nitrosative stress, and mitochondrial dysfunction (Duan et al., 2021). As a result of this loss in myofiber integrity, resident muscle stem cells undergo fibrogenesis rather than myogenesis, causing aberrant collagen deposition and subsequent necrosis (Wilschut et al., 2012; Kornegay, 2017). Through repeated cycles of necrosis and regeneration, muscle is gradually replaced with fibrous connective tissue and fat, producing the phenotypic characteristics of DMD (Venugopal and Pavlakis, 2022).

Skeletal muscle regeneration is carried out by the proliferation of quiescent muscle satellite cells (muscle stem cells) and the differentiation of myofibers. Activation of the Notch pathway is required to maintain the quiescent state of muscle satellite cells, and disruption of the Notch pathway leads to disruption of muscle satellite cell maintenance, thereby impairing muscle regeneration. Hence, disruption of the Notch pathway is one of the mechanisms of skeletal muscle disease. Currently, three muscle disease genes that interact with the Notch pathway have recently been identified—Jag2, MEGF10, and POGLUT1—whose mutation has been noted in muscular dystrophies. This review introduces the pathogenesis and treatment strategies for DMD, and discusses the biology of the Notch pathway and genetics in muscular dystrophies.

Pathology of DMD

DMD symptoms occur as early as 2–3 years of age and the disorder causes death prior to the third or fourth decade of life, usually around ages 19–25 (Mah, 2016; Duan et al., 2021; Iftikhar et al., 2021). DMD initially presents with symptoms of difficulties climbing stairs, a waddling gait, toe walking, Gowers' sign, and frequent falls (Birnkrant et al., 2018b; Duan et al., 2021). The physiological presentation of DMD goes on to primarily include progressive muscle degeneration, proximal weakness, and joint contractures (Mah, 2016; Coppens et al., 2021). Due to this, DMD patients are typically wheelchair-dependent by 10–12 years of age (Duan et al., 2021). DMD eventually brings about numerous secondary complications, including scoliosis, respiratory insufficiency, and cardiac issues (Mah, 2016). Dilated cardiomyopathy, myocardial necrosis, conduction defects, and arrhythmias are very common as well, with cardiorespiratory failure being the leading cause of mortality in DMD patients (Mah, 2016; Yao et al., 2021). This can be attributed to the absence of dystrophin in cardiomyocytes, which causes a loss of contractile function (Yucel et al., 2018). Additionally, though most DMD patients do not fit the criteria for intellectual disability, most do have some degree of cognitive impairment (Yucel et al., 2018). Many DMD patients do have a below-average IQ, as studies have reported that 20% of DMD patients have an IQ lower than 70 and 44% of DMD patients have learning disabilities (Yucel et al., 2018; Mohamadian et al., 2022). DMD patients also have been shown to be at increased risk for neurobehavioral comorbidities, such as attention-deficit/hyperactivity disorder, autism spectrum disorder, epilepsy, and anxiety (Mohamadian et al., 2022). There has been a suggestion of genotype-phenotype association with regards to *dystrophin* mutation and neurodevelopmental manifestations, as Ricotti et al. found that patients with distal mutations in the *dystrophin* gene were more likely to have neurodevelopmental problems, intellectual disability, memory deficits, and decreased grey matter volume. However, this study also demonstrated that emotional and behavioral problems were equally distributed among patients with proximal versus distal *dystrophin* mutations, calling into question this genotype-phenotype association (Ricotti et al., 2016). Cognitive impairments seen in DMD patients have typically been thought of as non-progressive, though recent studies have suggested otherwise (Bagdatlioglu et al., 2020). Studies in a mouse model of DMD have demonstrated that long-term memory and anxiety behaviors do worsen with age, which indicates that dystrophin

deficiency causes progressive cognitive impairment greater than that naturally seen with aging, and furthermore that the reduced life expectancy of human DMD patients may mask their potential for progressive cognitive impairment (Bagdatlioglu et al., 2020).

DMD is medically evaluated in several manners, including *via* laboratory work, muscle biopsy, gene analysis, electromyography, and cardiac testing (Venugopal and Pavlakis, 2022). The possibility of newborn screening has been extensively discussed, and a recent survey revealed that most DMD physicians would see a benefit in newborn screening and feel that the DMD care community is ready for this (Armstrong et al., 2022). This may be of greatly advantageous, as the majority of DMD physicians also indicated that they would recommend initiating therapies much earlier than the typical age at which DMD is currently diagnosed (Armstrong et al., 2022). However, this has not yet become standard (Birnkrant et al., 2018b). The diagnosis of DMD is usually confirmed after symptoms are present via a laboratory test for serum creatine kinase (CK), a muscle enzyme that, when elevated, reflects ongoing muscle damage (Duan et al., 2021). Serum CK is often elevated in DMD patients before the development of clinical symptoms, as levels peak by age two and its level is typically 10–20x greater than the upper limit of normal (Venugopal and Pavlakis, 2022). Other muscle enzymes, including aldolase, alanine transaminase (ALT), and aspartate aminotransferase (AST), are often elevated as well, though not used as a diagnostic measure (Duan et al., 2021). Though serial muscle biopsies from DMD patients are not usually necessary for diagnosis, they do reveal multiple dystrophic changes, which include disorganization, scattered degeneration, connective tissue proliferation, inflammation, muscle fiber necrosis, and extensive deposits of adipose tissue in place of muscle (Guiraud et al., 2015; Coppens et al., 2021; Venugopal and Pavlakis, 2022). Gene analysis of DMD patients shows a complete absence of the *dystrophin* gene, and dystrophin immunoblotting may be utilized in order to predict the severity of the disease (Venugopal and Pavlakis, 2022). In examining muscles, electromyography can detect nonspecific myopathic features associated with muscular dystrophy (Venugopal and Pavlakis, 2022). Finally, cardiac testing is used to evaluate for complications frequently seen with DMD; electrocardiogram reveals characteristic changes, telemetry identifies conduction abnormalities, and echocardiogram shows evidence of dilated cardiomyopathy, which is present in nearly all DMD patients by the time they reach their twenties (Venugopal and Pavlakis, 2022).

Current treatment for DMD

Despite its prevalence and severity, there is currently no cure for DMD and most available therapies simply act to manage symptoms and prolong ambulation and lifespan (Birnkrant et al., 2018b; Yao et al., 2021). As laid out clearly in a multi-part review by Birnkrant et al., a multidisciplinary approach to treatment is critical, typically led by a neuromuscular specialist. Corticosteroids and supportive measures have remained the standard of care over the past 30 years, since the molecular basis of DMD was defined (Motohashi et al., 2019). Corticosteroids, usually prednisone or deflazacort, are typically initiated around 4–5 years of age and provide numerous benefits for DMD patients, including deceleration of myofiber necrosis, improved pulmonary function, delayed development of scoliosis, prolonged independent ambulation, reduced progression of cardiomyopathy, improved mortality, and stabilization of muscle strength and function (Mah, 2016; Birnkrant et al., 2018b; Iftikhar et al., 2021; Venugopal and Pavlakis, 2022). That said, there is a slew of adverse side effects associated with corticosteroid use, including short stature, obesity, and cataracts, deeming it a suboptimal treatment (Mah, 2016). Corticosteroids also greatly increase the probability that DMD patients develop osteoporosis and skeletal fractures, including vertebral compression fractures, for which they are already at an elevated risk (Birnkrant et al., 2018a). Corticosteroid treatment is typically supplemented by supportive interventions that act to prolong survival and lessen symptom severity. To account for cardiac troubles, DMD patients are typically treated with angiotensin-converting enzyme (ACE) inhibitors and beta-blockers in order to slow the progression of cardiomyopathy and attempt to prevent heart failure (Venugopal and Pavlakis, 2022). It is recommended that spirometry be initiated when the patient is 5–6 years old, and noninvasive positive pressure ventilation and effective airway clearance are used to manage respiratory issues (Mah, 2016; Birnkrant et al., 2018a). Orthopedic management and physiotherapy are employed with the primary goals of minimizing joint contractures, maintaining a straight spine, and promoting bone health (Birnkrant et al., 2018a). Finally, endocrine and gastrointestinal management are also crucial to the appropriate treatment of DMD patients (Birnkrant et al., 2018b).

Recent scientific advances have garnered the potential for novel therapies to fight numerous neuromuscular diseases, including DMD. Currently, many therapeutic approaches aim to rescue dystrophin expression in skeletal muscle with hopes of improving function in dystrophic muscle, promoting muscle hypertrophy, and reducing muscle wasting (Cossu and Sampaolesi, 2007; Vieira et al., 2015). The goal of these therapies is not to cure DMD, but rather to improve severe DMD phenotypes to mimic more mild phenotypes, similar to BMD (Tominari and Aoki, 2022). A common limitation in the quest for effective DMD therapies is that there is no specific set of recommended or required outcome measures, making goals ambiguous (Shimizu-Motohashi et al., 2019). With regard to rescuing dystrophin expression, the level of dystrophin required for clinical efficacy has remained unclear; while restoring 15%–20% of normal dystrophin levels in mouse models has shown improvement, 33%–40% has been reported as necessary for

improvement in dog models (Sun et al., 2020). In humans, restoring 30% of normal dystrophin levels has been suggested as the standard for notable improvement (Sun et al., 2020). However, the relevance of this is still unknown, as some patients with low levels of dystrophin have been shown to maintain relatively normal muscle function, and studies in DMD patients that have extremely low but still detectable levels of dystrophin have suggested that even a small amount of dystrophin protein can mitigate skeletal muscle deficits (Nakamura et al., 2016; Waldrop et al., 2018).

Leading approaches in novel DMD therapies thus far have been gene-based, including gene replacement, endogenous gene repair, exon skipping, and read-through therapies (Yao et al., 2021). Multiple issues with these techniques have arisen, including immune response to the vector, difficulty delivering genes to post-mitotic muscle fibers, and the fact that many of these techniques only have potential for treating DMD patients with particular genetic mutations, of which there are several (Cossu and Sampaolesi, 2007; Iftikhar et al., 2021). Other methods being explored include upregulation of utrophin, inhibition of histone deacetylase, antagonization of the myostatin pathway, and increased angiogenesis (Cossu and Sampaolesi, 2007; Verma et al., 2018; Sun et al., 2020). Agents have also been explored in order to target downstream pathological changes seen in DMD, such as fibrosis, inflammation, ischemia, oxidative stress, loss of calcium homeostasis, and muscle atrophy (Yao et al., 2021). Though exon-skipping and read-through therapies in particular have shown promise, they have their drawbacks and other approaches have shown limited success in preclinical and clinical trials thus far; therefore, there is a distinct need for further research and development.

Of note, several model organisms have been used to study DMD and potential therapies, the most common of which is the *mdx* mouse. The *mdx* mouse has a mutation in the dystrophin gene itself, similar to human DMD patients (Yucel et al., 2018). However, *mdx* mice do not exhibit a shortened lifespan, severe muscle degeneration, or other key features of DMD, such as cardiomyopathy (Yucel et al., 2018; Gao et al., 2019). Their milder phenotype is likely attributable to the high regenerative capacity of mouse muscle, as well as the fact that utrophin is still active, whose expression may compensate for the lack of dystrophin (Plantié et al., 2015; Gao et al., 2019). The utrophin protein has a remarkably similar structure and function to dystrophin in linking the sarcolemma to the cytoskeleton, but is primarily expressed in skeletal muscle during fetal development and, in healthy muscle, is downregulated prior to birth (Yucel et al., 2018). Utrophin is usually upregulated in skeletal muscle when dystrophin is absent and has even been proposed as an alternative target protein to dystrophin, due to their similarities (Yao et al., 2021). However, due to key functional differences in the protein structure, utrophin cannot fully compensate for the loss of dystrophin in human DMD patients (Yucel et al., 2018). In order to account for this in murine models, double knockout (dKO) mice models have been utilized, which, in addition to knocking out *dystrophin*, also knock out one of a variety of genes that play important roles in myogenesis and muscle function (Yucel et al., 2018). Namely, *dystrophin*/*utrophin* dKO mice have been employed in studies, as they more closely resemble the clinical manifestations of DMD and have been deemed more suitable for gene therapy testing (Gao et al., 2019). Furthermore, a golden retriever muscular dystrophy (GRMD) dog model has come into use, as it better aligns with the progressive course of human DMD than most mouse models (Kornegay, 2017). GRMD studies have not always substantiated findings in *mdx* mouse studies, and have also illuminated various side effects of potential treatments that are not seen in *mdx* mice (Kornegay, 2017). GRMD has also been crucial in investigating the speed of disease progression, as RNA sequencing has been employed to identify biomarkers for this (Brinkmeyer-Langford et al., 2018). Despite their utility, practical considerations do limit the use of GRMD models, especially dog availability and expense (Kornegay, 2017). Finally, *drosophila* and zebrafish models of DMD have been studied, as these organisms have modeled many human diseases over the last several decades and comparative genomic studies have demonstrated sequence conservation of dystrophin in both organisms (Plantié et al., 2015). In particular, zebrafish *sapje* mutants have been useful, as they contain a mutation at *dystrophin* and do not express compensatory *utrophin*, so they exhibit features more similar to human DMD pathology (Plantié et al., 2015).

Skeletal muscle regeneration

Because muscular dystrophies, including DMD, are characterized by progressive degeneration of skeletal muscle, the structure and function of skeletal muscle must be understood in order to develop effective therapeutic strategies. In humans, skeletal muscle comprises approximately 40% of total body weight (Frontera and Ochala, 2015). It is responsible for converting chemical energy into mechanical energy, hence generating force and power to produce movement and perform voluntary functions (Frontera and Ochala, 2015). Skeletal muscle is necessary for the maintenance of homeostasis and other bodily functions as well, including respiration and metabolic function (Joanisse et al., 2017; Sousa-Victor et al., 2022).

Skeletal muscle is heterogeneous tissue, composed of different types of muscle fibers (Joanisse et al., 2017). Its architecture involves a specific arrangement of these muscle fibers, along with surrounding connective tissue (Frontera and Ochala, 2015). Skeletal muscle fibers are formed through the fusion of single cells and contain several hundred post-mitotic nuclei in their mature form (Tedesco et al., 2010). This

multinucleation presents a hurdle to the treatment of deficient skeletal muscle, as therapies face the task of restoring proper gene expression in hundreds of millions of post-mitotic nuclei (Tedesco et al., 2010).

Skeletal muscle tissue has the ability to regenerate new muscle fibers upon indication by homeostatic demand, hypertrophy, or need for repair secondary to injury, exercise, or disease (Tedesco et al., 2010; Sato et al., 2012). The regenerative capacity of skeletal muscle declines with aging (Sousa-Victor et al., 2022). The stem cells of postnatal muscle, known as satellite cells, are responsible for >99% of the regenerative potential of adult skeletal muscle (Conboy et al., 2003; Bröhl et al., 2012; Joanisse et al., 2017). Other progenitors, including pericytes, endothelial cells, and interstitial cells, have a limited amount of regenerative potential as well (Tedesco et al., 2010; Verma et al., 2018).

Satellite cells

Satellite cells are crucial to the regenerative capacity of skeletal muscle tissue; when they dysfunction, the skeletal muscle loses its regenerative ability, leading to the degeneration reminiscent of DMD (Asakura et al., 2002; Bröhl et al., 2012; Sato et al., 2012; Fuchs and Blau, 2020). During prenatal development, some muscle progenitor cells migrate into position as mononuclear cells between the basal lamina of the muscle fiber and its sarcolemma; these cells ultimately constitute the satellite cell pool and are defined by their unique molecular location (Tedesco et al., 2010; Wilschut et al., 2012). Satellite cells are mononuclear and comprise 2.5%–6% of all nuclei for any given skeletal muscle fiber (Tedesco et al., 2010). They play important roles both in establishing and growing muscle during development and in maintaining muscle in adults via regeneration (Bröhl et al., 2012). Satellite cells are distinct from other types of progenitors in that they are limited to myogenesis, rather than possessing a broader multilineage differentiation potential (Asakura et al., 2001; 2002; Wilschut et al., 2012).

Satellite cells can adopt several different states, including quiescence, activation, proliferation, and differentiation (Li et al., 2021). Initially, during the perinatal and postnatal periods, satellite cells are proliferative (Bröhl et al., 2012). Then, in healthy adult muscle, satellite cells maintain the essential feature of quiescence under homeostatic conditions (Bröhl et al., 2012). Quiescence is common to stem cells and is defined by reversible mitotic arrest: quiescent cells do not divide, but rather are still able to re-enter the cell cycle and proliferate upon stimulation (Bjornson et al., 2011). Quiescence permits self-renewal, allowing for the maintenance of stem cell populations throughout the lifetime of an animal (Bjornson et al., 2011). Furthermore, quiescence involves reduced metabolic activity, so that satellite cells are protected against endogenous stress from DNA replication and cellular respiration (Bjornson et al., 2011). On a genetic level, quiescent cells highly express the paired box 7 (*Pax7*) gene, which has been shown to be the most reliable marker for satellite cells (Mourikis et al., 2012; Fuchs and Blau, 2020; Starosta and Konieczny, 2021; Sousa-Victor et al., 2022). Mice null for *Pax7* are notably deficient in satellite cells, and misregulation of *Pax7* has been implicated in DMD (Gayraud-Morel et al., 2012; Coppens et al., 2021). Aside from satellite cells, *Pax7* is not expressed by any other cell type in muscle tissue (Fuchs and Blau, 2020).

Upon injury or due to homeostatic demand, satellite cells leave their quiescent state, re-entering the cell cycle and downregulating *Pax7* (Dumont et al., 2015; Kann et al., 2021). At this point, they instead express myogenic regulatory factors (MRFs), including *Myf5* and *MyoD*, which promote cell activation and the cells become myoblasts, poised to regenerate muscle tissue (Mourikis et al., 2012; Wilschut et al., 2012; Sousa-Victor et al., 2022). MRFs are specifically expressed in skeletal muscle lineage, and when transfected into certain other cell types, MRFs can induce them to adopt a myogenic fate (Biressi et al., 2013). Cell ablation studies have demonstrated that *Myf5* and *MyoD* can independently initiate myogenic differentiation, thus deeming them myogenic determination genes (Biressi et al., 2013). *Myf5* is the first MRF to be expressed during mammalian development (Biressi et al., 2013). Though *MyoD* is only expressed in a small percentage of quiescent satellite cells, all progenitors of satellite cells transcribe *MyoD* prenatally and express it prior to the first cell division (Kanisicak et al., 2009; Gayraud-Morel et al., 2012). Other MRFs include *Mrf4*, which only acts as a determination gene during embryonic development, and *myogenin*, which is never co-expressed with *Pax7* and acts as a differentiation factor downstream of *MyoD* and *Myf5* (Kottlors and Kirschner, 2010; Gayraud-Morel et al., 2012; Biressi et al., 2013).

Importantly, the satellite cell population is heterogenous, and subpopulations serve distinct functions (Dumont et al., 2015). Some primarily perform asymmetric divisions, which are more prevalent during homeostasis in order to generate myogenic progenitors while maintaining the satellite cell pool (Dumont et al., 2015; Sousa-Victor et al., 2022). Others predominantly perform symmetric divisions, which are more common after indication by injury or breakdown, as they act to expand the satellite cell pool (Dumont et al., 2015; Sousa-Victor et al., 2022). Satellite cells maintain a dynamic balance between symmetric and asymmetric division in accordance with the present needs of the muscle, and which type of division that satellite cells undergo is primarily governed by two factors: polarity and orientation (Dumont et al., 2015). Asymmetric division is driven by unequal distribution of polarity proteins, specifically members of the Partitioning-defective protein (PAR) family, which establish cell polarity in several different cell types (Dumont et al., 2015). With regard to orientation, symmetric divisions typically occur in a planar orientation, while asymmetric

divisions usually occur in an apical-basal orientation (Kuang et al., 2007). Furthermore, different subpopulations of satellite cells express genes associated with quiescence and myogenesis to varying degrees (Dumont et al., 2015). Though *MyoD* is consistently expressed in all activated satellite cells, there are populations of *Myf5*-positive and *Myf5*-negative satellite cells present in adult muscle; studies using fluorescent protein tagging have revealed that approximately 10% of satellite cells constitute a subpopulation that never expresses *Myf5* during development (Kuang et al., 2007; Dumont et al., 2015; Sousa-Victor et al., 2022). Interestingly, these *Myf5*-negative cells have shown a greater ability to self-renew and are more stem-like as compared to their *Myf5*-positive counterparts (Kuang et al., 2007; Sousa-Victor et al., 2022). Also, satellite cells demonstrate *Pax7* at different levels, and subpopulations of satellite cells that express higher levels of *Pax7* are less prone to differentiation (Rocheteau et al., 2012). This is not surprising since *Pax7* is so intimately associated with quiescence and proliferation.

The intrinsic regulatory mechanisms that govern quiescence, cell cycle progression, and cell fate determination of satellite cells are influenced by extrinsic cues (Mourikis et al., 2012; Dumont et al., 2015; Verma et al., 2018). These cues involve proximity to endothelial cells, as well as the specialized local niche between the myofiber sarcolemma and basal lamina in which satellite cells reside (Dumont et al., 2015; Verma et al., 2018). During quiescence, the basal lamina physically separates satellite cells from other local niche cells (Kann et al., 2021). Muscular injury induces changes in this niche, namely disruption of the basal lamina, which exposes satellite cells to the growth factors and signaling molecules that they are normally sequestered from (Kann et al., 2021). This external cue subsequently promotes satellite cell activation and proliferation.

Satellite cells as a therapeutic tool for DMD

Though it has been established that satellite cells drive muscle regeneration and that impaired regeneration drives the phenotype of DMD, the specific role of satellite cells in this impaired regeneration has been disputed (Dumont and Rudnicki, 2016).

Some studies have reported that satellite cell number remains the same or is even elevated in dystrophic muscle as compared with age-matched controls (Kottlors and Kirschner, 2010; Jiang et al., 2014). Further, some studies have suggested that impaired regeneration occurs secondary to the surrounding pathogenic environment rather than intrinsic issues with the regenerative capacity of satellite cells (Boldrin et al., 2015). This would indicate that lack of satellite cells is not the culprit for impaired regeneration. Similarly, other studies have suggested that insufficient regeneration may be caused by failure of differentiation rather than a lack of self-renewal and proliferation (Kottlors and Kirschner, 2010). This presents a direct link between dystrophin deficiency and impaired regeneration, as dystrophin is crucial for defining cell polarity, which strongly influences whether satellite cell division is asymmetric or symmetric and subsequently whether differentiation and myogenesis occur (Chang et al., 2016; Dumont and Rudnicki, 2016). Dystrophin influences polarity by interacting with MARK2, a cell polarity-regulating kinase (Chang et al., 2016). When dystrophin is deficient in DMD muscle, there is reduced expression of MARK2, which leads to loss of PARD3 polarization, a member of the PAR family (Chang et al., 2016). Consequently, asymmetric satellite cell divisions wither, so fewer myogenic progenitors are produced and muscle regeneration is impaired (Chang et al., 2016; Dumont and Rudnicki, 2016). This link between dystrophin and polarity demonstrates a direct role for dystrophin in the loss of regenerative capacity seen in DMD, and supports the idea that exhaustion of the satellite pool may not be the cause for impaired regeneration.

On the contrary, several studies have indicated that satellite cell pool exhaustion precipitates loss of regenerative capacity, and satellite cells do remain a key target for therapies combatting DMD (Wilschut et al., 2012). Due to their constant activation in an attempt to compensate for the unrelenting muscle degeneration of DMD, the satellite cell pool becomes depleted in dystrophic tissue, leading to failure of muscle repair and accelerated disease progression (Morgan and Zammit, 2010; Sacco et al., 2010; Wilschut et al., 2012; Jiang et al., 2014; Mu et al., 2015). Hence, rescuing satellite cell functionality has been a key target for DMD therapies (Liu et al., 2021).

The year 1990 saw the first successful satellite cell transplant into a boy with DMD, which achieved dystrophin production (Law et al., 1990). Though clinical trials throughout the 1990s demonstrated safety, no significant functional benefit was identified (Cossu and Sampaolesi, 2007). Approaches to satellite cell transplantation are still being explored in order to account for their drawbacks. For example, the heterogeneity of cultured satellite cells makes them somewhat unreliable in transfer therapies, so they have been cultured in various systems or on different mediums in order to select satellite cells that can best survive, engraft, and repopulate (Sun et al., 2020). Due to the lack of adequate success with satellite cell transfer thus far, the quest for optimization of this approach persists.

Though satellite cells have been looked to as a superior option, as they have self-renewal capacity and differentiation potential, myoblast-transfer therapies have been explored as well, as they have a high ability to generate muscle fibers (Shimizu-Motohashi et al., 2019). Pioneer myoblast-transfer studies demonstrated that intramuscular injection of healthy myoblasts into *mdx* mice resulted in fusion with host fibers and extensive dystrophin production (Tedesco et al., 2010).

These early suggestions of success led to several clinical trials in the early 1990s–2000s that unfortunately failed for various reasons, including poor survival, limited migration of donor cells after transplantation, and immune responses that caused the rejection of the donor cells (Tedesco et al., 2010; Shimizu-Motohashi et al., 2019). In the interim, numerous approaches with different transplantation techniques have been attempted to sidestep these concerns, including employing conditional proliferation-dependent suicide agents in order to combat the oncogenic potential of immortalized cells (Sun et al., 2020). However, ample success has not yet been achieved with myoblasts (Sakai et al., 2017).

In addition to satellite cells and myoblasts, several different myogenic progenitors have been investigated as potential candidates in transfer therapies as well, including mesenchymal stem cells, $CD133^{+}$ cells, mesangioblasts, embryonic stem cells, and induced pluripotent stem cells (Sakai et al., 2017; Shimizu-Motohashi et al., 2019; Tominari and Aoki, 2022). Despite the established efficacy of exon-skipping and read-through therapies, cell transplantation therapies are applicable to more patients, as they are not specific to patients with certain types of mutations (Tominari and Aoki, 2022). Cell transfer therapies have both explored using genetically unmodified cells from healthy donors, which are mutation-free but carry a greater risk of immune reaction, and using autologous genetically-corrected cells, which require gene manipulation prior to transplantation but carry a much lower risk of immune reaction (Shimizu-Motohashi et al., 2019; Duan et al., 2021). Clinical trials in human patients thus far have primarily focused on cells from healthy donors, while preclinical trials in animals have employed the autologous genetically-corrected cell approach (Shimizu-Motohashi et al., 2019). As discussed with regards to satellite cell- and myoblast-transfer therapies, promise for these approaches has been demonstrated but they have not been overwhelmingly successful thus far.

Notch signaling system

Satellite cells are an important target to consider in novel therapies since their depletion is a strong potential cause for DMD progression. Therefore, it is essential that we deepen our understanding of the various pathways that regulate their function. One of these regulators is the Notch signaling system, whose dysfunction has been shown to specifically deplete satellite cells, as is seen in DMD (Jiang et al., 2014). The Notch signaling pathway is highly conserved in both vertebrates and invertebrates and regulates cell proliferation, cell fate decisions, and induction of differentiation (Bröhl et al., 2012; Sato et al., 2012; Starosta and Konieczny, 2021). The Notch pathway serves important roles in both embryonic development and in adults (Luo et al., 2005). During development, Notch signaling is crucial for formation of

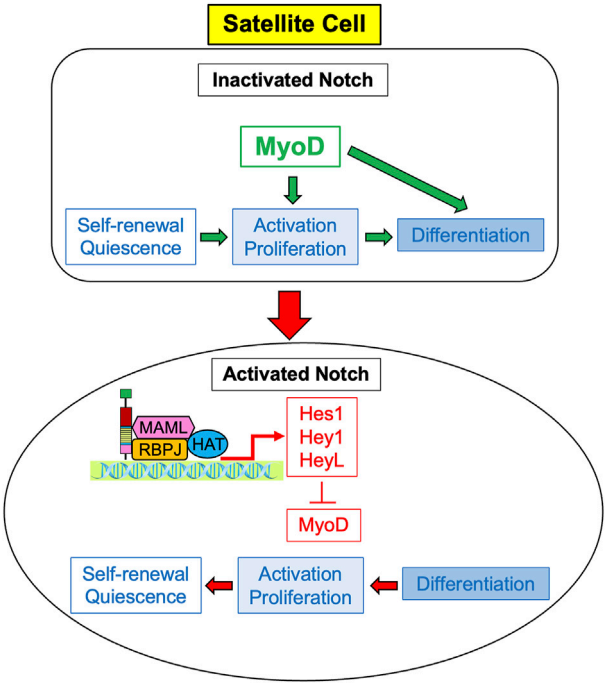

FIGURE 1
Notch signaling induces proliferation of satellite cells. Expression of MyoD causes activation, cell the proliferation and differentiation of satellite cells, so they ultimately cease cell division and differentiate into myocytes. Activated Notch signaling results in the expression of Notch target genes *Hes1*, *Hey 1*, and *HeyL*, which inhibit the transcription of MyoD. Without MyoD, satellite cells predominately proliferate rather than differentiate, and ultimately self-renew to return to quiescent cells.

healthy muscle, as elimination of the pathway has been shown to lead to premature differentiation of myogenic progenitors and ultimately to the development of small and weak muscle groups (Bröhl et al., 2012; Mourikis et al., 2012). Furthermore, embryonic knockouts of various components of the Notch pathway genes have been shown to be lethal in mice, deeming it essential for embryonic development (McIntyre et al., 2020). In adults, Notch signaling is crucial for tissue renewal and maintenance in multiple organ systems, with one of its primary roles being regulation of myogenesis and the regeneration of skeletal muscle tissue (Conboy and Rando, 2002; Sato et al., 2012; Coppens et al., 2021). With old age, Notch signaling decreases in skeletal muscle, leading to an age-related decline in the proliferative ability of satellite cells and subsequently to lower regenerative potential (Conboy et al., 2003). The pathway is context-dependent, altering based on factors such as cell type, timing, and mode of signaling, so that it can respond to the current needs of the organism (Kuroda et al., 1999).

In order to promote the regeneration of skeletal muscle in the adult, Notch signaling regulates satellite cells by suppressing

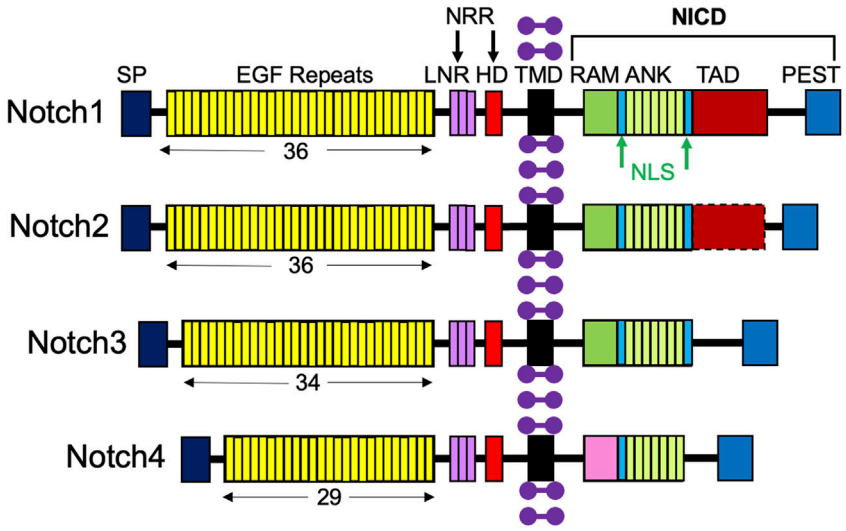

FIGURE 2
Structures of the four Notch receptors. The four Notch receptors identified in humans are depicted with their structural components: SP, signal peptide; EGF, repeats indicated by the number below; LNR, LIN12-Notch repeats; HD, heterodimerization domain; NRR, negative regulatory region; TMD, transmembrane domain; RAM, RBPJ-associated module; NLS, nuclear localization signal; ANK, ankyrin repeats; TAD, transcriptional activation domain; PEST (proline/glutamic acid/serine threonine-rich motif), and NICD, Notch intracellular domain. Purple dumbbells represent surrounding membrane phospholipids.

myogenic differentiation (Mourikis et al., 2012). When Notch is inactivated, MyoD activates satellite cells causing their differentiation. However, activated Notch promotes the expression of Hes and Hey family genes, particularly *Hes1*, *Hey1*, and *HeyL* (Sakai et al., 2017; D'Souza et al., 2008). These genes suppress MyoD, and therefore suppress differentiation while promoting satellite cell proliferation and self-renewal in order to maintain the satellite cell pool, as depicted in Figure 1 (Gioftsidi et al., 2022). Maintenance of the satellite cell pool then augments the regenerative ability of the skeletal muscle. Unsurprisingly, active Notch signaling is associated with the maintenance of quiescence; in quiescent satellite cells, Notch signaling is high and Notch target genes are more highly expressed to promote self-renewal and proliferation, whilst MyoD and differentiation are suppressed (Fukada et al., 2007; Bjornson et al., 2011; Baghdadi et al., 2018; Kann et al., 2021; Sousa-Victor et al., 2022). Several studies in both *mdx* mice and in satellite cell-derived myoblasts have also demonstrated that constitutive Notch activation upregulates *Pax7*, which is associated with satellite cell quiescence and self-renewal (Wen et al., 2012; Jiang et al., 2014).

It should be noted that Notch signaling plays a role in muscle cells beyond just satellite cells, as well. Importantly, Notch1 may be activated in myotubes, which serves to upregulate the expression of Notch ligands and enhance the regenerative capacity of adjacent satellite cells (Bi et al., 2016). This aspect enhances the ability of myotubes as a stem cell niche. Furthermore, it has been shown that in disuse and diabetes, multinucleated myofibers express Notch2 via activation by the Notch ligand Dll4 from the microvascular endothelium (Fujimaki et al., 2022). This ultimately leads to the progression of muscle atrophy seen in these conditions, making it a therapeutic target (Fujimaki et al., 2022).

Notch signaling scheme

A molecular scheme for the Notch signaling pathway has been established, lending insight into ways in which it can be targeted in therapies. Notch receptors are large type I transmembrane proteins comprised of an extracellular domain, a single transmembrane domain, and an intracellular region (Figure 2; Sato et al., 2012). There are four different Notch receptors in humans, Notch1-4, which are structurally distinct. Their extracellular domain includes a signal peptide, 29–36 epidermal growth factor (EGF) repeats, three conserved cysteine-rich Lin12-Notch repeats (LNR), and a heterodimerization domain (HD); together, the LNR and HD constitute the negative regulatory region (NRR), which keeps the receptor "off" when there are no ligands present (Sato et al., 2012). The Notch intracellular domain (NICD) consists of a recombining binding protein - J (RBPJ) association module domain (RAM), nuclear localization signals (NLS), seven ankyrin repeats (ANK), a transcriptional activation domain (TAD), and a C-terminal proline-glutamic acid/serine

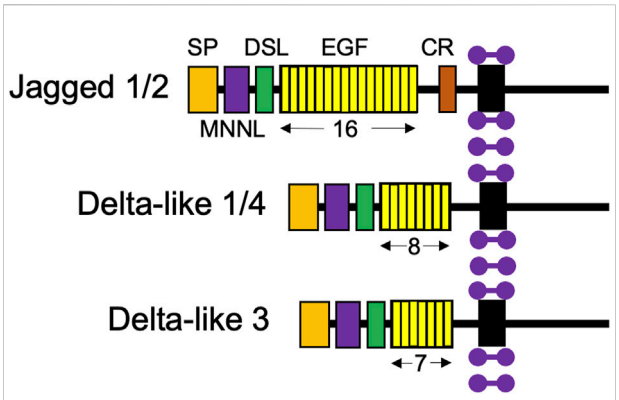

FIGURE 3
Structures of the five Notch ligand proteins. The five Notch ligands identified in humans are depicted with their structural components: SP, signal peptide; MNNL, modular N-terminal Notch ligand; DSL, Delta, Serrate, and LAG-2 domains; EGF, repeats indicated by number below; and CR, cysteine-rich domain. Purple dumbbells represent surrounding membrane phospholipids.

threonine-rich motif (PEST) (Sato et al., 2012). Importantly, Notch3 and Notch4 lack a TAD (Fujimaki et al., 2017).

Like Notch receptors, Notch ligands are also type 1 cell surface proteins with multiple tandem EGF repeats in their extracellular domains (Figure 3; D'Souza et al., 2008). There are five Notch ligands in humans, Jagged1, 2 (Jag1, 2) and Delta-like 1, 3, and 4 (Dll1, 3, 4), which each have unique structures. Notch ligands are presented on neighboring niche cells and activate Notch receptors through a juxtracrine pathway (Coppens et al., 2021; Kann et al., 2021). Of note, there has been evidence to demonstrate *cis*-inhibitory interactions between Notch ligands and receptors located on the same cell (Coppens et al., 2021).

After the ligand binds to the extracellular domain of the Notch receptor, a signal transduction cascade is initiated, known as the canonical Notch signaling pathway, depicted in Figure 4 (McIntyre et al., 2020). Initially, the receptor undergoes a series of proteolytic cleavages, first by an ADAM-family metalloproteinase in the extracellular domain and then by γ-secretase in the transmembrane region, in order to ultimately liberate the Notch intracellular domain (NICD) (McIntyre et al., 2020). This step presents an opportunity for regulation of the Notch pathway; if cells are treated with DAPT, γ-secretase is inhibited, NICD will therefore not be liberated, and transcription of target genes will not be activated (Dong et al., 2021). Once liberated under normal conditions, NICD translocates to the nucleus and associates with a DNA-binding protein that includes RBPJ (Nandagopal et al., 2018; Kann et al., 2021). Of note, RBPJ is also known as the CSL (CBF1/Suppressor of Hairless/LAG-1) (McIntyre et al., 2020). Without NICD, RBPJ binds transcriptional corepressors to inhibit the transcription of target genes (Bjornson et al., 2011). When NICD is present, it binds RBPJ, displaces the corepressors, and recruits coactivators, including Mastermind (Mastermind-like in mammals) and histone acetyltransferases to assemble a transcriptional complex and activate transcription of Notch target genes, including *Hes1, Hey1,* and *HeyL* (Figure 1, 2; McIntyre et al., 2020; D'Souza et al., 2008; Bröhl et al., 2012; Sato et al., 2012; Baghdadi et al., 2018). Intracellular Notch activity is regulated by protein turnover that occurs at the PEST at the C-terminal

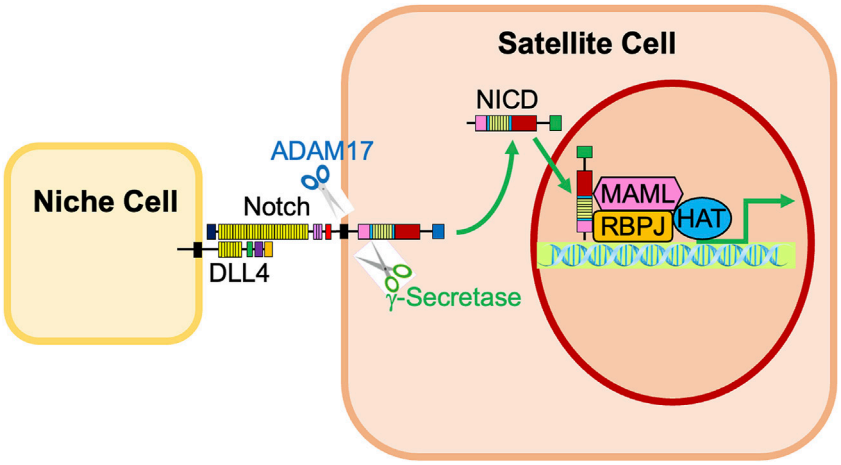

FIGURE 4
Activation of Notch signaling in satellite cells by neighboring niche cells. Notch receptors expressed in satellite cells are activated by interaction with Notch ligands, such as Dll4, on neighboring niche cells. The Notch receptor is cleaved by ADAM17 and γ-secretase, liberating the Notch Intracellular Domain (NICD). The NICD translocates into the nucleus, associates with RBPJ, and recruits transcriptional coactivators, including Mastermind (MAML) and histone acetyltransferases (HAT). This complex promotes the activation of Notch target genes *Hes1, Hey1,* and *HeyL*.

domain of the NICD, as the NICD rapidly degrades when targeted by ubiquitylation (Andersson et al., 2011).

Various notch receptors and ligands

Multiple studies have demonstrated that the Notch receptors and ligands are not functionally equivalent, having varied downstream effects on self-renewal, proliferation, and differentiation of satellite cells (Preuße et al., 2015; Nandagopal et al., 2018). These differences are important to understand, especially when considering how to optimally target Notch in novel therapies.

With regards to receptors, prior studies have demonstrated that Notch1 and Notch3 have different and even contradictory roles, with Notch3 acting as a repressor for Notch1 (Low et al., 2018). Whereas activity of the canonical Notch signaling pathway typically leads to an increase in proliferation of satellite cells, experiments have shown that cells only expressing Notch3 proliferate less than controls and, similarly, that deficiency of Notch3 even leads to increased muscle regeneration and higher numbers of satellite cells (Kitamoto and Hanaoka, 2010). Additionally, Fujimaki et al. demonstrated that knockout of either Notch1 or Notch2 in satellite cells in mice prevents proliferation and self-renewal, indicating that they are necessary for the maintenance of the satellite cell pool and adult muscle regeneration (Fujimaki et al., 2017). On the contrary, mice deficient in Notch3 were viable and fertile, and even exhibited elevated numbers of quiescent satellite cells and greater proliferative ability, again suggesting that Notch3 acts to negatively regulate satellite cell proliferation (Fujimaki et al., 2017).

Numerous studies have specifically evaluated the ability of ligands Dll1, Dll4, Jag1, and Jag2 to induce Notch signaling, with results proving to be somewhat contradictory (Sakai et al., 2017). In human cells, *in vitro* studies have shown that Dll4 and Jag1 more strongly induce Notch signaling than does Dll1 (Sakai et al., 2017). Moreover, differences between Dll1 and Dll4 have been identified with respect to both the manner in which they activate Notch1 and their downstream effects, and it has been established that they are unable to replace the function of one another in many tissues (Preuße et al., 2015). First, Dll4 is presented to satellite cells by adjacent myofibers during quiescence, whereas Dll1 is expressed by differentiating cells that provide a self-renewing signal during regeneration (Yartseva et al., 2020; Kann et al., 2021). Second, Dll1 and Dll4 activate Notch1 in distinct manners: Dll1 activates Notch1 in discrete, frequency-modulated pulses, while Dll4 activates Notch1 in a sustained, amplitude-modulated manner (Nandagopal et al., 2018). Satellite cells are able to discriminate between these two types of signals using dynamics, with the Dll1 signal primarily upregulating *Hes1* and the Dll4 signal primarily upregulating *Hey1* and *HeyL* (Nandagopal et al., 2018; Zhang et al., 2021). Different ligands also affect satellite cell activity differently in distinct environments as a stem cell niche. Recent work has demonstrated that proximity to blood vessels is associated with satellite cell self-renewal as a vascular niche, specifically when Dll4 induces quiescence, therefore creating a vascular niche for satellite cell maintenance (Verma et al., 2018).

Notch signaling in DMD

The absence of Notch signaling precipitates impaired muscle regeneration and phenotypic characteristics reminiscent of DMD (Siebel and Lendahl, 2017). Lin et al. showed that conditional knockout mice whose endogenous Notch signaling was blocked in the satellite cell compartment acquired several features of muscular dystrophy, namely impaired muscle regeneration (Lin et al., 2013). Furthermore, inhibition of Notch signaling in satellite cells led to reduced self-renewal capacity and proliferation as well as increased differentiation of myoblasts, which together exhaust the satellite cell pool (Lin et al., 2013; Verma et al., 2018; Fiore et al., 2020). Together, these results suggest that Notch signaling promotes processes necessary for muscle tissue regeneration, and it is thus likely that impaired Notch signaling contributes to the pathogenic mechanisms of DMD (Tables 1, 2). On that note, insufficient Notch signaling has been directly implicated in DMD, as recent works demonstrated that DMD muscle tissue contains decreased Notch signaling (Table 1; Church et al., 2014; Starosta and Konieczny, 2021), although an earlier work showed upregulation of Notch signaling genes in *mdx* mice (Table 1; Turk et al., 2005). Jiang et al. showed that satellite cells in the skeletal muscle of *mdx* mice exhibit reduced expression of multiple Notch receptors, ligands, and target genes such as *Hes1*, *Hey1* and *HeyL* (Table 1; Jiang et al., 2014). Matrix metalloproteinase-9 (MMP9) is an extracellular protease involved in tissue remodeling, inflammation, and development of interstitials in skeletal muscle (Hindi et al., 2013). Gene knockout of *Mmp9* increases the expression of Notch ligands and receptors, and Notch target genes in skeletal muscle of *mdx* mice, and dramatically improves myopathy and augments myofiber regeneration in *mdx* mice (Table 1; Hindi et al., 2013).

Fiore et al. demonstrated that loss of or pharmacological inhibition of protein kinase C-θ (PKCθ), which modulates various signaling pathways in muscle, led to increased Notch signaling in *mdx* mice, and consequently improved muscle regeneration and reduced muscle wasting. This study also noted that inhibition of PKCθ acted to upregulate the expression level of *Pax7* and *Notch1*; together, these results demonstrate an avenue for increasing Notch pathway activity to ameliorate the DMD phenotype (Table 1; Fiore et al., 2020).

Specific components of the Notch pathway, namely ligands Jag1 and Jag2, have been implicated in the dysfunction seen in muscular dystrophy. One large study identified the over-

TABLE 1 Aberrant expression of Notch signaling genes in muscular dystropjy.

Gene	Species	Function	Citation
DII3, Numb, Numbl, Notch1, Notch2	Mouse	Upregulated Notch signaling genes in mdx mice	Turk et al. (2005)
Notch2, Notch3, Jag2, Hes1, HeyL	Mouse	Upregulated Notch signaling genes inmdx:Mmp9$^{+/-}$mouse muscle compared with mdx mice	Hindi et al. (2013)
Jag2, Numb	Mouse	Both genes are downregulated in mdx mice	Church et al. (2014)
Jag2, Notch1, Notch2, Numb, Hes1	Mouse	These genes are downregulated in mdx:utrn−/− dKO mice	Church et al. (2014)
Numb, Notch3	Human	Both genes are upregulated in DMD.	Church et al. (2014)
Notch1, Hes1	Human	Both genes are downregulated in DMD.	Church et al. (2014)
Notch1, Notch3, Jag1, Hey1, HeyL	Mouse	Notch1, Notch3, Jag1, Hey1 and HeyL are reduced in the mdx myoblasts	Jiang et al. (2014)
Notch1, Notch2, Notch3, Jag2, Hes, Hey1	Mouse	Downregulation of these genes in the skeletal muscles of mdx, mice	Mu et al. (2015)
Notch1, Notch2, Notch3, Jag2, Hes1, Hey1	Mouse	Over-activation of these genes in the skeletal muscles of mdx:utrn−/− dKO mice	Mu et al. (2015)
Notch1	Human	POGLUT1-mutated muscular dystrophy patients revealed decrease in the level of the NOTCH1	Servián-Morilla et al. (2016)
Jag1, DII1	Mouse	Expression of DII1 and Jag1 is higher in mdx:PKCθ−/− mouse muscle compared with mdx mice	Fiore et al. (2020)

TABLE 2 Phenotypical changes of muscular dystrophy via modulation of Notch signaling.

Gene	Species	Function	Citation
MEGF10	Human	Early-onset myopathy, areflexia, respiratory distress and dysphagia (EMARDD) or MEGF10 myopathy is associated with mutations in MEGF10, in which satellite cells from the patients show impaired proliferation and differentiation	Logan et al. (2011)
Notch	Mouse	mdx satellite cells have reduced activation of Notch signaling	Jiang et al. (2014)
Notch1	Mouse	Notch1 activation is sufficient to rescue the self-renewal deficiencies of mdx satellite cells	Jiang et al. (2014)
Notch	Mouse	Notch inhibition produces functional defects in mdx muscle	Church et al. (2014)
Jag1	Dog	Overexpression of Jag1 rescues the DMD Phenotype in golden retriver muscular dystrophy (GRMD)	Vieira et a., 2015
Notch	Mouse	Inhibition of Notch by treatment with DAPT improves DMD phenotypes in mdx:utrn−/− dKO mice	Mu et al. (2015)
POGLUT1	Human	A POGLU1 mutation causes lim-girdle muscular dystrophy (LGMD) with reduced Notch	Servián-Morilla et al. (2016)
Notch1	Mouse	Myofiber-specific activiation of Notch1 improves muscle pathology in mdx mice	Bi et al. (2016)
Jag1	Human	Jag1 induced IL-1β in DMD but not by normal myogenic cells reduces proliferation and differentiation	Nagata et al. (2017)
MEGF10	Mouse	Satellite cells from Meg10−/− mice and Megf10−/−:mdx dKO mice also show impaired proliferation and migration	Saha et al. (2017)
Notch2NLC	Human	CGG expression in NOTCH2NLC is associated with oculopharyngodistal myopathy (OPDM)	Ogasawara et al. (2020)
Notch/TGFb	Human	Inhibition of Notch and TGFβ promotes mygenic differentiation of human DMD iPSCs	Choi et al. (2012)
Jag 2	Human	Jag2 mutations are associated with unsolved muscular dystrophy	Coppens et al. (2021)

representation of pathogenic *Jag2* variants in patients with genetically-unsolved muscular dystrophy (Table 2; Coppens et al., 2021). Also, the downregulation of *Jag2* in murine myoblasts has been connected with the downregulation of other components of the Notch pathway, suggesting its importance (Coppens et al., 2021). *Jag1* has been closely tied to DMD, especially in a GRMD DMD model dog (Table 2; Vieira et al., 2015). Whole genome studies have uncovered an SNP in the promoter region of GRMD *Jag1* that creates a novel myogenin binding site (Vieira et al., 2015; Gioftsidi et al., 2022). This allows for greater expression of *Jag1* via myogenin, a transcription factor in the MyoD family, which leads to greater proliferative potential (Vieira et al., 2015; Gioftsidi et al., 2022). Not only has greater proliferative capacity been observed with overexpression of *Jag1*, but this intervention can even ameliorate the DMD phenotype in GRMD, marking it as a potential therapeutic target and indicating that *Jag1* may act as a genetic modifier of DMD (Vieira et al., 2015; Gioftsidi et al., 2022). Similarly, overexpression of *Jag1* in the *sapje*, a zebrafish model of DMD, produced a fiber organization

resembling the wild-type phenotype (Vieira et al., 2015; Gioftsidi et al., 2022).

Despite promising evidence for restoration of Notch signaling or upregulation of components of the Notch pathway to benefit DMD, other reports have been inconsistent. In one study, genes for Notch signaling were downregulated in *mdx* satellite cells and Notch1 activation was sufficient to rescue the self-renewal deficiencies of *mdx* satellite cells, but failed to improve muscle pathology (Tables 1, 2; Jiang et al., 2014). Another study concluded that though Notch inhibition does produce slight functional defects in dystrophic muscle, Notch activation does not significantly improve muscle regeneration in mouse models (Table 2; Church et al., 2014). So, despite some promising experiments, further research is needed to clearly elucidate the link between muscular dystrophy and Notch signaling and set the stage for effective therapies.

To add to these contradictory findings, some studies have found overexpression of Notch signaling to actually be associated with the DMD phenotype, whereas deficiency of Notch signaling is usually thought to precede the satellite cell pool depletion implicated in DMD (Mu et al., 2015). Studies in *dystrophin*/*utrophin* dKO mice have exhibited sustained inflammation, impaired muscle regeneration, and rapid depletion and senescence of satellite cells associated with overactivation of Notch signaling genes (Table 1; Mu et al., 2015). The reasoning for this is that Notch signaling may repress myogenesis, which causes it to adversely affect muscle regeneration (Mu et al., 2015). Subsequent experiments showed that intramuscular injection of DAPT, a γ-secretase inhibitor, acted to inhibit Notch signaling and consequently upregulated expression of Pax7 and MyoD, and also improved the histopathology of dystrophic muscle (Table 2; Mu et al., 2015). This suggests that activated Notch signaling may participate in the pathology of DMD, and that downregulation of Notch may be an effective therapeutic approach (Mu et al., 2015). Importantly, these experiments utilized dKO mice, rather than the *mdx* mouse model that has been more frequently employed. It has been suggested that findings in dKO mice may more accurately reflect phenomena in human DMD, as these models more accurately mimic DMD pathology (Gao et al., 2019).

Notably, overexpression of Notch exhibits context-dependent effects, depending upon whether it is induced in satellite cells or in differentiated cells (Table 2; Bi et al., 2016). For example, Bi et al. found that overexpression of Notch signaling in satellite cells causes dedifferentiation into quiescent satellite cells, which causes defects in muscle growth and regeneration. However, myotube-specific constitutive Notch activation actually improves regeneration in aged and dystrophic muscles (Table 2; Bi et al., 2016).

With regards to DMD treatment development, Notch signaling has been targeted in prior attempts at transplant-based therapeutic approaches. For instance, for engraftment to be successful, cells must be expanded *ex vivo* since a single donor muscle biopsy does not provide enough cells to meaningfully affect the muscle mass of a DMD patient (Parker et al., 2012). The way in which satellite cells are cultured meaningfully affects their effectiveness after transplant for the repair of dystrophic muscle (Parker et al., 2012; Parker and Tapscott, 2013). Studies have demonstrated that *ex vivo* expansion on tissue culture plates coated with Dll1-IgG fusion protein inhibits differentiation and increases levels of genes normally expressed in satellite cells, which leads to more effective engraftment and regeneration (Parker et al., 2012; Parker and Tapscott, 2013). Therefore, approaches incorporating components of the Notch pathway may be beneficial in transplant-based therapies.

Furthermore, therapeutic applications of the Notch pathway have been explored with regard to other topics in developmental and cancer biology (Zohorsky and Mequanint, 2021). Some studies have tried delivering soluble ligands in an attempt to activate Notch signaling, though these attempts have been largely unsuccessful (Zohorsky and Mequanint, 2021). Hence, the focus is being directed to the embedded and immobilized delivery of Notch ligands in order to facilitate activation of the endogenous pathway (Zohorsky and Mequanint, 2021). Thus far, Notch ligands have been immobilized to two-dimensional surfaces to examine the behavior of various cell types, including satellite cells (Parker et al., 2012; Safaee et al., 2017; Zohorsky and Mequanint, 2021). This idea has been employed in practice to respond to several maladies. For instance, one study found that the delivery of Jag1 to wounds was able to enhance wound healing (Chigurupati et al., 2007). Another found that delivery of Jag1-containing hydrogels inhibited myofibroblast differentiation in order to counteract cardiac fibrosis and expedite cardiac repair (Boopathy et al., 2015). Utilizing a different approach, another group found that implementing soluble Jag1 via stents could inhibit Notch signaling and subsequently prevent restenosis in vein grafts (Zhou et al., 2015). Hence, research thus far has demonstrated success in targeting the Notch pathway via multiple approaches in order to achieve varied goals, suggesting promise for targeting the Notch pathway in DMD treatments. It should be noted that the Notch pathway has been successfully targeted in cancer therapies as well, given the wealth of Notch research done through the lens of cancer biology and the implication of abnormal activation and expression of the Notch pathway in cancers, especially breast cancer and liver cancer (Zhang et al., 2019; Jia et al., 2021). Over the past 10 years, several new classes of drugs have emerged to therapeutically target Notch in cancer, acting to limit Notch signaling to reduce the pathway's pro-oncogenic effects (Moore et al., 2020). Delivery of γ-secretase inhibitors such as DAPT has been effective, as well as receptor/ligand antibodies and Notch transcription complex inhibitors (Moore et al., 2020; Jia et al., 2021). A pro-inflammatory cytokine, IL-1β, is known to promote cell cycle progression of non-dystrophic myogenic cells but not

DMD myogenic cells. Jag1, which is induced by IL-1β in DMD but not by normal cells, reduces the proliferation and differentiation of myogenic cells. Therefore, up-regulation of Jag1 by IL-1β plays a crucial role in the loss of muscle regeneration capacity of DMD muscles (Table 2; Nagata et al., 2017). Finally, inhibition of Notch and TGF-β promotes myogenic differentiation of human DMD-derived induced Pluripotent Stem Cells (iPSCs) (Table 2; Choi et al., 2012). With respect to muscular dystrophy treatment, the opposite approach would likely be taken, attempting to increase Notch activity rather than decrease it as is done in cancer treatments.

Finally, mutations in several components of the Notch pathway have been implicated in other various hereditary disorders, in addition to muscular dystrophies (Table 2). Missense mutations in Notch ligands *Jag1*, *Dll1*, and *Dll4* have been linked to Alagille syndrome I (ALGS), nonspecific neurodevelopmental disorders, and Adams-Oliver Syndrome 6 (AOS6), respectively (Coppens et al., 2021). CGG repeat expansions in the noncoding region of the *NOTCH2NLC* gene, a Notch inhibitor (Fiddes et al., 2018), can enhance Notch signaling. These expansions have been associated with several diseases, including multiple system atrophy (MSA), leukoencephalopathy, and forms of dementia including Alzheimer's disease and frontotemporal dementia (Fiddes et al., 2018; Ogasawara et al., 2020). CGG repeats of *NOTCH2NLC* have also been implicated as a causative factor in neuronal intranuclear inclusion disease (NIID) and oculopharyngodistal myopathy (OPDM), both neurodegenerative diseases that involve progressive muscle weakness (Table 2; Ogasawara et al., 2020). Moreover, mutations at splice sites in different Notch receptors and ligands have also been shown to influence Notch signaling and have been implied in various pathologic phenotypes (Vargas-Franco et al., 2022). The splicing mechanism is somewhat unclear, though one study linked hnRNPL, a splicing regulator, to the Notch signaling pathway in several ways; overexpression of a partner of hnRNPL in zebrafish has been shown to destabilize the NICD and inhibit Notch signaling, studies in mice demonstrated that hnRNPL level is increased when Dll3 (a Notch inhibitory ligand) is lost, the fly homolog of hnRNPL (smooth) genetically modifies Notch, and hnRNPL downstream RNA targets include multiple components of the Notch pathway, including receptors Notch2 and Notch3 (Vargas-Franco et al., 2022). Though the specific mechanism remains unknown, possible splicing defects in Notch pathway components have been associated with many specific diseases. ALGS is normally caused by mutations in the *Jag1*, and heterozygous mutation at a splicing site just before exon 11 has been identified as a culprit (Zhu et al., 2021). Though much less frequently, ALGS is also caused by mutations in the *Notch2*, and a splice site mutation within the ankyrin repeats leads to decreased Notch signaling, playing a role in the pathology (Kamath et al., 2012). A variant in *Notch4* has been associated with schizophrenia, and recent analyses suggested that polymorphisms affecting the alternative splicing of *Notch4* may increase schizophrenia susceptibility (Shayevitz et al., 2012). Splice site mutations in *Notch3* have been linked to CASADIL (Cerebral Autosomal Dominant Arteriopathy with Subcortical Infarcts and Leukoencephalopathy) as a potential source of pathology (Lundkvist et al., 2005). A splice site variant of *Dll4*, which includes an in-frame insertion of 12 bp, has been associated with a variable neurodevelopmental phenotype (Fischer-Zirnsak et al., 2019). Lastly, studies in zebrafish have demonstrated that different splice variants of *deltaC*, a Notch ligand, cannot replace the function of one another during midline formation and somitogenesis (Mara et al., 2008).

Other proteins associated with the Notch pathway: MEGF10 and POGLUT1

It should be noted that there are several interactions between the Notch pathway and other components in satellite cells, which work together to govern satellite cell proliferation. Multiple EGF-like domains 10 (MEGF10) is a transmembrane receptor expressed in both developing muscle satellite cells and myoblasts, which has exhibited marked similarity to Notch (Saha et al., 2017; Draper et al., 2019; Li et al., 2021). MEGF10 regulates myogenesis in conjunction with the Notch pathway, and MEGF10 deficiency displays several characteristics similar to Notch deficiency (Draper et al., 2019; Li et al., 2021). Biallelic loss of function of *MEGF10* causes MEGF10 myopathy or Early-onset myopathy, areflexia, respiratory distress and dysphagia (EMARDD), which involves areflexia, respiratory distress, and dysphagia (Table 2; Logan et al., 2011; Saha et al., 2017). A suggested cellular mechanism for disease in MEGF10 myopathy is slower proliferation and migration of satellite cells (Li et al., 2021). This leads to reduced MyoD expression and subsequent defects in myogenesis, which contributes to impaired skeletal muscle regeneration after injury seen in MEGF10 myopathy (Li et al., 2021). Several similarities and relationships have been identified between MEGF10 and the Notch pathway. First, sequence alignment of mammalian MEGF10 and its *drosophila* homolog, Drpr, have highlighted the conservation of domains that are characteristic of the Notch ligands (Draper et al., 2019). *Drpr* deficiency has been shown to lead to muscle abnormalities in flies. In addition, flies that overexpress mouse MEGF10 or fly Drpr display developmental arrest

(Draper et al., 2019). In mice, there has been a suggestion for interaction between MEGF10 and the Notch pathway in regulating myogenesis (Table 2; Saha et al., 2017). Further, it has been shown that knockdown of *Megf10* results in downregulation of *Notch1*, *Notch2*, *Notch3*, and *Hes1*, hence suggesting that the extracellular domain of MEGF10 may act as a ligand to activate Notch signaling (Holterman et al., 2007). Also, MEGF10 myopathy involves impaired tyrosine phosphorylation, which causes impaired interaction between MEGF10 and the Notch signaling pathway (Li et al., 2021). Similarly to Notch, deficits seen with MEGF10 myopathy have suggested MEGF10 as a target for potential therapies for muscle diseases; rescuing MEGF10 may have therapeutic implications with regard to ameliorating impaired muscle regeneration (Li et al., 2021).

Protein glycosylation is one of the major regulatory mechanisms of the signaling pathway (Pandey et al., 2021). The extracellular domain of the Notch receptor is modified with *O*-fucose and *O*-glucose glycans, and this glycosylation is crucial for the activity of the pathway (Takeuchi et al., 2018). POGLUT1 is involved in the post-translational modification and function of Notch receptors and ligands by reducing *O*-glucosyltransferase activity on Notch, receptors and ligands and missense mutations in *POGLUT1* were identified in a family with autosomal recessive limb-girdle muscular dystrophy (LGMD) (Table 2; Servián-Morilla et al., 2016). Primary myoblasts from patients with *POGLUT1* mutations demonstrate slow proliferation, a decreased pool of quiescent satellite cells and a decreased Notch signaling in their muscle tissues (Table 1; Servián-Morilla et al., 2016). Studies have also identified potential interactions between POGLUT1 and Jag1, though the biological relevance is still unclear (Pandey et al., 2021).

α-Dystroglycan is a glycosylated protein and a key component of the dystrophin-glycoprotein complex (DCG), as it is essential for normal basement membrane development and muscle maintenance (Servián-Morilla et al., 2016). Its extracellular subunit is modified with *O*-linked glycans, which is necessary for the proliferation of satellite cells. One study focused on ribitol-phosphate modification, which is necessary for functional maturation of α-dystroglycan (Tokuoka et al., 2022). Cytidine-diphosphate (CDP-ribitol) is a donor substrate for ribitol-phosphate modification , and proof-of-concept work indicated that supplementation therapy with CDP-ribitol could accelerate development of therapeutic agents for diseases involving glycosylation defects, including DMD (Tokuoka et al., 2022). These results suggest that modulations of Notch protein and pathway may be a promising therapeutic target for muscular dystrophies.

Conclusion

Due to their prevalence and severity, it is imperative that we continue to search for effective therapies for muscular dystrophies, including DMD. The pathogenesis of DMD and other muscular dystrophies has been well-characterized, and there has been a convincing indication that depletion of the satellite cell pool is implicated in the degeneration that defines the muscular dystrophy phenotype. By targeting the Notch signaling pathway, therapies have the potential to selectively increase the proliferation of satellite cells, thereby hopefully ameliorating the muscular dystrophy phenotype and dramatically improving the quality of life for those living with the condition. Prior work has demonstrated some success with satellite cell-transfer therapies, as well as with targeted upregulation of certain components of the Notch signaling pathway, including the ligand Jag1. Further research is necessary for the optimization of these therapies and the exploration of different manners in which the power of the Notch signaling pathway can be harnessed in order to combat muscular dystrophies.

Author contributions

All authors listed have made a substantial, direct, and intellectual contribution to the work and approved it for publication.

Funding

This work was supported by NIHR01AR062142, NIHR21AR070319, and Regenerative Medicine Minnesota (RMM) Grant to AA.

Conflict of interest

The authors declare that the research was conducted in the absence of any commercial or financial relationships that could be construed as a potential conflict of interest.

Publisher's note

References

Andersson, E. R., Sandberg, R., and Lendahl, U. (2011). Notch signaling: Simplicity in design, versatility in function. *Development* 138, 3593–3612. doi:10.1242/dev.063610

Armstrong, N., Schrader, R., Fischer, R., and Crossnohere, N. (2022). Duchenne expert physician perspectives on Duchenne newborn screening and early Duchenne care. *Am. J. Med. Genet. Part C Semin. Med. Genet. n/a*. doi:10.1002/ajmg.c.31993

Asakura , A., Komaki, M., and Rudnicki, M. A. (200). Muscle satellite cells are multipotential stem cells that exhibit myogenic, osteogenic, and adipogenic differentiation. *Differentiation* 68, 245–253. doi:10.1046/j.1432-0436.2001.680412.x

Asakura, A., Seale, P., Girgis-Gabardo, A., and Rudnicki, M. A. (2002) Myogenic specification of side population cells in skeletal muscle. *J. Cell Biol.* 159, 123–134. doi:10.1083/jcb.200202092

Bagdatlioglu, E., Porcari, P., Greally, E., Blamire, A. M., and Straub, V. W. (2020). Cognitive impairment appears progressive in the mdx mouse. *Neuromuscul. Disord.* 30, 368–388. doi:10.1016/j.nmd.2020.02.018

Baghdadi, M. B., Castel, D., Machado, L., Fukada, S.-I., Birk, D. E., Relaix, F., et al. (2018). Reciprocal signalling by Notch-Collagen V-CALCR retains muscle stem cells in their niche. *Nature* 557, 714–718. doi:10.1038/s41586-018-0144-9

Balin, S. J., and Cascalho, M. (2010). The rate of mutation of a single gene. *Nucleic Acids Res.* 38, 1575–1582. doi:10.1093/nar/gkp1119

Bi, P., Yue, F., Sato, Y., Wirbisky, S., Liu, W., Shan, T., et al. (2016). Stage-specific effects of Notch activation during skeletal myogenesis. *Elife* 5, e17355, doi:10.7554/eLife.17355

Biressi, S., Bjornson, C. R. R., Carlig, P. M. M., Nishijo, K., Keller, C., and Rando, T. A. (2013). Myf5 expression during fetal myogenesis defines the developmental progenitors of adult satellite cells. *Dev. Biol.* 379, 195–207. doi:10.1016/j.ydbio.2013.04.021

Birnkrant, D. J., Bushby, K., Bann, C. M., Alman, B. A., Apkon, S. D., Blackwell, A., et al. (2018a). Diagnosis and management of Duchenne muscular dystrophy, part 2: Respiratory, cardiac, bone health, and orthopaedic management. *Lancet. Neurol.* 17, 347–361. doi:10.1016/S1474-4422(18)30025-5

Birnkrant, D. J., Bushby, K., Bann, C. M., Apkon, S. D., Blackwell, A., Brumbaugh, D., et al. (2018b). Diagnosis and management of Duchenne muscular dystrophy, part 1: Diagnosis, and neuromuscular, rehabilitation, endocrine, and gastrointestinal and nutritional management. *Lancet. Neurol.* 17, 251–267. doi:10.1016/S1474-4422(18)30024-3

Bjornson, C. R. R., Cheung, T. H., Liu, L., Tripathi, P. V., Steeper, K. M., and Rando, T. A. (2011). Notch signaling is necessary to maintain quiescence in adult muscle stem cells. *Stem Cells* 30, 232–242. doi:10.1002/stem.773

Boldrin, L., Zammit, P. S., and Morgan, J. E. (2015). Satellite cells from dystrophic muscle retain regenerative capacity. *Stem Cell Res.* 14, 20–29. doi:10.1016/j.scr.2014.10.007

Boopathy, A. V., Martinez, M. D., Smith, A. W., Brown, M. E., García, A. J., and Davis, M. E. (2015). Intramyocardial delivery of notch ligand-containing hydrogels improves cardiac function and angiogenesis following infarction. *Tissue Eng. Part A* 21, 2315–2322. doi:10.1089/ten.TEA.2014.0622

Brinkmeyer-Langford, C., Chu, C., Balog-Alvarez, C., Yu, X., Cai, J. J., Nabity, M., et al. (2018). Expression profiling of disease progression in canine model of Duchenne muscular dystrophy. *PLoS One* 13, e0194485, doi:10.1371/journal.pone.0194485

Bröhl, D., Vasyutina, E., Czajkowski, M. T., Griger, J., Rassek, C., Rahn, H.-P., et al. (2012). Colonization of the satellite cell niche by skeletal muscle progenitor cells depends on notch signals. *Dev. Cell* 23, 469–481. doi:10.1016/j.devcel.2012.07.014

Chang, N. C., Chevalier, F. P., and Rudnicki, M. A. (2016). Satellite cells in muscular dystrophy - lost in polarity. *Trends Mol. Med.* 22, 479–496. doi:10.1016/j.molmed.2016.04.002

Chigurupati, S., Arumugam, T. V., Son, T. G., Lathia, J. D., Jameel, S., Mughal, M. R., et al. (2007). Involvement of notch signaling in wound healing. *PLoS One* 2, e1167, doi:10.1371/journal.pone.0001167

Choi, I. Y., Lim, H. T., Che, Y. H., Lee, G., and Kim, Y. J. (2012). Inhibition of the combinatorial signaling of transforming growth factor-beta and NOTCH promotes myotube formation of human pluripotent stem cell-derived skeletal muscle progenitor cells. *Cells.* 10, 1649, doi:10.3390/cells10071649

Church, J. E., Trieu, J., Chee, A., Naim, T., Gehrig, S. M., Lamon, S., et al. (2014). Alterations in Notch signalling in skeletal muscles from mdx and dko dystrophic mice and patients with Duchenne muscular dystrophy. *Exp. Physiol.* 99, 675–687. doi:10.1113/expphysiol.2013.077255

Conboy, I. M., Conboy, M. J., Smythe, G. M., and Rando, T. A. (2003). Notch-mediated restoration of regenerative potential to aged muscle. *Science* 302, 1575–1577. doi:10.1126/science.1087573

Conboy, I. M., and Rando, T. A. (2002). The regulation of notch signaling controls satellite cell activation and cell fate determination in postnatal myogenesis. *Dev. Cell* 3, 397–409. doi:10.1016/s1534-5807(02)00254-x

Coppens, S., Barnard, A. M., Puusepp, S., Pajusalu, S., Õunap, K., Vargas-Franco, D., et al. (2021). A form of muscular dystrophy associated with pathogenic variants in JAG2. *Am. J. Hum. Genet.* 108, 1164–1856. doi:10.1016/j.ajhg.2021.04.018

Cossu, G., and Sampaolesi, M. (2007). New therapies for Duchenne muscular dystrophy: Challenges, prospects and clinical trials. *Trends Mol. Med.* 13, 520–526. doi:10.1016/j.molmed.2007.10.003

Crisafulli, S., Sultana, J., Fontana, A., Salvo, F., Messina, S., and Trifirò, G. (2020). Global epidemiology of Duchenne muscular dystrophy: An updated systematic review and meta-analysis. *Orphanet J. Rare Dis.* 15, 141, doi:10.1186/s13023-020-01430-8

Dong, Z., Huo, J., Liang, A., Chen, J., Chen, G., and Liu, D. (2021). Gamma-Secretase Inhibitor (DAPT), a potential therapeutic target drug, caused neurotoxicity in planarian regeneration by inhibiting Notch signaling pathway. *Sci. Total Environ.* 781, 146735, doi:10.1016/j.scitotenv.2021.146735

Draper, I., Saha, M., Stonebreaker, H., Salomon, R. N., Matin, B., and Kang, P. B. (2019). The impact of Megf10/Drpr gain-of-function on muscle development in Drosophila. *FEBS Lett.* 593, 680–696. doi:10.1002/1873-3468.13348

D'Souza, B., Miyamoto, A., and Weinmaster, G. (2008). The many facets of Notch ligands. *Oncogene* 27, 5148–5167. doi:10.1038/onc.2008.229

Duan, D., Goemans, N., Takeda, S., Mercuri, E., and Aartsma-Rus, A. (2021). Duchenne muscular dystrophy. *Nat. Rev. Dis. Prim.* 7, 13, doi:10.1038/s41572-021-00248-3

Dumont, N. A., and Rudnicki, M. A. (2016). Targeting muscle stem cell intrinsic defects to treat Duchenne muscular dystrophy. *Npj Regen. Med.* 1, 16006, doi:10.1038/npjregenmed.2016.6

Dumont, N. A., Wang, Y. X., and Rudnicki, M. A. (2015). Intrinsic and extrinsic mechanisms regulating satellite cell function. *Development* 142, 1572–1581. doi:10.1242/dev.114223

Fiddes, I. T., Lodewijk, G. A., Mooring, M., Bosworth, C. M., Ewing, A. D., Mantalas, G. L., et al. (2018). Human-specific NOTCH2NL genes affect notch signaling and cortical neurogenesis. *Cell* 173, 1356–1369. doi:10.1016/j.cell.2018.03.051e22

Fiore, P. F., Benedetti, A., Sandonà, M., Madaro, L., De Bardi, M., Saccone, V., et al. (2020). Lack of PKCθ promotes regenerative ability of muscle stem cells in chronic muscle injury. *Int. J. Mol. Sci.* 21, E932, doi:10.3390/ijms21030932

Fischer-Zirnsak, B., Segebrecht, L., Schubach, M., Charles, P., Alderman, E., Brown, K., et al. (2019). Haploinsufficiency of the notch ligand DLL1 causes variable neurodevelopmental disorders. *Am. J. Hum. Genet.* 105, 631–639. doi:10.1016/j.ajhg.2019.07.002

Frontera, W. R., and Ochala, J. (2015). Skeletal muscle: A brief review of structure and function. *Calcif. Tissue Int.* 96, 183–195. doi:10.1007/s00223-014-9915-y

Fuchs, E., and Blau, H. M. (2020). Tissue stem cells: Architects of their niches. *Cell Stem Cell* 27, 532–556. doi:10.1016/j.stem.2020.09.011

Fujimaki, S., Matsumoto, T., Muramatsu, M., Nagahisa, H., Horii, N., Seko, D., et al. (2022). The endothelial Dll4–muscular Notch2 axis regulates skeletal muscle mass. *Nat. Metab.* 4, 180–189. doi:10.1038/s42255-022-00533-9

Fujimaki, S., Seko, D., Kitajima, Y., Yoshioka, K., Tsuchiya, Y., Masuda, S., et al. (2017). Notch1 and Notch2 coordinately regulate stem cell function in the quiescent and activated states of muscle satellite cells. *Stem Cells* 36, 278–285. doi:10.1002/stem.2743

Fukada, S., Uezumi, A., Ikemoto, M., Masuda, S., Segawa, M., Tanimura, N., et al. (2007). Molecular signature of quiescent satellite cells in adult skeletal muscle. *Stem Cells* 25, 2448–2459. doi:10.1634/stemcells.2007-0019

Gao, Q. Q., and McNally, E. M. (2015). The dystrophin complex: Structure, function, and implications for therapy. *Compr. Physiol.* 5, 1223–1239. doi:10.1002/cphy.c140048

Gao, X., Tang, Y., Amra, S., Sun, X., Cui, Y., Cheng, H., et al. (2019). Systemic investigation of bone and muscle abnormalities in dystrophin/utrophin double knockout mice during postnatal development and the mechanisms. *Hum. Mol. Genet.* 28, 1738–1751. doi:10.1093/hmg/ddz012

Gayraud-Morel, B., Chrétien, F., Jory, A., Sambasivan, R., Negroni, E., Flamant, P., et al. (2012). Myf5 haploinsufficiency reveals distinct cell fate potentials for adult skeletal muscle stem cells. *J. Cell Sci.* 125, 1738–1749. doi:10.1242/jcs.097006

Gioftsidi, S., Relaix, F., and Mourikis, P. (2022). The Notch signaling network in muscle stem cells during development, homeostasis, and disease. *Skelet. Muscle* 12, 9, doi:10.1186/s13395-022-00293-w

Guiraud, S., Aartsma-Rus, A., Vieira, N. M., Davies, K. E., van Ommen, G.-J. B., and Kunkel, L. M. (2015). The pathogenesis and therapy of muscular dystrophies. *Annu. Rev. Genomics Hum. Genet.* 16, 281–308. doi:10.1146/annurev-genom-090314-025003

Hindi, S. M., Shin, J., Ogura, Y., Li, H., and Kumar, A. (2013). Matrix metalloproteinase-9 inhibition improves proliferation and engraftment of myogenic cells in dystrophic muscle of mdx mice. *PLoS One.* 8, e72121, doi:10.1371/journal.pone.0072121

Holterman, C. E., Le Grand, F., Kuang, S., Seale, P., and Rudnicki, M. A. (2007). Megf10 regulates the progression of the satellite cell myogenic program. *J. Cell Biol.* 179, 911–922. doi:10.1083/jcb.200709083

Iftikhar, M., Frey, J., Shohan, M. J., Malek, S., and Mousa, S. A. (2021). Current and emerging therapies for Duchenne muscular dystrophy and spinal muscular atrophy. *Pharmacol. Ther.* 220, 107719, doi:10.1016/j.pharmthera.2020.107719

Jia, H., Wang, Z., Zhang, J., and Feng, F. (2021). γ-Secretase inhibitors for breast cancer and hepatocellular carcinoma: From mechanism to treatment. *Life Sci.* 268, 119007, doi:10.1016/j.lfs.2020.119007

Jiang, C., Wen, Y., Kuroda, K., Hannon, K., Rudnicki, M., and Kuang, S. (2014). Notch signaling deficiency underlies age-dependent depletion of satellite cells in muscular dystrophy. *Dis. Model. Mech.* 7, 997, 1004. doi:10.1242/dmm.015917

Joanisse, S., Nederveen, J. P., Snijders, T., McKay, B. R., and Parise, G. (2017). Skeletal muscle regeneration, repair and remodelling in aging: The importance of muscle stem cells and vascularization. *Gerontology* 63, 91–100. doi:10.1159/000450922

Kamath, B. M., Bauer, R. C., Loomes, K. M., Chao, G., Gerfen, J., Hutchinson, A., et al. (2012). NOTCH2 mutations in Alagille syndrome. *J. Med. Genet.* 49, 138–144. doi:10.1136/jmedgenet-2011-100544

Kanisicak, O., Mendez, J. J., Yamamoto, S., Yamamoto, M., and Goldhamer, D. J. (2009). Progenitors of skeletal muscle satellite cells express the muscle determination gene, MyoD., *Dev. Biol.* 332, 131–141. doi:10.1016/j.ydbio.2009.05.554

Kann, A. P., Hung, M., and Krauss, R. S. (2021). Cell–cell contact and signaling in the muscle stem cell niche. *Curr. Opin. Cell Biol.* 73, 78–83. doi:10.1016/j.ceb.2021.06.003

Kitamoto, T., and Hanaoka, K. (2010). Notch3 null mutation in mice causes muscle hyperplasia by repetitive muscle regeneration. *Stem Cells* 28, 2205–2216. doi:10.1002/stem.547

Kornegay, J. N. (2017). The golden retriever model of Duchenne muscular dystrophy. *Skelet. Muscle* 7, 9, doi:10.1186/s13395-017-0124-z

Kottlors, M., and Kirschner, J. (2010). Elevated satellite cell number in Duchenne muscular dystrophy. *Cell Tissue Res.* 340, 541–548. doi:10.1007/s00441-010-0976-6

Kuang, S., Kuroda, K., Le Grand, F., and Rudnicki, M. A. (2007). Asymmetric self-renewal and commitment of satellite stem cells in muscle. *Cell* 129, 999–1010. doi:10.1016/j.cell.2007.03.044

Kuroda, K., Tani, S., Tamura, K., Minoguchi, S., Kurooka, H., and Honjo, T. (1999). Delta-induced notch signaling mediated by RBP-J inhibits MyoD expression and myogenesis*. *J. Biol. Chem.* 274, 7238–7244. doi:10.1074/jbc.274.11.7238

Law, P., Bertorini, T., Goodwin, T., Chen, M., Fang, Q., Li, H.-J., et al. (1990). Dystrophin production induced by myoblast transfer therapy in Duchenne muscular dystrophy. *Lancet* 336, 114–115. doi:10.1016/0140-6736(90)91628-n

Li, C., Vargas-Franco, D., Saha, M., Davis, R. M., Manko, K. A., Draper, I., et al. (2021). Megf10 deficiency impairs skeletal muscle stem cell migration and muscle regeneration. *FEBS Open Bio* 11, 114–123. doi:10.1002/2211-5463.13031

Lin, S., Shen, H., Jin, B., Gu, Y., Chen, Z., Cao, C., et al. (2013). Brief report: Blockade of Notch signaling in muscle stem cells causes muscular dystrophic phenotype and impaired muscle regeneration. *Stem Cells* 31, 823–828. doi:10.1002/stem.1319

Liu, Q., Deng, J., Qiu, Y., Gao, J., Li, J., Guan, L., et al. (2021). Non-coding RNA basis of muscle atrophy. *Mol. Ther. Nucleic Acids* 26, 1066–1078. doi:10.1016/j.omtn.2021.10.010

Logan, C. V., Lucke, B., Pottinger, C., Abdelhamed, Z. A., Parry, D. A., Szymanska, K., et al. (2011). Mutations in MEGF10, a regulator of satellite cell myogenesis, cause early onset myopathy, areflexia, respiratory distress and dysphagia (EMARDD). *Nat. Genet.* 43, 1189–1192. doi:10.1038/ng.995

Lovering, R. M., Porter, N. C., and Bloch, R. J. (2005). The muscular dystrophies: From genes to therapies. *Phys. Ther.* 85, 1372–1388. doi:10.1093/ptj/85.12.1372

Low, S., Barnes, J. L., Zammit, P. S., and Beauchamp, J. R. (2018). Delta-like 4 activates notch 3 to regulate self-renewal in skeletal muscle stem cells. *Stem Cells* 36, 458–466. doi:10.1002/stem.2757

Lundkvist, J., Zhu, S., Hansson, E. M., Schweinhardt, P., Miao, Q., Beatus, P., et al. (2005). Mice carrying a R142C Notch 3 knock-in mutation do not develop a CADASIL-like phenotype. *Genesis* 41, 13–22. doi:10.1002/gene.20091

Luo, D., Renault, V. M., and Rando, T. A. (2005). The regulation of Notch signaling in muscle stem cell activation and postnatal myogenesis. *Semin. Cell Dev. Biol.* 16, 612–622. doi:10.1016/j.semcdb.2005.07.002

Mah, J. K. (2016). Current and emerging treatment strategies for Duchenne muscular dystrophy. *Neuropsychiatr. Dis. Treat.* 12, 1795–1807. doi:10.2147/NDT.S93873

Mara, A., Schroeder, J., and Holley, S. A. (2008). Two deltaC splice-variants have distinct signaling abilities during somitogenesis and midline patterning. *Dev. Biol.* 318, 126–132. doi:10.1016/j.ydbio.2008.03.009

McIntyre, B., Asahara, T., and Alev, C. (2020). *Overview of basic mechanisms of Notch signaling in development and disease BT - Notch signaling in embryology and cancer. Molecular biology of Notch signaling.* J. Reichrath and S. Reichrath, eds. (Cham: Springer International Publishing), pp. 9–27. doi:10.1007/978-3-030-36422-9_2

Mohamadian, M., Rastegar, M., Pasamanesh, N., Ghadiri, A., Ghandil, P., and Naseri, M. (2022). Clinical and molecular spectrum of muscular dystrophies (MDs) with intellectual disability (ID): A comprehensive overview. *J. Mol. Neurosci.* 72, 9–23. doi:10.1007/s12031-021-01933-4

Moore, G., Annett, S., McClements, L., and Robson, T. (2020). Top notch targeting strategies in cancer: A detailed overview of recent insights and current perspectives. *Cells* 9. 1503. doi:10.3390/cells9061503

Morgan, J. E., and Zammit, P. S. (2010). Direct effects of the pathogenic mutation on satellite cell function in muscular dystrophy. *Exp. Cell Res.* 316, 3100–3108. doi:10.1016/j.yexcr.2010.05.014

Motohashi, N., Shimizu-Motohashi, Y., Roberts, T. C., and Aoki, Y. (2019). Potential therapies using myogenic stem cells combined with bio-engineering approaches for treatment of muscular dystrophies. *Cells* 8, 1066, doi:10.3390/cells8091066

Mourikis, P., Sambasivan, R., Castel, D., Rocheteau, P., Bizzarro, V., and Tajbakhsh, S. (2012). A critical requirement for notch signaling in maintenance of the quiescent skeletal muscle stem cell state. *Stem Cells* 30, 243–252. doi:10.1002/stem.775

Mu, X., Tang, Y., Lu, A., Takayama, K., Usas, A., Wang, B., et al. (2015). The role of Notch signaling in muscle progenitor cell depletion and the rapid onset of histopathology in muscular dystrophy. *Hum. Mol. Genet.* 24, 2923–2937. doi:10.1093/hmg/ddv055

Nagata, Y., Kiyono, T., Okamura, K., Goto, Y. I., Matsuo, M., Ikemoto-Uezumi, M., et al. (2017). Interleukin-1beta (IL-1β)-induced Notch ligand Jagged1 suppresses mitogenic action of IL-1β on human dystrophic myogenic cells. *PLoS One.* 12, e0188821, doi:10.1371/journal.pone.0188821

Nakamura, A., Fueki, N., Shiba, N., Motoki, H., Miyazaki, D., Nishizawa, H., et al. (2016). Deletion of exons 3-9 encompassing a mutational hot spot in the DMD gene presents an asymptomatic phenotype, indicating a target region for multiexon skipping therapy. *J. Hum. Genet.* 61, 663–667. doi:10.1038/jhg.2016.28

Nandagopal, N., Santat, L. A., LeBon, L., Sprinzak, D., Bronner, M. E., and Elowitz, M. B. (2018). Dynamic ligand discrimination in the notch signaling pathway. *Cell* 172, 869–880. doi:10.1016/j.cell.2018.01.002e19

Ogasawara, M., Iida, A., Kumutpongpanich, T., Ozaki, A., Oya, Y., Konishi, H., et al. (2020). CGG expansion in NOTCH2NLC is associated with oculopharyngodistal myopathy with neurological manifestations. *Acta Neuropathol. Commun.* 8, 204. doi:10.1186/s40478-020-01084-4

Pandey, A., Niknejad, N., and Jafar-Nejad, H. (2021). Multifaceted regulation of Notch signaling by glycosylation. *Glycobiology* 31, 8–28. doi:10.1093/glycob/cwaa049

Parker, M. H., Loretz, C., Tyler, A. E., Duddy, W. J., Hall, J. K., Olwin, B. B., et al. (2012). Activation of Notch signaling during *ex vivo* expansion maintains donor muscle cell engraftment. *Stem Cells* 30, 2212–2220. doi:10.1002/stem.1181

Parker, M. H., and Tapscott, S. J. (2013). Expanding donor muscle-derived cells for transplantation. *Curr. Protoc. Stem Cell Biol.* Chapter 2, Unit 2C.4. doi:10.1002/9780470151808.sc02c04s25*Chapter 2,* Unit-2C.4

Plantié, E., Migocka-Patrzałek, M., Daczewska, M., and Jagla, K. (2015). Model organisms in the fight against muscular dystrophy: Lessons from drosophila and zebrafish. *Molecules* 20, 6237–6253. doi:10.3390/molecules20046237

Preuße, K., Tveriakhina, L., Schuster-Gossler, K., Gaspar, C., Rosa, A. I., Henrique, D., et al. (2015). Context-dependent functional divergence of the notch ligands DLL1 and DLL4 *in vivo*. *PLoS Genet.* 11, e1005328. doi:10.1371/journal.pgen.1005328

Ricotti, V., Mandy, W. P. L., Scoto, M., Pane, M., Deconinck, N., Messina, S., et al. (2016). Neurodevelopmental, emotional, and behavioural problems in Duchenne

muscular dystrophy in relation to underlying dystrophin gene mutations. *Dev. Med. Child. Neurol.* 58, 77–84. doi:10.1111/dmcn.12922

Rocheteau, P., Gayraud-Morel, B., Siegl-Cachedenier, I., Blasco, M. A., and Tajbakhsh, S. (2012). A subpopulation of adult skeletal muscle stem cells retains all template DNA strands after cell division. *Cell* 148, 112–125. doi:10.1016/j.cell.2011.11.049

Sacco, A., Mourkioti, F., Tran, R., Choi, J., Llewellyn, M., Kraft, P., et al. (2010). Short telomeres and stem cell exhaustion model Duchenne muscular dystrophy in mdx/mTR mice. *Cell* 143, 1059–1071. doi:10.1016/j.cell.2010.11.039

Safaee, H., Bakooshli, M. A., Davoudi, S., Cheng, R. Y., Martowirogo, A. J., Li, E. W., et al. (2017). Tethered jagged-1 synergizes with culture substrate stiffness to modulate notch-induced myogenic progenitor differentiation. *Cell. Mol. Bioeng.* 10, 501–513. doi:10.1007/s12195-017-0506-7

Saha, M., Mitsuhashi, S., Jones, M. D., Manko, K., Reddy, H. M., Bruels, C. C., et al. (2017). Consequences of MEGF10 deficiency on myoblast function and Notch1 interactions. *Hum. Mol. Genet.* 26, 2984–3000. doi:10.1093/hmg/ddx189

Sakai, H., Fukuda, S., Nakamura, M., Uezumi, A., Noguchi, Y.-T., Sato, T., et al. (2017). Notch ligands regulate the muscle stem-like state *ex vivo* but are not sufficient for retaining regenerative capacity. *PLoS One* 12, e0177516. doi:10.1371/journal.pone.0177516

Sato, C., Zhao, G., and Ilagan, M. X. G. (2012). An overview of notch signaling in adult tissue renewal and maintenance. *Curr. Alzheimer Res.* 9, 227–240. doi:10.2174/156720512799361600

Servián-Morilla, E., Takeuchi, H., Lee, T. V., Clarimon, J., Mavillard, F., Area-Gómez, E., et al. (2016). A POGLUT1 mutation causes a muscular dystrophy with reduced Notch signaling and satellite cell loss. *EMBO Mol. Med.* 8, 1289–1309. doi:10.15252/emmm.201505815

Shayevitz, C., Cohen, O. S., Faraone, S. V., and Glatt, S. J. (2012). A re-review of the association between the NOTCH4 locus and schizophrenia. *Am. J. Med. Genet. B Neuropsychiatr. Genet.* 159B, 477–483. doi:10.1002/ajmg.b.32050

Shimizu-Motohashi, Y., Komaki, H., Motohashi, N., Takeda, S., Yokota, T., and Aoki, Y. (2019). Restoring dystrophin expression in Duchenne muscular dystrophy: Current status of therapeutic approaches. *J. Pers. Med.* 9, E1. doi:10.3390/jpm9010001

Siebel, C., and Lendahl, U. (2017). Notch signaling in development, tissue homeostasis, and disease. *Physiol. Rev.* 97, 1235–1294. doi:10.1152/physrev.00005.2017

Sousa-Victor, P., García-Prat, L., and Muñoz-Cánoves, P. (2022). Control of satellite cell function in muscle regeneration and its disruption in ageing. *Nat. Rev. Mol. Cell Biol.* 23, 204–226. doi:10.1038/s41580-021-00421-2

Starosta, A., and Konieczny, P. (2021). Therapeutic aspects of cell signaling and communication in Duchenne muscular dystrophy. *Cell. Mol. Life Sci.* 78, 4867–4891. doi:10.1007/s00018-021-03821-x

Sun, C., Shen, L., Zhang, Z., and Xie, X. (2020). *Therapeutic Strategies for Duchenne Muscular Dystrophy: An Update. Genes (Basel).* 11.doi:10.3390/genes11080837

Takeuchi, H., Schneider, M., Williamson, D. B., Ito, A., Takeuchi, M., Handford, P. A., et al. (2018). Two novel protein O-glucosyltransferases that modify sites distinct from POGLUT1 and affect Notch trafficking and signaling. *Proc. Natl. Acad. Sci. U. S. A.* 115, E8395–E8402. doi:10.1073/pnas.1804005115

Tedesco, F. S., Dellavalle, A., Diaz-Manera, J., Messina, G., and Cossu, G. (2010). Repairing skeletal muscle: Regenerative potential of skeletal muscle stem cells. *J. Clin. Invest.* 120, 11–19. doi:10.1172/JCI40373

Tokuoka, H., Imae, R., Nakashima, H., Manya, H., Masuda, C., Hoshino, S., et al. (2022). CDP-ribitol prodrug treatment ameliorates ISPD-deficient muscular dystrophy mouse model. *Nat. Commun.* 13, 1847. doi:10.1038/s41467-022-29473-4

Tominari, T., and Aoki, Y. (2022). Clinical development of novel therapies for Duchenne muscular dystrophy—current and future. *Neurol. Clin. Neurosci.*, 1–8. doi:10.1111/ncn3.12656

Turk, R., Sterrenburg, E., de Meijer, E. J., van Ommen, G. J., den Dunnen, J. T., and 't Hoen, P. A. (2005). Muscle regeneration in dystrophin-deficient mdx mice studied by gene expression profiling. *BMC Genomics.* 6, 98, doi:10.1186/1471-2164-6-98

Vargas-Franco, D., Kalra, R., Draper, I., Pacak, C. A., Asakura, A., and Kang, P. B. (2022). The Notch signaling pathway in skeletal muscle health and disease. *Muscle Nerve* 2022, 1–15. doi:10.1002/mus.27684

Venugopal, V., and Pavlakis, S. (2022). *Duchenne muscular dystrophy*. (Treasure Island, FL: StatPearls Publishing)

Verma, M., Asakura, Y., Murakonda, B. S. R., Pengo, T., Latroche, C., Chazaud, B., et al. (2018). Muscle satellite cell cross-talk with a vascular niche maintains quiescence via VEGF and notch signaling. *Cell Stem Cell* 23, 530–543. doi:10.1016/j.stem.2018.09.007e9

Vieira, N. M., Elvers, I., Alexander, M. S., Moreira, Y. B., Eran, A., Gomes, J. P., et al. (2015). Jagged 1 rescues the Duchenne muscular dystrophy phenotype. *Cell* 163, 1204–1213. doi:10.1016/j.cell.2015.10.049

Waldrop, M. A., Gumienny, F., El Husayni, S., Frank, D. E., Weiss, R. B., and Flanigan, K. M. (2018). Low-level dystrophin expression attenuating the dystrophinopathy phenotype. *Neuromuscul. Disord.* 28, 116–121. doi:10.1016/j.nmd.2017.11.007

Wen, Y., Bi, P., Liu, W., Asakura, A., Keller, C., and Kuang, S. (2012). Constitutive Notch activation upregulates Pax7 and promotes the self-renewal of skeletal muscle satellite cells. *Mol. Cell. Biol.* 32, 2300–2311. doi:10.1128/MCB.06753-11

Wilschut, K. J., Ling, V. B., and Bernstein, H. S. (2012). Concise review: Stem cell therapy for muscular dystrophies. *Stem Cells Transl. Med.* 1, 833–842. doi:10.5966/sctm.2012-0071

Yao, S., Chen, Z., Yu, Y., Zhang, N., Jiang, H., Zhang, G., et al. (2021). Current pharmacological strategies for Duchenne muscular dystrophy. *Front. Cell Dev. Biol.* 9, 689533, doi:10.3389/fcell.2021.689533

Yartseva, V., Goldstein, L. D., Rodman, J., Kates, L., Chen, M. Z., Chen, Y.-J. J., et al. (2020). Heterogeneity of satellite cells implicates DELTA1/NOTCH2 signaling in self-renewal. *Cell Rep.* 30, 1491–1503. doi:10.1016/j.celrep.2019.12.100

Yucel, N., Chang, A. C., Day, J. W., Rosenthal, N., and Blau, H. M. (2018). Humanizing the mdx mouse model of DMD: The long and the short of it. *NPJ Regen. Med.* 3, 4, doi:10.1038/s41536-018-0045-4

Zhang, Y., Lahmann, I., Baum, K., Shimojo, H., Mourikis, P., Wolf, J., et al. (2021). Author Correction: Oscillations of Delta-like1 regulate the balance between differentiation and maintenance of muscle stem cells. *Nat. Commun.* 12, 1766, doi:10.1038/s41467-021-22144-w

Zhang, Y., Xie, Z.-Y., Guo, X.-T., Xiao, X.-H., and Xiong, L.-X. (2019). Notch and breast cancer metastasis: Current knowledge, new sights and targeted therapy. *Oncol. Lett.* 18, 2743–2755. doi:10.3892/ol.2019.10653

Zhou, X., Xiao, Y., Mao, Z., Huang, J., Geng, Q., Wang, W., et al. (2015). Soluble Jagged-1 inhibits restenosis of vein graft by attenuating Notch signaling. *Microvasc. Res.* 100, 9–16. doi:10.1016/j.mvr.2015.01.009

Zhu, W., Cheng, Y.-S., Xu, M., Farkhondeh, A., Beers, J., Zou, J., et al. (2021). Generation of Alagille syndrome derived induced pluripotent stem cell line carrying heterozygous mutation in the JAGGED-1 gene at splicing site (Chr20: 10, 629, 709C>A) before exon 11. *Stem Cell Res.* 53, 102366, doi:10.1016/j.scr.2021.102366

Zohorsky, K., and Mequanint, K. (2021). Designing biomaterials to modulate notch signaling in tissue engineering and regenerative medicine. *Tissue Eng. Part B Rev.* 27, 383–410. doi:10.1089/ten.TEB.2020.0182

frontiers | Frontiers in Physiology

TYPE Original Research
PUBLISHED 14 February 2023
DOI 10.3389/fphys.2023.1109587

OPEN ACCESS

EDITED BY
Katsumasa Goto,
Toyohashi Sozo University, Japan

REVIEWED BY
Gavin Pinniger,
University of Western Australia, Australia
Dawn A. Lowe,
University of Minnesota Twin Cities, United States

*CORRESPONDENCE
Stewart I. Head,
S.head@westernsydney.edu.au

SPECIALTY SECTION
This article was submitted to Striated Muscle Physiology, a section of the journal Frontiers in Physiology

RECEIVED 28 November 2022
ACCEPTED 03 February 2023
PUBLISHED 14 February 2023

CITATION
Redwan A, Kiriaev L, Kueh S, Morley JW, Houweling P, Perry BD and Head SI (2023), Six weeks of N-acetylcysteine antioxidant in drinking water decreases pathological fiber branching in MDX mouse dystrophic fast-twitch skeletal muscle.
Front. Physiol. 14:1109587.
doi: 10.3389/fphys.2023.1109587

Six weeks of N-acetylcysteine antioxidant in drinking water decreases pathological fiber branching in MDX mouse dystrophic fast-twitch skeletal muscle

Asma Redwan[1], Leonit Kiriaev[2], Sindy Kueh[1], John W. Morley[1], Peter Houweling[2], Ben D. Perry[3] and Stewart I. Head[1,2]*

[1]School of Medicine, Western Sydney University, Sydney, NSW, Australia, [2]Murdoch Children's Research Institute, Melbourne, VIC, Australia, [3]School of Science, Western Sydney University, Sydney, NSW, Australia

Introduction: It has been proposed that an increased susceptivity to oxidative stress caused by the absence of the protein dystrophin from the inner surface of the sarcolemma is a trigger of skeletal muscle necrosis in the destructive dystrophin deficient muscular dystrophies. Here we use the mdx mouse model of human Duchenne Muscular Dystrophy to test the hypothesis that adding the antioxidant NAC at 2% to drinking water for six weeks will treat the inflammatory phase of the dystrophic process and reduce pathological muscle fiber branching and splitting resulting in a reduction of mass in mdx fast-twitch EDL muscles.

Methods: Animal weight and water intake was recorded during the six weeks when 2% NAC was added to the drinking water. Post NAC treatment animals were euthanised and the EDL muscles dissected out and placed in an organ bath where the muscle was attached to a force transducer to measure contractile properties and susceptibility to force loss from eccentric contractions. After the contractile measurements had been made the EDL muscle was blotted and weighed. In order to assess the degree of pathological fiber branching mdx EDL muscles were treated with collagenase to release single fibers. For counting and morphological analysis single EDL mdx skeletal muscle fibers were viewed under high magnification on an inverted microscope.

Results: During the six-week treatment phase NAC reduced body weight gain in three- to nine-week-old mdx and littermate control mice without effecting fluid intake. NAC treatment also significantly reduced the mdx EDL muscle mass and abnormal fiber branching and splitting.

Discussion: We propose chronic NAC treatment reduces the inflammatory response and degenerative cycles in the mdx dystrophic EDL muscles resulting

Abbreviations: ANOVA, Analysis of Variance; CN, Centrally nucleated; DMD, Duchenne Muscular Dystrophy; EC, Eccentric Contraction; EDL, Extensor Digitorum Longus; f, Stimulation frequency; FCS, Fetal Calf Serum; h, Hill coefficient; HRT, Half relaxation time; Kf, Half frequency; LC, Littermate controls, Lo, Optimal length; NAC, N-acetylcysteine; P, Force developed, Po, Initial Maximal Force from a single 2 s tetani at 125 Hz; Pmax, Maximal tetanic force; Pmin/Pmax, Force developed at minimum/Force developed at maximum; SD, Standard Deviation; TTP, Time to peak.

in a reduction in the number of complexed branched fibers reported to be responsible for the dystrophic EDL muscle hypertrophy.

KEYWORDS

mdx, skeletal muscle contraction, NAC, oxidative stress, fiber branching, muscle damage, dystrophy, split fiber

Introduction

It has been proposed that oxidative stress plays a role in the pathophysiology of Duchenne Muscular Dystrophy (DMD), despite this there is currently no effective antioxidant treatment for DMD (Mosca et al., 2021; Lian et al., 2022). N-acetylcysteine (NAC) is an antioxidant that is approved for use in humans, making it attractive as a potential therapeutic treatment for inflammatory conditions in humans (Mokhtari et al., 2017). In skeletal muscle NAC acts as a scavenger of free radicals and contributes to increasing levels of the powerful endogenous intracellular antioxidant glutathione (Kerksick and Willoughby, 2005). Oral dosing with NAC counteracts oxidative stress in skeletal muscles of humans and mice (Medved et al., 2004; Matuszczak et al., 2005; Terrill et al., 2012; Michelucci et al., 2017) and has been shown to ameliorate respiratory muscle dysfunction in animal models of hypoxic disease (O'Halloran and Lewis, 2017).

Several studies have used the mdx dystrophin deficient mouse, the most used animal model of the destructive human dystrophin deficient muscular dystrophy DMD, to study the chronic effects of oral administration of NAC in drinking water or by intraperitoneal injection on skeletal muscle pathology (Terrill et al., 2012; Pinto et al., 2013; Pinniger et al., 2017). These mdx mouse studies show NAC lowers markers of inflammation and oxidative stress in diaphragm and limb muscles and reduces necrotic damage.

There have been reports of a reduction in body weight gain in mice chronically dosed with NAC in their drinking water (Flurkey et al., 2010; Kim et al., 2013; Pinniger et al., 2017). However, rather than this being an adverse effect of NAC dosing it is commonly accepted that oral NAC supplementation reduces body mass gain by decreasing fat levels (Kim et al., 2013; Cao and Picklo, 2014; Ma et al., 2016) and this effect drops off with continued treatment with NAC (Cao and Picklo, 2014).

Previous studies from our laboratory and others have demonstrated a characteristic feature of the dystrophic pathology in mdx mice and DMD boys are the presence of abnormally regenerated branched limb skeletal muscle fibers which increase in number and complexity with age (Bell and Conen, 1968; Schmalbruch, 1976; Head et al., 1992; Chan and Head, 2011; Massopust et al., 2020; Kiriaev et al., 2021b). We and others have demonstrated the increase of these branched fibers mechanically weakens the muscle in the later stages of the dystrophic disease (Head et al., 1992; Chan and Head, 2011; Head, 2012; Pichavant et al., 2016; Kiriaev et al., 2018).

Since the first reports of the mdx mouse it has been noted that the fast-twitch muscles are more susceptible to eccentric (lengthening) contraction (EC) damage (Head et al., 1992; Moens et al., 1993). This susceptibility to EC damage increases as the dystrophic animal ages (Chan et al., 2007; Chan and Head, 2011; Head, 2012; Kiriaev et al., 2018; Kiriaev et al., 2021a). The reason for this increased susceptibility to EC damage is not clear and there have been several hypotheses put forward to explain this effect (Allen et al., 2016); 1) The absence of dystrophin mechanically weakens the sarcolemma making it more susceptible to rupture during EC, 2) Absence of dystrophin is responsible for cycles of necrosis/regeneration resulting in the increase of abnormally regenerated branched fibers structurally compromising the dystrophic membranes ability to resist EC damage 3) The absence of dystrophin results in an increased susceptibility to oxidative damage triggered by EC or 4) The absence of dystrophin sensitizes the ionic mechanisms of the electrical pathways that trigger muscle contraction to damage from EC. It is likely that the increased susceptibility of dystrophic fast-twitch muscle to EC damage involves some combination of these factors.

To test the efficacy of NAC as a possible treatment for DMD we gave it orally for 6 weeks to growing mdx and control mice and measured its effect on body weight gain, EDL muscle weight, fiber branching morphology, contractile function and response to EC. Its main efficacy was in reducing the number of abnormally branched fibers and reversing the increased muscle mass which results from the proliferation of branched fibers as the dystrophic phenotype progresses.

Materials and methods

Ethics approval

Animal use was approved by the Western Sydney University Animal Care and Ethics Committee (A14350). Experiments were conducted in compliance with the animal ethics checklist and ethical principles under which the journal operates.

Animals

Many previous studies on mdx mice have used a separate in-bred colony of wild-type (WT) mice to act as controls. These WT colonies have been separately in-bred since the discovery of the mdx mouse over 25 years ago. This raises the possibility of novel mutations in the WT control group confounding the interpretation of the data from the mdx dystrophic mouse. In our study littermates are bred to act as control animals for mdx mice. These are the gold standard controls for mdx dystrophic studies as both dystrophin negative and dystrophin positive animals are on identical genetic backgrounds, with the only difference being the mutation in the dystrophin gene on the X chromosome at locus Xp21. Mice were obtained from the Western Sydney University

animal facility. Male mice were used in the present study to reflect the sex linked DMD condition in boys. The colony of dystrophic mice and littermate controls (LC) used in this study were second generation offspring of C57BL/10ScSn DMD (mdx) mice. The LC were distinguished from dystrophic mice by genotyping. NAC treatment began at 3 weeks of age, and all mice were sampled at 9 weeks of age. The age of mice and duration of treatment were chosen as they reflect a period when the mdx mice have undergone at least one cycle of necrosis and regeneration. The three-to-nine-week age range in mice can be compared to the growth phase of adolescent in humans (Grounds et al., 2008). Mice were housed individually (1 animal per cage) in an environmentally controlled room with a 12 h light/dark cycle at 20°C–25°C and had access to food and water *ad libitum*.

NAC treatment

NAC (Sigma-Aldrich, Australia) treatment in drinking water was commenced post weaning at 3 weeks of age. NAC was dissolved in RO water and administered as 2% NAC in drinking water for 6 weeks. To overcome any NAC taste avoidance issues drinking water was flavored with banana and caramel (Australian Food Ingredient Suppliers, AFIS); diluted according to manufacturer's recommendation (0.1% v/v); and sweetened using 0.1% sucralose (Splenda®). Untreated animals received same flavored drinking water without NAC. The four experimental groups (n = 6 mice per group) were: 1) mdx NAC treated; 2) mdx untreated; 3) LC NAC treated; and 4) LC untreated. Each mouse was housed individually in its own cage. The cage water dispenser was weighed to determine each individual animals water consumption. The mice were weighed every 3 days.

Muscle preparation

After the 6 weeks NAC treatment, a mouse was placed in a transparent induction chamber and overdosed with isoflurane delivered at 4% in oxygen from a precision vaporizer. The mouse was removed from the chamber and a cervical dislocation carried out. The left and right fast-twitch EDL muscles were dissected from the hind limbs. Once isolated, the EDL muscle was suspended in an organ bath filled with 100% O2 bubbled Tyrode and tied by its tendons from one end to a dual force transducer/linear tissue puller (300 Muscle Lever; Aurora Scientific Instruments, Canada) and secured to a base at the other end using 6–0 silk sutures (Pearsalls Ltd., UK). The EDL data from each animal was averaged to give n = 6 (number of mice used). At all times during the dissection and prior to use the hind limb and muscles were kept under 100% oxygenated Tyrode solution to minimize any post-mortem deficits in initial maximum force (Po). Composition of Tyrode solution in mM (also used as dissection solution): 4 KCl, 135 NaCl, 0.33 NaH2PO4, 1 MgCl2, 10 HEPES, 2.5 CaCl2 and 11 glucose, 0.1% fetal calf serum (FCS).

Muscle force recordings

The muscle was stimulated to contract isometrically by applying a supramaximal voltage across parallel platinum electrodes (701C stimulator; Aurora Scientific Instruments) running the full length of the EDL muscle. Isometric force recordings and eccentric (lengthening) contractions (EC) were made on a 300C Muscle Lever (Aurora Scientific Instruments, Canada). Force responses were analyzed using the 615 A Dynamic Muscle Control and Analysis software (Aurora Scientific Instruments). At the start of each experiment, the muscle was set to optimal length (Lo) which produces maximal twitch force and maintained at this length throughput the experiment. All procedures were performed at a room temperature (20°C–22°C).

Initial maximum force (Po) and P_{max}

At the start of the contractile experiments a supramaximal stimulus was given at 125 Hz (1 ms pulses) for 1 s and the maximum force produced during the tetanic plateau was recorded as Po, the maximum force output of the muscle at optimal length Lo. For the force frequency P_{max} was obtained from the curve fitted to the sigmoidal equation given below. For the EC studies P_{max} was recorded from the isometric plateau of the first EC.

Force frequency curve

Force-frequency curves were generated at frequencies 2, 15, 25, 37.5, 50, 75, 100, 125 and 150 Hz. A 30s rest was given between each frequency to minimize the effects of fatigue. A sigmoid curve relating muscle force (P) to stimulation frequency (f) was fitted by using a sigmoidal equation. The curve had the equation.

From the fitted parameters of the curve, the following contractile properties were obtained: Half-frequency (Kf) where the force developed is half the sum of (Pmin) and (Pmax). The Hill coefficient (h) which quantifies the slope of the muscle force frequency sigmoidal curve. These were used for population statistics.

Eccentric contractions and recovery

A series of eccentric (lengthening) contractions (EC) were then performed on each EDL where the contracted muscle was stretched 20% from Lo. At t = 0s, the muscle was stimulated *via* supramaximal pulses of 1 ms duration and 125 Hz frequency. At t = 0.9s, after maximal isometric force was attained, each muscle was stretched 20% longer than their optimal length at a velocity of 2.4 mm/s then held at this length for 2s before returning to Lo. Electrical stimulus was stopped at t = 5s. The EC procedure was repeated 6 times with 3-min rest intervals in between each EC. On completion of the EC protocol, recovery force was measured *via* an isometric contraction given for 1s at 125 Hz (1 ms pulses) at the following time points; 0, 20, 40 and 60 min.

10.3389/fphys.2023.1109587

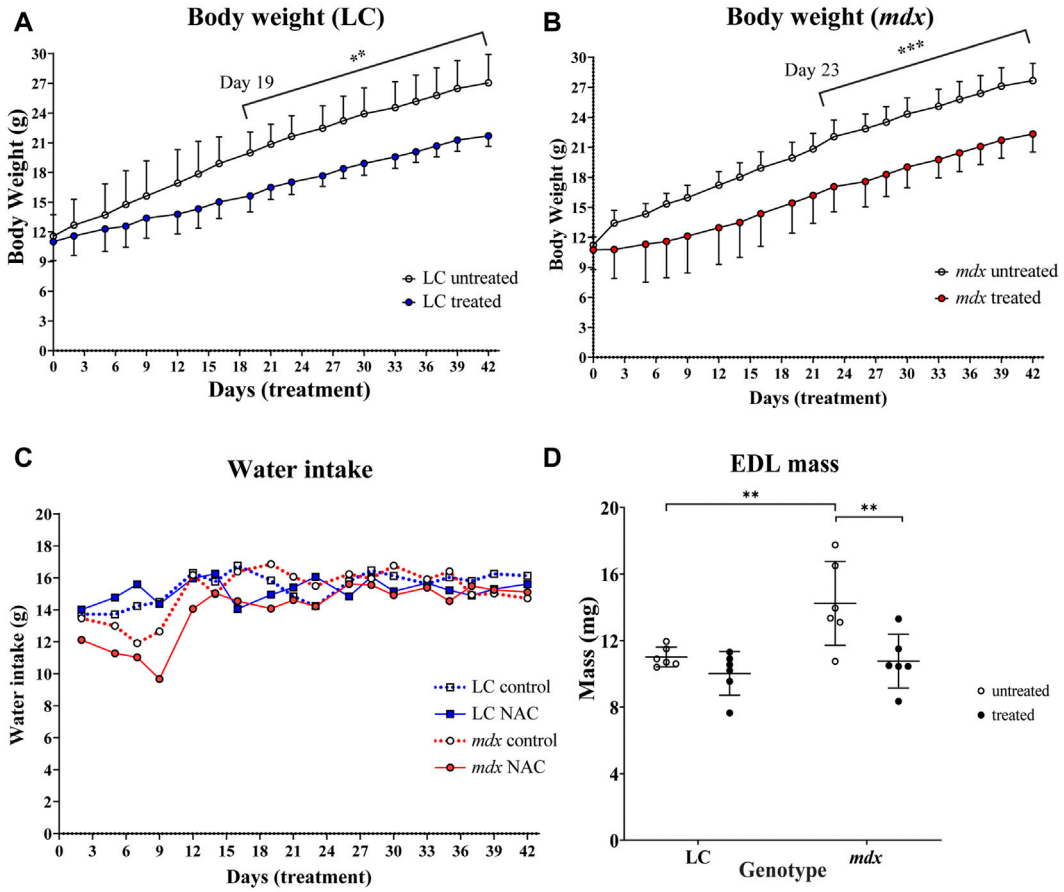

FIGURE 1
Effect of NAC on body weight **(A)** LC **(B)** mdx **(C)** water intake of animals throughout treatment period and **(D)** muscle mass **(A)** shows significant differences in weight gain from day 19 onward for LCs untreated vs. NAC treated ($p = 0.0015$). **(B)** shows significant differences in weight gain from day 23 onward for mdx mice untreated vs. NAC treated ($p = 0.0008$). **(C)** Line graph showing water intake of all animals throughout the treatment period (error bars omitted for clarity) ($n = 6$) LC untreated/treated and $n = 6$ mdx untreated/treated) **(D)** Scatterplots of EDL muscle mass for LC and mdx untreated and treated groups (n = 6 EDL from each group). Dystrophic EDL muscles from mice not treated with NAC were heavier compared to the treated mdx group ($p = 0.0034$).). Genotype differences between untreated mice show increased muscle mass in mdx EDL compared to LCs ($p = 0.0062$). Data set represent mean value ±SD. Statistical differences displayed within graphs are differences between genotypes and treatment groups assessed by two-way ANOVA, *post hoc* analysis using Sidak's multiple comparisons test with significance established at $p < 0.05$.

Muscle mass

After the contractile procedures were completed, the muscle was removed from the transducer, blotted on filter paper, and weighed.

Skeletal muscle single fiber enzymatic isolation and morphology

EDL muscles were digested in Tyrode solution (without FCS) containing 3 mg/mL collagenase type IVA (Sigma Aldrich,United States), gently bubbled with oxygen, and maintained at 37°C. After 25 min the muscle was removed from solution, rinsed in Tyrode solution containing 0.1% FCS and placed in a relaxing solution with the following composition (mM): 117 KCl, 36 NaCl, 1 MgSO4, 60 HEPES, 8 ATP, 50 EGTA). Each muscle was then gently agitated using pipette suction, releasing individual fibers from the muscle mass. Using a pipette 0.5 mL of solution was drawn and placed on a glass slide for counting. A total of 2025 fibers from 12 EDL muscles were counted: mdx untreated ($n = 1186$ fibers from 6 EDL) vs. mdx NAC treated ($n = 839$ fibers from 6 EDL). Only intact fibers with no evidence of digestion damage were selected for counting. All muscle fibers from LCs showed no branching and were not counted (Kiriaev et al., 2021a).

Statistical analyses

Data are presented as means ± SD. Differences occurring between genotypes and treatment groups were assessed by two-way ANOVA. Post hoc analysis was performed using Sidak's multiple comparisons test. Where indicated an unpaired *t*-test was used and significance was accepted at $p < 0.05$. All statistical tests and curve fitting were performed using a statistical software package Prism Version 10 (GraphPad, CA,United States).

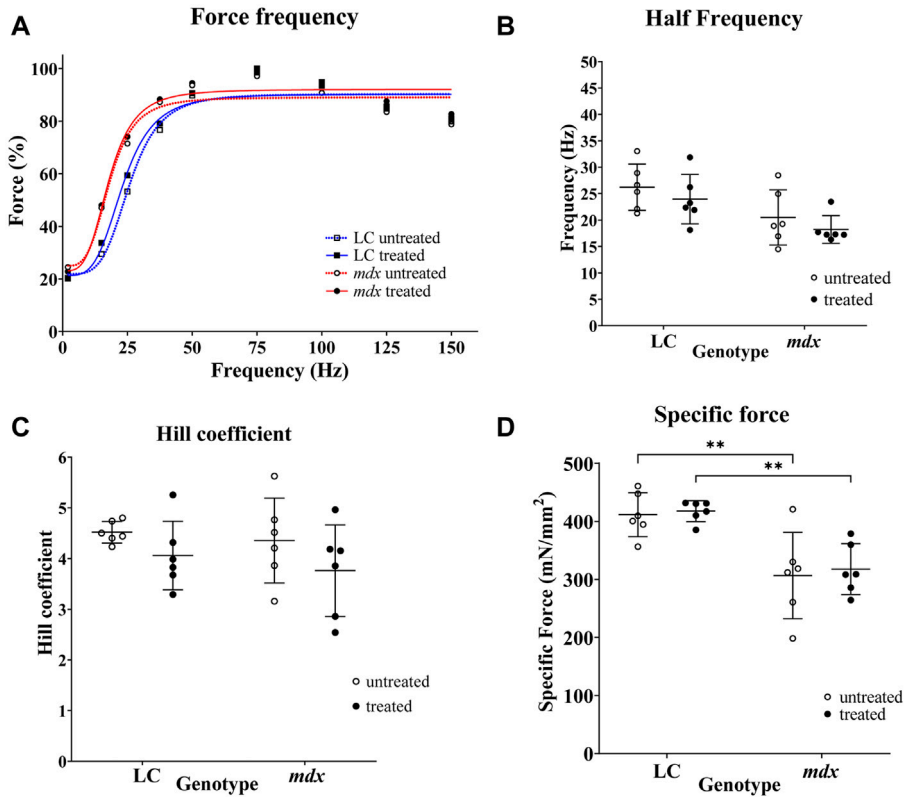

FIGURE 2
Force frequency curves and fitted parameters and specific force. **(A)** Force frequency data from individual EDL muscles were aggregated to produce a single curve for LC and mdx mice to visualize differences between treatment groups and genotypes (n = 6 EDL for each group). Forces are normalized to P_{max}. In graph **(A)** SD error bars are omitted for clarity. **(B,C)** are scatterplots of half-frequency and Hill coefficient obtained from force frequency curve shown in **(A)**. **(D)** Shows the maximum specific force (Po) produced by the EDL muscles, there was no effect of NAC treatment, however, as has been reported previously the dystrophin deficient mdx muscles produced significantly less force than LCs, both in NAC treated (p = 0.0035) and untreated (0.0023) conditions. Data set represent mean value ±SD.

Results

NAC treatment and water intake, body mass and EDL muscle mass

Figure 1 shows the effect on body weight gain, fluid intake and EDL muscle mass of 6 weeks 2% NAC in drinking water. The animals were given the NAC over 3–9 weeks of age which is the period of active growth for mice. Figures 1A, B shows NAC significantly reduced the rate of growth in LC from days 19–42 of treatment (p = 0.0015) and mdx animals from days 23–42 of treatment (p = 0.0008). Figure 1C shows that the application of NAC to the flavored drinking water did not markedly affect mean fluid intake during the period of the study (for clarity the SD bars have been omitted). Figure 1D shows in LC NAC did not affect the EDL mass, but in mdx NAC treated EDL muscles were significantly lower (p = 0.0034) in weight compared to untreated ones. Dystrophic EDL mass was heavier compared to LC (p = 0.0062).

Force-frequency curves and specific Po

The aggregate force–frequency curves for NAC treated and non-treated LC and mdx EDL muscles are shown in Figure 2. These curves are fitted with the sigmoidal equation given in the methods, the following best-fit parameters defining these curves were obtained from the group data, half frequency which produced 50% force and the Hill coefficient which is the slope of the rising portion of the sigmoidal curve Figures 2B, C. In Figure 2A forces are expressed as a percentage of the pre-EC P_{max}. There were no significant differences in half frequency and Hill coefficient with respect to genotype or treatment (Figures 2B, C). Figure 2D shows the maximum specific force (Po) produced by the EDL muscles, there was no effect of NAC treatment, however, as has been reported previously the dystrophin deficient mdx muscles produced significantly less force than LCs, both in NAC treated (p = 0.0035) and untreated (0.0023) conditions.

Percentage force loss resulting from a series of six ECs at 20% stretch from Lo

In Figure 3 force was normalized to the isometric plateau of the first EC, prior to stretching to Lo+20% for n = 6 EDL muscles of each group. Figure 3A shows that there was a graded reduction of force with each EC for both NAC treated and untreated muscles. As has been previously reported mdx muscle were significantly more susceptible to EC induced force loss when

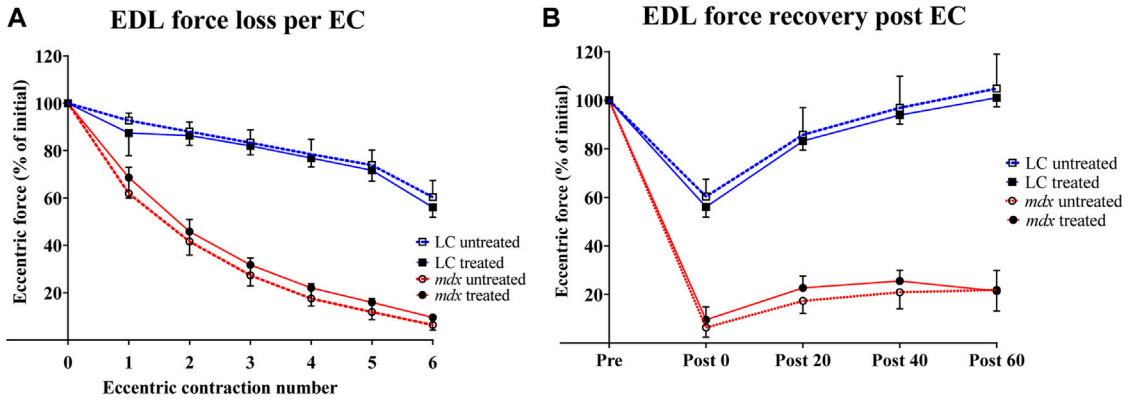

FIGURE 3
Percentage force loss and force recovery from EC protocol **(A)** Percentage force loss resulting from a series of six ECs at 20% stretch at 2.4 mm/s from Lo (n = 6). Force was normalized to the isometric plateau of the first EC in each group **(B)** Percentage force recovery recorded at 0, 20, 40, 60 -minute intervals post EC (n = 6). Data shown in both graphs are mean ± SD.

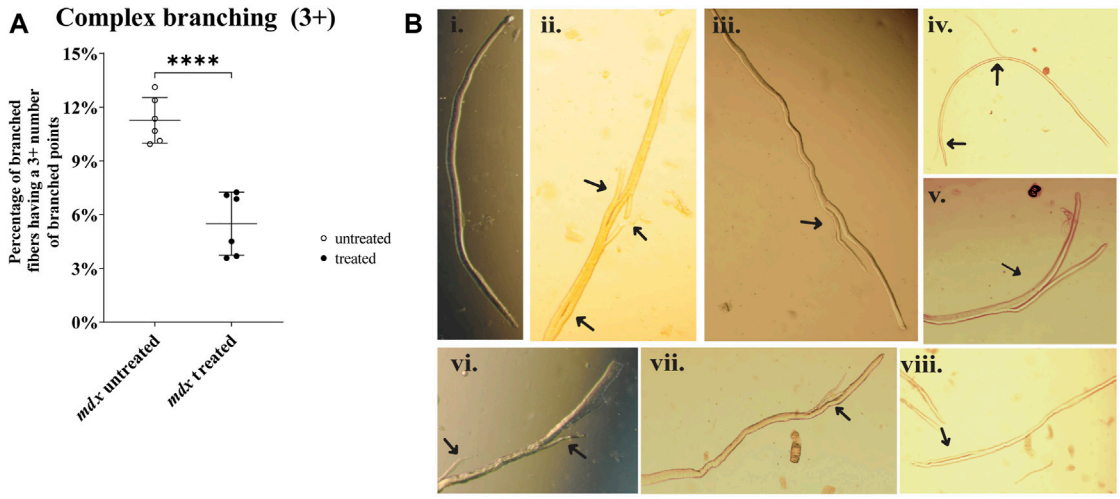

FIGURE 4
Enzymatically digested mdx EDL muscle fibers. **(A)** Scatterplots of complex fiber branching (3 +) between mdx untreated and mdx NAC treated (P= <0.0001). Fibers from LC were omitted due to no presence of fiber branching. Data shown in both graphs are mean ± SD. Statistical differences displayed in graph are assessed by unpaired t-test with significance established at $p < 0.05$ **(B)** Photomicrographs (X200) of enzymatically digested EDL muscle fibers (note in some cases the whole fiber is not shown.) a selection of NAC treated and untreated mdx are shown in **(Bi-viii) (Bi)** a straight mdx fiber with no branching. **(Bii)**: is a fiber with 3 branches **(Biii,v,vii)**: fibers with one branch **(Biv,vi)** fibers with 2 small branches **(Bviii)**: fiber has a split that is connected to the main **(i,iii,iv,v,vii)** are from mdx NAC; **(ii,vi,viii)** are from mdx untreated mice.

compared to age matched LC (Kiriaev et al., 2018; Kiriaev et al., 2021a) and this was not altered by treatment with NAC. Figure 3B shows the rate of recovery of force over 60 min, mdx muscles recovered ~20% and this recovery was not different in EDL muscles from NAC treated mdx. In contrast Figure 3B shows EDL muscle from both NAC treated and non-treated LC animals recovered ~100% force over 60 min.

Fiber branching morphology in mdx

Figure 4A compares complex fiber branching (3 + branches) between mdx untreated and mdx NAC treated (P= <0.0001). Figure 4B includes photomicrographs showing an example of a non-branched fiber Figure 4Bi and examples of fiber branching of differing complexity Figures 4Bii–viii.

Discussion

The effect of 6 weeks of 2% NAC in drinking water on body weight, muscle mass, and water intake

There have been findings of reduced body mass gain in NAC-supplemented rodents (Kim et al., 2006; Kondratov et al., 2009; Kim et al., 2013; Cao and Picklo, 2014). In particular (Pinniger et al., 2017) using 2% NAC in drinking water for 6 weeks concluded that the reduction of body weight gain in mdx mice was a red flag for considering the use of NAC as a treatment for boys with DMD. Commenting on Pinniger et al., 2017 study (O'Halloran et al., 2018), suggested that some of the reduced weight gain may be attributed to a decrease in body fat and not because of a reduction in lean mass and also that the acidification of the drinking water resulting from the addition of NAC may reduce fluid intake, accounting for some of the weight loss. To address this latter concern, we measured the fluid intake in NAC treated animals compared with no NAC and found no significant effect of NAC on fluid consumption. Confirming Pinniger et al., 2017 finding we also reported that 6 weeks of 2% NAC drinking water caused significant reduction in EDL muscle mass. It is unlikely that this reduction in muscle weight is entirely due to reduced lean body mass, as NAC treatment in LC mice did not cause a significant reduction in the weight of EDL muscles (Figure 1D). As mentioned above a component of the reduction in body weight gain with NAC supplementation has been shown to be due to NAC reducing fat (Kim et al., 2006) and increasing energy expenditure (Ma et al., 2016). It has been shown that fiber branching is responsible for the hypertrophy in the mdx mouse (Faber et al., 2014), so it is reasonable to hypothesize that a proportion of the reduction in EDL muscle mass we show here (Figure 1D) could be a consequence of the reduction in complex 3 + fiber branching we report (Figure 4A).

NAC does not reduce the susceptibility to EC force loss seen in dystrophin deficient fast-twitch muscles, nor does it improve recovery post EC force loss.

The fast twitch EDL muscles of mdx mice have long been known to be more susceptible to damage from EC compared to age match WT controls, as measured by a reduction in Po post EC (Head et al., 1992) and this was confirmed in later studies which utilized LCs for the mdx mice (Kiriaev et al., 2018). In the present study we use a strong eccentric contraction protocol that produced a ~90% Po force loss in mdx which only recovered to ~20% of Po after 60 min demonstrating that it was likely the EC had caused significant membrane damage (Olthoff et al., 2018). In contrast, the same EC protocol applied to age matched LC EDL muscle resulted in only a ~40% force loss which recovered to ~100% max Po after 60 min, suggesting that no significant membrane damage had occurred in LC as a result of the EC protocol. In the LC the rapidly reversible component of EC force loss fits well with a fatigue induced and/or a reversible ROS-mediated inhibition of contractile force and we conclude there is no muscle damage connected with insults to the sarcolemma integrity. In contrast, Post EC in the mdx muscle there was only 10% Po remaining which recovered to only 20% after 60 min, leading us to surmise that only 10% of the 90% EC induced force loss in the mdx was fatigue induced and/or a reversible ROS-mediated inhibition of contractile force, while the remaining 80% Po deficit is likely muscle damage connected with insults to the sarcolemma integrity disrupting its electrical and ionic control pathways. Six weeks treatment with 2% NAC did not ameliorate the EC induced force loss or improve recovery post EC either in LCs or mdx, in keeping with (Whitehead et al., 2008) who showed 6 weeks of treatment with NAC in drinking water did not protect from eccentric damage at 35°C and there was only a small ~7% significant improvement at room temperature. We hypothesize that the reduction in complex branching resulting from NAC treatment we report here was not sufficient to reduce the dystrophic muscle below the branched fiber "tipping point" (Chan and Head, 2011; Head, 2012; Kiriaev et al., 2021a). Supplementary Table S2 shows the absolute tetanic force, absolute twitch force, specific twitch force of NAC treated and untreated animals with respect to genotype before EC, after EC and recovery 60 min post EC. The twitch kinetics; time to peak (TTP) and half relaxation time (HRT) for NAC treated and untreated animals with respect to genotype for each of the experimental timepoints are also given in Supplementary Table S2. There was no effect of NAC treatment on any of the parameters.

Mdx EDL fiber branching in singly housed mice

When compared to our earlier studies (Kiriaev et al., 2018; Kiriaev et al. 2021a; Kiriaev et al. 2021b) the amount of complex 3 + fiber branching we report here from 9-week-old mdx is similar to the mdx EDL muscles from >4 months mdx, see Supplementary Figure S1 for graphical comparison. These current mdx EDL muscles from 9-week-old mice show a force deficit comparable with the mdx EDL muscles from mice aged >4 months. Additionally, 60 min after the EC protocol these current mdx EDL muscles from 9-week-old mice regained a similar amount of force to the mdx EDL muscles from mice aged >4 months. A major difference with our earlier study, where mice were housed ~ six per cage, is that in this current study mice were housed, one animal per cage. Here this single housing is associated with an accelerate dystrophic branching phenotype. It is possible that single housing may predispose the male mdx mice to greater locomotory activity, possibly associated with the increased space available per animal (Krohn et al., 2006), which would accelerate the appearance of the branching phenotype. It has long been reported that contractile activity is associated with muscle damage in the dystrophinopathies, in fact studies have demonstrated that if you immobilize dystrophic muscles, they do not undergo pathological changes (Allen et al., 2016). While we cannot rule out the possibility that the reduction in branching we see in mdx NAC treatment is due to NAC acting to reduce motor activity by reducing anxiety and stress, it would appear unlikely as a systematic review of clinical trials involving NAC reported that NAC does not reduce anxiety (Deepmala et al., 2015). Additionally, it has been demonstrated that single housing of male mice causes less stress when compared with group-housing of male mice (Kamakura et al., 2016). It is important to note that the force loss and recovery after EC is related to the degree of branching and

not the chronological age of the mdx mouse, which supports our long-standing hypothesis that it is the degree of branching which is responsible for the increased EC damage with age (Chan and Head, 2011; Head, 2012; Kiriaev et al., 2018). Supplementary Figure S1 and Supplementary Table S1 uses data from our earlier studies (Kiriaev et al., 2018; Kiriaev et al. 2021a; Kiriaev et al. 2021b) to illustrate the significant increase in 3 + complex branching that occurs from 3 weeks to >112 weeks of age. It is clear that while the degree of motor activity may have a small effect on complex 3 + branching between 9 and 16 weeks, the major phenotype seen across the lifespan of the mdx mouse is the transition from non-branched muscle fibers to the point where >80% of fast-twitch fibers have 3 + complexed branched fibers (Supplementary Figure S1 and Supplementary Table S1), with many fibers containing 10 or more branches (Kiriaev et al., 2021a; Kiriaev et al., 2021b).

Fiber branching, a marker of pathology in mdx muscle, is reduced in fast-twitch EDL muscles from NAC treated mdx.

We and others have shown that a striking pathological feature of regenerated skeletal muscle in the dystrophinopathies is the presence of abnormally branched fibers which dramatically increase in both number and complexity with age (Bell and Conen, 1968; Schmalbruch, 1976; Head et al., 1992; Chan and Head, 2011; Head, 2012; Massopust et al., 2020; Kiriaev et al., 2021a). The number and complexity of these fibers can be used as a marker of the progression of the dystrophinopathies (Bell and Conen, 1968; Kiriaev et al., 2021a). The presence of centrally nucleated (CN) fibers is commonly used as a measure of regeneration, however, it is accepted that by > 8 weeks of age over 90% of mdx mouse skeletal muscle fibers will have regenerated. From 24 weeks to >104 weeks mdx skeletal muscle fibers are 100% centrally nucleated (Massopust et al., 2020), and thus unlike fiber branching, which continues to increase in complexity (Kiriaev et al., 2021a) CN is not reliable indicator of the number of cycles of degeneration/regeneration. Here we show NAC treatment reduces the complexity of branched fibers in the fast-twitch mdx EDL muscle, demonstrating that NAC treatment improves mdx fast-twitch muscle pathology. In the dystrophinopahties it has been proposed that the absence of the protein, dystrophin, from the inner surface of the sarcolemma predispose the skeletal muscle to increased oxidative stress and free radical triggered necrosis, which has been identified as a major cause of muscle injury (Disatnik et al., 2000; Mosca et al., 2021; Lian et al., 2022). The reduction in fiber branching we report here is likely due to NAC reducing (Rando, 2002) the level of free radical triggered necrosis in the active phase of the disease. The reduction in branching we report here was not sufficient to confer a protective effect from the force deficit caused by EC (Chan and Head, 2011). As the mdx mouse model is characterized by a period of florid necrosis 3–20 weeks of age (Duddy et al., 2015) many biochemical changes which are indicative of oxidative damage could be a secondary result of the necrosis, inflammatory response, and subsequent regeneration (Rando, 2002). However, the fact that acute NAC application to the organ bath in *in vitro* experiments has shown that NAC can prevent eccentric contraction force loss in fast twitch mdx muscles (Whitehead et al., 2008; Olthoff et al., 2018; Lindsay et al., 2020) supports the hypothesis that the absence of dystrophin directly increases the susceptibility the muscle to oxidative triggered damage (Mosca et al., 2021; Lian et al., 2022). The present study provides further support for this in finding that 2% NAC in drinking water for 6 weeks prevents the increase in muscle mass characteristic of the dystrophinopathies and reduces the number of complex 3 + fiber branching. These are effects which could be predicted to occur if NAC does indeed reduce myonecrosis (Head, 2012).

Summary

In the current study we confirmed that 6 weeks of 2% NAC in drinking water significantly reduces body weight gain in both mdx and LC mice. This was not the result of a reduced fluid intake, as was reported in (Kondratov et al., 2009), because we monitored water intake and after some initial fluctuation it was the same for NAC treated mdx and LCs compared to non-treated mdx and LCs. We showed that NAC prevents the increase in skeletal muscle mass characteristic of the dystrophinopathies and reduces the number and complexity of branched fibers which have been shown to be responsible for this increase in mass (Faber et al., 2014; Froehner et al., 2015). This reduction in fiber branching suggests that the antioxidant action of NAC may have reduced the myonecrosis involved in the degeneration/regeneration cycles characteristic of the mdx skeletal muscle pathology. We have previously shown as the number of these cycles increases with age so does the number and complexity of branched fibers in the mdx EDL (Chan and Head, 2011; Kiriaev et al., 2018). However, in our present study NAC does not ameliorate the sensitivity of mdx dystrophic fast-twitch EDL muscle to damage caused by EC (Head et al., 1992) possibly because the reduction in 3 + complex branched fibers is not of sufficient magnitude to be protective.

Data availability statement

The raw data supporting the conclusion of this article will be made available by the authors, without undue reservation.

Ethics statement

The animal study was reviewed and approved by the animal study was reviewed and approved by Western Sydney University Animal Care and Ethics Committee.

Author contributions

AR and SK carried out the experiments. AR, LK, SK, and SH analyzed the data and interpreted results of experiments. AR and SH drafted the manuscript. AR, LK, SK, JM, PH, BP, and SH edited and revised the manuscript. All authors approved the final version of manuscript and agreed to be accountable for all aspects of the work in ensuring that questions related to the accuracy or integrity of any part of the work are appropriately investigated and resolved. All persons designated as authors quality for authorship, and all those who qualify for authorship are listed.

Funding

AR's Ph.D. research and open access publishing fees were supported by Western Sydney University, Australia RTP Fund 19246071. The research was supported by the Australian National Health and Medical Research Council Ideas Grants—2012362.

Conflict of interest

The authors declare that the research was conducted in the absence of any commercial or financial relationships that could be construed as a potential conflict of interest.

Publisher's note

Supplementary material

The Supplementary Material for this article can be found online at: https://www.frontiersin.org/articles/10.3389/fphys.2023.1109587/full#supplementary-material

References

Allen, D. G., Whitehead, N. P., and Froehner, S. C. (2016). 'Absence of dystrophin disrupts skeletal muscle signaling: Roles of Ca2+, reactive oxygen species, and nitric oxide in the development of muscular dystrophy. *Physiol. Rev.* 96, 253–305. doi:10.1152/physrev.00007.2015

Bell, C. D., and Conen, P. E. (1968). 'Histopathological changes in Duchenne muscular dystrophy. *J. Neurol. Sci.* 7, 529–544. doi:10.1016/0022-510x(68)90058-0

Cao, J. J., and Picklo, M. J. (2014). 'N-acetylcysteine supplementation decreases osteoclast differentiation and increases bone mass in mice fed a high-fat diet. *J. Nutr.* 144, 289–296. doi:10.3945/jn.113.185397

Chan, S., Head, S. I., and Morley, J. W. (2007). Branched fibers in dystrophic mdx muscle are associated with a loss of force following lengthening contractions. *Am. J. Physiology-Cell Physiology* 293, C985–C992. doi:10.1152/ajpcell.00128.2007

Chan, S., and Head, S. I. (2011). The role of branched fibres in the pathogenesis of Duchenne muscular dystrophy. *Exp. Physiol.* 96, 564–571. doi:10.1113/expphysiol.2010.056713

Deepmala, J. S., Kumar, N., Delhey, L., Berk, M., Dean, O., Spielholz, C., et al. (2015). Clinical trials of N-acetylcysteine in psychiatry and neurology: A systematic review. *Neurosci. Biobehav Rev.* 55, 294–321. doi:10.1016/j.neubiorev.2015.04.015

Disatnik, M. H., Chamberlain, J. S., and Rando, T. A. (2000). Dystrophin mutations predict cellular susceptibility to oxidative stress. *Muscle Nerve* 23, 784–792. doi:10.1002/(sici)1097-4598(200005)23:5<784::aid-mus17>3.0.co;2-y

Duddy, W., Duguez, S., Johnston, H., Cohen, T. V., Phadke, A., Gordish-Dressman, H., et al. (2015). Muscular dystrophy in the mdx mouse is a severe myopathy compounded by hypotrophy, hypertrophy and hyperplasia. *Skelet. muscle* 5.

Faber, R. M., Hall, J. K., Chamberlain, J. S., and Banks, G. B. (2014). 'Myofiber branching rather than myofiber hyperplasia contributes to muscle hypertrophy in mdx mice. *Skelet. Muscle* 4, 10. doi:10.1186/2044-5040-4-10

Flurkey, K., Astle, C. M., and Harrison, D. E. (2010). Life extension by diet restriction and N-acetyl-L-cysteine in genetically heterogeneous mice. *J. Gerontol. A Biol. Sci. Med. Sci.* 65, 1275–1284. doi:10.1093/gerona/glq155

Froehner, S. C., Reed, S. M., Anderson, K. N., Huang, P. L., and Percival, J. M. (2015). 'Loss of nNOS inhibits compensatory muscle hypertrophy and exacerbates inflammation and eccentric contraction-induced damage in mdx mice. *Hum. Mol. Genet.* 24, 492–505. doi:10.1093/hmg/ddu469

Grounds, M. D., Radley, H. G., Lynch, G. S., Nagaraju, K., and De Luca, A. (2008). 'Towards developing standard operating procedures for pre-clinical testing in the mdx mouse model of Duchenne muscular dystrophy. *Neurobiol. Dis.* 31, 1–19. doi:10.1016/j.nbd.2008.03.008

Head, S. (2012). "A two stage model of skeletal muscle necrosis in muscular dystrophy-the role of fiber branching in the terminal stage," in *Muscular dystrophy* Editor Dr Madhuri Hegde.

Head, S. I., Williams, D. A., and Stephenson, D. G. (1992). 'Abnormalities in structure and function of limb skeletal muscle fibres of dystrophic mdx mice. *Proc. Biol. Sci.* 248, 163–169. doi:10.1098/rspb.1992.0058

Kamakura, R., Kovalainen, M., Leppaluoto, J., Herzig, K. H., and Makela, K. A. (2016). The effects of group and single housing and automated animal monitoring on urinary corticosterone levels in male C57BL/6 mice. *Physiol. Rep.* 4, e12703. doi:10.14814/phy2.12703

Kerksick, C., and Willoughby, D. (2005). 'The antioxidant role of glutathione and N-acetyl-cysteine supplements and exercise-induced oxidative stress. *J. Int. Soc. Sports Nutr.* 2, 38–44. doi:10.1186/1550-2783-2-2-38

Kim, J. H., Kwak, H. B., Thompson, L. V., and Lawler, J. M. (2013). 'Contribution of oxidative stress to pathology in diaphragm and limb muscles with Duchenne muscular dystrophy. *J. Muscle Res. Cell Motil.* 34, 1–13. doi:10.1007/s10974-012-9330-9

Kim, J. R., Ryu, H. H., Chung, H. J., Lee, J. H., Kim, S. W., Kwun, W. H., et al. (2006). 'Association of anti-obesity activity of N-acetylcysteine with metallothionein-II down-regulation. *Exp. Mol. Med.* 38, 162–172. doi:10.1038/emm.2006.20

Kiriaev, L., Kueh, S., Morley, J. W., North, K. N., Peter, J. H., and Head, S. I. (2018). Branched fibers from old fast-twitch dystrophic muscles are the sites of terminal damage in muscular dystrophy. *Am. J. Physiology-Cell Physiology* 314, C662–C674. doi:10.1152/ajpcell.00161.2017

Kiriaev, L., Kueh, S., Morley, J. W., Houweling, P. J., Chan, S., North, K. N., et al. (2021b). 'Dystrophin-negative slow-twitch soleus muscles are not susceptible to eccentric contraction induced injury over the lifespan of the mdx mouse. *Am. J. Physiology Cell Physiology* 321, C704–C720. doi:10.1152/ajpcell.00122.2021

Kiriaev, L., Kueh, S., Morley, J. W., North, K. N., Houweling, P. J., and Head, S. I. (2021a). 'Lifespan analysis of dystrophic mdx fast-twitch muscle morphology and its impact on contractile function. *Front. Physiol.* 12, 771499. doi:10.3389/fphys.2021.771499

Kondratov, R. V., Vykhovanets, O., Kondratova, A. A., and Antoch, M. P. (2009). 'Antioxidant N-acetyl-L-cysteine ameliorates symptoms of premature aging associated with the deficiency of the circadian protein BMAL1. *Aging (Albany NY)* 1, 979–987. doi:10.18632/aging.100113

Krohn, T. C., Sørensen, D. B., Ottesen, J. L., and Hansen, A. K. (2006). The effects of individual housing on mice and rats: A review. *Anim. Welf.* 15, 343–352. doi:10.1017/s0962728600030669

Lian, D., Chen, M. M., Wu, H., Deng, S., and Hu, X. (2022). 'The role of oxidative stress in skeletal muscle myogenesis and muscle disease. *Antioxidants (Basel)* 11 (4), 755. doi:10.3390/antiox11040755

Lindsay, A., Baumann, C. W., Rebbeck, R. T., Yuen, S. L., Southern, W. M., Hodges, J. S., et al. (2020). 'Mechanical factors tune the sensitivity of mdx muscle to eccentric strength loss and its protection by antioxidant and calcium modulators. *Skelet. Muscle* 10, 3. doi:10.1186/s13395-020-0221-2

Ma, Y., Gao, M., and Liu, D. (2016). N-acetylcysteine protects mice from high fat diet-induced metabolic disorders. *Pharm. Res.* 33, 2033–2042. doi:10.1007/s11095-016-1941-1

Massopust, R. T., Thompson, W. J., Lee, Y. I., Pritchard, A. L., Nguyen, V-K. M., McCreedy, D. A., et al. (2020). Lifetime analysis of mdx skeletal muscle reveals a progressive pathology that leads to myofiber loss. *Sci. Rep.* 10, 17248–48. doi:10.1038/s41598-020-74192-9

Matuszczak, Y., Farid, M., Jones, J., Lansdowne, S., Smith, M. A., Taylor, A. A., et al. (2005). 'Effects of N-acetylcysteine on glutathione oxidation and fatigue during handgrip exercise. *Muscle Nerve* 32, 633–638. doi:10.1002/mus.20385

Medved, I., Brown, M. J., Bjorksten, A. R., Murphy, K. T., Petersen, A. C., Sostaric, S., et al. (2004). 'N-acetylcysteine enhances muscle cysteine and glutathione availability and attenuates fatigue during prolonged exercise in endurance-trained individuals. *J. Appl. Physiol.* 97, 1477–1485. doi:10.1152/japplphysiol.00371.2004

Michelucci, A., De Marco, A., Guarnier, F. A., Protasi, F., and Boncompagni, S. (2017). 'Antioxidant treatment reduces formation of structural cores and improves muscle function in RYR1(Y522S/WT) mice. *Oxid. Med. Cell Longev.* 2017, 6792694.

Moens, P., Baatsen, P. H., and Marechal, G. (1993). 'Increased susceptibility of EDL muscles from mdx mice to damage induced by contractions with stretch. *J. Muscle Res. Cell Motil.* 14, 446–451. doi:10.1007/BF00121296

Mokhtari, V., Afsharian, P., Shahhoseini, M., Kalantar, S. M., and Moini, A. (2017). A review on various uses of N-acetyl cysteine. *Cell J.* 19, 11–17. doi:10.22074/cellj.2016.4872

Mosca, N., Petrillo, S., Bortolani, S., Monforte, M., Ricci, E., Piemonte, F., et al. (2021). 'Redox homeostasis in muscular dystrophies. *Cells* 10, 1364. doi:10.3390/cells10061364

O'Halloran, K. D., and Lewis, P. (2017). 'Respiratory muscle dysfunction in animal models of hypoxic disease: Antioxidant therapy goes from strength to strength. *Hypoxia (Auckl)* 5, 75–84. doi:10.2147/HP.S141283

O'Halloran, K. D., Murphy, K. H., and Burns, D. P. (2018). Antioxidant therapy for muscular dystrophy: Caveat lector. *J. Physiol.* 596, 737–738. doi:10.1113/JP275598

Olthoff, J. T., Lindsay, A., Abo-Zahrah, R., Baltgalvis, K. A., Patrinostro, X., Belanto, J. J., et al. (2018). 'Loss of peroxiredoxin-2 exacerbates eccentric contraction-induced force loss in dystrophin-deficient muscle. *Nat. Commun.* 9, 5104. doi:10.1038/s41467-018-07639-3

Pichavant, C., Burkholder, T. J., and Pavlath, G. K. (2016). 'Decrease of myofiber branching via muscle-specific expression of the olfactory receptor mOR23 in dystrophic muscle leads to protection against mechanical stress. *Skelet. Muscle* 6, 2. doi:10.1186/s13395-016-0077-7

Pinniger, G. J., Jessica, R. T., Assan, E. B., MirandaGrounds, D., and Arthur, P. G. (2017). 'Pre-clinical evaluation of N-acetylcysteine reveals side effects in the mdx mouse model of Duchenne muscular dystrophy. *J. physiology* 595, 7093–7107. doi:10.1113/JP274229

Pinto, F., Moraes, N., Marques, M., and Neto, H. S. (2013). N-acetylcysteine treatment reduces TNF-α levels and myonecrosis in diaphragm muscle of mdx mice. *Clin. Nutr.* 32, 472–475. doi:10.1016/j.clnu.2012.06.001

Rando, T. A. (2002). 'Oxidative stress and the pathogenesis of muscular dystrophies. *Am. J. Phys. Med. Rehabil.* 81, S175–S186. doi:10.1097/00002060-200211001-00018

Schmalbruch, H. (1976). 'Muscle fibre splitting and regeneration in diseased human muscle. *Neuropathology Appl. Neurobiol.* 2, 3–19. doi:10.1111/j.1365-2990.1976.tb00558.x

Terrill, J. R., Radley-Crabb, H. G., Grounds, M. D., and Arthur, P. G. (2012). 'N-Acetylcysteine treatment of dystrophic mdx mice results in protein thiol modifications and inhibition of exercise induced myofibre necrosis. *Neuromuscul. Disord.* 22, 427–434. doi:10.1016/j.nmd.2011.11.007

Whitehead, N. P., Pham, C., Gervasio, O. L., and Allen, D. G. (2008). 'N-Acetylcysteine ameliorates skeletal muscle pathophysiology in mdx mice. *J. physiology* 586, 2003–2014. doi:10.1113/jphysiol.2007.148338

frontiers | Frontiers in Physiology

TYPE Review
PUBLISHED 14 February 2023
DOI 10.3389/fphys.2023.1130063

OPEN ACCESS

EDITED BY
Atsushi Asakura,
University of Minnesota Twin Cities,
United States

REVIEWED BY
Diego Fraidenraich,
The State University of New Jersey,
United States
Lucio Barile,
University of Italian Switzerland,
Switzerland

*CORRESPONDENCE
Maurilio Sampaolesi,
maurilio.sampaolesi@kuleuven.be

SPECIALTY SECTION
This article was submitted to Striated Muscle Physiology, a section of the journal Frontiers in Physiology

RECEIVED 22 December 2022
ACCEPTED 31 January 2023
PUBLISHED 14 February 2023

CITATION
Yedigaryan L and Sampaolesi M (2023), Extracellular vesicles and Duchenne muscular dystrophy pathology: Modulators of disease progression. *Front. Physiol.* 14:1130063. doi: 10.3389/fphys.2023.1130063

Extracellular vesicles and Duchenne muscular dystrophy pathology: Modulators of disease progression

Laura Yedigaryan[1] and Maurilio Sampaolesi[1,2]*

[1]Translational Cardiomyology Laboratory, Stem Cell and Developmental Biology, Department of Development and Regeneration, KU Leuven, Leuven, Belgium, [2]Histology and Medical Embryology Unit, Department of Anatomy, Histology, Forensic Medicine and Orthopaedics, Sapienza University of Rome, Rome, Italy

Duchenne muscular dystrophy (DMD) is a devastating disorder and is considered to be one of the worst forms of inherited muscular dystrophies. DMD occurs as a result of mutations in the dystrophin gene, leading to progressive muscle fiber degradation and weakness. Although DMD pathology has been studied for many years, there are aspects of disease pathogenesis and progression that have not been thoroughly explored yet. The underlying issue with this is that the development of further effective therapies becomes stalled. It is becoming more evident that extracellular vesicles (EVs) may contribute to DMD pathology. EVs are vesicles secreted by cells that exert a multitude of effects *via* their lipid, protein, and RNA cargo. EV cargo (especially microRNAs) is also said to be a good biomarker for identifying the status of specific pathological processes that occur in dystrophic muscle, such as fibrosis, degeneration, inflammation, adipogenic degeneration, and dilated cardiomyopathy. On the other hand, EVs are becoming more prominent vehicles for custom-engineered cargos. In this review, we will discuss the possible contribution of EVs to DMD pathology, their potential use as biomarkers, and the therapeutic efficacy of both, EV secretion inhibition and custom-engineered cargo delivery.

KEYWORDS

extracellular vesicles (EVs), exosomes, muscle regeneration, miRNAs, muscular dystrophies, cardiomyopathy, satellite cells, induced pluripotent stem cells (iPSCs)

1 Introduction

Duchenne muscular dystrophy (DMD) is an X-linked degenerative disease of cardiac and skeletal muscles, as a consequence of mutations in the dystrophin gene (Yao et al., 2021) (Verhaart & Aartsma-Rus, 2019). The dystrophin protein is a crucial member of the dystrophin glycoprotein complex (Ribeiro et al., 2019). Dystrophin plays a critical role in the integrity, maintenance, and normal functions of muscle cells. Under normal circumstances, muscle degeneration activates muscle-specific stem cells, namely satellite cells, that differentiate into mature muscle cells, contributing to muscle regeneration (Biera et al., 2018) (Bentzinger et al., 2012). Dystrophin has been described to play a vital role in the asymmetrical division of satellite cells as well as their regenerative capacity (Dumont et al., 2015) (Keefe & Kardon, 2015). Therefore, the absence of dystrophin leads to the replacement of degenerated muscle tissues with fibrotic and fat tissues (Emery, 2002). Copious amounts of different therapeutic approaches for treating DMD have been extensively explored. Some of these include exon-skipping oligonucleotides (Aartsma-Rus et al., 2017), anti-inflammatory and anti-fibrotic agents (Heier et al., 2013) (Levi et al., 2015), and stem cell-based therapies such as the

transplantation of satellite cells (Arpke et al., 2013), mesoangioblasts (Sampaolesi et al., 2006), pericytes (Valadares et al., 2014), etc. Although results in pre-clinical models were very encouraging, the clinical trial in five DMD patients based upon four consecutive systemic administrations of human leukocyte antigen (HLA)-matched donor cells (from a sibling) showed safety but no efficacy (Cossu et al., 2015). Thus, many research opportunities arose from the exploration of novel strategies to enhance the efficacy of transplanted cells, including signaling molecules that mediate the crosstalk between donor cells and the muscle regenerative niche.

Currently, the topic of extracellular vesicles (EVs) and their involvement in disease promotion and progression is gaining momentum (Gartz et al., 2020). EVs are nanosized vesicles released by cells (Rome et al., 2019). These vesicles are mediators of intercellular communication and are divided into three different types: apoptotic bodies, microvesicles, and exosomes. Research has shown that EVs derived from diseased cells or bodily fluids from patients or animal models, are most often enriched for pathogenic proteins and nucleic acids (Gartz et al., 2020). As a result, there is growing interest in synthesizing novel therapeutics targeting EVs. It is still debatable whether EVs are simply markers of disease or dynamic participants in the pathological advancement of any given disease (Yates et al., 2022). While EVs have already proven to be potential biomarkers and carriers of DMD-improving molecules, there is still much to be discovered in terms of their involvement in DMD pathophysiology (Meng et al., 2022). It has been discovered that microRNAs (miRNAs) may play the biggest role in EV-mediated disease progression. miRNAs are short non-coding RNAs that bind to messenger RNAs (mRNAs), leading to either translational repression or mRNA degradation (Matsuzaka et al., 2016) (Lee & Vasudevan, 2013). The significance of miRNAs in DMD has been studied extensively and EV-enclosed miRNAs are said to represent potentially effective biomarkers. On the other hand, EVs derived from healthy cells have also contributed to the improvement of DMD symptoms (Aminzadeh et al., 2018).

In this review, we wish to delve into the known aspects of EV involvement in DMD pathophysiology, in both types of striated muscle, and as stated previously, the more well-known aspects of EVs in this disease, namely as potential biomarkers and therapeutic agents. We will also briefly discuss potential therapeutic options with EVs and what the future may hold for nanoparticle therapy.

2 Duchenne muscular dystrophy

DMD, as an X-linked disorder, is one of the most severe muscle diseases. Unfortunately, there is still no cure for DMD (Verhaart & Aartsma-Rus, 2019). The incidence of DMD is approximately 1 in 5,136 male births (Crisafulli et al., 2020). Already between the ages of 8 and 10, it is difficult for patients to stand and walk, coaxing the need for assistive equipment such as braces or wheelchairs. Most DMD patients pass away due to cardiorespiratory failure (Meyers & Townsend, 2019) (Silva et al., 2019). However, due to improvements in both respiratory and cardiac care, the life expectancy of DMD patients has increased, with patients reaching their 30s, and even some living into their 40s and 50s (Landfeldt et al., 2020). Sadly, the condition is fatal in 100% of cases (Chemello et al., 2020).

Mutations in the dystrophin gene lead to the occurrence of DMD (Monaco et al., 1986) (Hoffman et al., 1987b) (Hoffman et al., 1987a) (Bonilla et al., 1988) (Haidet et al., 2008) (Okubo et al., 2020) and the severity of DMD strongly depends on the mutation type. 'In-frame' mutations generate a partially functional dystrophin protein, leading to a less severe form of DMD, namely Becker muscular dystrophy (Kunkel et al., 1986) (Haidet et al., 2008). On the other hand, "out of frame" mutations completely disrupt the reading frame, leading either to the complete lack of dystrophin or an entirely dysfunctional dystrophin (Aravind et al., 2019). This leads to the severe DMD phenotype. The absence of a functional dystrophin increases the fragility of muscle fibers and promotes ongoing cycles of muscle degradation and regeneration (Ribeiro et al., 2019). Under such circumstances, dysfunctional satellite cells, activation of calcium-dependent proteases and overall disruption of calcium homeostasis, mitochondrial disruption, and inflammatory cytokines greatly contribute to muscle being replaced by fibrotic and fatty tissues (Wakayama et al., 1979) (Klingler et al., 2012).

Current DMD therapeutics focus on dystrophin-targeted therapies and targeting the consequential pathological changes (Guiraud & Davies, 2017). Therapies such as cell therapies, gene therapies, and protein replacement therapies are all dystrophin-targeted therapies. Although much research has gone into these methods, significant challenges persist (Chamberlain & Chamberlain, 2017). Primarily, it is very difficult to target all muscle tissues, given the high abundance and the wide distribution of muscle throughout the whole body (Verhaart & Aartsma-Rus, 2019). On the other hand, such therapies may slow down the progression of the disease, however, the restoration of abnormal muscle tissues is unsubstantiated due to the deteriorating nature of DMD. Targeting downstream pathological processes in DMD also represents a promising but a yet not-fully understood therapy strategy. Much must still be researched, particularly for obtaining in-depth information of the secondary pathological changes since the specific mechanisms of such therapies remain obscure.

3 Extracellular vesicles and the prominence of their cargo

EVs are single outer membrane-bound vesicles that can be classified according to their size distribution, biogenesis, and function (Gabisonia et al., 2022). Exosomes represent the population of EVs with the smallest diameter, namely from 50 to 150 nm (Heijnen et al., 1999) (Logozzi, et al., 2021). These vesicles are produced *via* the endolysosomal pathway, formed from the invagination of late endosomes, housed in multivesicular bodies (MVBs) and released by exocytosis.

Briefly, MVBs accumulate intraluminal vesicles (ILVs) and may then either fuse with lysosomes and promote ILV destruction, or fuse with the cell membrane and release ILVs in the extracellular space (Huotari & Helenius, 2011). The biogenesis of MVBs may follow either the endosomal sorting complexes required for transport machinery (ESCRT)-dependent or -independent pathway. The ESCRT-dependent pathway consists of a complex machinery, facilitated by four main complexes and some additional proteins. This pathway leads to the formation of ILVs in a stepwise fashion. On the other hand, ESCRT-independent processes are based on the presence of lipid rafts inside the endosomal membranes. These lipid rafts consist of cholesterol and more importantly, sphingolipids, which are converted to ceramide through the action

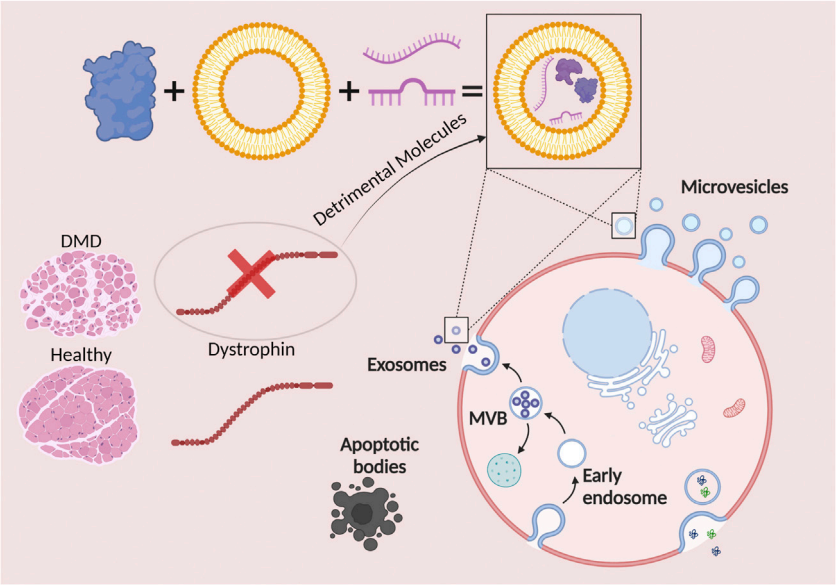

FIGURE 1
Extracellular vesicles (EVs) are hailed as potential modulators of Duchenne muscular dystrophy progression. EVs are represented by exosomes, microvesicles, and apoptotic bodies. The cargo of exosomes and microvesicles consists of effector molecules such as proteins, lipids, and nucleic acids. The lack of a functional dystrophin leads to the formation and release of exosomes and microvesicles with detrimental molecules, inducing both negative paracrine and endocrine effects.

of sphingomyelinase enzymes (Trajkovic, et al., 2008). The coalescence of ceramide forms microdomains that induce budding and subsequent formation of ILVs.

The next population of EVs are the microvesicles (MVs). These vesicles range from 50 to 1,000 nm in diameter, therefore, being mainly larger than exosomes (Heijnen et al., 1999) (Skog, et al., 2008). MV biogenesis occurs following the direct outward blebbing and pinching of the plasma membrane. Lastly, apoptotic bodies represent the largest (in size) population of EVs, considered to range from 1,000 to 5,000 nm in diameter (Atkin-Smith et al., 2015). As their name suggests, apoptotic bodies are released after programmed cell death, also known as apoptosis (Figure 1).

The cargo of EVs is what makes them incredibly intriguing to study. EVs are known to have a distinctive signature of proteins, lipids, and nucleic acids, analogous to their cell or tissue of origin. EVs are known to be enriched for proteins of the tetraspanin family, namely CD9, CD63, and CD81 (Gabisonia et al., 2022). While still not definitive, these proteins are said to contribute to membrane remodeling to mold the EV structure. EVs are enriched in a multitude of lipids. Although the composition of surface lipids has not been studied extensively, it has been hypothesized that these lipids are crucial for the regulation of EV release, as well as in their final composition (Subra et al., 2007). Lastly, EVs are highly enriched in nucleic acids (Mathivanan et al., 2010), of which mRNAs and miRNAs have been studied comprehensively. In particular, miRNAs are becoming increasingly popular in therapeutic research. miRNAs are non-coding RNAs that either block translation of target mRNAs or activate their degradation (Yedigaryan & Sampaolesi, 2021).

EVs secreted by skeletal and cardiac muscle carry a wide range of myokines, miRNAs, proteins, and mRNAs that are thought to play various roles in muscle homeostasis, development, and myogenesis (Vechetti et al., 2020). Overall, the EV cargo plays a significant role in the musculoskeletal system. In particular, miRNAs and specifically the myomiRs, which are muscle-oriented miRNAs (highly enriched in muscle) (Chen et al., 2006) (Annibalini et al., 2019), display key roles in controlling muscle homeostasis, proliferation, and differentiation of muscle stem cells (Coenen-Stass et al., 2016). As an example, miR-206 is one of the most abundant miRNAs in muscle-derived EVs which aids in muscle injury repair by promoting development and differentiation of tissues (Guescini et al., 2015). These EVs are not only muscle tissue-specific agents but have also been described to affect other tissues (Jalabert et al., 2016) (Rome, 2022). Therefore, much still remains to fully understand the muscle secretome and its extensive range of effects. Although not extensively studied, there has been evidence to show that EVs have an effect on disease pathophysiology. As an example, Gartz et al. showed that treatment with GW4869, a substance to reduce/inhibit exosome release, was protective against cardiac stress in *mdx* mice (a popular model of DMD) (Gartz et al., 2020) (Yates et al., 2022). They attributed this effect to the miRNA cargo. In another study, Matsuzaka et al. showed that the excision of the neutral sphingomyelinase 2/sphingomyelin phosphodiesterase 3 (nSMase2/Smpd3) (modulates the Ca^{2+}-dependent secretion of EVs) gene in *mdx* mice led to a decrease in muscle inflammation and overall improved functionality (Matsuzaka et al., 2020). These studies already point toward the multidimensional role of EVs in DMD.

EVs also participate in the physiological regulation of both skeletal and cardiac muscle. The roles of EVs released by cardiac and non-cardiac cells in the heart are difficult to define. Most current studies have not been able to mimic physiologically-relevant environments that can be closely associated with *in vivo* processes (Wagner & Radisic, 2021). On the other hand, in order to maintain the metabolic balance of the body, physiological regulation of organ cross-talk is essential (Wang et al., 2022). As an endocrine organ, skeletal muscle can release a multitude of factors that are absorbed by various tissues to produce regulatory effects (Leal et al., 2018). In addition to these factors, skeletal muscle can also release EVs, especially during physical exercise (Rome et al., 2019). EVs released during exercise are released by skeletal muscle and absorbed by other tissues,

leading to intercellular and interorgan communication, effectively altering the metabolism of receptor cells (Guay & Regazzi, 2017). In this sense, skeletal muscle promotes systemic health through the release of EVs after exercise. Physical therapy is a very important intervention method for DMD patients (Case et al., 2018), therefore, the importance of EVs released during exercise is also crucial in pathological settings.

4 The role of extracellular vesicles in the Duchenne muscular dystrophy skeletal muscle phenotype

It has become quite well-known that EVs derived from different sources (healthy) can elicit functional improvements in different disease models (Biera et al., 2018) (Leng et al., 2021). Most of this research has already indicated that EVs play a key role in the pathology of brain diseases in particular (Christoforidou et al., 2020) (Meldolesi, 2021). Not much has been revealed about the role of EVs in DMD pathology (mechanism), however, more studies are now focusing on this phenomenon. It is important to note that the paracrine actions displayed by skeletal muscle-released EVs is not exclusive to muscle physiology, they may also have an impact on whole-body homeostasis (Rome et al., 2019). Recently, our laboratory has pointed at the anti-myogenic role of EVs derived from dystrophic mice on C2C12 myoblasts and human mesoangioblasts (Yedigaryan et al., 2022b). As stated previously, the myomiRs represent muscle-oriented miRNAs and likely epitomize the most efficacious molecules found mainly in EVs, and tied to striated muscle physiology. Studies on myomiRs miR-1, miR-133, and miR-206 specifically, have gained tremendous attention in understanding muscle degeneration. Accordingly, we found that miR-206 was upregulated in mainly dystrophic, but also aged mice (Yedigaryan et al., 2022b). Consequently, one of the main targets of miR-206 is the ribosomal binding protein 1, a potent regulator of collagen biosynthesis specifically in fibrogenic recipient cells (Fry et al., 2017). Therefore, the upregulation of this miRNA would induce less extracellular matrix deposition, which would be the optimal setting for muscle remodeling, in particular, hypertrophy. However, in DMD, this could also explain the fibrotic pathogenesis, since satellite cell activity is perturbed and, therefore, the muscle cannot be properly regenerated.

Although not in the context of DMD, a recent study displayed that myoblasts incubated with EVs released from myotubes pre-treated with an oxidative stress-mimicking substance, namely hydrogen peroxide, lead to a significant reduction in the diameter of myotubes and to a stimulation of myoblast proliferation (Guescini et al., 2017). This goes in line with the grave role of oxidative stress involved in the pathogenesis of DMD (Petrillo et al., 2017) (Duelen et al., 2022). It has even been highlighted as being the prime cause for muscle degeneration in DMD (Salam et al., 2007). Therefore, under such diseased conditions, this could potentially be a role for skeletal muscle EVs to induce further oxidative stress.

Metabolically, Aswad et al. revealed that the excessive concentration of palmitate and saturated fatty acids in diet-induced obese mice increases intra-muscular ceramide levels that have been established to regulate EV release from muscle (Aswad et al., 2014). In a later study, it was found that an inhibitor of ceramide synthesis GW4869 (an inhibitor of exosome secretion) was able to improve muscle structure and function in *mdx* mice compared to untreated *mdx* mice (Matsuzaka et al., 2016). This gives more evidence to uphold the concept of deleterious organ cross-talks associated with the circulation of detrimental EV cargos.

Research has shown that fluorescently-labeled skeletal muscle-derived exosomes injected in mice are efficiently taken up by the heart (Aswad et al., 2014). On the other hand, cardiosphere-derived cell (CDC) exosomes have been found to be taken up by skeletal muscle (Aminzadeh et al., 2018). Cardiospheres are self-organized spherical clusters derived from human cardiac stem cells (Messina et al., 2004). These cells can be replated to yield CDCs (Smith et al., 2007). The connection between heart failure and idiosyncrasies in skeletal muscle morphology and biological function has been well documented (Lipkin et al., 1988) (Sullivan et al., 1990). Evidence suggests that myocardium-derived miRNAs released into circulation during heart failure progression may have a negative impact on skeletal muscle (Murach & McCarthy, 2017). This reveals another potential role of EVs released in dystrophic muscles, contributing to progressive muscle degeneration due to the cross-talk between skeletal and cardiac muscle EVs, as progressive cardiomyopathy progression and skeletal muscle dissociation in DMD ostensibly leads to the exchange of deleterious EVs from both organs, escalating disease progression. Both skeletal muscle and cardiac muscle partake in multiple organ cross-talks *via* EVs (Figure 2).

This also may contribute to the idea that therapy (cell or cell-free) targeting both cardiac and skeletal muscles would be of great interest when focusing on the most debilitating manifestations of muscular dystrophies, especially DMD. Recently, our laboratory developed induced pluripotent stem cell (iPSC)-derived mesodermal progenitors through differentiation in a monolayer and chemically-defined media (Breuls et al., 2021). We found that these cells are able to differentiate into the skeletal and cardiac muscle lineages both *in vitro* and *in vivo*. Therefore, these cells may house a secretome that could be beneficial to both striated muscle types.

As stated previously, for now, miRNAs appear to represent the most consequential population of EV cargos. This applies not only to the myomiRs, but also to more ubiquitously expressed miRNAs (Catapano et al., 2020). In animal models of DMD, some miRNAs have been found to be significantly up- or downregulated (Yedigaryan & Sampaolesi, 2021). These miRNAs include miR-199a-5p (upregulated in DMD muscle cells and downregulated in DMD fibroblasts (Zanotti et al., 2018)), involved in the wingless-related integration site (WNT) signaling pathway (targeting numerous myogenic cell proliferation and differentiation regulatory factors) (Alexander et al., 2013), and miR-29, a targeter of AKT Serine/Threonine Kinase 3 (AKT3)/nuclear factor kappa-light-chain-enhancer of activated B cells (NF-kB)/Yin Yang1 (YY1) signaling and fibrotic genes (Wang et al., 2012). Recently, miR-486 has also been revealed to play an essential role in muscle function and is found to be significantly downregulated in DMD (Samani et al., 2022). The loss of this miRNA has been associated with disrupted muscle architecture, reduced myofiber size, and increased cardiac fibrosis, just to name a few. Some miRNAs have been revealed to be exclusively upregulated in DMD *in vitro* and *in vivo* models. These miRNAs include, miR-200c, targeter of forkhead box protein O1 (FOXO1) and endothelial nitric oxide synthase (eNOS), essentially inhibiting myoblast differentiation (D'Agostino et al., 2018), miR-21, targeting phosphatase and tensin homolog (PTEN) and receptor tyrosine kinase (RTK) signaling, ultimately leading to more collagen production (Zanotti et al., 2015), and miR-31, directly targeting Myf5 and dystrophin, leading to satellite cell quiescence and a furthermore contribution to the lack of dystrophin (Young et al., 2016).

miRNAs also represent potentially exceptional biomarkers for DMD (Coenen-Stass et al., 2017). miRNAs are abundant, easily measured using low-cost techniques, stable in properly stored biofluid samples, and the discovery of candidate biomarkers is facile compared to novel protein biomarkers. Not only are most myomiRs great candidates for biomarkers, but additional putative biomarkers have been revealed to be

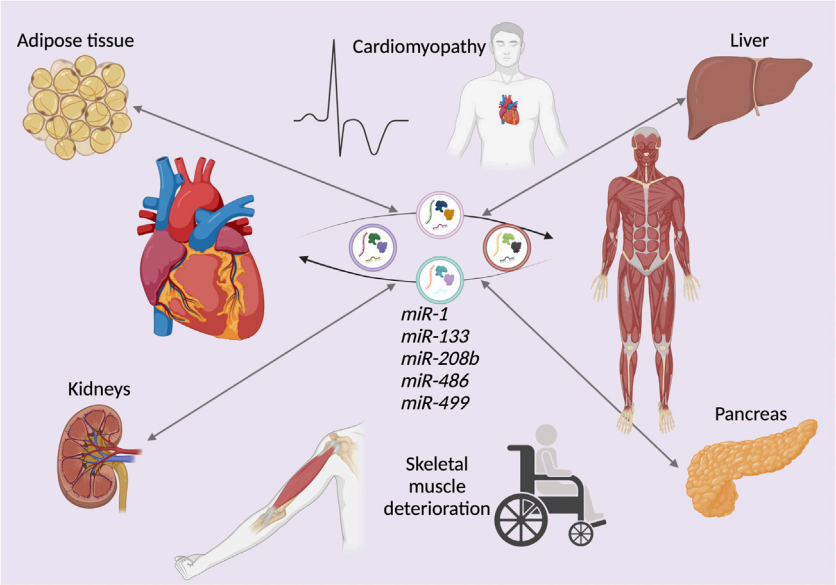

FIGURE 2
The deleterious effects of extracellular vesicle (EV)-mediated organ cross-talk. The exchange of microRNAs (miRNAs), either downregulated or upregulated in young and elderly Duchenne muscular dystrophy (DMD) patients. The depicted miRNAs represent examples of EV cargos exchanged between not only cardiac and skeletal muscle, but also various other organs and tissues such as kidneys, pancreas, liver, and adipose tissue. This cross-talk exacerbates the DMD phenotype.

associated with DMD, including: miR-30, miR-22, miR-95, miR-181, miR-193b, and miR-378 (Jeanson-Leh et al., 2014). Jeanson-Leh et al. also found that in the serum of the Golden Retriever muscular dystrophy model there is a class of dysregulated miRNAs, namely members of the delta like non-canonical Notch ligand 1-iodothyronine deiodinase 3 (*DLK-DIO3*) locus. This locus appears to have an involvement in muscle pathophysiology (Benetatos et al., 2013).

The specific types of surface antigens on EVs have also been considered in the realm of biomarker adaptation for DMD. As an example, Matsuzaka et al. found that an increase in the levels of muscle-abundant miRNAs appears to be tied to CD63 antigen levels on EVs (Matsuzaka et al., 2016). They found that CD63-and major histocompatibility complex (MHC) II-associated EVs collected from the serum of DMD patients were significantly enriched in myomiRs compared to healthy controls, especially miR-1, miR-133a, and miR-206 for CD63-associated EVs and miR-1 and miR-133a for MHC II-associated EVs. Additionally, in *mdx* mice, it was found that levels of miR-133a and miR-206 were significantly increased in CD81-, flotillin-1-, and MHC II-associated EVs, and flotillin-1- and MHC II-coupled EVs, respectively, compared to wild type mice.

Overall, skeletal muscle-released EVs from DMD models must still be additionally explored in order to truly understand their role in DMD pathophysiology and to start the establishment of further therapeutic strategies involving EVs.

5 Cardiac involvement of extracellular vesicles in Duchenne muscular dystrophy

It has become apparent that there is a wealth of molecular species released by cardiac muscle under both physiological and pathological circumstances (Valadi et al., 2007) (Pironti et al., 2015) (Gao et al., 2020). These molecules are said to employ paracrine and/or endocrine effects (Gabisonia et al., 2022). Contrariwise, humoral factors produced by other organs, such as adipose tissue (Crewe et al., 2021), liver (Zardi et al., 2010), kidney (Gao et al., 2020), or skeletal muscle (Murach & McCarthy, 2017), may impact the function of normal and diseased hearts. EVs represent one of the main means of delivering potent molecules to and from the heart. Furthermore, intracardiac cell-to-cell communication has also come to the forefront of understanding the paracrine and endocrine effects of EVs in the heart (Saheera et al., 2021) (Nguyen et al., 2021). It has been found that cardiomyocytes represent only approximately 30% of cardiac cells, therefore, they must have a means of communicating with neighboring endothelial cells, fibroblasts, smooth muscle cells, macrophages, and pericytes (Nag, 1980) (Banerjee et al., 2007). The proper communication between these cell types ensures the homeostatic state of the heart (Perbellini et al., 2018). A multitude of different proteins and nucleic acids have been identified in cardiomyocyte-released exosomes (Malik et al., 2013). Some examples include inflammatory factors such as interleukin-6 (IL-6) (Datta et al., 2017), IL-1β (Yu et al., 2019), tumor necrosis factor-α (TNF-α) (Yu et al., 2012), heat shock proteins such as heat-shock protein 20 (Hsp20) (Zhang et al., 2012), metabolic transporters such as glucose transporter type 4 (GLUT4) and type 1 (GLUT1) (Garcia et al., 2016), as well as enzymes such as lactate dehydrogenase (LDH), and proteins that play a major role in the cardiac development signaling pathway, such as Wnt-binding proteins (Korkut et al., 2009). As stated previously, nucleic acids, especially a wide variety of miRNAs are also present in cardiac EVs (Waldenström et al., 2012) (Wang et al., 2014) (Li et al., 2021). The specific cargo carried by these EVs is strongly tied to their biogenesis and by the different stimuli influencing the parent cells (Malik et al., 2013).

Since cardiomyopathy is one of the leading causes of early mortality in DMD patients, it is crucial to understand the molecular pathology leading to cardiac dysfunction. Gartz et al. demonstrated that short-term exposure to exosomes secreted by dystrophin-deficient iPSC-derived cardiomyocytes (Dys-iCM) had the same protective effect against stress-induced injury on Dys-iCMs as did wild type exosomes (Gartz et al., 2018). They revealed that the protective pathways stimulated in this process included p38 mitogen-activated protein kinase (p38 MAPK) and extracellular signal-regulated protein kinase 1/2 (ERK1/2). However, since this did not mimic physiological *in vivo* conditions where cells are exposed to secreted exosomes continuously, Gartz et al. made a follow-up study to see if long-term exposure to exosomes may represent physiological conditions better (Gartz et al., 2020). In this follow-up study, Gartz et al. tested the effects of DMD cardiac exosomes (acquired from iPSC-derived DMD cardiomyocytes) on iPSC-derived DMD cardiomyocytes, after long-term exposure (Gartz et al., 2020). They confirmed that DMD cardiomyocytes were more vulnerable to stress (higher levels of reactive oxygen species), exhibited a decrease in mitochondrial membrane potential, and experienced an increase in the level of cell death. Long-term exposure of these cardiomyocytes to non-affected exosomes revealed to be protective, however, exposure to DMD cardiac exosomes resulted in no protective effects, rather an increase in the vulnerability to stress of DMD cardiomyocytes. Furthermore, they found that the miRNA cargo was significantly implicated in the pathological effects of DMD cardiac exosomes. In particular, the miRNA cargo housed miRNAs that regulate adverse pathways such as tumor protein P53 (p53) and transforming growth factor-β (TGF-β) (Shirokova & Niggli, 2013) (Lin et al., 2015). Lastly, it was also revealed that exosome inhibition mitigated pathological events tied to DMD cardiomyopathy in an *mdx* mouse model. The most recent follow-up study surfaced where the authors tried to identify the exact mechanism by which DMD cardiac exosomes are able to alter crucial stress-responsive genes in recipient cells (Gartz et al., 2021). They revealed that iPSC-derived DMD cardiomyocyte exosomes contain a heavily-altered miRNA profile compared to healthy controls. In particular, miR-339-5p was upregulated in DMD cardiomyocytes, DMD cardiac exosomes, as well as in mouse cardiac tissue. Some of the important targets of this miRNA are mouse double minute 2 homolog (MDM2), glycogen synthase kinase-3 alpha (GSK3A), and mitogen-activated protein kinase kinase 3 (MAP2K3), genes that are important in stress-responsive signaling pathways (Betel et al., 2008) (Zhang et al., 2014) (Jansson et al., 2015) (Agarwal et al., 2015). Therefore, the upregulation of this miRNA diminishes the ability of DMD cardiomyocytes to protect against stress injury. In line with miRNA deregulation, the myomiRs also appear to be abnormally expressed in the heart of DMD models (Lee et al., 2022). A few examples include, miR-1, involved in the electrical remodeling of the heart and arrhythmia induction if dysregulated (Yang et al., 2007), miR-133, which in case of downregulation causes cardiac hypertrophy (Carè et al., 2007), and the miR-208 family that strongly contributes to cardiac hypertrophy and arrhythmias (Callis et al., 2009).

Other studies have focused more on the potential positive/negative effects of EVs derived from healthy/diseased cells and/or tissues. Research has shown that exosomes isolated from healthy wild-type CDCs *in vitro* are able to improve both cardiac function and skeletal muscle myopathy (Aminzadeh et al., 2018) (Rogers et al., 2019). This effect was the result of a decrease in inflammation and oxidative stress, as well as improved mitochondrial function. Additionally, miR-148a was identified as a potential facilitator of enhanced full-length dystrophin protein synthesis. Another study revealed that exosomes collected from progenitor or stem cells *in vitro*, are able to improve cardiac function *in vivo*, after injury (Lai et al., 2010). In other cardiac disorders, namely cardiac overload or diabetic cardiomyopathy, it was found that exosomes hamper cardiomyocyte metabolism (Halkein et al., 2013) (Bang et al., 2014) or induce cardiac hypertrophy (Bang et al., 2014) through the delivery of an abundance of pathogenic miRNAs. More recently, it was discovered that exosomes isolated from DMD muscle-derived fibroblasts stimulate fibrosis, mainly mediated by exosomal miR-199-5p (Zanotti et al., 2018). With regard to three dimensional (3D) cardiac models, recently, our laboratory unveiled that cardiac organoids derived from DMD iPSCs display DMD-like cardiomyopathy and disease progression phenotypes in long-term cultures compared to clustered regularly interspaced short palindromic repeats (CRISPR)/(CRISPR/Cas9) mutation-corrected isogenic controls (Marini et al., 2022). It was revealed that in the DMD cardiac organoid dysregulated gene network, three miRNAs were found to play crucial roles. These miRNAs were hsa-mir-335-5p, hsa-mir-124-3p, and hsa-mir-26b-5p and further studies are in progress to determine their gene targets and potential roles in DMD cardiac degeneration. miR-335-5p is said to play a critical role in cardiomyocyte apoptosis, calcium level increases, and cardiac hypertrophy in right ventricular remodeling due to pulmonary arterial hypertension (Ma et al., 2022). miR-124-3p has been described to promote cardiac fibroblast activation and proliferation in patients with atrial fibrillation (Zhu et al., 2022). Lastly, miR-26b-5p has been found to be highly expressed in phenylephrine-induced cardiac hypertrophy (Tang et al., 2020).

As with skeletal muscle, miRNAs are also becoming strong candidate biomarkers for DMD cardiomyopathy progression. Although less pronounced than skeletal muscle biomarkers, some miRNAs have been found to be tied to specific muscular dystrophy cardiac events (Becker et al., 2016). As an example, Becker et al. revealed that miR-222, miR-26a, and miR-378a-5p, are significantly upregulated in patients with proof of myocardial scarring compared to those without (Becker et al., 2016). A more recent study has revealed that serum levels of miR-1, miR-133a, miR-133b, and miR-499 were significantly higher in DMD patients with cardiac involvement compared to the no cardiac involvement group (Meng et al., 2022). It has come to attention that the lipid signature of EVs may also discriminate between diseased and control conditions. One such example was evidenced by Burrello et al., where they identified a significant shift in the amount, as well as the diversity of sphingolipid species in EVs derived from ST-segment-elevation myocardial infarction patients *versus* controls (Burrello et al., 2020).

Although research revealing the role of EVs in DMD cardiomyopathy is quite novel, there are some promising results that confirm the potential pathophysiological roles of diseased EVs. Indeed, as documented in the next section, some clinical trials reveal a central role of miRNAs in the positive action of cell secretome-mediated therapy. Please see Table 1 for an overview of important miRNAs described in the text.

TABLE 1 An overview of dysregulated microRNAs (miRNAs) in Duchenne muscular dystrophy (DMD) described in the text. The columns represent the miRNAs, up- or downregulated in skeletal and/or cardiac muscle, and their potential involvement in DMD due to dysregulation (*in vivo* and/or *in vitro*).

microRNAs	Sk—skeletal muscle, C—cardiac muscle Up- or downregulated (specified in text)	Study type and potential involvement in DMD due to dysregulation
miR-1	C: Up	*In vivo*; Arrhythmogenesis
miR-133a	C: Down	*In vivo* and *in vitro*; Cardiac hypertrophy
miR-206	Sk: Up	*In vitro*; Fibrosis
miR-199-5p	Sk: Up, C: Up	*In vivo* and *in vitro*; Fibrosis
miR-29	Sk: Down	*In vivo* and *in vitro*; Increased muscle fibrogenesis
miR-486	Sk: Down, C: Down	*In vivo*; Disrupted muscle architecture, reduced myofiber size, and increased cardiac fibrosis
miR-200c	Sk: Up	*In vivo* and *in vitro*; Reduced myofiber size
miR-21	Sk: Up	*In vivo* and *in vitro*; Fibrosis
miR-31	Sk: Up	*In vivo* and *in vitro*; Reduced myofiber size and disrupted muscle architecture
miR-339-5p	C: Up	*In vivo and in vitro*; Impairment of protection from stress injury, cell death
miR-208	C: Up	*In vivo*; Cardiac hypertrophy
miR-148a	C: Down	*In vivo* and *in vitro*; Facilitator of dystrophin synthesis
miR-335-5p	C:*	*In vitro*; DMD cardiac organoid dysregulation, cardiomyocyte apoptosis, increase in calcium levels, and cardiac hypertrophy
miR-124-3p	C:*	*In vitro*; DMD cardiac organoid dysregulation, cardiac fibrosis
miR-26b-5p	C:*	*In vitro*; DMD cardiac organoid dysregulation, cardiac hypertrophy

*These miRNAs are said to be dysregulated in DMD cardiac organoids (not specified yet if up- or downregulated).

6 From the bench to the bedside: Extracellular vesicles in clinical development

The use of human embryonic stem cells (hESCs) or hESC-derived cells in the field of cardiac regeneration has progressed towards a clinical trial (Menasché et al., 2018). Menasché et al. conducted a trial for the use of hESC-derived cardiovascular progenitors (embedded in a fibrin patch) on patients with severe ischemic left ventricular dysfunction. They demonstrated the feasibility of deriving these cells in a clinical-grade manner, as well as outlined the short- and medium-term safety of these cells. Although interpreted cautiously, the authors did detect improved contractility of the grafted segments. This improvement was hypothesized to be due to the secretion of biomolecules manifesting host-linked reparative mechanisms (Garbern & Lee, 2013). These biomolecules were found to be largely present in EVs. Furthermore, it was previously shown that the cardioprotective effects of the hESC-derived cardiac progenitors could be recapitulated by the sole administration of their released EVs (Kervadec et al., 2016). The authors assessed the content of these EVs and found that miR-302 appeared to be predominantly expressed. This miRNA is tied to cardiomyocyte proliferation stimulation (Tao et al., 2015). This revelation has caused a further understanding and a potential shift towards viewing hESC- or iPSC-derived progenitors as vital producers of a secretome able to induce a paracrine mechanism of action, explaining the long-term action of ESC derivatives in spite of their scarce long-standing engraftment potential (Menasché, 2022). Therefore, the secretome may be further considered as the "active substance", that includes not only cytokines, chemokines, growth factors, RNAs, and proteins, but also extracellular vesicles. This ongoing study also exudes a burgeoning high potency when it comes to a multitude of other cardiac diseases, including DMD-induced cardiomyopathy.

Early work reported by Aminzadeh et al. (Aminzadeh et al., 2014) (Aminzadeh et al., 2015) motivated the Halt cardiomyOPathy progrEssion in Duchenne (HOPE-Duchenne) clinical trial (Ascheim & Jefferies, 2016), which is now entering phase 3 (McDonald et al., 2022). Aminzadeh et al. unveiled the striking effect of CDCs in *mdx* mice. Although initially the main goal was to ameliorate some of the pathophysiological consequences of DMD in the heart, the authors later revealed the affinity of CDCs to also restore skeletal muscle function (Aminzadeh et al., 2018). This uncovered the major systemic benefits of CDC injection into the heart. CDCs are said to induce their beneficial effects through the secretion of exosomes. These exosomes may play a multitude of different roles such as targeting macrophages and altering them into a healing rather than pro-inflammatory state (de Couto et al., 2015), as well as targeting fibroblasts and ultimately having an antifibrotic effect (Tseliou et al., 2015). Among the cargo of CDC-derived exosomes, miRNAs (miR-146a and miR-181b) and Y RNA fragments are the known bioactive components (Cambier et al., 2017) (de Couto et al., 2017) (Marbán, 2018) (McDonald, 2022). miR-146b has been shown to suppress ischemia/reperfusion injury by targeting interleukin-1 receptor-associated kinase 1 (IRAK) and tumor necrosis factor receptor (TNFR)-associated factor 6 (TRAF6) (Cheng et al., 2013) (Ibrahim et al., 2014). These pro-inflammatory cytokines are involved in the toll-like receptor (TLR) signaling pathway (Wang et al., 2013). This miRNA was shown to also suppress nicotinamide adenine dinucleotide phosphate oxidase four (NOX4) and SMAD family member 4 (SMAD4), which are

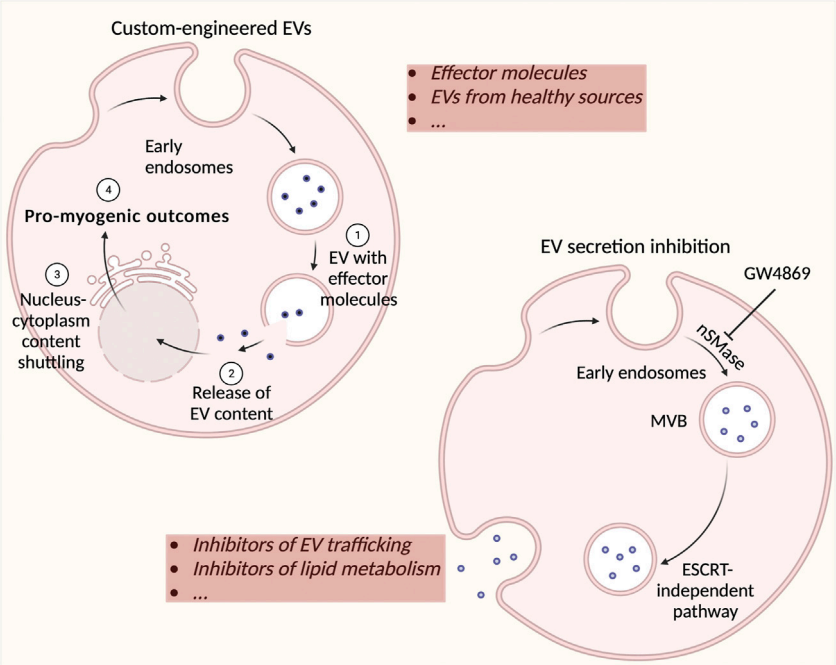

FIGURE 3
Possible strategies for using extracellular vesicles (EVs) as therapeutic agents. Custom cargos may be implemented in specific EVs (such as derived from healthy muscle) and potentially used as a Duchenne muscular dystrophy (DMD) therapeutic. Effector molecules may include nucleic acids, lipids, proteins, adeno-associated viruses (for gene therapy), and propeptides with limited efficacy via direct administration. The inhibition of EV formation and secretion is a new strategy for stopping the effect of detrimental EVs in DMD. Most commonly used compounds include inhibitors of EV trafficking such as calpeptin, manumycin A, Y27632, and inhibitors of lipid metabolism such as imipramine, pantethine, and GW4869. These inhibitors may either act on the endosomal sorting complexes required for transport machinery (ESCRT)-dependent (e.g. manumycin A) or –independent pathway (e.g. GW4869). There are a multitude of other drugs that have been investigated for their ability to inhibit EV secretion such as U0126, clopidogrel, indomethacin, and chloramidine. These strategies represent potentially highly efficacious therapeutics for DMD treatment.

involved in oxidative stress induction and the TGF-β profibrotic pathway, respectively (Infanger et al., 2010) (Vasa-Nicotera et al., 2011) (Liu et al., 2012). It has been found that miR-181b may be involved in the cardioprotective effect of CDC-derived exosomes by targeting protein kinase C-delta (PKC-δ) within distinctive macrophages, to induce a marked polarization state (de Couto et al., 2017). Cambier et al. revealed that a fragment of Y RNA, highly enriched in CDC-derived EVs, enhances IL-10 protein secretion by altering *Il10* gene expression (Cambier et al., 2017). IL-10 is a well-known cardioprotective cytokine, particularly in myocardial ischemia/reperfusion injury (Yang et al., 2000).

Phase 1 of the HOPE clinical study revealed that CDCs appeared to display an acceptable level of safety and were able to preserve upper limb and cardiac function after one-time delivery into the coronary arteries of DMD patients (Ascheim & Jefferies, 2016) (McDonald et al., 2022). Phase 2 of the HOPE clinical trial (HOPE-2) examined the safety and efficacy of sequential intravenous injections of human CDCs in patients with late-stage DMD (McDonald, 2018). This trial disclosed that CDCs are safe and efficacious with regard to reducing deterioration of upper limb function in late-stage DMD patients. Cardiac functional and structural benefits were also observed compared to the placebo group. Phase 3 of the HOPE clinical trial (HOPE-3) is currently recruiting participants and will entail testing the CDCs in a large number of patients, compared to phase 2 (McDonald et al., 2022). Therefore, the HOPE clinical trial represents a very promising therapeutic approach for DMD patients, as it continues on to the third phase of testing.

It is imperative to develop a large-scale production of EVs as a medicinal product in line with current good manufacturing processes (GMP) guidelines. Such methods are currently being studied and developed. Overcoming limitations such as contaminants, xeno-free reagents *in lieu* of animal-derived ones, and scalable and reliable isolation methods are some of the important aspects of establishing ready-to-use EV products (Andriolo et al., 2018). It is also critical that the robustness and the reproducibility be measurable with reliable and optimized analytical methods in order to follow GMP guidelines.

Overall, the future of research in the direction of understanding the importance of the cell secretome is gaining momentum and more revelations with regard to this topic will surely be made.

7 Conclusion and potential therapeutic applications

In retrospect, EVs represent a field of study that must be explored a lot more in depth. While recent studies have already established that EVs are very important mediators in cell-to-cell communication, it remains to be further seen exactly how they contribute to healthy compared to diseased physiology. There is an abundant amount of evidence suggesting that DMD EVs induce deleterious effects, so it may be beneficial to understand which molecules are responsible for the adverse effects and to explore the possibility of counteracting the release of these molecules from EVs. Nowadays, the focus of EV-related potential therapies lies with the delivery of either EVs

derived from healthy sources (Aminzadeh et al., 2018) (Yedigaryan et al., 2022a) or custom-cargo-engineered EVs that can efficiently deliver molecules to recipient cells (Matsuzaka et al., 2022). The inhibition of EV release represents a paradigm shift in the manner of treatment for diseases (Gartz et al., 2020) (Catalano & O'Driscoll, 2019) (Figure 3). However, compounds used to inhibit EV formation and/or release must be scrutinized closely for their off-target effects and under these circumstances, investigated for their influence on healthy cells. In the context of DMD, it appears that one of the most efficacious molecules in EVs are miRNAs. This also asserts a potential therapeutic strategy, as antagomiRs (anti-miRs), chemically engineered oligonucleotides intended for silencing endogenous miRNAs, may be utilized to block harmful miRNAs. On the other hand, miRNA mimics, chemically-designed double-stranded RNA molecules used to imitate endogenous miRNAs, may be used to enrich tissues with advantageous miRNAs (Rotini et al., 2018). These anti-miRs could potentially also be encapsulated in healthy EVs and delivered to patients. Although these ideas all seem to represent a highly compelling argument for their use in DMD therapy, much research and trials must be devised to understand their feasibility, safety, and final effectiveness (Villa et al., 2019). However, nano-therapy is becoming increasingly widespread and there will most likely come a time when exploratory cell therapy takes a backseat to cell-free therapeutic approaches.

Author contributions

LY wrote the first draft of the manuscript. LY and MS contributed to the conception and design of the manuscript, manuscript revision, re-reading, and approval of the final submitted version.

Funding

The work done in the authors' laboratory is supported by Small Research Infrastructure KU Leuven–BioAssemblyBot 400 (KA/20/088), Research Foundation Flanders (FWO) (#G066821N), INTERREG–Euregio Meuse-Rhine (GYM, Generate your muscle 2020-EMR116), and the Italian Ministry of Health, Ricerca Finalizzata (RF-2019-12369703). MS is a recipient of the Hercules Foundation grant (AKUL/19/34) for the financing provided to purchase the high throughput calcium imaging system.

Acknowledgments

The authors gratefully acknowledge Sylvia Sauvage for her technical assistance, as well as Christina Vochten and Vicky Raets for their administrative assistance. All figures were created with BioRender.com.

Conflict of interest

The authors declare that the research was conducted in the absence of any commercial or financial relationships that could be construed as a potential conflict of interest.

Publisher's note

All claims expressed in this article are solely those of the authors and do not necessarily represent those of their affiliated organizations, or those of the publisher, the editors and the reviewers. Any product that may be evaluated in this article, or claim that may be made by its manufacturer, is not guaranteed or endorsed by the publisher.

References

Aartsma-Rus, A., Straub, V., Hemmings, R., Haas, M., Schlosser-Weber, G., Stoyanova-Beninska, V., et al. (2017). Development of exon skipping therapies for Duchenne muscular dystrophy: A critical review and a perspective on the outstanding issues. *Nucleic Acid. Ther.* 27 (5), 251–259.

Agarwal, V., Bell, G. W., Nam, J.-W., and Bartel, D. P. (2015). Predicting effective microRNA target sites in mammalian mRNAs. *eLife* 4, e05005.

Alexander, M. S., Kawahara, G., Motohashi, N., Casar, J. C., Eisenberg, I., Myers, J. A., et al. (2013). MicroRNA-199a is induced in dystrophic muscle and affects WNT signaling, cell proliferation, and myogenic differentiation. *Cell Death Differ.* 20 (9), 1194–1208. doi:10.1038/cdd.2013.62

Aminzadeh, M. A., Tobin, R., Smith, R., Marbán, L., and Marbán, E. (2014). Heart-derived cell therapy for Duchenne cardiomyopathy: Cardiosphere-derived cells and their exosomes improve function, restore mitochondrial integrity and reverse degenerative changes in the hearts of mdx mice. *Circulation Res.* 115, e90.

Aminzadeh, M., Durvasula, P., Tobin, R., Guan, X., Andres, A., Taylor, D., et al. (2015). Exosome-mediated reversal of Duchenne cardiomyopathy. *Circulation* 132, A16015.

Aminzadeh, M., Rogers, R., Fournier, M., Tobin, R., Guan, X., Childers, M., et al. (2018). Exosome-mediated benefits of cell therapy in mouse and human models of Duchenne muscular dystrophy. *Stem Cell Rep.* 10 (3), 942–955. doi:10.1016/j.stemcr.2018.01.023

Andriolo, G., Provasi, E., Lo Cicero, V., Brambilla, A., Soncin, S., Torre, T., et al. (2018). Exosomes from human cardiac progenitor cells for therapeutic applications: Development of a GMP-grade manufacturing method. *Front. Physiology* 9, 1169. doi:10.3389/fphys.2018.01169

Annibalini, G., Contarelli, S., Lucertini, F., Guescini, M., Maggio, S., Ceccaroli, P., et al. (2019). Muscle and systemic molecular responses to a single flywheel based iso-inertial training session in resistance-trained men. *Front. Physiology* 10, 554. doi:10.3389/fphys.2019.00554

Aravind, S., Ashley, B., Mannan, A., Ganapathy, A., Ramesh, K., Ramachandran, A., et al. (2019). Targeted sequencing of the DMD locus: A comprehensive diagnostic tool for all mutations. *Indian J. Med. Res.* 150 (3), 282–289. doi:10.4103/ijmr.IJMR_290_18

Arpke, R. W., Darabi, R., Mader, T. L., Zhang, Y., Toyama, A., Lonetree, C.-l., et al. (2013). A new immuno-dystrophin-deficient model, the NSG-mdx4Cv mouse, provides evidence for functional improvement following allogeneic satellite cell transplantation. *Stem Cells* 31 (8), 1611–1620. doi:10.1002/stem.1402

Ascheim, D., and Jefferies, J. (2016). A randomized, open-label study of the safety and efficacy of multi-vessel intracoronary delivery of allogeneic cardiosphere-derived cells in patients with cardiomyopathy secondary to Duchenne muscular dystrophy. Available at: https://clinicaltrials.gov/ct2/show/NCT02485938.

Aswad, H., Forterre, A., Wiklander, O. P., Vial, G., Santy-Berger, E., Jalabert, A., et al. (2014). Exosomes participate in the alteration of muscle homeostasis during lipid-induced insulin resistance in mice. *Diabetologia* 57, 2155–2164. doi:10.1007/s00125-014-3337-2

Atkin-Smith, G. K., Tixeira, R., Paone, S., Mathivanan, S., Collins, C., Liem, M., et al. (2015). A novel mechanism of generating extracellular vesicles during apoptosis via a beads-on-a-string membrane structure. *Nat. Commun.* 6, 7439. doi:10.1038/ncomms8439

Banerjee, I., Fuseler, J. W., Price, R. L., Borg, T. K., and Baudino, T. A. (2007). Determination of cell types and numbers during cardiac development in the neonatal and adult rat and mouse. *Am. J. Physiology Heart Circulatory Physiology* 293 (3), H1883–H1891. doi:10.1152/ajpheart.00514.2007

Bang, C., Batkai, S., Dangwal, S., Gupta, S. K., Foinquinos, A., Holzmann, A., et al. (2014). Cardiac fibroblast-derived microRNA passenger strand-enriched exosomes mediate cardiomyocyte hypertrophy. *J. Clin. Investigation* 124 (5), 2136–2146. doi:10.1172/JCI70577

Becker, S., Florian, A., Patrascu, A., Rösch, S., Waltenberger, J., Sechtem, U., et al. (2016). Identification of cardiomyopathy associated circulating miRNA biomarkers in patients with muscular dystrophy using a complementary cardiovascular magnetic

resonance and plasma profiling approach. *J. Cardiovasc. Magnetic Reson.* 18, 25. doi:10.1186/s12968-016-0244-3

Benetatos, L., Hatzimichael, E., Londin, E., Vartholomatos, G., Loher, P., Rigoutsos, I., et al. (2013). The microRNAs within the DLK1-DIO3 genomic region: Involvement in disease pathogenesis. *Cell. Mol. Life Sci.* 70, 795–814. doi:10.1007/s00018-012-1080-8

Bentzinger, C. F., Wang, Y. X., and Rudnicki, M. A. (2012). Building muscle: Molecular regulation of myogenesis. *Cold Spring Harb. Perspect. Biol.* 4, a008342. doi:10.1101/cshperspect.a008342

Betel, D., Wilson, M., Gabow, A., Marks, D. A., and Sander, C. (2008). The microRNA.org resource: Targets and expression. *Nucleic Acids Res.* 36 (1), D149–D153. doi:10.1093/nar/gkm995

Biera, A., Berensteina, P., Kronfelda, N., Morgoulis, D., Ziv-Av, A., Hodaya, G., et al. (2018). Placenta-derived mesenchymal stromal cells and their exosomes exert therapeutic effects in Duchenne muscular dystrophy. *Biomaterials* 174, 67–78. doi:10.1016/j.biomaterials.2018.04.055

Bonilla, E., Samitt, C. E., Miranda, A. F., Hays, A. P., Salviati, G., DiMauro, S., et al. (1988). Duchenne muscular dystrophy: Deficiency of dystrophin at the muscle cell surface. *Cell* 54 (4), 447–452. doi:10.1016/0092-8674(88)90065-7

Breuls, N., Giarratana, N., Yedigaryan, L., Garrido, G. M., Carai, P., Heymans, S., et al. (2021). Valproic acid stimulates myogenesis in pluripotent stem cell-derived mesodermal progenitors in a NOTCH-dependent manner. *Cell Death Dis.* 12, 677. doi:10.1038/s41419-021-03936-w

Burrello, J., Biemmi, V., Dei Cas, M., Amongero, M., Bolis, S., Lazzarini, E., et al. (2020). Sphingolipid composition of circulating extracellular vesicles after myocardial ischemia. *Sci. Rep.* 10, 16182. doi:10.1038/s41598-020-73411-7

Callis, E, T., Pandya, K., Seok, H. Y., Tang, R.-H., Tatsuguchi, M., Huang, Z. P., et al. (2009). MicroRNA-208a is a regulator of cardiac hypertrophy and conduction in mice. *J. Clin. Investigation* 119 (9), 2772–2786. doi:10.1172/JCI36154

Cambier, L., de Couto, G., Ibrahim, A., Echavez, A. K., Valle, J., Liu, W., et al. (2017). Y RNA fragment in extracellular vesicles confers cardioprotection via modulation of IL-10 expression and secretion. *EMBO Mol. Med.* 9 (3), 337–352. doi:10.15252/emmm.201606924

Carè, A., Catalucci, D., Bonci, D., Addario, A., Gallo, P., Bang, M.-L., et al. (2007). MicroRNA-133 controls cardiac hypertrophy. *Nat. Med.* 13, 613–618. doi:10.1038/nm1582

Case, L. E., Apkon, S. D., Gulyas, A., Juel, L., Matthews, D., Newton, R. A., et al. (2018). Rehabilitation management of the patient with Duchenne muscular dystrophy. *Pediatrics* 142 (2), S17–S33. doi:10.1542/peds.2018-0333D

Catalano, M., and O'Driscoll, L. (2019). Inhibiting extracellular vesicles formation and release: A review of EV inhibitors. *J. Extracell. Vesicles* 9 (1), 1703244. doi:10.1080/20013078.2019.1703244

Catapano, F., Scaglioni, D., Maresh, K., Ala, P., Domingos, J., Selby, V., et al. (2020). Novel free-circulating and extracellular vesicle-derived miRNAs dysregulated in Duchenne muscular dystrophy. *Epigenomics* 12 (21), 1899–1915. doi:10.2217/epi-2020-0052

Chamberlain, J. R., and Chamberlain, J. S. (2017). Progress toward gene therapy for Duchenne muscular dystrophy. *Mol. Ther. J. Am. Soc. Gene Ther.* 25 (5), 1125–1131. doi:10.1016/j.ymthe.2017.02.019

Chemello, F., Wang, Z., Li, H., R, M. J., Liu, N., Bassel-Duby, R., et al. (2020). Degenerative and regenerative pathways underlying Duchenne muscular dystrophy revealed by single-nucleus RNA sequencing. *Proc. Natl. Acad. Sci. U. S. A.* 117 (47), 29691–29701. doi:10.1073/pnas.2018391117

Chen, J.-F., Mandel, E. M., Thomson, J. M., Wu, Q., Callis, T. E., Hammond, S. M., et al. (2006). The role of microRNA-1 and microRNA-133 in skeletal muscle proliferation and differentiation. *Nat. Genet.* 38 (2), 228–233. doi:10.1038/ng1725

Cheng, H. S., Sivachandran, N., Lau, A., Boudreau, E., Zhao, J. L., Baltimore, D., et al. (2013). MicroRNA-146 represses endothelial activation by inhibiting pro-inflammatory pathways. *EMBO Mol. Med.* 5 (7), 1017–1034. doi:10.1002/emmm.201202318

Christoforidou, E., Joilin, G., and Hafezparast, M. (2020). Potential of activated microglia as a source of dysregulated extracellular microRNAs contributing to neurodegeneration in amyotrophic lateral sclerosis. *J. Neuroinflammation* 17 (1), 135. doi:10.1186/s12974-020-01822-4

Coenen-Stass, A., Betts, C., Lee, Y., Mäger, I., Turunen, M., Andaloussi, S., et al. (2016). Selective release of muscle-specific, extracellular microRNAs during myogenic differentiation. *Hum. Mol. Genet.* 25 (18), 3960–3974. doi:10.1093/hmg/ddw237

Coenen-Stass, A. M., Wood, M. J., and Roberts, T. C. (2017). Biomarker potential of extracellular miRNAs in Duchenne muscular dystrophy. *Trends Mol. Med.* 23 (11), 989–1001. doi:10.1016/j.molmed.2017.09.002

Crewe, C., Funcke, J.-B., Li, S., Joffin, N., Gliniak, C. M., Ghaben, A. L., et al. (2021). Extracellular vesicle-based interorgan transport of mitochondria from energetically stressed adipocytes. *Cell Metab.* 33 (9), 1853–1868. doi:10.1016/j.cmet.2021.08.002

Crisafulli, S., Sultana, J., Andrea, F., Salvo, F., Messina, S., and Trifirò, G. (2020). Global epidemiology of Duchenne muscular dystrophy: An updated systematic review and meta-analysis. *Orphanet J. Rare Dis.* 15 (1), 141. doi:10.1186/s13023-020-01430-8

D'Agostino, M., Torcinaro, A., Madaro, L., Marchetti, L., Sileno, S., Beji, S., et al. (2018). Role of miR-200c in myogenic differentiation impairment via p66Shc: Implication in skeletal muscle regeneration of dystrophic mdx mice. *Oxidative Med. Cell. Longev.* 2018, 4814696. doi:10.1155/2018/4814696

Datta, R., Bansal, T., Rana, S., Datta, K., Chaudhuri, R. D., Chawla-Sarkar, M., et al. (2017). Myocyte-derived Hsp90 modulates collagen upregulation via biphasic activation of STAT-3 in fibroblasts during cardiac hypertrophy. *Mol. Cell. Biol.* 37 (6), e00611–e00616. doi:10.1128/MCB.00611-16

de Couto, G., Gallet, R., Cambier, L., Jaghatspanyan, E., Makkar, N., Dawkins, J. F., et al. (2017). Exosomal MicroRNA transfer into macrophages mediates cellular postconditioning. *Circulation* 136 (2), 200–214. doi:10.1161/CIRCULATIONAHA.116.024590

de Couto, G., Liu, W., Tseliou, E., Sun, B., Makkar, N., Kanazawa, H., et al. (2015). Macrophages mediate cardioprotective cellular postconditioning in acute myocardial infarction. *J. Clin. Investigation* 125 (8), 3147–3162. doi:10.1172/JCI81321

Duelen, R., Costamagna, D., Gilbert, G., De Waele, L., Goemans, N., Desloovere, K., et al. (2022). Human iPSC model reveals a central role for NOX4 and oxidative stress in Duchenne cardiomyopathy. *Stem Cell Rep.* 17 (2), 352–368. doi:10.1016/j.stemcr.2021.12.019

Dumont, N. A., Wang, Y. X., von Maltzahn, J., Pasut, A., Bentzinger, C. F., Brun, C. E., et al. (2015). Dystrophin expression in muscle stem cells regulates their polarity and asymmetric division. *Nat. Med.* 21, 1455–1463. doi:10.1038/nm.3990

Emery, A. E. (2002). THe muscular dystrophies. *Lancet* 359 (9307), 687–695. doi:10.1016/S0140-6736(02)07815-7

Fry, C. S., Kirby, T. J., Kosmac, K., McCarthy, J. J., and Peterson, C. A. (2017). Myogenic progenitor cells control extracellular matrix production by fibroblasts during skeletal muscle hypertrophy. *Cell Stem Cell* 20 (1), 56–69. doi:10.1016/j.stem.2016.09.010

Gabisonia, K., Khan, M., and Recchia, F. A. (2022). Extracellular vesicle-mediated bidirectional communication between heart and other organs. *Am. J. Physiology Heart Circulatory Physiology* 322 (5), H769–H784. doi:10.1152/ajpheart.00659.2021

Gao, L., Mei, S., Zhang, S., Qin, Q., Li, H., Liao, Y., et al. (2020). Cardio-renal exosomes in myocardial infarction serum regulate proangiogenic paracrine signaling in adipose mesenchymal stem cells. *Theranostics* 10 (3), 1060–1073. doi:10.7150/thno.37678

Garbern, J. C., and Lee, R. T. (2013). Cardiac stem cell therapy and the promise of heart regeneration. *Cell Stem Cell* 12 (6), 689–698. doi:10.1016/j.stem.2013.05.008

Garcia, N. A., Moncayo-Arlandi, J., Sepulveda, P., and Diez-Juan, A. (2016). Cardiomyocyte exosomes regulate glycolytic flux in endothelium by direct transfer of GLUT transporters and glycolytic enzymes. *Cardiovasc. Res.* 109 (3), 397–408. doi:10.1093/cvr/cvv260

Gartz, M., Beatka, M., Prom, M. J., Strande, J. L., and Lawlor, M. W. (2021). Cardiomyocyte-produced miR-339-5p mediates pathology in Duchenne muscular dystrophy cardiomyopathy. *Hum. Mol. Genet.* 30 (23), 2347–2361. doi:10.1093/hmg/ddab199

Gartz, M., Darlington, A., Afzal, M. Z., and Strande, J. L. (2018). Exosomes exert cardioprotection in dystrophin-deficient cardiomyocytes via ERK1/2-p38/MAPK signaling. *Sci. Rep.* 8 (1), 16519. doi:10.1038/s41598-018-34879-6

Gartz, M., Lin, C.-W., Sussman, M. A., Lawlor, M. W., and Strande, J. L. (2020). Duchenne muscular dystrophy (DMD) cardiomyocyte-secreted exosomes promote the pathogenesis of DMD-associated cardiomyopathy. *Dis. Models Mech.* 13 (11), 045559. doi:10.1242/dmm.045559

Guay, C., and Regazzi, R. (2017). Exosomes as new players in metabolic organ cross-talk. *Diabetes, Obes. Metabolism* 19 (S1), 137–146. doi:10.1111/dom.13027

Guescini, M., Canonico, B., Lucertini, F., Maggio, S., Annibalini, G., Barbieri, E., et al. (2015). Muscle releases alpha-sarcoglycan positive extracellular vesicles carrying miRNAs in the bloodstream. *PLOS One* 10 (5), e0125094. doi:10.1371/journal.pone.0125094

Guescini, M., Maggio, S., Ceccaroli, P., Battistelli, M., Annibalini, G., Piccoli, G., et al. (2017). Extracellular vesicles released by oxidatively injured or intact C2C12 myotubes promote distinct responses converging toward myogenesis. *INernational J. Mol. Sci.* 18 (11), 2488. doi:10.3390/ijms18112488

Guiraud, S., and Davies, K. E. (2017). Pharmacological advances for treatment in Duchenne muscular dystrophy. *Curr. Opin. Pharmacol.* 34, 36–48. doi:10.1016/j.coph.2017.04.002

Haidet, A. M., Rizo, L., Handy, C., Umapathi, P., Eagle, A., Shilling, C., et al. (2008). Long-term enhancement of skeletal muscle mass and strength by single gene administration of myostatin inhibitors. *Proc. Natl. Acad. Sci. U. S. A.* 105 (11), 4318–4322. doi:10.1073/pnas.0709144105

Halkein, J., Tabruyn, S. P., Ricke-Hoch, M., Haghikia, A., Nguyen, N.-Q.-N., Scherr, M., et al. (2013). MicroRNA-146a is a therapeutic target and biomarker for peripartum cardiomyopathy. *J. Clin. Investigation* 123 (5), 2143–2154. doi:10.1172/JCI64365

Heier, C. R., Damsker, J. M., Yu, Q., Dillingham, B. C., Huynh, T., Van der Meulen, J. H., et al. (2013). VBP15, a novel anti-inflammatory and membrane-stabilizer, improves muscular dystrophy without side effects. *EMBO Mol. Med.* 5, 1569–1585. doi:10.1002/emmm.201302621

Heijnen, H. F., Schiel, A. E., Fijnheer, R., Geuze, H. J., and Sixma, J. J. (1999). Activated platelets release two types of membrane vesicles: Microvesicles by surface shedding and exosomes derived from exocytosis of multivesicular bodies and alpha-granules. *Blood* 94 (11), 3791–3799. doi:10.1182/blood.v94.11.3791.423a22_3791_3799

Hoffman, E. P., Brown, R. H., Jr, and Kunkel, L. M. (1987a). Dystrophin: The protein product of the Duchenne muscular dystrophy locus. *Cell* 51 (6), 919–928. doi:10.1016/0092-8674(87)90579-4

Hoffman, E. P., Monaco, A. P., Feener, C. C., and Kunkel, L. M. (1987b). Conservation of the Duchenne muscular dystrophy gene in mice and humans. *Science* 238 (4825), 347–350. doi:10.1126/science.3659917

Huotari, J., and Helenius, A. (2011). Endosome maturation. *EMBO J.* 30, 3481–3500. doi:10.1038/emboj.2011.286

Ibrahim, A. G.-E., Cheng, K., and Marbán, E. (2014). Exosomes as critical agents of cardiac regeneration triggered by cell therapy. *Stem Cell Rep.* 2 (5), 606–619. doi:10.1016/j.stemcr.2014.04.006

Infanger, D. W., Cao, X., Butler, S. D., Burmeister, M. A., Zhou, Y., Stupinski, J. A., et al. (2010). Silencing nox4 in the paraventricular nucleus improves myocardial infarction-induced cardiac dysfunction by attenuating sympathoexcitation and periinfarct apoptosis. *Circulation Res.* 106 (11), 1763–1774. doi:10.1161/CIRCRESAHA.109.213025

Jalabert, A., Vial, G., Guay, C., Wiklander, O. P., Nordin, J. Z., Aswad, H., et al. (2016). Exosome-like vesicles released from lipid-induced insulin-resistant muscles modulate gene expression and proliferation of beta recipient cells in mice. *Diabetologia* 59 (5), 1049–1058. doi:10.1007/s00125-016-3882-y

Jansson, M. D., Damas, N. D., Lees, M., Jacobsen, A., and Lund, A. H. (2015). miR-339-5p regulates the p53 tumor-suppressor pathway by targeting MDM2. *Oncogene* 34, 1908–1918. doi:10.1038/onc.2014.130

Jeanson-Leh, L., Lameth, J., Krimi, S., Buisset, J., Amor, F., Le Guiner, C., et al. (2014). Serum profiling identifies novel muscle miRNA and cardiomyopathy-related miRNA biomarkers in golden retriever muscular dystrophy dogs and Duchenne muscular dystrophy patients. *Pthology* 184 (11), 2885–2898. doi:10.1016/j.ajpath.2014.07.021

Keefe, A. C., and Kardon, G. (2015). A new role for dystrophin in muscle stem cells. *Nat. Med.* 21, 1391–1393. doi:10.1038/nm.4006

Kervadec, A., Bellamy, V., El Harane, N., Arakélian, L., Vanneaux, V., Cacciapuoti, I., et al. (2016). Cardiovascular progenitor-derived extracellular vesicles recapitulate the beneficial effects of their parent cells in the treatment of chronic heart failure. *J. Heart Lung Translplantation Official Publ. Int. Soc. Heart Transplant.* 35 (6), 795–807. doi:10.1016/j.healun.2016.01.013

Klingler, W., Jurkat-Rott, K., Lehmann-Horn, F., and Schleip, R. (2012). The role of fibrosis in Duchenne muscular dystrophy. *Acta Myol.* 31 (3), 184–195.

Korkut, C., Ataman, B., Ramachandran, P., Ashley, J., Barria, R., Gherbesi, N., et al. (2009). Trans-synaptic transmission of vesicular Wnt signals through Evi/Wntless. *Cell* 139 (2), 393–404. doi:10.1016/j.cell.2009.07.051

Kunkel, L., Hejtmancik, J., Caskey, C., Speer, A., Monaco, A., Middlesworth, W., et al. (1986). Analysis of deletions in DNA from patients with Becker and Duchenne muscular dystrophy. *Nature* 322 (6074), 73–77. doi:10.1038/322073a0

Lai, C. R., Arslan, F., Lee, M. M., Sze, N. S., Choo, A., Chen, T. S., et al. (2010). Exosome secreted by MSC reduces myocardial ischemia/reperfusion injury. *Stem Cell Res.* 4 (3), 214–222. doi:10.1016/j.scr.2009.12.003

Landfeldt, E., Thompson, R., Sejersen, T., McMillan, H. J., Kirschner, J., and Lochmüller, H. (2020). Life expectancy at birth in Duchenne muscular dystrophy: A systematic review and meta-analysis. *Eur. J. Epidemiol.* 35 (7), 643–653. doi:10.1007/s10654-020-00613-8

Leal, L. G., Lopes, M. A., and Batista, M. L., Jr. (2018). Physical exercise-induced myokines and muscle-adipose tissue crosstalk: A review of current knowledge and the implications for health and metabolic diseases. *Front. Physiology* 9, 1307. doi:10.3389/fphys.2018.01307

Lee, A., Moon, J., and Kho, C. (2022). MicroRNAs in dystrophinopathy. *Int. J. Mol. Sci.* 23, 7785. doi:10.3390/ijms23147785

Lee, S., and Vasudevan, S. (2013). Post-transcriptional stimulation of gene expression by microRNAs. *Adv. Exp. Med. Biol.* 768, 97–126. doi:10.1007/978-1-4614-5107-5_7

Leng, L., Dong, X., Gao, X., Ran, N., Geng, M., Zuo, B., et al. (2021). Exosome-mediated improvement in membrane integrity and muscle function in dystrophic mice. *Mol. Ther. J. Am. Soc. Gene Ther.* 29 (4), 1459–1470. doi:10.1016/j.ymthe.2020.12.018

Levi, O., Genin, O., Angelini, C., Halevy, O., and Pines, M. (2015). Inhibition of muscle fibrosis results in increases in both utrophin levels and the number of revertant myofibers in Duchenne muscular dystrophy. *Oncotarget* 6 (27), 23249–23260. doi:10.18632/oncotarget.4021

Li, J., Salvador, A. M., Li, G., Valkov, N., Ziegler, O., Yeri, A., et al. (2021). Mir-30d regulates cardiac remodeling by intracellular and paracrine signaling. *Circulation Res.* 128 (1), e1–e23. doi:10.1161/CIRCRESAHA.120.317244

Lin, B., Li, Y., Han, L., Kaplan, A. D., Ao, Y., Kalra, S., et al. (2015). Modeling and study of the mechanism of dilated cardiomyopathy using induced pluripotent stem cells derived from individuals with Duchenne muscular dystrophy. *Dis. Models Mech.* 8 (5), 457–466. doi:10.1242/dmm.019505

Lipkin, D. P., Jones, D. A., Round, J. M., and Poole-Wilson, P. A. (1988). Abnormalities of skeletal muscle in patients with chronic heart failure. *Int. J. Cardiol.* 18 (2), 187–195. doi:10.1016/0167-5273(88)90164-7

Liu, Z., Lu, C.-L., Cui, L.-P., Hu, Y.-L., Yu, Q., Jiang, Y., et al. (2012). MicroRNA-146a modulates TGF-β1-induced phenotypic differentiation in human dermal fibroblasts by targeting SMAD4. *Archives Dermatological Res.* 304 (3), 195–202. doi:10.1007/s00403-011-1178-0

Logozzi, M., Mizzoni, D., Di Raimo, R., Hiuliani, A., Maggi, M., Sciarra, A., et al. (2021). Plasmatic exosome number and size distinguish prostate cancer patients from healthy individuals: A prospective clinical study. *Front. Oncol.* 11, 727317. doi:10.3389/fonc.2021.727317

Ma, H., Ye, P., Zhang, A.-k., Yu, W.-d., Lin, S., and Zheng, Y.-g. (2022). Upregulation of miR-335-5p contributes to right ventricular remodeling via calumenin in pulmonary arterial hypertension. *BioMed Res. Int.* 2022, 9294148. doi:10.1155/2022/9294148

Malik, Z. A., Kott, K. S., Poe, A. J., Kuo, T., Chen, L., Ferrara, K. W., et al. (2013). Cardiac myocyte exosomes: Stability, HSP60, and proteomics. *Am. J. Physiology Heart Circulatory Physiology* 304 (7), H954–H965. doi:10.1152/ajpheart.00835.2012

Marbán, E. (2018). A mechanistic roadmap for the clinical application of cardiac cell therapies. *Nat. Biomed. Eng.* 2, 353–361. doi:10.1038/s41551-018-0216-z

Marini, V., Marino, F., Aliberti, F., Giarratana, N., Pozzo, E., Duelen, R., et al. (2022). Long-term culture of patient-derived cardiac organoids recapitulated Duchenne muscular dystrophy cardiomyopathy and disease progression. *Front. Cell Dev. Biol.* 10, 878311. doi:10.3389/fcell.2022.878311

Mathivanan, S., Ji, H., and Simpson, R. J. (2010). Exosomes: Extracellular organelles important in intercellular communication. *J. Proteomics* 73 (10), 1907–1920. doi:10.1016/j.jprot.2010.06.006

Matsuzaka, Y., Hirai, Y., Hashido, K., and Okada, T. (2022). Therapeutic application of extracellular vesicles-capsulated adeno-associated virus vector via nSMase2/smpd3, satellite, and immune cells in Duchenne muscular dystrophy. *Int. J. Mol. Sci.* 23 (3), 1551. doi:10.3390/ijms23031551

Matsuzaka, Y., Tanihata, J., Komaki, H., Ishiyama, A., Oya, Y., Rüegg, U., et al. (2016). Characterization and functional analysis of extracellular vesicles and muscle-abundant miRNAs (miR-1, miR-133a, and miR-206) in C2C12 myocytes and mdx mice. *PLOS One* 11 (12), e0167811. doi:10.1371/journal.pone.0167811

Matsuzaka, Y., Tanihata, J., Ooshima, Y., Yamada, D., Sekiguchi, M., Miyatake, S., et al. (2020). The nSMase2/Smpd3 gene modulates the severity of muscular dystrophy and the emotional stress response in mdx mice. *BMC Med.* 18 (1), 343. doi:10.1186/s12916-020-01805-5

McDonald, C. (2018). A phase 2, randomized, double-blind, placebo-controlled trial evaluating the safety and efficacy of intravenous delivery of allogeneic cardiosphere-derived cells in subjects with Duchenne muscular dystrophy. Available at: https://clinicaltrials.gov/ct2/show/NCT03406780?term=cardiosphere&cond=Muscular+Dystrophies&draw=2&rank=3.

McDonald, C. (2022). A phase 3, randomized, double-blind, placebo-controlled trial evaluating the efficacy and safety of human allogeneic cardiosphere-derived cells for the treatment of Duchenne muscular dystrophy. Available at: https://clinicaltrials.gov/ct2/show/NCT05126758?term=exosome&cond=Muscular+Dystrophies&draw=2&rank=1.

McDonald, C. M., Marbán, E., Hendrix, S., Hogan, N., Smith, R. R., Eagle, M., et al. (2022). Repeated intravenous cardiosphere-derived cell therapy in late-stage Duchenne muscular dystrophy (HOPE-2): A multicentre, randomised, double-blind, placebo-controlled, phase 2 trial. *Lancet* 399 (10329), 1049–1058. doi:10.1016/S0140-6736(22)00012-5

Meldolesi, J. (2021). Extracellular vesicles (exosomes and ectosomes) play key roles in the pathology of brain diseases. *Mol. Biomed.* 2, 18. doi:10.1186/s43556-021-00040-5

Menasché, P. (2022). Human embryonic stem cells still have a place in the cell therapy landscape. *Cardiovasc. Res.* 118, e96–e97. doi:10.1093/cvr/cvac117

Menasché, P., Vanneaux, V., Hagège, A., Bel, A., Cholley, B., Parouchev, A., et al. (2018). Transplantation of human embryonic stem cell-derived cardiovascular progenitors for severe ischemic left ventricular dysfunction. *J. Am. Coll. Cardiol.* 71 (4), 429–438. doi:10.1016/j.jacc.2017.11.047

Meng, Q., Zhang, J., Zhong, J., Zeng, D., and Lan, D. (2022). Novel miRNA biomarkers for patients with Duchenne muscular dystrophy. *Front. Neurology* 13, 921785. doi:10.3389/fneur.2022.921785

Messina, E., De Angelis, L., Frati, G., Morrone, S., Chimenti, S., Fiordaliso, F., et al. (2004). Isolation and expansion of adult cardiac stem cells from human and murine heart. *Circulation Res.* 95 (9), 911–921. doi:10.1161/01.RES.0000147315.71699.51

Meyers, T. A., and Townsend, D. (2019). Cardiac pathophysiology and the future of cardiac therapies in Duchenne muscular dystrophy. *Int. J. Mol. Sci.* 20 (17), 4098. doi:10.3390/ijms20174098

Monaco, A. P., Neve, R. L., Colletti-Feener, C., Bertelson, C. J., Kurnit, D. M., and Kunkel, L. M. (1986). Isolation of candidate cDNAs for portions of the Duchenne muscular dystrophy gene. *Nature* 323 (6089), 646–650. doi:10.1038/323646a0

Murach, K. A., and McCarthy, J. J. (2017). MicroRNAs, heart failure, and aging: Potential interactions with skeletal muscle. *Heart Fail. Rev.* 22 (2), 209–218. doi:10.1007/s10741-016-9572-5

Nag, A. C. (1980). Study of non-muscle cells of the adult mammalian heart: A fine structural analysis and distribution. *Cytobios* 28 (109), 41–61.

Nguyen, B. Y., Azam, T., and Wang, X. (2021). Cellular signaling cross-talk between different cardiac cell populations: An insight into the role of exosomes in the heart diseases and therapy. *Am. J. Physiology Heart Circulatory Physiology* 320 (4), H1213–H1234. doi:10.1152/ajpheart.00718.2020

Okubo, M., Noguchi, S., Hayashi, S., Nakamura, H., Komaki, H., Matsuo, M., et al. (2020). Exon skipping induced by nonsense/frameshift mutations in DMD gene results in Becker muscular dystrophy. *Hum. Genet.* 139 (2), 247–255. doi:10.1007/s00439-019-02107-4

Perbellini, F., Watson, S. A., Bardi, I., and Terracciano, C. M. (2018). Heterocellularity and cellular cross-talk in the cardiovascular system. *Front. Cardiovasc. Med.* 5, 143. doi:10.3389/fcvm.2018.00143

Petrillo, S., Pelosi, L., Piemonte, F., Travaglini, L., Forcina, L., Catteruccia, M., et al. (2017). Oxidative stress in Duchenne muscular dystrophy: Focus on the NRF2 redox pathway. *Hum. Mol. Genet.* 26 (14), 2781–2790. doi:10.1093/hmg/ddx173

Pironti, G., Strachan, R. T., Abraham, D., Yu, S. M.-W., Chen, M., Chen, W., et al. (2015). Circulating exosomes induced by cardiac pressure overload contain functional

angiotensin II type 1 receptors. *Circulation* 131 (24), 2120–2130. doi:10.1161/CIRCULATIONAHA.115.015687

Ribeiro, A. F., Jr, Souza, L. S., Almeida, C. F., Ishiba, R., Fernandes, S. A., Guerrueri, D. A., et al. (2019). Muscle satellite cells and impaired late stage regeneration in different murine models for muscular dystrophies. *Sci. Rep.* 9 (1), 11842. doi:10.1038/s41598-019-48156-7

Rogers, R. G., Fournier, M., Sanchez, L., Ibrahim, A. G., Aminzadeh, M. A., Lewis, M. I., et al. (2019). Disease-modifying bioactivity of intravenous cardiosphere-derived cells and exosomes in mdx mice. *JCI Insight* 4 (7), e125754. doi:10.1172/jci.insight.125754

Rome, S., Forterre, A., Mizgier, M. L., and Bouzakri, K. (2019). Skeletal muscle-released extracellular vesicles: State of the art. *Front. Physiology* 10, 929. doi:10.3389/fphys.2019.00929

Rome, S. (2022). Muscle and adipose tissue communicate with extracellular vesicles. *Int. J. Mol. Sci.* 23, 7052. doi:10.3390/ijms23137052

Rotini, A., Martínez-Sarrà, E., Pozzo, E., and Sampaolesi, M. (2018). Interactions between microRNAs and long non-coding RNAs in cardiac development and repair. *Pharmacol. Res.* 127, 58–66. doi:10.1016/j.phrs.2017.05.029

Saheera, S., Jani, V. P., Witwer, K. W., and Kutty, S. (2021). Extracellular vesicle interplay in cardiovascular pathophysiology. *Am. J. Physiology Heart Circulatory Physiology* 320 (5), H1749–H1761. doi:10.1152/ajpheart.00925.2020

Salam, E. A., Abdel-Meguid, I., and Korraa, S. (2007). Markers of oxidative stress and aging in Duchene muscular dystrophy patients and the possible ameliorating effect of He: Ne laser. *Acta Myol.* 26 (1), 14–21.

Samani, A., Hightower, R. M., Reid, A. L., English, K. G., Lopez, M. A., Doyle, J. S., et al. (2022). miR-486 is essential for muscle function and suppresses a dystrophic transcriptome. *Life Sci. Alliance* 5 (9), e202101215. doi:10.26508/lsa.202101215

Sampaolesi, M., Blot, S., D'Antona, G., Granger, N., Tonlorenzi, R., Innocenzi, A., et al. (2006). Mesoangioblast stem cells ameliorate muscle function in dystrophic dogs. *Nature* 444, 574–579. doi:10.1038/nature05282

Shirokova, N., and Niggli, E. (2013). Cardiac phenotype of Duchenne muscular dystrophy: Insights from cellular studies. *J. Mol. Cell. Cardiol.* 58, 217–224. doi:10.1016/j.yjmcc.2012.12.009

Silva, I. S., Pedrosa, R., Azevedo, I. G., Forbes, A.-M., Fregonezi, G. A., Dourado Junior, M. E., et al. (2019). Respiratory muscle training in children and adults with neuromuscular disease. *Cochrane Database Syst. Rev.* 9 (9), CD011711. doi:10.1002/14651858.CD011711.pub2

Skog, J., Würdinger, T., van Rijn, S., Meijer, D. H., Gainche, L., Sena-Esteves, M., et al. (2008). Glioblastoma microvesicles transport RNA and proteins that promote tumour growth and provide diagnostic biomarkers. *Nat. Cell Biol.* 10 (12), 1470–1476. doi:10.1038/ncb1800

Smith, R. R., Barile, L., Cho, H. C., Leppo, M. K., Hare, J. M., Messina, E., et al. (2007). Regenerative potential of cardiosphere-derived cells expanded from percutaneous endomyocardial biopsy specimens. *Circulation* 115 (7), 896–908. doi:10.1161/CIRCULATIONAHA.106.655209

Subra, C., Laulagnier, K., Perret, B., and Record, M. (2007). Exosome lipidomics unravels lipid sorting at the level of multivesicular bodies. *Biochimie* 89 (2), 205–212. doi:10.1016/j.biochi.2006.10.014

Sullivan, M. J., Green, H. J., and Cobb, F. R. (1990). Skeletal muscle biochemistry and histology in ambulatory patients with long-term heart failure. *Circulation* 81 (2), 518–527. doi:10.1161/01.cir.81.2.518

Tang, L., Xie, J., Yu, X., and Zheng, Y. (2020). MiR-26a-5p inhibits GSK3β expression and promotes cardiac hypertrophy *in vitro*. *PeerJ* 8, e10371. doi:10.7717/peerj.10371

Tao, L., Bei, Y., Zhou, Y., Xiao, J., and Li, X. (2015). Non-coding RNAs in cardiac regeneration. *Oncotarget* 6, 42613–42622. doi:10.18632/oncotarget.6073

Trajkovic, K., Hsu, C., Chiantia, S., Rajendran, L., Wenzel, D., Wieland, F., et al. (2008). Ceramide triggers budding of exosome vesicles into multivesicular endosomes. *Science* 319 (5867), 1244–1247. doi:10.1126/science.1153124

Tseliou, E., Fouad, J., Reich, H., Slipczuk, L., de Couto, G., Aminzadeh, M., et al. (2015). Fibroblasts rendered antifibrotic, antiapoptotic, and angiogenic by priming with cardiosphere-derived extracellular membrane vesicles. *J. Am. Coll. Cardiol.* 66 (6), 599–611. doi:10.1016/j.jacc.2015.05.068

Valadares, M., Gomes, J., Castello, G., Assoni, A., Pellati, M., Bueno, C., et al. (2014). Human adipose tissue derived pericytes increase life span in utrn tm1Ked dmd mdx/J mice. *Stem Cell Rev. Rep.* 10, 830–840. doi:10.1007/s12015-014-9537-9

Valadi, H., Ekström, K., Bossios, A., Sjöstrand, M., Lee, J. J., and Lötvall, J. O. (2007). Exosome-mediated transfer of mRNAs and microRNAs is a novel mechanism of genetic exchange between cells. *Nat. Cell Biol.* 9 (6), 654–659. doi:10.1038/ncb1596

Vasa-Nicotera, M., Chen, H., Tucci, P., Yang, A. L., Saintigny, G., Menghini, R., et al. (2011). miR-146a is modulated in human endothelial cell with aging. *Atherosclerosis* 217 (2), 326–330. doi:10.1016/j.atherosclerosis.2011.03.034

Vechetti, I. J., Jr, Valentino, T., Mobley, C. B., and McCarthy, J. J. (2020). The role of extracellular vesicles in skeletal muscle and systematic adaptation to exercise. *J. Physiology* 599 (3), 845–861. doi:10.1113/JP278929

Verhaart, I. E., and Aartsma-Rus, A. (2019). Therapeutic developments for Duchenne muscular dystrophy. *Nat. Rev. Neurol.* 15, 373–386. doi:10.1038/s41582-019-0203-3

Villa, F., Quarto, R., and Tasso, R. (2019). Extracellular vesicles as natural, safe and efficient drug delivery systems. *Pharmaceutics* 11 (11), 557. doi:10.3390/pharmaceutics11110557

Wagner, K. T., and Radisic, M. (2021). A new role for extracellular vesicles in cardiac tissue engineering and regenerative medicine. *Adv. NanoBiomed Res.* 1 (11), 2100047. doi:10.1002/anbr.202100047

Wakayama, Y., Schotland, D. L., Bonilla, E., and Orecchio, E. (1979). Quantitative ultrastructural study of muscle satellite cells in Duchenne dystrophy. *Neurology* 29 (3), 401–407. doi:10.1212/wnl.29.3.401

Waldenström, A., Gennebäck, N., Hellman, U., and Ronquist, G. (2012). Cardiomyocyte microvesicles contain DNA/RNA and convey biological messages to target cells. *PLOS One* 7 (4), e34653. doi:10.1371/journal.pone.0034653

Wang, L., Zhou, L., Jiang, P., Lu, L., Chen, X., Lan, H., et al. (2012). Loss of miR-29 in myoblasts contributes to dystrophic muscle pathogenesis. *Mol. Ther. J. Am. Soc. Gene Ther.* 20 (6), 1222–1233. doi:10.1038/mt.2012.35

Wang, W., Li, M., Chen, Z., Xu, L., Chang, M., Wang, K., et al. (2022). Biogenesis and function of extracellular vesicles in pathophysiological processes of skeletal muscle atrophy. *Biochem. Pharmacol.* 198, 114954. doi:10.1016/j.bcp.2022.114954

Wang, X., Ha, T., Liu, L., Zou, J., Zhang, X., Kalbfleisch, J., et al. (2013). Increased expression of microRNA-146a decreases myocardial ischaemia/reperfusion injury. *Cardiovasc. Res.* 97 (3), 432–442. doi:10.1093/cvr/cvs356

Wang, X., Huang, W., Liu, G., Cai, W., Millard, R. W., Wang, Y., et al. (2014). Cardiomyocytes mediate anti-angiogenesis in type 2 diabetic rats through the exosomal transfer of miR-320 into endothelial cells. *J. Mol. Cell. Cardiol.* 74, 139–150. doi:10.1016/j.yjmcc.2014.05.001

Yang, B., Lin, H., Xiao, J., Lu, Y., Luo, X., Li, B., et al. (2007). The muscle-specific microRNA miR-1 regulates cardiac arrhythmogenic potential by targeting GJA1 and KCNJ2. *Nat. Med.* 13 (4), 486–491. doi:10.1038/nm1569

Yang, Z., Zingarelli, B., and Szabó, C. (2000). Crucial role of endogenous interleukin-10 production in myocardial ischemia/reperfusion injury. *Circulation* 101 (9), 1019–1026. doi:10.1161/01.cir.101.9.1019

Yao, S., Chen, Z., Yu, Y., Zhang, N., Jiang, H., Zhang, G., et al. (2021). Current pharmacological strategies for Duchenne muscular dystrophy. *Front. Cell Dev. Biol.* 9, 689533. doi:10.3389/fcell.2021.689533

Yates, A. G., Pink, R. C., Erdbrügger, U., Siljander, P. R.-M., Dellar, E. R., Pantazi, P., et al. (2022). In sickness and in health: The functional role of extracellular vesicles in physiology and pathology *in vivo*: Part II: Pathology: Part II: Pathology. *J. Extracell. Vesicles* 11 (1), e12190. doi:10.1002/jev2.12190

Yedigaryan, L., Gatti, M., Marini, V., Maraldi, T., and Sampaolesi, M. (2022a). Shared and divergent epigenetic mechanisms in cachexia and sarcopenia. *Cells* 11 (15), 2293. doi:10.3390/cells11152293

Yedigaryan, L., Martínez-Sarrà, E., Giacomazzi, G., Giarratana, N., van der Veer, B. K., Rotini, A., et al. (2022b). Extracellular vesicle-derived miRNAs improve stem cell-based therapeutic approaches in muscle wasting conditions. *Front. Immunol.* 13, 977617. doi:10.3389/fimmu.2022.977617

Yedigaryan, L., and Sampaolesi, M. (2021). Therapeutic implications of miRNAs for muscle-wasting conditions. *Cells* 10 (11), 3035. doi:10.3390/cells10113035

Young, C. S., Hicks, M. R., Ermolova, N. V., Nakano, H., Jan, M., Younesi, S., et al. (2016). A single CRISPR-cas9 deletion strategy that targets the majority of DMD patients restores dystrophin function in hiPSC-derived muscle cells. *Cell Stem Cell* 18 (4), 533–540. doi:10.1016/j.stem.2016.01.021

Yu, D.-W., Ge, P.-P., Liu, A.-L., Yu, X.-Y., and Liu, T.-T. (2019). HSP20-mediated cardiomyocyte exosomes improve cardiac function in mice with myocardial infarction by activating Akt signaling pathway. *Eur. Rev. Med. Pharmacol. Sci.* 23 (11), 4873–4881. doi:10.26355/eurrev_201906_18075

Yu, X., Deng, L., Wang, D., Li, N., Chen, X., Cheng, X., et al. (2012). Mechanism of TNF-α autocrine effects in hypoxic cardiomyocytes: Initiated by hypoxia inducible factor 1α, presented by exosomes. *J. Mol. Cell. Cardiol.* 53 (6), 848–857. doi:10.1016/j.yjmcc.2012.10.002

Zanotti, S., Gibertini, S., Blasevich, F., Bragato, C., Ruggieri, A., Saredi, S., et al. (2018). Exosomes and exosomal miRNAs from muscle-derived fibroblasts promote skeletal muscle fibrosis. *Matrix Biol. J. Int. Soc. Matrix Biol.* 74, 77–100. doi:10.1016/j.matbio.2018.07.003

Zanotti, S., Gibertini, S., Curcio, M., Savadori, P., Pasanisi, B., Morandi, L., et al. (2015). Opposing roles of miR-21 and miR-29 in the progression of fibrosis in Duchenne muscular dystrophy. *Biochimica Biophysica Acta* 1852 (7), 1451–1464. doi:10.1016/j.bbadis.2015.04.013

Zardi, E. M., Abbate, A., Zardi, D. M., Dobrina, A., Margiotta, D., Van Tassell, B. W., et al. (2010). Cirrhotic cardiomyopathy. *J. Am. Coll. Cardiol.* 56 (7), 539–549. doi:10.1016/j.jacc.2009.12.075

Zhang, C., Liu, J., Wang, X., Wu, R., Lin, M., Laddha, S. V., et al. (2014). MicroRNA-339-5p inhibits colorectal tumorigenesis through regulation of the MDM2/p53 signaling. *Oncotarget* 5 (19), 9106–9117. doi:10.18632/oncotarget.2379

Zhang, X., Wang, X., Zhu, H., Kranias, E. G., Tang, Y., Peng, T., et al. (2012). Hsp20 functions as a novel cardiokine in promoting angiogenesis via activation of VEGFR2. *PLOS One* 7 (3), e32765. doi:10.1371/journal.pone.0032765

Zhu, P., Li, H., Zhang, A., Li, Z., Zhang, Y., Ren, M., et al. (2022). MicroRNAs sequencing of plasma exosomes derived from patients with atrial fibrillation: miR-124-3p promotes cardiac fibroblast activation and proliferation by regulating AXIN1. *J. Physiology Biochem.* 78 (1), 85–98. doi:10.1007/s13105-021-00842-9

frontiers | Frontiers in Physiology

TYPE Original Research
PUBLISHED 10 April 2023
DOI 10.3389/fphys.2023.1094359

OPEN ACCESS

EDITED BY
Atsushi Asakura,
University of Minnesota Twin Cities,
United States

REVIEWED BY
So-ichiro Fukada,
Osaka University, Japan
Radbod Darabi,
University of Texas Health Science Center
at Houston, United States

*CORRESPONDENCE
Hidetoshi Sakurai,
hsakurai@cira.kyoto-u.ac.jp

SPECIALTY SECTION
This article was submitted to
Striated Muscle Physiology,
a section of the journal
Frontiers in Physiology

RECEIVED 10 November 2022
ACCEPTED 14 March 2023
PUBLISHED 10 April 2023

CITATION
Sato M, Goto M, Yamanouchi K and
Sakurai H (2023), A new immunodeficient
Duchenne muscular dystrophy rat model
to evaluate engraftment after human
cell transplantation.
Front. Physiol. 14:1094359.
doi: 10.3389/fphys.2023.1094359

A new immunodeficient Duchenne muscular dystrophy rat model to evaluate engraftment after human cell transplantation

Masae Sato[1], Megumi Goto[1], Keitaro Yamanouchi[2] and Hidetoshi Sakurai[1]*

[1]Department of Clinical Application, Center for iPS Cell Research and Application (CiRA), Kyoto University, Kyoto, Japan, [2]Department of Veterinary Physiology, Graduate School of Agricultural and Life Sciences, The University of Tokyo, Tokyo, Japan

Duchenne muscular dystrophy (DMD) is an X-linked fatal muscular disease, affecting one in 3,500 live male births worldwide. Currently, there is no cure for this disease, except for steroid-based treatment to attenuate disease progression. Cell transplantation therapy is a promising therapeutic approach, however, there is a lack of appropriate animal models to conduct large-scale preclinical studies using human cells, including biochemical and functional tests. Here, we established an immunodeficient DMD rat model and performed exhaustive pathological analysis and transplantation efficiency evaluation to assess its suitability to study DMD. Our DMD rat model exhibited histopathological characteristics similar to those observed in human patients with DMD. Human myoblasts demonstrated successful engraftment following transplantation into these rats. Therefore, this immunodeficient DMD rat model would be useful in preclinical studies to develop cellular transplantation therapies for DMD.

KEYWORDS

DMD, rat model, immunodeficient, cell transplantation, pathology

1 Introduction

Duchenne muscular dystrophy (DMD) is caused by multiple mutations in the *DMD* gene, which is located on the X chromosome (Hoffman et al., 1987). The *DMD* gene encodes dystrophin, which connects the muscle cell cytoskeleton to the extracellular matrix (Robert, 2001). DMD is an intractable and fatal muscle disease that causes chronic inflammation and muscle degradation. Patients with DMD are usually diagnosed at 3–5 years of age and lose the ability to walk at approximately 12 years of age. Subsequently, they require respiratory support and suffer from cardiomyopathy in their early teens (Fairclough et al., 2013). Currently, there is no curative treatment for DMD, however, dystrophin restoration is being investigated as a possible treatment option, and several therapeutic approaches have been investigated, including exon-skipping, gene therapy by oligonucleotides (Fairclough et al., 2013) (Beytía et al., 2012), and cell transplantation (Sun et al., 2020). Preclinical trials in dogs and mice have recently been reported using these approaches (Beytía et al., 2012) (Nowak and Davies, 2004). However, milder phenotypes were reported in C57BL/10-mdx mice than in humans (Nakamura and Takeda, 2011), while dogs showed greater individual variation.

Proof-of-concept studies using DMD model animals are necessary to develop novel therapies that restore dystrophin expression in DMD. Thus, we used a rat model with fewer genetic differences, and that was more symptomatic of DMD than C57BL/10-mdx mice (Larcher et al., 2014) (Nakamura et al., 2014) (Taglietti et al., 2022). Cell therapy is a promising therapeutic approach for DMD because adult muscle stem cells (MuSCs), or satellite cells (Marg et al., 2014) (Cerletti et al., 2008) (Sacco et al., 2008) (Tanaka et al., 2009) (Xu et al., 2015) (Montarras et al., 2005), retain robust regeneration potential for injured muscle cells. Recently, it was reported that skeletal MuSCs induced from induced pluripotent stem (iPS) cells can be grafted into mice, and we observed that muscle tone was restored after transplantation (Zhao et al., 2020). Preclinical studies of cell transplantation therapies involve transplanting human cells into animals, requiring immunosuppressive agents to prevent rejection of the transplanted human cells. Additionally, the prolonged use of immunosuppressive drugs is discouraged as it could modify the disease state (Samata et al., 2015). Nude rats with T cell dysfunction are capable of successful human cell engraftment and have been used as immunodeficient animal models (Hanes, 2006). Nude rats are also used in preclinical studies of induced pluripotent stem cell-derived dopaminergic progenitor cells for the treatment of Parkinson's disease (Doi et al., 2020) Therefore, future research regarding clinical applications and basic analysis of DMD should be conducted using an immunodeficient DMD rat model.

In this study, we generated an immunodeficient DMD rat model capable of human cell engraftment by crossing a DMD model rat which shows no revertant fiber in skeletal muscle (Nakamura et al., 2014) with a nude rat. We conducted histopathological evaluation of the novel rat model to confirm successful engraftment after immortalized human myoblast cell transplantation.

2 Materials and methods

2.1 Animals

All experiments involving the use of animals were performed in accordance with the Guide for the Care and Use of Laboratory Animals of the University of Kyoto, and the procedures were approved by the Institutional Animal Care and Use Committee of the University of Kyoto (approval number 19-119). Animals were maintained at 23°C with a 12/12 h light/dark cycle, with lights on at 08:00 a.m. and were fed *ad libitum*.

2.2 Generation of immunodeficient DMD rat model

We used the Wistar–Imamichi strain DMD rat model (DMD rat model: $X^{Dmd}Y$) carrying mutations in exons 3 and 16 of the *Dmd* gene (Nakamura et al., 2014). Immunodeficient F344/NJcl.Cg-Foxn1^{rnu} rats (nude rat: Foxn1$^{rnu/rnu}$) were purchased (CLEA Japan, Inc., Tokyo, Japan). Immunodeficient DMD rats were established by crossing a Foxn1$^{rnu/rnu}$ male rat with an $X^{Dmd}X$ female rat. X^{Dmd} was identified by genotyping the litter population (Nakamura et al., 2014). The following rat genotypes were used in this study: $X^{Dmd}Y$ Foxn1$^{rnu/rnu}$ (DMD nude rats), XX Foxn1$^{rnu/rnu}$ or XY Foxn1$^{rnu/rnu}$ rats (WT nude rats) and $X^{Dmd}Y$ Foxn1$^{rnu/+}$(immunocompetent DMD rat model).

2.3 Creatine kinase activity

Creatine kinase activity in the serum of DMD nude rats and their age-matched WT nude rats (1-, 5-, and 12-months-old) was measured using a Fuji Dri-Chem system by Oriental Yeast Co., Ltd. (Tokyo, Japan).

2.4 Urinary titin and creatine measurement

Urine samples were obtained from 1-, 5-, and 12-month-old WT nude and DMD nude rats. Urinary titin was measured using a Mouse Titin N-Fragment Assay Kit (27,602, Immuno-Biological Laboratories Co., Ltd.). Urinary creatinine (Cr) concentrations were measured using a Lab Assay Creatinine kit (636–51011, Fujifilm Wako Pure Chemical Corporation Ltd.) (Maruyama et al., 2016).

2.5 Grip test

Forelimb strength was determined by a muscle relaxation measurement device (no. BS-TM-RM, Brain Science idea, Osaka, Japan). The study was conducted on 5 to 6 and 9-month-old WT nude and DMD nude rats. Tails of rats gripping a wire mesh plate, which was equipped with a devise, were pulled horizontally and the maximum tension was recorded. In 3 serial times of pulling, the average forelimb muscle tension was used as the value for muscle strength. All trials were performed by one examiner.

2.6 Open-field test

The open-field test was used to assess vertical (rearing) activities. The rats were placed in a cylinder and their behavior was recorded using a camera for 3 min to count the number of rearing behaviors. The study was conducted on 12-month-old WT nude and DMD nude rats. All experiments were conducted at the same location (2 m above the floor) and under constant illumination.

2.7 Hu5/KD3 cell culture

Human immortalized myoblast cell line Hu5/KD3 was provided by the National Center for Geriatrics and Gerontology (Obu, Aichi, Japan) (Shiomi et al., 2011). The cells were maintained on collagen type I-coated dishes (4010-010, Iwaki Glass Co., Ltd.), in high glucose Dulbecco's modified Eagle's medium (DMEM; 08,488-55, Nacalai Tesque) supplemented with 20% fetal bovine serum (FBS; 556-33865, Gibco, ThermoFisher Scientific), 2% Ultroser G (15,950-017, Biosepta, Pall Life Sciences), 1% L-glutamine (15,950-017, Invitrogen), and 0.5% penicillin streptomycin mixed solution (09,367-34, Nacalai Tesque).

2.8 Preparation of polymer solution

Gelatin (Kindly provided from Dr. Yasuhiko Tabata, Kyoto University) and hyaluronic acid (Kindly provided from Dr. Yasuhiko Tabata, Kyoto University) were dissolved in 20% FBS DMEM without Ultroser G, at 1% w/v at 37°C in a water bath. A mixed polymer solution was prepared by mixing the hyaluronic acid solution with gelatin solution in a 1:4 volume ratio (Miura et al., 2022).

2.9 Transplantation studies

4-week-old WT and DMD nude rats were anesthetized with 2% isoflurane (704239096, VIATRIS) and cryoinjury was performed to model muscle injury. The tibialis anterior (TA) was exposed, and cryoinjury was performed on both TA muscles three times for 12 s each by direct contact of the TA muscles with a cryoprobe dipped in liquid nitrogen (Nalbandian et al., 2021). Following cryoinjury, 6×10^6 Hu5/KD3 cells were mixed with the polymer solution, as described above, and injected into the left and right TA muscles. The rats were sacrificed either 3 weeks or 3 months after transplantation, and the TA muscle samples were collected and analyzed by immunohistochemical staining.

2.10 Histological analyses of skeletal muscle tissues

Histological analyses were performed as previously described (Takenaka-Ninagawa et al., 2021). The skeletal muscle tissues were mounted in tragacanth gum (206–02242, Fujifilm Wako Pure Chemical Corporation Ltd.) and frozen using liquid nitrogen-cooled isopentane. Paraffin-embedded skeletal muscle tissues were used for hematoxylin & eosin (H&E) staining. Additionally, the heart and the diaphragm were also stained with H&E and Sirius red (SR), which was performed by Applied Medical Research, Inc. (Osaka, Japan). Cryosections (12 μm) of TA muscles were obtained using a cryostat (Leica Biosystems). For samples used for immunostaining, the sections were fixed with 4% paraformaldehyde (PFA; 09154-85, Nacalai Tesque) in phosphate-buffered saline (PBS; 11,482-15, Nacalai Tesque) at 24°C for 20 min. For quantitative analysis of the myofiber minimal Feret's diameter, cryosections were fixed with methanol at −20°C for 7 min. After fixation, sections were blocked with Blocking one (03,953-95, Nacalai Tesque) for 1 h, followed by incubation with primary antibodies (Supplementary Table S1) diluted in Can Get Signal B (NKB-601X4, Toyobo) overnight at 4°C. Sections were then washed twice with 0.2% Triton X in PBS and incubated with secondary antibodies (Supplementary Table S1) diluted in Can Get Signal B for 1 h. Subsequently, the sections were washed twice with 0.2% Triton X in PBS and the immunostained sections were mounted using Vectashield mounting medium with DAPI (H-1200, Vector Laboratories). Immunofluorescence images were acquired using a Zeiss LSM 700 laser scanning confocal microscope (Carl Zeiss). For quantitative analysis of myofiber minimal Feret's diameters, 10 fields were randomly selected from sections stained with anti-Pan laminin antibody. The minimal Feret's diameter and SR-stained positive area per section were calculated using Keyence image analyzer (Keyence Corporation, Osaka, Japan)

2.11 Histological analysis of transverse sections

For transverse sections, WT and DMD nude rats were reflux-fixed using 10% formalin (37,152-51, Nacalai Tesque) and then decalcified and paraffin-embedded by Applied Medical Research, Inc. Both H&E and SR staining were performed by Applied Medical Research, Inc. Images were captured using a BZ-X700 microscope (Keyence, Osaka, Japan).

2.12 Statistical analysis

All statistical analyses were performed using GraphPad Prism version 9.2.0 for Mac OS (GraphPad Software). Data are expressed as the mean ± SEM. Differences between the groups were analyzed using the two-tailed paired Student's t-test. A p-value <0.05 was considered statistically significant. GraphPad Prism was used to calculate survival curves (Kaplan-Meier) with Mantel-Cox test and to construct graphs for each group. All live WT nude rats were discontinued for follow-up at 76 weeks.

3 Results

3.1 Physical, behavioral, and biochemical characteristics of immunodeficient DMD rats

F344/NJcl.Cg-Foxn1^{rnu} rats are immunodeficient nude rats with defective T cell function (Hanes, 2006). We crossed Wistar–Imamichi strain DMD model rats (Nakamura et al., 2014) with F344/NJcl.Cg-Foxn1^{rnu} rats (WT nude rat) to establish an immunodeficient DMD rat model (DMD nude rat). The body size of 12-month-old DMD nude rats was smaller than that of the WT nude rats (Figure 1A). DMD nude rats often remained close to the floor due to decreased muscle strength in their extremities (Figure 1A) and weighed less than WT nude rats starting at 4-week-old (Figure 1B). The survival curves for WT and DMD nude rats revealed that half of the DMD nude rats died at 60-week-old, with no surviving animals beyond 68-week-old. The life span of DMD nude rats was significantly shorter than that of WT nude rats, as seen from the survival curves (Figure 1C). Human patients with DMD display muscle damage characterized by increased CK activity in the serum and increased titin levels in urea (Goto et al., 1967) (Maruyama et al., 2016). The CK activity level in 1-month-old DMD nude rats was significantly increased compared to that in WT nude rats, which decreased after 12-month-old (Figure 1D). A similar trend was observed for urinary titin (Figure 1E). Furthermore, to measure the muscle function impairments of DMD nude rats quantitatively, grip tests were performed on 5 to 6 and 9-month-old WT nude rats and DMD nude rats. Analysis of grip force showed significant reduction of muscle function in DMD nude rats compared to WT nude rats at both 5 to 6-month-old and 9-month-old (Figure 1F, left). Considering the low body weight in DMD nude rats, a statistically

10.3389/fphys.2023.1094359

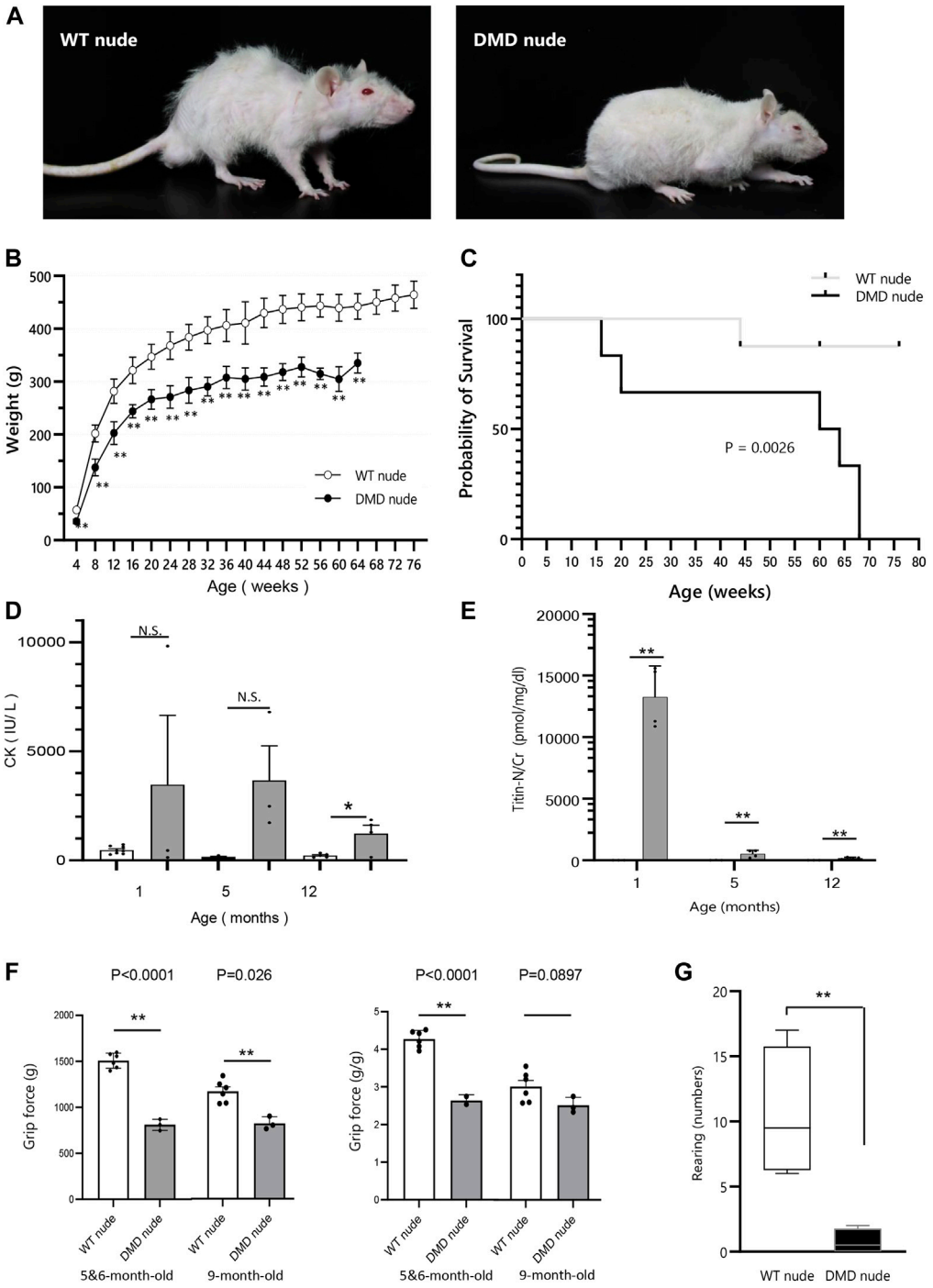

FIGURE 1
Generation of immunodeficient Duchenne muscular dystrophy (DMD) rat model. **(A)** Representative images of 12-month-old wild type (WT) and DMD nude rats. **(B)** Body weight comparison of WT and DMD nude rats. (WT nude rat: n = 8, DMD nude rat: n = 7). **(C)** Kaplan-Meier curves comparing survival rates of WT and DMD nude rats. Mantel-Cox test, p = 0.0026. (WT nude rat: n = 8, DMD nude rat: n = 7). **(D)** The serum creatine kinase (CK) activity in WT and DMD nude rats (WT nude rats: n = 8, 3, and 5; DMD nude rat: n = 3, 3, and 3). **(E)** The urinary titin concentrations in WT and DMD nude rats (WT nude rats: n = 3 for all groups; DMD nude rat: n = 4 for all groups). **(F)** Quantification of maximum muscle strength by grip test. The study was conducted on 5 to 6 and 9-month-old WT nude and DMD nude rats. (WT nude rat: n = 2, 2, DMD nude rat: n = 1, 1). **(G)** Motor behavior was examined using an open-field test. WT and DMD nude rats at 12-month-old were individually placed in the cylinder for 3 min (WT nude rat: n = 4, DMD nude rat: n = 4). *p < 0.05, **p < 0.01.

TABLE 1 Total body weight and weights of various skeletal muscles in WT and DMD nude rats at 1, 5, and over 12-month-old.

Age	1month-old		5 month-old		Over 12 months old	
	WT	DMD	WT	DMD	WT	DMD
Muscle weight (mg)						
Tibialis anterior muscle	324.4 ± 26.6	217.8* ±13.0	629.7 ± 20.3	763.4 ± 60.6	734.7 ± 15.3	700.9 ± 51.7
Gastrocnemius	863.1 ± 57.8	804.2 ± 5.0	2034.1 ± 39.3	2058.0 ± 171.4	2338.4 ± 104.3	2114.9 ± 196.6
Quadriceps femoris	1284.3 ± 82.5	1254.6 ± 7.0	3166.3 ± 84.4	2702.6 ± 107.2	3734.8 ± 96.3	2643.8** ±171.9
Diaphragm	601.0 ± 47.8	698.4 ± 79.0	1281.9 ± 67.3	1375.4 ± 42.2	1587.3 ± 91.1	1396.3 ± 112.4
Heart	743.8 ± 70.4	773.4 ± 25.4	1328.6 ± 41.4	1327.6 ± 70.0	1630.5 ± 73.4	1807.3 ± 82.1
Number of samples	n = 4	n = 3	n = 3	n = 5	n = 8	n = 6

Data show the means and ±SEM., The number of samples is 4 for the Tibialis anterior muscle only over 12-month-old WT nude rat. *$p < 0.05$; **$p < 0.01$.

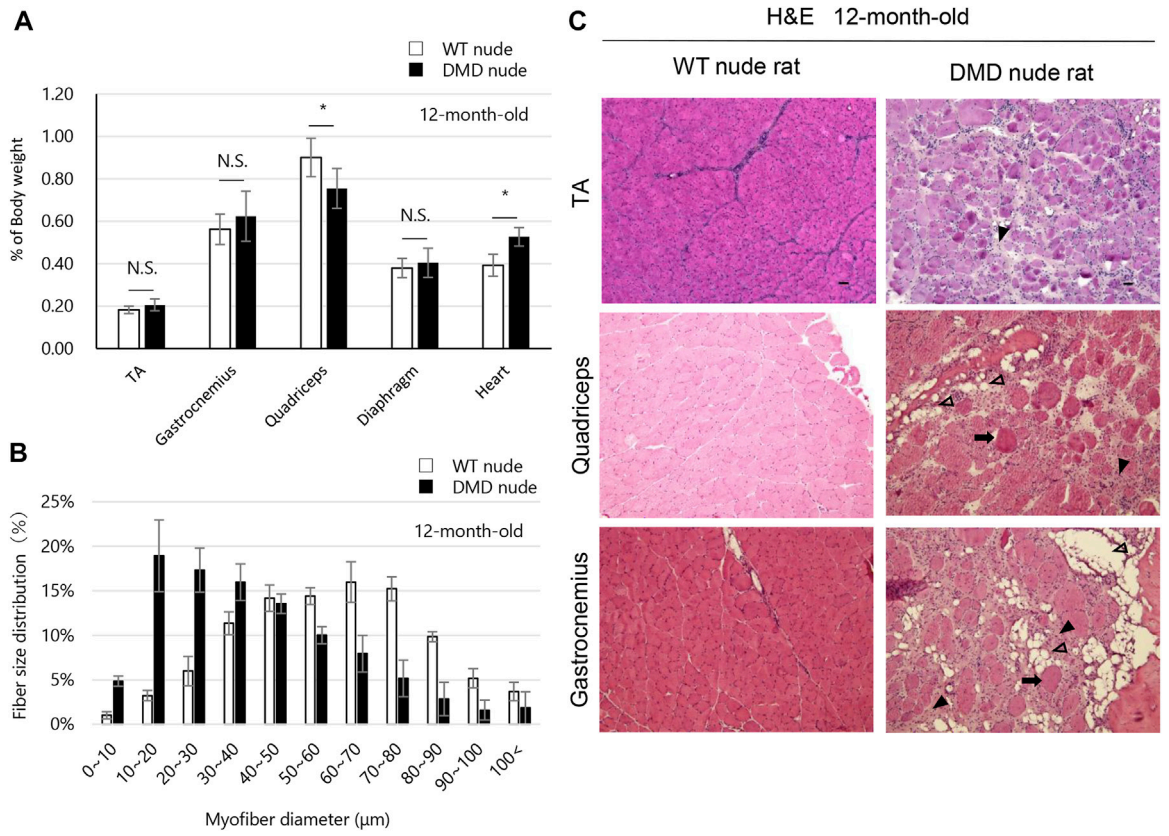

FIGURE 2
Phenotypic analysis of the skeletal muscles of DMD nude rats. **(A)** The percentage of body weight represented by each muscle tissue at the indicated ages in WT and DMD nude rats. N.S. non-significant, *$p < 0.05$. **(B)** Histological changes in the fiber diameter in 12-month-old WT and DMD nude rats. **(C)** Representative images of hematoxylin & eosin (H&E) staining of the tibialis anterior (TA), quadriceps, and gastrocnemius muscle sections in 12-month-old WT and DMD nude rats. The symbols, ➡, ▼, and ▽, indicate necrotic myofibers, fibrosis, and adipogenesis, respectively. Scale bar = 50 μm.

significant reduction of approximately 36% in grip force normalized by body weight was also observed in DMD nude rats (approximately 2.74 g/g) compared to WT nude rats (approximately 4.27 g/g) at 5 to 6-month-old (Figure 1F, right). Spontaneous locomotion measurement is an important analysis to confirm the phenotype in DMD animal models (Larcher et al., 2014). Thus, we measured a horizontal activity such as rearing and observed a significant reduction of 93% ± 0.1% in DMD nude rats compared to that in WT nude rats (Figure 1G). These results indicate that DMD nude rats display progressive muscle tissue damage followed by severe muscle weakness. In addition, significant weight loss was observed in DMD rats, with a shorter life span compared to WT nude rats.

10.3389/fphys.2023.1094359

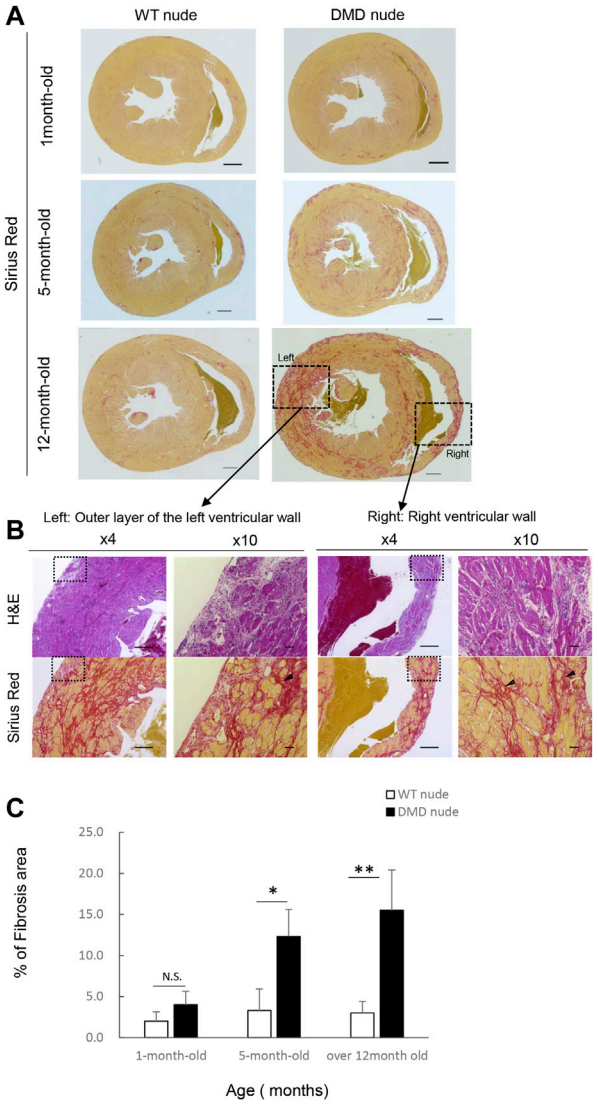

FIGURE 3
Severe and progressive muscle changes in the heart of DMD nude rats. **(A)** Representative images of Sirius red (SR)-stained hearts of WT and DMD nude rats, showing the degree of fibrosis at each respective age. WT nude rats are shown on the left, and DMD nude rats are shown on the right. Scale bar = 1 mm (one-month-old), scale bar = 500 μm (5- and 12- month-old) **(B)** Detailed analysis of severe and progressive changes in the heart of a DMD nude rat. The upper row shows hematoxylin & eosin (H&E) staining, and the lower row shows SR staining images. The right panel shows magnified views of the left panel. Magnified area denoted by the square in panel **(A,B)** ×4, scale bar = 500 μm; ×10, scale bar = 50 μm. **(C)** Bar graph summarizing SR-positive areas in WT and DMD nude rats at 1, 5, and over 12 months of age. N.S. non-significant, $*p < 0.05$, $**p < 0.01$.

3.2 Pathological analysis of the skeletal muscle tissues in DMD nude rats

The weights of each skeletal muscle tissue, the diaphragm, and the heart of WT nude and DMD nude rats were compared at 1, 5, and over 12-month-old (Table 1). We observed decreased skeletal muscle weights in DMD nude rats compared to that in WT nude rats, reflecting the small body size of DMD nude rats, except for the weight of the TA muscle at 5 months (Table 1). Although no statistically significant difference was observed, the increased TA muscle weight in DMD nude rats indicated a tendency towards pseudohypertrophy. Due to body weight differences between WT and DMD nude rats (Figure 1B), we normalized the weights of various skeletal muscles, such as the diaphragm and the heart, to their respective body weights (% of body weight for each tissue). Among skeletal muscles, the percentage of body weight for the quadriceps muscle was significantly lower in 12-month-old DMD nude rats than in WT nude rats (Figure 2A), indicating that the proximal muscle atrophied more than the distal muscle. However, no significant differences were observed between the two groups in the percentage of body weight for the muscles at 1 and 5-month-old (Supplementary Figure S1). Furthermore, quantification of histological changes in the fiber diameter on the quadriceps muscle revealed an overall decreased fiber size in 12-month-old DMD nude rats compared to that in WT nude rats (Figure 2B). Moreover, histopathological evaluation of the TA, quadriceps, and gastrocnemius muscles using H&E staining revealed necrotic fibers and inflammatory cell infiltration in 12-month-old DMD nude rats compared to that in age-matched WT nude rats (Figure 2C), and increased adipogenesis in the quadriceps and gastrocnemius muscles in DMD nude rats (Figure 2C). We also observed significantly increased percentage of body weight of the heart in 12-month-old DMD nude rats compared to that in WT nude rats (Figure 2A). Thus, DMD nude rats displayed cardiac hypertrophy and pathological heart dysfunction at 12-month-old.

3.3 Pathological analysis of the heart in DMD nude rats

We performed histopathological evaluation of the heart using H&E and SR staining in 12-month-old DMD and WT nude rats due to the observed cardiac hypertrophy in DMD nude rats (Figure 2A). Figures 3A, B show histological images of the hearts from DMD and WT nude rats with H&E and SR staining. We observed minor fibrosis in the heart of 1-month-old DMD nude rats compared to that in WT nude rats. However, the fibrotic area expanded progressively in the hearts of 5 and 12-month-old DMD nude rats (Figure 3A), indicating progressive fibrosis of the heart with age in DMD nude rats. In addition to severe fibrosis, mononuclear cells and necrotic myofibers were also observed in the outer layer of the left and right ventricular walls of the hearts in DMD nude rats (Figure 3B). We evaluated the progression of fibrosis by quantifying the percentage of fibrotic area in transverse sections of the hearts using SR staining and observed an age dependent increase in the fibrotic area in DMD nude rats compared to that in WT nude rats (Figure 3C).

3.4 Pathological analysis of the diaphragm in DMD nude rats

We examined fibrosis of the diaphragm using H&E and SR staining as decreased respiratory function is a characteristic of DMD. Figure 4A shows the histological images of the diaphragms from DMD and WT nude rats with SR staining. 1-month-old DMD nude rats displayed mild

10.3389/fphys.2023.1094359

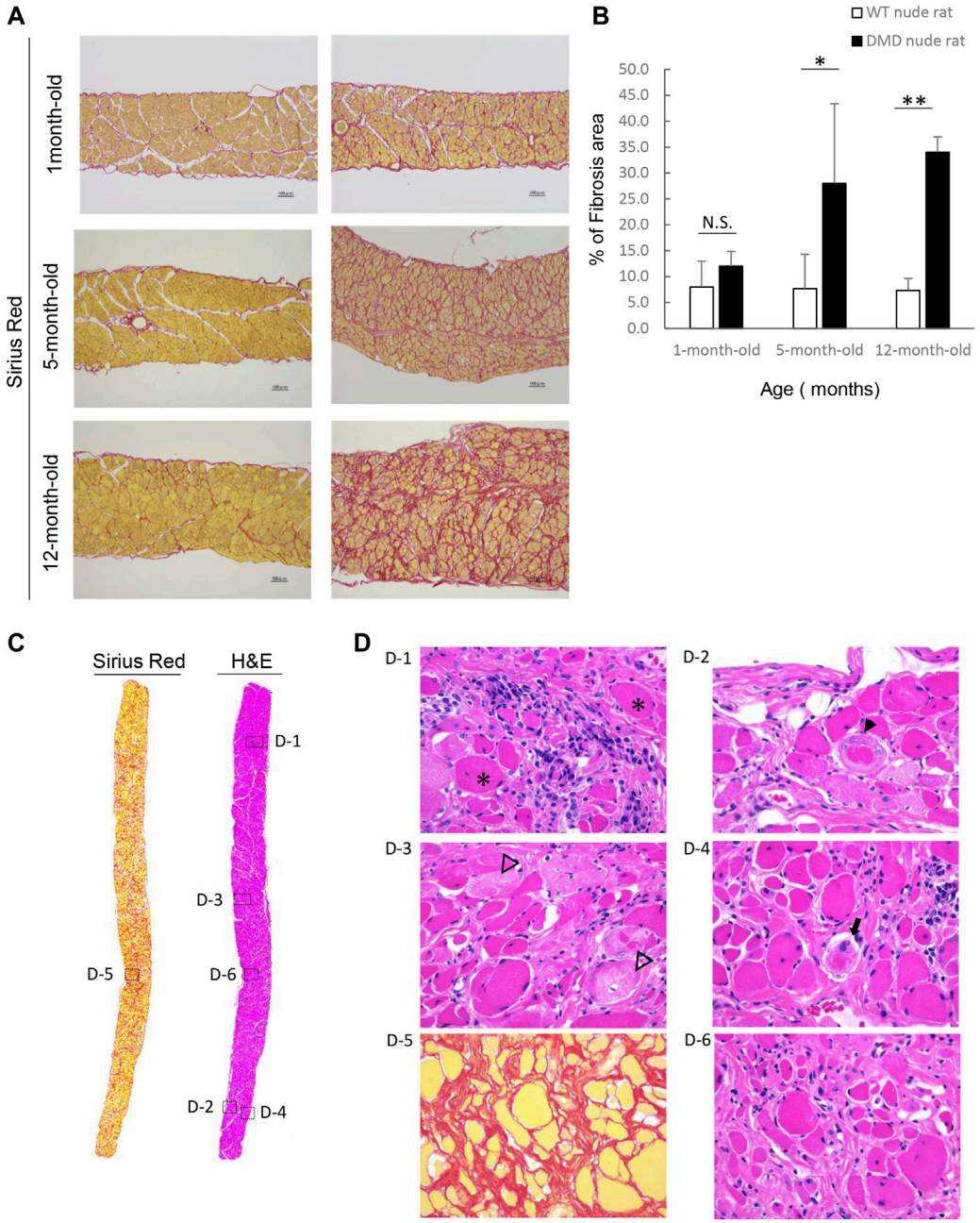

FIGURE 4
Detailed analysis of severe changes in the diaphragm in DMD nude rats. **(A)** Representative Sirius red (SR)-stained images of the detailed analysis of severe and progressive changes in the diaphragm in DMD nude rats. The left row shows the results from wild type (WT) nude rats, and the right row shows the results from DMD nude rats. Scale bar = 100 μm. **(B)** Bar graph summarizing SR-positive areas in the diaphragm from rats at 1, 5, and over 12-month-old. N.S. non-significant, $^{**}p < 0.01$. **(C)** Representative images of SR and hematoxylin & eosin (H&E) staining showing the degree of fibrosis in the diaphragm of a DMD nude rat. The right row shows H&E staining, and the left row shows SR staining. **(D)** Representative images of H&E staining of the diaphragm of 12-month-old DMD nude rats. Magnified area denoted by the square in panel **(C)**. The symbols, *, ▼, ▽, and ➡, indicate hypercontraction (opaque) fiber (D-1), ring-fiber (D-2), pale necrotic fiber (D-3), and moth-eaten fiber (D-4), respectively. Comparative images of H&E and SR staining of the same location are shown (D-5 & D-6).

fibrosis in the diaphragm compared to that in WT nude rats. We observed progressing fibrosis in the diaphragm in 5- and 12-month-old DMD nude rats. We evaluated the progression of fibrosis by quantifying the percentage of fibrotic area using SR staining. Similar to that in the heart, we observed an age dependent increase in the fibrotic area in DMD nude rats compared to that in WT nude rats (Figure 4B). Figure 4C shows H&E- and SR-stained cross-sections of the diaphragms of 12-month-old DMD nude rats. The H&E-stained image shows a marked difference in the size of muscle fiber, while the SR-stained images show fibrotic areas throughout the diaphragm

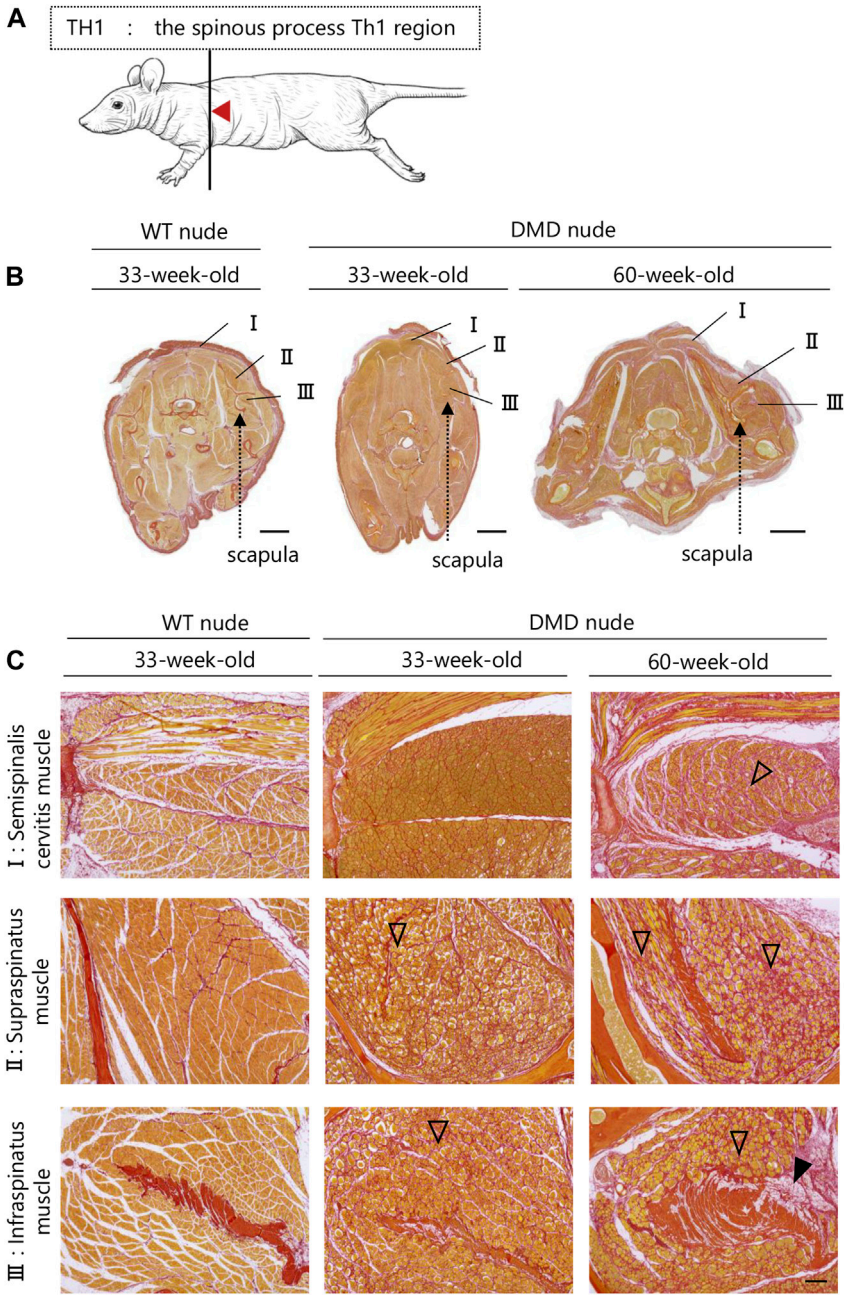

FIGURE 5
Lesion distribution within the skeletal muscle in transverse sections in DMD nude rats. **(A)** Schematic drawing showing the sectioning location of the shoulder and rump. The cuts were made in the spinous process of the Th1 region (Th1). **(B)** Representative images of Sirius red (SR) staining in Th1 shoulder sections of each rat type to evaluate the degree of fibrosis. Scale bar = 5 mm. **(C)** Magnified views of I, II, and III indicated by arrows are shown in the lower columns. Scale bar = 300 μm. The symbols, ▽ and ▼, indicate fibrosis and adipogenesis, respectively.

(Figure 4C). Magnified the H&E-stained images show Opaque fiber (Figure 4 D–1), ring-fiber (Figure 4 D–2), pale necrotic fiber (Figure 4 D–3), and moth-eaten (Figure 4 D–4). Progressive fibrosis in the interstitium (Figure 4 D–5), regenerating muscle with small muscle fiber caliber and central nuclei observed (Figure 4 D–6). These characteristic pathological findings in the diaphragms of DMD nude rats are typical human DMD patient-like diaphragmatic lesions.

3.5 Transverse histological analysis of whole muscle tissue of DMD model rats

A transverse sectional analysis was performed to comprehensively evaluate the body's musculature. The muscles in the shoulder region were analyzed by sectioning the spine at the Th1 position (Figure 5A). Figures 5B, C and Supplementary Figure S2 present the representative

10.3389/fphys.2023.1094359

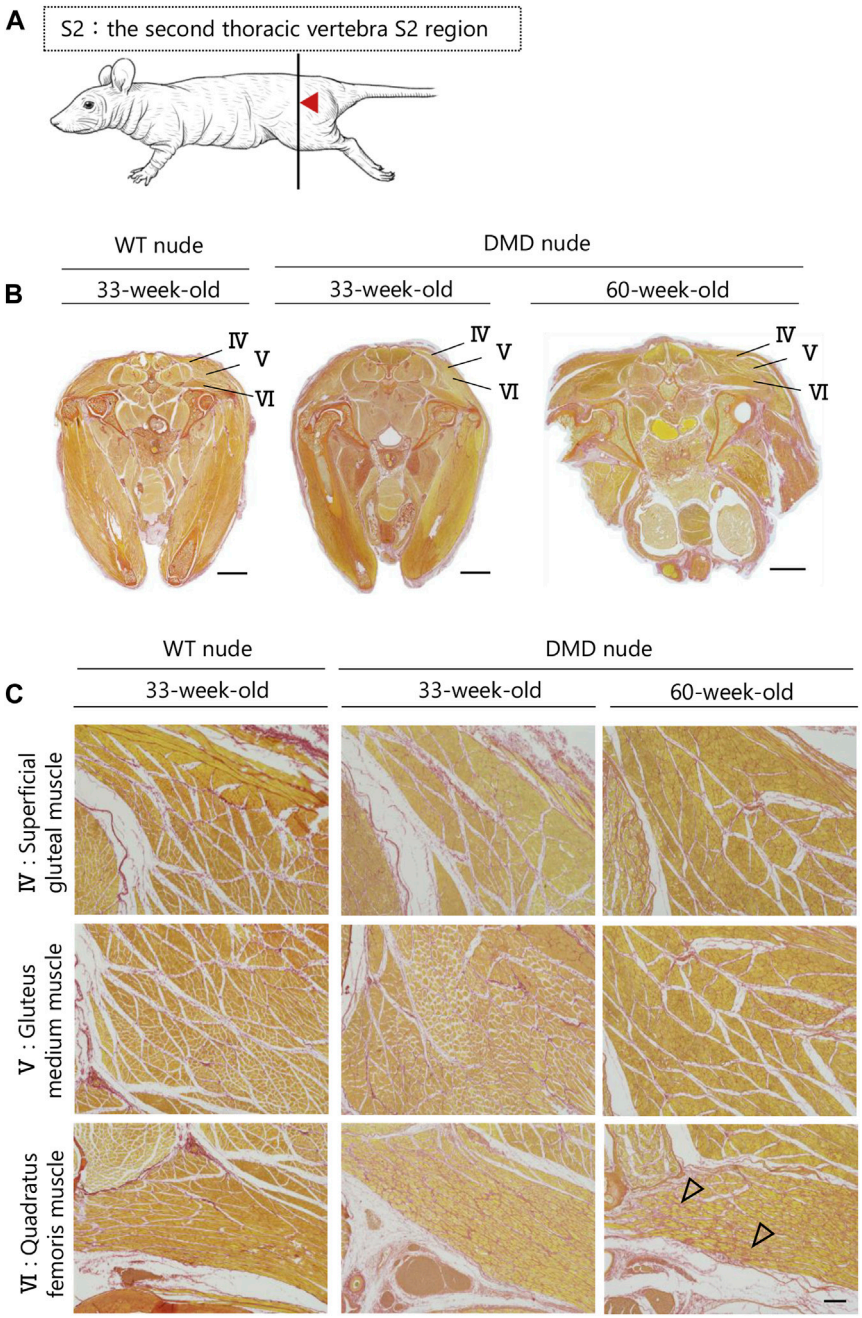

FIGURE 6
Lesion distribution within the skeletal muscle in transverse sections in DMD nude rats. **(A)** Schematic drawing showing the sectioning location of the rump. The cuts were made in the spinous process of the second thoracic vertebra S2 region (S2). **(B)** Representative images of Sirius red (SR) staining at the S2 lumbar section of each type of rat to evaluate the degree of fibrosis. Scale bar = 5 mm. **(C)** Magnified views of IV, V, and VI from **(B)** indicated by arrows are shown in the lower columns. Scale bar = 300 μm. The symbols, ▽ indicates fibrosis.

H&E and SR-stained images of the shoulder and buttock muscles from 33 to 60-week-old DMD and WT nude rats. The skeletal muscles around the scapula of the Th1 region showed increased fibrosis in 60-week-old DMD nude rats (Figure 5B), and progressive fibrosis was also observed in semispinalis cervitis (I), supraspinatus muscle (II), and infraspinatus muscle (III) with positive SR staining (Figure 5C). The muscles in the buttock region were analyzed by sectioning the lumbar vertebra at the S2 position (Figure 6A). We observed similar levels of fibrosis between DMD and WT nude rats in the gluteal muscles, including the superficial gluteal (IV) and gluteus medium (V) muscles. We did not observe pronounced fattening (Figures 6B, C; Supplementary Figure S2), in contradiction to that reported in the magnetic resonance imaging results of human patients with DMD (Polavarapu et al., 2016). However, the muscles associated with moving joints, such as the quadratus femoris muscle (VI), were revealed to be impaired (Figure 6C).

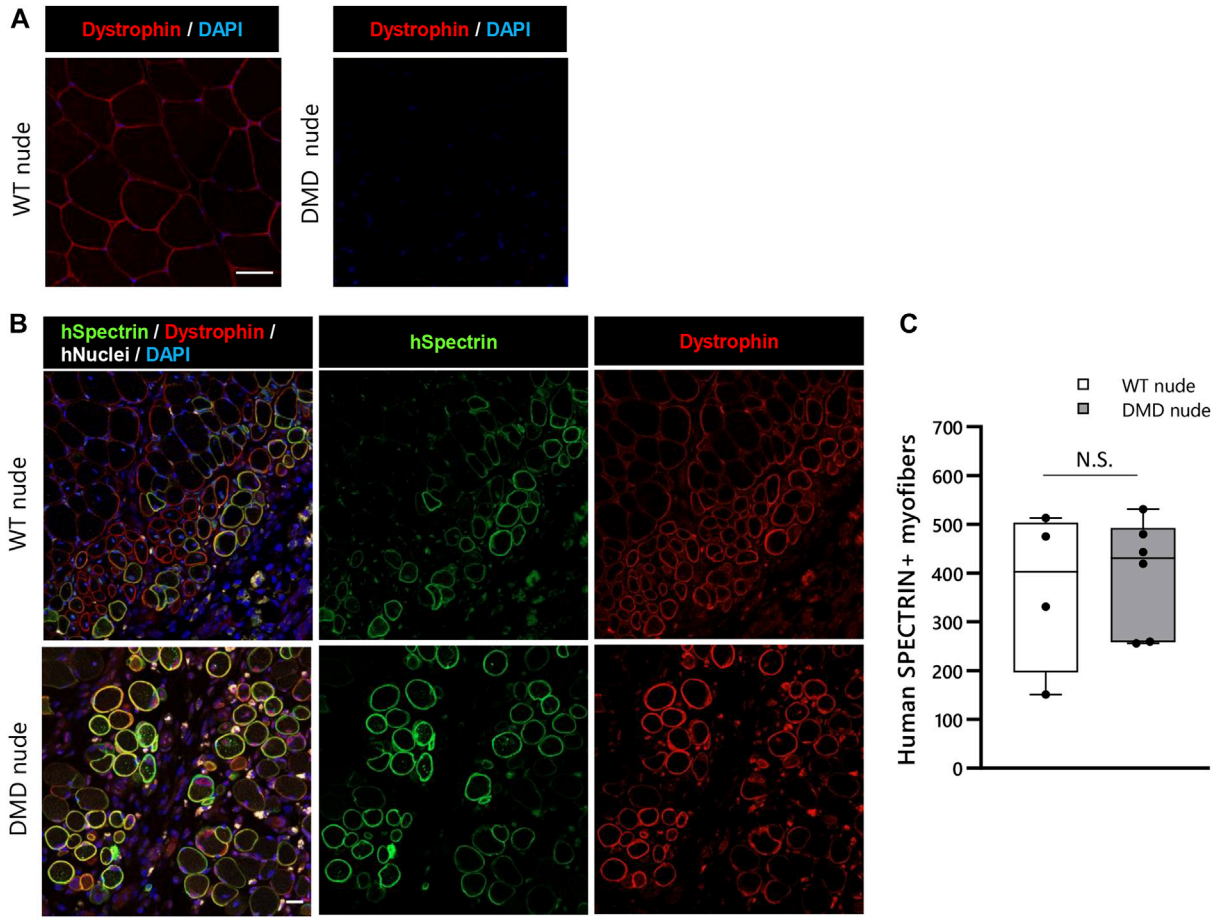

FIGURE 7
Suitability of the immunodeficient DMD rat model for engraftment after human cell transplantation. **(A)** Representative images of immunostaining with dystrophin antibodies in cryosections of the TA muscle of WT nude rat. **(B)** Representative images showing engraftment of transplanted Hu5/KD3 cells in 4-week-old WT and DMD nude rats. The engrafted cells were evaluated 3 weeks after transplantation using immunohistochemistry for human spectrin. Human spectrin (green), dystrophin (red), nuclei (white), and DAPI (blue). Scale bars = 25 μm. **(C)** The number of engrafted myofibers in 1 TA muscle. N.S. non-significant.

3.6 Validation of human cell engraftment in DMD nude rats

We conducted transplantation studies to evaluate the acceptance of human cells by WT and DMD nude rats. First, we performed immunohistochemistry using an anti-dystrophin antibody to confirm the absence of dystrophin protein expression in DMD nude rats (Figure 7A). After cryo-injury treatment, we injected immortalized human myoblasts (Hu5/KD3) into the TA muscles of WT and DMD nude rats. Three weeks post-transplantation, the rats were euthanized, and TA muscles were collected for cryosectioning. Evaluation of human myoblast engraftment, through the detection of human spectrin-positive fibers (Figure 7B), revealed almost 400 human spectrin-positive myofibers in both DMD and WT nude rats (Figure 7C). We observed dystrophin expression in the spectrin-positive fibers in the DMD nude rat muscle (Figure 7B), indicating that regeneration of dystrophin positive myofibers by human cells can be assessed using the DMD nude rat. In WT nude rats, Hu5/KD3 cells were still engrafted 3 months after transplantation (Supplementary Figure S3). On the other hand, when Hu5/KD3 cells were transplanted into the immunocompetent DMD model rats ($X^{Dmd}Y$ $Foxn1^{+/rnu}$), no engraftment was observed (Supplementary Figure S4).

4 Discussion

In this study, we generated an immunodeficient DMD rat model (DMD nude rat) and confirmed that it exhibited the DMD pathology similar to that seen in human patients. Furthermore, we confirmed that engraftment of immortalized human myoblasts followed by muscle regeneration could be assessed in DMD nude rats.

Several DMD model animals have been established and reported to date, including dogs (Kornegay, 2017), rats (Larcher et al., 2014; Nakamura et al., 2014; Taglietti et al., 2022), and mice (Tanabe, 1986). However, to study the use of cell transplantation as a possible therapy for DMD, immunodeficient animal models should be used to enable grafting different types of donor cells without the risk of immune rejection. The NSG-mdx^{4Cv} mouse has been reported as an

optimal immunodeficient DMD model enabling the engraftment of human cells (Arpke et al., 2013). The mdx4^{Cv} mouse harbors a point mutation in exon 53 of the *dmd* gene resulting in a premature stop codon (Im et al., 1996) and has been used for validating dystrophin restoration procedures because it has 10-times fewer revertant fibers than the C57BL/10-mdx mouse (Danko et al., 1992). The NSG-mdx^{4Cv} mouse was established by breeding the mdx^{4Cv} mouse with the NSG mouse, which is severely immunodeficient, lacking T, B, and NK cells (Cao et al., 1995) and shows significant engraftment of transplanted xenogeneic cells (Arpke et al., 2013). Although the NSG-mdx^{4Cv} mouse displayed slightly enhanced fibrosis in the diaphragm and quadriceps compared to that in the C57BL/10-mdx mouse, no adipogenesis was observed in the NSG-mdx^{4Cv} mouse. Moreover, muscle function was identical between the NSG-mdx^{4Cv} and C57BL/10-mdx mice, revealing a milder DMD phenotype than that exhibited in human patients (Arpke et al., 2013). DMD nude rat model is characterized by lower body weight and shorter life span compared to WT nude rats. DMD nude rats had significantly lower body weight than WT nude rats at 4 weeks of age and died by 68-week-old. In contrast, C57BL/10-mdx mice show no significant weight loss compared to controls (Tanabe, 1986) and have a mean lifespan that is 19% reduce than controls at 21.5-month-old (Chamberlain et al., 2007). Furthermore, the forelimb grip strength of C57BL/10-mdx mice show 13.0% of reduction from WT mice (Spurney et al., 2009), while DMD nude rats show 36.0% reduction from WT mice at 5-6-month-old.We also observed increased muscle breakdown markers including serum CK activity and urine titin level, in the early stages of disease progression, which decreased as the disease progressed. Thus, our DMD nude rat model showed a more severe phenotype than the C57BL/10-mdx mouse, making it suitable for evaluating the efficacy of cell transplantation therapy in preclinical studies.

Next, we performed histopathological evaluation of the degree of skeletal muscle degradation and observed overall decreased skeletal muscle weights in DMD nude rats compared to those in WT nude rats. In addition, we observed progressive fibrosis of the heart and diaphragm, which are closely related to rat survival, in DMD nude rats, with increasing severity as the rats aged. SR-stained images also showed advanced fibrosis and adipogenesis, with markedly small fiber diameter in the quadriceps muscle of DMD nude rats, which has not been reported in the DMD mouse model. DMD nude rats showed severe fibrosis and adipogenesis of skeletal muscle, similar to previously reported DMD rat models (Larcher et al., 2014; Nakamura et al., 2014; Taglietti et al., 2022). In DMD nude rat, muscle fibers of different sizes due to repeated necrosis and regeneration of muscle fibers characteristic of patient with DMD were observed. Cardiac fibrosis and respiratory fibrosis also progressively and age-dependently worsen, comparable to previously reported DMD rat models (Larcher et al., 2014; Nakamura et al., 2014; Taglietti et al., 2022). A transverse histological analysis of DMD nude rat muscle tissues revealed damaged muscles around the scapula in the shoulder area. In contrast, despite progressive fibrosis of the deep gluteal muscles, we did not observe any severe damage to the buttocks. The lack of adipogenesis in the buttocks, unlike that seen in human patients with DMD (Polavarapu et al., 2016), could be explained by differences between bipedal and tetrapodal animals (Vlahovic et al., 2017; Veenvliet et al., 2020). Further, we confirmed that our DMD nude rats can receive transplanted human myoblasts for preclinical studies. The injected Hu5/KD3 cells showed similar engraftment in WT and DMD nude rats, analyzed using spectrin and dystrophin positive human fibers. Moreover, we detected Hu5/KD3 cells in the TA muscles in WT nude rats *via* positive spectrin and dystrophin staining even after 3 months, indicating strong engraftment. Notably, since DMD nude rats show no revertant fiber which some DMD model rats have (Larcher et al., 2014; Taglietti et al., 2022), such phenotype would be an advantage to assess the engraftment efficiency accurately after cell transplantation. Future cell transplantation studies should be conducted using these DMD nude rats to administer skeletal MuSCs derived from iPS cells (Zhao et al., 2020) and to evaluate their engraftment and function. However, we observed some instances of accidental death with isoflurane anesthesia at about 5 months of age and after treadmill exercise at the age of 7 months (data not shown). Additionally, since natural breeding of DMD nude rat is difficult, we have confirmed that artificial insemination can produce fertilized eggs, although the probability is low (data not shown). Thus, studies should be carefully designed to analyze the effects of cell therapy and other drugs, because the symptoms of DMD nude rat are more severe than those of NSG-mdx^{4Cv} mouse.

In summary, we have developed immunodeficient DMD rat model that exhibits a pathology similar to human patients with DMD and that accepts human myoblast transplantation, making it suitable for basic DMD research as well as for preclinical studies investigating cell transplantation therapy. We report no revertant fiber and an appropriately sized animal model for evaluating skeletal muscle after human MuSC transplantation with more severe symptoms than in the previously established NSG-mdx^{4Cv} mouse model with milder symptoms.

Data availability statement

The original contributions presented in the study are included in the article/Supplementary Material, further inquiries can be directed to the corresponding author.

Ethics statement

Ethical review and approval was not required for the study on human participants in accordance with the local legislation and institutional requirements. Written informed consent for participation was not required for this study in accordance with the national legislation and the institutional requirements. The animal study was reviewed and approved by the Institutional Animal Care and Use Committee of the University of Kyoto.

Author contributions

Conceptualization, HS, KY, and MS; Methodology, MS and MG; formal analysis, MS; Investigation, MS and MG; Resources, HS and KY; Data curation, MS; Discussions, MS and HS; Writing—Original

draft, MS; Writing—Review and Editing, MS and HS; Visualization, MS; Supervision, HS and KY; Funding acquisition, HS.

Funding

This work was primarily supported by a grant from the Acceleration Transformative Research for Medical Innovation Set-up Scheme (ACT-MS) (JP18im0210817) and partially by a grant from The Core Center for iPS Cell Research (JP13bm0104001), both of which are provided by the Japan Agency for Medical Research and Development, AMED (to HS).

Acknowledgments

We thank Dr. Naohiro Hashimoto from the National Center for Geriatrics and Gerontology, Japan, for providing the human immortalized myoblast cell line Hu5/KD3, and Dr. Yasuhiko Tabata from Kyoto University for Gelatin and hyaluronic acid. We also thank Dr. Yasuhiro Miura, Ms. Sayaka Ichinoseki, Ms. Yukiko Nakagawa, and Ms. Tomoka Sabuta for technical assistance.

Conflict of interest

The authors declare that the research was conducted in the absence of any commercial or financial relationships that could be construed as a potential conflict of interest.

Publisher's note

Supplementary material

The Supplementary Material for this article can be found online at: https://www.frontiersin.org/articles/10.3389/fphys.2023.1094359/full#supplementary-material

References

Arpke, R. W., Darabi, R., Mader, T. L., Zhang, Y., Toyama, A., Lonetree, C. L., et al. (2013). A new immuno-dystrophin-deficient model, the NSG-mdx(4Cv) mouse, provides evidence for functional improvement following allogeneic satellite cell transplantation. *Stem Cells*. 31 (8), 1611–1620. doi:10.1002/stem.1402

Beytía, M. A., Vry, J., and Kirschner, J. (2012). Drug treatment of duchenne muscular dystrophy: Available evidence and perspectives. *Acta Myol.* 31, 4–8.

Cao, X., Shores, E. W., Hu-Li, J., Anver, M. F., Kelsall, B. L., Rssell, S. M., et al. (1995). Defective lymphoid development in mice lacking expression of the common cytokine receptor γ chain. *Immunity* 2, 223–238.

Cerletti, M., Jurga, S., Witczak, C. A., Hirshman, M. F., Shadrach, J. L., Goodyear, L. J., et al. (2008). Highly efficient, functional engraftment of skeletal muscle stem cells in dystrophic muscles. *Cell* 134 (1), 37–47. doi:10.1016/j.cell.2008.05.049

Chamberlain, J. S., Metzger, J., Reyes, M., Townsend, D., Faulkner, J. A., Reyes, M., et al. (2007). Dystrophin deficient mdx mice display a reduced life span and are susceptible to spontaneous rhabdomyosarcoma. *FASEB J.* 21 (9), 2195–2204.

Danko, I., Chapman, V., and Wolff, J. A. (1992). The frequency of revertants in mdx mouse genetic models for Duchenne muscular dystrophy. *Pediatr. Res.* 32, 128–131.

Doi, D., Magotani, H., Kikuchi, T., Ikeda, M., Hiramatsu, S., Yoshida, K., et al. (2020). Pre-clinical study of induced pluripotent stem cell-derived dopaminergic progenitor cells for Parkinson's disease. *Nat. Commun.* 11 (1), 3369. doi:10.1038/s41467-020-17165-w

Fairclough, R. J., Wood, M. J., and Davies, K. E. (2013). Therapy for duchenne muscular dystrophy: Renewed optimism from genetic approaches. *Nat. Rev. Genet.* 14 (6), 373–378. doi:10.1038/nrg3460

Goto, I., Peters, H. A., and Reese, H. H. (1967). Creatine phosphokinase in neuromuscular disease. Patients and families. *Activity Progressive Muscular Dystrophy Neuromuscul. Dis. Aquatic Org.* 16 (5), 529–535. doi:10.1001/archneur.1967.00470230081011

Hanes, M. A. (2006). *The nude rat* American College of Laboratory Animal Medicine, 2nd Edition. The Laboratory Rat.

Hoffman, E. P., Brown, R. H., Jr., and Kunkel, L. M. (1987). Dystrophin: The protein product of the duchenne muscular dystrophy locus. *Cell* 51, 919–928.

Im, W. B., Phelps, S. F., Copen, E. H., Adams, E. G., Slightom, J. L., Chamberlain, J. S., et al. (1996). Differential expression of dystrophin isoforms in strains of mdx mice with different mutations. *Hum. Mol. Genet.* 5 (8), 1149–1153.

Kornegay, J. N. (2017). The golden retriever model of Duchenne muscular dystrophy. *Skelet. Muscle* 7 (1), 9. doi:10.1186/s13395-017-0124-z

Larcher, T., Lafoux, A., Tesson, L., Remy, S., Thepenier, V., Francois, V., et al. (2014). Characterization of dystrophin deficient rats: A new model for duchenne muscular dystrophy. *PLoS One* 9 (10), e110371. doi:10.1371/journal.pone.0110371

Marg, A., Escobar, H., Gloy, S., Kufeld, M., Zacher, J., Spuler, A., et al. (2014). Human satellite cells have regenerative capacity and are genetically manipulable. *J. Clin. Investigation* 124 (10), 4257–4265. doi:10.1172/JCI63992

Maruyama, N., Asai, T., Abe, C., Inada, A., Kawauchi, T., Miyashita, K., et al. (2016). Establishment of a highly sensitive sandwich ELISA for the N-terminal fragment of titin in urine. *Sci. Rep.* 6, 39375. doi:10.1038/srep39375

Miura, Y., Sato, M., Kuwahara, T., Ebata, T., Tabata, Y., Sakurai, H., et al. (2022). Transplantation of human iPSC-derived muscle stem cells in the diaphragm of Duchenne muscular dystrophy model mice. *PLoS One* 17 (4), e0266391. doi:10.1371/journal.pone.0266391

Montarras, D., Morgan, J., Collins, C., Relaix, F., Zaffran, S., Cumano, A., et al. (2005). Direct isolation of satellite cells for skeletal muscle regeneration. *Science* 309, 2064–2067.

Nakamura, A., and Takeda, S. (2011). Mammalian models of duchenne muscular dystrophy: Pathological characteristics and therapeutic applications. *J. Biomed. Biotechnol.* 2011, 184393. doi:10.1155/2011/184393

Nakamura, K., Fujii, W., Tsuboi, M., Tanihata, J., Teramoto, N., Takeuchi, S., et al. (2014). Generation of muscular dystrophy model rats with a CRISPR/Cas system. *Sci. Rep.* 4, 5635. doi:10.1038/srep05635

Nalbandian, M., Zhao, M., Sasaki-Honda, M., Jonouchi, T., Lucena-Cacace, A., Mizusawa, T., et al. (2021). Characterization of hiPSC-derived muscle progenitors reveals distinctive markers for myogenic cell purification toward cell therapy. *Stem Cell Rep.* 16 (4), 883–898. doi:10.1016/j.stemcr.2021.03.004

Nowak, K. J., and Davies, K. E. (2004). Duchenne muscular dystrophy and dystrophin: Pathogenesis and opportunities for treatment. *EMBO Rep.* 5 (9), 872–876. doi:10.1038/sj.embor.7400221

Polavarapu, K., Manjunath, M., Preethish-Kumar, V., Sekar, D., Vengalil, S., Thomas, P., et al. (2016). Muscle MRI in Duchenne muscular dystrophy: Evidence of a distinctive pattern. *Neuromuscul. Disord.* 26 (11), 768–774. doi:10.1016/j.nmd.2016.09.002

Roberts, R. G. (2001). Dystrophins and dystrobrevins. *Genome Biol.* 2 (4), reviews3006.3001–3006.3007.

Sacco, A., Doyonnas, R., Kraft, P., Vitorovic, S., Blau, H. M., Kraft, P., et al. (2008). Self-renewal and expansion of single transplanted muscle stem cells. *Nature* 456 (7221), 502–506. doi:10.1038/nature07384

Samata, B., Kikuchi, T., Miyawaki, Y., Morizane, A., Mashimo, T., Nakagawa, M., et al. (2015). X-linked severe combined immunodeficiency (X-SCID) rats for xeno-transplantation and behavioral evaluation. *J. Neurosci. Methods* 243, 68–77. doi:10.1016/j.jneumeth.2015.01.027

Shiomi, K., Kiyono, T., Okamura, K., Uezumi, M., Goto, Y., Yasumoto, S., et al. (2011). CDK4 and cyclin D1 allow human myogenic cells to recapture growth property without compromising differentiation potential. *Gene Ther.* 18 (9), 857–866. doi:10.1038/gt.2011.44

Spurney, C. F., Gordish-Dressman, H., Guerron, A. D., Sali, A., Pandey, G. S., Rawat, R., et al. (2009). Preclinical drug trials in the mdx mouse: Assessment of reliable and sensitive outcome measures. *Muscle Nerve* 39 (5), 591–602. doi:10.1002/mus.21211

Sun, C., Serra, C., Lee, G., Wagner, R. K., Lee, G., and Wagner, K. R. (2020). Stem cell-based therapies for Duchenne muscular dystrophy. *Exp. Neurol.* 323, 113086. doi:10.1016/j.expneurol.2019.113086

Taglietti, V., Kefi, K., Bronisz-Budzynska, I., Mirciloglu, B., Rodrigues, M., Cardone, N., et al. (2022). Duchenne muscular dystrophy trajectory in R-DMDdel52 preclinical rat model identifies COMP as biomarker of fibrosis. *Acta Neuropathol. Commun.* 10 (1), 60. doi:10.1186/s40478-022-01355-2

Takenaka-Ninagawa, N., Kim, J., Zhao, M., Sato, M., Jonouchi, T., Goto, M., et al. (2021). Collagen-VI supplementation by cell transplantation improves muscle regeneration in Ullrich congenital muscular dystrophy model mice. *Stem Cell Res. Ther.* 12 (1), 446. doi:10.1186/s13287-021-02514-3

Tanabe, Y., Esaki, K., Nomura, T., and Nomura, T. (1986). Skeletal muscle pathology in X chromosome-linked muscular dystrophy (mdx) mouse. *Acta Neuropathol. (Bet1)* 69, 91–95.

Tanaka, K. K., Hall, J. K., Troy, A. A., Cornelison, D. D., Majka, S. M., Olwin, B. B., et al. (2009). Syndecan-4-expressing muscle progenitor cells in the SP engraft as satellite cells during muscle regeneration. *Cell Stem Cell* 4 (3), 217–225. doi:10.1016/j.stem.2009.01.016

Veenvliet, J. V. B., Adriano, K., Helene, H., Leah, S-W., Manuela, S., Dennis, K., et al. (2020). Mouse embryonic stem cells self-organize into trunklike structures with neural tube and somites. *Science* 370, eaba4937. doi:10.1101/2020.03.04.974949

Vlahovic, H., Bazdaric, K., Marijancic, V., Soic-Vranic, T., Malnar, D., Arbanas, J., et al. (2017). Segmental fibre type composition of the rat iliopsoas muscle. *J. Anat.* 230 (4), 542–548. doi:10.1111/joa.12588

Xu, X., Wilschut, K. J., Kouklis, G., Tian, H., Hesse, R., Garland, C., et al. (2015). Human satellite cell transplantation and regeneration from diverse skeletal muscles. *Stem Cell Rep.* 5 (3), 419–434. doi:10.1016/j.stemcr.2015.07.016

Zhao, M., Tazumi, A., Takayama, S., Takenaka-Ninagawa, N., Nalbandian, M., Nagai, M., et al. (2020). Induced fetal human muscle stem cells with high therapeutic potential in a mouse muscular dystrophy model. *Stem Cell Rep.* 15 (1), 80–94. doi:10.1016/j.stemcr.2020.06.004

frontiers | Frontiers in Physiology

TYPE Original Research
PUBLISHED 25 April 2023
DOI 10.3389/fphys.2023.1152576

OPEN ACCESS

EDITED BY
Katsumasa Goto,
Toyohashi Sozo University, Japan

REVIEWED BY
Túlio De Almeida Hermes,
Federal University of Alfenas, Brazil
Kyle Bohnert,
St. Ambrose University, United States
Yann Simon Gallot,
University of Évry Val d'Essonne, France

*CORRESPONDENCE
Joshua T. Selsby,
jselsby@iastate.edu

RECEIVED 27 January 2023
ACCEPTED 10 April 2023
PUBLISHED 25 April 2023

CITATION
Krishna S, Spaulding HR, Koltes JE, Quindry JC, Valentine RJ and Selsby JT (2023), Indicators of increased ER stress and UPR in aged D2-mdx and human dystrophic skeletal muscles.
Front. Physiol. 14:1152576.
doi: 10.3389/fphys.2023.1152576

Indicators of increased ER stress and UPR in aged D2-mdx and human dystrophic skeletal muscles

Swathy Krishna[1], Hannah R. Spaulding[1], James E. Koltes[1], John C. Quindry[2], Rudy J. Valentine[3] and Joshua T. Selsby[1]*

[1]Department of Animal Science, Iowa State University, Ames, IA, United States, [2]School of Integrative Physiology and Athletic Training, University of Montana, Missoula, MT, United States, [3]Department of Kinesiology, Iowa State University, Ames, IA, United States

Duchenne muscular dystrophy (DMD) is a progressive muscle disease that results in muscle wasting, wheelchair dependence, and eventual death due to cardiac and respiratory complications. In addition to muscle fragility, dystrophin deficiency also results in multiple secondary dysfunctions, which may lead to the accumulation of unfolded proteins causing endoplasmic reticulum (ER) stress and the unfolded protein response (UPR). The purpose of this investigation was to understand how ER stress and the UPR are modified in muscle from D2-mdx mice, an emerging DMD model, and from humans with DMD. We hypothesized that markers of ER stress and the UPR are upregulated in D2-mdx and human dystrophic muscles compared to their healthy counterparts. Immunoblotting in diaphragms from 11-month-old D2-mdx and DBA mice indicated increased ER stress and UPR in dystrophic diaphragms compared to healthy, including increased relative abundance of ER stress chaperone CHOP, canonical ER stress transducers ATF6 and pIRE1α S724, and transcription factors that regulate the UPR such as ATF4, XBP1s, and peIF2α S51. The publicly available Affymetrix dataset (GSE38417) was used to analyze the expression of ER stress and UPR-related transcripts and processes. Fifty-eight upregulated genes related to ER stress and the UPR in human dystrophic muscles suggest pathway activation. Further, based on analyses using iRegulon, putative transcription factors that regulate this upregulation profile were identified, including ATF6, XBP1, ATF4, CREB3L2, and EIF2AK3. This study adds to and extends the emerging knowledge of ER stress and the UPR in dystrophin deficiency and identifies transcriptional regulators that may be responsible for these changes and be of therapeutic interest.

KEYWORDS

DMD, mdx, dystrophin, unfolded protein response, transcription factor

Introduction

Duchenne muscular dystrophy (DMD) is a fatal muscle disease that affects approximately 1 in 5,000–6,000 boys born worldwide (Mendell et al., 2012; Mah et al., 2014; Ryder et al., 2017; Duan et al., 2021). This disease is caused by the absence of a functional dystrophin protein, a structural component of the dystrophin-glycoprotein complex (DGC), present on the sarcolemmal membrane (Hoffman et al., 1987; Koenig

et al., 1987). The absence of dystrophin leads to contraction-induced muscle injuries, fatty and fibrotic infiltration, and muscle wasting (Petrof et al., 1993; Ehmsen et al., 2002; Morris et al., 2010). Dystrophin deficiency also causes a host of cellular dysfunctions including, but not limited to, inflammation, calcium mishandling, impaired autophagy, and oxidative stress (Chen et al., 2005; Selsby et al., 2010; Selsby, 2011; Selsby et al., 2012; Moorwood and Barton, 2014; Spaulding et al., 2018).

The extent to which independent and interdependent modes of cellular dysfunction contribute to DMD pathology remain an active area of scientific inquiry. For instance, the pathophysiological changes associated with DMD may result in perturbations of cellular homeostasis, causing an accumulation of misfolded or unfolded proteins and subsequent ER stress (Moorwood and Barton, 2014; Hulmi et al., 2016; Pauly et al., 2017). In response to these alterations, the unfolded protein response (UPR) is activated in muscle cells. In general, the UPR is thought to be activated primarily through the translocation of three transmembrane sensors: PERK, IRE1α, and ATF6 (Walter and Ron, 2011; Adams et al., 2019; Afroze and Kumar, 2019; Hetz et al., 2020; Gallot and Bohnert, 2021). The most common restorative mechanisms of cellular homeostasis by the UPR are through translational repression to regulate the accumulation of misfolded proteins and through the production of protein chaperones, which facilitate protein folding (Adams et al., 2019; Afroze and Kumar, 2019; Hetz et al., 2020; Gallot and Bohnert, 2021). ER stress may also stimulate proteolysis via activation of the calpain and proteasome systems (Afroze and Kumar, 2019), which may decrease accumulation of misfolded proteins via degradation. This process may be complicated; however, via decreased autophagy in dystrophic muscle (De Palma et al., 2012; Spitali et al., 2013; Spaulding et al., 2018; Krishna et al., 2021), which ostensibly limits removal of protein aggregates.

PERK, IRE1α, and ATF6 are the most studied ER stress transducers that initiate the UPR. Upon accumulation of misfolded proteins in the ER lumen, the chaperone BiP/GRP78/HSPA5 is dissociated from PERK, IRE1α, and ATF6, allowing their activation through phosphorylation and subsequent initiation of the UPR (Walter and Ron, 2011; Hetz, 2012; Afroze and Kumar, 2019). Activated PERK phosphorylates eIF2α at S51, which inhibits global translation, but selectively upregulates ATF4 and ER stress chaperones such as CHOP and BiP/GRP78/HSPA5 (Walter and Ron, 2011; Hetz, 2012; Afroze and Kumar, 2019). eIF2α can also be phosphorylated by PKR/EIF2AK2 as well as GCN2 and HRI, among other kinases (Clemens, 2001). IRE1α-mediated activation of the UPR is initiated by dimerization and phosphorylation of IRE1α. This facilitates splicing of XBP1, forming XBP1s, which promotes transcription (along with translocated and cleaved ATF6) of ER stress chaperones and activation of ERAD (ER-associated degradation) (Walter and Ron, 2011; Hetz, 2012; Afroze and Kumar, 2019). Prolonged ER stress and UPR can also lead to inflammatory signaling and apoptosis. Inflammatory signaling is activated through JNK-AP1 by IRE1α and through NFκB by PERK and IRE1α (Walter and Ron, 2011; Hetz, 2012). Skeletal muscle has an extensive ER; however, a detailed understanding of the role of ER stress in skeletal muscle, particularly under pathophysiological conditions such as DMD, is lacking.

DMD is frequently modeled by the mdx mouse, which has a relatively mild disease phenotype that largely fails to accurately recapitulate progressive degeneration in skeletal muscle as observed in dystrophin-deficient human muscle, with the notable exception of the diaphragm (Stedman et al., 1991; Grounds et al., 2008). In the mdx model, lifespan is only slightly shortened, and heart function is largely preserved (Chamberlain et al., 2007; Grounds et al., 2008; Yucel et al., 2018). Despite this, the mdx mouse model has been instrumental for the determination of disease mechanisms and cellular dysfunction and as an early screen of therapeutic interventions. Consistent with the aforementioned understanding of cellular dysfunction, a limited body of work suggests dystrophin deficiency causes ER stress in muscles from mdx mice and those with DMD (Moorwood and Barton, 2014; Hulmi et al., 2016; Pauly et al., 2017). Given the relatively mild phenotype in the mdx mouse model, the mdx mutation was backcrossed to a DBA line, resulting in a more severe model (D2-mdx), which better recapitulates human disease pathology (Coley et al., 2016; Putten et al., 2019; Spaulding et al., 2019; Hammers et al., 2020). The extent to which ER stress may be stimulated in this emerging murine model is unknown and in muscles from boys/men with DMD has only been briefly considered (Moorwood and Barton, 2014). Therefore, the purpose of this investigation was to determine the extent to which ER stress is modified in dystrophin-deficient skeletal muscle in an emerging mouse model and in boys/men with DMD. This improved understanding will be beneficial in the development of therapeutics aimed at correcting secondary dysfunctions associated with DMD. We hypothesized that markers of ER stress and UPR would be upregulated in 11-month-old D2-mdx diaphragm and human dystrophic muscles.

Methods

Animal treatments

Animal treatments were approved by the Institutional Animal Care and Use Committees at the University of Montana and the University of Florida. Detailed methods and data from limb muscle (Spaulding et al., 2019), and diaphragm (Spaulding et al., 2020; Krishna et al., 2021), from these animals have been previously published. In brief, 11-month-old DBA (n = 7) or D2-mdx (n = 7) male mice were anesthetized to a surgical level, and diaphragms were collected, and then the mice were euthanized by exsanguination. The collected muscles were frozen in liquid nitrogen for further analyses. Previously reported functional analyses from these diaphragms indicated reduced specific force and histopathological analyses indicated increased fibrotic area and reduced contractile area in diaphragms from D2-mdx compared to diaphragms from DBA mice (Spaulding et al., 2020). Given these previously established functional, histological, and biochemical alterations, the diaphragm was selected for experiments described herein.

TABLE 1 Primary and secondary antibodies used for Western blotting.

Antibody	Product id	Company	Host	Primary	Secondary
AP1	A5968	Sigma aldrich	Rabbit	1:1000 TBST	1:2000 TBST
ATF4	97038 S	Cell signaling	Mouse	1:1000 TBST	1:2000 TBST
ATF6	65880 S	Cell signaling	Rabbit	1:1000 TBST	1:2000 TBST
BiP	3,177	Cell signaling	Rabbit	1:1000 TBST	1:2000 TBST
CHOP	2,895	Cell signaling	Mouse	1:1000 TBST	1:2000 TBST
eIF2α	9722 S	Cell signaling	Rabbit	1:1000 TBST	1:2000 TBST
IRE1α	3,294	Cell signaling	Rabbit	1:1000 TBST	1:2000 TBST
IκBα	4,812	Cell signaling	Rabbit	1:1000 TBST	1:2000 TBST
NFκB	8,242	Cell signaling	Rabbit	1:1000 TBST	1:2000 TBST
peIF2α S51	3,398	Cell signaling	Rabbit	1:1000 TBST	1:2000 TBST
pIRE1α S724	Ab48187	Abcam	Rabbit	1:1,000 2.5% milk	1:1000 TBST
PKR	SC-6282	Santa cruz biotechnology	Rabbit	1:1000 TBST	1:2000 TBST
pNFκB S536	3,033	Cell signaling	Rabbit	1:1000 TBST	1:2000 TBST
pPERK T980	3,179	Cell signaling	Rabbit	1:3,000 2.5% milk	1:3,000 5% milk
pPKR T446	Ab32036	Abcam	Rabbit	1:1000 TBST	1:2000 TBST
XBP1s	40435 S	Cell signaling	Rabbit	1:1000 TBST	1:2000 TBST

Protein extraction and Western blotting in D2-mdx

Diaphragms were prepared for Western blotting as previously described (Krishna et al., 2021). In brief, protein was extracted in whole muscle buffer (10 mM sodium phosphate, 2% SDS, pH 7.0) and the concentration was determined using BCA (Thermo Fisher Pierce™ BCA protein assay, #23225). Protein was diluted to a concentration of 4 μg/μL and precisely 40 μg of protein was loaded into each lane. Protein was separated by molecular mass and then transferred to a nitrocellulose membrane. Equal loading was confirmed by quantification of total lane optical density following a Ponceau S stain and objective measurement using AzureSpot software (Azure Biosystems, Version 2.0.062). The stain was removed, membranes were blocked in 5% milk in Tris-buffered saline with 0.1% Tween 20 (TBST), and membranes were incubated with primary and secondary antibodies (Table 1). The membranes were then exposed to enhanced chemiluminescence blotting substrate (ECL, BioRad Clarity™) for 5 min, imaged using Azure™ C600, and quantified using AzureSpot software using automated band detection.

Human affymetrix chip data analysis

To evaluate ER stress in human dystrophic muscle, the publicly available Affymetrix microarray dataset accession ID: GSE38417 (alternate ID: EGEOD-38417) (Dorsey and Ward, 2016) was analyzed using the Bioconductor package, Limma (Ritchie et al., 2015) in R (Team, 2021). The microarray data were generated from muscle biopsy samples from boys with (n = 12; range: 0.92–8 years; mean: 3.75 ± 2.25 years)) or without (n = 6; age unknown) DMD using Human U1133 2.0 arrays. Gene Ontology (GO) analysis and network constructions were performed using ClueGO in Cytoscape version 8.0 (Bindea et al., 2009). String database (Szklarczyk et al., 2021) was used to identify the interactions between the genes of interest. Specifically, the experimentally determined and predicted interactions, based on curated databases and text mining, between the genes were mapped into the network. The transcriptional regulators of the genes of interest were identified using the iRegulon plugin (Janky et al., 2014) in Cytoscape.

Statistics

For the statistical analysis of western blots, an unpaired t-test was performed in GraphPad Prism version 8.0.0. Significance was established at $p < 0.05$. For differential expression in the microarray, the Limma package in R was used (Ritchie et al., 2015), and significance for differential expression was established at a $\log_2$ fold change (FC) > 0.2 and false-discovery rate (FDR) < 0.1 [applying Benjamini and Hochberg (BH) correction (Benjamini and Hochberg, 1995)] for all analyses. For the ontology analyses, an FDR < 0.1 was applied.

Results

ER stress in D2-mdx mice

These mice and tissues have been used to support previous investigations. Through this previous work, we have established that diaphragms from these D2-mdx mice have histopathological injury

10.3389/fphys.2023.1152576

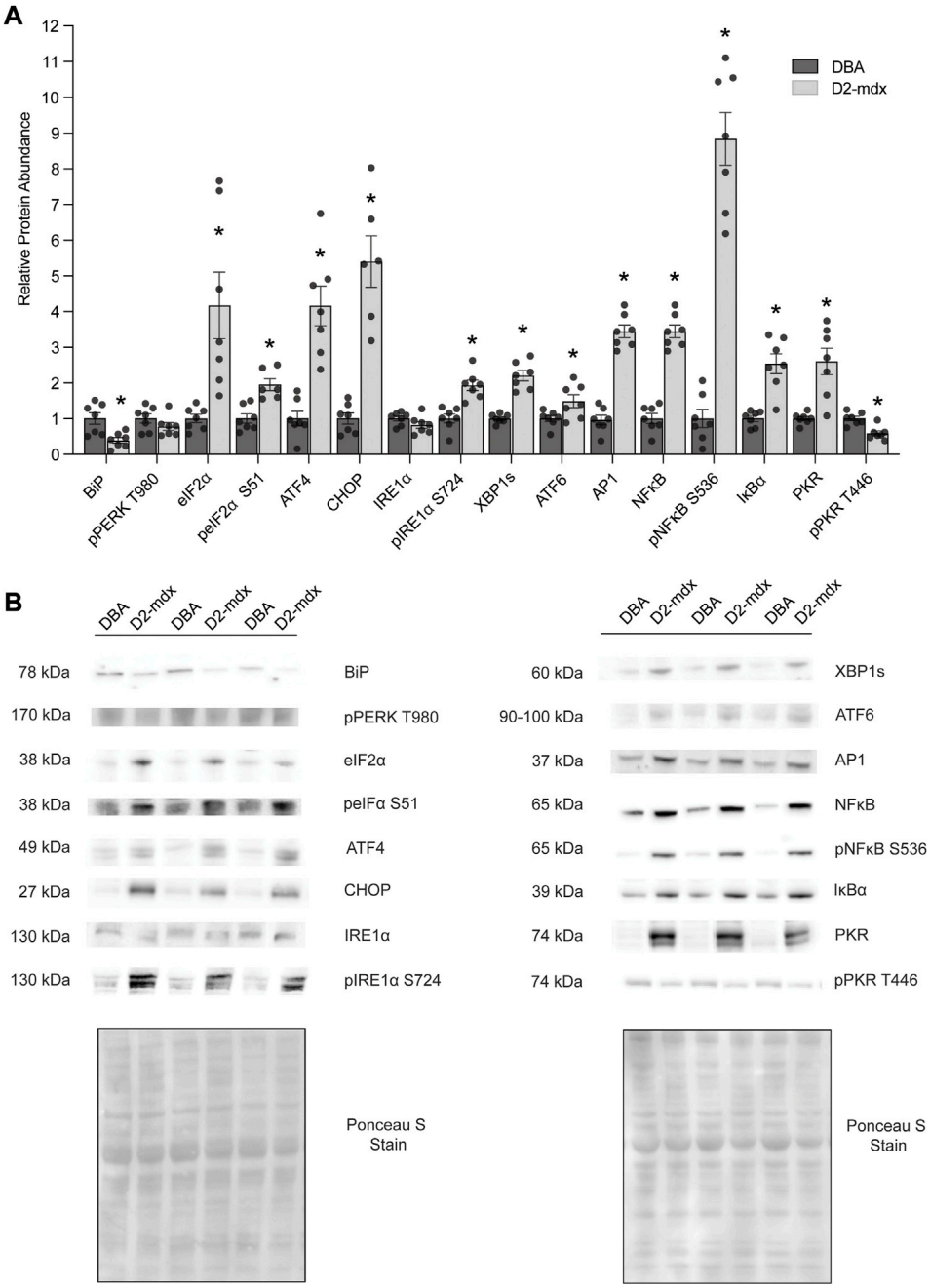

FIGURE 1
Increased abundance of markers of ER stress and the UPR in D2-mdx mice (n = 7) compared to DBA (n = 7). **(A)** Increased relative abundance except for BiP/GRP78/HSPA5 and pPKR T446 (decreased), IRE1α (similar), and pPERK T980 (similar). **(B)** Representative Western blot and Ponceau S stain images. Unpaired t-test used for statistical analysis. Significance established at $p < 0.05$.

and impaired specific tension compared to DBA controls (Spaulding et al., 2020) as well as impaired autophagy (Krishna et al., 2021). We have also established that limb muscle from these D2-mdx mice have smaller mass (absolute and relative), decreased function, and increased histopathological injury compared to DBA mice (Spaulding et al., 2020) as well as alterations in autophagy (Krishna et al., 2021).

In 11-month-old D2-mdx diaphragm, the ER chaperone BiP/GRP78/HSPA5 was decreased by approximately 60% (p = 0.0054) compared to DBA (Figure 1). Similarly, pPERK T980 (PERK phosphorylated at T980) was numerically, albeit non-significantly, decreased (p = 0.0560). Dystrophin deficiency increased eIF2α approximately 4-fold (p = 0.0056) and peIF2α S51 was increased approximately 2-fold (p = 0.0009) compared to DBA. ATF4 was increased approximately 4-fold (p = 0.0002) and CHOP was increased approximately 6.2-fold ($p < 0.0001$) in D2-mdx compared to DBA. While IRE1α (p = 0.1572) was similar between groups, activated pIRE1α S724 was

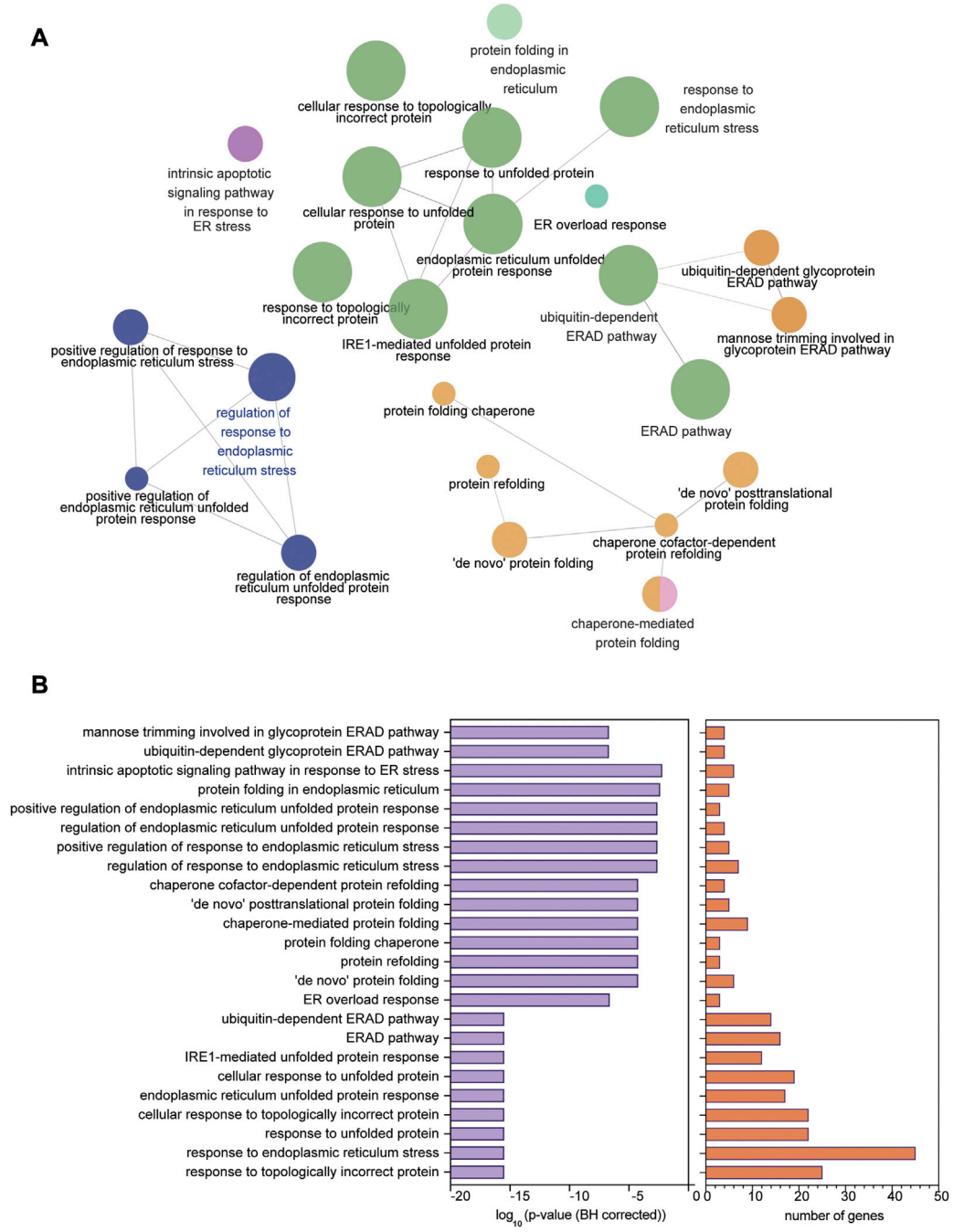

FIGURE 2
ER stress and UPR-related processes identified in human dystrophic muscle. **(A)** Ontology processes related to ER stress and the UPR analyzed using ClueGO in upregulated genes from the human Affymetrix data chip analysis mapped in Cytoscape. **(B)** *p*-value (BH corrected) and number of genes in each of the 24 processes identified. Significance of enrichment established at FDR < 0.01 (BH correction).

increased approximately 2-fold ($p = 0.0003$) compared to DBA. Further, the IRE1α-mediated spliced XBP1 (XBP1s) was increased by 2.2-fold ($p < 0.0001$), and ATF6 by approximately 1.5-fold ($p = 0.0298$) in D2-mdx compared to DBA.

In addition to chronic muscle injury, prolonged ER stress and UPR cause activation of inflammatory signaling. In D2-mdx, relative abundance of AP1 was increased by approximately 2.5-fold compared to DBA. There was an increased relative abundance of NFκB (by approximately 3.5-fold, $p < 0.0001$) and pNFκB S536 (by 8.8-fold, $p < 0.0001$) in D2-mdx, despite increased IκBα (an inhibitor of NFκB activity; 2.5-fold, $p = 0.0002$), compared to healthy muscles. Interestingly pPKR T446, which regulates ER stress and inflammatory pathways, was decreased by approximately 40% ($p = 0.0010$), although total PKR/EIF2AK2 was increased by 2.6-fold ($p = 0.0011$).

TABLE 2 Gene ontology (GO) processes identified for the 58 upregulated ER stress- and UPR-related genes from the human Affymetrix chip analysis with p-adjusted (BH) < 0.1. The ontology analyses for all the differentially expressed genes were performed in ClueGO in Cytoscape. No significantly enriched ER stress- and UPR-related processes were identified with downregulated genes.

	GO terms	Process	Genes
1	GO: 0035966	response to topologically incorrect protein	[ARFGAP3, ATXN3, CANX, CREB3L2, DNAJB11, DNAJB14, EDEM1, EDEM3, EXTL2, FKBP14, HSP90B1, HSPA13, KDELR3, PDIA5, PIK3R1, PTPN2, SERP1, SERPINH1, SSR1, THBS1, TM7SF3, TMEM33, TPP1, UFL1, UGGT2]
2	GO: 0034976	response to ER stress	[ALOX5, ARFGAP3, ATXN3, BID, CANX, CASP4, CAV1, CCDC47, CREB3L2, DNAJB11, DNAJB14, DNAJC10, EDEM1, EDEM3, ERLIN1, ERLIN2, EXTL2, FKBP14, HSP90B1, ITPR1, KDELR3, MAN1A1, MAN1B1, MAP3K5, OS9, PDIA3, PDIA5, PIK3R1, PTPN2, SEC16A, SERP1, SRPX, SSR1, THBS1, TMCO1, TMEM33, TMTC3, TMX1, TP53, TPP1, TRIM25, UBE2J1, UFL1, UFM1, UGGT2]
3	GO: 0006986	response to unfolded protein	[ARFGAP3, CANX, CREB3L2, DNAJB11, EDEM1, EDEM3, EXTL2, FKBP14, HSP90B1, HSPA13, KDELR3, PDIA5, PIK3R1, PTPN2, SERP1, SERPINH1, SSR1, THBS1, TM7SF3, TMEM33, TPP1, UFL1]
4	GO: 0035967	cellular response to topologically incorrect protein	[ARFGAP3, ATXN3, CANX, CREB3L2, DNAJB11, DNAJB14, EDEM1, EXTL2, FKBP14, HSP90B1, HSPA13, KDELR3, PDIA5, PIK3R1, PTPN2, SERP1, SSR1, TM7SF3, TMEM33, TPP1, UFL1, UGGT2]
5	GO: 0030968	ER unfolded protein response	[ARFGAP3, CANX, CREB3L2, DNAJB11, EDEM1, EXTL2, FKBP14, HSP90B1, KDELR3, PDIA5, PIK3R1, PTPN2, SERP1, SSR1, TMEM33, TPP1, UFL1]
6	GO: 0034620	cellular response to unfolded protein	[ARFGAP3, CANX, CREB3L2, DNAJB11, EDEM1, EXTL2, FKBP14, HSP90B1, HSPA13, KDELR3, PDIA5, PIK3R1, PTPN2, SERP1, SSR1, TM7SF3, TMEM33, TPP1, UFL1]
7	GO: 0036498	IRE1-mediated unfolded protein response	[ARFGAP3, DNAJB11, EDEM1, EXTL2, FKBP14, KDELR3, PDIA5, SERP1, SSR1, TMEM33, TPP1, UFL1]
8	GO: 0036503	ERAD pathway	[ATXN3, CAV1, CCDC47, DNAJB14, DNAJC10, EDEM1, EDEM3, ERLIN1, ERLIN2, HSP90B1, MAN1A1, MAN1B1, OS9, TRIM25, UBE2J1, UGGT2]
9	GO: 0030433	ubiquitin dependent ERAD pathway	[CAV1, CCDC47, DNAJB14, DNAJC10, EDEM1, EDEM3, ERLIN1, ERLIN2, HSP90B1, MAN1A1, MAN1B1, OS9, TRIM25, UBE2J1]
10	GO: 0006983	ER overload response	[BID, CCDC47, TMCO1]
11	GO: 0006458	"*de novo*" protein folding	[CD74, DNAJB14, FKBP1B, GAK, HSPA13, SELENOF]
12	GO: 0042026	protein refolding	[B2M, FKBP1B, HSPA13]
13	GO: 0044183	protein folding chaperone	[CCDC47, CD74, HSPA13]
14	GO: 0061077	chaperone-mediated protein folding	[CD74, CRTAP, CSNK2A2, DNAJB14, FKBP1B, GAK, HSPA13, P3H1, PPIB]
15	GO: 0051084	"*de novo*" post translational protein folding	[CD74, DNAJB14, GAK, HSPA13, SELENOF]
16	GO: 0051085	chaperone cofactor-dependent protein refolding	[CD74, DNAJB14, GAK, HSPA13]
17	GO: 1905897	regulation of response to ER stress	[ALOX5, ATXN3, CAV1, PIK3R1, PTPN2, TMEM33, UFL1]
18	GO: 1905898	positive regulation of response to ER stress	[ATXN3, CAV1, PIK3R1, PTPN2, TMEM33]
19	GO: 1900101	regulation of ER unfolded protein response	[PIK3R1, PTPN2, TMEM33, UFL1]
20	GO: 1900103	positive regulation of ER unfolded protein response	[PIK3R1, PTPN2, TMEM33]
21	GO: 0034975	protein folding in ER	[CANX, DNAJC10, HSP90B1, PDIA3, VAPA]
22	GO: 0070059	intrinsic apoptotic signaling pathway in response to ER stress	[CASP4, DNAJC10, ITPR1, MAP3K5, PTPN2, TP53]

(Continued on following page)

TABLE 2 (*Continued*) Gene ontology (GO) processes identified for the 58 upregulated ER stress- and UPR-related genes from the human Affymetrix chip analysis with p-adjusted (BH) < 0.1. The ontology analyses for all the differentially expressed genes were performed in ClueGO in Cytoscape. No significantly enriched ER stress- and UPR-related processes were identified with downregulated genes.

	GO terms	Process	Genes
23	GO: 0097466	ubiquitin-dependent glycoprotein ERAD pathway	[EDEM1, EDEM3, MAN1A1, MAN1B1]
24	GO: 1904382	mannose trimming involved in glycoprotein ERAD pathway	[EDEM1, EDEM3, MAN1A1, MAN1B1]

ER stress in skeletal muscle from boys with DMD

Ontology analyses (for biological processes and cell components) to identify processes related to the ER were performed separately on the upregulated (FDR<0.1 and $\log_2$ FC > 0.2) and downregulated (FDR<0.1 and $\log_2$ FC < 0.2) genes. We did not identify enriched ER-related processes using the ontology analysis of the downregulated genes. We identified 553 genes using GO biological processes and 449 genes using GO cellular components related to the ER following ontology analyses on the upregulated genes. When combined, a total of 868 unique genes were used for a refined search to identify specific processes related to ER stress and the UPR. Through this approach, we identified 24 processes comprised of a total of 58 genes (Figures 2A,B; Table 2). The processes identified suggest possible disruptions in protein folding, calcium storage and release, and activation of the UPR and ERAD (Table 2). Of note, among the processes identified, "response to endoplasmic reticulum stress" had the most identified genes (45 genes) (Figure 2B).

The 58 upregulated genes had $\log_2$ FC ranging from 0.3699 to 3.3031 (Figure 3A), and FDR ranged from 2E-09 to 0.03 (Supplementary Table S1) in dystrophic muscles compared to healthy muscles. Additionally, a subset of the human genes that correspond to the proteins measured in D2-mdx and DBA mice were also detected in the microarray dataset (Figure 3B). Among these genes, only PKR/EIF2AK2 was upregulated considering the stringent cut-off of FDR < 0.1 ($\log_2$ FC of 0.08, FDR = 0.003, p < 0.01), whereas if p-value ($p < 0.05$) was considered several additional transcripts were also upregulated.

Next, we identified transcription factors that may contribute to the regulation of the identified 58 genes. Based on sequence analysis and motif searches, we identified 30 putative transcription factors (normalized enrichment score (NES) cut-off 3%) that regulate ER stress and UPR-related genes of interest (Table 3). This analysis identified transcription factors that regulate the majority (86.2%) of the upregulated ER stress and UPR-related genes identified in our analysis. Next, we queried our dataset and discovered that, of these 30 transcription factors, 27 were differentially expressed (FDR<0.1; 14 downregulated and 13 upregulated; Supplementary Table S2). In order to identify the most plausible transcriptional regulatory profile, the top 13 transcriptional regulators (NES cut-off 4.00) and the identified ER-stress-related genes regulated by these transcription factors were mapped into a network (Figure 3C) along with known and predicted interactions identified using String. Of interest, the transcriptional regulators TAF9, NFYA, and TP53 were among the identified String interactions that were experimentally determined (Supplementary Figure S1), providing additional confidence in this approach.

An ontology analysis on the identified transcriptional regulators and their orthologues was performed to determine if they were previously described in association with ER and ER stress. Our analysis confirmed CREB3L2, ATF6, ATF4, ATF6B, TP53, EIF2AK3, XBP1, CREB3L1, and CREB3 (Figure 4A) were associated with ER and ER stress. Additionally, our analysis also suggested that transcription factors TAF9, ELK1, MYB, and NFATC3, which had a high NES value, were also associated with ER and ER stress (Figure 4B).

Discussion

Dystrophin deficiency causes multiple, deleterious changes to cellular processes and leads to oxidative stress, impaired calcium homeostasis, inflammation, and impaired autophagy. Disruption of cellular homeostasis may also result in accumulation of misfolded proteins and subsequent ER stress, which can lead to the activation of the UPR as well as inflammation and ultimately activation of cell death pathways (Hetz, 2012; Moorwood and Barton, 2014; Pauly et al., 2017; Afroze and Kumar, 2019; Gallot and Bohnert, 2021). The extent to which ER stress and the UPR occur in dystrophic muscle remain poorly understood. The purpose of this study was to better understand ER stress and the UPR in the emerging D2-mdx model and in human dystrophic skeletal muscles. Herein, we provide new evidence for ER stress and the UPR in a murine dystrophinopathy model and in human dystrophic muscle. Additionally, based on sequence and motif analysis from humans, we identified potential transcriptional regulators of ER stress and the UPR in dystrophic skeletal muscle.

The D2-mdx model is an emerging mouse model of DMD and may better recapitulate disease pathology and progression than other commonly used dystrophin-deficient mouse models (Putten et al., 2019; Spaulding et al., 2019; Hammers et al., 2020; Spaulding et al., 2020). The extent to which ER stress and the UPR are modified in the D2-mdx model is unclear, although ER stress and the UPR were previously described in the well-studied DMD model, the mdx mouse (Moorwood and Barton, 2014; Hulmi et al., 2016). Herein, we report that markers of ER stress and the UPR were upregulated in diaphragm from 11-month-old D2-mdx mice, in good agreement with findings in dystrophic muscle from mdx mice (Moorwood and Barton, 2014; Hulmi et al., 2016; Pauly et al., 2017). In dystrophic diaphragms from mdx mice, markers of ER stress and the UPR were increased, but these processes may be mediated in part by age or

10.3389/fphys.2023.1152576

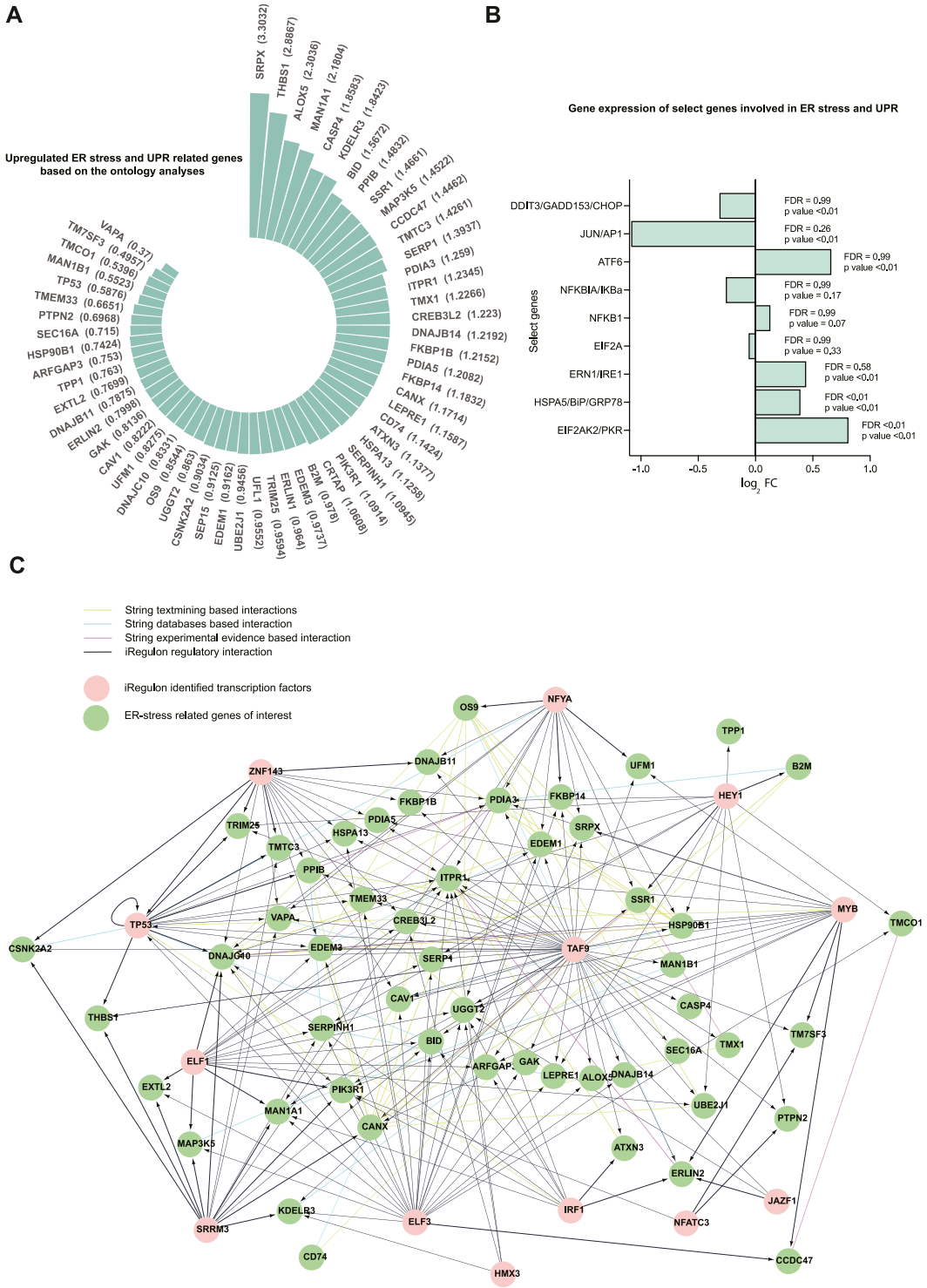

FIGURE 3
A total of 58 upregulated genes related to ER stress and the UPR were identified in the human Affymetrix chip data analyzed. **(A)** Fold changes (log_2 FC) for the 58 upregulated ER stress and UPR-related genes (FDR ranged from 2E-09 to 0.03). Differential expression was analyzed using the Limma package in R. The 58 genes were selected from the 24 GO processes that are related to ER stress and the UPR. **(B)** Representation of gene expression of select genes subsetted from the human Affymetrix chip data corresponding to the proteins immunoblotted in DBA and D2-mdx mice. **(C)** The network for the genes of interest and their transcriptional regulators is created using Cytoscape incorporating the String interactions (with a high interaction score of 0.7) and transcription factors identified using iRegulon (NES cutoff = 4). The top 13 transcriptional regulators are used.

TABLE 3 Putative transcription factors with their orthologues and target genes identified based on motif and track searches in iRegulon. Transcription factors with a normalized enrichment score (NES) > 3% and higher area under curve (AUC) are listed. The iRegulon analysis was performed on the 58 upregulated genes from the identified ER stress- and UPR-related processes.

Transcription factors	Target genes	NES	AUC
TAF9, CREB3L1, CREB3, XBP1, ATF6, ATF6B, CREB3L2	SERPINH1, SSR1, LEPRE1, FKBP14, KDELR3, CANX, THBS1, PDIA5, UBE2J1, DNAJC10, TMEM33, HSP90B1, MAN1A1, PPIB, TMX1, CAV1, FKBP1B, CSNK2A2, EDEM3, DNAJB11, BID, EDEM1, ALOX5, SERP1, TM7SF3, UGGT2	8.896	0.1161
CREB3L2	SERPINH1, LEPRE1, FKBP14, KDELR3, PDIA5, MAN1A1, CAV1, ARFGAP3, ALOX5	7.6388	0.1013
ZNF143, TP53	VAPA, TMTC3, EDEM3, ITPR1, DNAJC10, TP53, PDIA3, PIK3R1	5.7753	0.0792
ELF3, ELK1, GABPA, ERF, ELK3, ETV3, ETS1, ETV1, FEV, ERG, ELK4, FLI1, ETV5, ETV4, ETS2, GABPB1, ETV2, ELF1, ETV6, ELF4, ELF5	EDEM3, TMCO1, SERP1, UGGT2, TMEM33, EXTL2, TP53, ITPR1, PIK3R1, LEPRE1, DNAJC10, DNAJB14, MAP3K5, MAN1A1, HSPA13	4.9077	0.0689
CDX1, MYB, NFE2L1, TLX2, HNF1B, HNF1A, PAX4	ERLIN2, PIK3R1, CSNK2A2, ITPR1, UGGT2, CAV1, SRPX, MAN1A1, LEPRE1, DNAJC10	4.8236	0.0679
NFATC3, ZEB1	PTPN2, PIK3R1, TM7SF3	4.5491	0.0646
NFYC, NFYA, NFYB, HNF1B, HNF1A, POLE3	DNAJB11, FKBP14, HSP90B1, VAPA	4.3964	0.0628
SRRM3	MAN1A1, PIK3R1, MAP3K5, EXTL2, CSNK2A2	4.2415	0.061
HEY1	DNAJC10, TMCO1, LEPRE1, SERP1, B2M, UBE2J1, TPP1, TRIM25, PDIA3, SSR1, SERPINH1, HSP90B1, PTPN2	4.2012	0.0857
ELF1, NEUROD1, TAL1	UBE2J1, EDEM1, MAN1A1, PIK3R1, MAP3K5, SERPINH1, EDEM3, UGGT2, DNAJC10, CREB3L2, ITPR1, BID, ARFGAP3	4.1884	0.0604
HMX3, HMX1	ITPR1, CREB3L2, UGGT2, KDELR3	4.1485	0.0599
SPI1	ITPR1, MAP3K5, B2M, BID, EDEM3, PPIB, PTPN2, EDEM1	4.0795	0.0838
IRF1, IRF7, IRF8	MAN1A1, PIK3R1, ATXN3, BID	4.0688	0.059
JAZF1	ERLIN2, ITPR1, UGGT2	4.0556	0.0588
SPIB, SPI1, SPIC, ETV6, ELF5, ELK1, ETV7, ETS1, SIRT6, GABPB1, ELF4, ELF2, ELK4, FLI1, YY1, NFATC3, TCF4, TBP	BID, ALOX5, MAP3K5, HSPA13, DNAJC10, EDEM3, TMCO1, PIK3R1, ITPR1, CD74	3.9626	0.0577
CEBPG, CEBPB, CEBPE, CEBPD, TBP	TMEM33, CCDC47, CSNK2A2, TM7SF3, ERLIN2	3.9427	0.0575
HOXC13, HOXA13, HOXB13, HOXD13, HOXD12, HOXC10, HOXC12, HOXC11, HOXA11, HOXA10, CDX1, OVOL1	TM7SF3, ITPR1, PIK3R1, MAP3K5, CAV1, TMEM33	3.5244	0.0525
EBF1	ARFGAP3, ALOX5, TMX1, EDEM1, PTPN2, CREB3L2, UFM1, MAP3K5	3.4896	0.0745
POLR2A	TP53, B2M, TPP1, TRIM25, EXTL2	3.4463	0.0738
TFAP4, FOXO1, FOXA1	SERPINH1, KDELR3, CREB3L2, PIK3R1, ITPR1	3.3761	0.0507
GFI1,GFI1B	SERPINH1, TMEM33, TMTC3	3.365	0.0506
YY1	HSPA13, CANX, TP53, EDEM1, B2M	3.3413	0.0722
MAX	ATXN3, PDIA5, MAN1B1, ARFGAP3, CCDC47, TMEM33	3.2547	0.0708
TEAD4	THBS1, UGGT2, TMCO1, CAV1, TRIM25	3.2513	0.0708
HNF4A, NR2F1, NR2F2, HNF4G, RXRG, PPARG, RXRB, RXRA, NR2C2	TM7SF3, PIK3R1, CSNK2A2, MAN1A1, UFM1	3.2101	0.0488
HSF1, HSF4	PIK3R1, SERPINH1, CD74, TMEM33	3.0839	0.0473
GATA2, GATA5, ZNF217, GATA6, GATA4, GATA3, GATA1	ITPR1, TM7SF3, SRPX	3.0773	0.0472
MZF1	CANX, PPIB, PDIA3, GAK, MAN1B1, UGGT2, DNAJC10, SERP1, TRIM25, TMTC3, SSR1, LEPRE1, SRPX, PTPN2, OS9, EXTL2, TP53, B2M, VAPA, UBE2J1, CCDC47	3.0197	0.0671
RFX5	B2M, TPP1, CD74	3.0164	0.0671

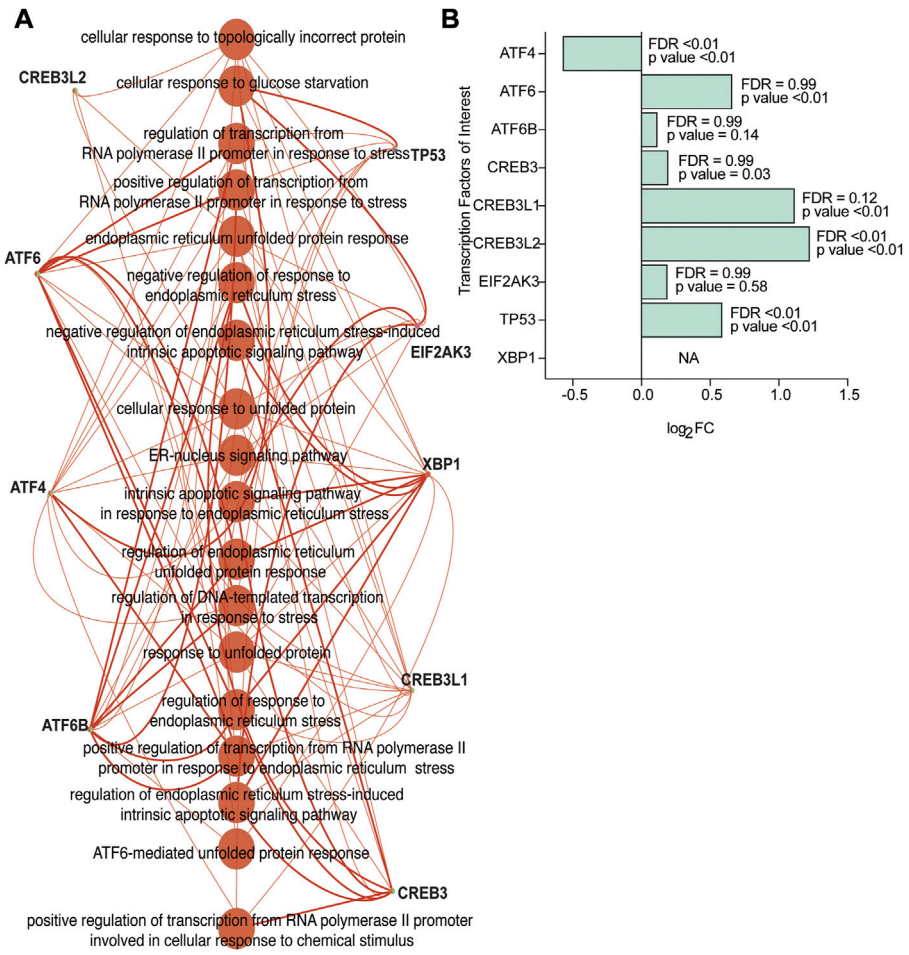

FIGURE 4
Transcriptional regulators from the human Affymetrix dataset confirmed as linked to ER stress and UPR-related processes. **(A)** The transcriptional regulators CREB3L2, ATF6, ATF4, ATF6B, TP53, EIF2AK3, XBP1, CREB3L1, and CREB3 correspond to ER-stress and UPR-related enriched processes based on gene ontology analysis on all the identified transcription factors, and orthologues (NES>3.00) identified using iRegulon. **(B)** Gene expression levels of the transcription factors of interest (based on a higher NES value and ontology analysis on transcription factors) subsetted from the human Affymetrix chip data analysis. FDR and *p*-values from differential expression using the Limma package are included.

disease progression. When viewed within this context, our data expand upon existing knowledge that indicates increased ER stress and the UPR have a more severe phenotype in the advanced disease model (D2-mdx mice) than in the less severe mdx model (Moorwood and Barton, 2014; Pauly et al., 2017). Moreover, and contrary to findings from studies reporting increased BiP/GRP78/HSPA5 in skeletal muscles from mdx mice (Moorwood and Barton, 2014; Pauly et al., 2017), we discovered BiP/GRP78/HSPA5 was decreased in diaphragms from D2-mdx mice likely due to age, genetic background, or advanced disease severity in animals used herein. Reduced expression of some ER chaperones with aging has been reported in skeletal muscle, suggestive of decreased ability to cope with ER stress (Ogata et al., 2009; Deldicque, 2013; O'Leary et al., 2013). These findings of increased ER stress and UPR due to the accumulation of misfolded proteins are complementary to our previous findings of an accumulation of autophagosomes in these dystrophic diaphragms (Krishna et al., 2021). It seems reasonable to suggest that an accumulation of damaged proteins and protein aggregates due to blunted autophagy, despite increased activation of calpain and proteasome systems (Selsby et al., 2010; Selsby et al., 2012; Hollinger and Selsby, 2013) is sufficient to cause ER stress and the UPR.

As a consequence of the UPR, eIF2α may be phosphorylated (S51) by a variety of kinases including PKR/EIF2AK2 and PERK, which antagonizes translation (Clemens, 2001). This flexibility supports our finding of increased peIF2α S51 despite similar pPERK T986 and decreased pPKR T446. Furthermore, PKR/EIF2AK2 regulates additional cell signaling and stress-related responses, including inflammatory signaling in response to ER stress (Gal-Ben-Ari et al., 2018). As increased activation of NFκB, as reported herein, is a hallmark of dystrophic muscle, these data raise the possibility that ER stress may contribute to this outcome. The associated elevation of the endogenous NFκB inhibitor, IκBα, may represent an attempt to limit inflammatory signaling despite the overwhelming pro-inflammatory muscle environment. Pharmacologic inhibition of ER stress in dystrophic muscle improved sarcoplasmic reticulum (SR)/ER-mitochondria interaction, calcium homeostasis, and muscle contractility (Pauly

et al., 2017), suggesting increased ER stress, or at least damage or dysfunction of the ER, is part of the disease sequala. Moreover, that disease severity was attenuated in a dystrophic mouse model following the knockout of caspase-12, an ER-specific caspase activated in muscles from mdx mice and humans with DMD (Moorwood and Barton, 2014), further supports this notion. Collectively, these studies raise the possibility of the therapeutic importance of ER stress- and UPR-related changes in DMD.

Despite a growing body of literature supporting ER stress and the UPR in dystrophic muscle from mouse models, human data is limited, to our knowledge, to increased relative abundance of cleaved caspase-4 and BiP in muscle from boys with DMD (Moorwood and Barton, 2014). Publicly available datasets from human dystrophic biopsies are an important resource to address novel research questions as they do not require new biopsies or experimentation, which may consume limited available tissue. Despite the paucity of human data for comparison, data presented in the present investigation are consistent with this previous report (Moorwood and Barton, 2014) in that processes related to ER stress and the UPR were upregulated. Specifically, within the transcriptomic dataset, we identified 58 upregulated genes related to ER stress and the UPR that were involved in processes associated with the disruption of calcium storage and release, protein folding and secretion, lipid biogenesis, and activation of ERAD, inflammation, and apoptosis in dystrophic muscles.

We also directly compared our protein expression data from D2-mdx mice to our gene expression data to identify commonalities. Although BiP/GRP78/HSPA5 protein abundance was decreased in D2-mdx mice and gene expression was similar in healthy and dystrophic human muscles, gene expression of BiP/GRP78/HSPA5 family member HSPA13A was increased in human dystrophic muscles. Likewise, HSP90B1, a molecular chaperone involved in quality control, protein folding, calcium homeostasis, and ERAD (Eletto et al., 2010), was upregulated by dystrophin deficiency. Distinct from the D2-mdx mice, CHOP/DDIT3/GADD153 was similar in healthy and dystrophin-deficient muscle from humans. PDIA5 and PDIA3, PDI genes that enable the formation of disulfide bonds and facilitate protein folding (Kranz et al., 2017; Adams et al., 2019), were upregulated in human dystrophic muscles. PTPN2, which regulates ER stress (Kasper et al., 2015), and, in concordance with previous findings (Moorwood and Barton, 2014), CASP4 expression were upregulated in human dystrophic muscles. Resolution to discordant expression of protein from D2-mdx mice and transcripts from boys with DMD will require further inquiry, but may be driven by differences in disease progression, animal type, and/or translation, among other factors.

To better understand the regulation of the genes involved in ER stress and the UPR in dystrophic muscles, we used iRegulon, a Cytoscape plugin based on motif detection and track discovery (Janky et al., 2014). Through the cis-regulatory sequence analyses in iRegulon (Janky et al., 2014), we identified transcriptional regulators of the genes of interest. Our approach revealed a total of 55 transcriptional regulators and orthologues at NES > 3.00. Among the putative transcription factors and orthologues identified, experimental evidence demonstrates that XBP1, ATF6, and CEBP are directly involved in the upregulation of UPR genes (Afroze and Kumar, 2019). In addition, the FOXO transcription factors (FOXO1 and FOXA1) were also identified in our analysis, and are well-known to regulate skeletal muscle homeostasis through their involvement in the modulation of energy homeostasis, proteolysis pathways, apoptosis, and regeneration (Sanchez et al., 2014; Parolo et al., 2018). Furthermore, based on predicted String interactions, the transcriptional regulators, TAF9, NFYA, and TP53, have previous experimental evidence of existing interactions between these transcriptional regulators and genes. These transcriptional regulators, to our knowledge, were not previously implicated in relation to ER stress in DMD. Interestingly, NFYA was previously identified as a regulator of regeneration and tissue repair (Musarò, 2020). Since ER stress and the UPR may also play a role in other myopathies, including LGMDs and Miyoshi myopathy (Ikezoe et al., 2003; Boito et al., 2007; Bohnert et al., 2018), findings reported herein may extend to a broader array of disease states.

In total, we provide novel evidence that dystrophin deficiency causes upregulation of ER stress and UPR markers in muscle from D2-mdx mice. Parallel to this important finding, we also demonstrated that similar alterations in ER stress and the UPR occur in human dystrophic muscle at the transcript level, and we identified key transcription factors, which appear to be involved in the regulation of these processes. We found that some genes are unpaired in terms of ER stress and UPR regulation in D2-mdx mice and human dystrophic skeletal muscles, requiring further studies to clarify the pattern of these events in the proposed experimental model. While acute activation of ER stress and the UPR and subsequent stimulation of proteolytic systems are likely a means to counter cell stress, it is likely that in dystrophic muscle chronic activation of ER stress and the UPR contributes to pathology, particularly as inhibition of ER stress via ablation of caspase-12 attenuates disease severity in mdx mice (Moorwood and Barton, 2014). Likewise, the therapeutic impact of calpain and proteasome inhibition are equivocal and collectively range from supportive of and antagonistic of cell health (Spencer and Mellgren, 2002; Gazzerro et al., 2010; Selsby et al., 2010; Selsby et al., 2012). It is reasonable to suggest that the UPR, autophagy, and proteolytic systems are entangled, however, their integrated responses to acute and chronic activation underscore the complexities of these systems and make clear that there are distinctions between outcomes driven acute and chronic activation. These data provide valuable insight regarding the regulation of ER stress in dystrophic muscle and support the possibility that strategies for maintenance of ER homeostasis may be of therapeutic importance.

Data availability statement

Publicly available datasets were analyzed in this study. This data can be found here: https://www.ncbi.nlm.nih.gov/geo/query/acc.cgi?acc=GSE38417. Affymetrix microarray data set accession ID: GSE38417 (alternate ID: EGEOD-38417).

Ethics statement

Ethical review and approval was not required for the study on human participants in accordance with the local legislation and

institutional requirements. Written informed consent from the participants' legal guardian/next of kin was not required to participate in this study in accordance with the national legislation and the institutional requirements. The animal study was reviewed and approved by the Institutional Animal Care and Use Committees at the University of Montana and the University of Florida.

Author contributions

JS, RV, and SK conceived the idea for this experiment. JS and JQ designed the animal experiment. Tissue collection was performed by HS and JQ. SK, JK, RV, and JS contributed to data collection, analysis, and interpretation. JS and SK drafted the manuscript. All authors contributed to manuscript revision and editing.

Funding

This work was funded in part by Michael's Cause and Ryan's Quest (JS and JQ) and Parent Project Muscular Dystrophy (JS and JQ).

Conflict of interest

The authors declare that the research was conducted in the absence of any commercial or financial relationships that could be construed as a potential conflict of interest.

Publisher's note

All claims expressed in this article are solely those of the authors and do not necessarily represent those of their affiliated organizations, or those of the publisher, the editors and the reviewers. Any product that may be evaluated in this article, or claim that may be made by its manufacturer, is not guaranteed or endorsed by the publisher.

Supplementary material

The Supplementary Material for this article can be found online at: https://www.frontiersin.org/articles/10.3389/fphys.2023.1152576/full#supplementary-material

References

Adams, C. J., Kopp, M. C., Larburu, N., Nowak, P. R., and Ali, M. M. U. (2019). Structure and molecular mechanism of ER stress signaling by the unfolded protein response signal activator IRE1. *Front. Mol. Biosci.* 6, 11. doi:10.3389/fmolb.2019.00011

Afroze, D., and Kumar, A. (2019). ER stress in skeletal muscle remodeling and myopathies. *FEBS J.* 286 (2), 379–398. doi:10.1111/febs.14358

Benjamini, Y., and Hochberg, Y. (1995). Controlling the false discovery rate: A practical and powerful approach to multiple testing. *J. R. Stat. Soc. Ser. B Methodol.* 57 (1), 289–300. doi:10.1111/j.2517-6161.1995.tb02031.x

Bindea, G., Mlecnik, B., Hackl, H., Charoentong, P., Tosolini, M., Kirilovsky, A., et al. (2009). ClueGO: A Cytoscape plug-in to decipher functionally grouped gene ontology and pathway annotation networks. *Bioinforma. Oxf. Engl.* 25 (8), 1091–1093. doi:10.1093/bioinformatics/btp101

Bohnert, K. R., McMillan, J. D., and Kumar, A. (2018). Emerging roles of ER stress and unfolded protein response pathways in skeletal muscle health and disease. *J. Cell Physiol.* 233 (1), 67–78. doi:10.1002/jcp.25852

Boito, C. A., Fanin, M., Gavassini, B. F., Cenacchi, G., Angelini, C., and Pegoraro, E. (2007). Biochemical and ultrastructural evidence of endoplasmic reticulum stress in LGMD2I. *Virchows Arch.* 451 (6), 1047–1055. doi:10.1007/s00428-007-0515-3

Chamberlain, J. S., Metzger, J., Reyes, M., Townsend, D., and Faulkner, J. A. (2007). Dystrophin-deficient mdx mice display a reduced life span and are susceptible to spontaneous rhabdomyosarcoma. *FASEB J.* 21 (9), 2195–2204. doi:10.1096/fj.06-7353com

Chen, Y. W., Nagaraju, K., Bakay, M., McIntyre, O., Rawat, R., Shi, R., et al. (2005). Early onset of inflammation and later involvement of TGFbeta in Duchenne muscular dystrophy. *Neurology* 65 (6), 826–834. doi:10.1212/01.wnl.0000173836.09176.c4

Clemens, M. J. (2001). Initiation factor eIF2 alpha phosphorylation in stress responses and apoptosis. *Prog. Mol. Subcell. Biol.* 27, 57–89. doi:10.1007/978-3-662-09889-9_3

Coley, W. D., Bogdanik, L., Vila, M. C., Yu, Q., Van Der Meulen, J. H., Rayavarapu, S., et al. (2016). Effect of genetic background on the dystrophic phenotype in mdx mice. *Hum. Mol. Genet.* 25 (1), 130–145. doi:10.1093/hmg/ddv460

De Palma, C., Morisi, F., Cheli, S., Pambianco, S., Cappello, V., Vezzoli, M., et al. (2012). Autophagy as a new therapeutic target in Duchenne muscular dystrophy. *Cell Death Dis.* 3 (11), e418–e410. doi:10.1038/cddis.2012.159

Deldicque, L. (2013). Endoplasmic reticulum stress in human skeletal muscle: Any contribution to sarcopenia? *Front. Physiol.* 4, 236. doi:10.3389/fphys.2013.00236

Dorsey, S., and Ward, C. (2016). "Gene expression data from Duchenne muscular dystrophy patients versus controls," in *BioStudies* (Cambridge: European Bioinformatics Institute).

Duan, D., Goemans, N., Takeda, S., Mercuri, E., and Aartsma-Rus, A. (2021). Duchenne muscular dystrophy. *Nat. Rev. Dis. Prim.* 7 (1), 13. doi:10.1038/s41572-021-00248-3

Ehmsen, J., Poon, E., and Davies, K. (2002). The dystrophin-associated protein complex. *J. Cell Sci.* 115 (14), 2801–2803. doi:10.1242/jcs.115.14.2801

Eletto, D., Dersh, D., and Argon, Y. (2010). GRP94 in ER quality control and stress responses. *Seminars Cell & Dev. Biol.* 21 (5), 479–485. doi:10.1016/j.semcdb.2010.03.004

Gal-Ben-Ari, S., Barrera, I., Ehrlich, M., and Rosenblum, K. (2018). Pkr: A kinase to remember. *Front. Mol. Neurosci.* 11, 480. doi:10.3389/fnmol.2018.00480

Gallot, Y. S., and Bohnert, K. R. (2021). Confounding roles of ER stress and the unfolded protein response in skeletal muscle atrophy. *Int. J. Mol. Sci.* 22 (5), 2567. doi:10.3390/ijms22052567

Gazzerro, E., Assereto, S., Bonetto, A., Sotgia, F., Scarfì, S., Pistorio, A., et al. (2010). Therapeutic potential of proteasome inhibition in Duchenne and Becker muscular dystrophies. *Am. J. Pathol.* 176 (1525-2191), 1863–1877. doi:10.2353/ajpath.2010.090468

Grounds, M. D., Radley, H. G., Lynch, G. S., Nagaraju, K., and De Luca, A. (2008). Towards developing standard operating procedures for pre-clinical testing in the mdx mouse model of Duchenne muscular dystrophy. *Neurobiol. Dis.* 31 (1), 1–19. doi:10.1016/j.nbd.2008.03.008

Hammers, D. W., Hart, C. C., Matheny, M. K., Wright, L. A., Armellini, M., Barton, E. R., et al. (2020). The D2.mdx mouse as a preclinical model of the skeletal muscle pathology associated with Duchenne muscular dystrophy. *Sci. Rep.* 10 (1), 14070. doi:10.1038/s41598-020-70987-y

Hetz, C. (2012). The unfolded protein response: Controlling cell fate decisions under ER stress and beyond. *Nat. Rev. Mol. Cell Biol.* 13 (2), 89–102. doi:10.1038/nrm3270

Hetz, C., Zhang, K., and Kaufman, R. J. (2020). Mechanisms, regulation and functions of the unfolded protein response. *Nat. Rev. Mol. Cell Biol.* 21 (8), 421–438. doi:10.1038/s41580-020-0250-z

Hoffman, E. P., Brown, R. H., and Kunkel, L. M. (1987). Dystrophin: The protein product of the duchenne muscular dystrophy locus. *Cell* 51 (6), 919–928. doi:10.1016/0092-8674(87)90579-4

Hollinger, K., and Selsby, J. T. (2013). The physiological response of protease inhibition in dystrophic muscle. *Acta Physiol. (Oxf)* 208 (3), 234–244. doi:10.1111/apha.12114

Hulmi, J. J., Hentila, J., DeRuisseau, K. C., Oliveira, B. M., Papaioannou, K. G., Autio, R., et al. (2016). Effects of muscular dystrophy, exercise and blocking activin receptor IIB ligands on the unfolded protein response and oxidative stress. *Free Radic. Biol. Med.* 99, 308–322. doi:10.1016/j.freeradbiomed.2016.08.017

Ikezoe, K., Furuya, H., Ohyagi, Y., Osoegawa, M., Nishino, I., Nonaka, I., et al. (2003). Dysferlin expression in tubular aggregates: Their possible relationship to endoplasmic reticulum stress. *Acta Neuropathol.* 105 (6), 603–609. doi:10.1007/s00401-003-0686-1

Janky, R. s., Verfaillie, A., Imrichová, H., Van de Sande, B., Standaert, L., Christiaens, V., et al. (2014). iRegulon: From a gene list to a gene regulatory network using large motif and track collections. *PLOS Comput. Biol.* 10 (7), e1003731. doi:10.1371/journal.pcbi.1003731

Koenig, M., Hoffman, E. P., Bertelson, C. J., Monaco, A. P., Feener, C., and Kunkel, L. M. (1987). Complete cloning of the duchenne muscular dystrophy (DMD) cDNA and preliminary genomic organization of the DMD gene in normal and affected individuals. *Cell* 50 (3), 509–517. doi:10.1016/0092-8674(87)90504-6

Kranz, P., Neumann, F., Wolf, A., Classen, F., Pompsch, M., Ocklenburg, T., et al. (2017). PDI is an essential redox-sensitive activator of PERK during the unfolded protein response (UPR). *Cell Death Dis.* 8 (8), e2986. doi:10.1038/cddis.2017.369

Krishna, S., Spaulding, H. R., Quindry, T. S., Hudson, M. B., Quindry, J. C., and Selsby, J. T. (2021). Indices of defective autophagy in whole muscle and lysosome enriched fractions from aged D2-mdx mice. *Front. Physiol.* 12, 691245. doi:10.3389/fphys.2021.691245

Mah, J. K., Korngut, L., Dykeman, J., Day, L., Pringsheim, T., and Jette, N. (2014). A systematic review and meta-analysis on the epidemiology of Duchenne and Becker muscular dystrophy. *Neuromuscul. Disord.* 24 (6), 482–491. doi:10.1016/j.nmd.2014.03.008

Mendell, J. R., Shilling, C., Leslie, N. D., Flanigan, K. M., al-Dahhak, R., Gastier-Foster, J., et al. (2012). Evidence-based path to newborn screening for Duchenne muscular dystrophy. *Ann. Neurol.* 71 (3), 304–313. doi:10.1002/ana.23528

Moorwood, C., and Barton, E. R. (2014). Caspase-12 ablation preserves muscle function in the mdx mouse. *Hum. Mol. Genet.* 23 (20), 5325–5341. doi:10.1093/hmg/ddu249

Morris, C. A., Selsby, J. T., Morris, L. D., Pendrak, K., and Sweeney, H. L. (2010). Bowman-Birk inhibitor attenuates dystrophic pathology in mdx mice. *J. Appl. physiology (Bethesda, Md, 1985)* 109(5), 1492–1499. doi:10.1152/japplphysiol.01283.2009

Musarò, A. (2020). Muscle homeostasis and regeneration: From molecular mechanisms to therapeutic opportunities. *Cells* 9 (9), 2033. doi:10.3390/cells9092033

O'Leary, M. F., Vainshtein, A., Iqbal, S., Ostojic, O., and Hood, D. A. (2013). Adaptive plasticity of autophagic proteins to denervation in aging skeletal muscle. *Am. J. Physiol. Cell Physiol.* 304 (5), C422–C430. doi:10.1152/ajpcell.00240.2012

Ogata, T., Machida, S., Oishi, Y., Higuchi, M., and Muraoka, I. (2009). Differential cell death regulation between adult-unloaded and aged rat soleus muscle. *Mech. Ageing Dev.* 130 (5), 328–336. doi:10.1016/j.mad.2009.02.001

Parolo, S., Marchetti, L., Lauria, M., Misselbeck, K., Scott-Boyer, M. P., Caberlotto, L., et al. (2018). Combined use of protein biomarkers and network analysis unveils deregulated regulatory circuits in Duchenne muscular dystrophy. *PLoS One* 13 (3), e0194225. doi:10.1371/journal.pone.0194225

Pauly, M., Angebault-Prouteau, C., Dridi, H., Notarnicola, C., Scheuermann, V., Lacampagne, A., et al. (2017). ER stress disturbs SR/ER-mitochondria Ca2+ transfer: Implications in Duchenne muscular dystrophy. *Biochimica Biophysica Acta (BBA) - Mol. Basis Dis.* 1863 (9), 2229–2239. doi:10.1016/j.bbadis.2017.06.009

Petrof, B. J., Shrager, J. B., Stedman, H. H., Kelly, A. M., and Sweeney, H. L. (1993). Dystrophin protects the sarcolemma from stresses developed during muscle contraction. *Proc. Natl. Acad. Sci. U. S. A.* 90 (8), 3710–3714. doi:10.1073/pnas.90.8.3710

Putten, M. v., Putker, K., Overzier, M., Adamzek, W. A., Pasteuning-Vuhman, S., Plomp, J. J., et al. (2019). Natural disease history of the D2-mdx mouse model for Duchenne muscular dystrophy. *FASEB J.* 33 (7), 8110–8124. doi:10.1096/fj.201802488R

Ritchie, M. E., Phipson, B., Wu, D., Hu, Y., Law, C. W., Shi, W., et al. (2015). Limma powers differential expression analyses for RNA-sequencing and microarray studies. *Nucleic Acids Res.* 43 (7), e47. doi:10.1093/nar/gkv007

Ryder, S., Leadley, R. M., Armstrong, N., Westwood, M., de Kock, S., Butt, T., et al. (2017). The burden, epidemiology, costs and treatment for duchenne muscular dystrophy: An evidence review. *Orphanet J. Rare Dis.* 12 (1), 79. doi:10.1186/s13023-017-0631-3

Sanchez, A. M. J., Candau, R. B., and Bernardi, H. (2014). FoxO transcription factors: Their roles in the maintenance of skeletal muscle homeostasis. *Cell. Mol. Life Sci.* 71 (9), 1657–1671. doi:10.1007/s00018-013-1513-z

Selsby, J., Morris, C., Morris, L., and Sweeney, L. (2012). A proteasome inhibitor fails to attenuate dystrophic pathology in mdx mice. *PLoS Curr.* 4, e4f84a944d8930. doi:10.1371/4f84a944d8930

Selsby, J., Pendrak, K., Zadel, M., Tian, Z., Pham, J., Carver, T., et al. (2010). Leupeptin-based inhibitors do not improve the mdx phenotype. *Am. J. Physiol. Regul. Integr. Comp. Physiol.* 299 (5), R1192–R1201. doi:10.1152/ajpregu.00586.2009

Selsby, J. T. (2011). Increased catalase expression improves muscle function in mdx mice. *Exp. Physiol.* 96 (2), 194–202. doi:10.1113/expphysiol.2010.054379

Spaulding, H. R., Kelly, E. M., Quindry, J. C., Sheffield, J. B., Hudson, M. B., and Selsby, J. T. (2018). Autophagic dysfunction and autophagosome escape in the mdx mus musculus model of Duchenne muscular dystrophy. *Acta Physiol.* 222 (2), 129444–e13011. doi:10.1111/apha.12944

Spaulding, H. R., Quindry, T., Hammer, K., Quindry, C. J., and Selsby, J. T. (2019). Nutraceutical and pharmaceutical cocktails did not improve muscle function or reduce histological damage in D2-mdx mice. *J. Appl. Physiology* 127 (4), 1058–1066. doi:10.1152/japplphysiol.00162.2019

Spaulding, H. R., Quindry, T., Quindry, C. J., and Selsby, J. T. (2020). Nutraceutical and pharmaceutical cocktails did not preserve diaphragm muscle function or reduce muscle damage in D2-mdx mice. *Exp. Physiol.* 105 (6), 989–999. doi:10.1113/EP087887

Spencer, M. J., and Mellgren, R. L. (2002). Overexpression of a calpastatin transgene in mdx muscle reduces dystrophic pathology. *Hum. Mol. Genet.* 11 (0964-6906), 2645–2655. doi:10.1093/hmg/11.21.2645

Spitali, P., Grumati, P., Hiller, M., Chrisam, M., Aartsma-Rus, A., and Bonaldo, P. (2013). Autophagy is impaired in the tibialis anterior of dystrophin null mice. *PLoS Curr.* 5, 1–11. doi:10.1371/currents.md.e1226cefa851a2f079bbc406c0a21e80

Stedman, H. H., Sweeney, H. L., Shrager, J. B., Maguire, H. C., Panettieri, R. A., Petrof, B., et al. (1991). The mdx mouse diaphragm reproduces the degenerative changes of Duchenne muscular dystrophy. *Nature* 352, 536–539. doi:10.1038/352536a0

Szklarczyk, D., Gable, A. L., Nastou, K. C., Lyon, D., Kirsch, R., Pyysalo, S., et al. (2021). Correction to 'the STRING database in 2021: Customizable protein-protein networks, and functional characterization of user-uploaded gene/measurement sets'. *Nucleic Acids Res.* 49, 10800–14962. doi:10.1093/nar/gkab835

Team, R. C. (2021). *R: A language and environment for statistical computing*. Vienna, Austria: R Foundation for Statistical Computing.

Walter, P., and Ron, D. (2011). The unfolded protein response: From stress pathway to homeostatic regulation. *Science* 334 (6059), 1081–1086. doi:10.1126/science.1209038

Yucel, N., Chang, A. C., Day, J. W., Rosenthal, N., and Blau, H. M. (2018). Humanizing the mdx mouse model of DMD: The long and the short of it. *npj Regen. Med.* 3 (1), 4. doi:10.1038/s41536-018-0045-4

Glossary

AP1	Activator protein 1
ATF4	Activating transcription factor 4
ATF6	Activating transcription factor 6
BCA	Bicinchoninic acid
BiP	Binding-immunoglobulin protein
CEBP	CCAAT-enhancer-binding proteins
CHOP	C/EBP homologous rotein
CREB3	Cyclic-AMP response element binding protein 3
CREB3L1	Cyclic-AMP response element binding protein 3L1
CREB3L2	Cyclic-AMP response element binding protein 3L2
DDIT3	DNA damage inducible transcript 3
EIF2AK2	Eukaryotic translation initiation factor 2 alpha kinase 2
EIF2AK3	Eukaryotic translation initiation factor 2 alpha kinase 3
eIF2α	Eukaryotic translation initiation factor 2 alpha
ERK	Extracellularly regulated kinases
FOXA1	Forkhead
FOXO	Forkhead box O
FOXO1	Forkhead box O1
GADD153	Growth arrest and DNA damage-inducible gene
GCN2	General control non-derepressible 2
GRP78	78 kDa glucose-regulated protein
HRI	Heme-regulated inhibitor
HSP90B1	Heat shock 70 kDa protein 90B1
HSPA13A	Heat shock 70 kDa protein 13 A
HSPA5	Heat shock 70 kDa protein 5
IRE1α	Inositol-requiring enzyme 1alpha
JNK	C-Jun N-terminal kinase
LGMD	Limb girdle muscular dystrophy
NFYA	Nuclear transcription factor Y subunit alpha
NFκB	Nuclear factor of kappa light polypeptide gene enhancer in B-cells
PDIA3	Protein disulfide isomerase family A member 6
PDIA5	Protein disulfide isomerase family A member 5
PKR	Protein kinase R
PTPN2	Protein tyrosine phosphatase non-receptor type 2
SDS	Sodium dodecyl sulfate
TAF9	TATA box binding protein (TBP)-associated factor 9
TP53	Tumor protein 53
XBP1	X-box binding protein 1

frontiers | Frontiers in Physiology

TYPE Original Research
PUBLISHED 09 May 2023
DOI 10.3389/fphys.2023.1190524

OPEN ACCESS

EDITED BY
Katsumasa Goto,
Toyohashi Sozo University, Japan

REVIEWED BY
Congshan Sun,
Johns Hopkins University, United States
Chrissa Kioussi,
Oregon State University, United States

*CORRESPONDENCE
April D. Pyle,
apyle@mednet.ucla.edu

RECEIVED 21 March 2023
ACCEPTED 17 April 2023
PUBLISHED 09 May 2023

CITATION
Saleh KK, Switzler C, Hicks MR, Gane L, Gibbs DE and Pyle AD (2023), Duchenne muscular dystrophy disease severity impacts skeletal muscle progenitor cells systemic delivery.
Front. Physiol. 14:1190524.
doi: 10.3389/fphys.2023.1190524

Duchenne muscular dystrophy disease severity impacts skeletal muscle progenitor cells systemic delivery

Kholoud K. Saleh[1,2], Corey Switzler[1], Michael R. Hicks[1,2], Lily Gane[1,2], Devin E. Gibbs[1,2,3] and April D. Pyle[1,2,3]*

[1]Department of Microbiology, Immunology and Molecular Genetics, University of California Los Angeles, Los Angeles, CA, United States, [2]Eli and Edythe Broad Center of Regenerative Medicine and Stem Cell Research, University of California Los Angeles, Los Angeles, CA, United States, [3]Molecular Biology Institute, University of California Los Angeles, Los Angeles, CA, United States

Duchenne muscular dystrophy (DMD) is caused by an out-of-frame mutation in the DMD gene that results in the absence of a functional dystrophin protein, leading to a devastating progressive lethal muscle-wasting disease. Muscle stem cell-based therapy is a promising avenue for improving muscle regeneration. However, despite the efforts to deliver the optimal cell population to multiple muscles most efforts have failed. Here we describe a detailed optimized method of for the delivery of human skeletal muscle progenitor cells (SMPCs) to multiple hindlimb muscles in healthy, dystrophic and severely dystrophic mouse models. We show that systemic delivery is inefficient and is affected by the microenvironment. We found that significantly less human SMPCs were detected in healthy gastrocnemius muscle cross-sections, compared to both dystrophic and severely dystrophic gastrocnemius muscle. Human SMPCs were found to be detected inside blood vessels distinctly in healthy, dystrophic and severely dystrophic muscles, with prominent clotting identified in severely dystrophic muscles after intra arterial (IA) systemic cell delivery. We propose that muscle microenvironment and the severity of muscular dystrophy to an extent impacts the systemic delivery of SMPCs and that overall systemic stem cell delivery is not currently efficient or safe to be used in cell based therapies for DMD. This work extends our understanding of the severe nature of DMD, which should be taken into account when considering stem cell-based systemic delivery platforms.

KEYWORDS

skeletal muscle, systemic delivery, duchenne muscular dystrophy, skeletal muscle progenitor cells, intra-arterial cell delivery

1 Introduction

Duchenne Muscular Dystrophy (DMD) is a genetic disease characterized by progressive muscle degeneration and weakness due to the absence of dystrophin protein. Without dystrophin, the sarcolemma is rendered fragile and compromised causing the muscle fibers to go through progressive rounds of contraction-induced damage, and Ca^{2+} influx into the muscle fiber which results in cell death. In DMD, continuous cycles of contraction-induced damage elicit a constant need for regeneration. However, it has been suggested that there is impaired regeneration because either the muscle stem cell population, satellite cells (SCs), are

rendered dysfunctional due to impaired polarity establishment or because of progressive exhaustion (Webster and Blau, 1990; Sacco et al., 2010; Dumont et al., 2015). Eventually, lack of proper regeneration leads to muscle fiber necrosis and generation of excess fibrotic tissue (Klingler et al., 2012).

Cell-based therapies were proposed for DMD by transplantation of myoblasts in which the enthusiasm of restoring dystrophin in the mdx mouse model by intra-muscular (IM) myoblast transplantation, resulted in 4 clinical trials in humans, that ultimately all failed to restore sufficient dystrophin to provide functional benefit (Partridge et al., 1989; Law et al., 1991; Gussoni et al., 1992; 1997; Huard et al., 1992; Karpati et al., 1993; Miller et al., 1997). The systemic delivery of various myogenic cell types to DMD muscles have been reported including mesoangioblasts, DLL4 and PDGF-BB treated satellite cells, skeletal muscle-derived CD133+ cells, and induced *Pax3* embryonic stem cell derived cells among others (Guttinger et al., 2006; Sampaolesi et al., 2006; Darabi et al., 2008; Tedesco et al., 2011; Sitzia et al., 2016; Gerli et al., 2019; Ausems et al., 2021). An overlooked parameter in developing systemic cell therapeutics is the context of disease severity and the diseased microenvironment. Genetic modifiers that regulate disease severity in the mdx mouse model is affected by the genetic background. Once the mdx mouse model is crossed to the DBA/2 genetic background, creating the mdxD2 strain, the mice exhibit increased fat and fibrosis deposition, muscle weakness, reduced skeletal muscle function, and fewer central myonuclei indicating the increased severity of dystrophy phenotype (Fukada et al., 2010; Coley et al., 2016). Thus, the mdxD2 mouse model better recapitulates the human disease and is useful in evaluating therapies for DMD. We have previously shown the complexity of muscle environment as DMD disease severity increases in mdx-NSG and mdxD2-NSG mice (Saleh et al., 2022). In this work, the mdx SCID mouse model was crossed with the severely immunocompromised mouse model NSG to generate mdx-NSG model. Moreover, the mdxD2 mouse was crossed with NSG to generate mdxD2-NSG mouse model. Mutations in the NSG mouse model renders B cells, T cells and natural killer cells deficient. These DMD severely immunocompromised mouse models are ideal for stem cell engraftment studies and cell delivery assessment as they permit evaluation of stem cell engraftment without the potential for immune-rejection of human cells.

Here we describe a detailed protocol to deliver human skeletal muscle progenitor cells (SMPCs) from fetal week 18 muscles to multiple hindlimb muscles in immunocompromised healthy, wt-NSG, dystrophic, mdx-NSG, and severely dystrophic, mdxD2-NSG, mouse models using intra-arterial (IA) delivery. This protocol has been optimized from other published protocols in two aspects, restoring blood flow into the artery after cell injection, and delivering the cells using a pump to maintain constant flow rate during cell delivery (Gerli et al., 2014; Matthias et al., 2015). We further investigated the detection and localization of SMPCs by quantifying the cells in at least 16 cross-sections taken across the length of the gastrocnemius muscles. We found overall that systemic delivery of SMPCs was inefficient in all models. However, significantly less human SMPCs were detected in wt-NSG gastrocnemius muscle cross-sections, compared to both mdx-NSG and mdxD2-NSG. Human SMPCs were found to be detected inside blood vessels distinctly in healthy, dystrophic and severely dystrophic muscles, with prominent clotting identified in mdxD2-NSG after IA systemic cell delivery. We propose that muscle microenvironment and the severity of muscular dystrophy to an extent impacts the systemic delivery of SMPCs and that overall systemic stem cell delivery is not currently efficient or safe to be used in cell based therapies for DMD.

2 Materials and methods

2.1 Institutional permissions

Human fetal muscle tissues were obtained from the University of California Los Angeles (UCLA) Center for AIDS Research (CFAR) Gene and Cellular Therapy Core and Advanced Bioscience Resources (ABR). Use of human tissues was institutional review board-approved by the UCLA Office of the Human Research Protection Program. Human fetal tissue work is IRB exempt. The work was reviewed and approved as exempt with IRB #20-000197 and IRB #15-000959. All animal work was conducted under protocols approved by the UCLA Animal Research Committee (ARC) (ARC-2006-119). Animals used in this study were housed in an immunocompromised core facility.

2.2 Animals

Animals used in this study were housed in UCLA Humanized Mouse Core, an immunocompromised core facility. C57BL/6 mice were crossed with NSG mice to generate C57-NSG mice (referred to as wt-NSG). mdx-NSG mice: mdx/C57BL/10 mice were crossed to NSG mice to generate mdx-NSG mice. mdxDBA2 mice were a generous gift from Dr. Melissa Spencer, UCLA, and were crossed to NSG mice to generate mdxD2-NSG mice. Pax7-Zsgreen mice were purchased from The Jackson Laboratory (#029549) and bred in house. Pups were genotyped using TransnetYX to ensure allele mutations. All animals used in this study were backcrossed to the original C57Bl/6 and mdxC57Bl/10 backgrounds for at least five generations.

2.3 Human muscle digestion

Muscles were first washed with 10% fetal bovine serum (FBS) in DMEM/F12% and 0.5% penicillin/streptomycin (P/S) for 10 min. The muscles were then finely chopped in digestion buffer consisting of 5% FBS in DMEM/F12, 0.5% P/S, 0.5% amphotericin (Ampho), 1 mg/ml collagenase II and 1 mg/ml dispase. The suspension was then incubated in 37°C on a shaker for 20–25 min, with intermittent trituration with 5 ml serological pipette. Once incubation time was over, 10% FBS wash buffer was added to the digested muscle to stop enzymatic digestion and the suspension spun at 2000 rpm at 10°C for 5 min. Then the supernatant was discarded and pellet was resuspended with sort buffer consisting of PBS -Mg^{2+}/Ca^{2+}, 1.5%–2% FBS and 0.5% P/S. The suspension was then passed through first 100 µm, then 70 µm and finally a 40 µm filters. The suspension was then spun at 2000 rpm at 10°C for 5 min and the pellet was resuspended with 5–6 ml of sort buffer. Cells were counted and blocked with Human TruStain FcX, then incubated with conjugated antibodies against CD31, CD235a, CD45, CD73, PDGFRα, CD11b and viability dye for 30 min. Lineage depleted cells were then sorted at UCLA Broad Stem Cell Research Center Flow Cytometry Core. Negatively depleted cells were then spun down at 1500 rpm for 5 min at room temperature, the pellet resuspended in

SKGM-2 supplemented with 20 ng/ml bFGF and cultured overnight in 6 well plate, incubated for 60 min with matrigel (1 million counted cells/well). The cells were dissociated with TrypLE (Thermo Fisher) the following day for IA delivery or qRT-PCR quantification. Human fetal tissue was obtained from ABR and is IRB exempt. The work was reviewed and approved as exempt with IRB #20-000197.

2.4 Quantitative real time-PCR

Overnight cultured SMPCs were dissociated with TrypLE and RNA was extracted using the RNeasy Plus Micro Kit (Qiagen). cDNA was synthesized using the iScript Reverse Transcription Supermix (Bio-Rad) and quantitative RT-PCR was performed using SsoAdvanced Universal SYBR Green Supermix (Bio-Rad) with technical triplicates on a Thermo Fisher Scientific QuantStudio 6 Pro Real-Time PCR system or a CFX384 Touch Real-Time PCR Detection system (Bio-Rad). Primers used in this study are previously described in (Xi et al., 2017).

2.5 Intravenous cell delivery

Human SMPCs were isolated as previously described, with a change in the sorting strategy. ERBB3 and NGFR positive cells were sorted and propagated for a week before their IV tail vein injection. Mice were sacrificed 48 h after cell delivery.

2.6 Intra-arterial cell delivery protocol

Before cell delivery we included a 45-min downhill exercise regimen similar to described (Mathur et al., 2011) to induce muscle injury in the lower hindlimbs of mice before systemic SMPCs delivery. SMPCs can delivered through the femoral artery of either the left or right leg of the mouse. During the surgery, the mouse needs to be kept on a heating pad. All equipment used should be sterilized by wiping with 70% ethanol. Surgical tools need to be autoclaved the day before the surgery. A hot bead sterilizer was used to sterilize the surgical tools between mice. With an experienced hand, the surgery may take between 45 min to 1 h. The surgery should be done under the microscope in a biohazard BSL class II cabinet, to ensure the maintenance of sterility. It is important to prepare a cage with a heating pad under it to warm up the bedding for the recovering mouse after the surgery. Typically, 800K-1M cells were IA delivered/mouse. Cell dissociation was performed ahead the start of surgery of each mouse. The surgery was performed by making an incision at the inguinal region on the right hindlimb parallel to the femoral vascular bundle, and the femoral vascular bundle is exposed. The femoral artery is then isolated, two 6–0 sutures are passed under it, and one suture is used to obstruct blood flow, upstream of the injection site. In a proximal location to the body, a small cut is made in the femoral artery using a 32 G needle. A 32 G catheter is then inserted (cannulation site) into the femoral artery. Using a pump one million dissociated SMPCs (cultured overnight) are delivered at a flow rate of 50 ul/min in a volume of 100–150 µl of HBSS. After the cell injection, saline is flushed through the catheter to deliver any remaining cells in the catheter. The catheter then is retracted slowly, and while obstructing blood flow upstream of the injection site, a cautery is used to seal the femoral artery at the cannulation site. After sealing the femoral artery and removing the suture obstructing the blood flow, blood should be seen flushing again through the femoral artery. The opened incision area is filled with saline and the incision is sutured using a 5–0 absorbable suture. Mice are monitored after the surgery and kept in cages over a heating pad for recovery. Mice are provided with Carprofen 5 mg/kg of body weight. After 48 h mice were sacrificed and their lungs and muscles were collected and embedded in OCT and frozen in isopentane cooled in liquid nitrogen. Surgeries were performed on $n = 3$ mice/mouse model for human SMPCs delivery with about 800 K- 1 M cells delivered/mouse. For Zsgreen satellite cells delivery, cells were delivered after sorting and about 50k cells were delivered in each mouse.

2.7 Digital droplet PCR

Alternative sections were collected from muscles and lungs, and genomic DNA was isolated using the zymogen Quick DNA MiniPrep kit according to manufacturer instructions. Samples then were provided for the CFAR Virology Core Lab and Tissue Culture/PCR Facility for further ddPCR processing.

2.8 Immunofluorescence staining

Frozen muscles embedded in OCT were serially sectioned at 10 µm thick cryosections. A hydrophobic barrier was drawn around sections, then washed with 0.1% Tween in PBS (PBST). The sections were then fixed with 4% PFA for 10 min. A permeabilization step, if necessary, followed by washing with 0.3% Triton X-100 in PBS at room temperature for 10 min. Sections were then blocked with 0.25% Gelatin, 0.1% Tween, 3% bovine serum albumin (BSA) and 10% goat serum (GS) in distilled water for 60 min at room temperature. Sections were then incubated in humidified chambers with primary antibodies overnight at 4°C in 0.25% gelatin, 0.1% Tween, 3% BSA and 1% GS. Sections were next incubated for 60 min with fluorophore-conjugated secondary antibodies diluted in PBS and 1% goat serum. DAPI vecatshield mounting media was then used to counterstain nuclei, coverslips were applied and nail polish was used to seal the coverslips. Images were captured using a Zeiss Axio Observer. Z1 microscope equipped with an AxioCamMR3 camera.

2.9 Imaris quantification

At least 16–18 cross-sectional areas along the depth of the gastroc muscle were used for human cells (LaminA/C+ nuclei) quantification in each mouse (n = 3 wt-NSG, n = 3 mdx-NSG and n = 3 mdxD2-NSG) after IA cell delivery. Tile images (at 20X) of each cross-section were captured by Zeiss Axio Observer. Z1 microscope equipped with an AxioCamMR3 with Zen (2.6) blue edition. Zen files with Czi extension were converted and stitched in Imaris File Converter and Imaris Stitcher to an ims format. Images were then analyzed in Imaris software version 9.6 where each image included an endothelial cell marker (CD31-488), human cell marker (LaminA/C-568) and DAPI. Spots feature was used to quantify human cells on the 568 channel, surface feature was used to quantify blood vessels with areas >100 µm^2 on the 488 channel, and then the object-object statistics was used to count the number of human cells

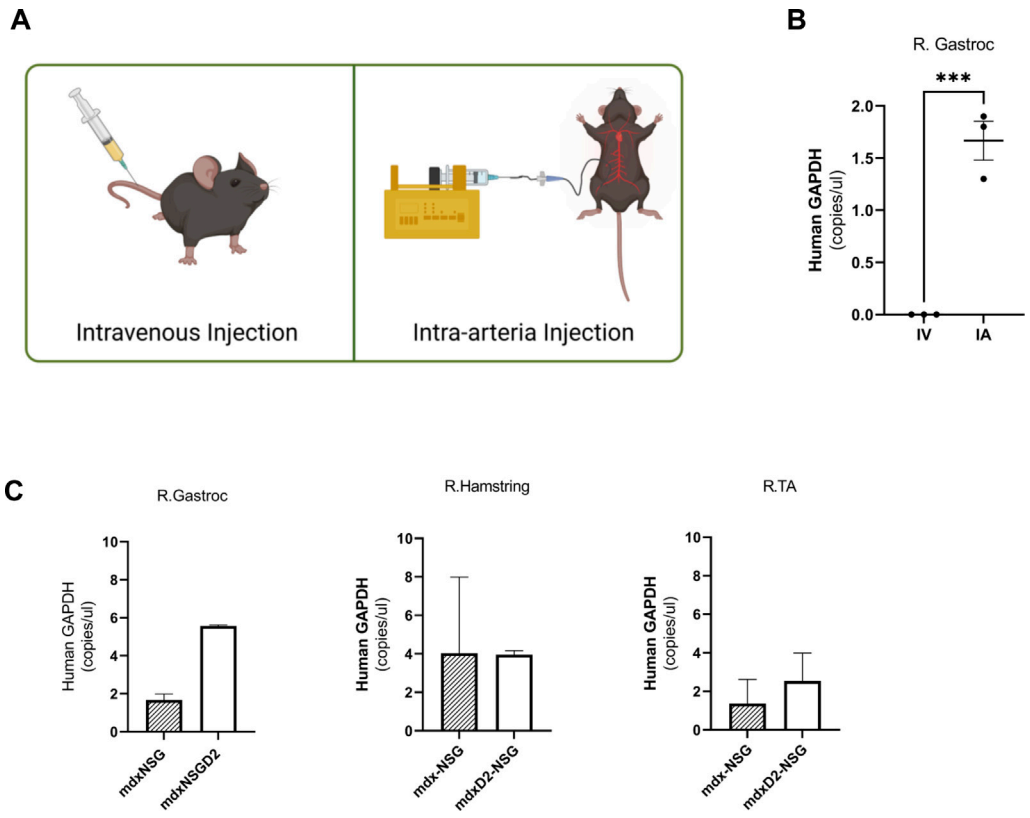

FIGURE 1
Intra-arterial cell delivery route improves delivery of human skeletal muscle progenitor cells to lower hindlimb gastrocnemius muscle. **(A)** Intravenous (IV) injection is performed by tail vein injection while intra-arterial (IA) cell delivery is performed by injecting the cells into the femoral artery of either the right or left hindlimb. **(B)** Human specific-GAPDH concentration measured in homogenized cross sections in mdx-NSG right gastrocnemius muscle (R. Gastroc) after IV and IA delivery utilizing digital droplet polymerase chain reaction. Alternative sections were collected for gDNA isolation, error bars showing mean ± SD. **(C)** Human specific-GAPDH concentration measured in homogenized cross sections of mdx-NSG and mdxD2-NSG right hindlimb muscles (where IA surgery was performed). Error bars showing mean + SD.

inside specified blood vessels. Quantification is shown as mean + SD, One way ANOVA with Tukey's multiple comparisons was used to compare the means of cells detected inside large vessels in wt-NSG, mdx-NSG and mdxD2-NSG.

3 Results

3.1 Optimized intra-arterial cell delivery protocol to lower hindlimb muscles

Lineage depleted SMPCs derived from FW 18 muscles were differentiated *in vitro* for 5 days in N2 media to validate their myogenic potential (Supplementary Figures S1A, B). We explored two routes of delivery of human SMPCs to lower hindlimb muscles, the first is an intravenous route (IV) where cells were injected into the tail vain of mice, and the second is intra-arterial (IA) where cells were delivered at a flow to the femoral artery (Figure 1A). We evaluated SMPC delivery by measuring human-specific GAPDH in muscle cross-sections using digital droplet polymerase chain reaction (ddPCR). Muscles were serially sectioned, at 10 µm thick cryosections, across the entire muscles with alternative sections collected for ddPCR. Human specific-GAPDH was detected in gastrocnemius muscles with IA delivered cells, but not IV delivered cells (Figure 1B) in mdx-NSG mice. Because cells were not detected in the gastrocnemius muscle after IV delivery in mdx-NSG mouse, we focused our efforts in optimizing the IA delivery method in mdx-NSG and mdxD2-NSG mice. We were able to detect human-specific GAPDH in the right hindlimb muscles, where surgery is performed, of mdx-NSG and mdxD2-NSG mice 48 h after cell delivery (Figure 1C), but not in the contralateral hindlimb (data not shown). In intramuscular (IM) cell engraftment experiments, muscles are typically injured 24 h before cell delivery using cardiotoxin, barium chloride, or cryoinjury, to induce muscle damage and assist in cell engraftment (Brimah et al., 2004; Ehrhardt et al., 2007; Darabi et al., 2008; Sacco et al., 2010; Sakai et al., 2013; Hicks et al., 2018). As this is not feasible for systemic delivery, we included a 45-min downhill exercise regimen similar to described to induce muscle injury in the lower hindlimbs of mice before systemic SMPC delivery (Mathur et al., 2011). Matthias et al. (2015) described a detailed method for IA cell delivery through the femoral artery with successful detection of human cells in the muscle. However, in the previous protocol after cell delivery the femoral artery is ligated, which in our hands caused a prominent ischemia injury detected in the gastrocnemius muscle of mdx-NSG mice (Supplementary Figure S1C). Femoral artery ligation has been demonstrated to cause ischemic gastrocnemius muscle injury with a

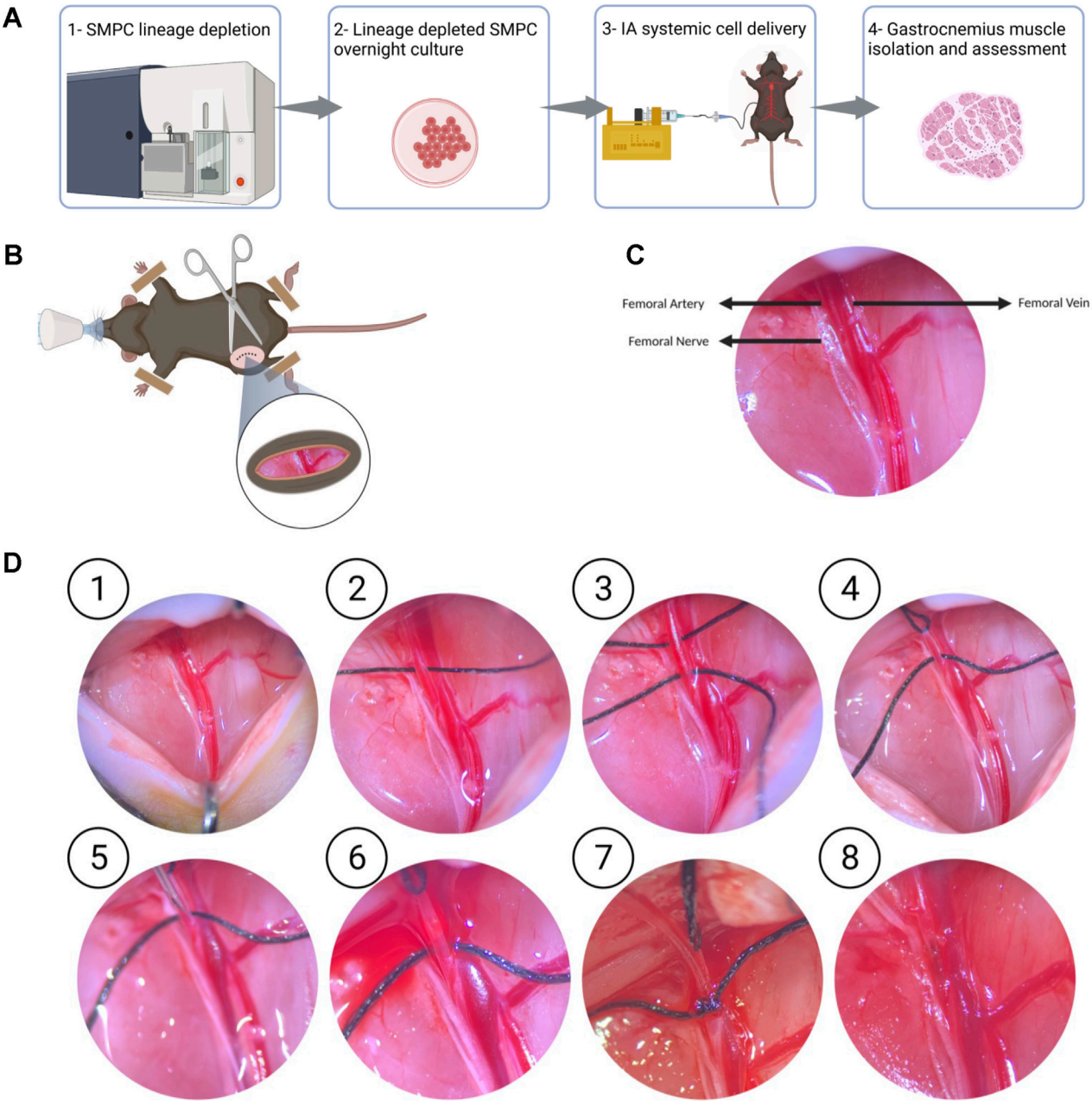

FIGURE 2
Optimized intra-arterial cell delivery protocol to lower hindlimb muscles **(A)** Schematic of experimental flow of IA systemic cell delivery. FW18/19 are lineage depleted and cultured overnight, cells are dissociated, and IA delivered at a 50 µl/min flow rate, and lower hindlimb muscles, including gastrocnemius muscle, are collected 48 h after surgery. **(B, C)** The femoral bundle consisting of the femoral artery, femoral nerve and femoral vein are exposed once retractors are used to open the incision site. **(D)** Detailed protocol of intra-arterial cell delivery where ① the femoral nerve and femoral artery are dissected away from the femoral vein. ② and ③ Two 6–0 size silk sutures, are passed underneath the femoral artery. ④ the silk suture upstream of the injection site is pulled to stop blood flow. ⑤ and ⑥ A 30 G needle is used to make a small puncture in the femoral artery downstream of the blood occlusion site ⑦ 32G catheter is then inserted into the femoral artery and secured with the second suture downstream of the injection site. Cell infusion is started at 50 µl/min ⑧ After untying the suture securing the catheter and retrieving the catheter from the femoral artery, a cauterizer is used to seal the infusion site. After removing the suture occluding the blood flow to the femoral artery, blood flow should be seen restored into the femoral artery.

decreased blood flow to the limb below the ligation site (Paoni et al., 2002; Padgett et al., 2016; Tu et al., 2021). Another IA cell delivery protocol described by Gerli et al. (2014) re-establishes blood flow in the femoral artery after cell delivery, however, the cells are not delivered at a constant flow rate. Our approach is optimized from other IA delivery strategies by combining both delivery of the cells at a constant flow rate of 50 µl/min of cell suspension using a catheter, and by restoring blood flow after cell delivery, to prevent muscle ischemic injury (Figures 2A–D). Approximately 800K-1M SMPCs were delivered to male wt-NSG, mdx-NSG or mdxD2-NSG mice.

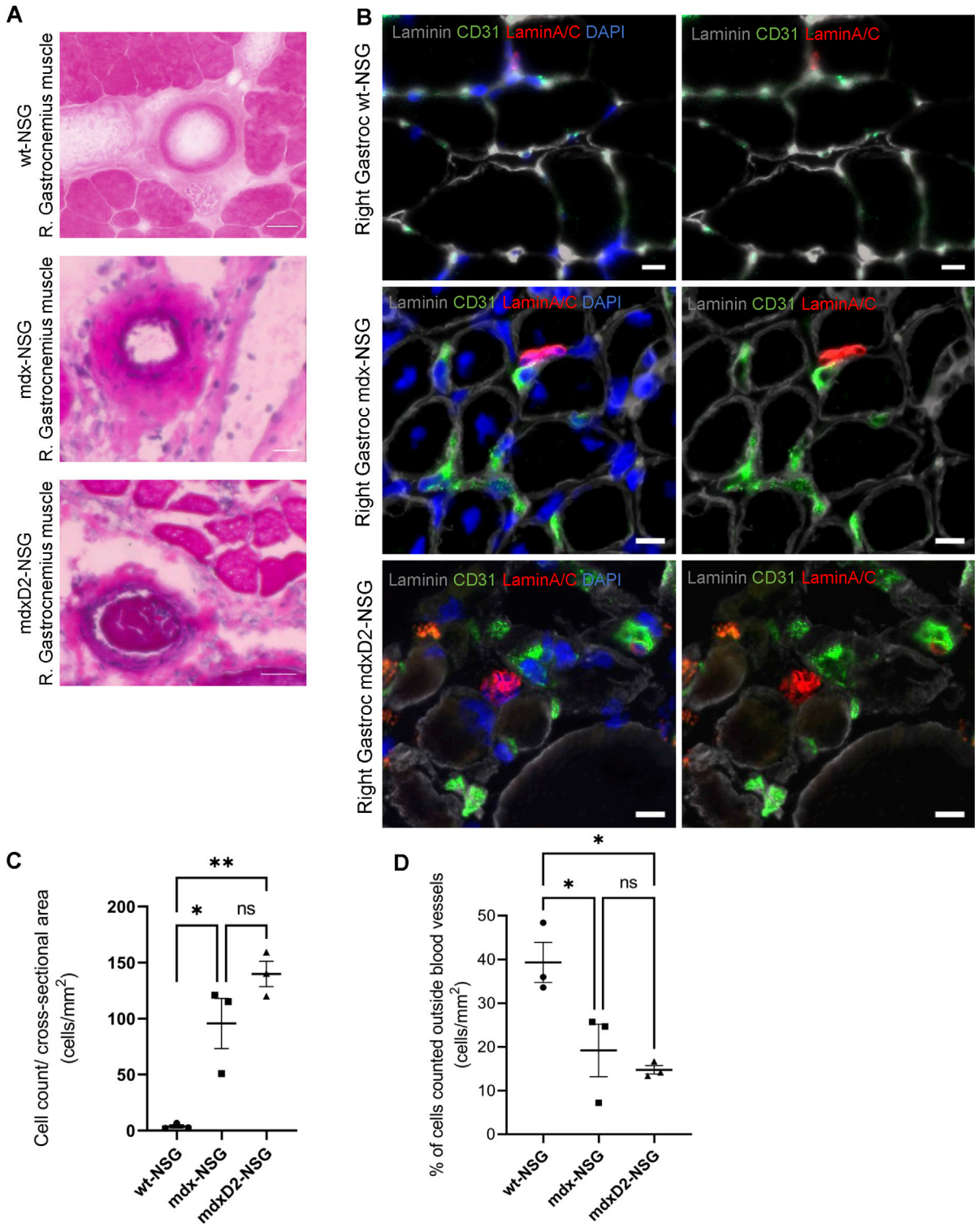

FIGURE 3
The severity of DMD mouse model impacts systemic human skeletal muscle progenitor cells delivery into lower hindlimb muscles. **(A)** Histological analysis of right gastrocnemius muscle after intra-arterial cell delivery in wt-NSG, mdx-NSG and mdxD2-NSG muscles. **(B)** Gastrocnemius muscle cross-sections staining for human skeletal muscle progenitors cells (marked by human nuclie marker LaminA/C, red) and blood vessels (marked by endothelial cells marker CD31, green) with human cells detected outside the blood vessels. Scale bars at 10 µm. **(C)** Plot of the total human cells quantified/ cross-sectional area of the gastrocnemius muscles of wt-NSG, mdx-NSG and mdxD2-NSG mouse models. (*N* = 3/mouse model, One Way ANOVA with Tukey's multiple comparisons, errors bars show mean ± SD, $*p \leq 0.01$, $**p << 0.01$). **(D)** Plot of the percentage of the total cells quantified outside blood vessels/cross-sectional area in wt-NSG, mdx-NSG and mdxD2-NSG muscles. (*N* = 3/mouse model, One Way ANOVA with Tukey's multiple comparisons, errors bars show mean±SD, $*p \leq 0.05$).

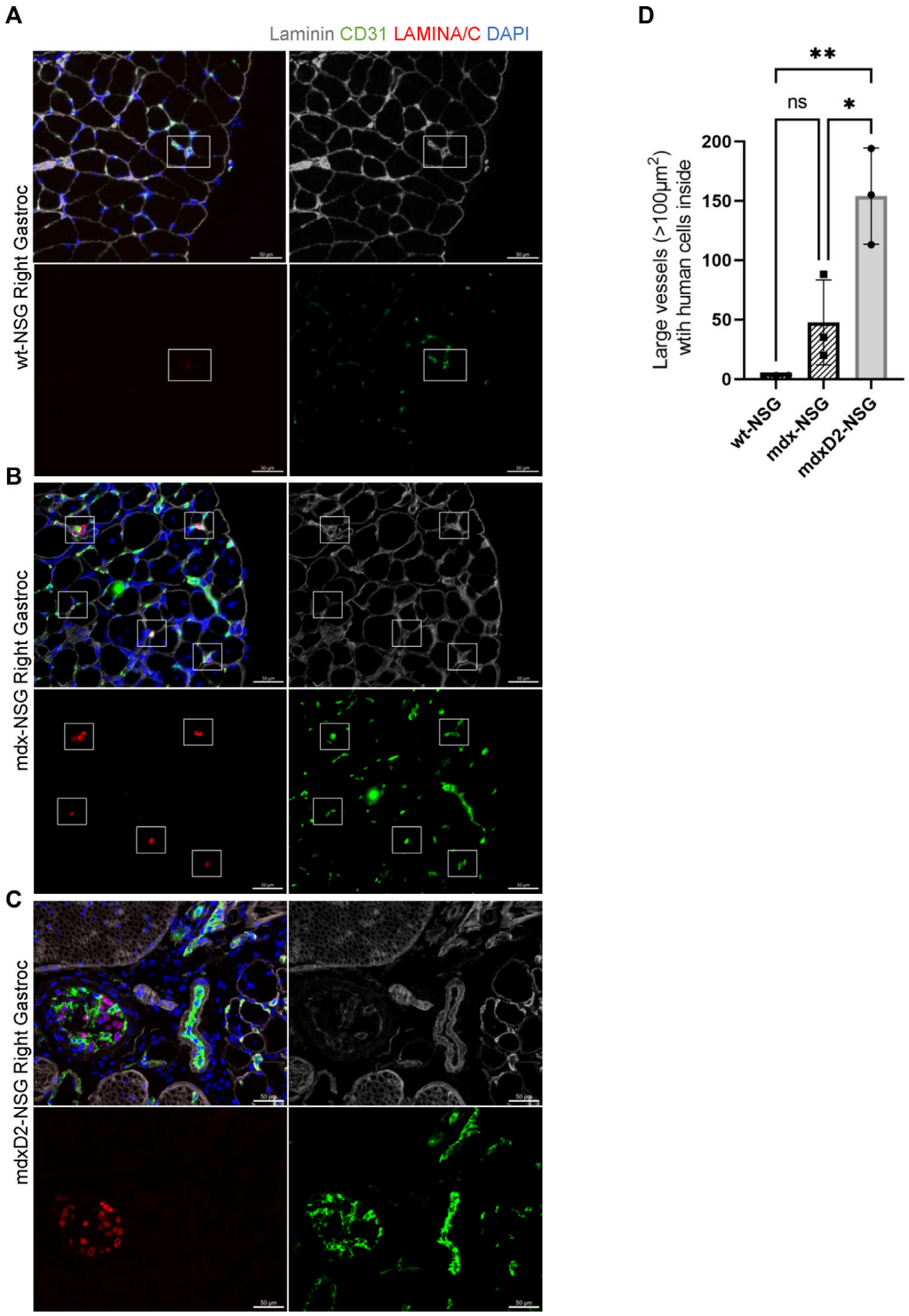

FIGURE 4
Significantly more human skeletal muscle progenitor cells are detected in large blood vessels in severely dystrophic gastrocnemius muscles. **(A–C)** Cross sections of right gastrocnemius muscles of wt-NSG, mdx-NSG, and mdxD2-NSG showing human nuclei (H-laminA/C, red) 48 h post IA cell delivery. SMPCs are detected inside blood vessels. Scale bars at 50 µm. **(D)** Comparison of the average number of blood vessels with a cross-sectional area >100 µm^2 with SMPCs detected inside in wt-NSG, mdx-NSG and mdxD2-NSG gastrocnemius muscles. (One way ANOVA with Tukey's multiple comparisons, error bars represent mean ± SD, *$p < 0.05$, **$p < 0.01$).

10.3389/fphys.2023.1190524

3.2 The severity of DMD mouse model impacts systemic human skeletal muscle progenitor cells delivery into lower hindlimb muscles

Despite our efforts to prevent muscle injury after optimization of IA systemic delivery procedure, severe injury was detected in the lower limb muscles in mdxD2-NSG mouse model, but not in mdx-NSG or wt-NSG (Supplementary Figure S2). To further investigate this finding, we performed histological analysis using hematoxylin and eosin staining on gastrocnemius muscle cross-sections of wt-NSG, mdx-NSG and mdxD2-NSG after SMPCs IA delivery. We observed prominent clotting occurring in large blood vessels in mdxD2-NSG, but not in wt-NSG and mdx-NSG (Figure 3A). These findings indicate a pronounced difference in SMPC IA cell delivery in severely dystrophic mouse model compared to healthy and dystrophic mouse models. To evaluate SMPC localization after their IA systemic delivery and whether the cells home to the muscle, right gastrocnemius muscles cross-sections were analyzed from all mouse models. In a successful cell delivery procedure, the human cells are expected to be detected outside the blood vessels and homing to the muscle (Figure 3B). Using both Zen 2.6 and Imaris Cell Imaging software we quantified human LaminA/C cells, a human cell perinuclear marker, in at least 16 cross-sections taken across the length of the muscle. Interestingly, we found significantly more human cells detected in gastrocnemius muscles per total cross-sectional area quantified in mdx-NSG and mdxD2-NSG compared to wt-NSG (Figure 3C). Of the total counted cells, significantly higher number of SMPCs, about 40%, quantified in wt-NSG gastrocnemius muscle cross-sections were detected outside the blood vessels, while only about an average of 20% and 18% were detected outside blood vessels in mdx-NSG and mdxD2-NSG, respectively (Figure 3D).

Because of the high frequency of detecting human SMPCs inside blood vessels, we then focused on evaluating the localization of SMPCs within blood vessels (Figures 4A–C). On average of the total SMPCs quantified in all gastrocnemius muscle cross-sections, 60%, 84%, and 62% of cells were observed inside the smallest blood vessel unit, the capillaries, in wt-NSG, mdx-NSG and mdxD2-NSG, respectively (not shown). We next sought to determine the differences in cell localization in large blood vessels between wt-NSG, mdx-NSG and mdxD2-NSG gastrocnemius muscles. Using Imaris Cell Imaging software we measured the area of larger vessels (veins/venules and arteries/arterioles) with human cells inside them and found that in mdx-NSG gastrocnemius muscles an average of 74 blood vessels with cross-sectional areas greater than 100 μm^2 had SMPCs detected in them, compared to an average of 154 blood vessels in mdxD2-NSG (Figure 4D). SMPCs detected inside 100 μm^2 blood vessel or greater in wt-NSG was negligible. Taken together we found that human SMPCs engraft inefficiently to lower hindlimb healthy and dystrophic muscles and are mainly detected inside blood vessels. We observed that human SMPCs localize in blood vessels distinctly in wt-NSG and mdx-NSG and mdxD2- NSG, with prominent clotting identified in mdxD2-NSG after human SMPCs IA systemic delivery. These findings indicate that the severity of DMD impacts human SMPC systemic delivery.

To verify that the previous findings were not influenced by cell size of human SMPCs, we IA delivered SCs to mdx-NSG mice (n = 2). For easier detection of the mouse SCs after delivery, we used a Pax7-ZsGreen transgenic mouse model that express enhanced green fluorescent protein for SCs isolation (Figure 5A). Because SCs are

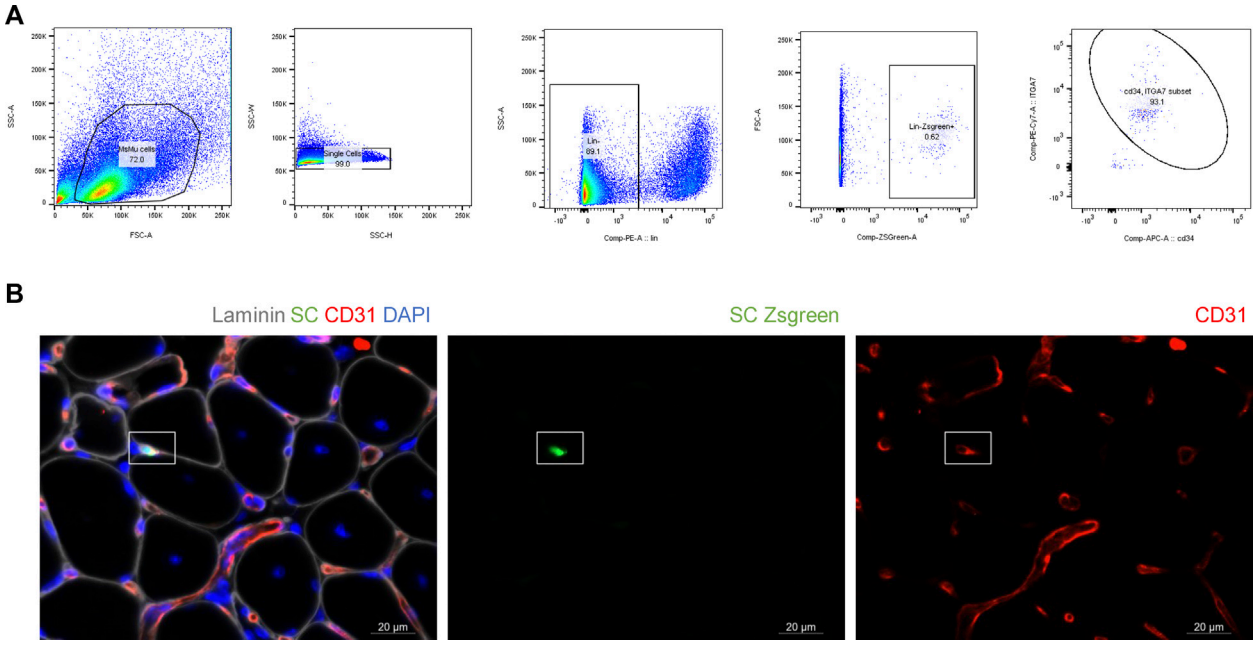

FIGURE 5
Mouse satellite cells do not efficiently extravasate. **(A)** Isolation of Zsgreen positive satellite cells for IA delivery in mdx-NSG mouse model. To confirm that Zsgreen cells isolated are indeed satellite cells, CD34 and ITGα7 staining was also performed on ZsGreen cells. Of the total Zsgreen + cells analyzed, 93% were CD34 and ITGα7 positive. **(B)** 50 K of healthy mouse Zsgreen satellite cells (green) were IA delivered to mdx-NSG mice (n = 2) and they were detected in capillaries. Scale bar 20 µm.

fewer in adult mouse muscle tissue, only about 50 K Zsgreen + SCs were delivered after their sort. The Zsgreen SCs were still detected inside capillaries in the mdx-NSG model, suggesting that the size of human SMPCs is not a main factor for their detection in capillaries (Figure 4B). This finding also suggests that human SMPC and mouse SCs are equally not equipped with the machinery that would enable them to home to the muscle.

Discussion

Cell based therapies for muscle diseases including DMD offer enormous potential for personalized therapies especially in combination with gene correction (Young et al., 2016; Hicks et al., 2018). The challenge faced is the lack of the ability to efficiently deliver cells to multiple muscles, which will be needed for neuromuscular diseases where multiple muscles are affected. Previously published reports for systemic delivery targeting multiple muscles did not deliver cells at a constant flow rate or were not able to re-establish blood flow back into the artery after cell delivery. Therefore, it was imperative to optimize an IA cell delivery protocol that provides delivered cells with the optimal conditions for muscle homing. Here we developed an optimized protocol for IA cell delivery by delivering the cells at a constant flow rate using a pump and catheter, and by establishing blood flow back into the femoral artery after cell delivery. This protocol confirmed its versatility with SMPCs delivered in three different mouse models, immunocompromised healthy and two dystrophic mouse models. Although this protocol has been developed for the delivery of SMPCs, it can be adapted for the delivery of other cell types, which we demonstrated by the delivery of mouse SCs, or for the delivery of modalities important for gene therapies.

The optimization of the IA protocol led us to focus on evaluating the systemic delivery potential of SMPCs in healthy and DMD mouse models. We found that although SMPCs can reach multiple lower limb muscles after IA systemic delivery, the efficiency is too low to lead to robust long-term engraftment. Moreover, cells are detected in the tibialis anterior, gastrocnemius, hamstring and lateral thigh muscles of the injected leg (right or left) where the procedure is performed, but not in the contralateral hindlimb muscle (data not shown). Evaluation of gastrocnemius muscle structure after IA delivery showed severe clotting evident in mdxD2-NSG, but not in wt-NSG or mdx-NSG muscles. Despite the fact that about the same number of cells were delivered to all mice across the mouse models, significantly fewer human SMPCs were detected in the wt-NSG gastrocnemius muscles in overall quantified cross-sectional areas. Interestingly, of the total human SMPCs quantified in the wt-NSG gastrocnemius muscle cross-sections, significantly higher number of cells were detected outside blood vessels compared to mdx-NSG and mdxD2-NSG. We therefore propose that less human SMPCs adhered to blood vessels in wt-NSG muscles compared to both DMD mouse models, which indicates a role the diseased microenvironment plays in the efficiency of systemic cell delivery.

Nonetheless, our current findings do not suggest that human SMPCs are homing efficiently to healthy muscle, as the majority of human SMPCs quantified were still detected inside blood vessels in all mouse models. However, interestingly, the localization of human SMPCs was distinct between the mouse models, with cells in the mdxD2-NSG observed in large blood vessels forming clots, not observed in mdx-NSG and wt-NSG muscles. These findings suggest that SMPCs are not endowed with the machinery to escape blood vessels to the surrounding muscle. Due to technical limitations, low number of SCs were delivered to the hindlimb muscle of mdx-NSG mice. However, as a proof of concept, we have shown that the gold standard mouse muscle stem cells also do not have the potential to extravasate efficiently. This challenge could perhaps be overcome by overexpressing the components needed to enable cells to extravasate utilizing the machinery used by leukocytes (Ley et al., 2007), but will require extensive optimization and a combination of cell and gene therapy approaches to overcome this large barrier to systemic based deliveries to muscle.

In summary, here we optimized an IA cell delivery protocol that can be utilized for both cell delivery and potentially combination cell and gene therapy applications. We have shown that IA systemic based cell delivery can be performed using human SMPCs, but the efficiency is too low to be considered for use in therapeutic applications. Indeed, in severely dystrophic mouse models it could be detrimental. We have shown differences in human SMPCs delivery in healthy, dystrophic and severely dystrophic muscles. These findings highlight the need to further understand the differences in skeletal muscle microenvironment between healthy, dystrophic and severely dystrophic mouse models, namely, endothelial cells that line the interior surface of blood vessels. Future studies will likely need to develop combination therapies targeting both the diseased microenvironment as well as generating a better SMPC that can be engineered to extravasate in parallel prior to use in regenerative medicine approaches for muscular dystrophy.

Data availability statement

The original contributions presented in the study are included in the article/Supplementary Material, further inquiries can be directed to the corresponding author.

Ethics statement

All animal work was conducted under protocols approved by the UCLA Animal Research Committee (ARC) *#ARC-2006-119-AM-006*. Human work was IRB exempt IRB#20-000197.

Author contributions

KS and AP designed the study and prepared the manuscript. KS performed IA surgeries with assistance from CS, MH, LG, and DG. KS and MH performed IV cell delivery. CS and LG contributed to cell counting and IF staining and imaging.

Funding

First author was supported by fellowship from Qatar National Research Fund (QNRF)-Qatar Research Leadership Program (QLRLP9-G-3330003). MH was funded by Muscular Dystrophy

Association (MDA) grant (#629098) and by Broad Stem Cell Research Center at UCLA (BSCRC). This work was funded by CIRM Quest grant (#DISC2-08824) and NIAMS/NIH grant (R01AR064327) to AP.

Acknowledgments

We would like to thank Luisa Iruela-Arispe and post-doctoral fellow in her lab Georg Hilfenhaus for their support and crucial discussions. We would like to thank Haun Meng and post-doctoral fellow in his lab Xiangsheng Liu for their support with IV cell delivery. We acknowledge FACS support provided by BSCRC Flow Cytometry Core at UCLA, we'd like to especially thank Felicia Codrea, Jessica Scholes, and Jeffrey Calimlim for their support. We acknowledge UCLA CFAR- Humanized Mouse Core for mouse colony husbandry. We acknowledge UCLA CFAR grant AI028697, the James B. Pendleton Charitable Trust and the McCarthy Family Foundation for ddPCR services especially provided by Alex E. Bollinger and Ting-Ting Wu. We acknowledge UCLA CFAR- Gene and Cellular Therapy Core and ABR for providing human muscle tissue. Illustrations in this paper were created with BioRender.com.

Conflict of interest

AP is co-founder and SAB member of MyoGene Bio.

The remaining authors declare that the research was conducted in the absence of any commercial or financial relationships that could be construed as a potential conflict of interest.

Publisher's note

Supplementary material

The Supplementary Material for this article can be found online at: https://www.frontiersin.org/articles/10.3389/fphys.2023.1190524/full#supplementary-material

SUPPLEMENTARY FIGURE 1
Optimized intra-arterial cell delivery prevents severe muscle ischemia injury **(A)** qRT-PCR of myogenic markers of lineage depleted human skeletal muscle progenitor cells (FW18). n = 3 biological samples, data are normalized to GAPDH as mean ± SD of technical triplicates. **(B)** Lineage depleted human skeletal muscle progenitor cells (FW18) fuse and form PAX7+ cells when differentiated *in vitro* for 5 days in N2 media. Scale bar at 100 µm. **(C)** Histological analysis, hematoxylin and eosin, staining of mdx-NSG gastrocnemius muscle 48 h after intra-arterial cells delivery in the right femoral artery. Top: control left gastrocnemius muscle, bottom left: mdx-NSG right gastrocnemius muscle with femoral artery ligation, bottom right: right gastrocnemius muscle with intra-arterial cell delivery procedure optimization fibrotic areas.

SUPPLEMENTARY FIGURE 2
Lower hindlimb morphology after intra-arterial cell delivery in mdx-NSG and mdxD2-NSG mice. mdxD2-NSG muscles show severe ischemia with H&E staining showing blood clots inside large blood vessels whereas control hindlimbs do not.

References

Ausems, C. R. M., Engelen, B. G. M. V., Bokhoven, H., and Wansink, D. G. (2021). Systemic cell therapy for muscular dystrophies. *Stem Cell Rev. Rep.* 17, 878–899. doi:10.1007/s12015-020-10100-y

Coley, W. D., Bogdanik, L., Vila, M. C., Yu, Q., Meulen, J. H. V. D., Rayavarapu, S., et al. (2016). Effect of genetic background on the dystrophic phenotype in mdx mice. *Hum. Mol. Genet.* 25, 130–145. doi:10.1093/hmg/ddv460

Darabi, R., Gehlbach, K., Bachoo, R. M., Kamath, S., Osawa, M., Kamm, K. E., et al. (2008). Functional skeletal muscle regeneration from differentiating embryonic stem cells. *Nat. Med.* 14, 134–143. doi:10.1038/nm1705

Dumont, N. A., Wang, Y. X., Maltzahn, J., Pasut, A., Bentzinger, C. F., Brun, C. E., et al. (2015). Dystrophin expression in muscle stem cells regulates their polarity and asymmetric division. *Nat. Med.* 21, 1455–1463. doi:10.1038/nm.3990

Fukada, S., Morikawa, D., Yamamoto, Y., Yoshida, T., Sumie, N., Yamaguchi, M., et al. (2010). Genetic background affects properties of satellite cells and mdx phenotypes. *Am. J. Pathol.* 176, 2414–2424. doi:10.2353/ajpath.2010.090887

Gerli, M. F. M., Maffioletti, S. M., Millet, Q., and Tedesco, F. S. (2014). Transplantation of induced pluripotent stem cell-derived mesoangioblast-like myogenic progenitors in mouse models of muscle regeneration. *J. Vis. Exp. Jove*, e50532. doi:10.3791/50532

Gerli, M. F. M., Moyle, L. A., Benedetti, S., Ferrari, G., Ucuncu, E., Ragazzi, M., et al. (2019). Combined notch and PDGF signaling enhances migration and expression of stem cell markers while inducing perivascular cell features in muscle satellite cells. *Stem Cell Rep.* 12, 461–473. doi:10.1016/j.stemcr.2019.01.007

Gussoni, E., Blau, H. M., and Kunkel, L. M. (1997). The fate of individual myoblasts after transplantation into muscles of DMD patients. *Nat. Med.* 3, 970–977. doi:10.1038/nm0997-970

Gussoni, E., Pavlath, G. K., Lanctot, A. M., Sharma, K. R., Miller, R. G., Steinman, L., et al. (1992). Normal dystrophin transcripts detected in Duchenne muscular dystrophy patients after myoblast transplantation. *Nature* 356, 435–438. doi:10.1038/356435a0

Guttinger, M., Tafi, E., Battaglia, M., Coletta, M., and Cossu, G. (2006). Allogeneic mesoangioblasts give rise to alpha-sarcoglycan expressing fibers when transplanted into dystrophic mice. *Exp. Cell Res.* 312, 3872–3879. doi:10.1016/j.yexcr.2006.08.012

Hicks, M. R., Hiserodt, J., Paras, K., Fujiwara, W., Eskin, A., Jan, M., et al. (2018). ERBB3 and NGFR mark a distinct skeletal muscle progenitor cell in human development and hPSCs. *Nat. Cell Biol.* 20, 46–57. doi:10.1038/s41556-017-0010-2

Huard, J., Bouchard, J. P., Roy, R., Malouin, F., Dansereau, G., Labrecque, C., et al. (1992). Human myoblast transplantation: Preliminary results of 4 cases. *Muscle Nerve* 15, 550–560. doi:10.1002/mus.880150504

Karpati, G., Ajdukovic, D., Arnold, D., Gledhill, R. B., Guttmann, R., Holland, P., et al. (1993). Myoblast transfer in duchenne muscular dystrophy. *Ann. Neurol.* 34, 8–17. doi:10.1002/ana.410340105

Klingler, W., Jurkat-Rott, K., Lehmann-Horn, F., and Schleip, R. (2012). The role of fibrosis in Duchenne muscular dystrophy. *Acta Myol. Myopathies Cardiomyopathies Off. J. Mediterr. Soc. Myol.* 31, 184–195.

Law, P. K., Goodwin, T. G., Fang, Q., Chen, M., Li, H., Florendo, J. A., et al. (1991). Myoblast transfer therapy for duchenne muscular dystrophy. *Pediatr. Int.* 33, 206–215. doi:10.1111/j.1442-200x.1991.tb01545.x

Ley, K., Laudanna, C., Cybulsky, M. I., and Nourshargh, S. (2007). Getting to the site of inflammation: The leukocyte adhesion cascade updated. *Nat. Rev. Immunol.* 7, 678–689. doi:10.1038/nri2156

Mathur, S., Vohra, R. S., Germain, S. A., Forbes, S., Bryant, N. D., Vandenborne, K., et al. (2011). Changes in muscle T2 and tissue damage after downhill running in mdx Mice. *Muscle Nerve* 43, 878–886. doi:10.1002/mus.21986

Matthias, N., Hunt, S. D., Wu, J., and Darabi, R. (2015). Skeletal muscle perfusion and stem cell delivery in muscle disorders using intra-femoral artery canulation in mice. *Exp. Cell Res.* 339, 103–111. doi:10.1016/j.yexcr.2015.08.018

Miller, R. G., Sharma, K. R., Pavlath, G. K., Gussoni, E., Mynhier, M., Yu, P., et al. (1997). Myoblast implantation in Duchenne muscular dystrophy: The San Francisco study. *Muscle Nerve* 20, 469–478. doi:10.1002/(sici)1097-4598(199704)20:4<469::aid-mus10>3.0.co;2-u

Partridge, T. A., Morgan, J. E., Coulton, G. R., Hoffman, E. P., and Kunkel, L. M. (1989). Conversion of mdx myofibres from dystrophin-negative to -positive by injection of normal myoblasts. *Nature* 337, 176–179. doi:10.1038/337176a0

Sacco, A., Mourkioti, F., Tran, R., Choi, J., Llewellyn, M., Kraft, P., et al. (2010). Short telomeres and stem cell exhaustion model duchenne muscular dystrophy in mdx/mTR mice. *Cell* 143, 1059–1071. doi:10.1016/j.cell.2010.11.039

Saleh, K. K., Xi, H., Switzler, C., Skuratovsky, E., Romero, M. A., Chien, P., et al. (2022). Single cell sequencing maps skeletal muscle cellular diversity as disease severity increases in dystrophic mouse models. *Iscience* 25, 105415. doi:10.1016/j.isci.2022.105415

Sampaolesi, M., Blot, S., D'Antona, G., Granger, N., Tonlorenzi, R., Innocenzi, A., et al. (2006). Mesoangioblast stem cells ameliorate muscle function in dystrophic dogs. *Nature* 444, 574–579. doi:10.1038/nature05282

Sitzia, C., Farini, A., Jardim, L., Razini, P., Belicchi, M., Cassinelli, L., et al. (2016). Adaptive immune response impairs the efficacy of autologous transplantation of engineered stem cells in dystrophic dogs. *Mol. Ther.* 24, 1949–1964. –1964. doi:10.1038/mt.2016.163

Tedesco, F. S., Hoshiya, H., D'Antona, G., Gerli, M. F. M., Messina, G., Antonini, S., et al. (2011). Stem cell–mediated transfer of a human artificial chromosome ameliorates muscular dystrophy. *Sci. Transl. Med.* 3, 96ra78. doi:10.1126/scitranslmed.3002342

Webster, C., and Blau, H. M. (1990). Accelerated age-related decline in replicative lifespan of Duchenne muscular dystrophy myoblasts: Implications for cell and gene therapy. *Somat. Cell Molec Gen.* 16, 557–565. doi:10.1007/bf01233096

Xi, H., Fujiwara, W., Gonzalez, K., Jan, M., Liebscher, S., Handel, B. V., et al. (2017). *In vivo* human somitogenesis guides somite development from hPSCs. *Cell Rep.* 18, 1573–1585. doi:10.1016/j.celrep.2017.01.040

Young, C. S., Hicks, M. R., Ermolova, N. V., Nakano, H., Jan, M., Younesi, S., et al. (2016). A single CRISPR-cas9 deletion strategy that targets the majority of DMD patients restores dystrophin function in hiPSC-derived muscle cells. *Cell Stem Cell* 18, 533–540. doi:10.1016/j.stem.2016.01.021

frontiers | Frontiers in Physiology

TYPE Original Research
PUBLISHED 17 May 2023
DOI 10.3389/fphys.2023.1145047

OPEN ACCESS

EDITED BY
Masatoshi Suzuki,
University of Wisconsin-Madison,
United States

REVIEWED BY
Nicolas Wein,
The Research Institute at Nationwide Children's Hospital, United States
Keitaro Yamanouchi,
The University of Tokyo, Japan

*CORRESPONDENCE
Rachele Rossi,
r.rossi@ucl.ac.uk

RECEIVED 15 January 2023
ACCEPTED 03 May 2023
PUBLISHED 17 May 2023

CITATION
Rossi R, Torelli S, Ala P, Weston W, Morgan J, Malhotra J and Muntoni F (2023), MyoD-induced reprogramming of human fibroblasts and urinary stem cells *in vitro*: protocols and their applications.
Front. Physiol. 14:1145047.
doi: 10.3389/fphys.2023.1145047

MyoD-induced reprogramming of human fibroblasts and urinary stem cells *in vitro*: protocols and their applications

Rachele Rossi[1,2]*, Silvia Torelli[1,2], Pierpaolo Ala[1,2], William Weston[1,2], Jennifer Morgan[1,2], Jyoti Malhotra[3] and Francesco Muntoni[1,2]

[1]The Dubowitz Neuromuscular Centre, UCL Great Ormond Street Institute of Child Health, London, United Kingdom, [2]National Institute for Health Research, Great Ormond Street Institute of Child Health Biomedical Research Centre, University College London, London, United Kingdom, [3]Sarepta Therapeutics Inc., Cambridge, MA, United States

The conversion of fibroblasts into myogenic cells is a powerful tool to both develop and test therapeutic strategies and to perform in-depth investigations of neuromuscular disorders, avoiding the need for muscle biopsies. We developed an easy, reproducible, and high-efficiency lentivirus-mediated transdifferentiation protocol, that can be used to convert healthy donor fibroblasts and a promising new cellular model, urinary stem cells (USCs), into myoblasts, that can be further differentiated into multinucleated myotubes *in vitro*. Transcriptome and proteome profiling of specific muscle markers (desmin, myosin, dystrophin) was performed to characterize both the myoblasts and myotubes derived from each cell type and to test the transdifferentiation-inducing capacity of MYOD1 in fibroblasts and USCs. Specifically, the Duchenne muscular dystrophy (DMD) transcripts and proteins, including both the full-length Dp427 and the short Dp71 isoform, were evaluated. The protocol was firstly developed in healthy donor fibroblasts and USCs and then used to convert DMD patients' fibroblasts, with the aim of testing the efficacy of an antisense drug *in vitro*. Technical issues, limitations, and problems are explained and discussed. We demonstrate that MyoD-induced-fibroblasts and USCs are a useful *in vitro* model of myogenic cells to investigate possible therapies for neuromuscular diseases.

KEYWORDS

duchenne muscular dystrophy, MyoD-induction, reprogramming, fibroblasts, urinary stem cells, lentivirus

1 Introduction

Duchenne muscular dystrophy (DMD) (OMIM # 310200) is a rare X-linked genetic disease affecting 21.4 children per 100,000 live male births. It is caused by mutations affecting the *DMD* gene resulting in reduction or complete absence of the related protein: dystrophin (DYS) (Crisafulli et al., 2020) (Muntoni et al., 2003). The most common mutations in *DMD* are large deletions and duplications, followed by small ins/del, point mutations, and splicing or deep intronic copy number variations (CNVs)/small mutations. Although the most frequent mutations are easily identifiable by a DNA test (i.e., MLPA, Sanger sequencing, gene panel), approximately 1% of atypical mutations require RNA analysis to be identified (Neri

et al., 2020). In recent years, many therapeutic strategies have been developed aiming to restore functional dystrophin in DMD muscles or to ameliorate the DMD patient's symptoms (Iftikhar et al., 2021). Other therapeutic strategies are now in development or in clinical trials (Fortunato et al., 2021), requiring a robust and reliable *in-vitro* model for their development. Neuromuscular disease-specific *in-vitro* models are more readily available than *in vivo* models, and are relevant for mutations present in patients that do not occur in existing rodent models (Fralish et al., 2021). However, these cellular models are frequently obtained from myoblasts isolated from skeletal muscle biopsies (San Miguel and Vargas, 2006). Muscle biopsies are also required to perform the in-depth analysis on RNA to study and confirm the occurrence of atypical mutations. Unfortunately, muscle biopsies are invasive procedures, and require particular attention in boys affected by DMD in view of the well-known general anesthesia related adverse events in this population (Thavorntanaburt et al., 2018). In this scenario, cellular genetic reprogramming offers a great advantage, allowing the use of other mesoderm derived cells instead of myoblasts derived from skeletal muscle biopsies. Indeed, the *MyoD* gene, the master regulatory factor, is able, once delivered into non-muscle lineage cells, such as dermal fibroblasts, to transdifferentiate them into muscle-like cells able to reproduce the disease phenotypic characteristics (Fujii et al., 2006). The most common delivery system is viral vector-mediated, but it has some limitations. For example, retroviral vectors have a very low transduction efficiency in slow-growing cells (Roest et al., 1999), whereas adenoviral vectors potentially offer a better transduction efficiency but exhibit cytotoxicity at high titres, require expression of the receptor of interest in the cells under study and do not integrate, leading to dilution following cell division (Fujii et al., 2006). To address these issues, we have developed a lentiviral vector, that is able to transduce both dividing and non-dividing cells, and efficiently and is reproducibly capable to reprogram dermal fibroblasts, derived from a skin biopsy, into myotubes *in vitro*. We also used the same lentiviral vector carrying the *MyoD* gene to transfect urinary stem cells (USCs) (Falzarano et al., 2016), to explore an entirely non-invasive cellular model. Aiming to test a DMD morpholino antisense oligomer (PMO) to skip *DMD* exon 53, golodirsen (Anwar and Yokota, 2020), we optimized an *in vitro* strategy of drug administration in MyoD-lentiviral transfected fibroblasts from both healthy donors and DMD patients. Protein and RNA extracted from these transfected and treated fibroblasts were analysed by qPCR with TaqMan systems and with highly efficient capillary Western blot (Wes), to evaluate the drug efficacy on DMD transcript and dystrophin protein restoration (Rossi et al., 2021) (Rossi et al., 2022). Considerations about the effect of transdifferentiation on DMD transcripts and DYS expression on healthy donor fibroblasts and USCs are discussed. We also characterized in detail two dystrophin protein isoforms, the short Dp71 and the full-length Dp427 m expression in these cellular models. Previous work had suggested that Dp71 expression is ubiquitously expressed with the exception of adult differentiated skeletal muscle, Dp427 m is the major isoform expressed in skeletal muscle fibers and it is only expressed in myofibers and muscle stem cells (de León et al., 2005). Thus, we analysed Dp71 and Dp427 m transcript and protein expression in induced and non-induced fibroblasts and urinary stem cells.

2 Materials and equipment

2.1 Materials, chemical

- DMEM high-glucose (Gibco, cat. no. 41966-052)
- Fetal bovine serum (FBS) (GIBCO) (Thermo Fisher, cat no. 26140)
- Horse serum (HS) (Thermo Fisher, cat no. 16050130)
- Penicillin/streptomycin (Pen/Strep) (Sigma, cat. no. P0781)
- Mega Cell (Sigma, cat. no. M3942)
- Non-Essential Amino Acids (NEAA) (Gibco, cat. no. 11140-050)
- 100X Glutamax (Gibco, cat. no. 35050-038)
- Skeletal Muscle Cell Differentiation Medium, ready to use, (Promocell, cat. no. C-23061)
- Trypsin-EDTA (Gibco, cat no. 15400-050)
- Phosphate-buffered saline (PBS) (Gibco, cat. no. 14190-094)
- Corning Matrigel Basement Membrane Matrix Growth Factor Reduced (Corning, cat. no. 354230)
- Doxycycline Hyclate (Sigma-Aldrich, cat. no. D9891)
- Puromycin: (Gibco, cat. no. A11138-03)
- Recombinant human epidermal growth factor (hEGF) (Lonza Bioscience, cat. no. CC-4107)
- Basic recombinant human fibroblast growth factor (bFGF) (Prospec-Tany, cat. no. CYT-218)
- Platelet-derived growth factor (PDGF-AB) (Prospec-Tany, cat. no. CYT-342)
- REBM Basal Medium (Lonza, cat. no.CC-3191)
- REGM renal epithelial SingleQuots Kit (Lonza, cat. no.CC-4127)
- Gibco Ham's F-12 Nutrient Mix (Gibco, cat. no. 11765054)
- Antibiotic/antimycotic solution (Sigma-Aldrich, cat. no. 120M0827)
- Ultrapure water with 0.1% gelatin (gelatin) (Millipore, cat. no. ECM0011B)
- Complete Protease Inhibitor Cocktail (Roche, cat. no. 11697498001)
- Plasmid: LV-TRE-VP64 mouse MyoD-T2A-dsRedExpress2 (donated by Dr Charles Gersbach but commercially available from Addgene plasmid no. 60625)
- Antisense PMO, Stock solution 1 mM.
- Endo-porter (PEG, Gene-Tools, cat. no. 2922498000)
- EndoFree Plasmid Giga Kit (QUIGEN, cat. no. 12391)
- RNeasy Mini Kit (QUIAGEN, cat. no. 74104)
- DNase I enzyme, Deoxyribonuclease I (Thermo fisher, cat. no.18068015)
- High-Capacity cDNA Reverse Transcription Kit (Applied Biosystems, cat. no. 4368814)
- TaqMan Universal PCR Master Mix (Thermo Fischer scientific, cat. no 4304437)
- Customized TaqMan systems (Thermo Fischer scientific, cat. no.4331348)
- Commercial TaqMan system for ACTBL2 gene, Hs01101944_s1 (Thermo Fischer scientific, cat. no.4331182)
- DNAse enzyme (Thermo Fisher cat. no. 1847019)
- Pierce BCA kit (Thermo Fisher Scientific, cat. no. 23250)
- Rabbit anti-dystrophin antibody (ab15277, Abcam, UK, dilution 1/50; ab154168)

TABLE 1 MyoD Lentiviral Titres obtained using two different commercial cell lines, HEK293T and LentiX HEK293T. Titres were obtained using cells harvested after 48 h of culturing.

Cell Line	Lentiviral Titre
HEK293T (48h harvest)	7.10E6
LentiX HEK293T (48h harvest)	5.21E6

TABLE 2 Multiplicity Of Infection (MOI) volumes to optimize transduction with increasing MOIs.

HEK293T 48h (1E5 cells)	Volumes
MOI 1	14.08ul
MOI 5	70.42ul
MOI 7	98.59ul

- Anti Mf20 antibody (Developmental Studies Hybridoma Bank, United States, 1:200)
- Anti Desmin antibody clone D33 (Dako, Agilent, 1:50)
- Anti-Human Fibroblast Surface Protein (Sigma, 1:500)
- Anti-rabbit (DM-001) and anti-mouse (DM-002) detection modules (Protein Simple, Bio-Techne)
- 66-440kD WES separation module 8 × 25 capillary cartridge (SM-W008, Bio-Techne)
- EZ Standard Pack 3 (PS-ST03EZ-8, Bio-techne)
- Alexa Fluor-488 goat anti mouse and anti rabbit antibodies (1: 1000, ThermoFisher, United States)

2.2 Materials, single-use plastic

- Steripipettes
- Counting Slides
- 15 mL sterile Falcon tubes
- 50 mL sterilie Falcon tubes
- T75 sterile flasks
- T175 sterile flasks
- 12 sterile well plate, flat bottom
- 6 sterile well plate, flat bottom

2.3 Equipment

- Wes system (ProteinSimple, Bio-Techne, United States)
- Real-Time PCR System (StepOnePlus™, Applied Biosystems, MA, United States)

2.4 Reagent setup

- Fibroblast Growth Medium: DMEM high-glucose, 10% FBS, 1% Pen/Strep
- Priming Differentiation Medium (MegaCell): Mega Cell, 2% FBS, 1% NEAA, 1% 100X Glutamax
- Secondary Differentiation Medium (PromoCell): PromoCell Skeletal Muscle Cell Differentiation Medium added with the provided supplement.
- Mesenchymal Proliferation Medium: DMEM high glucose, 10% FBS, 1% 100X GlutaMAX, 1% NEAA, 1% antibiotic/antimycotic solution, 5 ng/mL bFGF, 5 ng/mL PDGF-AB, 5 ng/mL EGF.
- USC Proliferation Medium: RE cell basal medium added with Renal Epithelial SingleQuots Kit (following company instruction) and Mesenchymal proliferation medium mixed at a 1:1 ratio.
- USC transfection Medium: DMEM high-glucose, 2% HS, 1% antibiotic/antimycotic solution.
- Corning Matrigel Basement Membrane working stock (Matrigel): to dilute the master stock to 0.1 mg/mL in DMEM-serum free, keeping Matrigel master stock on ice, see detailed protocol (Muses et al., 2011). Working solution should be stored at 4°C for no longer than 1 month.
- Puromycin working stock (Puromycin): experimentally determined (see below) to be 0.75 µg/mL with a maximum ratio of 10,000cells/100 µL medium.
- Doxycycline Hyclate working stock (Doxycycline): 3 µg/mL stock solution diluted to 103 diluted (1 µL in 10 mL of medium).
- Lysis buffer A: urea 4M, Tris 125 mM pH 6.8, SDS 4%.

3 Methods

3.1 Cells

This work was performed under the NHS National Research Ethics: setting up of a rare diseases biological samples bank (biobank) for research to facilitate pharmacological, gene and cell therapy trials in neuromuscular disorders (REC reference number: 06/Q0406/33), and the use of cells as a model system to study pathogenesis and therapeutic strategies for Neuromuscular Disorders (REC reference 13/LO/1826).

1 HEK-293-T Cell Line (Merck KGaA, Darmstadt, Germany, cat.no. 12022001-1VL) and 1 Lenti-X™ 293T Cell Line (Takara, 2022, cat.no. 632180) were used for large-scale vector production (Albrecht et al., 2015.). 1 Human fibrosarcoma HT1080 cell line (ATCC, cat. no. CCL-121) was used to perform lentiviral titration and to establish the protocol. Fibroblasts from 5 human adult healthy donors, were isolated from skin biopsies collected after obtaining written informed consent, to test the protocol reproducibility and to perform the RNA and protein tests. Urinary stem cells were previously isolated from 2 human adult healthy donors and cultured following the Falzarano et al. protocol (Falzarano et al., 2016).

3.2 Lentivirus and protocol set up

3.2.1 Plasmid

In this study was used the plasmid LV-TRE-VP64 mouse MyoD-T2A-dsRedExpress2 kindly donated by Dr Charles

Gersbach. Briefly we cloned the MyoD gene fused with Vp64 activation domain into a Tet-ON lentiviral vector. The lentiviral vector constitutively expresses the reverse tetracycline transactivator (rtTA2S-M2) and the puromycin resistance gene (PuroR) from the human phosphoglycerate kinase (hPGK) promoter. It also contains a DsRed Cassette downstream of the tetracycline response element (TRE) promoter. The rtTA2S-M2 binds to the TRE and activates expression of the downstream genes in the presence of doxycycline. Vp64 enhances the expression of the downstream gene, the MyoD factor. The puromycin selection cassette enables enrichment of transduced cells, while the DsRed cassette enables assessment of transduction efficiency.

3.2.2 Lentiviral production

Lentiviral production was undertaken using either HEK293T or the commercial LentiX HEK293T cell lines. A 24-flask production system was utilized, with separate harvests and ultracentrifugation steps at 48 and 72 h. The time of lentiviral harvest is critical to the titer that will be achieved (TAKARA BIO INC.). The LentiX cell line was used in an attempt to increase viral titer, but it appears to give a slightly lower titer than the HEK293T cells (data not shown). All the transduction experiments were conducted using only the HEK293T 48h samples.

3.2.3 Lentiviral titration

50,000 HT1080 cells (Schwartz et al., 2013) were transduced with two different volumes of lentivirus (Table 1) and cultured for 7 days (virus was added to cell cultures on day 1 and cells were collected on day 7), to ensure lentiviral integration. DNA was harvested, diluted to 20 ng/µL, and assessed by qPCR using both custom TaqMan system for the LTR virus gene and commercial TaqMan system for human beta actin genes, alongside plasmid serial 7-points dilution ranging from 10E10 to 10E3. qPCR experiment conditions are described in Kutner, *et al* (2009) (Kutner et al., 2009).

3.2.4 Determination of the optimal multiplicity of infection (MOI)

Lentiviral transductions were undertaken on 1E5 HT1080 cells, in 6 well-plates. To determine the baseline of transduction we analysed the DsRed reporter gene expression by FACS, using increasing multiplicity of infections (MOIs) (MOI 1, MOI 5, MOI 7) listed in Table 2. Each analysis was conducted pre and post 10 days of puromycin selection (Figure 1A). DsRed positive cells count take advantage of the DsRed fluorescent label cassette within plasmid #60625. After puromycin selection, MOI 1 and 5-transfected cells showed comparable DsRed expression as shown by FACs profiles and positive cell counts (Figures 1A, B). Cells transfected with MOI 7 had a slightly reduced number of cells compared to the other MOIs (Figure 1B). The DsRed positive cell count reveals a correlation between MOIs and the initial baseline transduction efficiency. However, following approximately 10 days of puromycin selection, the proportion of DsRed positive cells appeared to be similar between groups, especially between MOI 1 and 5. MOI 1 was selected to avoid cell stress and save virus stocks, achieving the same result compared to the other MOIs.

3.2.5 Determination of the optimal puromycin concentration

The puromycin working concentration recommended by the manufacturer (Gibco) ranges from 0.2 to 5.0 µg/mL, although the company website reports toxicity in eukaryotic cells at concentrations of 1 µg/mL. We tested two concentrations: 1 µg/mL and 0.75 µg/mL. We found that a dose of 1 µg/mL results in reduced proliferation, granulations and markers of stress in transfected fibroblast populations. On the contrary, a dose of

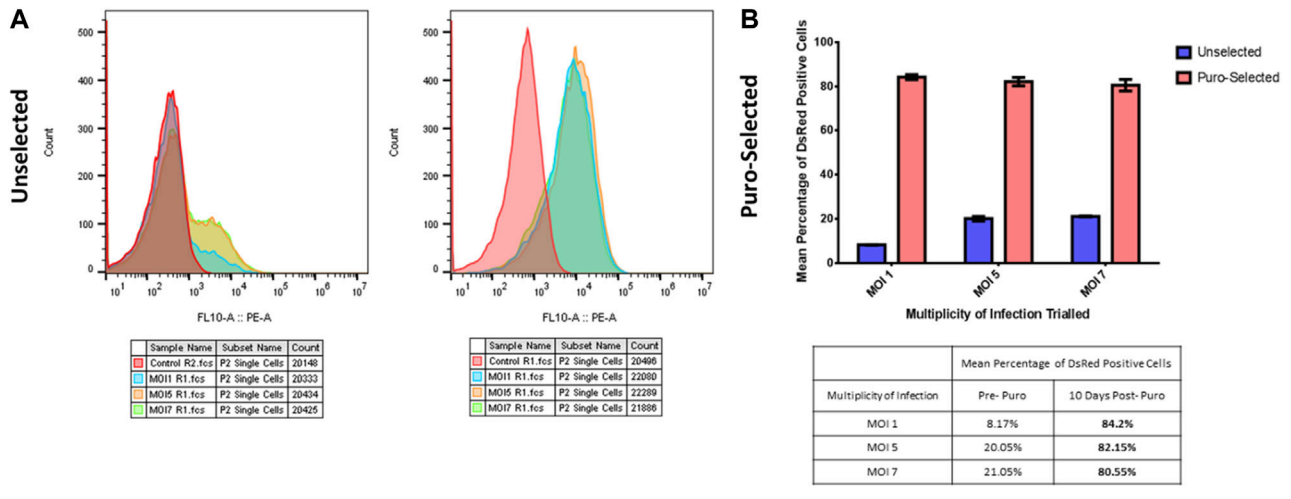

FIGURE 1
MOIs selection. **(A)** FACs profiles of human healthy fibroblasts infected with increasing multiplicity of infections (MOIs), pre (left graph) and post (right graph) puromycin selection. Red peak corresponds to non-transfected cells used as control sample, light blue peak to MOI 1, orange peak to MOI 5 and green peak to MOI 7. **(B)** DsRed positive cell count of human healthy fibroblasts infected with increasing multiplicity of infections (MOIs), pre (blue bars) and post (red bars) puromycin selection. Y-axis is the percentage of red signal from the DsRed Fluorescent label cassette present within the plasmid. The X-axis shows the different MOIs tested. Table below the graph shows the peak values.

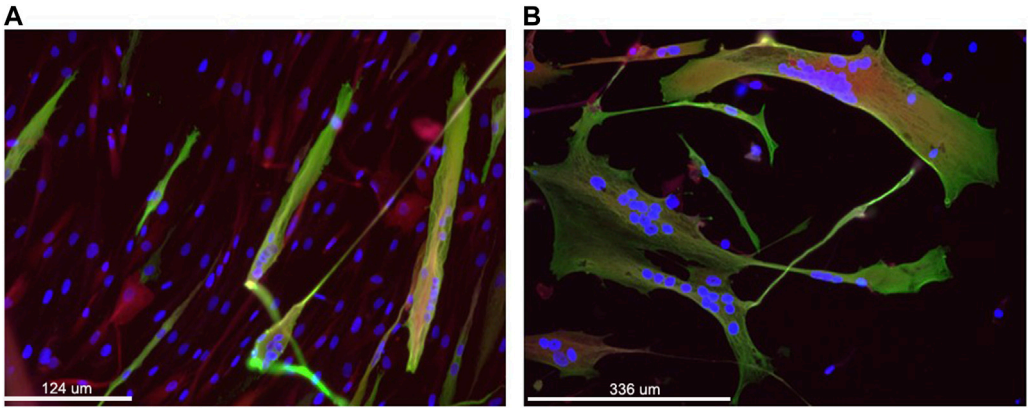

FIGURE 2
Immunofluorescence staining of transduced fibroblasts to assess MyoD-mediated differentiation and fusion of cells. Nuclei are stained in blue (DAPI), Sarcomeric myosin heavy chain in green using MF20 antibody and in red the residual DsRed associated with the transgene expression. Panel **(A)** shows cells grown for 10 days in primary culture medium and panel **(B)** shows cells grown for 10 days in the secondary culture medium. Magnification: bar 124 and 336 microns in panel A, B, respectively.

0.75 μg/mL allows selection of transfected cells without interfering with proliferation or causing excessive cell stress. Thus, 0.75 μg/mL was chosen as working concentration for human fibroblast selection. Moreover, at this concentration, we found that puromycin causes toxicity if it is administrated with a ratio greater than 100 μL of medium containing 0.75 μg/mL of puromycin for 10,000 cells.

3.2.6 Medium selection

After puromycin selection (11 days in total), fibroblasts were seeded on Matrigel-coated flasks and differentiated using two different media (MegaCell and PromoCell differentiation medium), both containing doxycycline (0.1 μL/mL), to test their effect on myogenic differentiation. After 10 days, cells cultured with both media were analyzed for the expression of myosin as a myotube marker, by IHC (Figure 2). The analysis revealed that MegaCell medium resulted in better viability (Figure 2A), whereas PromoCell differentiation medium resulted in better fusion (Figure 2B). It was decided to move to a culture system using both media: MegaCell for 5 or 9 days (see below) from the start of transdifferentiation and PromoCell for the 5 remining days, for a total of 14 days in differentiation media, in order to achieve a reasonable viability and fusion.

3.3 Fibroblast MyoD transduction protocol

Expand human fibroblast cells to reach 70%–80% confluence, in a T75 flask containing 5 mL of fibroblast growth medium. Then, trypsinise cells (remove all medium, wash cells with 5 mL of PBS, add 3 mL of trypsin-EDTA to each flask, place in an incubator until the cells have detached (approximately 2- 3 min), inactivate trypsin with 5 mL of fresh growth medium), count and seed 10^5 cells/well in a 6 well plate, using 1mL/well of fibroblast growth medium. Gently agitate thawed lentiviral aliquots and pipette a volume consistent with the selected MOI. In this case we used 14.08 μL of MyoD Lentiviral prep "HEK293T 48hrs" at multiplicity of infection 1 (MOI 1) to infect 100,000 cells in 1 mL. Apply gently using a dropwise circular motion. Wet tips with medium before taking up the virus to reduce the possibility of the virus adhering to the plastic tip.

Place cells with freshly applied lentivirus into an incubator at (37°C/5% CO_2) for 24 h. Ensure you close the incubator door gently. After 24 h of incubation, change the medium to 2 mL of fresh fibroblast growth medium and continue to grow the cells until they reach 80%–90% of confluency (around 3–4 days).

3.3.1 Expansion of MyoD transduced fibroblasts from a 6 well plate

Trypsinise cells and plate them into a T75 flask with 10 mL of fresh fibroblast growth medium. Change the medium every 2–3 days. Examine cells every day, they should reach 70%–80% confluency in 3–4 days post seeding.

3.3.2 Puromycin selection of MyoD transduced cells

Once cells have reached 70%–80% confluence, add puromycin (at previously determined concentration of 0.75 μg/mL) to fresh fibroblast growth medium. Change the medium with puromycin every 2–3 days, for either a total of 11 days, or until 80%–90% confluency is reached.

3.3.3 MyoD trans-differentiation of transduced and cell selection

Coat wells of 6-well plates with Matrigel (add 700 μL of the Matrigel per well, rock the plate gently, put in an incubator 37°C/5% CO_2 for 1 h, aspirate the excess Matrigel). Without allowing the Matrigel to dry out, seed 10^5 of puromycin-selected-cells per well in 2 mL of fibroblast growth medium without puromycin. Once cells are confluent, apply a Matrigel top layer to each well (aspirate all the medium, add 700 μL of Matrigel working solution to the cells, incubate for an hour, then remove excess Matrigel). From this step it is essential to work extremely carefully to prevent cell detachment. Add 2mL/well of Priming Differentiation Medium supplemented with doxycycline. This represents the start of the

trans-differentiation process. Perform complete media changes using Priming Differentiation Medium supplemented with doxycycline every 2 -3 days. Myotube formation will be evident after 3–5 days. After 7 days from the start of the transdifferentiation (step 12), the top layer of Matrigel should be re-applied, as described in step 11. After 5 or 9 days* in Priming Differentiation medium, cells are transitioned to the Second Differentiation medium supplemented with doxycycline and maintained for 5 days * 9 days are recommended for functional tests such as drug tests or to evaluate proteins expressed at a later stage of myogenic differentiation.

3.4 USCs MyoD transduction protocol

Grow human USCs until they reach 80%–90% confluence, in a 6-well plate using 2 mL of USC proliferation medium/well. Trypsinise the cells (remove all medium, wash wells twice with 500 µL of trypsin-EDTA, add 500 µL of trypsin-EDTA to each well, place the plate in an incubator until the cells have detached (around 2- 3 min), inactivate trypsin with 2 ml of USC Proliferation medium/well). Mix cells from two wells in a 15 mL Falcon tube and count them. Centrifuge Falcon tubes (10 min at 400x g at room temperature (RT)), discard supernatant and wash pellets with 5 mL of USC transfection medium. Centrifuge Falcon tubes (10 min at 400x g, RT), discard supernatant and resuspend each pellet with 1 mL of USC transfection medium. Add 14.08 µL of MyoD Lentiviral preparation "HEK293T 48hrs" at MOI 1 to 10^5 cells. Perform the infection in Falcon tubes. Wet tips with medium before taking up the virus to reduce the possibility of the virus adhering to the plastic tip. Incubate Falcon tubes at 37°C/5% CO_2 for an hour (lid should be not completely closed), mixing gently once, after 30 min of incubation. Coat T25 flasks with 0.1% gelatin (add 2.5 mL of gelatin/flask, rock the plate gently, put in an incubator at 37°C/5% CO_2 for 30 min, aspirate the excess of gelatin, wash with 3 mL of PBS containing 1% of antibiotic/antimycotic solution, remove excess washing solution). Transfer infected cells from Falcon tubes into gelatin-coated T25 flasks (one flask for each Falcon tube). Place flasks into an incubator at (37°C/5% CO_2) for 24 h. Ensure you close the incubator door gently. After 24 h of incubation, replace the medium with 2.5 mL of USC Proliferation medium and continue to grow cells until they reach 70%–80% confluency (about 2–3 days).

Follow Fibroblast MyoD transduction protocol from the "Puromycin Selection of MyoD Transduced Cells" section (step 7). For USCs is recommended not to exceed 7 passages.

3.5 Antisense oligonucleotide treatment of trans-differentiated fibroblasts

This drug test protocol is set up for an antisense phosphorodiamidate morpholino oligomers (PMO) inducing exon skipping in the *DMD* gene. Two doses of antisense were administered to cultured MyoD-induced fibroblasts, the first one for 24 h and the second for 48 h of incubation.

At day 6 from the start of trans-differentiation (step 17), remove medium from each well and apply 1mL/well of the Priming Differentiation medium supplemented with doxycycline. Apply 10µL/well of 1 mM PMO antisense using a circular dropwise motion.

Apply 6 µL of Endoporter using a circular dropwise motion, in every well. Incubate plates for 24 h then change the medium: 1mL/well of Priming Differentiation containing doxycycline. After 2 days, change medium to 2mL/well of the Second Differentiation medium supplemented with doxycycline. After 5 days (from the first antisense administration) remove medium from each well and replace it with 1mL/well of the Second Differentiation medium supplemented with doxycycline. Repeat steps 2 and 3. Incubate plates for 48 h (prolonged incubation time can be associated with toxicity). Cells are ready to be collected for further studies/analysis.

3.6 RNA extraction and analysis

RNAs were extracted from cells using the Quiagen RNeasy Micro Kit, treated with DNase I enzyme and retrotranscribed into cDNA by High-Capacity cDNA Reverse Transcription Kit. All the procedures were performed following the manufacturers' instructions. cDNAs were analyzed using single system TaqMan qPCR, complementary to DMD Dp427 m 5′UTR exon 1 boundary (custom, sequence available under request), DMD Dp71 5′UTR exon 1 boundary (custom, sequence available under request). Different expression between DMD Dp427 m and Dp71 isoforms was evaluated using Ct, using the formula: $2^{\wedge(Ct\ Dp427-Ct\ Dp71)}$.

3.7 Capillary western immunoassay (Wes)

Proteins were extracted adding Lysis buffer A to the harvested cells (50 µL of Lysis buffer A/well), transferred to Eppendorf microtubes, boiled for 3 min, treated with DNAse enzyme (6µL/tube of DNAse incubated for 30 min at 4°C), centrifugation at 14,000 g for 10 min, at RT. Collect the supernatant and discard the pellet if you can see it. Protein quantification was performed using the Pierce BCA kit (ThermoFisher Scientific, United States). Capillary Western immunoassay (Wes) analysis was performed on a Wes system (ProteinSimple, Bio-Techne, United States) following the manufacturer's instructions for the 66–440 kDa Separation Module, using 1 µg of sample lysate for each well. The following primary and secondary antibodies were used: rabbit anti-dystrophin antibody, anti MF20, anti-rabbit, and anti-mouse antibodies.

3.8 Immunostaining

Non-infected fibroblasts and differentiated MyoD lentiviral transfected fibroblasts and USCs were plated on coverslips coated with collagen. After 5 days in the Priming Differentiation medium and 5 days in the Secondary Differentiation medium (both doxycycline supplemented), cells were fixed in 4% paraformaldehyde for 10 min and then washed (3 × 10 min) in PBS. Coverslips were then incubated with primary antibodies against desmin, myosin heavy chain and dystrophin proteins for 1 h at RT and then washed (3 × 10 min) in PBS. After incubation with 488-conjugated secondary antibodies for 30 min at RT and washes in PBS, the coverslips were mounted in Hydromount + Dapi. Images were acquired using a Leica DMR microscope interfaced to MetaMorph (Molecular Devices).

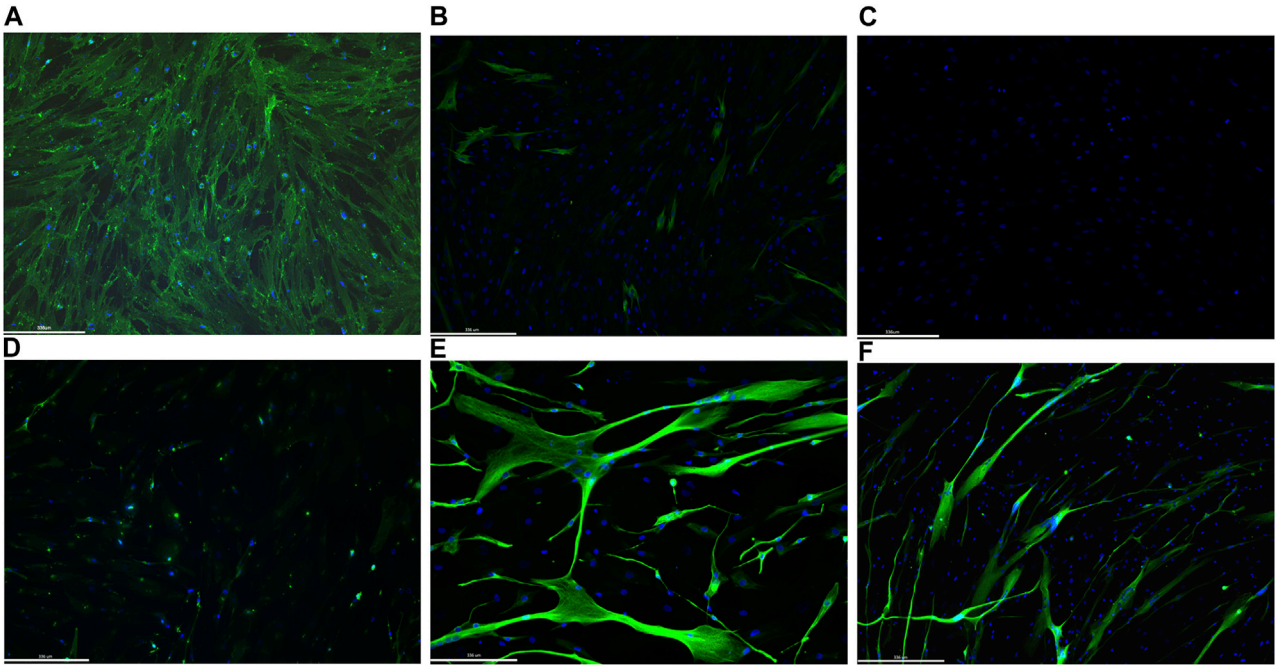

FIGURE 3
Representative images of immunofluorescence staining on 1 human healthy donor non-infected fibroblasts and differentiated MyoD lentivirally-transfected fibroblasts. Non-infected fibroblasts were immunolabelled with fibroblast surface protein antibodies **(A)**, desmin **(B)** and Mf20 **(C)**. Differentiated MyoD lentivirally-transfected fibroblasts were stained after 10 days in differentiation medium (5 days in priming and 5 days in secondary differentiation medium) with antibodies against fibroblast surface protein **(D)**, desmin **(E)** and Mf20 **(F)**. Nuclei are stained in blue (DAPI). Magnification: bar 336 microns.

4 Results

We demonstrated the reproducibility and efficacy of the MyoD-lentivirus protocol and used it to evaluate DMD Dp427 m and Dp71transcripts and proteins from healthy donor transduced fibroblasts and USCs.

4.1 MyoD-induced myogenic conversion of fibroblasts

In order to test the efficiency of our protocol in inducing myogenic conversion of fibroblasts, we immunostained (IHC) non-infected fibroblasts and differentiated MyoD lentiviral transfected fibroblasts for desmin and myosin heavy chain (MF20) expression. Desmin, an intermediate filament protein, is well-recognized to be one of the earliest expressed proteins during muscle development. Differentiated myotubes express high level of desmin, whereas myoblasts and satellite cells express lower levels of desmin, and fibroblasts do not express the protein (Paulin and Li., 2004). Sarcomeric myosin is expressed in striated and cardiac muscle where it confers contractile properties to the muscle fibers. Due to its tissue specificity, it has been used as a myoblast differentiation marker (Lee et al., 2019) (Shimizu et al., 1985). Immunostaining of non-infected fibroblasts, from one donor, shows only fibroblast surface protein expression (Figure 3A), while there was no signal for either desmin or myosin heavy chain (Figures 3B, C, respectively). On the contrary, after MyoD lentiviral infection and 10 days of transdifferentiation (5 days in primary differentiation medium and 5 days in secondary differentiation medium), fibroblasts express the two skeletal muscle markers, desmin and MF20 (Figures 3E, F, respectively). Moreover, immunostaining with an antibody against desmin (Figure 3E) reveals the characteristic elongate shape of myotubes formed from myoblast fusion. A slight background of fibroblast surface proteins expression was detected on differentiated MyoD lentiviral transfected fibroblasts (Figure 3D).

4.2 MyoD-induced myogenic conversion of USCs

The two skeletal muscle markers, desmin and MF20, were also used to test the myogenic differentiation process on MyoD lentiviral infected and non-infected USC cultures. Figure 4 shows immunostaining of USCs from one healthy donor. Non-infected USCs do not express either desmin (Figure 4A) or MF20 (Figure 4B). Conversely, differentiated MyoD lentiviral transfected USCs, immunostained after 10 days in differentiation media (5 days in primary and 5 days in secondary differentiation medium) showed signal from both antibodies desmin (Figure 4C) and MF20 (Figure 4D).

4.3 Myosin heavy chain, sarcomere (MHC) capillary western blot (Wes)

To better evaluate myosin protein expression, proteins extracted from the same healthy donor cells tested for IHC were analysed

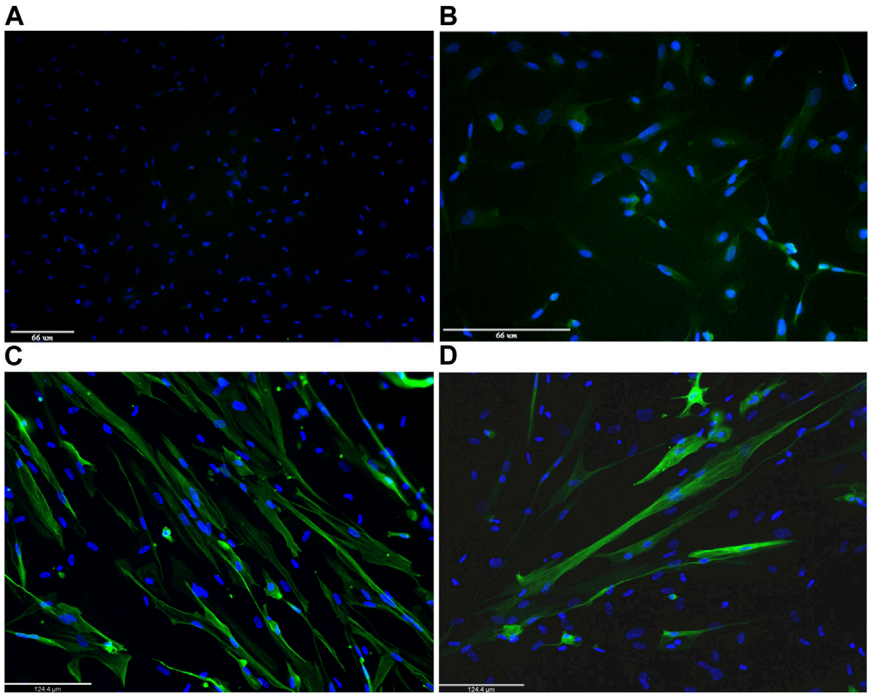

FIGURE 4
Representative images of immunofluorescence staining on 1 human healthy donor non-infected urinary stem cells (USCs) and differentiated MyoD lentivirally-transfected USCs. Non-infected USCs were immunolabelled with desmin **(A)** and Mf20 **(B)**. Differentiated MyoD lentivirally-transfected USCs were stained after 10 days in differentiation medium (5 days in Priming Differentiation Medium and 5 days in Secondary Differentiation Medium) with antibodies against desmin **(C)** and Mf20 **(D)**. Nuclei are stained in blue (DAPI). Magnification: bar 66 microns in panels A and B and bar 124.4 microns in panels C and D.

using MF20 antibody (that recognises the myosin heavy chain, sarcomere (MHC), in the fully automated capillary system (Wes). In order to increase protein expression, especially DYS, both fibroblasts and USCs were grown in differentiation media for a total of 14 days. As expected, non-transfected cells, either fibroblasts or USCs, did not express myosin heavy chain (data not shown). On the contrary, differentiated MyoD lentiviral transfected fibroblasts show a unique peak of 212 kDa corresponding to the molecular weight expected for myosin heavy chain (Figure 5A). Similarly, differentiated MyoD lentiviral transfected USCs also have only one peak at the same molecular weight (Figure 5B).

4.4 DMD Dp427 m and Dp71 isoforms expression

This protocol was developed in order to generate DMD cellular models useful for drug testing and *DMD* transcript/dystrophin protein analysis. For this reason, we evaluated dystrophin expression, before and after the MyoD induction, by Wes on proteins extracted from fibroblasts and USCs. As expected, non-infected fibroblasts express only the short DYS isoform Dp71 and not the full-length muscle isoform Dp427 m (Figure 5C). Interestingly, differentiated MyoD lentivirally-transfected fibroblasts express Dp427 m but still maintain Dp71 expression (Figure 5D), unlike mature muscle fibers, that express Dp71 at very low level and only in some subjects (Kawaguchi et al., 2018) (Chesshyre et al., 2022). Similarly, non-transfected USCs expressed only the Dp71 DYS isoform (Figure 5E). After differentiation, the Dp71 isoform continued to be expressed, but at a low level, especially if compared to the Dp427 m full -length isoform (Figure 5F). Using the same cells, we evaluated the difference between the DMD Dp427 m and the Dp71 transcript expression in transfected and non-transfected fibroblasts and USCs. The Dp427 m isoform transcript is always present, even in non-muscle (non-infected) cells but with low levels of expression; Dp427 expression is 0.5% and 1% of Dp71 expression in fibroblasts and USCs, respectively. In differentiated MyoD lentivirally-transfected fibroblasts, the Dp427 transcript increased its expression, becoming comparable to Dp71, (98.6% of the Dp71 expression). Also, in the differentiated MyoD lentiviral transfected USCs, the Dp427 transcript increased its expression becoming substantially more expressed than the Dp71 isoform (Dp71 expression is 85.7% less than Dp427 expression) (Table 3).

5 Discussion

Currently, 4 antisense morpholinos for treating DMD patients have been approved by the FDA, etelpilsen (exon 51) golodirsen and viltolarsen (exon 53), and casimersen (exon 45). The skipping of these exons could be beneficial for around 30% of DMD patients but skipping of other exons will be needed to treat

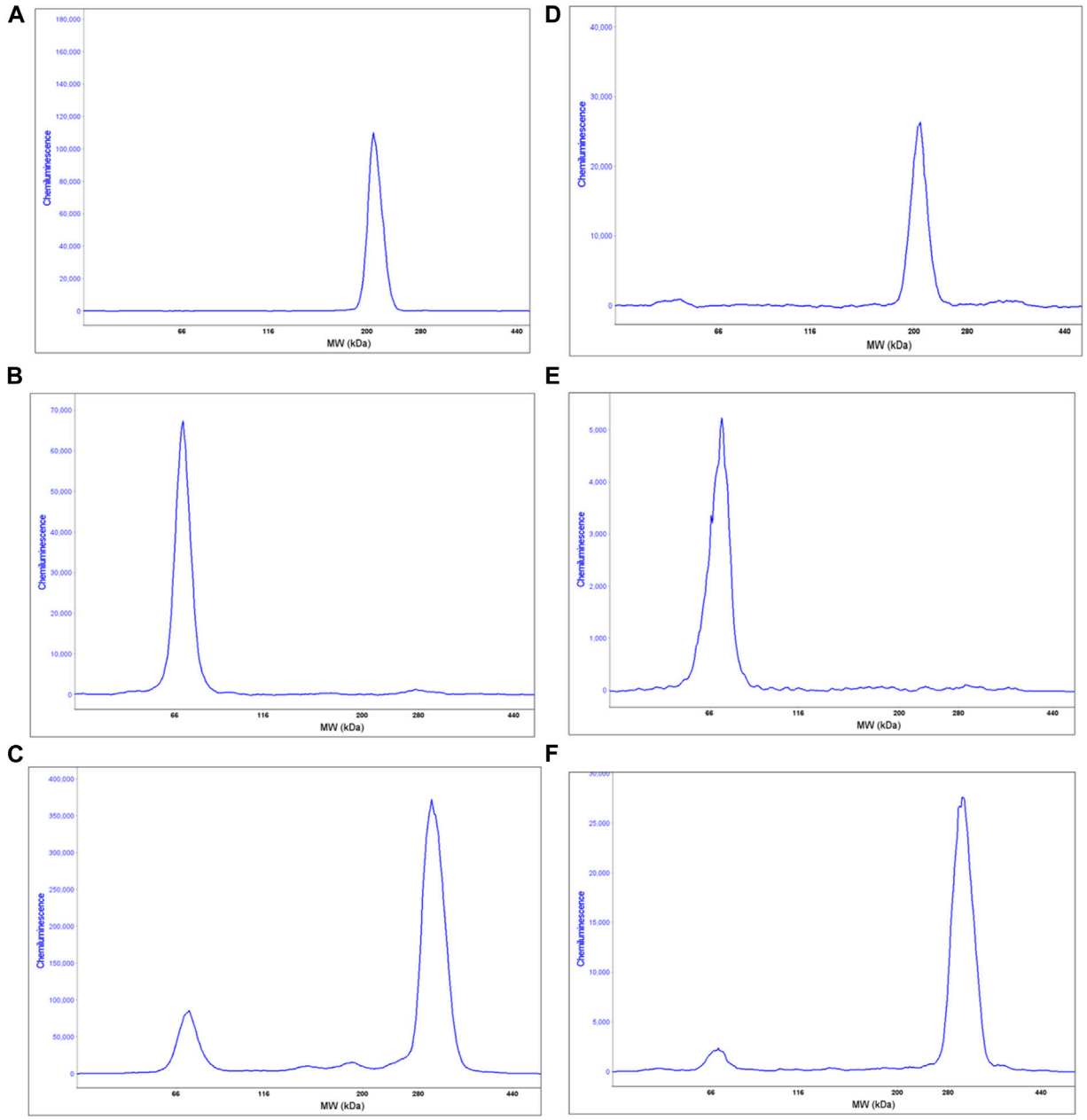

FIGURE 5
Wes analysis of proteins extracted from 1 human healthy donor non-infected and differentiated MyoD lentivirally-transfected fibroblasts and USCs. Graphs **(A, B)** show the sarcomeric myosin heavy chain expression in differentiated MyoD lentivirally-transfected fibroblasts and USCs respectively, using the anti Mf20 antibody. Graphs **(C, D)** show the DYS analysis on non-infected and on differentiated MyoD lentiviral transfected fibroblasts, respectively, using the Ab 154168 against the DMD C-terminal domain. The non-infected fibroblasts analysis shows only one peak at the molecular weight corresponding to the Dp71 DYS short isoform **(C)**. However, in differentiated MyoD-transduced fibroblasts **(D)** two peaks are present - one corresponding to the Dp71 DYS short isoform and the second to the full length Dp421 m DYS isoform. Graphs E and F show the DYS analysis on non-infected and differentiated MyoD lentivirally-transfected USCs, respectively. Like fibroblasts, non-infected USCs show only one peak, corresponding to the Dp71 DYS short isoform **(E)** while differentiated USCs show two peaks, corresponding to the Dp71 (lower) and the full length DYS isoform (higher) **(F)**.

more DMD patients (Aartsma-Rus and Corey., 2020; Anderson, 2021). To this end, more oligonucleotides need to be developed and their uptake into relevant tissues needs to be improved (e.g., by using different chemistries like peptide-phosphorodiamidate morpholino oligonucleotide (PPMO) conjugates (Moulton and Moulton, 2010). Another important aspect to be tackled is the inter-patient variability in response to the same antisense oligonucleotide (Arechavala-Gomeza et al., 2012) (Frank et al., 2020). Other therapeutic strategies for types of mutations other than deletions (i.e., nonsense mutation and readthrough therapies) and gene therapies are under testing or development (Yao et al., 2021). The availability of good cellular models is required to test these approaches *in vitro*. Considering the young average age of DMD patients and their

TABLE 3 DMD transcripts Dp427 and Dp71 expression by qPCR. For each isoform transcript, the corresponding Ct value obtained by qPCR and the relative ratio percentage in fibroblasts and USCs without lentivirus infections (Non Myo-D induced) and after the complete differentiation induced by MyoD-lentiviral transfection (Myo-D induced) are shown. The ratio between the two isoforms is expressed as a percentage and calculated using the following formula: $2^{-(Ct\ Dp427-Ct\ Dp71)}$.

		Non infected cells		differentiated MyoD lentiviral transfected	
	DMD isoforms	Ct	ratio percentage	Ct	ratio percentage
Fibroblasts	Dp427 m	31.3	0.50%	28.63	98.60%
	Dp71	23.9		28.61	
USCs	Dp427 m	31	1.10%	26	696%
	Dp71	24.6		28.8	

already compromised muscular tissue, avoiding skeletal muscle biopsies and, instead, having an easy reproducible, low invasively cellular model should be a priority. In this paper, we detailed a highly efficient transdifferentiation protocol, based on the study of Kabadi and colleagues (Kabadi et al., 2015). Specifically, we used the described protocol to convert both human dermal fibroblasts and stem cells from urine into differentiated myotubes *in vitro*, using the myogenic factor (MyoD gene) delivered by a lentiviral vector. Protein and RNA isolated from both differentiated MyoD lentiviral transfected cells were used to evaluate the cell reprogramming influence on the dystrophin isoforms expression. Moreover, fibroblasts from 25 DMD patients, differentiated using the protocol we describe here, were used to test antisense PMO for the treatment of Duchenne muscular dystrophy; results of this study are summarized in Rossi et al., 2021 (Rossi et al., 2021) and Rossi et al., 2022 (Rossi et al., 2022).The protocol was set up using a commercially available line of immortalized fibroblasts to test the best multiplicity of infection (MOI) and have the highest efficiency with the lowest possible toxicity. The concentration of puromycin required to select transfected cells and the differentiation media to achieve good cell proliferation and subsequently a good fusion index, was determined. Once the protocol was established, it was extended to fibroblasts derived from 5 healthy donors and to USCs from 2 healthy donors, to assess its reproducibility and efficacy in converting cells into the myogenic lineage. All the biological replicates, either fibroblasts or USCs, gave similar immunohistochemistry results. Muscle markers, desmin and myosin heavy chain, were expressed only in MyoD-transfected cells, with the desmin signal being stronger than myosin heavy chain, in both fibroblasts and USC-derived cells. These may be explained by the nature of these markers itself; desmin is well known to be expressed at an early stage of muscle development and precedes all other known muscle structural proteins (Capetanaki et al., 1997) (Clemen et al., 2013). A concomitant factor that might have affected myosin heavy chain expression, is the time cells are left in differentiation media. Although myotubes are evident after 3–5 days in primary differentiation medium, 9 days of culture in primary differentiation medium and 5 in secondary differentiation medium (i.e., for a total of 14 days in differentiation media), give a better myogenic differentiation. For IHC evaluation, cells were maintained for 5 days in primary medium, to reduce the risk that cells would detach from the glass substrate and to confirm the presence of myotubes after a shorter differentiation time. Wes analysis for myosin and DYS were instead performed on proteins extracted from cells that had been in the primary differentiation medium for 9 days. The MF20 peak, in both transduced cell lines, is associated with high chemiluminescence, suggesting that myosin heavy chain is abundant after transfection and its expression seems to be proportionate to their time in primary differentiation medium. The expression of dystrophin isoforms before and after MyoD transfection is very interesting. The full-length Dp427 m isoform is expressed only in muscle and glial cells (Muntoni et al., 2003), while the short isoform Dp71 was believed to have a ubiquitous expression except in skeletal muscle. However, it has been recently demonstrated that the Dp71 isoform is also expressed in healthy human skeletal muscle, even if at low levels and detected only using a high amount of muscle lysate on the Wes (Kawaguchi et al., 2018). On the other hand, several studies found a higher level of Dp71 expression in DMD patients and mdx mouse muscle than in healthy subjects, suggesting a correlation between its expression and the muscle degeneration-regeneration phenomenon observed in the disease (Chesshyre et al., 2022). Using Wes, we confirmed that the Dp427 isoform is expressed only in MyoD induced fibroblasts and USCs, but these cells also expressed the Dp71 isoform at a higher level than in healthy donor skeletal muscle. Although we did not quantify this, it is possible to appreciate the different Dp71 chemiluminescent signal from the non-transfected and the transfected cells, suggesting a reduction in Dp71 expression in the latter compared to the non-transfected cells. This suggests that although MyoD can trigger myogenic conversion, it is not able to completely switch off the proteome of the original cells. In MyoD transfected fibroblasts, for example, the Dp427 m expression is part of the myogenic proteome while the Dp71 is part of the fibroblasts' proteome. We observed that dystrophin transcripts behave differently to the corresponding proteins. The Dp427 and Dp71 transcripts are expressed in all cells but with different levels according to the cell type: Dp427 transcript is more abundant in myogenic cells, whereas Dp71 transcript is more highly expressed in non-transfected cells. These differences are seen in both our cell models. In fibroblasts, the expression of the two DMD transcripts does not change dramatically after conversion: Dp427 expression changes from being around half of Dp71 levels in non-treated fibroblasts to become similar to each other in transfected differentiated cells. USCs have a more dramatic difference in DMD isoform expression: the

Dp427 transcript is present at 1% of the Dp71 transcript expression level in non-converted cells, but after myogenic conversion Dp71 expression is reduced to 14% of the expression level of the Dp427 transcript. This transcript expression evaluation was conducted only in two healthy donors: one for fibroblasts and one for USCs. USCs, obtained from urine samples, may represent an ideal source to study DMD disease (Falzarano et al., 2016) considering the great advantage over conventional cell sources collected through invasive and time-consuming procedures (Falzarano and Ferlini, 2019). But further in-depth studies on USCs are needed either to confirm our preliminary findings on DMD transcript expression differences compare to fibroblasts and to validate them as proper *in vitro* model for drug-testing. The protocol here described could help in this aim, considering that, at the moment, only three MyoD-conversion protocols are described in the literature (Falzarano et al., 2016; Kim et al., 2016; Takizawa et al., 2019) but only one uses the efficient lentivirus as vector (Kim et al., 2016). Moreover, this direct cell reprogramming protocol, is a useful way, in terms of cost and time, to obtain muscular-specific cell types than generate them by reprogramming techniques of induced pluripotent stem (Falzarano and Ferlini, 2019).

In conclusion, being able to obtain a robust patient-derived cell model capable, to some extent, to reproduce the muscle physiological and pathological phenotypes, and avoiding invasive procedures, is a great advantage for scientists and patients, especially in childhood-onset diseases such as DMD. The MyoD gene is effective in myogenic conversion of different cell types (Weintraub et al., 1989) and being able to transfect it into cells using a highly efficient integrating virus, which has low cytotoxicity, provides, in our opinion, a clear advantage compared to other methods in use. Our MyoD lentiviral transduction protocol is able to efficiently and reproducibly convert two different types of human cells, dermal fibroblasts and USCs, into the myogenic lineage. Fibroblasts have been used to test the efficacy of antisense PMO on DMD patients pre-clinically, with reliable results (Rossi et al., 2021) (Rossi et al., 2022) and USCs would be a completely non-invasive cellular model. Future work will be required to assess whether MyoD-induced USCs are indeed a good model for *in vitro* drug testing, which would substantially reduce the need for taking muscle or skin biopsies from patients.

Data availability statement

The raw data supporting the conclusion of this article will be made available by the authors, without undue reservation.

Ethics statement

The studies involving human participants were reviewed and approved by the NHS National Research Ethics: setting up of a rare diseases biological samples bank (biobank) for research to facilitate pharmacological, gene and cell therapy trials in neuromuscular disorders (REC reference number: 06/Q0406/33), and the use of cells as a model system to study pathogenesis and therapeutic strategies for Neuromuscular Disorders (REC reference 13/LO/1826). The patients/participants provided their written informed consent to participate in this study.

Author contributions

RR is responsible of USCs protocol development, cells culturing, transcript analysis, data analyses, manuscript preparation, manuscript review and revisions. ST is responsible for Wes and ICH experiments, data analyses, manuscript review and revisions. PA is responsible for cell culturing and cell storage. WW is responsible for ICH experiments. JeM and FM are responsible for the study design, study investigator and manuscript review. All authors contributed to the article and approved the submitted version.

Funding

This study was sponsored by Sarepta Therapeutics, Inc., to FM and JeM.

Acknowledgments

We wish to thank Dr Charles Gersbach who kindly donated the plasmid (LV-TRE-VP64 mouse MyoD-T2A-dsRedExpress2). The MRC Centre for Neuromuscular Diseases Biobank London, supported by the National Institute for Health Research Biomedical Research Centres at Great Ormond Street Hospital for Children NHS Foundation Trust and at University College London Hospitals NHS Foundation Trust and University College London, is acknowledged for providing fibroblasts and UCSs used in this paper. We want to thank Dr. Marc Moore for his precious contribution to fibroblast protocol set-up, and Dr. John Counsell and Dr. Jinhong Meng for their help with the plasmid experiments.

Conflict of interest

JyM was employed by the Sarepta Therapeutics Inc. FM has received consulting fees from Biogen, Italfarmaco, Pfzer, PTC Therapeutics, Roche, Sarepta Therapeutics, and Wave Therapeutics; and is supported by the National Institute of Health Research Biomedical Research Centre at Great Ormond Street Hospital for Children NHS Foundation Trust, and University College London.

The remaining authors declare that the research was conducted in the absence of any commercial or financial relationships that could be construed as a potential conflict of interest.

Publisher's note

All claims expressed in this article are solely those of the authors and do not necessarily represent those of their affiliated

organizations, or those of the publisher, the editors and the reviewers. Any product that may be evaluated in this article, or claim that may be made by its manufacturer, is not guaranteed or endorsed by the publisher.

References

Aartsma-Rus, A., and Corey, D. R. (2020). The 10th oligonucleotide therapy approved: Golodirsen for Duchenne muscular dystrophy. *Nucleic acid. Ther.* 30 (2), 67–70. doi:10.1089/nat.2020.0845

Albrecht, C., Hosiner, S., Tichy, B., Aldrian, S., Hajdu, S., and Nürnberger, S. (2015). Comparison of lentiviral packaging mixes and producer cell lines for RNAi applications. *Mol. Biotechnol.* 57 (6), 499–505. doi:10.1007/s12033-015-9843-8

Anderson, L. A. (2021). What are the new drugs for Duchenne muscular dystrophy? *Drugs*. Available at: https://www.drugs.com/medical-answers/new-drugs-duchenne-muscular-dystrophy-3172658/.

Anwar, S., and Yokota, T. (2020). Golodirsen for Duchenne muscular dystrophy. *Drugs today* 56 (8), 491–504. doi:10.1358/dot.2020.56.8.3159186

Arechavala-Gomeza, V., Anthony, K., Morgan, J., and Muntoni, F. (2012). Antisense oligonucleotide-mediated exon skipping for Duchenne muscular dystrophy: Progress and challenges. *Curr. gene Ther.* 12 (3), 152–160. doi:10.2174/156652312800840621

Capetanaki, Y., Milner, D. J., and Weitzer, G. (1997). Desmin in muscle formation and maintenance: Knockouts and consequences. *Cell Struct. Funct.* 22 (1), 103–116. doi:10.1247/csf.22.103

Chesshyre, M., Ridout, D., Hashimoto, Y., Ookubo, Y., Torelli, S., Maresh, K., et al. (2022). Investigating the role of dystrophin isoform deficiency in motor function in Duchenne muscular dystrophy. *J. cachexia, sarcopenia muscle* 13 (2), 1360–1372. doi:10.1002/jcsm.12914

Clemen, C. S., Herrmann, H., Strelkov, S. V., and Schröder, R. (2013). Desminopathies: Pathology and mechanisms. *Acta Neuropathol.* 125, 47–75. doi:10.1007/s00401-012-1057-6

Crisafulli, S., Sultana, J., Fontana, A., Salvo, F., Messina, S., and Trifirò, G. (2020). Global epidemiology of Duchenne muscular dystrophy: An updated systematic review and meta-analysis. *Orphanet J. rare Dis.* 15 (1), 141. doi:10.1186/s13023-020-01430-8

de León, M. B., Montañez, C., Gómez, P., Morales-Lázaro, S. L., Tapia-Ramírez, V., Valadez-Graham, V., et al. (2005). Dystrophin Dp71 expression is down-regulated during myogenesis: Role of Sp1 and Sp3 on the Dp71 promoter activity. *J. Biol. Chem.* 280 (7), 5290–5299. doi:10.1074/jbc.M411571200

Falzarano, M. S., D'Amario, D., Siracusano, A., Massetti, M., Amodeo, A., La Neve, F., et al. (2016). Duchenne muscular dystrophy myogenic cells from urine-derived stem cells recapitulate the dystrophin genotype and phenotype. *Hum. gene Ther.* 27 (10), 772–783. doi:10.1089/hum.2016.079

Falzarano, M. S., and Ferlini, A. (2019). Urinary stem cells as tools to study genetic disease: Overview of the literature. *J. Clin. Med.* 8 (5), 627. doi:10.3390/jcm8050627

Fortunato, F., Rossi, R., Falzarano, M. S., and Ferlini, A. (2021). Innovative therapeutic approaches for Duchenne muscular dystrophy. *J. Clin. Med.* 10 (4), 820. doi:10.3390/jcm10040820

Fralish, Z., Lotz, E. M., Chavez, T., Khodabukus, A., and Bursac, N. (2021). Neuromuscular development and disease: Learning from *in vitro* and *in vivo* models. *Front. Cell Dev. Biol.* 9, 764732. doi:10.3389/fcell.2021.764732

Frank, D. E., Schnell, F. J., Akana, C., El-Husayni, S. H., Desjardins, C. A., Morgan, J., et al. 2020. Increased dystrophin production with golodirsen in patients with Duchenne muscular dystrophy. *Neurology*, 94(21), e2270. doi:10.1212/WNL.0000000000009233

Fujii, I., Matsukura, M., Ikezawa, M., Suzuki, S., Shimada, T., and Miike, T. (2006). Adenoviral mediated MyoD gene transfer into fibroblasts: Myogenic disease diagnosis. *Brain and Dev.* 28 (7), 420–425. doi:10.1016/j.braindev.2005.12.007

Iftikhar, M., Frey, J., Shohan, M. J., Malek, S., and Mousa, S. A. (2021). Current and emerging therapies for Duchenne muscular dystrophy and spinal muscular atrophy. *Pharmacol. Ther.* 220, 107719. doi:10.1016/j.pharmthera.2020.107719

Kabadi, A. M., Thakore, P. I., Vockley, C. M., Ousterout, D. G., Gibson, T. M., Guilak, F., et al. (2015). Enhanced MyoD-induced transdifferentiation to a myogenic lineage by fusion to a potent transactivation domain. *ACS Synth. Biol.* 4 (6), 689–699. doi:10.1021/sb500322u

Kawaguchi, T., Niba, E., Rani, A., Onishi, Y., Koizumi, M., Awano, H., et al. (2018). Detection of dystrophin Dp71 in human skeletal muscle using an automated capillary western assay system. *Int. J. Mol. Sci.* 19 (6), 1546. doi:10.3390/ijms19061546

Kim, E. Y., Page, P., Delle fave-Castillo, L. M., McNally, E. M., and Wyatt, E. J. (2016). Direct reprogramming of urine-derived cells with inducible MyoD for modeling human muscle disease. *Skelet. muscle* 6, 32. doi:10.1186/s13395-016-0103-9

Kutner, R., Zhang, X. .Y., and Reiser, J. (2009). Production, concentration and titration of pseudotyped HIV-1-based lentiviral vectors. *Nat. Protoc.* 4, 495–505. doi:10.1038/nprot.2009.22

Lee, L. A., Karabina, A., Broadwell, L. J., and Leinwand, L. A. (2019). The ancient sarcomeric myosins found in specialized muscles. *Skelet. muscle* 9 (1), 7. doi:10.1186/s13395-019-0192-3

Moulton, H. M., and Moulton, J. D. (2010). Morpholinos and their peptide conjugates: Therapeutic promise and challenge for Duchenne muscular dystrophy. *Biochimica biophysica acta* 1798 (12), 2296–2303. doi:10.1016/j.bbamem.2010.02.012

Muntoni, F., Torelli, S., and Ferlini, A. (2003). Dystrophin and mutations: One gene, several proteins, multiple phenotypes. *Lancet Neurology* 2 (12), 731–740. doi:10.1016/s1474-4422(03)00585-4

Muses, S., Morgan, J. .E., and Wells, D. .J. (2011). A new extensively characterised conditionally immortal muscle cell-line for investigating therapeutic strategies in muscular dystrophies. *PLoS One* 6 (9), e24826. doi:10.1371/journal.pone.0024826

Neri, M., Rossi, R., Trabanelli, C., Mauro, A., Selvatici, R., Falzarano, M. S., et al. (2020). The genetic landscape of dystrophin mutations in Italy: A Nationwide study. *Front. Genet.* 11, 131. doi:10.3389/fgene.2020.00131

Paulin, D., and Li, Z. (2004). Desmin: A major intermediate filament protein essential for the structural integrity and function of muscle. *Exp. Cell Res.* 301 (1), 1–7. doi:10.1016/j.yexcr.2004.08.004

Roest, P. A., Bakker, E., Fallaux, F. J., Verellen-Dumoulin, C., Murry, C. E., and den Dunnen, J. T. (1999). New possibilities for prenatal diagnosis of muscular dystrophies: Forced myogenesis with an adenoviral MyoD-vector. *Lancet* 353 (9154), 727–728. doi:10.1016/S0140-6736(98)05471-3

Rossi, R., Moore, M., Torelli, S., Ala, P., Catapano, F., Phadke, R., et al. (2021). Evaluation of DMD transcripts after golodirsen treatment of MyoD-converted fibroblasts from 4053-101 clinical trial patients. *Neuromuscul. Disord.* 31 (1), S93. doi:10.1016/j.nmd.2021.07.170

Rossi, R., Moore, M., Torelli, S., Ala, P., Catapano, F., Rahul, P., et al. (2022). VP.58 Golodirsen induced DMD transcripts localization and dystrophin production in MyoD-converted fibroblasts from 4053-101 clinical trial patients. *Neuromuscul. Disord.* 32 (1), S103. doi:10.1016/j.nmd.2022.07.252

San Miguel, M. T., and Vargas, E. (2006). Drug evaluation and approval process in the European Union. *Arthritis rheumatism* 55 (1), 12–14. doi:10.1002/art.21712

Schwartz, M. P., Rogers, R. E., Singh, S. P., Lee, J. Y., Loveland, S. G., Koepsel, J. T., et al. (2013). A quantitative comparison of human HT-1080 fibrosarcoma cells and primary human dermal fibroblasts identifies a 3D migration mechanism with properties unique to the transformed phenotype. *PloS one* 8 (12), e81689. doi:10.1371/journal.pone.0081689

Shimizu, T., Dennis, J. E., Masaki, T., and Fischman, D. A. (1985). Axial arrangement of the myosin rod in vertebrate thick filaments: Immunoelectron microscopy with a monoclonal antibody to light meromyosin. *J. Cell Biol.* 101 (3), 1115–1123. doi:10.1083/jcb.101.3.1115

TAKARA (2022). Takara BIO INC. Available at: https://www.takarabio.com/learning-centers/gene-function/viral-transduction/lentivirus/lentiviral-tips. n.d.

Takizawa, H., Hara, Y., Mizobe, Y., Ohno, T., Suzuki, S., Inoue, K., et al. (2019). Modelling Duchenne muscular dystrophy in MYOD1-converted urine-derived cells treated with 3-deazaneplanocin A hydrochloride. *Sci. Rep.* 9, 3807. doi:10.1038/s41598-019-40421-z

Thavorntanaburt, S., Tanboon, J., Likasitwattanakul, S., Sangruchi, T., Nishino, I., Ngerncham, M., et al. (2018). Impact of muscle biopsy on diagnosis and management of children with neuromuscular diseases: A 10-year retrospective critical review. *J. Pediatr. Surg.* 53 (3), 489–492. doi:10.1016/j.jpedsurg.2017.06.006

Weintraub, H., Tapscott, S. J., Davis, R. L., Thayer, M. J., Adam, M. A., Lassar, A. B., et al. (1989). Activation of muscle-specific genes in pigment, nerve, fat, liver, and fibroblast cell lines by forced expression of MyoD. *Proc. Natl. Acad. Sci. U. S. A.* 86 (14), 5434–5438. doi:10.1073/pnas.86.14.5434

Yao, S., Chen, Z., Yu, Y., Zhang, N., Jiang, H., Zhang, G., et al. (2021). Current pharmacological strategies for Duchenne muscular dystrophy. *Front. Cell Dev. Biol.* 9, 689533. doi:10.3389/fcell.2021.689533

frontiers | Frontiers in Physiology

TYPE Review
PUBLISHED 30 May 2023
DOI 10.3389/fphys.2023.1180980

OPEN ACCESS

EDITED BY
Masatoshi Suzuki,
University of Wisconsin-Madison,
United States

REVIEWED BY
Young il Lee,
University of Florida, United States
Elen H. Miyabara,
University of São Paulo, Brazil
Keitaro Yamanouchi,
The University of Tokyo, Japan

*CORRESPONDENCE
Michael A. Rudnicki,
mrudnicki@ohri.ca

RECEIVED 06 March 2023
ACCEPTED 23 May 2023
PUBLISHED 30 May 2023

CITATION
Kodippili K and Rudnicki MA (2023), Satellite cell contribution to disease pathology in Duchenne muscular dystrophy.
Front. Physiol. 14:1180980.
doi: 10.3389/fphys.2023.1180980

Satellite cell contribution to disease pathology in Duchenne muscular dystrophy

Kasun Kodippili[1,2] and Michael A. Rudnicki[1,2]*

[1]The Sprott Centre for Stem Cell Research, Regenerative Medicine Program, Ottawa Hospital Research Institute, Ottawa, ON, Canada, [2]Department of Cellular and Molecular Medicine, Faculty of Medicine, University of Ottawa, Ottawa, ON, Canada

Progressive muscle weakness and degeneration characterize Duchenne muscular dystrophy (DMD), a lethal, x-linked neuromuscular disorder that affects 1 in 5,000 boys. Loss of dystrophin protein leads to recurrent muscle degeneration, progressive fibrosis, chronic inflammation, and dysfunction of skeletal muscle resident stem cells, called satellite cells. Unfortunately, there is currently no cure for DMD. In this mini review, we discuss how satellite cells in dystrophic muscle are functionally impaired, and how this contributes to the DMD pathology, and the tremendous potential of restoring endogenous satellite cell function as a viable treatment strategy to treat this debilitating and fatal disease.

KEYWORDS

Duchenne muscular dystrophy, satellite cells, skeletal muscle stem cells, muscle regeneration, myogenesis, dystrophin, asymmetric cell division, symmetric cell division

Introduction

Duchenne muscular dystrophy (DMD) is a rare yet well-characterized, severe and progressive muscle wasting disease. It is the most common type of muscular dystrophy with a global incidence of 1 in 5,000 live male births (Mendell et al., 2012; Mah et al., 2014; Ryder et al., 2017). Patients first present with symptoms such as difficulty climbing stairs and rising from a sitting or lying position, frequent falls, waddling gate, trouble running and jumping, etc., around 2–3 years of age. The progressive nature of this degenerative disease means that patients are often wheel-chair bound by the age of 10–12, and require assisted ventilation by the third decade of their life. Despite improvements in patient care and treatment strategies in the last few decades, most DMD patients die between 20–40 years of age from respiratory and/or cardiac complications (Mercuri et al., 2019).

Etiology

DMD is a genetic disease caused by mutations in the dystrophin-encoding *DMD* gene on the X chromosome. Consequently, DMD is presented primarily in males, and is maternally inherited. With 79 exons, and spanning 2.2 Mb, the *DMD* gene is the largest known human gene (Koenig et al., 1987). The gene also carries a relatively high mutation rate, with about a third of all DMD cases caused by *de novo* germline mutations. Approximately one-third of all mutations in DMD patients are caused by deletions of one or more exons. Another 5%–15% are duplications, and about 20% are small mutations such as point mutations, deletions, or insertions (Aartsma-Rus et al., 2006). While these large deletions or duplications can occur anywhere in the gene,

two mutation hotspots have been identified between exons 45–55 and 2–10 (Duan et al., 2021). In general, if mutations do not disrupt the open reading frame, a partially functional dystrophin protein, albeit shorter or longer in the middle, will be produced and result in a milder disease called Becker muscular dystrophy (BMD) (Koenig et al., 1989; Duan et al., 2021).

Mechanisms and pathophysiology

DMD results in the loss of the muscle isoform of dystrophin (Dp427m) (Hoffman et al., 1987). The dystrophin protein plays a key structural role in muscle where it links the internal cytoskeleton to the extracellular matrix and the dystrophin-associated protein complex (DAPC) (Ervasti and Campbell, 1993; Ervasti, 2007). The loss of dystrophin protein results in the disassembly of the DAPC, reduced expression levels of certain DAPC components, and the loss of the interaction between F-actin in cytoskeleton and the extracellular matrix (Figure 1). This, together with the loss of crucial signaling roles played by DAPC member proteins, leads to wide-ranging consequences including loss of myofiber integrity, membrane leakage, impaired muscle fiber contractile activity, and progressive muscle degeneration (Nowak and Davies, 2004; Guiraud et al., 2015).

Muscle degeneration

Dystrophin, along with the DAPC, function as a molecular scaffold serving a mechanical function during muscle contraction. In healthy muscle, this linkage between the cytoskeleton, sarcolemma and extracellular matrix is crucial for weathering the force output and significant mechanical stress arising from each bout of muscle contraction. Even so, repetitive contractions can cause sarcolemmal defects and tears in healthy muscle as well, leading to muscle degeneration and inflammation (Ervasti and Sonnemann, 2008; Abdel-Salam et al., 2009). In response, tissue resident skeletal muscle stem cells (MuSCs, also called satellite cells) are activated and mobilized to repair the damage and replace lost muscle fibers (Dumont et al., 2015a). In dystrophic muscle, the sarcolemma is further susceptible to contraction-induced damage, and this increased sarcolemmal permeability results in the influx of calcium and other small molecules leading to cell dysfunction and death. Continued cell death ultimately leads to an imbalance in muscle degeneration and regeneration, and the deposition of fibrotic tissue in place of functional muscle, further exacerbating disease pathology. Unfortunately for DMD patients, lack of dystrophin protein has direct consequences on the function of satellite cells as well (Dumont and Rudnicki, 2016). This stem cell phenotype and its contribution to disease in DMD, along with the remarkable potential of stem cell-based treatments to alter the rates of muscle degeneration and regeneration, and disease progression will be the focus of this mini review.

Satellite cells

Adult skeletal muscle, which accounts for about 30%–40% of the adult human body weight, is stable under homeostatic conditions, with only sporadic proliferation and fusion of satellite cells to compensate for muscle turnover from normal

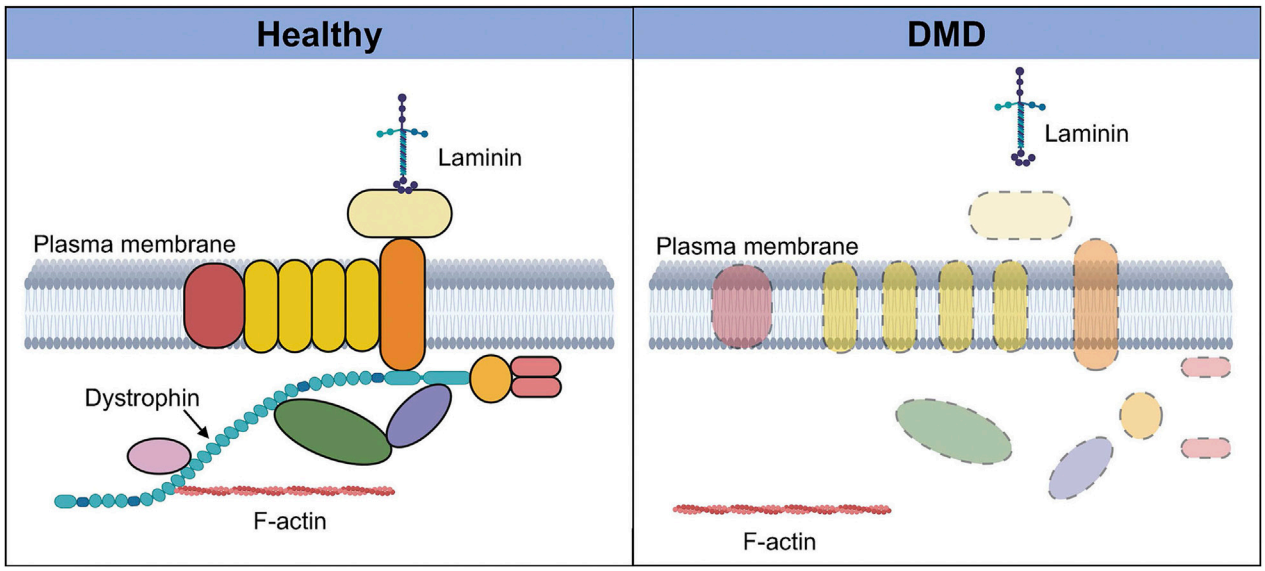

FIGURE 1
Dystrophin-associated protein complex in healthy and Duchenne muscular dystrophy (DMD) muscle. In healthy muscle (left), dystrophin and its binding partners together form a protein complex called the dystrophin-associated protein complex, which plays numerous signaling and structural roles. This highly organized transmembrane protein complex links the intracellular cytoskeleton with the sarcolemma and the extra-cellular matrix via laminin. In the absence of dystrophin in DMD muscle (right), this protein complex is disassembled, and there is delocalization and loss of expression of several components of the complex. The interaction between F-actin and the extracellular matrix is also lost, resulting in a wide range of deleterious effects that severely compromise the integrity and function of the tissue. Created with BioRender.com.

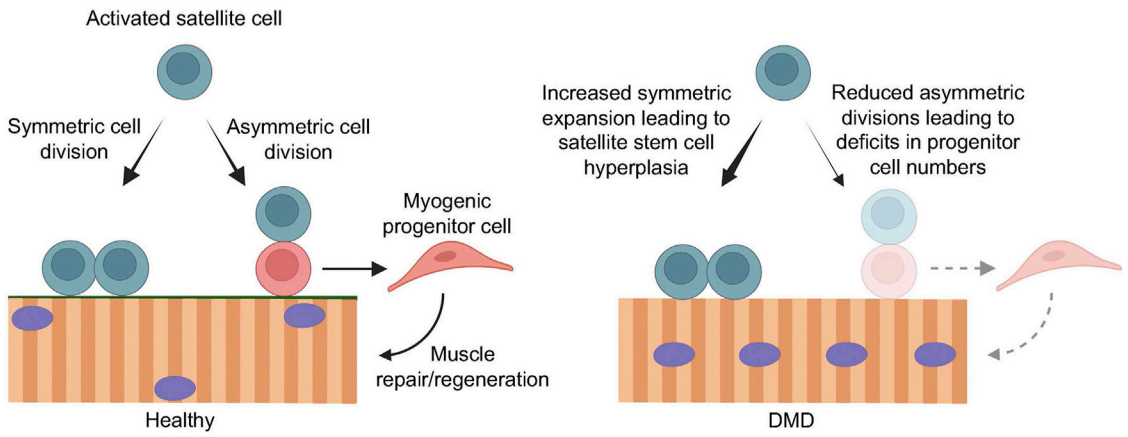

FIGURE 2
Loss of dystrophin compromises efficient muscle regeneration. In healthy muscle (left), regenerative myogenesis is initiated by activated satellite cells that undergo symmetric cell division to maintain the muscle stem cell pool, as well as asymmetric cell division to give rise to myogenic progenitor cells that expand and contribute to efficient muscle repair and regeneration. In the context of DMD (right), the loss of dystrophin in activated satellite cells results in impaired cell polarity cues, leading to mitotic defects and reduced asymmetric cell divisions. Consequently, the balance favors symmetric stem cell expansion, resulting in satellite cell hyperplasia, and greatly reduced asymmetric cell divisions and myogenic progenitor cell numbers. This impairs muscle regeneration, leading to progressive muscle degeneration and wasting. Created with BioRender.com.

wear and tear. Yet, upon tissue injury, skeletal muscle demonstrates an incredible ability to regenerate. This is enabled by satellite cells, the tissue resident stem cell population. Satellite cells, independently discovered in 1961 by Alexander Mauro and Bernard Katz, are cells "wedged" between the basal lamina and plasma membrane of the muscle fiber (Mauro, 1961; Scharner and Zammit, 2011). Satellite cells provide new myonuclei during postnatal growth, and then become mitotically quiescent in mature muscle, while also retaining the ability to supply myoblasts for muscle hypertrophy and repair when called upon to do so (Yablonka-Reuveni, 2011).

In adult muscle, MuSCs can be identified by the transcription factor Pax7, which is expressed in all quiescent and proliferating satellite cells, across many different species (Yin et al., 2013). Prenatal and postnatal myogenesis are regulated by a family of basic helix-loop-helix transcription factors known as myogenic regulatory factors (MRFs). These include Myf5, MyoD, Myogenin and MRF4, and they orchestrate the progression of satellite cells through the myogenic program, along with Pax7 (Yablonka-Reuveni et al., 2008; Schmidt et al., 2019; Shirakawa et al., 2022). While the dynamics of their temporal and spatial expression have allowed for the characterization of a sequential and hierarchical relationship between these factors, the full scope of their mechanisms of action is still being worked out. In general, upregulation of Myf5 marks the earliest phase of myogenic commitment, followed by expression of MyoD, which marks a majority of activated and proliferating satellite cells. Downregulation of Pax7 and concomitant upregulation of MRF4 and myogenin then signal the terminal differentiation of satellite cells into skeletal muscle progenitor cells (Relaix and Zammit, 2012; Wang and Rudnicki, 2012; Forcina et al., 2020; Relaix et al., 2021).

Satellite cell differentiation and self-renewal

While satellite cell differentiation is the process by which newly formed myofibers are available for muscle repair and regeneration, satellite cell self-renewal is required to replenish the stem cell pool. Maintenance of this balance between differentiation and self-renewal is critical for muscle homeostasis. Following activation, a satellite cell can undergo either symmetric or asymmetric cell division (Figure 2). In symmetric cell division, one stem cell can generate two functionally identical daughter cells. In asymmetric satellite cell division, the asymmetric segregation of intrinsic cell fate determinants prior to cell division can give rise two daughter cells with divergent cell fates, where one cell will be a self-renewing stem cell, while the other will be a committed myogenic progenitor that can differentiate and fuse, either with each other to form new myotubes or to existing muscle fibers (Kuang et al., 2007; Dumont et al., 2015a; Feige et al., 2018) (Figure 2). Consequently, a defect in self-renewal ability results in depleted satellite cell numbers and the stem cell pool, and impaired muscle regeneration capacity. Reduced asymmetric divisions, on the other hand, lead to a reduced rate of myogenic progenitor cell generation, which also impairs muscle regeneration (Figure 2). As such, a tightly regulated balance between satellite cell self-renewal and differentiation is paramount for maintaining the stem cell pool and for generating enough progenitors to support efficient growth and regeneration of muscle.

Satellite cells in DMD

Our previous work established that, in addition to the myofiber, dystrophin protein is also expressed at high levels in activated

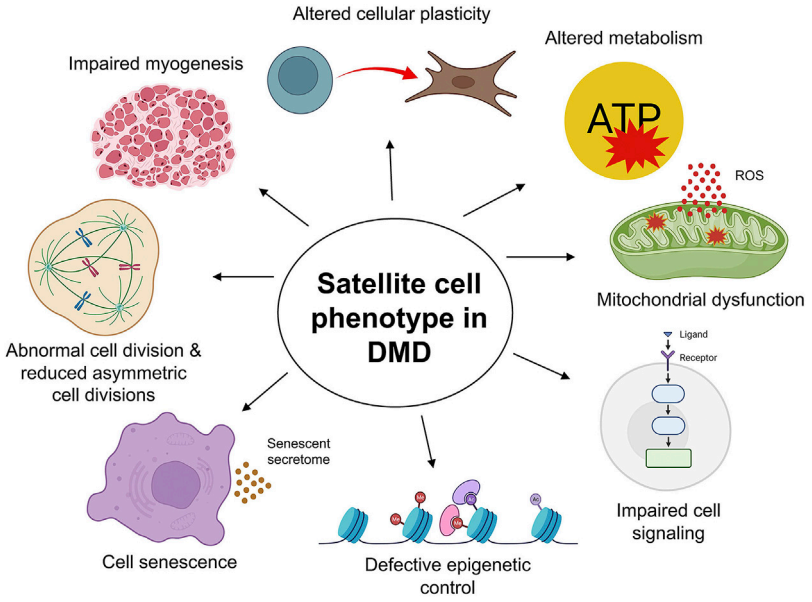

FIGURE 3
The satellite cell phenotype in Duchenne muscular dystrophy (DMD). The cell-intrinsic phenotype of satellite cells in DMD muscle manifests in a variety of ways. The loss of dystrophin impairs satellite cell division, leading to reduced asymmetric cell divisions, myogenic progenitor cells, and compromised regenerative myogenesis. Altered cellular plasticity of satellite cells in response to chronic injury and inflammation contributes to connective tissue deposition. Aberrant mitochondrial morphology, function, and metabolic profile lead to reduced proliferation and functional loss of satellite cells, further exacerbating DMD pathology, particularly in advanced stages of the disease. Elevated expression of senescence markers, mitotic defects, and increased oxidative stress and inflammation are all characteristic of DMD satellite cells and muscle pathology. Further, satellite cells maintain tightly regulated epigenetic control and cell signaling for optimal function. Loss of dystrophin in DMD satellite cells compromises these regulatory mechanisms, affecting satellite cell function at all stages, including maintenance of quiescence, activation, division, proliferation, and differentiation, ultimately contributing to the severe disease pathology in DMD. Created with BioRender.com.

satellite cells where it regulates satellite cell fate and myogenesis (Dumont et al., 2015b). Dystrophin binds the cell polarity effector Mark2 (also known as Par1b) in activated satellite cells. This interaction promotes the asymmetric segregation of the cell polarity regulator Pard3 to the opposite pole of the cell, and establishes the polarized distribution of the PAR complex (Dumont et al., 2015b). This results in the apicobasal orientation of mitotic spindle and asymmetric cell division. Asymmetric cell division enables satellite cells to maintain their reserve cell pool (via the self-renewing stem cell), and contribute to the myogenic progenitor population at the same time (via the differentiating cell).

In the absence of dystrophin in DMD satellite cells, cellular polarity is disrupted, resulting in increased mitotic stress, and abnormal mitotic spindle orientation and cell division. Further, there is a loss of asymmetric cell divisions and a reduction in myogenic progenitor cell numbers and muscle regeneration (Dumont et al., 2015b; Chang et al., 2016; Feige et al., 2018).

Pathophysiology of the satellite cell phenotype in DMD

It is now well established that muscle fibers from human DMD patients as well as dystrophin-deficient mdx mice show significantly elevated numbers of Pax7$^+$ satellite cells (Kottlors and Kirschner, 2010; Bankole et al., 2013; Dumont et al., 2015b; Ribeiro et al., 2019) (Figure 2). This is contrary to the initial hypothesis that satellite cell numbers are exhausted in DMD (Heslop et al., 2000; Luz et al., 2002). Instead, accumulating evidence from our group and others points to a cell intrinsic defect in dystrophic satellite cells, resulting in reduced asymmetric cell division and myogenic commitment, as well as increased mitotic stress, abnormal cell division events and cellular senescence (Figure 3).

Reduced asymmetric cell division and impaired myogenesis

In dystrophic muscle, the expression of Mark2 is reduced, and the PAR complex remains uniformly distributed, which greatly affects cell polarity establishment and asymmetric cell division. We have previously shown that satellite cells from mdx mice display a 5-fold reduction in the proportion of asymmetric divisions (Dumont et al., 2015b). Consequently, the number of myogenic progenitors that are available for efficient muscle regeneration is also significantly reduced (Figure 2). Further exacerbating this defect is the altered differentiation kinetics of dystrophic myoblasts. Yablonka-Reuveni and Anderson previously showed that dystrophic myoblasts in cell culture displayed an earlier reduction in MyoD expression and an earlier than normal expression of myogenin, compared to wild-type cells (Yablonka-Reuveni and Anderson, 2006). Dystrophic cells also differentiated more rapidly in cell culture than did wild-type cells. Consistent with these early findings, more recent evidence

using transcriptomic, genome-scale metabolic modeling and functional analyses have also established cell-autonomous defects in DMD myoblasts. Gosselin et al. showed significantly altered expression of 170 genes in mdx myoblasts, including MyoD and key genes controlled by MyoD such as myogenin, Mymk (myomaker), Mymx (myomixer), epigenetic regulators, extracellular matrix interactors, calcium signaling and fibrosis genes (Gosselin et al., 2022). Functionally, these changes resulted in increased myoblast proliferation, altered chemotaxis, and accelerated differentiation in myoblasts derived from mdx mice as well as human DMD patients (Gosselin et al., 2022). Myoblasts are the effector cells of muscle growth and repair, and these data underline the cell autonomous abnormalities in DMD that negatively impact cell cycle exit, migration to the site of muscle damage, and cell fusion; three processes that are critical for efficient myogenesis.

Myotubes derived from DMD myoblasts have also been observed to have reduced expression of sarcomeric genes, likely contributing to the characteristic sarcomeric instability seen in DMD skeletal muscle (Barthélémy et al., 2022). Moreover, DMD patient derived human induced pluripotent stem cells differentiated into myotubes have also been shown to undergo pronounced calcium ion (Ca^{2+}) influx upon *in vitro* contraction (Shoji et al., 2015; Yoshioka et al., 2021). Increased susceptibility to sarcolemmal injury and excess calcium ion influx are generally regarded as the initial triggers for skeletal muscle damage in DMD, and these lines of evidence once again highlight the stem cell phenotype that contributes to DMD pathology.

Mitochondrial dysfunction

Currently, there is a large body of data implicating mitochondrial dysfunction as a secondary contributor to muscle pathology in DMD (Vila et al., 2017; Ramos et al., 2020; Reid and Alexander, 2021; Bellissimo et al., 2022) (Figure 3). Moore et al. showed aberrant mitochondrial morphology, reduced cristae number, and large mitochondrial vacuoles in mdx mouse muscle prior to onset of myofiber necrosis, which progresses with disease severity (Moore et al., 2020). Further, microtubule disorganization has been noted in dystrophin-deficient mouse muscle which was associated with impaired ADP control of mitochondrial bioenergetics (Ramos et al., 2020). While a low-level production of reactive oxygen species (ROS) is required for cell-cell signaling in normal cells, dysfunctional mitochondria in dystrophic muscle release abnormal levels of ROS, which can then activate pro-inflammatory pathways which further exacerbate disease pathology (Chen et al., 2022b). Further, it has been shown using nuclear magnetic resonance spectroscopy, that such elevated ROS production and damaged mitochondrial membrane in human and mouse dystrophic mitochondria are associated with reduced ATP generation and oxidative capacity (Kuznetsov et al., 1998; Griffin et al., 2001; Sharma et al., 2003). And restoring mitochondrial bioenergetic function ameliorated the DMD pathology in mouse models (Pauly et al., 2012; Luan et al., 2021).

So what role do satellite cells play in this context? Onopiuk et al. (2009) previously showed that mdx myoblasts displayed reduced oxygen consumption and mitochondrial membrane potential, and elevated ROS formation. Matre et al. (2019) provided further insight into the role of dystrophin deficiency in satellite cells with respect to bioenergetics and stress resistance. By restoring dystrophin expression in mdx satellite cells via CRISPR/Cas9, they showed significantly reduced oxidative stress, ROS formation, and mitochondrial membrane potential in edited cells. Dystrophin restoration also improved mitochondrial function in mdx satellite cells in terms of oxygen consumption rate, ATP production, maximal respiratory capacity, and mitochondrial coupling efficiency. These dystrophin-restored mdx satellite cells also displayed increased tricarboxylic acid (TCA) cycle activity and levels of Krebs cycle metabolites such as citrate and malate. Finally, transplantation of these edited mdx satellite cells in dystrophic mice resulted in significantly better survival and cell engraftment compared to unedited mdx satellite cells (Matre et al., 2019).

In regenerating muscle, mitochondrial homeostasis is maintained by removing damaged mitochondria by mitophagy, and adding newly synthesized mitochondria derived from satellite cells to reconstitute the mitochondrial network in regenerating myofibers. Using a satellite cell transplantation model, Mohiuddin et al. (2020) show that dystrophic satellite cells have altered mitochondrial gene expression and content, and a significant reduction in mitochondrial respiration. Further, DMD satellite cells, which carry defective mitochondria, fuse with existing fibers to propagate their mitochondrial dysfunction during muscle regeneration (Pant et al., 2015; Mohiuddin et al., 2020). They also show that functional satellite cells from healthy donors can reconstitute the mitochondrial network in dystrophic host muscle and improve mitochondrial function. Therefore, the quality of the mitochondrial network of the satellite cells that are fusing to existing fibers during muscle repair determine the oxidative capacity of the muscle undergoing repair.

Satellite cell senescence

Cell senescence is a permanent (i.e., irreversible) cell cycle arrest, which is a normal occurrence during embryonic development, tissue repair, and regeneration (Kumari and Jat, 2021). Once the growth and regeneration processes are completed, these senescent cells are eliminated. Cell senescence can be induced by stressors such as DNA damage stress, oxidative stress, etc. However, a progressive accumulation of senescent cells is a hallmark of muscle pathology, such as in DMD, due to elevated levels of oxidative stress and inflammation (Sugihara et al., 2020; Saito and Chikenji, 2021; Young et al., 2021). Senescent cells are metabolically active and secrete inflammatory cytokines and chemokines that lead to a further increase in chronic inflammation (Kwon et al., 2019). They can also induce other nearby non-senescent cells to undergo senescence by releasing juxtacrine and paracrine effectors, a phenomenon termed secondary senescence (Kirschner et al., 2020). Therefore, senescent cells can have widespread effects in exacerbating tissue pathologies.

In a recent study, Sugihara et al. (2020) provided new insights into the role of satellite cell senescence in DMD progression (Figure 3). They show elevated expression of senescence markers such as CDKN2A, p16, and p19 in a rat model of DMD, as well as

skeletal muscle tissue of human DMD patients. By reversing senescence via genetic ablation of p16, the authors observed a functional recovery of satellite cells, enhanced muscle regeneration, and the amelioration of the DMD phenotype in the rat model (Sugihara et al., 2020). In addition, depleting senescent cells via pharmacological means in late-stage DMD rats resulted in significantly decreased expression of senescence markers and improved muscle regeneration. These results are evidence that the presence of senescent cells is detrimental and exacerbates disease progression in DMD.

In another study, mdx mice carrying shortened telomeres in satellite cells displayed severe muscular dystrophy that worsened with age (Sacco et al., 2010). In these mice, the cell-autonomous defect of satellite cells to maintain the damage-repair cycle of dystrophic muscle was further worsened by a decreased telomere length. Since telomere shortening is one of the causes of cell senescence, these data could be supportive of the deleterious impact of senescent cells in dystrophic muscle.

Altered cellular plasticity

As mentioned previously, one of the hallmarks of DMD pathology is the excessive and dysregulated deposition of fibrotic tissue in skeletal muscle in response to chronic tissue injury and inflammation. The extent of the accumulation of connective and fat tissue often corresponds to the severity of the disease. TGFβ activity and the expression of its downstream signaling mediators (such as activated SMAD2/3) increase with age in mdx mice, contributing to impaired muscle regeneration and function (Vidal et al., 2008; Mann et al., 2011; Kharraz et al., 2014). While the role of muscle resident fibro-adipogenic progenitors (FAPs) that differentiate into fibroblasts and adipocytes and contribute to fibrosis has been well characterized, accumulating evidence of altered cellular plasticity of satellite cells shows that a fraction of these muscle stem cells can undergo a mesenchymal-like/fibrogenic transition in DMD muscle (Figure 3).

Previous *in vitro* data using satellite cells isolated from old (18-mo) mdx mice or from muscles of DMD patients showed that a fraction of these myoblasts was reprogrammed to attain a profibrotic function, producing higher amounts of collagen in culture compared to control cells (Ionasescu and Ionasescu, 1982; Alexakis et al., 2007). Subsequently, Biressi et al. (2014) provided *in vivo* evidence that satellite cells obtained from dystrophic muscles of mdx mice showed compromised myogenic potential and enhanced expression of fibrogenic genes due to increased TGFβ activity. They showed elevated canonical Wnt signaling in mdx mouse muscles which in turn induced the expression of TGFβ2. This Wnt-TGFβ2 signaling axis promoted the acquisition of fibrogenic features by myoblasts. Furthermore, *in vivo* inhibition of the TGFβ pathway in mdx mice with anti-TGFβ antibody or by drug treatment reduced the expression of fibrotic genes and markers such as collagen type I and fibronectin 1, and rescued the satellite cell phenotype and partially ameliorated the dystrophic pathology (Biressi et al., 2014).

Consistent with these data, Pessina et al. (2015) also provided evidence of TGFβ-induced alterations in cellular plasticity in advanced dystrophic muscles of humans and mice where a fraction of myogenic cells (in addition to endothelial and inflammatory cells) lost their cell identity and acquired the capacity to produce extra cellular matrix proteins such as α-smooth muscle actin, collagen type I, and fibronectin. Interestingly, this fibrogenic process in response to elevated TGFβ signaling also resulted in the acquisition of a mesenchymal progenitor multipotent status, where myogenic cells that had acquired fibrogenic traits were also more prone to undergo osteogenic or adipogenic conversions (Pessina et al., 2015). These alterations in cellular plasticity of dystrophic satellite cells directly contributed to impaired muscle regeneration and worsened disease pathology.

Defective epigenetic control of satellite cell function

Satellite cells are subjected to strict epigenetic control at various stages of myogenesis (Segalés et al., 2015; Massenet et al., 2021; Cicciarello et al., 2022). For example, we now know that satellite cell quiescence is an active and reversible state, controlled by specific epigenetic mechanisms (Gopinath et al., 2014; Boonsanay et al., 2016; Li and Dilworth, 2016; García-Prat et al., 2020). Our group and others have shown that quiescent satellite cell activation, division, and proliferation are also under tight epigenetic control (Tapscott, 2005; McKinnell et al., 2008; Dilworth and Blais, 2011; Diao et al., 2012). Pax7 plays a critical role in the transcriptional regulation of satellite cells (Soleimani et al., 2012; Lilja et al., 2017). Moreover, Pax7 also triggers Myf5 synthesis in committed progenitor cells, via its interaction with the arginine methyltransferase CARM1 (coactivator-associated arginine methyltransferase 1). This interaction is crucial for establishing polarity-regulated gene expression during asymmetric satellite cell division by methylating Pax7 at several arginine residues, thereby leading to the expression of Myf5 (Kawabe et al., 2012; Saber and Rudnicki, 2022).

In a previous study, we showed that CARM1 is a specific substrate of p38γ, and that phosphorylation of CARM1 prevented its nuclear translocation (Chang et al., 2018; Saber and Rudnicki, 2022). β1-syntrophin, a component of the dystrophin-associated protein complex, is required for the basal localization of the p38γ/p-CARM1 complex in satellite cells. Specifically, p38γ localization is restricted to the basal surface by β1-syntrophin during asymmetric satellite cell division. This leads to the phosphorylation of CARM1, and subsequent inhibition of Myf5 activation (Chang et al., 2018).

Importantly, we also showed that in dystrophin-deficient mdx satellite cells, the p38γ and β1-syntrophin interaction was completely absent. Consequently, there was increased phosphorylation of CARM1, and decreased nuclear translocation and interaction with Pax7, leading to impaired epigenetic activation of Myf5 and reduced myogenic progenitor cell production (Chang et al., 2018).

In another study, Acharyya et al. (2010) showed an additional role for TNFα and NFκB to impact myogenesis by negatively regulating satellite cell activation through epigenetic silencing of notch 1 via hypermethylation of its promoter region. Moreover, mdx skeletal muscles show higher histone deacetylase (HDAC) activity compared to wild type mouse muscle (Renzini et al., 2022). And

mdx satellite cells derived from single myofibers also show increased global deacetylase activity and higher expression levels of HDAC2 (Colussi et al., 2008). Furthermore, treatment with histone deacetylase inhibitors ameliorated dystrophic pathology (Bajanca and Vandel, 2017). Interestingly, it has been reported that nitric oxide (NO) donors also improved the dystrophic phenotype in a manner similar to histone deacetylase inhibitors, perhaps suggesting a common mechanism of action (Colussi et al., 2008). The absence of dystrophin in DMD muscle results in the loss of sarcolemmal localization and reduced expression of neuronal nitric oxide synthase (nNOS), a key component of the dystrophin associated protein complex that is involved in several functional roles in skeletal muscle including contraction, glucose uptake, blood flow regulation, and muscle regeneration (Lai et al., 2009). This loss of nNOS and subsequent nitric oxide signaling results in a decrease in NO-dependent S-nitrosylation of HDAC2 in mdx muscle. And restoring this NO-signaling-dependent inhibition of HDAC2 showed significant therapeutic effect in dystrophic mouse muscle (Colussi et al., 2008; Colussi et al., 2009).

Restoring satellite cell function as a treatment strategy for DMD

Antisense oligonucleotide (AON) mediated exon skipping, Adeno associated virus (AAV) mediated gene therapy, gene editing using the CRISPR/Cas9 system, as well as cell therapy with dystrophin competent cells have all received considerable research focus in recent decades as viable treatment options for DMD (Sun et al., 2020; Duan et al., 2021; Happi Mbakam et al., 2022). However, these therapeutic strategies largely target the dystrophic myofibers, and do not address the cell-autonomous defects of dystrophin-deficient satellite cells that we have outlined thus far.

One challenge of CRISPR/Cas9 mediated gene editing in correcting the genetic defect of DMD cells is the long-term maintenance of the edited gene (Chen et al., 2022a). Satellite cell transduction and editing by CRISPR/Cas9 have traditionally been limited, and consequently, the edited nuclei may be diluted out as new muscle cells are generated. However, recent reports have explored the possibility of successfully editing satellite cells with the use of more efficient genetic tools. Kwon et al. (2020) reported that by systematically assessing a panel of AAV serotypes with different tissue tropisms, they identified AAV9 as having the highest transduction rate in satellite cells in mdx mice via both local injections and systemic tail-vein injections. Paired with muscle specific promoters, they were able to achieve up to ~60% Cre-mediated recombination. Unfortunately, however, the percentage of total gene editing in satellite cells was drastically lower at ~1.5% (Kwon et al., 2020). Consistent with these data, Nance et al. (2019) also reported using AAV9 to successfully perform gene editing and restore dystrophin expression in mdx satellite cells. In another recent study, Domenig et al. (2022) reported the use of a novel *in vitro* cellular model in combination with CRISPR/Cas9 gene editing to restore dystrophin expression in dystrophic mice. Specifically, they reprogrammed fibroblasts obtained from dystrophic mice into highly proliferative induced myogenic progenitor cells (iMPCs), and then performed CRISPR/Cas9 mediated exon skipping to correct the genetic mutation in these cells and restore dystrophin expression. Engraftment of these corrected DMD iMPCs into the muscle of dystrophic mice restored dystrophin expression *in vivo* and contributed to the muscle stem cell pool as well (Domenig et al., 2022).

There is accumulating evidence now showing that restoring satellite cell function can have tremendous therapeutic potential for DMD. One such strategy is to augment asymmetric satellite cell divisions and significantly increase the number of myogenic progenitors available for muscle regeneration. For example, the epidermal growth factor receptor (EGFR)—aurora kinase A (Aurka) signaling pathway is an alternative effector pathway to regulate asymmetric satellite stem cell divisions (Wang et al., 2019). Specifically, EGF treatment drives its receptor (EGFR) that is localized at the basal surface of satellite cells to recruit the mitotic spindle assembly protein Aurka and induce asymmetric divisions (Wang et al., 2019). Crucially, this cell polarity pathway is independent of dystrophin or the DAPC, and therefore, can rescue the deficit in asymmetric stem cell divisions seen in DMD satellite cells. Indeed, mdx mice treated with exogenous EGF showed significantly increased progenitor numbers, enhanced muscle regeneration as well as muscle strength (Wang et al., 2019). Lending further credence to this notion, Flanigan et al. (2021) have recently identified PARD6G as a genetic modifier capable of influencing disease severity in DMD patients. In a large genome-wide association study (GWAS) of loss of ambulation in patients, the group discovered PARD6G, a member of the PAR polarity complex (PAR3-PAR6-aPKC) that involved in the control of asymmetric cell division of satellite cells, as a genetic modifier in a substantial cohort of DMD patients who showed significantly prolonged ambulation (Flanigan et al., 2021).

Various other signaling pathways involved in cell polarity establishment and satellite cell proliferation and differentiation could also be targeted as a therapeutic strategy. For example, the canonical notch signaling pathway governs satellite cell fate decisions, cell proliferation and induction of differentiation (Gioftsidi et al., 2022). Further, interactions between a variety of notch ligands and receptors need to be precisely regulated temporally and spatially for optimal results. Several lines of evidence show that impaired notch signaling contributes to the pathogenic mechanisms of DMD (Church et al., 2014; Jiang et al., 2014; Den Hartog and Asakura, 2022). Mu et al. (2015) showed an overactivation of notch signaling in dystrophic mouse skeletal muscle, and the repression of notch signaling reduced the depletion and senescence of muscle progenitor cells and restored myogenic capacity. Moreover, it was revealed that overexpression of Jagged 1, a notch ligand, acted as a genetic modifier that dramatically improved muscle regeneration and function in two dystrophic "escaper" dogs that were phenotypically normal (Vieira et al., 2015). The notch signaling pathway is also involved in asymmetric satellite cell divisions via its interacting partner numb, which is asymmetrically inherited by the committed daughter cell (Conboy and Rando, 2002). It remains to be seen whether pharmacological modulation of this notch/numb signaling dynamic can rescue the asymmetric cell division deficit observed in DMD satellite cells.

The Jak/Stat signaling pathway is another example of a signaling axis that regulates asymmetric cell divisions and drives myogenic

progenitor formation (Price et al., 2014). Stat3 signaling promotes myogenic lineage progression via its regulation of MyoD (Tierney et al., 2014). And the use of Stat3 inhibitors has been shown to promote tissue repair and partially restore muscle regeneration in dystrophic muscle (Sala and Sacco, 2016). We have also previously shown that Wnt7a, which is known to stimulate the planar cell polarity pathway via its interaction with the Fzd7 receptor, can also be manipulated to promote satellite stem cell expansion and improve muscle regeneration and function in mdx muscle (Le Grand et al., 2009; von Maltzahn et al., 2012).

As discussed in the previous section, the confluence of chronic inflammation, oxidative stress, and satellite cell senescence greatly exacerbates the disease pathology in DMD. The senescence associated secretory phenotype (SASP) is where senescent cells secrete various cytokines such as TGFβ and Interluekin-6 (IL-6) that contribute to fibrosis and inflammation. Since SASP of senescent muscle satellite cells compromises muscle regeneration, removal of these senescent cells is expected to be of therapeutic value in DMD muscle. To test this hypothesis, Sugihara et al. (2020) treated 8-mo old DMD rats with the senolytic drug ABT263, which specifically depletes senescent cells. ABT263 treatment successfully decreased the expression of senescence markers and senescent cells, and increased the number of newly regenerating muscle fibers in treated dystrophic muscle (Sugihara et al., 2020). In another recent study, Moiseeva et al. (2023) developed a lifetime atlas of *in vivo* senescent cells in regenerating skeletal muscle, using single-cell transcriptomics and a method to separate senescent cells from subsets of various niche cell types. They show increased presence of senescent cells in the dystrophic muscles of mdx mice, and reducing the accumulation of senescent cells in mdx mice by treating with the senolytic compounds dasatinib and quercetin increased the size of regenerating myofibers and decreased inflammation and matrix deposition (Moiseeva et al., 2023). Furthermore, they show that senescent cells can reduce satellite cell expansion through paracrine pro-inflammatory and pro-fibrotic SASP activity, which may impair muscle regeneration, particularly in advanced stages of the disease (Moiseeva et al., 2023).

Increased levels of Ca^{2+} influx lead to myofiber necrosis and a severe inflammatory response in DMD. This response is mainly mediated by the NF-kB pro-inflammatory pathway. TNF-α and IL-6 are primarily responsible for regulating this pathway. While current strategies that target muscle inflammation in DMD include the use of glucocorticoids such as prednisone, prednisolone, and deflazacort, their long-term usage carries severe immune modulatory side effects (Szabo et al., 2021). Several small molecule drug candidates are currently in clinical trials that aim to modulate these pro-inflammatory immune responses in DMD muscle, and improve the satellite cell niche and promote muscle regeneration. These also include histone deacetylases inhibitors, that have been shown to be especially effective at treating inflammation in dystrophic muscle over corticosteroids. In several preclinical studies, small molecule HDAC inhibitors yielded significant functional and morphological benefits to dystrophic muscle, including decreasing the inflammatory infiltrate, and increasing muscle size, quality, and function, as well as improving the therapeutic efficacy of gene therapy approaches (Consalvi et al., 2011; Sincennes et al., 2016; Licandro et al., 2021; Bizot et al., 2022). Importantly, they have also been shown to directly modulate the function of satellite cells. For example, Murray et al. investigated the role of dietary tributyrin, an HDAC inhibitor, on satellite cell activity and muscle regeneration in a piglet model. They showed that tributyrin treatment in these piglets enhanced the terminal differentiation of satellite cells and improved muscle growth (Murray et al., 2018; Murray et al., 2021). Moreover, treatment with trichostatin A (TSA), valproic acid, or sodium butyrate, which are all inhibitors of class I and II HDACs, has been shown to enhance myogenic differentiation and improve the efficiency of myoblast recruitment and fusion (Iezzi et al., 2002; Iezzi et al., 2004).

Concluding remarks

It is now evident that a truly effective treatment for DMD will need to account for the myofiber phenotype as well as the muscle stem cell phenotype. In the absence of dystrophin, the myofiber phenotype manifests in the form of contraction-induced sarcolemmal injury, membrane leakage, impaired muscle contraction and loss of force, increased Ca^{2+} influx, inflammation, progressive muscle degeneration, and fibrotic tissue deposition. The muscle stem cell phenotype, on the other hand, leads to reduced asymmetric stem cell divisions and impaired myogenesis, accelerated differentiation, altered metabolism and mitochondrial dysfunction, satellite cell senescence, defective epigenetic control, and impaired cell signaling (Figure 3). These phenotypes converge to result in a devastating and fatal muscle disease that currently has no cure. While groundbreaking research into gene therapy (including gene replacement and gene editing) aim to tackle the primary defect of dystrophin loss in myofibers in DMD, these strategies fail to adequately address the muscle stem cell phenotype. Here we have outlined several exciting and viable treatment avenues to target the stem cell phenotype and to ameliorate the dystrophic pathology and improve the quality of life for patients.

However, it is worth noting that a disease with such widespread pathogenesis will require a synergistic therapeutic approach for optimal results. For example, improving the stem cell phenotype by increasing asymmetric cell divisions and the number of myogenic progenitor cells available for muscle regeneration will need to be executed in a way that satellite cell self-renewal and replenishment of the stem cell pool are not compromised. Otherwise, the stem cell pool may be exhausted, resulting in impaired muscle regeneration, once again. Further, as we have described here, dystrophic satellite cells carry an inherent pathology in terms of their altered gene expression, metabolism, elevated inflammation and oxidative stress, and propensity for cell senescence. While increasing myogenic progenitor numbers in this dystrophic milieu will undoubtedly improve myogenesis and muscle function, these progenitors will continue to propagate their intrinsic defects via fusion to each other or existing myofibers. However, it remains to be determined whether a pharmacological rescue of the impairment in asymmetric division will ameliorate these intrinsic deficits. Therefore, we must continue our efforts to lay the groundwork for a more comprehensive understanding

of the pathophysiology of this disease, while leaving no stone unturned in our progress towards an all-encompassing treatment for these patients.

Author contributions

Conceptualization and writing: KK. Review and funding acquisition: MR. All authors contributed to the article and approved the submitted version.

Funding

The studies from the laboratory of MR were carried out with support of grants from the US National Institutes for Health (R01AR044031), the Canadian Institutes for Health Research (FDN-148387), E-Rare-3 (Canadian Institutes of Health Research/Muscular Dystrophy Canada), Defeat Duchenne Canada, the Muscular Dystrophy Association, and the Stem Cell Network.

Conflict of interest

MR is a Founding Scientist and CSO of Satellos Bioscience, and KK is supported from a research contract from Satellos Bioscience.

Publisher's note

All claims expressed in this article are solely those of the authors and do not necessarily represent those of their affiliated organizations, or those of the publisher, the editors and the reviewers. Any product that may be evaluated in this article, or claim that may be made by its manufacturer, is not guaranteed or endorsed by the publisher.

References

Aartsma-Rus, A., Van Deutekom, J. C., Fokkema, I. F., Van Ommen, G. J., and Den Dunnen, J. T. (2006). Entries in the leiden duchenne muscular dystrophy mutation database: An overview of mutation types and paradoxical cases that confirm the reading-frame rule. *Muscle Nerve* 34, 135–144. doi:10.1002/mus.20586

Abdel-Salam, E., Abdel-Meguid, I., and Korraa, S. S. (2009). Markers of degeneration and regeneration in Duchenne muscular dystrophy. *Acta Myol.* 28, 94–100.

Acharyya, S., Sharma, S. M., Cheng, A. S., Ladner, K. J., He, W., Kline, W., et al. (2010). TNF inhibits notch-1 in skeletal muscle cells by Ezh2 and DNA methylation mediated repression: Implications in duchenne muscular dystrophy. *PLoS One* 5, e12479. doi:10.1371/journal.pone.0012479

Alexakis, C., Partridge, T., and Bou-Gharios, G. (2007). Implication of the satellite cell in dystrophic muscle fibrosis: A self-perpetuating mechanism of collagen overproduction. *Am. J. Physiol. Cell Physiol.* 293, C661–C669. doi:10.1152/ajpcell.00061.2007

Bajanca, F., and Vandel, L. (2017). Epigenetic regulators modulate muscle damage in duchenne muscular dystrophy model. *PLoS Curr.* 9. doi:10.1371/currents.md.f1e2379fa632f8135577333dd92ca83b

Bankole, L. C., Feasson, L., Ponsot, E., and Kadi, F. (2013). Fibre type-specific satellite cell content in two models of muscle disease. *Histopathology* 63, 826–832. doi:10.1111/his.12231

Barthélémy, F., Santoso, J. W., Rabichow, L., Jin, R., Little, I., Nelson, S. F., et al. (2022). Modeling patient-specific muscular dystrophy phenotypes and therapeutic responses in reprogrammed myotubes engineered on micromolded gelatin hydrogels. *Front. Cell Dev. Biol.* 10, 830415. doi:10.3389/fcell.2022.830415

Bellissimo, C. A., Garibotti, M. C., and Perry, C. G. R. (2022). Mitochondrial stress responses in duchenne muscular dystrophy: Metabolic dysfunction or adaptive reprogramming? *Am. J. Physiol. Cell Physiol.* 323, C718–c730. doi:10.1152/ajpcell.00249.2022

Biressi, S., Miyabara, E. H., Gopinath, S. D., Carlig, P. M., and Rando, T. A. (2014). A Wnt-TGFβ2 axis induces a fibrogenic program in muscle stem cells from dystrophic mice. *Sci. Transl. Med.* 6, 267. 267ra176. doi:10.1126/scitranslmed.3008411

Bizot, F., Goossens, R., Tensorer, T., Dmitriev, S., Garcia, L., Aartsma-Rus, A., et al. (2022). Histone deacetylase inhibitors improve antisense-mediated exon-skipping efficacy in mdx mice. *Mol. Ther. Nucleic Acids* 30, 606–620. doi:10.1016/j.omtn.2022.11.017

Boonsanay, V., Zhang, T., Georgieva, A., Kostin, S., Qi, H., Yuan, X., et al. (2016). Regulation of skeletal muscle stem cell quiescence by suv4-20h1-dependent facultative heterochromatin formation. *Cell Stem Cell* 18, 229–242. doi:10.1016/j.stem.2015.11.002

Chang, N. C., Chevalier, F. P., and Rudnicki, M. A. (2016). Satellite cells in muscular dystrophy - lost in polarity. *Trends Mol. Med.* 22, 479–496. doi:10.1016/j.molmed.2016.04.002

Chang, N. C., Sincennes, M. C., Chevalier, F. P., Brun, C. E., Lacaria, M., Segalés, J., et al. (2018). The dystrophin glycoprotein complex regulates the epigenetic activation of muscle stem cell commitment. *Cell Stem Cell* 22, 755–768. doi:10.1016/j.stem.2018.03.022

Chen, G., Wei, T., Yang, H., Li, G., and Li, H. (2022a). CRISPR-based therapeutic gene editing for duchenne muscular dystrophy: Advances, challenges and perspectives. *Cells* 11, 2964. doi:10.3390/cells11192964

Chen, T. H., Koh, K. Y., Lin, K. M., and Chou, C. K. (2022b). Mitochondrial dysfunction as an underlying cause of skeletal muscle disorders. *Int. J. Mol. Sci.* 23, 12926. doi:10.3390/ijms232112926

Church, J. E., Trieu, J., Chee, A., Naim, T., Gehrig, S. M., Lamon, S., et al. (2014). Alterations in Notch signalling in skeletal muscles from mdx and dko dystrophic mice and patients with Duchenne muscular dystrophy. *Exp. Physiol.* 99, 675–687. doi:10.1113/expphysiol.2013.077255

Cicciarello, D., Schaeffer, L., and Scionti, I. (2022). Epigenetic control of muscle stem cells: Focus on histone lysine demethylases. *Front. Cell Dev. Biol.* 10, 917771. doi:10.3389/fcell.2022.917771

Colussi, C., Gurtner, A., Rosati, J., Illi, B., Ragone, G., Piaggio, G., et al. (2009). Nitric oxide deficiency determines global chromatin changes in Duchenne muscular dystrophy. *Faseb J.* 23, 2131–2141. doi:10.1096/fj.08-115618

Colussi, C., Mozzetta, C., Gurtner, A., Illi, B., Rosati, J., Straino, S., et al. (2008). HDAC2 blockade by nitric oxide and histone deacetylase inhibitors reveals a common target in Duchenne muscular dystrophy treatment. *Proc. Natl. Acad. Sci. U. S. A.* 105, 19183–19187. doi:10.1073/pnas.0805514105

Conboy, I. M., and Rando, T. A. (2002). The regulation of Notch signaling controls satellite cell activation and cell fate determination in postnatal myogenesis. *Dev. Cell* 3, 397–409. doi:10.1016/s1534-5807(02)00254-x

Consalvi, S., Saccone, V., Giordani, L., Minetti, G., Mozzetta, C., and Puri, P. L. (2011). Histone deacetylase inhibitors in the treatment of muscular dystrophies: Epigenetic drugs for genetic diseases. *Mol. Med.* 17, 457–465. doi:10.2119/molmed.2011.00049

Den Hartog, L., and Asakura, A. (2022). Implications of notch signaling in duchenne muscular dystrophy. *Front. Physiol.* 13, 984373. doi:10.3389/fphys.2022.984373

Diao, Y., Guo, X., Li, Y., Sun, K., Lu, L., Jiang, L., et al. (2012). Pax3/7BP is a Pax7-and Pax3-binding protein that regulates the proliferation of muscle precursor cells by an epigenetic mechanism. *Cell Stem Cell* 11, 231–241. doi:10.1016/j.stem.2012.05.022

Dilworth, F. J., and Blais, A. (2011). Epigenetic regulation of satellite cell activation during muscle regeneration. *Stem Cell Res. Ther.* 2, 18. doi:10.1186/scrt59

Domenig, S. A., Bundschuh, N., Lenardič, A., Ghosh, A., Kim, I., Qabrati, X., et al. (2022). CRISPR/Cas9 editing of directly reprogrammed myogenic progenitors restores dystrophin expression in a mouse model of muscular dystrophy. *Stem Cell Rep.* 17, 321–336. doi:10.1016/j.stemcr.2021.12.003

Duan, D., Goemans, N., Takeda, S. I., Mercuri, E., and Aartsma-Rus, A. (2021). Duchenne muscular dystrophy. *Nat. Rev. Dis. Prim.* 7, 13. doi:10.1038/s41572-021-00248-3

Dumont, N. A., Bentzinger, C. F., Sincennes, M. C., and Rudnicki, M. A. (2015a). Satellite cells and skeletal muscle regeneration. *Compr. Physiol.* 5, 1027–1059. doi:10.1002/cphy.c140068

Dumont, N. A., and Rudnicki, M. A. (2016). Targeting muscle stem cell intrinsic defects to treat Duchenne muscular dystrophy. *NPJ Regen. Med.* 1, 16006. doi:10.1038/npjregenmed.2016.6

Dumont, N. A., Wang, Y. X., Von Maltzahn, J., Pasut, A., Bentzinger, C. F., Brun, C. E., et al. (2015b). Dystrophin expression in muscle stem cells regulates their polarity and asymmetric division. *Nat. Med.* 21, 1455–1463. doi:10.1038/nm.3990

Ervasti, J. M., and Campbell, K. P. (1993). A role for the dystrophin-glycoprotein complex as a transmembrane linker between laminin and actin. *J. Cell Biol.* 122, 809–823. doi:10.1083/jcb.122.4.809

Ervasti, J. M. (2007). Dystrophin, its interactions with other proteins, and implications for muscular dystrophy. *Biochim. Biophys. Acta* 1772, 108–117. doi:10.1016/j.bbadis.2006.05.010

Ervasti, J. M., and Sonnemann, K. J. (2008). Biology of the striated muscle dystrophin-glycoprotein complex. *Int. Rev. Cytol.* 265, 191–225. doi:10.1016/S0074-7696(07)65005-0

Feige, P., Brun, C. E., Ritso, M., and Rudnicki, M. A. (2018). Orienting muscle stem cells for regeneration in homeostasis, aging, and disease. *Cell Stem Cell* 23, 653–664. doi:10.1016/j.stem.2018.10.006

Flanigan, K. M., Waldrop, M. A., Martin, P. T., Alles, R., Dunn, D. M., Alfano, L. N., et al. (2021). *Candidate gene modifiers of dystrophinopathy identified by the uniform application of genome-wide datasets to novel GWAS-identified loci*. medRxiv.

Forcina, L., Cosentino, M., and Musarò, A. (2020). Mechanisms regulating muscle regeneration: Insights into the interrelated and time-dependent phases of tissue healing. *Cells* 9, 1297. doi:10.3390/cells9051297

García-Prat, L., Perdiguero, E., Alonso-Martín, S., Dell'Orso, S., Ravichandran, S., Brooks, S. R., et al. (2020). FoxO maintains a genuine muscle stem-cell quiescent state until geriatric age. *Nat. Cell Biol.* 22, 1307–1318. doi:10.1038/s41556-020-00593-7

Gioftsidi, S., Relaix, F., and Mourikis, P. (2022). The Notch signaling network in muscle stem cells during development, homeostasis, and disease. *Skelet. Muscle* 12, 9. doi:10.1186/s13395-022-00293-w

Gopinath, S. D., Webb, A. E., Brunet, A., and Rando, T. A. (2014). FOXO3 promotes quiescence in adult muscle stem cells during the process of self-renewal. *Stem Cell Rep.* 2, 414–426. doi:10.1016/j.stemcr.2014.02.002

Gosselin, M. R. F., Mournetas, V., Borczyk, M., Verma, S., Occhipinti, A., Róg, J., et al. (2022). Loss of full-length dystrophin expression results in major cell-autonomous abnormalities in proliferating myoblasts. *Elife* 11, e75521. doi:10.7554/eLife.75521

Griffin, J. L., Williams, H. J., Sang, E., Clarke, K., Rae, C., and Nicholson, J. K. (2001). Metabolic profiling of genetic disorders: A multitissue (1)H nuclear magnetic resonance spectroscopic and pattern recognition study into dystrophic tissue. *Anal. Biochem.* 293, 16–21. doi:10.1006/abio.2001.5096

Guiraud, S., Aartsma-Rus, A., Vieira, N. M., Davies, K. E., Ommen, G.-J. B. V., and Kunkel, L. M. (2015). The pathogenesis and therapy of muscular dystrophies. *Annu. Rev. Genomics Hum. Genet.* 16, 281–308. doi:10.1146/annurev-genom-090314-025003

Happi Mbakam, C., Lamothe, G., and Tremblay, J. P. (2022). Therapeutic strategies for dystrophin replacement in duchenne muscular dystrophy. *Front. Med. (Lausanne)* 9, 859930. doi:10.3389/fmed.2022.859930

Heslop, L., Morgan, J. E., and Partridge, T. A. (2000). Evidence for a myogenic stem cell that is exhausted in dystrophic muscle. *J. Cell Sci.* 113 (12), 2299–2308. doi:10.1242/jcs.113.12.2299

Hoffman, E. P., Brown, R. H., and Kunkel, L. M. (1987). Dystrophin: The protein product of the duchenne muscular dystrophy locus. *Cell* 51, 919–928. doi:10.1016/0092-8674(87)90579-4

Iezzi, S., Cossu, G., Nervi, C., Sartorelli, V., and Puri, P. L. (2002). Stage-specific modulation of skeletal myogenesis by inhibitors of nuclear deacetylases. *Proc. Natl. Acad. Sci. U. S. A.* 99, 7757–7762. doi:10.1073/pnas.112218599

Iezzi, S., Di Padova, M., Serra, C., Caretti, G., Simone, C., Maklan, E., et al. (2004). Deacetylase inhibitors increase muscle cell size by promoting myoblast recruitment and fusion through induction of follistatin. *Dev. Cell* 6, 673–684. doi:10.1016/s1534-5807(04)00107-8

Ionasescu, V., and Ionasescu, R. (1982). Increased collagen synthesis by Duchenne myogenic clones. *J. Neurol. Sci.* 54, 79–87. doi:10.1016/0022-510x(82)90220-9

Jiang, C., Wen, Y., Kuroda, K., Hannon, K., Rudnicki, M. A., and Kuang, S. (2014). Notch signaling deficiency underlies age-dependent depletion of satellite cells in muscular dystrophy. *Dis. Model Mech.* 7, 997–1004. doi:10.1242/dmm.015917

Kawabe, Y., Wang, Y. X., Mckinnell, I. W., Bedford, M. T., and Rudnicki, M. A. (2012). Carm1 regulates Pax7 transcriptional activity through MLL1/2 recruitment during asymmetric satellite stem cell divisions. *Cell Stem Cell* 11, 333–345. doi:10.1016/j.stem.2012.07.001

Kharraz, Y., Guerra, J., Pessina, P., and Serrano, A. L. (2014). Understanding the process of fibrosis in duchenne muscular dystrophy. *BioMed Res. Int.* 2014, 965631. doi:10.1155/2014/965631

Kirschner, K., Rattanavirotkul, N., Quince, M. F., and Chandra, T. (2020). Functional heterogeneity in senescence. *Biochem. Soc. Trans.* 48, 765–773. doi:10.1042/BST20190109

Koenig, M., Beggs, A. H., Moyer, M., Scherpf, S., Heindrich, K., Bettecken, T., et al. (1989). The molecular basis for duchenne versus becker muscular dystrophy: Correlation of severity with type of deletion. *Am. J. Hum. Genet.* 45, 498–506.

Koenig, M., Hoffman, E. P., Bertelson, C. J., Monaco, A. P., Feener, C., and Kunkel, L. M. (1987). Complete cloning of the Duchenne muscular dystrophy (DMD) cDNA and preliminary genomic organization of the DMD gene in normal and affected individuals. *Cell* 50, 509–517. doi:10.1016/0092-8674(87)90504-6

Kottlors, M., and Kirschner, J. (2010). Elevated satellite cell number in Duchenne muscular dystrophy. *Cell Tissue Res.* 340, 541–548. doi:10.1007/s00441-010-0976-6

Kuang, S., Kuroda, K., Le Grand, F., and Rudnicki, M. A. (2007). Asymmetric self-renewal and commitment of satellite stem cells in muscle. *Cell* 129, 999–1010. doi:10.1016/j.cell.2007.03.044

Kumari, R., and Jat, P. (2021). Mechanisms of cellular senescence: Cell cycle arrest and senescence associated secretory phenotype. *Front. Cell Dev. Biol.* 9, 645593. doi:10.3389/fcell.2021.645593

Kuznetsov, A. V., Winkler, K., Wiedemann, F. R., Von Bossanyi, P., Dietzmann, K., and Kunz, W. S. (1998). Impaired mitochondrial oxidative phosphorylation in skeletal muscle of the dystrophin-deficient mdx mouse. *Mol. Cell Biochem.* 183, 87–96. doi:10.1023/a:1006868130002

Kwon, J. B., Ettyreddy, A. R., Vankara, A., Bohning, J. D., Devlin, G., Hauschka, S. D., et al. (2020). *In vivo* gene editing of muscle stem cells with adeno-associated viral vectors in a mouse model of duchenne muscular dystrophy. *Mol. Ther. Methods Clin. Dev.* 19, 320–329. doi:10.1016/j.omtm.2020.09.016

Kwon, S. M., Hong, S. M., Lee, Y. K., Min, S., and Yoon, G. (2019). Metabolic features and regulation in cell senescence. *BMB Rep.* 52, 5–12. doi:10.5483/BMBRep.2019.52.1.291

Lai, Y., Thomas, G. D., Yue, Y., Yang, H. T., Li, D., Long, C., et al. (2009). Dystrophins carrying spectrin-like repeats 16 and 17 anchor nNOS to the sarcolemma and enhance exercise performance in a mouse model of muscular dystrophy. *J. Clin. Invest.* 119, 624–635. doi:10.1172/JCI36612

Le Grand, F., Jones, A. E., Seale, V., Scimè, A., and Rudnicki, M. A. (2009). Wnt7a activates the planar cell polarity pathway to drive the symmetric expansion of satellite stem cells. *Cell Stem Cell* 4, 535–547. doi:10.1016/j.stem.2009.03.013

Li, Y., and Dilworth, F. J. (2016). Compacting chromatin to ensure muscle satellite cell quiescence. *Cell Stem Cell* 18, 162–164. doi:10.1016/j.stem.2016.01.009

Licandro, S. A., Crippa, L., Pomarico, R., Perego, R., Fossati, G., Leoni, F., et al. (2021). The pan HDAC inhibitor Givinostat improves muscle function and histological parameters in two Duchenne muscular dystrophy murine models expressing different haplotypes of the LTBP4 gene. *Skelet. Muscle* 11, 19. doi:10.1186/s13395-021-00273-6

Lilja, K. C., Zhang, N., Magli, A., Gunduz, V., Bowman, C. J., Arpke, R. W., et al. (2017). Pax7 remodels the chromatin landscape in skeletal muscle stem cells. *PLoS One* 12, 0176190. doi:10.1371/journal.pone.0176190

Luan, P., D'Amico, D., Andreux, P. A., Laurila, P. P., Wohlwend, M., Li, H., et al. (2021). Urolithin A improves muscle function by inducing mitophagy in muscular dystrophy. *Sci. Transl. Med.* 13, 0319. doi:10.1126/scitranslmed.abb0319

Luz, M. A., Marques, M. J., and Santo Neto, H. (2002). Impaired regeneration of dystrophin-deficient muscle fibers is caused by exhaustion of myogenic cells. *Braz J. Med. Biol. Res.* 35, 691–695. doi:10.1590/s0100-879x2002000600009

Mah, J. K., Korngut, L., Dykeman, J., Day, L., Pringsheim, T., and Jette, N. (2014). A systematic review and meta-analysis on the epidemiology of Duchenne and Becker muscular dystrophy. *Neuromuscul. Disord.* 24, 482–491. doi:10.1016/j.nmd.2014.03.008

Mann, C. J., Perdiguero, E., Kharraz, Y., Aguilar, S., Pessina, P., Serrano, A. L., et al. (2011). Aberrant repair and fibrosis development in skeletal muscle. *Skelet. Muscle* 1, 21. doi:10.1186/2044-5040-1-21

Massenet, J., Gardner, E., Chazaud, B., and Dilworth, F. J. (2021). Epigenetic regulation of satellite cell fate during skeletal muscle regeneration. *Skelet. Muscle* 11, 4. doi:10.1186/s13395-020-00259-w

Matre, P. R., Mu, X., Wu, J., Danila, D., Hall, M. A., Kolonin, M. G., et al. (2019). CRISPR/Cas9-Based dystrophin restoration reveals a novel role for dystrophin in bioenergetics and stress resistance of muscle progenitors. *Stem Cells* 37, 1615–1628. doi:10.1002/stem.3094

Mauro, A. (1961). Satellite cell of skeletal muscle fibers. *J. Biophys. Biochem. Cytol.* 9, 493–495. doi:10.1083/jcb.9.2.493

Mckinnell, I. W., Ishibashi, J., Le Grand, F., Punch, V. G., Addicks, G. C., Greenblatt, J. F., et al. (2008). Pax7 activates myogenic genes by recruitment of a histone methyltransferase complex. *Nat. Cell Biol.* 10, 77–84. doi:10.1038/ncb1671

Mendell, J. R., Shilling, C., Leslie, N. D., Flanigan, K. M., Al-Dahhak, R., Gastier-Foster, J., et al. (2012). Evidence-based path to newborn screening for Duchenne muscular dystrophy. *Ann. Neurol.* 71, 304–313. doi:10.1002/ana.23528

Mercuri, E., Bönnemann, C. G., and Muntoni, F. (2019). Muscular dystrophies. *Lancet* 394, 2025–2038. doi:10.1016/S0140-6736(19)32910-1

Mohiuddin, M., Choi, J. J., Lee, N. H., Jeong, H., Anderson, S. E., Han, W. M., et al. (2020). *Transplantation of muscle stem cell mitochondria rejuvenates the bioenergetic function of dystrophic muscle*. bioRxiv. 017822.

Moiseeva, V., Cisneros, A., Sica, V., Deryagin, O., Lai, Y., Jung, S., et al. (2023). Senescence atlas reveals an aged-like inflamed niche that blunts muscle regeneration. *Nature* 613, 169–178. doi:10.1038/s41586-022-05535-x

Moore, T. M., Lin, A. J., Strumwasser, A. R., Cory, K., Whitney, K., Ho, T., et al. (2020). Mitochondrial dysfunction is an early consequence of partial or complete dystrophin loss in mdx mice. *Front. Physiol.* 11, 690. doi:10.3389/fphys.2020.00690

Mu, X., Tang, Y., Lu, A., Takayama, K., Usas, A., Wang, B., et al. (2015). The role of Notch signaling in muscle progenitor cell depletion and the rapid onset of histopathology in muscular dystrophy. *Hum. Mol. Genet.* 24, 2923–2937. doi:10.1093/hmg/ddv055

Murray, R. L., Zhang, W., Iwaniuk, M., Grilli, E., and Stahl, C. H. (2018). Dietary tributyrin, an HDAC inhibitor, promotes muscle growth through enhanced terminal differentiation of satellite cells. *Physiol. Rep.* 6, e13706. doi:10.14814/phy2.13706

Murray, R. L., Zhang, W., Liu, J., Cooper, J., Mitchell, A., Buman, M., et al. (2021). Tributyrin, a butyrate pro-drug, primes satellite cells for differentiation by altering the epigenetic landscape. *Cells* 10, 3475. doi:10.3390/cells10123475

Nance, M. E., Shi, R., Hakim, C. H., Wasala, N. B., Yue, Y., Pan, X., et al. (2019). AAV9 edits muscle stem cells in normal and dystrophic adult mice. *Mol. Ther.* 27, 1568–1585. doi:10.1016/j.ymthe.2019.06.012

Nowak, K. J., and Davies, K. E. (2004). Duchenne muscular dystrophy and dystrophin: Pathogenesis and opportunities for treatment. *EMBO Rep.* 5, 872–876. doi:10.1038/sj.embor.7400221

Onopiuk, M., Brutkowski, W., Wierzbicka, K., Wojciechowska, S., Szczepanowska, J., Fronk, J., et al. (2009). Mutation in dystrophin-encoding gene affects energy metabolism in mouse myoblasts. *Biochem. Biophys. Res. Commun.* 386, 463–466. doi:10.1016/j.bbrc.2009.06.053

Pant, M., Sopariwala, D. H., Bal, N. C., Lowe, J., Delfin, D. A., Rafael-Fortney, J., et al. (2015). Metabolic dysfunction and altered mitochondrial dynamics in the utrophin-dystrophin deficient mouse model of duchenne muscular dystrophy. *PLoS One* 10, 0123875. doi:10.1371/journal.pone.0123875

Pauly, M., Daussin, F., Burelle, Y., Li, T., Godin, R., Fauconnier, J., et al. (2012). AMPK activation stimulates autophagy and ameliorates muscular dystrophy in the mdx mouse diaphragm. *Am. J. Pathol.* 181, 583–592. doi:10.1016/j.ajpath.2012.04.004

Pessina, P., Kharraz, Y., Jardi, M., Fukada, S., Serrano, A. L., Perdiguero, E., et al. (2015). Fibrogenic cell plasticity blunts tissue regeneration and aggravates muscular dystrophy. *Stem Cell Rep.* 4, 1046–1060. doi:10.1016/j.stemcr.2015.04.007

Price, F. D., Von Maltzahn, J., Bentzinger, C. F., Dumont, N. A., Yin, H., Chang, N. C., et al. (2014). Inhibition of JAK-STAT signaling stimulates adult satellite cell function. *Nat. Med.* 20, 1174–1181. doi:10.1038/nm.3655

Ramos, S. V., Hughes, M. C., Delfinis, L. J., Bellissimo, C. A., and Perry, C. G. R. (2020). Mitochondrial bioenergetic dysfunction in the D2.mdx model of Duchenne muscular dystrophy is associated with microtubule disorganization in skeletal muscle. *PLOS ONE* 15, 0237138. doi:10.1371/journal.pone.0237138

Reid, A. L., and Alexander, M. S. (2021). The interplay of mitophagy and inflammation in duchenne muscular dystrophy. *Life (Basel)* 11, 648. doi:10.3390/life11070648

Relaix, F., Bencze, M., Borok, M. J., Der Vartanian, A., Gattazzo, F., Mademtzoglou, D., et al. (2021). Perspectives on skeletal muscle stem cells. *Nat. Commun.* 12, 692. doi:10.1038/s41467-020-20760-6

Relaix, F., and Zammit, P. S. (2012). Satellite cells are essential for skeletal muscle regeneration: The cell on the edge returns centre stage. *Development* 139, 2845–2856. doi:10.1242/dev.069088

Renzini, A., Marroncelli, N., Cavioli, G., Di Francescantonio, S., Forcina, L., Lambridis, A., et al. (2022). Cytoplasmic HDAC4 regulates the membrane repair mechanism in Duchenne muscular dystrophy. *J. Cachexia Sarcopenia Muscle* 13, 1339–1359. doi:10.1002/jcsm.12891

Ribeiro, A. F., Souza, L. S., Almeida, C. F., Ishiba, R., Fernandes, S. A., Guerrieri, D. A., et al. (2019). Muscle satellite cells and impaired late stage regeneration in different murine models for muscular dystrophies. *Sci. Rep.* 9, 11842. doi:10.1038/s41598-019-48156-7

Ryder, S., Leadley, R. M., Armstrong, N., Westwood, M., De Kock, S., Butt, T., et al. (2017). The burden, epidemiology, costs and treatment for duchenne muscular dystrophy: An evidence review. *Orphanet J. Rare Dis.* 12, 79. doi:10.1186/s13023-017-0631-3

Saber, J., and Rudnicki, M. A. (2022). Carm1 and the epigenetic control of stem cell function. *Stem Cells Transl. Med.* 11, 1143–1150. doi:10.1093/stcltm/szac068

Sacco, A., Mourkioti, F., Tran, R., Choi, J., Llewellyn, M., Kraft, P., et al. (2010). Short telomeres and stem cell exhaustion model Duchenne muscular dystrophy in mdx/mTR mice. *Cell* 143, 1059–1071. doi:10.1016/j.cell.2010.11.039

Saito, Y., and Chikenji, T. S. (2021). Diverse roles of cellular senescence in skeletal muscle inflammation, regeneration, and therapeutics. *Front. Pharmacol.* 12, 739510. doi:10.3389/fphar.2021.739510

Sala, D., and Sacco, A. (2016). Signal transducer and activator of transcription 3 signaling as a potential target to treat muscle wasting diseases. *Curr. Opin. Clin. Nutr. Metab. Care* 19, 171–176. doi:10.1097/MCO.0000000000000273

Scharner, J., and Zammit, P. S. (2011). The muscle satellite cell at 50: The formative years. *Skelet. Muscle* 1, 28. doi:10.1186/2044-5040-1-28

Schmidt, M., Schüler, S. C., Hüttner, S. S., Von Eyss, B., and Von Maltzahn, J. (2019). Adult stem cells at work: Regenerating skeletal muscle. *Cell. Mol. Life Sci.* 76, 2559–2570. doi:10.1007/s00018-019-03093-6

Segalés, J., Perdiguero, E., and Muñoz-Cánoves, P. (2015). Epigenetic control of adult skeletal muscle stem cell functions. *Febs J.* 282, 1571–1588. doi:10.1111/febs.13065

Sharma, U., Atri, S., Sharma, M. C., Sarkar, C., and Jagannathan, N. R. (2003). Skeletal muscle metabolism in duchenne muscular dystrophy (DMD): An *in-vitro* proton NMR spectroscopy study. *Magn. Reson Imaging* 21, 145–153. doi:10.1016/s0730-725x(02)00646-x

Shirakawa, T., Toyono, T., Inoue, A., Matsubara, T., Kawamoto, T., and Kokabu, S. (2022). Factors regulating or regulated by myogenic regulatory factors in skeletal muscle stem cells. *Cells* 11, 1493. doi:10.3390/cells11091493

Shoji, E., Sakurai, H., Nishino, T., Nakahata, T., Heike, T., Awaya, T., et al. (2015). Early pathogenesis of Duchenne muscular dystrophy modelled in patient-derived human induced pluripotent stem cells. *Sci. Rep.* 5, 12831. doi:10.1038/srep12831

Sincennes, M. C., Brun, C. E., and Rudnicki, M. A. (2016). Concise review: Epigenetic regulation of myogenesis in Health and disease. *Stem Cells Transl. Med.* 5, 282–290. doi:10.5966/sctm.2015-0266

Soleimani, V. D., Punch, V. G., Kawabe, Y., Jones, A. E., Palidwor, G. A., Porter, C. J., et al. (2012). Transcriptional dominance of Pax7 in adult myogenesis is due to high-affinity recognition of homeodomain motifs. *Dev. Cell* 22, 1208–1220. doi:10.1016/j.devcel.2012.03.014

Sugihara, H., Teramoto, N., Nakamura, K., Shiga, T., Shirakawa, T., Matsuo, M., et al. (2020). Cellular senescence-mediated exacerbation of Duchenne muscular dystrophy. *Sci. Rep.* 10, 16385. doi:10.1038/s41598-020-73315-6

Sun, C., Shen, L., Zhang, Z., and Xie, X. (2020). Therapeutic strategies for duchenne muscular dystrophy: An update. *Genes (Basel)* 11, 837. doi:10.3390/genes11080837

Szabo, S. M., Salhany, R. M., Deighton, A., Harwood, M., Mah, J., and Gooch, K. L. (2021). The clinical course of duchenne muscular dystrophy in the corticosteroid treatment era: A systematic literature review. *Orphanet J. Rare Dis.* 16, 237. doi:10.1186/s13023-021-01862-w

Tapscott, S. J. (2005). The circuitry of a master switch: Myod and the regulation of skeletal muscle gene transcription. *Development* 132, 2685–2695. doi:10.1242/dev.01874

Tierney, M. T., Aydogdu, T., Sala, D., Malecova, B., Gatto, S., Puri, P. L., et al. (2014). STAT3 signaling controls satellite cell expansion and skeletal muscle repair. *Nat. Med.* 20, 1182–1186. doi:10.1038/nm.3656

Vidal, B., Serrano, A. L., Tjwa, M., Suelves, M., Ardite, E., De Mori, R., et al. (2008). Fibrinogen drives dystrophic muscle fibrosis via a TGFbeta/alternative macrophage activation pathway. *Genes Dev.* 22, 1747–1752. doi:10.1101/gad.465908

Vieira, N. M., Elvers, I., Alexander, M. S., Moreira, Y. B., Eran, A., Gomes, J. P., et al. (2015). Jagged 1 rescues the duchenne muscular dystrophy phenotype. *Cell* 163, 1204–1213. doi:10.1016/j.cell.2015.10.049

Vila, M. C., Rayavarapu, S., Hogarth, M. W., Van Der Meulen, J. H., Horn, A., Defour, A., et al. (2017). Mitochondria mediate cell membrane repair and contribute to Duchenne muscular dystrophy. *Cell Death Differ.* 24, 330–342. doi:10.1038/cdd.2016.127

Von Maltzahn, J., Renaud, J. M., Parise, G., and Rudnicki, M. A. (2012). Wnt7a treatment ameliorates muscular dystrophy. *Proc. Natl. Acad. Sci. U. S. A.* 109, 20614–20619. doi:10.1073/pnas.1215765109

Wang, Y. X., Feige, P., Brun, C. E., Hekmatnejad, B., Dumont, N. A., Renaud, J. M., et al. (2019). EGFR-aurka signaling rescues polarity and regeneration defects in dystrophin-deficient muscle stem cells by increasing asymmetric divisions. *Cell Stem Cell* 24, 419–432. doi:10.1016/j.stem.2019.01.002

Wang, Y. X., and Rudnicki, M. A. (2012). Satellite cells, the engines of muscle repair. *Nat. Rev. Mol. Cell Biol.* 13, 127–133. doi:10.1038/nrm3265

Yablonka-Reuveni, Z., and Anderson, J. E. (2006). Satellite cells from dystrophic (mdx) mice display accelerated differentiation in primary cultures and in isolated myofibers. *Dev. Dyn.* 235, 203–212. doi:10.1002/dvdy.20602

Yablonka-Reuveni, Z., Day, K., Vine, A., and Shefer, G. (2008). Defining the transcriptional signature of skeletal muscle stem cells. *J. Anim. Sci.* 86, E207–E216. doi:10.2527/jas.2007-0473

Yablonka-Reuveni, Z. (2011). The skeletal muscle satellite cell: Still young and fascinating at 50. *J. Histochem Cytochem* 59, 1041–1059. doi:10.1369/0022155411426780

Yin, H., Price, F., and Rudnicki, M. A. (2013). Satellite cells and the muscle stem cell niche. *Physiol. Rev.* 93, 23–67. doi:10.1152/physrev.00043.2011

Yoshioka, K., Ito, A., Horie, M., Ikeda, K., Kataoka, S., Sato, K., et al. (2021). Contractile activity of myotubes derived from human induced pluripotent stem cells: A model of duchenne muscular dystrophy. *Cells* 10, 2556. doi:10.3390/cells10102556

Young, L. V., Morrison, W., Campbell, C., Moore, E. C., Arsenault, M. G., Dial, A. G., et al. (2021). Loss of dystrophin expression in skeletal muscle is associated with senescence of macrophages and endothelial cells. *Am. J. Physiol. Cell Physiol.* 321, C94–c103. doi:10.1152/ajpcell.00397.2020

frontiers | Frontiers in Physiology

TYPE Review
PUBLISHED 26 June 2023
DOI 10.3389/fphys.2023.1183101

OPEN ACCESS

EDITED BY
Masatoshi Suzuki,
University of Wisconsin-Madison,
United States

REVIEWED BY
Mai ElMallah,
Duke University, United States
Ornella Cappellari,
University of Bari Aldo Moro, Italy

*CORRESPONDENCE
Joseph M. Metzger,
metzgerj@umn.edu

RECEIVED 09 March 2023
ACCEPTED 24 May 2023
PUBLISHED 26 June 2023

CITATION
Bez Batti Angulski A, Hosny N, Cohen H, Martin AA, Hahn D, Bauer J and Metzger JM (2023), Duchenne muscular dystrophy: disease mechanism and therapeutic strategies.
Front. Physiol. 14:1183101.
doi: 10.3389/fphys.2023.1183101

Duchenne muscular dystrophy: disease mechanism and therapeutic strategies

Addeli Bez Batti Angulski, Nora Hosny, Houda Cohen, Ashley A. Martin, Dongwoo Hahn, Jack Bauer and Joseph M. Metzger*

Department of Integrative Biology and Physiology, University of Minnesota Medical School, Minneapolis, MN, United States

Duchenne muscular dystrophy (DMD) is a severe, progressive, and ultimately fatal disease of skeletal muscle wasting, respiratory insufficiency, and cardiomyopathy. The identification of the dystrophin gene as central to DMD pathogenesis has led to the understanding of the muscle membrane and the proteins involved in membrane stability as the focal point of the disease. The lessons learned from decades of research in human genetics, biochemistry, and physiology have culminated in establishing the myriad functionalities of dystrophin in striated muscle biology. Here, we review the pathophysiological basis of DMD and discuss recent progress toward the development of therapeutic strategies for DMD that are currently close to or are in human clinical trials. The first section of the review focuses on DMD and the mechanisms contributing to membrane instability, inflammation, and fibrosis. The second section discusses therapeutic strategies currently used to treat DMD. This includes a focus on outlining the strengths and limitations of approaches directed at correcting the genetic defect through dystrophin gene replacement, modification, repair, and/or a range of dystrophin-independent approaches. The final section highlights the different therapeutic strategies for DMD currently in clinical trials.

KEYWORDS

muscle disease, therapeutic strategies, skeletal muscle, dystrophin, Duchenne muscular dystrophy, pathophysiology

1 Genetic basis and clinical presentation of DMD

Duchenne muscular dystrophy (DMD) is a severe X-linked recessive disorder caused by mutations in the dystrophin gene and consequent complete loss of dystrophin protein expression (Hoffman et al., 1987). The incidence of DMD is estimated at 1:5,000 boys worldwide, making it one of the most common recessive disorders in humans. The DMD gene that encodes dystrophin is located at position Xp21.1 of the X chromosome. DMD is the largest known gene in the human body, spanning 2.5 MB of DNA with 79 exons and 78 introns (Cohn and Campbell, 2000). The corresponding 14 kb mRNA transcript generates a 427 kDa protein with 3,685 amino acids (Hoffman et al., 1987; Emery, 2002).

Due to its massive size, the mutation rate for the dystrophin gene is quite high, with about one-third of mutations occurring *de novo* and the remaining caused by germline mosaicism or inheritance from a carrier mother (Nallamilli et al., 2021). More than 7,000 different dystrophin mutations have been identified in patients with DMD or Becker muscular dystrophy (BMD) (Bladen et al., 2015). Approximately 60% of

mutations in patients with DMD are deletions, and 11% are duplications, with the remainder being small mutations affecting the coding sequence and splice sites (Bladen et al., 2015). Deletions and duplications occur predominantly in two hotspots of the DMD gene, located at exons 3–9 and 45–55 (Min et al., 2019a). The high mutation rate, along with the many different ways in which a frameshift could occur, raises significant challenges for the development of gene correction therapies applicable to patients with different dystrophin mutations.

DMD mutations preventing the production of dystrophin hold dire consequences for protection against muscle membrane stress. Dystrophin forms a mechanical link between cytoskeletal actin and the extracellular matrix (ECM), which protects the sarcolemma from the force associated with stretch and contraction (Campbell and Kahl, 1989; Boland et al., 1996; Houang et al., 2018). Secondary to deficient membrane stability is the disorganization of numerous proteins associated with dystrophin, as well as impairment of their distribution and cell signaling, both leading to severe and progressive muscle wasting (Emery, 1993; Jungbluth et al., 2018). Women act as carriers, and although affected men appear normal at birth, steady muscle weakness and wasting are first apparent in proximal limb muscles before spreading to more distal muscles (Mercuri et al., 2019), leading to the disease being typically diagnosed in the first few years of life (Tyler, 2003; Birnkrant et al., 2018). The earliest symptoms such as a waddling gait, frequent falls, difficulties standing up from a sitting position (Gower's sign), and struggling to climb stairs can be seen between ages 2 and 3 (Emery, 2002). Affected children exhibit delayed gross motor development, and at ages 10–12, most patients require a wheelchair (Tsuda, 2018). As muscle weakness progresses, scoliosis and joint contractures develop, which promote restrictive lung disease (Bushby et al., 2010). Assisted ventilation is necessary by about 15–20 years of age, and the majority of DMD patients die from cardiac/respiratory failure between 20 and 30 years of age, even when optimal care has been administered (Mendell et al., 2012; Mercuri et al., 2019). Additionally, the corresponding immobility hastens the decline in bone density and increases the risk of fracture (McDonald et al., 2002).

The cardiac muscle must withstand significant mechanical stress to pump blood throughout the body, and the consequences of this stress are greatly exacerbated in DMD patients. Membrane instability leads to gradual cardiac myocyte death, resulting in fibrosis and secondary fatty infiltration (Townsend et al., 2011; Houang et al., 2018; Tsuda, 2018). This process decreases diastolic/systolic function, which plays a role in the atrophy and remodeling that gives rise to heterogeneous pathological alterations to the ventricular myocardium (Amin et al., 2002; Desguerre et al., 2009; Spurney, 2011a; Lee et al., 2014). Life-threatening consequences of cardiac muscle dystrophin deficiency include dilated cardiomyopathy, arrhythmias, and congestive heart failure (Kamdar and Garry, 2016; McNally and Wyatt, 2017; Buddhe et al., 2019; Meyers and Townsend, 2019). Along with these debilitating effects on cardiac function, the pulmonary ramifications of DMD are a key co-contributor to patient mortality (Emery, 2002). Weakened respiratory muscles, particularly the diminishment of diaphragm function, cause severe ventilatory insufficiency (Benditt and Boitano, 2005; Bushby et al., 2010). Additionally, incidences of otherwise benign upper respiratory tract infections can lead to serious acute respiratory failure in DMD, as patients cannot cough effectively. Diminished cough capacity causes airway secretions to be retained that in turn increases the risk of pneumonia and atelectasis (Bushby et al., 2010). Reduction in vital capacity and elevated residual volume due to impaired expiratory muscle function is also exhibited, which further necessitates assisted ventilation later in the disease progression (Bach et al., 1997; Benditt and Boitano, 2005; Bushby et al., 2010).

Although dystrophin deficiency in muscle tissues is the primary cause of the life-limiting issues associated with DMD, a lack of brain dystrophin has consequences as well (Duan et al., 2021). DMD patients reportedly have a higher susceptibility to seizures as compared to dystrophin replete individuals. Additionally, cognitive, neuropsychological, and neurobehavioral abnormalities are more likely to occur in DMD patients (Boyce et al., 1991; Kim et al., 1995). The general intelligence of affected boys is one standard deviation below the normal mean IQ, with 34.8% of patients reported to have intellectual disabilities (Cotton et al., 2001). Moreover, ADHD, autism spectrum disorder, and moderate-to-severe reading problems were exhibited in 11.7%, 3.1%, and 20% of patients, respectively (Hendriksen and Vles, 2006; Hendriksen and Vles, 2008).

The survival of patients with DMD has improved over time. With optimal care, patients with DMD can survive to live in their thirties and forties, mainly owing to the development of guidelines for care and management and improved treatment for cardiopulmonary dysfunction (Birnkrant et al., 2018).

2 Dystrophin function

Dystrophin is an essential cytoskeletal protein in muscle that localizes to the inner surface of the muscle cell membrane and is enriched at the costameres and sites of cell–cell contact (Ervasti and Campbell, 1993). Dystrophin is the connection point joining the actin cytoskeleton to the inner surface of the sarcolemma (Hoffman et al., 1987; Ahn and Kunkel, 1993). Dystrophin has the characteristic biochemical properties of a membrane cytoskeletal protein and is recognized as a major member of the spectrin-type superfamily of actin-binding proteins (Petrof et al., 1993; Straub et al., 1997). In muscle cells, dystrophin plays an important role in maintaining membrane integrity and preventing membrane rupture (Emery, 2002; Gao and McNally, 2015).

The dystrophin protein has four main functional domains: 1) an N-terminal region with homologies to the actin-binding domains of α-actinin that anchors the protein to the cytoskeleton; 2) a central rod domain containing 24 spectrin-like repeats separated by four hinge regions; 3) a cysteine-rich domain that anchors dystrophin to the muscle membrane via interaction with the transmembrane protein β-dystroglycan; and 4) a C-terminal domain that binds dystrobrevin and syntrophins, mediating sarcolemma localization (Ervasti, 2013). The N-terminal domain includes two calponin homology domains (CH1 and CH2). This conventional CH-actin binding domain binds directly to F actin, anchoring dystrophin to the cytoskeleton (Rybakova et al., 1996). The spectrin-like repeats in the central rod of dystrophin indicate that dystrophin works as a shock absorber, helping to resist repeated rounds of muscle contraction and relaxation. The rod domain also harbors a

second actin-binding motif (ABD2). ABD2 is found near the middle of the rod and works in concert with ABD1 to form a strong lateral association with actin filaments (Straub et al., 1992). The rod domain also mediates dystrophin interaction with microtubules via spectrin-like repeats 20–23 and is required for the organization of the microtubule lattice in skeletal muscle cells. Furthermore, the rod forms a flexible linker between the amino- and carboxy-termini. Four short proline-rich spacers, called "hinges," are interspersed in the mid-rod domain providing elasticity to the protein (Koenig et al., 1988). Hinge 4 is at the end of the rod domain and contains a WW domain, a domain implicated in protein–protein interactions (Koenig and Kunkel, 1990; Straub et al., 1992). The WW domain, along with two neighboring EF-hands, binds the carboxy-terminus of β-dystroglycan, anchoring dystrophin at sarcolemma (Koenig et al., 1988). In dystrophin, the two EF-hands are located in the cysteine-rich domain, which resides between the central rod and the C-terminus. The cysteine-rich domain also contains a zinc finger (ZZ) domain (Ishikawa-Sakurai et al., 2004). The carboxy-terminal (CT) domain is α-helical and provides binding sites for dystrobrevin and syntrophins, mediating their sarcolemma localization.

Connection is achieved through the dystrophin-glycoprotein complex (DGC), which consists of extracellular (α-dystroglycan), transmembrane (sarcoglycans, β-dystroglycan, sarcospan), and cytoplasmic proteins (dystrophin, syntrophins, neuronal nitric oxide synthase, dystrobrevin), providing a link between the intracellular cytoskeleton and the ECM (Campbell and Kahl, 1989; Ervasti and Campbell, 1991).

It has been shown that α-dystroglycan resides on the extracellular surface of the sarcolemma and functions as a receptor for extracellular ligands such as laminin (Montanaro et al., 1999). Here, α-dystroglycan is tightly associated with β-dystroglycan, a transmembrane protein that also interacts with dystrophin. At the sarcolemma, β-dystroglycan is tightly associated with the sarcoglycan subcomplex, which is composed of four single-pass transmembrane proteins: α-sarcoglycan, β-sarcoglycan, γ-sarcoglycan, and δ-sarcoglycan (Ervasti and Campbell, 1993). The sarcoglycan complex is also tightly associated with sarcospan, a small transmembrane protein. On the cytoplasmic side of the sarcolemma, dystrophin maintains its membrane localization by interacting with β-dystroglycan. Dystrophin binds to the intracellular actin network to link the cytoskeleton to DGC, which in turn connects to basal lamina by interacting with ECM ligands. Other cytoplasmic components of DGC include α-dystrobrevin, syntrophins, and neuronal nitric oxide synthase (nNOS) (Ervasti, 2013). The α-dystrobrevin/syntrophin triplet associates with dystrophin and anchors nNOS to the sarcolemma (Guiraud et al., 2015).

3 Pathophysiological mechanisms of Duchenne muscular dystrophy

3.1 Membrane instability

In striated muscle, force is generated through cycles of contraction and relaxation of muscle fibers as driven via the sarcomere (Gordon et al., 2000). As discussed previously, in healthy muscle, the integrity of the sarcolemma is maintained through interactions between the sarcolemma, cytoskeleton, and ECM through the DGC and the integrin complex (Houang et al., 2018; Duan et al., 2021). However, in DMD, due to the lack of dystrophin and its associated proteins, the physical connection between the sarcolemma, cytoskeleton, and ECM is lost, causing the sarcolemma to become leaky and highly susceptible to injury (Guiraud et al., 2015; Houang et al., 2018; Duan et al., 2021). This mechanism is supported by several observations. Previous work has identified hallmarks of muscle injury in DMD patients in the form of sarcolemmal tears (so-called "delta" lesions) (Mokri and Engel, 1975; Pestronk et al., 1982; Duan et al., 2021), increased levels of creatine kinase in the serum, and the uptake of large proteins including albumin and Evans blue dye (Houang et al., 2018; Duan et al., 2021). As levels of muscle damage are directly linked to levels of muscle stress, those muscles that undergo higher levels of stress are more likely to incur higher levels of damage. This can be seen in skeletal muscles involved in the exercise, specifically those muscles undergoing lengthening contractions, where it has been shown that repetitive contractions lead to increases in sarcolemmal damage (Petrof et al., 1993; Allen et al., 2016). This can also be seen in the diaphragm, where increased levels of injury are seen in DMD patients (Stedman et al., 1991). Taken together, these works demonstrate the need for the dystrophin complex to maintain the structural integrity of the muscle sarcolemma and highlight the devastating consequences of muscle fiber membrane stability in DMD.

3.2 Calcium dysregulation

A major consequence of the increased levels of membrane instability and leakiness in DMD muscles is an increase in intracellular calcium levels and disrupted calcium homeostasis within the muscle (Hopf et al., 1996; Mareedu et al., 2021). There is some debate over the mechanisms leading to increased intracellular calcium in the DMD muscle. Previous work has suggested that calcium can enter the muscle fibers through membrane tears (Yasuda et al., 2005; Houang et al., 2018), through a number of different calcium channels, including store-operated, voltage-gated, or stretch-activated (Mareedu et al., 2021), or through sodium channels (Mareedu et al., 2021).

Although the mechanism of calcium entry is not fully resolved, it is clear that increased calcium levels in DMD muscles have a significant negative impact on function. This can be seen through the myriad of calcium-signaling pathways in the cell, including calmodulin (Pertille et al., 2010), calpains (Gailly et al., 2007), and dysferlin (Bansal et al., 2003; Houang et al., 2018), all of which can negatively impact calcium cycling and muscle repair. Another possible mechanism of calcium dysfunction in DMD that has become a recent area of focus is the sarcoplasmic reticulum (SR) (Duan et al., 2021). In DMD muscle fibers, it has been shown that there is an increase in passive calcium leak from the SR, and therefore sarco-endoplasmic reticulum calcium ATPase (SERCA) function is reduced, leading to an increase in cytosolic calcium levels (Duan et al., 2021; Mareedu et al., 2021). It has been suggested that this process may occur through SR crosstalk with reactive oxygen species (ROS) (Papa and Skulachev, 1997; Houang et al., 2018;

Mareedu et al., 2021). Further damage in the muscle can also be the result of calcium-mediated changes in mitochondrial function, which can lead to a reduction in ATP production and loss of membrane potential (Kyrychenko et al., 2015; Houang et al., 2018; Kang et al., 2018; Mareedu et al., 2021). Both of these mechanisms are discussed in more detail as follows. It is evident in dystrophic muscle fibers that the number of ways calcium-signaling can negatively impact muscle function and the increased levels of cytosolic calcium in DMD muscle is unmistakably a driving force in the pathology of the disease.

3.3 Inflammation

Immune cell infiltration is a main feature of DMD and is strongly associated with disease severity (Rosenberg et al., 2015; Villalta et al., 2015; Saclier et al., 2021). In DMD patients, inflammation onset precedes the onset of clinical symptoms (Pescatori et al., 2007). The involvement of the immune system after DMD onset, when there is already marked muscle damage, is well established (Vidal et al., 2008; Burzyn et al., 2013; Mojumdar et al., 2014; Mázala et al., 2020; Saclier et al., 2021). However, little is known about the role of inflammation in the earliest phase of DMD prior to the clinical onset (Evans et al., 2009).

Skeletal muscle is host to a heterogeneous combination of endothelial, stem, and immune cells, including macrophages, natural killer (NK) cells, T cells, B cells, and neutrophils (Tidball and Villalta, 2010). Immune cells play an important role in skeletal muscle homeostasis, repair, and regeneration (Tidball and Villalta, 2010; Castiglioni et al., 2015; Sciorati et al., 2016). The unique immune-privileged status of skeletal muscle (Sciorati et al., 2016) relies on the absence of constitutive MHCI expression and the lower number of antigen-presenting cells and pro-inflammatory cells in homeostasis, resulting in less necrosis and a lower capacity to generate abscesses (Evans et al., 2009; Tibdall et al., 2018). In the setting of acute muscle injury, neutrophils and pro-inflammatory macrophages are early players and are essential in clearing damaged fibers. They are then gradually replaced by anti-inflammatory pro-regenerative macrophages to stimulate fibers regeneration and fibrosis (Evans et al., 2009; Tidball and Villalta, 2010; Castiglioni et al., 2015; Tidball et al., 2018; Gehlert and Jacko, 2019). A distinct population of regulatory T cells (Foxp3+ Treg) drives the transition to a pro-regenerative state and potentiates muscle regeneration and repair (Burzyn et al., 2013).

As detailed previously, membrane instability is a primary defect in DMD. In healthy muscles, intense exercise causes membrane damage and leakage of cytoplasmic content into the extracellular compartment (Sorichter et al., 1998; Sorichter et al., 1999). This is associated with increased circulating levels of muscle proteins such as fatty acid binding protein and muscle-specific creatine kinase that can be used as biomarkers to detect and evaluate these injuries (Sorichter et al., 1998). Due to the muscle's unique immune privilege, rapid membrane repair mechanisms, and membrane stability conferred by intact dystrophin, this inflammatory response is limited, controlled, and quickly resolved in healthy muscle (Sciorati et al., 2016). In DMD, the muscle loses its immune privilege. Membrane instability caused by dystrophin deficiency leads to the continuous release of cytoplasmic content, in particular, damage-associated molecular patterns (DAMPs) that are ligands to toll-like receptors (TLRs), purinoceptors (P2RX7), and other pattern recognition receptors (PRRs) on muscle and immune cells (Henriques-Pons et al., 2014; Giordano et al., 2015; Sinadinos et al., 2015). Upon activation, PRR downstream signaling cascades initiate the innate immune response. Moreover, pro-inflammatory cytokines induce the expression of MHCI and MHCII on muscle fibers, thus breaking down the muscle immune privilege. In addition to membrane instability, intracellular calcium overload and increased oxidative stress further induce tissue damage, contributing to triggering the inflammatory cascade in dystrophin-deficient muscles (Wehling et al., 2001; Henriques-Pons et al., 2014).

The immune cell infiltration in young DMD patients is predominantly formed by macrophages and T cells (Evans et al., 2009). Similar findings were revealed in dystrophin-deficient murine muscles (Lozanoska-Ochser et al., 2018). Early in the DMD time course, degenerated muscle fibers are cleared and repaired by regeneration (Tidball and Villalta, 2010; Tidball et al., 2018). The co-existence of lesions of different ages and the overlapping of pro-inflammatory and anti-inflammatory signaling prevent the full resolution of inflammation and sustain a chronic inflammatory response, which further progresses muscle damage. As the disease progresses, the impaired regenerative capacity and the chronic inflammatory environment of dystrophic muscle lead to fibrosis and adipose tissue accumulation (Vidal et al., 2008; Evans et al., 2009; Rosenberg et al., 2015; Mázala et al., 2020).

Macrophages play a key role in the disease progression of DMD (Rosenberg et al., 2015). Genetic ablation of CCR2 in a dystrophin-deficient mouse model (mdx), which prevents the monocytes from exiting the bone marrow, reduces the pro-inflammatory macrophage infiltration into the dystrophin-deficient muscle and is shown to improve muscle histology and function (Mojumdar et al., 2014). Bhattarai et al. (2022) showed, in the necrotic phase, a TLR4-dependent alteration of the inflammatory phenotype of the mdx mice bone-marrow-derived macrophages, with implications in major remodeling of the macrophage metabolic and epigenetic landscape. These changes correspond to characteristics of trained immunity and indicate that trained immunity can play an important role in DMD pathogenesis and progression (Bhattarai et al., 2022). T cells also play a crucial role in DMD pathogenesis (Lozanoska-Ochser et al., 2018; Tidball et al., 2018). $CD4^+$ helper T cells promote the immune response by producing inflammatory cytokines (Spencer et al., 2001). $CD8^+$ T-cell perforin-mediated cytotoxicity and fatty acid synthetase-induced cytotoxicity cause muscle fiber apoptosis (Spencer et al., 1997; Cai et al., 2000; Spencer et al., 2001). Effector T cells were recently shown to be one of the earliest cell types infiltrating the dystrophic skeletal muscle (in 2-week-old mdx mice) via a protein kinase C θ-(PKCθ-) dependent mechanism (Lozanoska-Ochser et al., 2018). The absence of PKCθ, a key regulator of effector T-cell activation, significantly reduced T-cell infiltration and the innate immune cell infiltrate in mdx/$Prkcq^{-/-}$ muscle (mdx lacking Prkcq, the PKCθ-coding gene), and improved the muscle phenotype (Lozanoska-Ochser et al., 2018).

3.4 Mitochondrial energetics

Mitochondria play a pivotal role in the bioenergetics of muscle fibers via oxidative phosphorylation. The electron transport chain oxidizes NADH or $FADH_2$ through Complexes I and II in the matrix of the mitochondria and generates a proton gradient across the inner membrane of the mitochondria while transporting the electrons (Ahmad et al., 2022). The ATP synthase utilizes this proton gradient to synthesize ATP from ADP and inorganic phosphate. Fine orchestration of the electron transport chain complexes is essential for normal bioenergetics. DMD results in an abnormal environment that is not favorable for mitochondrial homeostasis (Cole et al., 2002; Allen et al., 2016). Instability in the DMD muscle membrane triggers extracellular Ca^{2+} inflow, leading to mitochondrial Ca^{2+} overload (Turner et al., 1988; Mareedu et al., 2021; Garcia-Castaneda et al., 2022). Although Ca^{2+} buffering is another key function of the mitochondria in the muscle through the mitochondrial Ca^{2+} uniporter (MCU), pathogenically high levels of cytoplasmic [Ca^{2+}] can lead to Ca^{2+} overload in the mitochondria and trigger the opening of the mitochondrial permeability transition pore (mPTP) (Hurst et al., 2017; Briston et al., 2019).

Morphologically, mitochondria in dystrophin-deficient muscle display decreased size and sparse cristae formation, which are attributed to an increased mitochondrial fission/fusion cycle (Pant et al., 2015; Kang et al., 2018; Moore et al., 2020). Furthermore, diminished protein expression involved in PINK1/PARKIN mitophagy also causes structural damage and mitochondrial dysfunction in dystrophic cardiac muscles (Pant et al., 2015). These observations combined suggest that increased mitochondrial dynamics and suppressed mitophagy in dystrophin-deficient muscle also contribute to mitochondrial dysfunction (Pant et al., 2015).

ATP synthesis capacity has also been found to be disrupted in dystrophin-deficient muscle, and this is shown by a reduction in mitochondrial density and maximal ATP synthesis rate (Percival et al., 2013), as well as mitochondrial respiration (Passaquin et al., 2002; Onopiuk et al., 2009; Schuh et al., 2012). Interestingly, mitochondrial dysfunction and metabolic abnormalities were found to precede the onset of myofiber necrosis in young mdx mice (Townsend et al., 2011; Moore et al., 2020).

3.5 Reactive oxygen species dysregulation

In healthy muscle, a basal level of reactive oxygen species (ROS) is produced, and this is required for optimal cellular function, such as contraction (Reid et al., 1992; Reid, 2001; Powers et al., 2011). Muscles from animal models and patients with DMD produce significantly more free radicals than normal muscle, making the dystrophic muscle more vulnerable than healthy muscle to oxidative stress. Electrons leaked from the electron transport chain in mitochondria are one of the major sources of ROS production in muscle fiber cells (Fridovich, 2004). Specifically, electrons leaked from Complexes I and III combine with oxygen to form superoxide and eventually hydrogen peroxide by superoxide dismutase ($e^- + O_2 \rightarrow O_2^- \rightarrow H_2O_2$) at the mitochondrial matrix and cytosol (Chance et al., 1979). Within a healthy cell, ROS and antioxidants maintain a delicate balance, referred to as the optimal redox state. However, an uncontrolled amount of ROS production in pathology that exceeds the capacity of innate antioxidants generates redox unbalance leading to pathological dysfunction and even cell death (Powers et al., 2011).

Within the muscle fiber, mitochondria form a reticular network that surrounds the contractile apparatus, providing a short distance for the ATP supply within the healthy muscle (Glancy et al., 2015). In pathology, however, this proximity becomes deleterious for the redox-sensitive contractile proteins. Myofilament structures, including troponin, tropomyosin, myosin, and actin, contain a thiol group that is sensitive to redox balance, and exposure to an excessive amount of ROS disrupts myofilament Ca^{2+} sensitivity and cross-bridge kinetics causing muscle contraction dysfunction (Andrade et al., 1998; Terrill et al., 2013).

DMD is noted for pathologically elevated ROS production from the mitochondria in muscle. Specifically, Complex I-supported maximal H_2O_2 production has been found to be markedly elevated in skeletal muscle from young mdx mice (Godin et al., 2012; Hughes et al., 2019). Furthermore, skeletal muscles from mdx mice display decreased Ca^{2+} retention capacity, leading to susceptibility to Ca^{2+}-induced mitochondrial permeability transition pore (mPTP) opening, as discussed previously. Interestingly, mdx skeletal and cardiac muscle have an adaptive elevation in ROS buffering capacity that counteracts the elevated ROS production from the mitochondria (Godin et al., 2012; Hughes et al., 2019; Hughes et al., 2020), and although this can temporarily dampen ROS, it still leads to an increase in oxidative damage as the disease progresses. Chronic inflammation due to sarcolemma damage and myofiber necrosis in dystrophin-deficient cardiac and skeletal muscle is a central feature of DMD, and this contributes to elevated ROS production from mitochondria (Terrill et al., 2016; Tulangekar and Sztal, 2021). Lastly, pathological conditions, including DMD, that impact mitochondrial function can cause more severe effects on the diaphragm than on limb muscle due to the relatively greater ROS emission rates per mass and mitochondrial content (Hahn et al., 2019). This suggests that the mitochondria as a crucial therapeutic target when considering the involvement of diaphragm weakness and wasting leads to cardiorespiratory failure in DMD patients (Mead et al., 2014).

NADPH oxidase 2 (NOX2) also has a considerable role in the pathology of DMD muscle as a source of ROS (Williams and Allen, 2007; Jung et al., 2008; Whitehead et al., 2010). NOX2 is activated by the microtubule-associated protein Rac1 upon mechanical stretching of the muscle, leading to ROS production. This process is greatly increased in DMD as the microtubule lattice becomes disorganized and dense due to the lack of dystrophin-microtubule interaction (Khairallah et al., 2012). NOX2 in phagocytic cells produces superoxide during respiratory bursts for host immunity against bacteria and infections. In DMD, continuous contraction-induced muscle membrane damage also leads to NOX2 activation (Moe et al., 2011; Zhao et al., 2015). Furthermore, biopsies from DMD patients showed greater gene expression of NOX2 compared to age-matched controls (Petrillo et al., 2017), and inhibition of NOX2 expression improved muscle function in mdx mice (Whitehead et al., 2015). Another important source of free radicals in dystrophin-deficient muscles is reactive nitrogen species produced by the cytosolic activation of delocalized

nNOS. Together, this free-radical production leads to increased DNA, protein, and lipid oxidation in dystrophin-deficient muscles (Kim et al., 2013; Grounds et al., 2020). Mitochondria and NOX2 have shown potential targets for ROS production.

Indeed, there have been several reports showing significant improvements in muscle function, as well as prevention of myofiber necrosis and membrane permeability from mdx skeletal muscle by N-acetylcysteine supplementation (Whitehead et al., 2008; Terrill et al., 2012; Pinniger et al., 2017).

3.6 Fibrosis

Fibrosis is a wound-healing process wherein an excessive amount of connective tissue is formed, leading to permanent scar tissue. The fraction of ECM in normal muscle is ~5%, which can be drastically increased in diseased or injured muscles (Lieber and Ward, 2013). Repeated injury/regeneration cycles and chronic inflammation cause fibrosis and loss of function, and this is another phenotypic feature of DMD (Kharraz et al., 2014; Gallardo et al., 2021). In DMD, fibrosis decreases contractile function and reduces the amount of healthy muscle for therapy (Kharraz et al., 2014). Muscle membrane damage in DMD and the subsequent accumulation of acidic metabolites and inflammation amplification initiate fibrotic tissue production by extracellular fluid containing fibronectin, glycosaminoglycans, and proteoglycans (Klingler et al., 2012). Specifically, transforming growth factor-β (TGF-β) is released from the skeletal muscle in injury or inflammation, and this activates myofibroblasts, leading to excessive production of ECM dominated by type I and type III collagen (Zhou et al., 2006; Lieber and Ward, 2013; Meng et al., 2016). Myostatin, which is a negative regulator of muscle mass, also stimulates muscle fibroblasts to proliferate ECM proteins (Li et al., 2008). In addition, angiotensin II, collagen triple helix repeat-containing 1 (Cthrc1) protein, and Wnt signaling regulate fibrogenic turnovers of the muscle cells (Bedair et al., 2008; Li et al., 2011; Cisternas et al., 2014).

The ECM functions as the major source of passive load-bearing in muscles. When comparing the normalized stiffness of a single muscle fiber, fiber bundle (ECM intact), and fiber alone (ECM non-intact), muscle fiber bundles had much higher stress, and this demonstrated that the ECM provides a large portion of the load-bearing function (Meyer and Lieber, 2011). In this light, DMD skeletal muscle displays significantly greater stiffness (Lacourpaille et al., 2015; Lacourpaille et al., 2017; Yu et al., 2022). In animal models of DMD, the lower limbs of mdx mice displayed an increase in the amount of collagen, and this was reported to have a close relationship with increased stiffness in the muscle (Brashear et al., 2021).

Because the fibrotic process begins early in DMD, therapeutic approaches aiming to reduce fibrosis have gained increased interest as a potential strategy for DMD. Therapeutic approaches inhibiting fibrosis (collagen type 1) have been shown to increase the expression of utrophin and the number of revertant myofibers (Levi et al., 2015). Other therapeutic targets that have shown the ability to limit the accumulation of fibrosis in DMD models and in patients include the renin-angiotensin system, cytokines, and tyrosine kinase receptors (Kharraz et al., 2014), ACE inhibitors, ARBs, and mineralocorticoid receptor antagonists (Heier et al., 2019; Kim et al., 2019).

4 Therapeutic strategies for DMD

Despite major therapeutic advances over the past 30 years, there is no curative treatment for DMD (McNally and Pytel, 2007; Mercuri et al., 2019). Nonetheless, a multidisciplinary medical, surgical, and rehabilitative approach targeting the symptoms of DMD can alter the natural course of the disease, improving longevity and quality of life. Glucocorticosteroids, such as deflazacort or prednisone, are the current standard of care and the most widely used treatment for DMD patients (Bushby et al., 2004). The exact mechanism by which glucocorticosteroids delay disease progression in DMD is not fully understood. However, it has been suggested that glucocorticosteroids increase total muscle mass and strength in patients with DMD through the stimulation of insulin-like growth factors, decreased inflammation, decreased lymphocyte reaction and cytokine production, and enhanced myoblast proliferation (for more information on this topic, please see earlier reviews (Angelini and Peterle, 2012; McDonald et al., 2018; McDonald et al., 2020). Although glucocorticosteroids and many other pharmacological strategies can delay symptoms by targeting the secondary effects of DMD, many are only partially effective because they treat just one aspect of DMD pathogenesis. Nevertheless, long-term corticosteroid treatment has a variety of unfavorable side effects, including weight gain, short stature, puberty delay, behavioral issues, and pathologic bone fractures (Connolly et al., 2002). A promising oral glucocorticosteroid analog named VBP-15 was recently shown to improve muscle strength without side effects in the mdx mouse (Damsker et al., 2013; Heier et al., 2013), and a phase 1 clinical trial is currently underway on healthy human volunteers.

As reviewed before, there has been great interest in developing genetic approaches to treat DMD. Herein, we highlight some of the most promising therapeutic strategies that have been used to treat DMD, including gene therapy approaches via direct replacement of dystrophin and newer approaches involving the manipulation of the cellular machinery at the level of gene transcription, mRNA processing, or translation.

4.1 Microdystrophin viral gene therapy

Viral-mediated gene therapy has long been considered a potential therapeutic strategy to treat DMD based on its capability to restore the missing dystrophin by providing a functional copy of the dystrophin gene or repairing dystrophin, thereby restoring dystrophin throughout the body. The fact that DMD patients can be candidates for replacement gene therapy regardless of the underlying dystrophin mutation makes this a very attractive approach to correct DMD defects (Gregorevic et al., 2004; Chamberlain and Chamberlain, 2017; Duan, 2018a; Crudele and Chamberlain, 2019).

Implementing DMD gene therapy has turned out to be a very challenging endeavor, involving two main challenges. The first problem is the dystrophin gene's immense size. The dystrophin

TABLE 1 Viral vector comparison in terms of their applicability to DMD gene therapy.

Characteristics	Adenovirus	Lentivirus	AAV
Genome	dsDNA	ssRNA	ssDNA
Capacity (kb)	Up to 30 kb	Up to 10 kb	Up to 4.7 kb
Genome integration	NO	Yes	On rare events
Expression duration	Transient	Persistent	Intermediate
Non-dividing cell transduction	Yes	Yes	Yes
Ability to target satellite cells	NO	Yes	NO
Immune response	High	Low	Very low
Risk	Elicits viral-induced inflammation/cytotoxicity	Insertional mutagenesis/potential for replication of competent virus	High safety profile

gene, including its coding sequence, poses a problem for viral vector packaging (Roberts et al., 1993). The second hurdle involves systemic delivery to treat all the striated muscles in the body. Thus, a whole-body systemic therapy approach is required (Townsend et al., 2007; Chamberlain and Chamberlain, 2017). Numerous truncated dystrophin designs and body-wide systemic viral gene transfer approaches have been investigated in many labs to overcome these barriers (Gregorevic et al., 2004; Odom et al., 2007; Duan, 2016a; Duan, 2018b; Ramos et al., 2019).

The most common viral vectors implemented for neuromuscular disorders are lentiviruses and adeno-associated viruses (AAV). Table 1 provides a comparison of different vector systems for treating DMD. Among all the virus-based technologies in use for DMD clinical trials, adeno-associated viral (AAV) vectors encoding mini- or microdystrophins show encouraging treatment results in the preclinical setting (Kawecka et al., 2015; Duan, 2018b). The full-length dystrophin cDNA is far larger than the 4.7 kb packaging capacity of AAVs. Hence, these vectors are unable to deliver the full-length dystrophin cDNA. Two or three AAV vector (tri-AAV) *in vivo* recombination systems have been reported to deliver full-length dystrophin, albeit at very low efficiency (Lostal et al., 2014; Morgan and Muntoni, 2021). Studies have been directed to generate engineered AAVs with increased packaging capacity that induces efficient transduction associated with a modest immune response (Rogers et al., 2011). The currently used recombinant AAVs (rAAV) are erased of all viral genes, specifically the rep and cap genes that encode the nonstructural and structural proteins, and replaced by a sequence of interest, resulting in a maximum encapsidation capacity of around 5 kb (Dong et al., 1996). These vectors mostly remain episomal as extrachromosomal concatemers and rarely integrate into the genome. However, Schnepp et al. (2003) reported rAAV integration rates of about 0.5% in muscles from adult mice. AAV serotypes display a variety of cellular tropisms with a range of efficiency for targeting different muscles (Gao et al., 2004; Zincarelli et al., 2008).

Initial studies featuring direct AAV vector injection into muscle showed high-level and durable gene transfer (Kessler et al., 1996; Xiao et al., 1996), although this was limited to the injected muscles and represents a non-clinically feasible condition as a continuous injection would be necessary for a therapeutic treatment modality. A major advancement was achieved when the Chamberlain lab (Gregorevic et al., 2004) and Xiao lab (Wang et al., 2005) demonstrated the success of using effective systemic gene transfer to cause whole-body muscle transduction in rodents with AAV pseudotype-6 vectors. Subsequently, the Duan lab reported the success of using systemic AAV-9 transduction in canines (Yue et al., 2008). Currently, a broad variety of AAV capsids that are either isolated from nature or engineered in laboratories have been used to accomplish systemic delivery (Townsend et al., 2007; Kotterman and Schaffer, 2014; Duan, 2016b). For instance, in rodents and large animals, a single intravenous administration of AAV-6, AAV-8, and AAV-9 led to whole-body muscle transduction. Additionally, limiting the expression to tissues of interest can be achieved by utilizing cell type-specific promoters. These advances spurred the development of AAV as the vector of choice for muscle gene therapy (Salva et al., 2007; Wang et al., 2014; Duan, 2016b).

Because AAV vectors rarely integrate into the muscle fiber genome, it follows that with muscle turnover, the microdystrophin transgenes will be diluted and lose effectiveness over time. As AAV vectors do not effectively target satellite cells, upon muscle injury, the satellite cells that are recruited to take part in the repair process will not contain the therapeutic transgene, causing the transduced cells to become diluted and eventually disappear with time (Arnett et al., 2014).

AAV administration may also induce an innate or cellular immune response to the vector, including anti-AAV capsid-neutralizing antibody production. In addition, some patients already have pre-existing AAV-neutralizing antibodies, which exclude them from receiving this treatment (Calcedo et al., 2009; Boutin et al., 2010). Strategies to counter this antibody response, such as by plasmapheresis, alternative AAV serotype, or immune-modulating drugs, are being investigated. The high safety profile of AAVs is evident by the fact that the most severe side effect to date using various AAV serotypes in several clinical trials was a temporary tissue inflammation that did not result in any long-term damage (Büning and Schmidt, 2015). Several clinical trials are investigating the safety and tolerability of this promising therapy in DMD patients (for more details, see *Clinical trials* section).

As clinical trials continue to develop, other factors controlling the function and stability of the transgene are being evaluated. The Chamberlain group reported that AAV-mediated delivery of

microdystrophin resulted in continued expression that was maintained for at least 27 months in both skeletal and cardiac muscles (Ramos et al., 2019). Conversely, Dupont et al. (2015) reported short-lived AAV-derived therapeutic mRNAs in the dystrophic milieu. This finding highlights the necessity for additional elements to be considered when rAAV-mediated gene therapy is being optimized. Designing improved gene therapy treatments for DMD will be made possible with continued research into vector development, optimization of expression cassettes, and further investigations, including immune modulation.

As previously indicated, the coding sequence of the muscle isoform of the dystrophin gene is approximately 11 kb long, and this length presents a significant difficulty in developing gene transfer therapy (Duan, 2018a). Observations in patients with BMD, typically a milder and less common form of muscular dystrophy, have suggested that the transfer of the full-length dystrophin open reading frame (ORF) may not be necessary for developing effective gene therapy. Thus, the disease phenotype may be alleviated with a smaller dystrophin gene construct. In BMD, mutations cause the loss of some exons but do not abolish dystrophin expression, as in the case of DMD (England et al., 1990).

The capacity to excise specific coding regions within the dystrophin gene while maximizing protein function has been made possible by the availability of the full-length sequence of dystrophin together with the knowledge of related protein domains (Jung et al., 1995; Rafael et al., 1996; Lai et al., 2009). Some domains of the dystrophin sequence are reported to be somewhat dispensable for protein function. Hence, a series of internally truncated dystrophin constructs lacking regions of the rod domain and/or the C-terminal domain were devised to be used in place of the full dystrophin (Yuasa et al., 1998; Harper et al., 2002; Goyenvalle et al., 2011; Chamberlain and Chamberlain, 2017). Microdystrophins are partially functional proteins that lack more than half of the typical amino acid sequence of dystrophin. Early versions of microdystrophin, which are about one-third the size of the human dystrophin cDNA (around 3.7 kb in size), lacked the C-terminal domain and up to 20 SRs. In pre-clinical studies, these were very successful at reducing necrosis in dystrophic mdx mouse muscles (Phelps et al., 1995; Gregorevic et al., 2006). They have also been successful in enhancing force generation in striated muscles of dystrophic mouse and canine models for DMD and in preserving the sarcolemma from the injury induced by contraction (Harper et al., 2002; Watchko et al., 2002; Abmayr and Chamberlain, 2006; Le Guiner et al., 2017). These characteristics are attained via micro-dys binding to γ-actin filaments and β-dystroglycan through the N-terminal actin-binding domain and the cystine-rich β-dystroglycan binding domain, respectively. Thus, microdystrophin can form a mechanically robust connection between the subsarcolemmal cytoskeleton and the ECM (Corrado et al., 1996; Rafael et al., 1996; Harper et al., 2002; Gardner et al., 2006; Ervasti, 2013).

Dystrophin structure-function studies have suggested that at least four SRs from the central rod domain are required to connect the crucial N-terminal and cysteine-rich domains. There are a variety of strategies to build such miniature dystrophins. Although it has been demonstrated that a variety of microdystrophins containing various SR combinations can alleviate the dystrophic pathophysiology, other SR arrangements have produced proteins with low or reduced functional capacity (Harper et al., 2002). For example, microdystrophin, ΔR4-R23/ΔCT (also known as mDysH2), one of the most used designs, reduces muscle necrosis and enhances muscle strength, but it has also been reported to cause ringbinden in some myofibers after myotendinous junction injury (Harper et al., 2002; Banks et al., 2008). Ringbinden was caused by a polyproline tract in hinge 2, which was corrected by replacing hinge 2 with hinge 3 (Banks et al., 2010). It is worth mentioning that Sarepta is testing this first-generation ΔR4-R23/ΔCT microdystrophin derived under the striated muscle-specific MHCK7 regulatory cassette in a human clinical trial (ClinicalTrials.gov: NCT03375164) (Figure 1) (Table 2) (Harper et al., 2002; Salva et al., 2007). (For more details, see *Clinical trials* section.)

Several other mini-/microdystrophin designs with clinical potential have been generated and tested in animal models (Banks et al., 2007; 2010; Jørgensen et al., 2009; Lai et al., 2009; Koo et al., 2011; McCourt et al., 2015; Hakim et al., 2017; Le Guiner et al., 2017; Duan, 2018b; Nelson et al., 2018). Among these, Δ3990 (mini-dystrophin), ΔR4–23/ΔCT (microdystrophin with deletion of repeats 4–23 and deletion of the C-terminal domain), and R16/17-containing microdystrophin (μDys-5R) are particularly noteworthy given the high safety profile and potency of these constructs in the murine and canine models (Figure 1) (Wang et al., 2000; Harper et al., 2002; Hakim et al., 2017). Strategic design of these microgenes to increase therapeutic efficacy includes codon optimization—a modification that switches a particular DNA sequence by changing its codons to match the most prevalent tRNAs, resulting in a more efficient translation (Foster et al., 2008) and the inclusion of nNOS-binding domain (repeats 16 and 17) (Lai et al., 2009).

Although all microdystrophins currently in clinical trials include hinges H1 and H4 (Figure 1), Wasala et al. (2022) recently studied the importance of including hinge 1/4 in microdystrophin gene therapy. They reported that hinge 1 is essential for the correct sarcolemmal localization of microdystrophin, restores the DGC, and enhances specific muscle force significantly compared to hinge 4. However, the construct including H1 and H4 outperformed the H1-only or H4-only microdystrophins. The Chamberlain group has been a leader in the field of testing microdystrophins with different structural configurations, including modification with central rod and/or various hinge domains (Harper et al., 2002; Wang et al., 2012). Here, vectors were evaluated in mdx^{4cv} mice and delivered using recombinant AAV6 vector. When compared to first-generation microdystrophins, two of the new microdystrophins were found to improve force generation while also localizing neuronal nitric oxide synthase to the sarcolemma, namely, μDys5 (ΔR2-R15/ΔR18-R22/ΔCT) and μDys7 (ΔH2-R15 + H3/ΔR18-R23/ΔCT) (Ramos et al., 2019).

It is worth noting that studies are needed to fully investigate the stability, function, and proper localization of the several different micro/mini-dystrophin constructs, as it is not entirely clear if the proteins will localize correctly within the cytoskeletal network.

Additional research is required to assess how functional these microdystrophins are in humans, including their therapeutic effectiveness. A functional improvement in DMD patients may

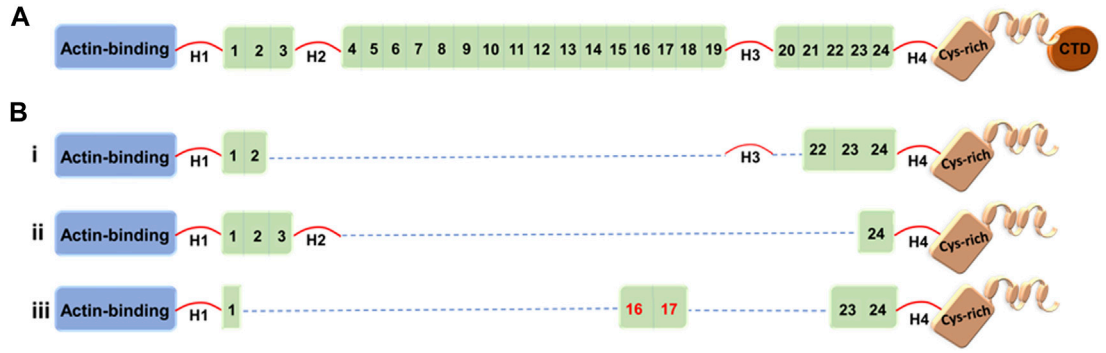

FIGURE 1
Full-length dystrophin and representative truncated dystrophins currently in use in clinical trials. **(A)** Full-length dystrophin *versus* **(B)** the truncated dystrophin constructs: i) mini-dystrophin Δ3990, ii) microdystrophin ΔR4-23/ΔCT (μDysH2) and iii) microdystrophin μDys-5R. Domains are identified as the N-terminal actin-binding domain, 1–24 spectrin-like repeats, four hinges (H1–H4), a cysteine-rich domain, and a C-terminal domain (CTD). The nNOS-binding domain is shown by the red numbers (repeats 16 and 17).

TABLE 2 Clinical trials using adeno-associated virus- (AAV-) mediated microdystrophin transfer for DMD therapy.

Company	Solid biosciences	Sarepta therapeutics	Pfizer	Nationwide Children's hospital
Description	Genetic: SGT-001	Genetic: rAAVrh74.MHCK7 microdystrophin	Genetic: PF-06939926	Administration of rAAVrh74.MCK.GALGT2 to DMD patients
Clinical trial number	NCT03368742	NCT03375164	NCT03362502	NCT03333590
Trial title	Microdystrophin gene transfer study in adolescents and children with DMD (IGNITE DMD)	A randomized, double-blind, placebo-controlled study of SRP-90001	A study to evaluate the safety and tolerability of PF-06939926 gene therapy in DMD	Gene transfer clinical trial to deliver rAAVrh74.MCK.GALGT2 for DMD
Delivery route	Intravenous injection	Intravenous injection into peripheral arm vein	Intravenous injection	Intravascular
AAV serotype	AAV9	AAVrh74	AAV9	AAVrh74
Current stage	Active, but no longer recruiting participants	Active, but no longer recruiting participants	Active, but no longer recruiting participants	Active, not recruiting
Primary outcome	Safety	Safety	Safety and tolerability	Safety and tolerability

also be more challenging to predict, given that the DMD animal models (where preclinical studies are tested) frequently exhibit a milder skeletal and cardiac muscle phenotype than humans. Additionally, because microdystrophins are shorter than the typical length of truncated dystrophins in BMD patients, microdystrophin therapy in DMD patients may not fully achieve the goal of attaining a BMD-like phenotype (Mercuri and Muntoni, 2013). Accordingly, the loss of functionality owing to the deletion of specific dystrophin protein subdomains continues to be problematic in terms of treatment effectiveness. It will also be crucial to achieve significant therapeutic efficacy in the heart since treating skeletal muscle without also treating the associated cardiomyopathy could paradoxically add more strain on the myocardium, due to increased physical activity, and hasten the development of heart disease (Townsend et al., 2008; 2009). This may be a general concern with treatments that more specifically target skeletal muscles without also addressing heart tissue.

4.2 Exon-skipping therapy

Exon skipping has been proposed and studied as a possible treatment for DMD for more than two decades. The goal of exon skipping therapy is to restore the disrupted open reading frame (ORF) of the dystrophin gene transcripts in DMD patients, allowing them to make a Becker's muscular dystrophy-like protein (Figure 2) (Niks and Aartsma-Rus, 2017). It is based on manipulating the pre-mRNA splicing of dystrophin transcripts to bypass a defective exon from the splicing machinery, restoring the reading frame and producing a partially functional, internally deleted dystrophin (Figure 2) (Schneider and Aartsma-Rus, 2021). The resulting dystrophin proteins are usually larger than the majority of mini- and microdystrophin gene therapy constructs currently under investigation.

Exon-skipping entails three experimental approaches: CRISPR DNA editing system, U7 snRNP-mediated splice

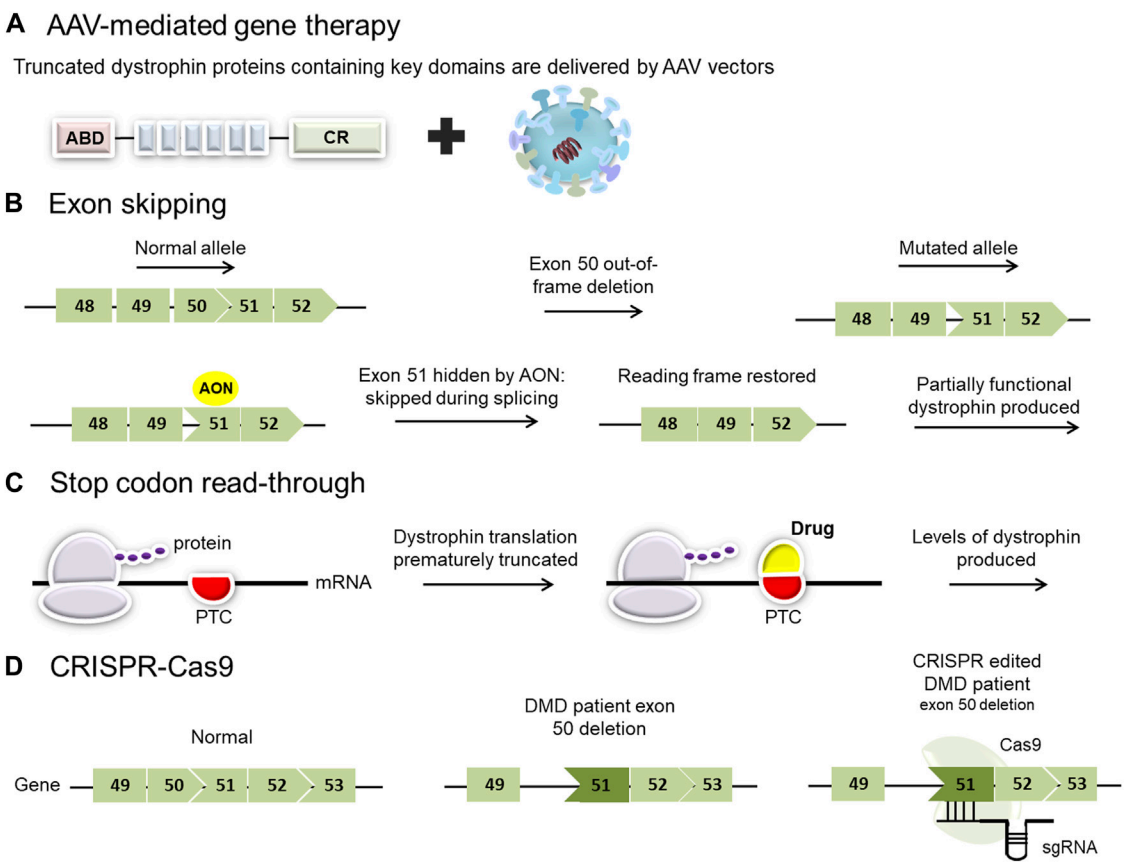

FIGURE 2
Overview of current and proposed experimental therapies for Duchenne muscular dystrophy (DMD). **(A)** AAV-mediated gene therapy employs viral vectors to deliver micro- or mini-dystrophin genes. Clinical trials using different adeno-associated virus (AAV) serotypes have shown promise for the treatment of patients with DMD. **(B)** Exon-skipping strategies seek to mask exons adjacent to others that have been deleted. This results in the restoration of the reading frame and permits the translation of a slightly smaller dystrophin product. **(C)** Stop codon read-through is a small molecule therapy aimed at reducing ribosomal sensitivity to mRNA stop codons, thus promoting ongoing dystrophin translation in those patients with nonsense mutations. (PTC: premature termination codon). **(D)** Genome editing, employing a CRISPR/Cas9 platform, has the potential to target specific pathogenic variants in the DMD gene but carries a risk of off-target effects.

blocking, and antisense oligonucleotides (AONs) (Takeda et al., 2021). CRISPR DNA editing techniques work at the DNA level to change myofiber genomic DNA in converting a DMD out-of-frame deletion into a BMD-like in-frame deletion. CRISPR relies on viral vectors to deliver the DNA editing technology (for more information on CRISPR-mediated exon skipping, see *CRISPR-Cas9 mediated gene editing strategies*). U7 snRNP-mediated inhibition of splicing is another approach for exon-skipping where modified U7 snRNP genes are delivered via AAV vectors (Vulin et al., 2004; Gadgil and Raczyńska, 2021). In this instance, an antisense sequence that targets the exon takes the place of the typical antisense portion that hybridizes to histone RNA. This does not target mRNA but pre-mRNA (similar to the mechanism of AON) (Gushchina et al., 2021). The third approach to accomplishing exon skipping is using oligonucleotide drugs that bind to the pre-mRNA (prior to splicing) to modulate RNA splicing. These oligonucleotide techniques have used a variety of drug chemistry with variable success, and this approach will be the focus of the following section.

4.2.1 AONs-mediated exon-skipping therapy

AONs are small 20–30 nucleotides of modified DNA or RNA homologs that specifically bind to their target exon prior to pre-mRNA splicing in a Watson-Crick-like manner, hiding the target exon from the splicing machinery so that it is spliced out with its flanking introns blocking its incorporation to the mature mRNA (Schneider and Aartsma-Rus, 2021). Antisense-mediated exon skipping is a method that targets a specific mutation (Bladen et al., 2015). For the reading frame to be restored, different exons have to be skipped depending on the location and size of the mutations (Aartsma-Rus et al., 2009; Bladen et al., 2015). Accordingly, different dystrophin proteins will be generated after skipping different exons for different mutations. Hence, it is crucial to have a precise genetic diagnosis of the disease to be able to design effective AONs (Arechavala-Gomeza et al., 2007).

For AON therapy, the majority of DMD patients would have one or more exons deleted. Overall, in DMD patients, 70% of the reading frame can be restored by single exon skipping, whereas another 8% would benefit from double exon skipping to restore the reading frame (Bladen et al., 2015). DMD deletions frequently

cluster in hotspots between exons 45 and 55; therefore, skipping target exons in this area could be of benefit to a large group of patients. Certain exons have been reported to have the highest applicability for skipping. Namely, exon 51 could be applied for (13%–14%) of patients, exon 45 and exon 53 both could be skipped for another 8%–10% of patients, and exon 44 could be skipped for an additional 6% of the patients (Mann et al., 2001; Van Deutekom et al., 2001).

Different chemical modifications have been tested to give the AONs drug-like characteristics in trying to enhance their bioavailability, improving their resistance to exonucleases and endonucleases, and increasing their affinity to the target RNA transcripts (Saleh et al., 2012). 2′-O-methyl phosphorothioate (2OMePS) AONs and phosphorodiamidate morpholino oligomers (PMOs) are used among other chemistries for DMD exon skipping clinical development approaches (Verma, 2018; Schneider and Aartsma-Rus, 2021).

A major challenge for the success of AON approaches centers on achieving adequate delivery to the myofiber nuclei so that the drug can hit its pre-mRNA target in the nucleus (prior to splicing) and prevent the splicing of the targeted exon (Takeda et al., 2021). Three different techniques have been used for the delivery of the oligonucleotides to the myofiber, namely, cell transfections, *in vivo* intramuscular injections, and *in vivo* systemic delivery (intravenous, intraperitoneal, or subcutaneous). Depending on the delivery technique, various oligonucleotide chemistries exhibit different degrees of myofiber delivery efficacy and exon-skipping efficiency (Heemskerk et al., 2009; Hoffman et al., 2011; Takeda et al., 2021).

The use of nanoparticles as a delivery vehicle has been investigated for enhancing AON uptake and reducing possible immune reactions. Polymethyl methacrylate (PMMA) nanoparticles include two subgroups: T1 and ZM2 have been tested for AON therapy in mdx mice (Schneider and Aartsma-Rus, 2021). T1 nanoparticles were shown to have slow biodegradability; however, they formed aggregates that precluded their use via intravenous administration and raised concerns about possible adverse effects (Rimessi et al., 2009). Regarding ZM2-encapsulated AONs, intraperitoneal delivery was accompanied by higher dystrophin restoration levels in skeletal muscle and hearts as compared to naked 2OMePs AONs (Rimessi et al., 2009; Ferlini et al., 2010). Moreover, the effect lasted for 90 days after the course of treatment (7 weeks) (Bassi et al., 2012). Still, more studies are needed to better understand the pharmacodynamics, pharmacokinetics, and any related side effects of this type of delivery.

2OMePS molecules possess a negative charge. They can effectively transfect cells *in vitro* and can be absorbed via intramuscular injection. Unfortunately, their use in clinical trials has been stopped, as no detectable dystrophin production in patient muscle was observed (Mann et al., 2001; Lu et al., 2003). Morpholinos (PMO) are uncharged compounds that are challenging to introduce into cells *in vitro*. They show little or no systemic distribution to normal myofibers but exhibit high levels of systemic delivery and efficient exon skipping in dystrophic muscle (Heemskerk et al., 2009; Hoffman et al., 2011; Novak et al., 2017). The effective delivery of PMOs was limited to the inflammatory foci and active muscle-regenerating regions of the dystrophic muscle tissue, where the macrophages seem to play a role in their delivery (Novak et al., 2017). Morpholinos have shown an acceptable safety profile at very large systemic doses in mouse, dog, and human studies (Yokota et al., 2009; Wu et al., 2010; Clemens et al., 2020; Komaki et al., 2020). Nevertheless, as the underlying mutations that cause DMD disease remain and due to transcript and protein turnover, repeated drug injection is required. Overall, the highest levels of dystrophin restoration have been achieved via morpholino chemistry using systemic delivery (Schneider and Aartsma-Rus, 2021).

Several strategies have been proposed to increase the effectiveness of AONs and their uptake by skeletal muscles and in the heart for multi-exons skipping or enhancing their delivery using muscle-homing peptide conjugation (e.g., arginine-rich peptide) or via nanoparticles. Multi-exon skipping approaches, which permit the skipping of several adjacent exons at once, are under investigation in order to broaden the range of mutations eligible for treatment (Goyenvalle et al., 2012). Cocktails of antisense oligonucleotides have been developed to target two or more neighboring exons within a particular area to induce multi-exon skipping, such as the major mutational hotspots (exons 45–55) (Taglia et al., 2015). Another favorable approach is conjugating AONs to arginine-rich cell-penetrating peptides (CPPs) to enhance cellular uptake. The conjugated PMO-based AONs are termed peptide phosphorodiamidate morpholino oligomers (PPMO). In mdx mice and canine X-linked muscular dystrophy model of DMD, PPMOs were shown to be safe and permitted a longer duration of effective exon skipping in the tissues evaluated, including the heart and diaphragm (Jearawiriyapaisarn et al., 2008; Wu et al., 2008; Echigoya et al., 2017).

Despite the attractiveness and applicability of single or multiple exon(s) skipping techniques and the fact that four AONs have already been approved for clinical trials, it is becoming clear that their delivery efficiency is not satisfactory (Sheikh and Yokota, 2021). This could be concluded from the low levels of dystrophin restoration in skeletal muscle biopsies and the lower levels observed in heart muscle (Heemskerk et al., 2009; Wu et al., 2009; Heemskerk et al., 2010; Jearawiriyapaisarn et al., 2010; Wu et al., 2010; Malerba et al., 2011; Yin et al., 2011). Therefore, ultimate clinical effectiveness will necessitate repeated injections. For exon skipping to reach clinical milestones, drug-induced dystrophin needs to be produced at higher levels in both skeletal and heart muscles. Hence, it is crucial to understand the underlying pathogenesis to maximize the treatment benefit. Epigenetic modulators that enhance or abolish the inhibitory effect of gene expression need to be considered with this treatment to retain and stabilize dystrophin transcripts and protein at multiple levels.

Taken together, the exon-skipping technique has advanced from *in vitro* proof of concept research of the clinical trial stage to FDA approval (Eser and Topaloğlu, 2022). Only single exon skipping has been approved for clinical trials (for more details, see *Clinical trials* section). The multiple exon-skipping approach is still facing hurdles (e.g., higher drug doses required, differential uptake and efficiency of the used ASOs) (Mitrpant et al., 2009; Yokota et al., 2009; Aartsma-Rus et al., 2014).

4.3 Stop codon read-through

Around 10%–15% of patients with DMD have a nonsense mutation that induces a premature termination codon (PTC) in the mRNA, causing the ribosome to terminate translation and failing to synthesize the remainder of the protein (Flanigan, 2014; Bladen et al., 2015). The principle of stop codon read-through is to induce the ribosome to continue translating the mRNA through the premature stop codon and continue through the rest of the transcript. The drug works by binding to the ribosome and its partners, disrupting its ability to recognize the premature stop codon, leading to the transformation of the PTC into a correct codon, thereby resulting in the continuation of the translation (Figure 2) (Bordeira-Carriço et al., 2012). This mechanism ideally needs to be specific to premature stop codons, without read-through of bona fide stop codons, to efficiently enable partial restoration of dystrophin expression in muscle (Welch et al., 2007). A number of drugs can induce stop codon read-through, and their efficacies rely on the nature of the nonsense mutation and the surrounding nucleotide sequences. These drugs can be divided into two main groups: aminoglycoside antibiotics (e.g., gentamycin; amikacin, tobramycin, and paromomycin) or chemical compounds without known analogs (e.g., ataluren or negamycin) (Bidou et al., 2012). Although gentamycin demonstrated efficacy in inducing stop codon read-through for numerous pathologies, including DMD (Barton-Davis et al., 1999; Wagner et al., 2001; Politano et al., 2003; Malik et al., 2010), toxicity remains a major concern limiting gentamycin from clinical considerations (Prayle and Smyth, 2010; Beringer and Winter 2011). In the past few years, several studies have aimed to select molecules capable of promoting mRNA translation despite the presence of a PTC. Ataluren (Translarna TM, previously known as PTC124) is a small oral molecule developed by PTC Therapeutics as a potentially safer alternative to induce stop codon read-through (Welch et al., 2007).

4.4 CRISPR-Cas9 mediated gene editing strategies

Over the past decade, gene editing has moved to the forefront with the identification of mechanisms of DNA repair (Stephenson and Flanigan, 2021). The CRISPR-Cas system has made it possible for research labs all around the world to successfully incorporate gene editing into their work (Jinek et al., 2012; Mali et al., 2013; Perez-Pinera et al., 2013). The two main components of the CRISPR/Cas9 system are the CRISPR-associated (Cas) endonuclease and a single guide RNA (sgRNA), which directs Cas9 to a particular ~20-nucleotide region in the genome that contains the complementary sequence (Figure 2).

Numerous engineered Cas endonucleases have been generated using naturally occurring Cas enzymes as guides. Targeted modifications have improved enzyme fidelity, reduced off-target mutations, increased editing efficiency, and used a more dispensable PAM sequence (Mali et al., 2013; Makarova et al., 2020). Engineered Cas proteins have extended to include nickase Cas9 (nCas9) (Ran et al., 2013) and deactivated Cas9 (dCas9) (Qi et al., 2013) that have been engineered to retain their programmable DNA-binding ability while decreasing or abolishing the Cas9 endonuclease activity, respectively. This has increased the safety of the CRISPR/Cas9 system owing to the absence of any DSBs (Dominguez et al., 2016). These may be combined with other elements, such as precise base editors (Komor et al., 2016; Yuan et al., 2018) or transcriptional activators (Qi et al., 2013; Wojtal et al., 2016), for alternative therapeutic strategies (Chen et al., 2022). Thus, the toolkit of CRISPR gene-editing systems has advanced, providing a growing number of options for CRISPR-based therapies.

The potential treatment of DMD using CRISPR/Cas9-mediated therapeutic techniques and the difficulties of CRISPR/Cas9-mediated therapeutic genome editing will be the main topics of this section.

4.4.1 CRISPR technology as a gene-editing therapeutic for DMD

A single infusion of CRISPR genome-editing components can theoretically treat DMD by correcting genetic mutations at the genome level utilizing CRISPR/Cas programmable nucleases (Olson, 2021; Chen et al., 2022), a concept that represents a promising therapeutic strategy for the long-term correction of genetic illnesses (Knott and Doudna, 2018). Several of the disease characteristics of DMD make gene editing an exciting treatment modality. First, owing to the relative dispensability of certain dystrophin domains, it is possible to remove mutant exons from the rod domain of the gene and restore the ORF yielding partially functional truncated dystrophins, as discussed previously. Second, a genetic repair of even a small percentage of muscle nuclei could enable the generation of dystrophin and its dissemination throughout the myofibers as skeletal fibers are multinucleated. Moreover, because the dystrophin gene is located on the X chromosome, affected boys only have one mutant allele that needs to be repaired. Therefore, unintentionally altering a wild-type copy of the gene is obviated (Long et al., 2014).

Both *in vitro* and *in vivo* studies using CRISPR-mediated gene editing for DMD have been conducted. Therapeutic effects have been reported in human cells and mice, rats, dogs, and piglets with various DMD mutations (Ousterout et al., 2015; Young et al., 2016; Amoasii et al., 2018; Duchene et al., 2018; Min et al., 2019a; Moretti et al., 2020; Pickar-Oliver et al., 2021; Szabo et al., 2021; Zhang et al., 2021). Attaining greater insights using sequence-humanized animal models will be required prior to any clinical translation. This would include providing crucial information such as the required dose, delivery vehicle, route of administration, and the percentage levels required for functional dystrophin recovery (Aartsma-Rus and van Putten, 2020; Olson, 2021). Off-target effects are also a concern and must be addressed prior to human trials.

4.4.2 Exon deletion

Exon excision, exon skipping, exon reframing, and exon knock-in are the main approaches for the CRISPR-mediated therapeutic repair of DMD mutations. Additionally, newly engineered CRISPR system technologies like the base or prime editors have been used to enable more accurate gene editing.

The majority (~60%) of DMD patients have a deletion of one or more exons. Deleting the out-of-frame exon to restore the ORF is a typical method for achieving single or multiple exon deletions. This can be accomplished by double-cut exon deletion to one exon or over the entire hotspot region. To cut out single or multiple mutant

exons, two sgRNAs flanking these sites can be targeted with Cas9, and this will cause the ORF to be restored by splicing the neighboring in-frame exons together (Ousterout et al., 2015; Maggio et al., 2016a; Young et al., 2016). Importantly, because this approach is less mutation-specific and permits the ablation of many exons in a mutational hotspot, it is applicable to a higher percentage of DMD patients. However, this is at the expense of shorter dystrophins compared to other correction strategies. This method, though appealing, has a number of drawbacks, including the increased risk of off-target mutations and a sharp decline in editing efficiency simply because two directed DSBs must occur at the same time for the edit/correction to be successful. Added to this issue is the challenge of delivering the two sgRNAs simultaneously.

DMD mutational hot spot deletion has the potential to cure around 60% of DMD patients, based on BMD patients with more mild symptoms, at least in skeletal muscles (Aartsma-Rus et al., 2006; Doo et al., 2012; Ousterout et al., 2015). Ousterout et al. (2015) designed multiplexed sgRNAs to restore the dystrophin reading frame by targeting the mutational hotspot in ΔEx48-50 DMD patient-derived myoblasts. Here, dystrophin expression was restored *in vitro* following gene editing. However, this correction was not as efficient as deleting exon 51 alone, and this raised concerns about the editing efficiency for deleting a larger DNA fragment. Other groups targeted this same region *in vitro* and demonstrated a successful restoration of dystrophin in multiple DMD cell lines (Maggio et al., 2016b; Young et al., 2016; Duchene et al., 2018). *In vivo* studies have also been conducted in the humanized DMD del45/mdx mouse model. Exons 45–55 were successfully deleted, and dystrophin expression was observed after gene correction (Young et al., 2017).

In vitro and *in vivo* studies using the double-cut gene-editing approach have been used to target single-exon deletions (Maggio et al., 2016b; Long et al., 2016; Tabebordbar et al., 2016; Zhang et al., 2017; Long et al., 2018; Matre et al., 2019; Moretti et al., 2020). Although removing a smaller region lessens some of the problems with the double-cut method, it also eliminates the multi-exon deletion advantages noted previously. Postnatal single exon deletion editing has been studied in the mdx mouse model. Here, dystrophin expression was partially restored in cardiac and skeletal muscle and was shown to last up to 1 year in some studies after a single intravenous injection of an adeno-associated virus that encodes the CRISPR cassette (Nelson et al., 2016; Nelson et al., 2019).

Exon duplication mutations, which affect 5% of DMD patients, can also be corrected using exon deletion techniques. One duplicate exon can be targeted with a single sgRNA designed against the intron region next to the duplicated exon. In the presence of Cas9, sgRNA will produce two cuts and eliminate one of the duplicate exons. Thus, in principle, the dystrophin gene ORF can be restored, resulting in the production of full-length dystrophin protein identical to normal dystrophin (Long et al., 2018). However, exon duplication excision is presently challenging to investigate *in vivo* owing to the lack of animal models with this mutation (Bladen et al., 2015). CRISPR/Cas9 technology was recently used to develop a mouse model with a muti-exon tandem duplication of exon 50. This duplication mutation was then corrected using the sgRNA CRISPR/Cas9 technique. This method removed the duplication mutation, restored the expression of full-length dystrophin, and improved muscle functionality *in vivo* (Maino et al., 2021). Thus, this approach has the potential to treat duplication mutations in DMD.

4.4.3 Exon skipping by gene editing

In comparison to AON-based exon skipping therapy that modulates dystrophin mRNA, CRISPR gene editing corrects the underlying mutation in the genome. Thus, it is regarded as a permanent genomic correction. The conservative CRISPR-based exon skipping approach using only one sgRNA, instead of two sgRNAs flanking a mutant exon, to abolish either the splice acceptor site or splice donor site of the out-of-frame exon is the commonly used method for exon skipping (Amoasii et al., 2018). The sequence encoding the exon splice acceptor or donor site is then deleted by NHEJ induced via CRISPR system-triggered DSB, leading to out-of-frame exon skipping and splicing to the next accessible exon. Compared to utilizing two sgRNAs to flank the exon for removal, a single-sgRNA method for exon skipping increases editing efficiency (Long et al., 2018).

Several *in vitro* and *in vivo* studies have been conducted to evaluate this approach. *In vitro*, single-cut exon skipping has been used to skip exons 43, 45, 51, and 53 by NHEJ-induced disruption of splice acceptor sites, and successful skipping was demonstrated in iPSCs-derived skeletal muscle myoblasts isolated from DMD patients. Dystrophin restoration and functional improvement were observed in the gene-edited cell lines (Maggio et al., 2016b; Long et al., 2018; Min et al., 2019b). This approach has also been tested *in vivo* in both mouse (Amoasii et al., 2017; Min et al., 2019b; Wei et al., 2020) and canine models (Amoasii et al., 2018). Targeting the splice acceptor site of exon 51 results in skipping exon 51 and restoration of the dystrophin ORF. Dystrophin expression restoration and improved muscle function were demonstrated in both the DMD mouse and canine models that lack exon 50 (Amoasii et al., 2017; Amoasii et al., 2018). Exon 45 skipping via CRISPR/Cas9 has also been demonstrated to restore the reading frame in the ΔEx44 mouse model, allowing exon 43 to splice to exon 46, thus restoring the dystrophin reading frame (Nelson et al., 2017; Min et al., 2019b).

4.4.4 Exon reframing by gene editing

Another strategy to restore the dystrophin ORF involves Cas9 induction of a single NHEJ (Li et al., 2015; Iyombe-Engembe et al., 2016; Amoasii et al., 2017; Long et al., 2018). This form of gene editing is designed to "reframe" the ORF of the dystrophin transcript by introducing small insertions and deletions (INDELS) via NHEJ of double-stranded DNA breaks generated by CRISPR-Cas9. When using a sgRNA to induce NHEJ in an out-of-frame exon, the generated indels result in a targeted frameshift to restore the dystrophin gene back in frame (Min et al., 2018). This method is often referred to as single-cut myoediting because only one sgRNA is used to direct Cas9 editing, requiring only a single cut to restore the dystrophin ORF in targeted muscle cells. A number of groups have shown efficient restoration of the dystrophin ORF through exon reframing in human iPSC-derived cardiac myocytes, mouse models, and large animal models of DMD (Ousterout et al., 2015; Amoasii et al., 2017; 2018; Bengtsson et al., 2017; Kyrychenko et al., 2017; Zhang et al., 2017; Long et al., 2018; Yuan et al., 2018). Exon reframing

produces small indels during the repair and serves as an efficient strategy to preserve a large portion of the dystrophin genomic sequence while bypassing the DMD mutation. This strategy offers the possibility of permanently correcting specific DMD mutations.

4.4.5 Exon knock-in

In contrast to NHEJ-mediated exon deletion, skipping or reframing HDR-mediated exon knock-in can restore the full-length dystrophin gene expression. This approach incorporates a DNA donor template with the appropriate sequence as a part of the editing components. HDR-mediated genome editing has been demonstrated in small and large animal models of DMD (Long et al., 2014; Bengtsson et al., 2017; Zhang et al., 2017; Zhu et al., 2017; Mata López et al., 2020). An example of this strategy is the correction of exon 23 in the germline of mdx mice via SpCas9 with a 180-nt single-stranded DNA oligonucleotide template. Correction rates ranged from 2% to 100% correction of the *Dmd* gene in the resultant mosaic mice (Long et al., 2014). HDR is not active in quiescent or G1-arrested cells, rendering it unsuitable in mature myofibers and cardiac myocytes. Additionally, the approach cannot be used to correct DMD deletion mutations because of the length restriction on the donor DNA template (Zhang et al., 2021).

Homology-independent targeted integration (HITI) is a gene editing method with a relatively high efficiency in postmitotic cells. HITI can accurately knock in a missing exon(s) at a specific locus using NHEJ, which bypasses the requirement of HDR. HITI has been developed to overcome the HDR-related challenges noted previously (Suzuki et al., 2016). Delivering a donor plasmid with two Cas9 cleavage sites flanking the desired donor sequence is a key component of HITI. Following the Cas9 cleavage of the targeted genomic DNA and the donor plasmid, the NHEJ repair pathway will then incorporate the donor sequence. Although this exon knock-in strategy to restore full-length dystrophin protein is promising, it has not yet been extensively evaluated in the setting of DMD. Pickar-Oliver et al. examined the HITI-mediated approach to insert the missing human exon 52 or a superexon encoding the human dystrophin cDNA sequence downstream of exon 51 into its corresponding position within the dystrophin gene in a humanized mouse model of DMD. The DMD model used contained an out-of-frame deletion of exon 52, and full-length dystrophin restoration in skeletal and cardiac muscles was demonstrated (Pickar-Oliver et al., 2021). This technique enables the entire restoration of full-length dystrophin, even though the insertion efficiencies were low, and would be applicable to about 20% of DMD patients.

4.4.6 Base editing

Roughly 25%–30% of patients with DMD have point mutations (Aartsma-Rus et al., 2006; Bladen et al., 2015). Base editing is a recently developed approach to expand the toolbox of gene editing strategies to treat DMD (Chemello et al., 2020). In base editing, there are two major categories of DNA base editors: cytosine base editors (CBEs), which convert the C:G base pair into a T:A base pair (Komor et al., 2016; Nishida et al., 2016; Gaudelli et al., 2017) and adenine base editors (ABEs), which convert A:T base pairs to G:C base pairs (Gaudelli et al., 2017). In this strategy, Cas9 nickase (nCas9) or deactivated Cas9 (dCas9) is fused to a cytidine deaminase or an engineered adenine deaminase protein, allowing precise single-base pair conversations without double-stranded breaks (Gaudelli et al., 2017; Huang et al., 2021). These RNA-guided nucleotide-specific base editors do not rely on the NHEJ repair pathway, and as a consequence, small indels through error-prone NHEJ at the target site are not produced. Furthermore, a donor DNA template for HDR is not required (Min et al., 2018). Recently, a CRISPR/Cas9 adenine base editor (ABE7.10) was used to substitute a single adenine with guanine in a DMD mouse model containing a nonsense mutation on exon 20 (Ryu et al., 2018). This strategy has also been used to induce exon skipping by mutating target DNA bases of splice motifs (Gapinske et al., 2018). In this context, a CBE base editor (hAID P182X) was implemented in various canonical intronic motifs to modulate the splicing of different genes (Yuan et al., 2018).

4.4.7 Prime editing

More recently, a new strategy, termed prime editing, has been developed, which has been added to the CRISPR techniques to treat DMD point mutations (Anzalone et al., 2019). Prime editing takes advantage of a catalytically inactive nCas9. As a result, no DSBs are produced. The nCas9 is coupled to an engineered reverse transcriptase and delivered with an extended sgRNA termed the "prime editing" guide RNA (pegRNA). Reverse transcriptase uses the pegRNA as a template to add a DNA alteration at the target location (Anzalone et al., 2020). This approach enables single-base transitions or transversions, as well as site-specific genomic insertions and deletions, without introducing DSBs or the need for an exogenous donor DNA as a template for HDR repair. With the aid of endogenous DNA repair pathways, this newly generated DNA flap is then incorporated into the genome. While size restrictions still pose a problem for *in vivo* distribution, prime editing provides the ability to correct a number of DMD-causing mutations. In a proof-of-concept study by Chemello et al. (2021), prime editing was tested in the context of DMD. The approach was shown to be capable of reframing the dystrophin ORF in DMD (ΔEx51) cardiac myocytes derived from human iPSCs (Chemello et al., 2021). Subsequently, the Tremblay group reported the correction of point mutations in exon 6 in human DMD myoblasts using the prime editing technique (Happi Mbakam et al., 2022b).

4.4.8 Delivery of CRISPR *in vivo*

An effective delivery mechanism is necessary to accomplish efficient *in vivo* postnatal genome editing. Cas9 and sgRNA, the two components of the CRISPR system, can be administered to the target organs via a variety of forms. DNA/DNA, mRNA/sgRNA, and protein/sgRNA are the possible nucleotide forms for Cas9 and sgRNA, respectively. The CRISPR delivery strategies frequently employed in DMD include viral and nonviral methods (Min et al., 2019a).

4.4.8.1 Viral delivery

For the delivery of CRISPR/Cas9 components, lentivirus, adenovirus, and adeno-associated virus (AAV) have been employed (Min et al., 2019a), and clinical trials using AAV for gene replacement therapy have been approved by the FDA (Mendell et al., 2017). AAV serotypes 1, 6, 8, 9, rh10, and rh74 have tropism for skeletal muscle and heart. These serotypes have been successfully

used in numerous preclinical investigations to deliver CRISPR gene editing components for postnatal genome editing (Lau and Suh, 2017; Wang et al., 2017).

The SpCas9 ORF is about 4.2 kb in length, which is close to the AAV cargo limit. Thus, a second AAV vector that carries the donor template or sgRNA is required. Hepatocytes and muscle cells have been successfully edited *in vivo* using a dual-AAV approach (Yang et al., 2016). *Staphylococcus aureus* (Sa) Cas9, a smaller Cas9 protein encoded by a 3.2-kb cDNA, has been employed for gene editing in mdx mice to avoid the requirement for a dual-vector system (Nelson et al., 2016; Tabebordbar et al., 2016; Bengtsson et al., 2017). For more flexibility with promoter usage in DMD gene therapy, new AAV serotypes have been engineered, such as the MyoAAV 2A serotype, which appears more efficient than AAV9 in muscle fibers. This serotype can be employed with genome-specific modifiers, including base or prime editors, to maximize therapeutic potential (Mendell et al., 2020; Tabebordbar et al., 2021; Happi Mbakam et al., 2022a).

4.4.8.2 Nonviral delivery

Cas9 and sgRNAs can be delivered *in vivo* through nonviral delivery mechanisms in a variety of forms, including DNA, mRNA, and ribonucleoproteins (RNP). Electroporation has been used to deliver negatively charged DNA or mRNA into muscle cells (Xu et al., 2016). Direct delivery of Cas9 and sgRNA constructs into the skeletal muscle of mdx mice using this technique led to the restoration of dystrophin expression (Xu et al., 2016). Another delivery method for CRISPR components, such as RNP or mRNA/sgRNA, is via lipid-mediated nanoparticles (Zuris et al., 2015; Miller et al., 2017). The cationic lipid nanoparticles can enclose the complex, which can then be transported into cells via endocytosis and pinocytosis. This method is relatively inexpensive compared to other approaches (Kim et al., 2014). Gold nanoparticles coupled to DNA and complexed with cationic endosomal disruptive polymers have also been reported to successfully deliver CRISPR RNP to mdx mice (Lee et al., 2017). Even though it seems to be an appealing strategy for delivering the RNP complex, a major challenge is the systemic delivery requirement to reach the heart, diaphragm, and skeletal muscles through the body. This, together with issues of efficiency, needs to be addressed before effective clinical applications can be investigated.

4.4.9 Gene editing: clinical considerations

Theoretically, gene editing has the potential to cure the disease with a single treatment, "one and done," by correcting the genetic defect causing the condition. Gene editing can enable the expression of normal or nearly normal dystrophin to maximize functional outcomes. The resultant dystrophin, post-gene editing, is anticipated to be larger than microdystrophins which are undergoing clinical trials. Physiological temporal-spatial expression is expected to be normal because the expression of dystrophin after gene editing will be driven under the control of the endogenous dystrophin gene locus. This is compared to therapeutic microdystrophin gene therapy, where expression is dependent on the cis-regulatory sequences designed and incorporated in the construct within the AAV vector (Min et al., 2019b).

4.4.10 Gene editing: future challenges

Despite recent advances, the gene-editing experimental approach is still in the early stages of development for DMD therapy, with several concerns that should be addressed. Notably, off-target mutation risk *in vivo* is a significant concern. Muscle-specific promoters have been used to drive the CRISPR cassette expression to reduce possible off-target effects in non-muscle tissues (Young et al., 2016; Miller et al., 2017). Other issues to be addressed are the delivery efficiency to all the affected skeletal muscles and the heart, in addition to issues related to the maintenance of long-term dystrophin expression. Cardiac myocytes are long-lived cells with minimal regeneration capacity; thus, upon adequate delivery of the editing cassette and precise correction, myocytes are anticipated to exhibit long-term dystrophin expression. However, skeletal muscle fibers have a remarkable regeneration capacity (Ma et al., 2022). Skeletal muscle cells are generated via satellite cell recruitment, the muscle stem cells that are not efficiently transduced by AAV (Arnett et al., 2014; Min et al., 2019b). Thus, the skeletal edited muscle cell proportion will be diluted with every regeneration cycle, ultimately reducing dystrophin expression in the fibers.

Furthermore, there are a number of immunological issues to take into account, such as immunogenicity toward Cas protein or the likelihood of immune reaction toward the replaced dystrophin, a possibility that remains with all gene replacement therapies. More research is required to fully address these concerns (Min et al., 2019b). Thus, further studies focusing on the safety and efficiency of the gene editing CRISPR system are necessary prior to clinical translation (Erkut and Yokota, 2022). The CRISPR system has recently been introduced into clinical trials for other diseases, such as cancer; allergy; and cardiovascular, immunological, and neurological disorders (Sharma et al., 2021). Even though the CRISPR system faces several challenges, it has undoubtedly created new possibilities for treating monogenic diseases that will certainly pave the way for many applications in the upcoming years.

4.5 Cell transplantation therapy

DMD cell-based therapeutics aim to transplant cells with functional dystrophin into dystrophin-deficient muscles. This is one of the earliest genetic approaches attempting to treat DMD (Smythe et al., 2000; Skuk et al., 2004; Skuk et al., 2006). However, multiple factors must be considered for successful muscle recovery. Autogenic cell transplantation, relying on genetic engineering of the host's induced pluripotent stem cells (iPSCs) to restore functional dystrophin expression, is associated with lower immunogenic risk than allogenic cell transplantation (obtained from a healthy donor) requiring immunosuppression (Maffioletti et al., 2014). Ideally, the transplanted cells should be competent to cross the vascular wall (blood–muscle barrier) upon systemic delivery to target different striated muscle entities (heart, diaphragm, and limb muscles) to limit the requirement for multiple injection sites into individual muscles. Moreover, to provide a long-term effect and reduce the risks of inducing an immune response from repeated deliveries, the transplanted cells must have a high muscle engraftment rate, incorporate into the host myocytes, and persist through self-renewal (Wallace et al., 2008).

Various cell types are candidates for transplantation and are being studied for DMD therapy. Satellite cells (myoblasts) are quiescent muscle stem cells that reside beneath the basal lamina (Mauro, 1961; Moss and Leblond, 1971). Upon muscle damage, myoblasts are activated to proliferate, self-renew, and repair. Other cell types, notably bone marrow-derived cells, pericytes, mesoangioblasts, and mesenchymal stem cells, are also under investigation because of their ability to access the muscle compartment and their myogenic potential. However, the limited capacity of these cells to be expanded *in vitro* constitutes a limitation for wide therapeutic usage. Nonetheless, based on the early successes in preclinical studies, a clinical trial is underway to transplant skeletal muscle-derived mesoangioblasts into the circulation of patients with DMD. Induced pluripotent stem cells (iPSCs), featuring an infinite self-renewal capacity, can be differentiated into myogenic lineages. However, iPSCs-derived myogenic progenitors could carry the risk of unlimited growth and teratoma development *in vivo* (Rong et al., 2012).

One of the most challenging hurdles for cell-based clinical applications centers on delivery. Although preclinical studies show promise (Rouger et al., 2011), most systemic studies report only limited engraftment of dystrophin restoration (Briggs and Morgan, 2013; Hogrel et al., 2013). Myoblasts lack extravasation ability, and continuous efforts are being made to improve their trans-endothelial migration ability (Choi et al., 2022). As for extravasation-competent stem cells, only a small fraction of transplanted stem cells appears to reach the muscle upon systemic delivery (Dellavalle et al., 2007). Additionally, although local high-density myoblast injections (intra-muscular injections) produce some dystrophin restoration around the needle track (Skuk et al., 2004; 2006), this approach is only practical for superficial small muscles.

On another note, cardiosphere-derived stem cells offer a transplantable cell type with therapeutic potential. Preliminary results from the randomized, phase I/II HOPE-Duchenne clinical trial (NCT02485938) revealed that the intra-coronary infusion of cardiosphere-derived cells was well tolerated and suggested a positive effect on upper limb and heart function for up to 12 months (Taylor et al., 2019). Furthermore, phase II of the Hope-2 clinical trial (NCT04428476) recently revealed that intravenous delivery of cardiosphere-derived cells is safe and has beneficial effects in slowing the deterioration of muscle function in patients with late-stage DMD (McDonald et al., 2022).

5 Small molecule therapy for DMD: copolymers

Despite the numerous trials exploring potential therapeutics, there remains a dearth of effective treatments available for DMD patients. In this context, it is worth considering additional strategic approaches that target the primary defect of DMD: severe muscle membrane fragility. As discussed previously, as the primary pathophysiological defect in DMD is the marked susceptibility to contraction-induced membrane stress, a unique therapeutic approach is the use of synthetic membrane stabilizers to prevent muscle damage by directly stabilizing the dystrophin-deficient muscle membrane (Houang et al., 2015; 2017).

Poloxamers emerged from industrial applications in the 1940s. Recently, however, amphiphilic characteristics of poloxamer have shown a protective effect on the cell membrane. Poloxamer 188 (P188; PEO_{75}-PPO_{30}-PEO_{75}, 8400 g/mol) is a non-ionic copolymer consisting of a triblock—a hydrophobic chain of poly(propylene oxide) (PPO) in the middle flanked by two hydrophilic poly(ethylene oxide) (PEO) chains on each side (Bates and Fredrickson, 1990). Studies using P188 have reported positive results in skeletal muscle fibers with electric injury (Lee et al., 1992; Lee et al., 1999; Collins et al., 2007), ischemia-reperfusion injuries (Hunter et al., 2010), heat injury (Merchant et al., 1998), radiation injury (Hannig et al., 1999), and sickle cell disease (Adams-Graves et al., 1997; Ballas et al., 2004). These results are due to the interactions between the phospholipid bilayer of the cells and the amphiphilic copolymer (Houang et al., 2017). Similar to these trials, DMD has been considered a potential candidate for the P188 treatment due to the fragile muscle cell membrane caused by dystrophin deficiency. In DMD, P188 is hypothesized to be beneficial in preventing cardiac myocyte damage induced by passive stretch and extracellular Ca^{2+} inflow triggered by micro-tears in the cell membrane (Yasuda et al., 2005) (Figure 3).

P188-treatment in isolated cardiac myocytes from mdx mice *in vitro* restored compliance and blocked susceptibility to stretch-induced Ca^{2+} overload (Yasuda et al., 2005). P188 delivery *in vivo* to mdx mice rapidly improved the geometry of the ventricles and suppressed the acute cardiac failure induced by a dobutamine stress test (Yasuda et al., 2005). P188 also prevented cardiomyopathy induced by isoproterenol in mdx mice (Spurney et al., 2011b). Similarly, systemic delivery of P188 for 8 weeks to dystrophic dogs (Golden retriever muscular dystrophy model) markedly reduced myocardial fibrosis, prevented left-ventricular remodeling, and inhibited the increase in cardiac Troponin I (TnI) and brain natriuretic peptide (BNP) in serum (Townsend et al., 2010). Furthermore, the direct application of P188 to isolated canine cardiac myocytes instantly restored poor myocyte compliance (Townsend et al., 2010).

For dystrophic skeletal muscle, the delivery method of P188 was found to be an important factor in the effectiveness of rescue of function. Interestingly, subcutaneous delivery of P188 showed protection against lengthening contraction-induced force loss, but this was not seen by intraperitoneal delivery. Furthermore, P188 significantly decreased baseline and lengthening contraction-induced membrane instability, as shown by reduced Evans Blue dye uptake in the mdx skeletal muscles (Houang et al., 2015). Skeletal muscles such as the diaphragm were also found to be protected by longer-term systemic delivery of P188 showing improved respiratory parameters, reduced centralized myonuclei, reduced variation in fiber size, and reduced collagen deposition (Markham et al., 2015).

Poloxamers can be manufactured in diverse forms by differing weight ratios of the PEO chain, molecular weight, and end group (Houang et al., 2018). Variations in hydrophilic and hydrophobic block lengths alter the hydrophobicity balance that determines the insertion of the molecule into the lipid bilayer of the cell and, thus, stabilization (Demina et al., 2005; Houang et al., 2017; Kim et al., 2017; Houang et al., 2018). For example, more hydrophobic poloxamers, such as P335 (PEO_{38}–PPO_{54}–PEO_{38}), P333 (PEO_{20}–PPO_{54}–PEO_{20}), and P181 (PEO_2–PPO_{30}–PEO_2), insert

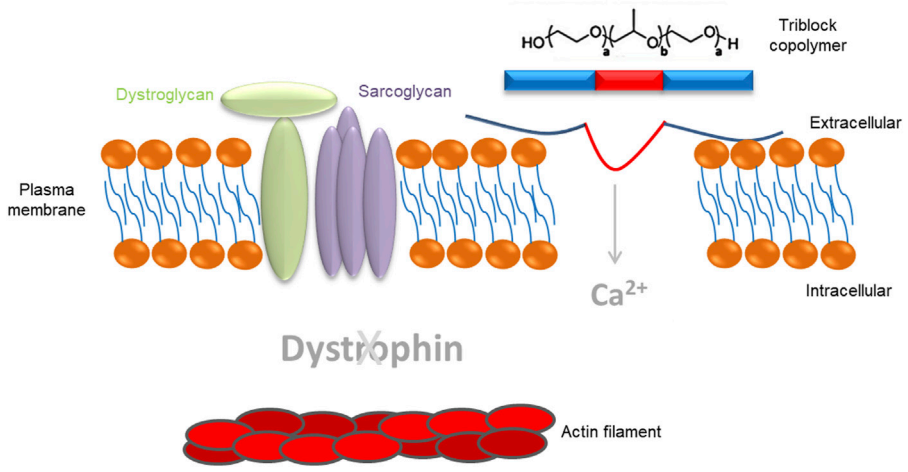

FIGURE 3
Copolymer-based muscle membrane stabilization of dystrophic muscle. Representation of copolymer-based stabilization of the damaged membrane via the interface of its hydrophobic PPO block (red) with stabilization by PEO blocks (blue) to prevent the entry of extracellular Ca^{2+} into the cell.

into the liposomal membrane and eventually lyse the cell (Houang et al., 2018). Compared to P188, extended P188 (PEO_{140}-PPO_{44}-PEO_{140}, 14,600 g/mol) also showed a robust protective effect at lower concentrations against the intracellular enzyme lactate dehydrogenase release induced by hypoosmotic stress (Houang et al., 2015). Furthermore, diblock copolymers (PEO_{75}-PPO_{15}) with a tert-butoxy end group (-C_4) showed significant protection against lengthening contraction-induced force loss in mdx mice, whereas a hydroxyl end group (-H) did not show any protection (Houang et al., 2017). This finding showed that the hydrophobicity of the end group also directly influences interactions with the cell membrane and stabilization.

For membrane stabilizers in DMD, Phrixus Pharmaceuticals, Inc. has initiated a Phase 2 single-site, open-labeled trial for skeletal limb, cardiac, and respiratory muscle endpoints in non-ambulatory DMD patients (ClinicalTrials.gov Identifier: NCT03558958). Further research to determine the optimal structure-function of synthetic membrane-protecting copolymers will be useful in seeking a full therapeutic effect in DMD.

6 Non-dystrophin-based therapeutics

This section focuses on the genetic strategies related to the correction of or compensation for the lack of dystrophin via meaningful alternatives to direct dystrophin reconstitution. The advantage of dystrophin complementary approaches is that they may be applied to a number of MD patients, regardless of the type of mutation. Several pharmacological strategies to slow down the disease progress, such as those reducing inflammation or fibrosis, are also in development, and these have been reviewed by different groups (Spinazzola and Kunkel, 2016) and will not be covered in this review.

6.1 Utrophin modulation

Utrophin is a structural and functional autosomal paralog of dystrophin encoded by the UTRN gene (Love et al., 1989). This large cytoskeletal protein (395 kDa) shows sequence and structural similarity to dystrophin. Unlike dystrophin, utrophin is highly expressed in developing muscle and is localized at the sarcolemma in early human development (Love et al., 1989; Pons et al., 1993) when dystrophin is absent or present only at low levels. As the myofiber matures, utrophin levels decrease and become enriched at the neuromuscular junction (McNally, 2012).

Utrophin content is increased at the sarcolemma of skeletal muscle in DMD and BMD patients compared to healthy individuals (Weir et al., 2004; Arechavala et al., 2010; Mamchaoui, 2018). The baseline mild phenotype observed in the mdx mouse has been proposed to result from the efficient regeneration process in this model along with utrophin upregulation as a compensatory mechanism to mitigate the lack of dystrophin (Guiraud et al., 2015). This view is supported by the fact that mice deficient in both utrophin and dystrophin display a much more severe pathology compared to mdx mice (Deconinck et al., 1997). Furthermore, proof of principle that utrophin could play a role as a dystrophin surrogate comes from preclinical studies which established that an increase in utrophin protein levels in transgenic mdx mice prevented pathology, and this prevention was dependent on the amount of utrophin expressed (Tinsley et al., 1998). Studies in animal models have provided compelling evidence that utrophin functions in these scenarios to directly protect the muscle against dystrophin-deficient membrane instability. Because utrophin is an endogenous protein that can substitute for dystrophin, several approaches have been initiated to upregulate utrophin expression (Soblechero-Martín et al., 2021), including direct mechanisms, such as gene or protein replacement (Sonnemann et al., 2009), and indirect methods, such as transcriptional upregulation of the

utrophin promoter or by stabilization of the protein or RNA (Michel et al., 2008).

Utrophin is expressed from at least two promoters, known as promoters A and B (Burton et al., 1999). Expression from promoter B is predominantly in endothelial cells in blood vessels, whereas expression from promoter A occurs in muscle and other tissues (Weir et al., 2002). Utrophin upregulation by stimulating promoter A activity is a promising pharmacological approach that has been extensively investigated. Thousands of small molecule candidates from drug libraries have been tested by high-throughput screening (HTS) assays to identify molecules acting at the utrophin A promotor site. Numerous small molecules, including heregulin (Krag et al., 2004), nabumetone (Moorwood et al., 2011), L-arginine (Voisin et al., 2005), and okadaic acid, have shown promising results at the preclinical level, with dose-dependent activation of the utrophin promoter. Ezutromid (SMTC1100) was the first orally bioavailable utrophin regulator that showed increased UTRN transcription (Soblechero-Martín et al., 2021). Pre-clinical results with the small molecule drug Ezutromid led Summit Therapeutics to initiate clinical trials as a potential treatment for DMD and BMD. Promising results from a Phase 1 healthy volunteer study showed that SMTC1100 is safe and well tolerated, with plasma levels achieved above those thought to be required to modulate utrophin (Ricotti et al., 2016). However, a Phase 2 clinical study (NCT02858362) failed to achieve both the primary (changes in leg muscle magnetic resonance parameters) and secondary (increased utrophin levels and decreased muscle damage) endpoints (Soblechero-Martín et al., 2021). Based on these results, Summit Therapeutics abandoned the development program of Ezutromid (Ricotti et al., 2016; Muntoni et al., 2019).

Direct utrophin protein replacement using recombinant full-length or truncated utrophin is another potential strategy to increase utrophin levels *in vivo*. The TAT protein transduction domain of the human immunodeficiency virus (HIV1) has been used to generate chimeric protein microutrophin (TAT-μUtr) and utrophin protein (TAT-Utr) (Sonnemann et al., 2009). Preclinical studies in mdx and dko mice were promising; however, further progress has not been reported. A similar pathway to micro-dys gene therapy has been pursued in the development of utrophin gene therapy. A number of preclinical studies using "micro-utrophin" (μUtrn) gene delivery have been reported recently, with some studies reporting restoration of the DGC, prevention of myofiber degeneration, normalization of serum CK levels, and improvement of muscle function (Ebihara et al., 2022). Furthermore, additional studies on double knockout (dko) mice and canine X-linked muscular dystrophy dogs have shown that μUtrn improves the severe pathological dystrophic phenotype in these models (Cerletti et al., 2003). One advantage to delivering utrophin is that it is less likely to elicit an immune response. It has been shown that viral gene delivery of dystrophin into DMD patients has been associated with an immune response, which limits the expression of dystrophin (Mendell et al., 2010). A protein such as utrophin, which is normally expressed in DMD patients, should not be associated with a similar immune response.

Utrophin, while highly similar to dystrophin, does not share all of the dystrophin binding domains. Therefore, it may not be able to fully substitute for dystrophin. Nonetheless, utrophin upregulation has been shown as a promising therapeutic approach, applicable to all DMD and BMD patients, irrespective of their dystrophin mutation. Many pathways involved in utrophin expression are currently being investigated. However, the amount of utrophin required by dystrophic patients to achieve a relevant clinical benefit remains to be determined. Further research is required before utrophin therapies can apply to DMD and BMD patients.

6.2 α7-Integrin upregulation

The α7β1 integrin protein is the predominant laminin-binding integrin in skeletal, cardiac, and vascular smooth muscle (Burkin and Kaufman, 1999). The integrin/laminin complex serves as a mechano-signaling anchor that binds laminin and links the ECM on the surface of muscle cells with the intracellular actin cytoskeleton (Hynes, 1992). α7 is present throughout the sarcolemma and is enriched at the myotendinous and neuromuscular junction. In particular, α7β1-integrin/laminin-211 plays a critical role in the functional integrity and maintenance of skeletal myoblasts and adult myofibers (Hodges et al., 1997; Mayer et al., 1997). α7 has been shown to be an important modifier of dystrophic symptoms, and defects in the components of this complex cause muscular dystrophy, illustrating the essential role of the α7 chain (Hodges et al., 1997; Guo et al., 2006). Interestingly, α7-integrin expression is increased at the sarcolemma in the mdx mouse and DMD patients (Hodges et al., 1997), demonstrating evidence that integrin upregulation may serve to functionally compensate for the lack of dystrophin. Moreover, knockout of both dystrophin and α7 integrin has been shown to produce a significantly more severe dystrophic phenotype, further supporting the evidence of a compensatory role for α7 integrin for dystrophin (Rooney et al., 2006).

Burkin et al. (2001, 2005) showed that transgenic overexpression of α7-integrin in dystrophin/utrophin double knockout mice (*mdx*/utrn$^{-/-}$) alleviates pathology, extends viability and mobility, and reduces kyphosis. In addition, increased expression of α7 in mdx mice significantly protected against loss of force, reversed muscle pathology, and stabilized sarcolemmal integrity (Heller et al., 2013). Importantly, eightfold overexpression of α7-integrin does not demonstrate detectable toxicity or disruption to global gene expression profiles (Liu et al., 2008). Therefore, similar to utrophin, small compound screens for α7-integrin modulators appear to be a viable approach (Gurpur et al., 2009).

Laminin-111 is another potential candidate of interest (Rooney et al., 2009a). Injection of laminin-111 protein in the mdx mouse increased the expression of α7-integrin, stabilized the sarcolemma, and protected muscle from exercise-induced damage (Rooney et al., 2009a; 2009b). Conversely, transgenic expression of the laminin α1 chain to enhance heterotrimer formation of laminin-111 in the mdx mouse reported no improvement of the dystrophic symptoms (Gawlik et al., 2011), showing that further studies are necessary to validate the functionality of laminin-111 protein therapy in DMD.

6.3 Myostatin, follistatin, and other muscle growth strategies

Myostatin is a transforming growth factor-β-superfamily member that acts as a negative regulator of skeletal muscle

growth (Mcpherron et al., 1997). The biological relevance of myostatin was addressed in mice through gene overexpression studies using normal or dominant-negative forms of the protein, systemic administration of myostatin protein or inactivating antibody, and gene inactivation (Zhu et al., 2000; Yang et al., 2001; Nishi et al., 2002; Grobet et al., 2003; Walsh and Celeste, 2005; Reisz-porszasz et al., 2022). Regardless of the approach used to induce myostatin inhibition, studies have shown functional improvement of the dystrophic muscle, such as increasing body weight, muscle mass, and muscle size, along with a significant decrease in muscle degeneration. Based on these studies and others carried out in cultured cells, the general consensus is that myostatin regulates postnatal muscle-fiber size by maintaining satellite cells in a quiescent state and inhibiting protein synthesis. Myostatin also regulates the number of muscle fibers during development by blocking the proliferation and differentiation of myoblasts (Lee, 2004; Tobin and Celeste, 2005).

However, some concerns have been raised about whether myostatin inhibition leads to a truly healthy muscle, as an exercise in myostatin-deficient cattle leads to early exhaustion. Moreover, it can even be deleterious, as disused muscle atrophy is markedly more severe in the context of myostatin deficiency (Mcmahon et al., 2022). Nonetheless, considering the effect of myostatin on muscle growth, inhibition of myostatin has been considered a therapeutic target in the treatment of muscle-degenerative and wasting conditions, such as muscular dystrophies, and clinical trials have been designed to increase muscle mass and strength in several of the most common forms of adult muscular dystrophy. Nevertheless, clinical trials in humans have been disappointing owing to a lack of improvement in muscle strength (Wagner et al., 2008) or adverse effects (Attie et al., 2013). Despite these negative results, other clinical trials based on blocking myostatin activity have been initiated (Mulivor et al., 2014; Pfizer, 2014).

7 Clinical trials and approved therapies

A growing number of pharmaceutical companies and startups have directed efforts toward DMD therapeutics. Many challenges remain, and the problem of delivery to all muscles of the body needs to be resolved. Nevertheless, there is little doubt that although a cure remains elusive, there has been a rapid expansion in the number of treatments entering clinical trials that have the potential to provide a significant clinical impact on the quality of life of DMD patients (ClinicalTrials.gov). Some of these approaches have received regulatory approval in the USA, Europe, and Japan (Mercuri et al., 2019). The increase in the number of patient registries and the ability to link natural histories significantly enhance opportunities to examine inter-individual differences to best evaluate disease progression/regression. These opportunities will greatly facilitate the emerging field of personalized/combinatory therapies, which represent the future of effective DMD treatments and will set the stage for other rare disease therapeutics.

Gene therapy has been elevated in the DMD field due to the promise that this approach could "stably" correct DMD defects via restoring dystrophin throughout the body (Gregorevic et al., 2006; Chamberlain and Chamberlain, 2017). Adeno-associated virus-(AAV) mediated gene therapies have advanced significantly since their clinical trial debut in 2003 (Kuzmin et al., 2021). Several studies have demonstrated the body-wide expression and therapeutic effect of this approach following intravascular AAV microdystrophin delivery (Mendell et al., 2021). Based on the many positive efficacy reports from experiments in the mdx mouse model and golden retrievers with muscular dystrophy (GRMD dog model) (Birch et al., 2023), four microdystrophin constructs have moved forward and are currently being investigated in clinical trials (Figure 1) (Table 2). The clinical trials were initiated in the United States in December 2017 and are now ongoing in Europe.

Clinical trial PF-06939926 is an AAV9-mediated transfer of microdystrophin currently tested in a Pfizer Phase 1b open-label clinical trial evaluating dose, safety, and tolerability of a single IV infusion of microdystrophin in ambulatory and non-ambulatory DMD patients (NCT03362502 and NCT04281485) (Table 2). PF-06939926 has been tested in men with DMD, ages 4 and older, at 21 sites, and two doses have been used: a low dose of 1×10^{14} vector genomes (vg)/kg) and a higher dose of 2×10^{14} vg/kg. Early data from five of six boys showed some evidence of improvement (or at least no decline) in the NorthStar Ambulatory Assessment (NSAA), compared with participants given a placebo during previous clinical trials. Side effects and serious adverse events were reported in some patients. Tragically, a death of a patient was reported, which led to the trial being put on hold due to questions about Pfizer's potency tests. Recently, the FDA announced the removal of the clinical hold after the company had addressed the agency's request regarding a potency assay and implementation of a protocol amendment.

SGT-001, an AAV9-mediated transfer of microdystrophin from Solid Biosciences, is also being evaluated in a phase I clinical trial, IGNITE DMD (NCT03368742) (Table 2). After a suspension due to a serious adverse effect in one patient, the study was recently re-activated with an amended clinical protocol and using SGT-001 manufactured with a second-generation process (Solid Bioscience). A clinical trial by Sarepta Therapeutics, Inc. is ongoing to investigate the safety and efficacy of the IV infusion of rAAVrh74.MHCK7 microdystrophin (SRP-9001), in a first open-label phase I/II trial (NCT03375164). Some evidence of 12-week dystrophin expression and a good safety profile was communicated from the first 11 participants enrolled in Study SRP-9001–103 (NCT04626674), another open-label Phase I study being conducted in partnership with Roche (Sarepta therapeutics).

Overall, to date, clinical trials have accrued preliminary results that have unfortunately demonstrated a lack of clinically meaningful success and missed milestones for efficacy (Mullard, 2021a). Thus far, the human trial data do not report the same success reported in animal works, indicating this promising approach requires significant further enhancement (Mullard, 2021b).

There is a clear need for caution as several serious treatment-related adverse events have been reported. Hepatic transaminitis, classed as severe, was reported in participants in trials in DMD, following SGT001 (Wagner et al., 2021) and rAAVrh74.MHCK7.microdystrophin (NCT03375164) (Mendell et al., 2020). One incidence of vomiting requiring hospital admission was reported as a severe adverse event with the PF-06939926 microdystrophin product (NCT03362502) (Belluscio et al., 2021). Moreover, two patients receiving rAAVrh74.MHCK7.microdystrophin (NCT03375164) experienced

TABLE 3 Clinical trials using stop codon read-through and exon skipping for DMD therapy in 2023.

Drug name	Description	Company	Delivery route	Current stage	Clinical trial number
Stop codon read-through					
Ataluren	Nonsense suppression	PTC Therapeutics	Oral	Phase III	NCT01557400
Exon skipping					
Eteplirsen (AVI-4568)	PMO morpholino targeting exon 51	Sarepta Therapeutics	Intravenous	Phase II	NCT03218995
				Phase II	NCT04179409
				Phase III	NCT03992430
				Phase III	NCT03985878
Golodirsen (SRP4053)	PMO morpholino targeting exon 53	Sarepta Therapeutics	Intravenous	Phase II	NCT04179409
				Phase III	NCT02500381
				Phase III	NCT03532542
Casimersen (SRP4053)	PMO morpholino targeting exon 45	Sarepta Therapeutics	Intravenous	Phase II	NCT04179409
Viltolarsen (NCNP-01)	PMO morpholino targeting exon 53	Nippon Shinyaku Co. Ltd	Intravenous	Phase II	NCT03167255
Drisapersen (PRO051)	2′-O-methyl PS Targeting exon 51	BioMarin Pharmaceutical Inc	Intravenous	Extension	NCT02636686

severe rhabdomyolysis (Today MDN, 2019; Novack et al., 2021). Significant issues remain to be considered, such as pre-existing DMD population immunity to certain AAV serotypes, the efficacy of the specific truncated micro- or mini-dystrophin variants used, and re-administration challenges and serotype switching considerations.

Consequently, other approaches aim to produce nearly full-length dystrophin by targeting only the region that encompasses the mutation in an effort to bypass the genetic defect. During the last decade, numerous approaches have been developed to directly correct genetic defects at the RNA level (Hanson et al., 2021), as discussed previously. In the case of dystrophin, such approaches are designed to either restore the expression of a full-length transcript or a nearly full-length *DMD*.

Ataluren (Translarna™, previously known as PTC124) is an orally bioavailable small molecule developed by PTC Therapeutics designed to enable the formation of a functioning protein in patients with genetic disorders caused by a nonsense mutation (Politano, 2021). Ataluren has demonstrated its efficacy *in vivo* using the mdx mouse model (Welch et al., 2007). However, laboratories failed to replicate this finding, questioning the specificity of Ataluren against stop codons (Auld et al., 2009; McElroy et al., 2013). Nonetheless, supported by evidence for functional improvement in a cell model of Hurler syndrome (Goldmann et al., 2012) and in mouse models of nonsense mutation-associated cystic fibrosis (Kerem et al., 2014), Ataluren advanced to clinical trials and was granted conditional marketing authorization by EMA in 2014 (https://www.ema.europa.eu/en/medicines/human/EPAR/translarna) for DMD ambulatory patients and those aged ≥2 years (Table 3). To date, two randomized, double-blind, placebo-controlled trials of Ataluren in DMD patients have been conducted: a Phase IIb trial (NCT00592553) on 174 randomized patients and a Phase III trial (NCT01826487) on 230 randomized patients (Table 3). In both trials, Ataluren was well-tolerated (Campbell et al., 2020). However, the trials failed to achieve the 48-week primary endpoint of improved distance walked in the 6-min walk test (SMWT) compared with patients who received placebo treatment. Nonetheless, these trials reported a trend of therapeutic efficacy, specifically a 29-m increase in the SMWT and an improvement in timed function tests in those who received Ataluren compared with placebo (Campbell et al., 2020; Politano, 2021). Unfortunately, very little evidence exists to inform the question of whether Ataluren displays any degree of efficiency or delivers a benefit in the heart.

A number of chemical versions of AONs exist to be applied for exon-skipping, including 2′-*O*-methyl-modified RNA, phosphorodiamidate morpholino oligomers (PMO), and tricycloDNA antisense. All of them have been used *in vitro* and *in vivo* in mouse and dog models and demonstrated efficient skipping that resulted in histology and functional improvements (Niks and Aartsma-Rus, 2017), as previously discussed. Several PMO compounds are in development to target the exons that represent the highest proportions of deletions amenable to exon-skipping. Eteplirsen (marketed under the trade name Exondys 51) is a morpholino ASO from Sarepta Therapeutics designed to mask a splice acceptor sequence in exon 51 of the dystrophin gene, thereby promoting exon skipping and restoration of the reading frame in the 13% of patients with amenable frame-shifting mutations. This was the first drug approved by the FDA as a specific DMD therapy. Patients' muscle biopsies after approximately a year of systemic dosing showed modest efficacy in the production of dystrophin protein expression (~1%), which is considered to be inadequate to confer significant clinical benefits (NCT01396239, NCT01540409, NCT02255552) (Table 3) (Mendell et al., 2016; Niks and Aartsma-Rus, 2017).

Regardless, the drug was approved, and efforts are underway to develop more effective oligonucleotide therapies. Tissue penetration and longevity of PMOs have remained an ongoing concern. To address these shortcomings, other delivery systems for AONs are

currently being investigated to identify the modifications that can optimize cellular penetration and systemic safety, with a major focus on PPMOs (Nguyen and Yokota, 2019). Additionally, multiple other exon-skipping AONs are being actively developed, with the FDA recently giving approval for Golodirsen (SRP-4053) and Viltolarsen, designed to skip exon 53, and Casimersen (SRP-4045), designed to skip exon 45 (Table 3). So far, data collected from DMD patients show that PMO AONs are well tolerated and safe in DMD following weekly intravenous (IV) administration (Frank et al., 2020; Komaki et al., 2020; Wagner et al., 2021).

8 Conclusion

The identification of the dystrophin gene as the cause of DMD has led to improved diagnosis while providing deep insights into the biochemistry and cellular physiology of the striated muscle cytoskeleton-membrane-ECM interface. The preceding decades have been marked by careful mechanistic studies aiming to tease apart the molecular processes disrupted by dystrophin loss in an effort to understand and correct the underlying pathology of DMD. These insights have greatly impacted DMD diagnosis and care, including the opportunity to develop novel, personalized, and effective therapeutic strategies to prolong and improve the quality of life of patients with DMD.

9 Future directions

The future of heart/skeletal muscle therapy in DMD will likely require a combination of approaches to achieve optimal outcomes, including a therapeutic approach to correct the genetic defect and target the secondary effects caused by the lack of dystrophin. Advances in technology have made many of the problems with therapeutic approaches more tractable. Despite that, two crucial and challenging issues shared by all new drugs are delivery and targeting. Finding an appropriate vehicle is critical to consistently reach the proper drug target at minimal, effective dosing. This is especially significant considering the enormous healthcare costs associated with these proposed therapies. Nonetheless, there is little doubt that although a cure remains elusive, there has been a rapid expansion in the number of treatments entering clinical trials that have the potential to provide a significant clinical impact on the quality of life for DMD patients. This turning point in the development of DMD therapies marks the beginning of a new mission for correcting monogenic muscular disorders. In turn, these approaches set an example for research progress for other related disorders.

Author contributions

ABBA searched the literature, organized the article structure, prepared tables and figures, and wrote and guided the manuscript for this review. NH searched the literature, prepared tables and figures, and wrote the manuscript. HC, AM, DH, and JB searched the literature and wrote the manuscript. JM guided the manuscript, provided critical input, and revised the manuscript for this review. All authors contributed to the article and approved the submitted version.

Funding

National Institutes of Health (R01)—Title: Copolymer-based sarcolemma stabilization for protecting dystrophic skeletal muscles *in vivo* (1R01AR071349). National Institutes of Health (R01)—Title: Skeletal muscle sarcomere function in health and disease (R01AR079477). National Institutes of Health (R01)—Title: Targeted membrane integrity in cardiac ischemia and reperfusion (R01HL122323). Regenerative Medicine Minnesota—Title: Advancing a genetically edited biosensor platform in human induced pluripotent stem cell-derived cardiac muscle for personalized medicine and drug discovery. This work was supported by grants from the NIH, the American Heart Association, the Muscular Dystrophy Association, and Regenerative Medicine Minnesota.

Conflict of interest

JM is on the scientific advisory board of and holds shares in Phrixus Pharmaceuticals Inc., a company developing novel therapeutics for heart failure. The terms of this arrangement have been reviewed and approved by the University of Minnesota in accordance with its conflict-of-interest policies.

Publisher's note

References

Aartsma-Rus, A., Ferlini, A., Goemans, N., Pasmooij, A. M., Wells, D. J., Bushby, K., et al. (2014). Translational and regulatory challenges for exon skipping therapies. *Hum. Gene Ther.* 25, 885–892. doi:10.1089/hum.2014.086

Aartsma-Rus, A., Fokkema, I., Verschuuren, J., Ginjaar, I., van Deutekom, J., van Ommen, G. J., et al. (2009). Theoretic applicability of antisense-mediated exon skipping for Duchenne muscular dystrophy mutations. *Hum. Mutat.* 30, 293–299. doi:10.1002/humu.20918

Aartsma-Rus, A., and van Putten, M. (2020). The use of genetically humanized animal models for personalized medicine approaches. *Dis. Model Mech.* 13, dmm041673. doi:10.1242/dmm.041673

Aartsma-Rus, A., Van Deutekom, J. C. T., Fokkema, I. F., Van Ommen, G. B., and Den Dunnen, J. T. (2006). Entries in the leiden duchenne muscular dystrophy mutation database: An overview of mutation types and paradoxical cases that confirm the reading-frame rule. *Muscle and Nerve Official J. Am. Assoc. Electrodiagn. Med.* 34, 135–144. doi:10.1002/mus.20586

Abmayr, S., and Chamberlain, J. (2006). The structure and function of dystrophin. Molecular mechanisms of muscular dystrophies. *Georget. Landes Biosci.*, 14–34.

Adams-Graves, P., Kedar, A., Koshy, M., Steinberg, M., Veith, R., Ward, D., et al. (1997). RheothRx (poloxamer 188) injection for the acute painful episode of sickle cell disease: A pilot study. *Blood* 90, 2041–2046. doi:10.1182/blood.V90.5.2041

Ahmad, M., Wolberg, A., and Kahwaji, C. I. (2022). "Biochemistry, electron transport chain," in StatPearls *(treasure island (FL).*

Ahn, A. H., and Kunkel, L. M. (1993). The structural and functional diversity of dystrophin. *Nat. Genet.* 3 (4), 283–291. doi:10.1038/ng0493-283

Allen, D. G., Whitehead, N. P., and Froehner, S. C. (2016). Absence of dystrophin disrupts skeletal muscle signaling: Roles of Ca2+, reactive oxygen species, and nitric oxide in the development of muscular dystrophy. *Physiol. Rev.* 96, 253–305. doi:10.1152/physrev.00007.2015

Amin, R. S., Kimball, T. R., Bean, J. A., Jeffries, J. L., Paul Willging, J., Cotton, R. T., et al. (2002). Left ventricular hypertrophy and abnormal ventricular geometry in children and adolescents with obstructive sleep apnea. *Am. J. Respir. Crit. Care Med.* 165, 1395–1399. doi:10.1164/rccm.2105118

Amoasii, L., Hildyard, J. C. W., Li, H., Sanchez-Ortiz, E., Mireault, A., Caballero, D., et al. (2018). Gene editing restores dystrophin expression in a canine model of Duchenne muscular dystrophy. *Science* 362, 86–91. doi:10.1126/science.aau1549

Amoasii, L., Long, C., Li, H., Mireault, A. A., Shelton, J. M., Sanchez-Ortiz, E., et al. (2017). Single-cut genome editing restores dystrophin expression in a new mouse model of muscular dystrophy. *Sci. Transl. Med.* 9, eaan8081. doi:10.1126/scitranslmed.aan8081

Andrade, F. H., Reid, M. B., Allen, D. G., and Westerblad, H. (1998). Effect of hydrogen peroxide and dithiothreitol on contractile function of single skeletal muscle fibres from the mouse. *J. Physiol.* 509 (2), 565–575. doi:10.1111/j.1469-7793.1998.565bn.x

Angelini, C., and Peterle, E. (2012). Old and new therapeutic developments in steroid treatment in Duchenne muscular dystrophy. *Acta Myol.* 31, 9–15.

Anzalone, A. V., Koblan, L. W., and Liu, D. R. (2020). Genome editing with CRISPR-Cas nucleases, base editors, transposases and prime editors. *Nat. Biotechnol.* 38, 824–844. doi:10.1038/s41587-020-0561-9

Anzalone, A. V., Randolph, P. B., Davis, J. R., Sousa, A. A., Koblan, L. W., Levy, J. M., et al. (2019). Search-and-replace genome editing without double-strand breaks or donor DNA. *Nature* 576, 149–157. doi:10.1038/s41586-019-1711-4

Arechavala, V., Kinali, M., Feng, L., Brown, S. C., Sewry, C., Morgan, J. E., et al. (2010). Immunohistological intensity measurements as a tool to assess sarcolemma-associated protein expression. *Neuropathol. Appl. Neurobiol.* 36, 265–274. doi:10.1111/j.1365-2990.2009.01056.x

Arechavala-Gomeza, V., Graham, I. R., Popplewell, L. J., Adams, A. M., Aartsma-Rus, A., Kinali, M., et al. (2007). Comparative analysis of antisense oligonucleotide sequences for targeted skipping of exon 51 during dystrophin pre-mRNA splicing in human muscle. *Hum. Gene Ther.* 18, 798–810. doi:10.1089/hum.2006.061

Arnett, A. L. H., Konieczny, P., Ramos, J. N., Hall, J., Odom, G., Yablonka-Reuveni, Z., et al. (2014). Adeno-associated viral vectors do not efficiently target muscle satellite cells. *Mol. Therapy-Methods Clin. Dev.* 1, 14038. doi:10.1038/mtm.2014.38

Attie, K. M., Borgstein, N. G., Yang, Y., Condon, C. H., Seehra, J. A. S. S., and Sherman, M. L. (2013). *A single ascending-dose study of muscle regulator ace-031 in healthy volunteers*. doi:10.1002/mus.23539

Auld, D. S., Thorne, N., Maguire, W. F., and Inglese, J. (2009). Mechanism of PTC124 activity in cell-based luciferase assays of nonsense codon suppression. *Proc. Natl. Acad. Sci. U. S. A.* 106, 3585–3590. doi:10.1073/pnas.0813345106

Bach, J. R., Ishikawa, Y., and Kim, H. (1997). Prevention of pulmonary morbidity for patients with Duchenne muscular dystrophy. *Chest* 112, 1024–1028. doi:10.1378/chest.112.4.1024

Ballas, S. K., Files, B., Luchtman-Jones, L., Benjamin, L., Swerdlow, P., Hilliard, L., et al. (2004). Safety of purified poloxamer 188 in sickle cell disease: phase I study of a non-ionic surfactant in the management of acute chest syndrome. *Hemoglobin* 28, 85–102. doi:10.1081/hem-120035919

Banks, G. B., Combs, A. C., Chamberlain, J. R., and Chamberlain, J. S. (2008). Molecular and cellular adaptations to chronic myotendinous strain injury in mdx mice expressing a truncated dystrophin. *Hum. Mol. Genet.* 17, 3975–3986. doi:10.1093/hmg/ddn301

Banks, G. B., Gregorevic, P., Allen, J. M., Finn, E. E., and Chamberlain, J. S. (2007). Functional capacity of dystrophins carrying deletions in the N-terminal actin-binding domain. *Hum. Mol. Genet.* 16, 2105–2113. doi:10.1093/hmg/ddm158

Banks, G. B., Judge, L. M., Allen, J. M., and Chamberlain, J. S. (2010). The polyproline site in hinge 2 influences the functional capacity of truncated dystrophins. *PLoS Genet.* 6, e1000958. doi:10.1371/journal.pgen.1000958

Bansal, D., Miyake, K., Vogel, S. S., Groh, S., Chen, C. C., Williamson, R., et al. (2003). Defective membrane repair in dysferlin-deficient muscular dystrophy. *Nature* 423, 168–172. doi:10.1038/nature01573

Barton-Davis, E. R., Cordier, L., Shoturma, D. I., Leland, S. E., and Sweeney, H. L. (1999). Aminoglycoside antibiotics restore dystrophin function to skeletal muscles of mdx mice. *J. Clin. Investigation* 104, 375–381. doi:10.1172/JCI7866

Bassi, E., Falzarano, S., Fabris, M., Gualandi, F., Merlini, L., Vattemi, G., et al. (2012). Persistent dystrophin protein restoration 90 days after a course of intraperitoneally administered naked $2^{\prime}$ OMePS AON and ZM2 NP-AON complexes in mdx mice. *J. Biomed. Biotechnol.* 2012, 897076. doi:10.1155/2012/897076

Bates, F. S., and Fredrickson, G. H. (1990). Block copolymer thermodynamics: Theory and experiment. *Annu. Rev. Phys. Chem.* 41, 525–557. doi:10.1146/annurev.pc.41.100190.002521

Bedair, H. S., Karthikeyan, T., Quintero, A., Li, Y., and Huard, J. (2008). Angiotensin II receptor blockade administered after injury improves muscle regeneration and decreases fibrosis in normal skeletal muscle. *Am. J. Sports Med.* 36, 1548–1554. doi:10.1177/0363546508315470

Benditt, J. O., and Boitano, L. (2005). Respiratory support of individuals with Duchenne muscular dystrophy: Toward a standard of care. *Phys. Med. Rehabil. Clin. N. Am.* 16, 1125–1139. doi:10.1016/j.pmr.2005.08.017

Bengtsson, N. E., Hall, J. K., Odom, G. L., Phelps, M. P., Andrus, C. R., Hawkins, R. D., et al. (2017). Muscle-specific CRISPR/Cas9 dystrophin gene editing ameliorates pathophysiology in a mouse model for Duchenne muscular dystrophy. *Nat. Commun.* 8, 14454–14510. doi:10.1038/ncomms14454

Beringer, P., and Winter, M. E. (2011). "Aminoglycoside antibiotics," in *Basic clinical pharmacokinetics* Fifth Edition, 134–181. doi:10.1002/9783527678679.dg00403

Bhattarai, S., Li, Q., Ding, J., Liang, F., Gusev, E., Lapohos, O., et al. (2022). TLR4 is a regulator of trained immunity in a murine model of Duchenne muscular dystrophy. *Nat. Commun.* 13, 879. doi:10.1038/s41467-022-28531-1

Bidou, L., Allamand, V., Rousset, J. P., and Namy, O. (2012). Sense from nonsense: Therapies for premature stop codon diseases. *Trends Mol. Med.* 18, 679–688. doi:10.1016/j.molmed.2012.09.008

Birch, S. M., Lawlor, M. W., Conlon, T. J., Guo, L. J., Crudele, J. M., Hawkins, E. C., et al. (2023). Assessment of systemic AAV-microdystrophin gene therapy in the GRMD model of Duchenne muscular dystrophy. *Sci. Transl. Med.* 15, eabo1815. doi:10.1126/scitranslmed.abo1815

Birnkrant, D. J., Bushby, K., Bann, C. M., Apkon, S. D., Blackwell, A., Colvin, M. K., et al. (2018). Diagnosis and management of duchenne muscular dystrophy, part 3: Primary care, emergency management, psychosocial care, and transitions of care across the lifespan. *Lancet Neurol.* 17, 445–455. doi:10.1016/S1474-4422(18)30026-7

Bladen, C. L., Salgado, D., Monges, S., Foncuberta, M. E., Kekou, K., Kosma, K., et al. (2015). The TREAT-NMD DMD global database: Analysis of more than 7,000 duchenne muscular dystrophy mutations. *Hum. Mutat.* 36, 395–402. doi:10.1002/humu.22758

Boland, B. J., Silbert, P. L., Groover, R. V., Wollan, P. C., and Silverstein, M. D. (1996). Skeletal, cardiac, and smooth muscle failure in Duchenne muscular dystrophy. *Pediatr. Neurol.* 14, 7–12. doi:10.1016/0887-8994(95)00251-0

Bordeira-Carriço, R., Pêgo, A. P., Santos, M., and Oliveira, C. (2012). Cancer syndromes and therapy by stop-codon readthrough. *Trends Mol. Med.* 18, 667–678. doi:10.1016/j.molmed.2012.09.004

Boutin, S., Monteilhet, V., Veron, P., Leborgne, C., Benveniste, O., Montus, M. F., et al. (2010). Prevalence of serum IgG and neutralizing factors against adeno-associated virus (AAV) types 1, 2, 5, 6, 8, and 9 in the healthy population: Implications for gene therapy using AAV vectors. *Hum. Gene Ther.* 21, 704–712. doi:10.1089/hum.2009.182

Boyce, F. M., Beggs, A. H., Feener, C., and Kunkel, L. M. (1991). Dystrophin is transcribed in brain from a distant upstream promoter. *Proc. Natl. Acad. Sci. U. S. A.* 88, 1276–1280. doi:10.1073/pnas.88.4.1276

Brashear, S. E., Wohlgemuth, R. P., Gonzalez, G., and Smith, L. R. (2021). Passive stiffness of fibrotic skeletal muscle in mdx mice relates to collagen architecture. *J. Physiol.* 599, 943–962. doi:10.1113/JP280656

Briggs, D., and Morgan, J. E. (2013). Recent progress in satellite cell/myoblast engraftment - relevance for therapy. *FEBS J.* 280, 4281–4293. doi:10.1111/febs.12273

Briston, T., Selwood, D. L., Szabadkai, G., and Duchen, M. R. (2019). Mitochondrial permeability transition: A molecular lesion with multiple drug targets. *Trends Pharmacol. Sci.* 40, 50–70. doi:10.1016/j.tips.2018.11.004

Buddhe, S., Cripe, L., Friedland-little, J., Eghtesady, P., Finder, J., Hor, K., et al. (2019)., 142. Cardiac, S72–S81. doi:10.1542/peds.2018-0333ICardiac management of the patient with duchenne muscular dystrophy*HHS Public Access*

Büning, H., and Schmidt, M. (2015). Adeno-associated vector toxicity—To be or not to be? *Mol. Ther.* 23, 1673–1675. doi:10.1038/mt.2015.182

Burkin, D. J., and Kaufman, S. J. (1999). *The α 7 β 1 integrin in muscle development and disease*, 183–190.

Burkin, D. J., Wallace, G. Q., Milner, D. J., Chaney, E. J., Mulligan, J. A., and Kaufman, S. J. (2005). Transgenic expression of {alpha}7{beta}1 integrin maintains muscle integrity, increases regenerative capacity, promotes hypertrophy, and reduces cardiomyopathy in dystrophic mice. *Increases Regen. Capacity , Promot. Hypertrophy , Reduces Cardiomyopathy Dystrophic Mice* 166, 253–263. doi:10.1016/s0002-9440(10)62249-3

Burkin, D. J., Wallace, G. Q., Nicol, K. J., Kaufman, D. J., and Kaufman, S. J. (2001). Enhanced expression of the alpha 7 beta 1 integrin reduces muscular dystrophy and restores viability in dystrophic mice *Dystrophy Restores Viability Dystrophic Mice* 152, 1207–1218. doi:10.1083/jcb.152.6.1207

Burton, E. A., Tinsley, J. M., Holzfeind, P. J., Rodrigues, N. R., and Davies, K. E. (1999). *A second promoter provides an alternative target for therapeutic up-regulation of utrophin in Duchenne muscular dystrophy*, 96.

Burzyn, D., Kuswanto, W., Kolodin, D., Shadrach, J. L., Cerletti, M., Jang, Y., et al. (2013). A special population of regulatory T cells potentiates muscle repair. *Cell* 155, 1282–1295. doi:10.1016/j.cell.2013.10.054

Bushby, K., Finkel, R., Birnkrant, D. J., Case, L. E., Clemens, P. R., Cripe, L., et al. (2010). Diagnosis and management of duchenne muscular dystrophy, part 2: Implementation of multidisciplinary care. *Lancet Neurol.* 9, 177–189. doi:10.1016/S1474-4422(09)70272-8

Bushby, K., Muntoni, F., Urtizberea, A., Hughes, R., and Griggs, R. (2004). Report on the 124th ENMC International Workshop. Treatment of Duchenne muscular dystrophy; defining the gold standards of management in the use of corticosteroids 2-4 April 2004, Naarden, The Netherlands. *Neuromuscul. Disord.* 14, 526–534. doi:10.1016/j.nmd.2004.05.006

Cai, B., Spencer, M. J., Nakamura, G., Tseng-Ong, L., and Tidball, J. G. (2000). Eosinophilia of dystrophin-deficient muscle is promoted by perforin-mediated cytotoxicity by T cell effectors. *Am. J. Pathol.* 156, 1789–1796. doi:10.1016/S0002-9440(10)65050-X

Calcedo, R., Vandenberghe, L. H., Gao, G., Lin, J., and Wilson, J. M. (2009). Worldwide epidemiology of neutralizing antibodies to adeno-associated viruses. *J. Infect. Dis.* 199, 381–390. doi:10.1086/595830

Campbell, C., Barohn, R. J., Bertini, E., Chabrol, B., Comi, P., Darras, B. T., et al. (2020). Meta-analyses of ataluren randomized controlled trials in nonsense mutation Duchenne muscular dystrophy. *J. Comp. Eff. Res.* 9, 973–984. doi:10.2217/cer-2020-0095

Campbell, K. P., and Kahl, S. D. (1989). Association of dystrophin and an integral membrane glycoprotein. *Nature* 338, 259–262. doi:10.1038/338259a0

Castiglioni, A., Corna, G., Rigamonti, E., Basso, V., Vezzoli, M., Monno, A., et al. (2015). FOXP3+ T cells recruited to sites of sterile skeletal muscle injury regulate the fate of satellite cells and guide effective tissue regeneration. *PLoS One* 10, e0128094. doi:10.1371/journal.pone.0128094

Cerletti, M., Negri, T., Cozzi, F., Colpo, R., Andreetta, F., Croci, D., et al. (2003). Dystrophic phenotype of canine X-linked muscular dystrophy is mitigated by adenovirus-mediated utrophin gene transfer. *Gene Ther.* 10, 750–757. doi:10.1038/sj.gt.3301941

Chamberlain, J. R., and Chamberlain, J. S. (2017). Progress toward gene therapy for duchenne muscular dystrophy. *Mol. Ther.* 25, 1125–1131. doi:10.1016/j.ymthe.2017.02.019

Chance, B., Sies, H., and Boveris, A. (1979). Hydroperoxide metabolism in mammalian organs. *Physiol. Rev.* 59, 527–605. doi:10.1152/physrev.1979.59.3.527

Chemello, F., Bassel-duby, R., and Olson, E. N. (2020). *Correction of muscular dystrophies by CRISPR gene editing*, 130.

Chemello, F., Chai, A. C., Li, H., Rodriguez-Caycedo, C., Sanchez-Ortiz, E., Atmanli, A., et al. (2021). Precise correction of Duchenne muscular dystrophy exon deletion mutations by base and prime editing. *Sci. Adv.* 7, eabg4910. doi:10.1126/sciadv.abg4910

Chen, G., Wei, T., Yang, H., Li, G., and Li, H. (2022). CRISPR-based therapeutic gene editing for duchenne muscular dystrophy: Advances, challenges and perspectives. *Cells* 11, 2964. doi:10.3390/cells11192964

Choi, S., Ferrari, G., Moyle, L. A., Mackinlay, K., Naouar, N., Jalal, S., et al. (2022). Assessing and enhancing migration of human myogenic progenitors using directed iPS cell differentiation and advanced tissue modelling. *EMBO Mol. Med.* 14, e14526. doi:10.15252/emmm.202114526

Cisternas, P., Vio, C. P., and Inestrosa, N. C. (2014). Role of Wnt signaling in tissue fibrosis, lessons from skeletal muscle and kidney. *Curr. Mol. Med.* 14, 510–522. doi:10.2174/1566524014666140414210346

Clemens, P. R., Rao, V. K., Connolly, A. M., Harper, A. D., Mah, J. K., Smith, E. C., et al. (2020). Safety, tolerability, and efficacy of viltolarsen in boys with duchenne muscular dystrophy amenable to exon 53 skipping: A phase 2 randomized clinical trial. *JAMA Neurol.* 77, 982–991. doi:10.1001/jamaneurol.2020.1264

Cohn, R. D., and Campbell, K. P. (2000). Molecular basis of muscular dystrophies. *Muscle Nerve* 23, 1456–1471. doi:10.1002/1097-4598(200010)23:10<1456:AID-MUS2>3.0.CO;2-T

Cole, M. A., Rafael, J. A., Taylor, D. J., Lodi, R., Davies, K. E., and Styles, P. (2002). A quantitative study of bioenergetics in skeletal muscle lacking utrophin and dystrophin. *Neuromuscul. Disord.* 12, 247–257. doi:10.1016/s0960-8966(01)00278-4

Collins, J. M., Despa, F., and Lee, R. C. (2007). Structural and functional recovery of electropermeabilized skeletal muscle *in-vivo* after treatment with surfactant poloxamer 188. *Biochim. Biophys. Acta* 1768, 1238–1246. doi:10.1016/j.bbamem.2007.01.012

Connolly, A. M., Schierbecker, J., Renna, R., and Florence, J. (2002). High dose weekly oral prednisone improves strength in boys with Duchenne muscular dystrophy. *Neuromuscul. Disord.* 12, 917–925. doi:10.1016/S0960-8966(02)00180-3

Corrado, K., Rafael, J. A., Mills, P. L., Cole, N. M., Faulkner, J. A., Wang, K., et al. (1996). Transgenic mdx mice expressing dystrophin with a deletion in the actin-binding domain display a "'mild becker'" phenotype. *J. Cell Biol.* 134, 873–884. doi:10.1083/jcb.134.4.873

Cotton, S., Voudouris, N. J., and Greenwood, K. M. (2001). Intelligence and Duchenne muscular dystrophy: Full-scale, verbal, and performance intelligence quotients. *Dev. Med. Child. Neurol.* 43, 497–501. doi:10.1017/s0012162201000913

Crudele, J. M., and Chamberlain, J. S. (2019). AAV-based gene therapies for the muscular dystrophies. *Hum. Mol. Genet.* 28, R102–R107. doi:10.1093/hmg/ddz128

Damsker, J. M., Dillingham, B. C., Rose, M. C., Balsley, M. A., Heier, C. R., Watson, A. M., et al. (2013). VBP15, a glucocorticoid analogue, is effective at reducing allergic lung inflammation in mice. *PLoS One* 8, e63871–e63879. doi:10.1371/journal.pone.0063871

Deconinck, A. E., Rafael, J. A., Skinner, J. A., Brown, S. C., Potter, A. C., Metzinger, L., et al. (1997). Utrophin-dystrophin-deficient mice as a model for Duchenne muscular dystrophy. *Cell* 90, 717–727. doi:10.1016/S0092-8674(00)80532-2

Dellavalle, A., Sampaolesi, M., Tonlorenzi, R., Tagliafico, E., Sacchetti, B., Perani, L., et al. (2007). Pericytes of human skeletal muscle are myogenic precursors distinct from satellite cells. *Nat. Cell Biol.* 9, 255–267. doi:10.1038/ncb1542

Demina, T., Grozdova, I., Krylova, O., Zhirnov, A., Istratov, V., Frey, H., et al. (2005). Relationship between the structure of amphiphilic copolymers and their ability to disturb lipid bilayers. *Biochemistry.* 44, 4042–4054. doi:10.1021/bi048373q

Desguerre, I., Christov, C., Mayer, M., Zeller, R., Becane, H. M., Bastuji-Garin, S., et al. (2009). Clinical heterogeneity of Duchenne muscular dystrophy (DMD): Definition of sub-phenotypes and predictive criteria by long-term follow-up. *PLoS One* 4, e4347. doi:10.1371/journal.pone.0004347

Dominguez, A. A., Lim, W. A., and Qi, L. S. (2016). Beyond editing: Repurposing CRISPR-cas9 for precision genome regulation and interrogation. *Nat. Rev. Mol. Cell Biol.* 17, 5–15. doi:10.1038/nrm.2015.2

Dong, J. Y., Fan, P. D., and Frizzell, R. A. (1996). Quantitative analysis of the packaging capacity of recombinant adeno-associated virus. *Hum. Gene Ther.* 7, 2101–2112. doi:10.1089/hum.1996.7.17-2101

Doo, K. H., Ryu, H. W., Kim, S. S., Lim, B. C., Hwang, H., Kim, K. J., et al. (2012). A case of Becker muscular dystrophy with early manifestation of cardiomyopathy. *Korean J. Pediatr.* 55, 350–353. doi:10.3345/kjp.2012.55.9.350

Duan, D. (2016a). Dystrophin gene replacement and gene repair therapy for duchenne muscular dystrophy in 2016: An interview. *Hum. Gene Ther. Clin. Dev.* 27, 9–18. doi:10.1089/humc.2016.001

Duan, D., Goemans, N., Takeda, S., Mercuri, E., and Aartsma-Rus, A. (2021). Duchenne muscular dystrophy. *Nat. Rev. Dis. Prim.* 7, 13. doi:10.1038/s41572-021-00248-3

Duan, D. (2018a). Micro-dystrophin gene therapy goes systemic in duchenne muscular dystrophy patients. *Hum. Gene Ther.* 29, 733–736. doi:10.1089/hum.2018.012

Duan, D. (2018b). Systemic AAV micro-dystrophin gene therapy for duchenne muscular dystrophy. *Mol. Ther.* 26, 2337–2356. doi:10.1016/j.ymthe.2018.07.011

Duan, D. (2016b). Systemic delivery of adeno-associated viral vectors. *Curr. Opin. Virol.* 21, 16–25. doi:10.1016/j.coviro.2016.07.006

Duchene, B. L., Cherif, K., Iyombe-Engembe, J. P., Guyon, A., Rousseau, J., Ouellet, D. L., et al. (2018). CRISPR-induced deletion with SaCas9 restores dystrophin expression in dystrophic models *in vitro* and *in vivo*. *Mol. Ther.* 26, 2604–2616. doi:10.1016/j.ymthe.2018.08.010

Dupont, J. B., Tournaire, B., Georger, C., Marolleau, B., Jeanson-Leh, L., Ledevin, M., et al. (2015). Short-lived recombinant adeno-associated virus transgene expression in dystrophic muscle is associated with oxidative damage to transgene mRNA. *Mol. Therapy-Methods Clin. Dev.* 2, 15010. doi:10.1038/mtm.2015.10

Ebihara, S., Guibinga, G., Gilbert, R., Nalbantoglu, J., Massie, B., Karpati, G., et al. (2022). *Differential effects of dystrophin and utrophin gene transfer in immunocompetent muscular dystrophy (mdx) mice*, 133–144.

Echigoya, Y., Nakamura, A., Nagata, T., Urasawa, N., Lim, K. R. Q., Trieu, N., et al. (2017). Effects of systemic multiexon skipping with peptide-conjugated morpholinos in the heart of a dog model of Duchenne muscular dystrophy. *Proc. Natl. Acad. Sci. U. S. A.* 114, 4213–4218. doi:10.1073/pnas.1613203114

Emery, A. E. H. (1993). Duchenne muscular dystrophy-Meryon's disease. *Neuromuscul. Disord.* 3, 263–266. doi:10.1016/0960-8966(93)90018-F

Emery, A. E. H. (2002). "The muscular dystrophies," in *Lancet* (Elsevier Limited), 687–695. doi:10.1016/S0140-6736(02)07815-7

England, S. B., Nicholson, L. V. B., Johnson, M. A., Forrest, S. M., Love, D. R., Zubrzycka-Gaarn, E. E., et al. (1990). Very mild muscular dystrophy associated with the deletion of 46% of dystrophin. *Nature* 343, 180–182. doi:10.1038/343180a0

Erkut, E., and Yokota, T. (2022). CRISPR therapeutics for duchenne muscular dystrophy. *Int. J. Mol. Sci.* 23, 1832. doi:10.3390/ijms23031832

Ervasti, J. M., and Campbell, K. P. (1993). A role for the dystrophin-glycoprotein complex as a transmembrane linker between laminin and actin. *J. Cell Biol.* 122, 809–823. doi:10.1083/jcb.122.4.809

Ervasti, J. M., and Campbell, K. P. (1991). Membrane organization of the dystrophin-glycoprotein complex. *Cell* 66, 1121–1131. doi:10.1016/0092-8674(91)90035-W

Ervasti, J. M. (2013). "Structure and function of the dystrophin-glycoprotein complex," in *Madame curie bioscience database. [Internet]* (Landes Bioscience).

Eser, G., and Topaloğlu, H. (2022). Current outline of exon skipping trials in duchenne muscular dystrophy. *Genes (Basel)* 13, 1241. doi:10.3390/genes13071241

Evans, N. P., Misyak, S. A., Robertson, J. L., Bassaganya-Riera, J., and Grange, R. W. (2009). Dysregulated intracellular signaling and inflammatory gene expression during

initial disease onset in duchenne muscular dystrophy. *Am. J. Phys. Med. Rehabil.* 88, 502–522. doi:10.1097/PHM.0b013e3181a5a24f

Ferlini, A., Sabatelli, P., Fabris, M., Bassi, E., Falzarano, S., Vattemi, G., et al. (2010). Dystrophin restoration in skeletal, heart and skin arrector pili smooth muscle of mdx mice by ZM2 NP-AON complexes. *Gene Ther.* 17, 432–438. doi:10.1038/gt.2009.145

Flanigan, K. M. (2014). Duchenne and becker muscular dystrophies. *Neurol. Clin.* 32, 671–688. doi:10.1016/j.ncl.2014.05.002

Foster, H., Sharp, P. S., Athanasopoulos, T., Trollet, C., Graham, I. R., Foster, K., et al. (2008). Codon and mRNA sequence optimization of microdystrophin transgenes improves expression and physiological outcome in dystrophic mdx mice following AAV2/8 gene transfer. *Mol. Ther.* 16, 1825–1832. doi:10.1038/mt.2008.186

Frank, D. E., Schnell, F. J., Akana, C., and El-husayni, S. H. (2020). *Increased dystrophin production with golodirsen in patients with Duchenne muscular dystrophy*. doi:10.1212/WNL.0000000000009233

Fridovich, I. (2004). Mitochondria: Are they the seat of senescence? *Aging Cell* 3, 13–16. doi:10.1046/j.1474-9728.2003.00075.x

Gadgil, A., and Raczyńska, K. D. (2021). U7 snRNA: A tool for gene therapy. *J. Gene Med.* 23, 1–15. doi:10.1002/jgm.3321

Gailly, P., De Backer, F., Van Schoor, M., and Gillis, J. M. (2007). *In situ* measurements of calpain activity in isolated muscle fibres from normal and dystrophin-lacking mdx mice. *J. Physiology* 582, 1261–1275. doi:10.1113/jphysiol.2007.132191

Gallardo, F. S., Cordova-Casanova, A., and Brandan, E. (2021). The linkage between inflammation and fibrosis in muscular dystrophies: The axis autotaxin-lysophosphatidic acid as a new therapeutic target? *J. Cell Commun. Signal* 15, 317–334. doi:10.1007/s12079-021-00610-w

Gao, G., Vandenberghe, L. H., Alvira, M. R., Lu, Y., Calcedo, R., Zhou, X., et al. (2004). Clades of Adeno-associated viruses are widely disseminated in human tissues. *J. Virol.* 78, 6381–6388. doi:10.1128/JVI.78.12.6381-6388.2004

Gao, Q., and McNally, E. (2015). The dystrophin complex: Structure, function, and implications for therapy. *Compr. Physiol.* 5, 1223–1239. doi:10.1002/cphy.c140048

Gapinske, M., Luu, A., Winter, J., Woods, W. S., Kostan, K. A., and Shiva, N. (2018). *CRISPR-SKIP: Programmable gene splicing with single base editors*, 1–11.

Garcia-Castaneda, M., Michelucci, A., Zhao, N., Malik, S., and Dirksen, R. T. (2022). Postdevelopmental knockout of Orai1 improves muscle pathology in a mouse model of Duchenne muscular dystrophy. *J. Gen. Physiol.* 154, e202213081. doi:10.1085/jgp.202213081

Gardner, K. L., Kearney, J. A., Edwards, J. D., and Rafael-Fortney, J. A. (2006). Restoration of all dystrophin protein interactions by functional domains in trans does not rescue dystrophy. *Gene Ther.* 13, 744–751. doi:10.1038/sj.gt.3302686

Gaudelli, N. M., Komor, A. C., Rees, H. A., Packer, M. S., Badran, A. H., Bryson, D. I., et al. (2017). Programmable base editing of A ● T to G ● C in genomic DNA without DNA cleavage. *Nat. Publ. Group* 551, 464–471. doi:10.1038/nature24644

Gawlik, K. I., Oliveira, B. M., and Durbeej, M. (2011). Transgenic expression of laminin 1 chain does not prevent muscle disease in the mdx mouse model for duchenne muscular dystrophy. *AJPA* 178, 1728–1737. doi:10.1016/j.ajpath.2010.12.030

Gehlert, S., and Jacko, D. (2019). The role of the immune system in response to muscle damage. *Dtsch. Z Sportmed* 70, 242–249. doi:10.5960/dzsm.2019.390

Giordano, C., Mojumdar, K., Liang, F., Lemaire, C., Li, T., Richardson, J., et al. (2015). Toll-like receptor 4 ablation in mdx mice reveals innate immunity as a therapeutic target in Duchenne muscular dystrophy. *Hum. Mol. Genet.* 24, 2147–2162. doi:10.1093/hmg/ddu735

Glancy, B., Hartnell, L. M., Malide, D., Yu, Z. X., Combs, C. A., Connelly, P. S., et al. (2015). Mitochondrial reticulum for cellular energy distribution in muscle. *Nature* 523, 617–620. doi:10.1038/nature14614

Godin, R., Daussin, F., Matecki, S., Li, T., Petrof, B. J., and Burelle, Y. (2012). Peroxisome proliferator-activated receptor gamma coactivator1-gene alpha transfer restores mitochondrial biomass and improves mitochondrial calcium handling in post-necrotic mdx mouse skeletal muscle. *J. Physiol.* 590, 5487–5502. doi:10.1113/jphysiol.2012.240390

Goldmann, T., Overlack, N., Möller, F., Belakhov, V., van Wyk, M., Baasov, T., et al. (2012). A comparative evaluation of NB30, NB54 and PTC124 in translational read-through efficacy for treatment of an USH1C nonsense mutation. *EMBO Mol. Med.* 4, 1186–1199. doi:10.1002/emmm.201201438

Gordon, A. M., Homsher, E., and Regnier, M. (2000). Regulation of contraction in striated muscle. *Physiol. Rev.* 80, 853–924. doi:10.1152/physrev.2000.80.2.853

Goyenvalle, A., Seto, J. T., Davies, K. E., and Chamberlain, J. (2011). Therapeutic approaches to muscular dystrophy. *Hum. Mol. Genet.* 20, R69–R78. doi:10.1093/hmg/ddr105

Goyenvalle, A., Wright, J., Babbs, A., Wilkins, V., Garcia, L., and Davies, K. E. (2012). Engineering multiple U7snRNA constructs to induce single and multiexon-skipping for Duchenne muscular dystrophy. *Mol. Ther.* 20, 1212–1221. doi:10.1038/mt.2012.26

Gregorevic, P., Allen, J. M., Minami, E., Blankinship, M. J., Haraguchi, M., Inn, E., et al. (2006). rAAV6-microdystrophin preserves muscle function and extends lifespan in severely dystrophic mice. *Nat. Med.* 12, 787–789. doi:10.1038/nm1439

Gregorevic, P., Blankinship, M. J., Allen, J. M., Crawford, R. W., Meuse, L., Miller, D. G., et al. (2004). Systemic delivery of genes to striated muscles using adeno-associated viral vectors. *Nat. Med.* 10, 828–834. doi:10.1038/nm1085

Grobet, L., Pirottin, D., Poncelet, D., Royo, L. J., Christians, E., Desmecht, D., et al. (2003). Modulating skeletal muscle mass by postnatal, muscle-specific inactivation of the myostatin gene. *Muscle-Specific Inact. Myostatin Gene* 238, 227–238. doi:10.1002/gene.10188

Grounds, M. D., Terrill, J. R., Al-Mshhdani, B. A., Duong, M. N., Radley-Crabb, H. G., and Arthur, P. G. (2020). Biomarkers for Duchenne muscular dystrophy: Myonecrosis, inflammation and oxidative stress. *DMM Dis. Models Mech.* 13, dmm043638–12. doi:10.1242/DMM.043638

Guiraud, S., Aartsma-Rus, A., Vieira, N. M., Davies, K. E., Van Ommen, G. J. B., and Kunkel, L. M. (2015). The pathogenesis and therapy of muscular dystrophies. *Annu. Rev. Genomics Hum. Genet.* 16, 281–308. doi:10.1146/annurev-genom-090314-025003

Guo, C., Willem, M., Werner, A., Raivich, G., Emerson, M., Neyses, L., et al. (2006). Absence of alpha 7 integrin in dystrophin-deficient mice causes a myopathy similar to Duchenne muscular dystrophy. *Hum. Mol. Genet.* 15, 989–998. doi:10.1093/hmg/ddl018

Gurpur, P. B., Liu, J., Burkin, D. J., and Kaufman, S. J. (2009). Valproic acid activates the PI3K/Akt/mTOR pathway in muscle and ameliorates pathology in a mouse model of Duchenne muscular dystrophy. *Dystrophy* 174, 999–1008. doi:10.2353/ajpath.2009.080537

Gushchina, L. V., Frair, E. C., Rohan, N., Bradley, A. J., Simmons, T. R., Chavan, H. D., et al. (2021). Lack of toxicity in nonhuman primates receiving clinically relevant doses of an AAV9.U7snRNA vector designed to induce DMD exon 2 skipping. *Hum. Gene Ther.* 32, 882–894. doi:10.1089/hum.2020.286

Hahn, D., Kumar, R. A., Ryan, T. E., and Ferreira, L. F. (2019). Mitochondrial respiration and H2O2 emission in saponin-permeabilized murine diaphragm fibers: Optimization of fiber separation and comparison to limb muscle. *Am. J. Physiol. Cell Physiol.* 317, C665–C673. doi:10.1152/ajpcell.00184.2019

Hakim, C. H., Wasala, N. B., Pan, X., Kodippili, K., Yue, Y., Zhang, K., et al. (2017). A five-repeat micro-dystrophin gene ameliorated dystrophic phenotype in the severe DBA/2J-mdx model of duchenne muscular dystrophy. *Mol. Ther. Methods Clin. Dev.* 6, 216–230. doi:10.1016/j.omtm.2017.06.006

Hannig, J., Yu, J., Beckett, M., Weichselbaum, R., and Lee, R. C. (1999). Poloxamine 1107 sealing of radiopermeabilized erythrocyte membranes. *Int. J. Radiat. Biol.* 75, 379–385. doi:10.1080/095530099140555

Hanson, B., Wood, M. J. A., and Roberts, T. C. (2021). Molecular correction of Duchenne muscular dystrophy by splice modulation and gene editing. *RNA Biol.* 18, 1048–1062. doi:10.1080/15476286.2021.1874161

Happi Mbakam, C., Lamothe, G., Tremblay, G., and Tremblay, J. P. (2022a). CRISPR-Cas9 gene therapy for duchenne muscular dystrophy. *Neurotherapeutics* 19, 931–941. doi:10.1007/s13311-022-01197-9

Happi Mbakam, C., Rousseau, J., Tremblay, G., Yameogo, P., and Tremblay, J. P. (2022b). Prime editing permits the introduction of specific mutations in the gene responsible for duchenne muscular dystrophy. *Int. J. Mol. Sci.* 23, 6160. doi:10.3390/ijms23116160

Harper, S. Q., Hauser, M. A., DelloRusso, C., Duan, D., Crawford, R. W., Phelps, S. F., et al. (2002). Modular flexibility of dystrophin: Implications for gene therapy of duchenne muscular dystrophy. *Nat. Med.* 8, 253–261. doi:10.1038/nm0302-253

Heemskerk, H. A., de Winter, C. L., de Kimpe, S. J., van Kuik-Romeijn, P., Heuvelmans, N., Platenburg, G. J., et al. (2009). *In vivo* comparison of 2'-O-methyl phosphorothioate and morpholino antisense oligonucleotides for Duchenne muscular dystrophy exon skipping. *J. Gene Med.* 11, 257–266. doi:10.1002/jgm.1288

Heemskerk, H., de Winter, C., van Kuik, P., Heuvelmans, N., Sabatelli, P., Rimessi, P., et al. (2010). Preclinical PK and PD studies on 2'-O-methyl-phosphorothioate RNA antisense oligonucleotides in the mdx mouse model. *Mol. Ther.* 18, 1210–1217. doi:10.1038/mt.2010.72

Heier, C. R., Damsker, J. M., Yu, Q., Dillingham, B. C., Huynh, T., Van der Meulen, J. H., et al. (2013). VBP15, a novel anti-inflammatory and membrane-stabilizer, improves muscular dystrophy without side effects. *EMBO Mol. Med.* 5, 1569–1585. doi:10.1002/emmm.201302621

Heier, C. R., Yu, Q., Fiorillo, A. A., Tully, C. B., Tucker, A., Mazala, D. A., et al. (2019). Vamorolone targets dual nuclear receptors to treat inflammation and dystrophic cardiomyopathy. *Life Sci. Alliance* 2, e201800186. doi:10.26508/LSA.201800186

Heller, K. N., Montgomery, C. L., Janssen, P. M., Clark, K. R., Mendell, J. R., and Rodino-Klapac, L. R. (2013). AAV-mediated overexpression of human α7 integrin leads to histological and functional improvement in dystrophic mice. *Mol. Ther.* 21, 520–525. doi:10.1038/mt.2012.281

Hendriksen, J. G. M., and Vles, J. S. H. (2006). Are males with duchenne muscular dystrophy at risk for reading disabilities? *Pediatr. Neurol.* 34, 296–300. doi:10.1016/j.pediatrneurol.2005.08.029

Hendriksen, J. G. M., and Vles, J. S. H. (2008). Neuropsychiatric disorders in males with duchenne muscular dystrophy: Frequency rate of attention-deficit hyperactivity disorder (ADHD), autism spectrum disorder, and obsessive-compulsive disorder. *J. Child. Neurol.* 23, 477–481. doi:10.1177/0883073807309775

Henriques-Pons, A., Yu, Q., Rayavarapu, S., Cohen, T. v., Ampong, B., Cha, H. J., et al. (2014). Role of toll-like receptors in the pathogenesis of dystrophin-deficient skeletal and heart muscle. *Hum. Mol. Genet.* 23, 2604–2617. doi:10.1093/hmg/ddt656

Hodges, B. L., Hayashi, Y. K., Nonaka, I., Wang, W., Arahata, K., and Kaufman, S. J. (1997). Altered expression of the alpha7beta1 integrin in human and murine muscular dystrophies. *J. Cell Sci.* 2881, 2873–2881. doi:10.1242/jcs.110.22.2873

Hoffman, E. P., Bronson, A., Levin, A. A., Takeda, S., Yokota, T., Baudy, A. R., et al. (2011). Restoring dystrophin expression in duchenne muscular dystrophy muscle progress in exon skipping and stop codon read through. *Am. J. Pathology* 179, 12–22. doi:10.1016/j.ajpath.2011.03.050

Hoffman, E. P., Brown, R. H., and Kunkel, L. M. (1987). Dystrophin: The protein product of the duchenne muscular dystrophy locus. *Cell* 51, 919–928. doi:10.1016/0092-8674(87)90579-4

Hogrel, J.-Y., Zagnoli, F., Canal, A., Fraysse, B., Bouchard, J.-P., Skuk, D., et al. (2013). Assessment of a symptomatic Duchenne muscular dystrophy carrier 20years after myoblast transplantation from her asymptomatic identical twin sister. *Neuromuscul. Disord.* 23, 575–579. doi:10.1016/j.nmd.2013.04.007

Hopf, F. W., Turner, P. R., Denetclaw, W. F., Reddy, P., and Steinhardt, R. A. (1996). A critical evaluation of resting intracellular free calcium regulation in dystrophic mdx muscle. *Am. J. Physiol. - Cell Physiol.* 271, C1325–C1339. doi:10.1152/ajpcell.1996.271.4.c1325

Houang, E. M., Haman, K. J., Filareto, A., Perlingeiro, R. C., Bates, F. S., Lowe, D. A., et al. (2015). Membrane-stabilizing copolymers confer marked protection to dystrophic skeletal muscle *in vivo*. *Mol. Ther. Methods Clin. Dev.* 2, 15042. doi:10.1038/mtm.2015.42

Houang, E. M., Haman, K. J., Kim, M., Zhang, W., Lowe, D. A., Sham, Y. Y., et al. (2017). Chemical end group modified diblock copolymers elucidate anchor and chain mechanism of membrane stabilization. *Mol. Pharm.* 14, 2333–2339. doi:10.1021/acs.molpharmaceut.7b00197

Houang, E. M., Sham, Y. Y., Bates, F. S., and Metzger, J. M. (2018). Muscle membrane integrity in duchenne muscular dystrophy: Recent advances in copolymer-based muscle membrane stabilizers. *Skelet. Muscle* 8, 31. doi:10.1186/s13395-018-0177-7

Huang, T. P., Newby, G. A., and Liu, D. R. (2021). Precision genome editing using cytosine and adenine base editors in mammalian cells. *Nat. Protoc.* 16, 1089–1128. doi:10.1038/s41596-020-00450-9

Hughes, M. C., Ramos, S. V., Turnbull, P. C., Edgett, B. A., Huber, J. S., Polidovitch, N., et al. (2020). Impairments in left ventricular mitochondrial bioenergetics precede overt cardiac dysfunction and remodelling in Duchenne muscular dystrophy. *J. Physiol.* 598, 1377–1392. doi:10.1113/JP277306

Hughes, M. C., Ramos, S. V., Turnbull, P. C., Rebalka, I. A., Cao, A., Monaco, C. M. F., et al. (2019). Early myopathy in Duchenne muscular dystrophy is associated with elevated mitochondrial H2 O2 emission during impaired oxidative phosphorylation. *J. Cachexia Sarcopenia Muscle* 10, 643–661. doi:10.1002/jcsm.12405

Hunter, R. L., Luo, A. Z., Zhang, R., Kozar, R. A., and Moore, F. A. (2010). Poloxamer 188 inhibition of ischemia/reperfusion injury: Evidence for a novel anti-adhesive mechanism. *Ann. Clin. Lab. Sci.* 40, 115–125.

Hurst, S., Hoek, J., and Sheu, S. S. (2017). Mitochondrial Ca2+ and regulation of the permeability transition pore. *J. Bioenerg. Biomembr.* 49, 27–47. doi:10.1007/s10863-016-9672-x

Hynes, R. (1992). Integrins: Versatility, modulation, and signaling in cell adhesion. *Cell* 69 (1), 11–25. doi:10.1016/0092-8674(92)90115-s

Ishikawa-Sakurai, M., Yoshida, M., Imamura, M., Davies, K. E., and Ozawa, E. (2004). ZZ domain is essentially required for the physiological binding of dystrophin and utrophin to β-dystroglycan. *Hum. Mol. Genet.* 13, 693–702. doi:10.1093/hmg/ddh087

Iyombe-Engembe, J.-P., Ouellet, D. L., Barbeau, X., Rousseau, J., Chapdelaine, P., Lagüe, P., et al. (2016). Efficient restoration of the dystrophin gene reading frame and protein structure in DMD myoblasts using the CinDel method. *Mol. Therapy-Nucleic Acids* 5, e283. doi:10.1038/mtna.2015.58

Jearawiriyapaisarn, N., Moulton, H. M., Buckley, B., Roberts, J., Sazani, P., Fucharoen, S., et al. (2008). Sustained dystrophin expression induced by peptide-conjugated morpholino oligomers in the muscles of mdx mice. *Mol. Ther.* 16, 1624–1629. doi:10.1038/mt.2008.120

Jearawiriyapaisarn, N., Moulton, H. M., Sazani, P., Kole, R., and Willis, M. S. (2010). Long-term improvement in mdx cardiomyopathy after therapy with peptide-conjugated morpholino oligomers. *Cardiovasc Res.* 85, 444–453. doi:10.1093/cvr/cvp335

Jinek, M., Chylinski, K., Fonfara, I., Hauer, M., Doudna, J. A., and Charpentier, E. (2012). A programmable dual-RNA-guided DNA endonuclease in adaptive bacterial immunity. *Science* 337, 816–821. doi:10.1126/science.1225829

Jørgensen, L. H., Larochelle, N., Orlopp, K., Dunant, P., Dudley, R. W. R., Stucka, R., et al. (2009). Efficient and fast functional screening of microdystrophin constructs *in vivo* and *in vitro* for therapy of duchenne muscular dystrophy. *Hum. Gene Ther.* 20, 641–650. doi:10.1089/hum.2008.162

Jung, C., Martins, A. S., Niggli, E., and Shirokova, N. (2008). Dystrophic cardiomyopathy: Amplification of cellular damage by Ca2+ signalling and reactive oxygen species-generating pathways. *Cardiovasc Res.* 77, 766–773. doi:10.1093/cvr/cvm089

Jung, D., Yang, B., Meyer, J., Chamberlain, J. S., and Campbell, K. P. (1995). Identification and characterization of the dystrophin anchoring site on beta-dystroglycan. *J. Biol. Chem.* 270, 27305–27310. doi:10.1074/jbc.270.45.27305

Jungbluth, H., Treves, S., Zorzato, F., Sarkozy, A., Ochala, J., Sewry, C., et al. (2018). Congenital myopathies: Disorders of excitation-contraction coupling and muscle contraction. *Nat. Rev. Neurol.* 14, 151–167. doi:10.1038/nrneurol.2017.191

Kamdar, F., and Garry, D. J. (2016). Dystrophin-deficient cardiomyopathy. *J. Am. Coll. Cardiol.* 67, 2533–2546. doi:10.1016/j.jacc.2016.02.081

Kang, C., Badr, M. A., Kyrychenko, V., Eskelinen, E. L., and Shirokova, N. (2018). Deficit in PINK1/PARKIN-mediated mitochondrial autophagy at late stages of dystrophic cardiomyopathy. *Cardiovasc Res.* 114, 90–102. doi:10.1093/cvr/cvx201

Kawecka, K., Theodoulides, M., Hasoglu, Y., Jarmin, S., Kymalainen, H., Le-Heron, A., et al. (2015). Adeno-associated virus (AAV) mediated dystrophin gene transfer studies and exon skipping strategies for duchenne muscular dystrophy (DMD). *Curr. Gene Ther.* 15, 395–415. doi:10.2174/1566523215666150710123830

Kerem, E., Konstan, M. W., De Boeck, K., Accurso, F. J., Sermet-Gaudelus, I., Wilschanski, M., et al. (2014). Ataluren for the treatment of nonsense-mutation cystic fibrosis: A randomised, double-blind, placebo-controlled phase 3 trial. *Lancet Respir. Med.* 2, 539–547. doi:10.1016/S2213-2600(14)70100-6

Kessler, P. D., Podsakoff, G. M., Chen, X., McQuiston, S. A., Colosi, P. C., Matelis, L. A., et al. (1996). Gene delivery to skeletal muscle results in sustained expression and systemic delivery of a therapeutic protein. *Proc. Natl. Acad. Sci. U. S. A.* 93, 14082–14087. doi:10.1073/pnas.93.24.14082

Khairallah, R. J., Shi, G., Sbrana, F., Prosser, B. L., Borroto, C., Mazaitis, M. J., et al. (2012). Microtubules underlie dysfunction in duchenne muscular dystrophy. *Sci. Signal* 5, ra56. doi:10.1126/scisignal.2002829

Kharraz, Y., Guerra, J., Pessina, P., Serrano, A. L., and Munoz-Canoves, P. (2014). Understanding the process of fibrosis in Duchenne muscular dystrophy. *Biomed. Res. Int.* 2014, 965631. doi:10.1155/2014/965631

Kim, J. H., Kwak, H. B., Thompson, L. V., and Lawler, J. M. (2013). Contribution of oxidative stress to pathology in diaphragm and limb muscles with Duchenne muscular dystrophy. *J. Muscle Res. Cell Motil.* 34, 1–13. doi:10.1007/s10974-012-9330-9

Kim, M., Haman, K. J., Houang, E. M., Zhang, W., Yannopoulos, D., Metzger, J. M., et al. (2017). PEO-PPO diblock copolymers protect myoblasts from hypo-osmotic stress *in vitro* dependent on copolymer size, composition, and architecture. *Biomacromolecules* 18, 2090–2101. doi:10.1021/acs.biomac.7b00419

Kim, M. J., Bible, K. L., Regnier, M., Adams, M. E., Froehner, S. C., and Whitehead, N. P. (2019). Simvastatin provides long-term improvement of left ventricular function and prevents cardiac fibrosis in muscular dystrophy. *Physiol. Rep.* 7, e14018. doi:10.14814/phy2.14018

Kim, S., Kim, D., Cho, S. W., Kim, J., and Kim, J. S. (2014). Highly efficient RNA-guided genome editing in human cells via delivery of purified Cas9 ribonucleoproteins. *Genome Res.* 24, 1012–1019. doi:10.1101/gr.171322.113

Kim, T. -W., Wu, K., and Black, I. B. (1995). Deficiency of brain synaptic dystrophin in human duchenne muscular dystrophy. *Ann. Neurol.* 38, 446–449. doi:10.1002/ana.410380315

Klingler, W., Jurkat-Rott, K., Lehmann-Horn, F., and Schleip, R. (2012). The role of fibrosis in Duchenne muscular dystrophy. *Acta Myol.* 31, 184–195.

Knott, G. J., and Doudna, J. A. (2018). CRISPR-Cas guides the future of genetic engineering. *Science* 361, 866–869. doi:10.1126/science.aat5011

Koenig, M., and Kunkel, L. M. (1990). Detailed analysis of the repeat domain of dystrophin reveals four potential hinge segments that may confer flexibility. *J. Biol. Chem.* 265, 4560–4566. doi:10.1016/s0021-9258(19)39599-7

Koenig, M., Monaco, A. P., and Kunkel, L. M. (1988). The complete sequence of dystrophin predicts a rod-shaped cytoskeletal protein. *Cell* 53, 219–228. doi:10.1016/0092-8674(88)90383-2

Komaki, H., Takeshima, Y., Matsumura, T., Ozasa, S., Funato, M., Takeshita, E., et al. (2020). Viltolarsen in Japanese duchenne muscular dystrophy patients: A phase 1/2 study. *Ann. Clin. Transl. Neurol.* 7, 2393–2408. doi:10.1002/acn3.51235

Komor, A. C., Kim, Y. B., Packer, M. S., Zuris, J. A., and Liu, D. R. (2016). Programmable editing of a target base in genomic DNA without double-stranded DNA cleavage. *Nature* 533, 420–424. doi:10.1038/nature17946

Koo, T., Malerba, A., Athanasopoulos, T., Trollet, C., Boldrin, L., Ferry, A., et al. (2011). Delivery of AAV2/9-microdystrophin genes incorporating helix 1 of the coiled-coil motif in the C-terminal domain of dystrophin improves muscle pathology and restores the level of α1-syntrophin and α-dystrobrevin in skeletal muscles of mdx mice. *Hum. Gene Ther.* 22, 1379–1388. doi:10.1089/hum.2011.020

Kotterman, M. A., and Schaffer, D. V. (2014). Engineering adeno-associated viruses for clinical gene therapy. *Nat. Rev. Genet.* 15, 445–451. doi:10.1038/nrg3742

Krag, T. O. B., Bogdanovich, S., Jensen, C. J., Fischer, M. D., Hansen-schwartz, J., Javazon, E. H., et al. (2004). Heregulin ameliorates the dystrophic phenotype in mdx mice. *Proc. Natl. Acad. Sci. U. S. A.* 101, 13856–13860. doi:10.1073/pnas.0405972101

Kuzmin, D. A., Shutova, M. V., Johnston, N. R., Smith, O. P., Johnstone, E. C., Kukushkin, Y. S., et al. (2021). The clinical landscape for AAV gene therapies. *Nat. Rev. Drug Discov.* 20, 173–174. doi:10.1038/d41573-021-00017-7

Kyrychenko, V., Kyrychenko, S., Tiburcy, M., Shelton, J. M., Long, C., Schneider, J. W., et al. (2017). Functional correction of dystrophin actin binding domain mutations by genome editing. *JCI Insight* 2, e95918. doi:10.1172/jci.insight.95918

Kyrychenko, V., Poláková, E., Janíček, R., and Shirokova, N. (2015). Mitochondrial dysfunctions during progression of dystrophic cardiomyopathy. *Cell Calcium* 58, 186–195. doi:10.1016/j.ceca.2015.04.006

Lacourpaille, L., Gross, R., Hug, F., Guevel, A., Pereon, Y., Magot, A., et al. (2017). Effects of duchenne muscular dystrophy on muscle stiffness and response to electrically-induced muscle contraction: A 12-month follow-up. *Neuromuscul. Disord.* 27, 214–220. doi:10.1016/j.nmd.2017.01.001

Lacourpaille, L., Hug, F., Guevel, A., Pereon, Y., Magot, A., Hogrel, J. Y., et al. (2015). Non-invasive assessment of muscle stiffness in patients with Duchenne muscular dystrophy. *Muscle Nerve* 51, 284–286. doi:10.1002/mus.24445

Lai, Y., Thomas, G. D., Yue, Y., Yang, H. T., Li, D., Long, C., et al. (2009). Dystrophins carrying spectrin-like repeats 16 and 17 anchor nNOS to the sarcolemma and enhance exercise performance in a mouse model of muscular dystrophy. *J. Clin. Invest.* 119, 624–635. doi:10.1172/JCI36612

Lau, C.-H., and Suh, Y. (2017). *In vivo* genome editing in animals using AAV-CRISPR system: Applications to translational research of human disease. *F1000Res* 6, 2153. doi:10.12688/f1000research.11243.1

Le Guiner, C., Servais, L., Montus, M., Larcher, T., Fraysse, B., Moullec, S., et al. (2017). Long-term microdystrophin gene therapy is effective in a canine model of Duchenne muscular dystrophy. *Nat. Commun.* 8, 16105–16115. doi:10.1038/ncomms16105

Lee, K., Conboy, M., Park, H. M., Jiang, F., Kim, H. J., Dewitt, M. A., et al. (2017). Nanoparticle delivery of Cas9 ribonucleoprotein and donor DNA *in vivo* induces homology-directed DNA repair. *Nat. Biomed. Eng.* 1, 889–901. doi:10.1038/s41551-017-0137-2

Lee, R. C., Hannig, J., Matthews, K. L., Myerov, A., and Chen, C. T. (1999). Pharmaceutical therapies for sealing of permeabilized cell membranes in electrical injuries. *Ann. N. Y. Acad. Sci.* 888, 266–273. doi:10.1111/j.1749-6632.1999.tb07961.x

Lee, R. C., River, L. P., Pan, F. S., Ji, L., and Wollmann, R. L. (1992). Surfactant-induced sealing of electropermeabilized skeletal muscle membranes *in vivo*. *Proc. Natl. Acad. Sci. U. S. A.* 89, 4524–4528. doi:10.1073/pnas.89.10.4524

Lee, S. J. (2004). Regulation of muscle mass by myostatin. *Annu. Rev. Cell Dev. Biol.* 20, 61–86. doi:10.1146/annurev.cellbio.20.012103.135836

Lee, T. H., Eun, L. Y., Choi, J. Y., Kwon, H. E., Lee, Y. M., Kim, H. D., et al. (2014). Myocardial atrophy in children with mitochondrial disease and Duchenne muscular dystrophy. *Korean J. Pediatr.* 57, 232–239. doi:10.3345/kjp.2014.57.5.232

Levi, O., Genin, O., Angelini, C., Halevy, O., and Pines, M. (2015). Inhibition of muscle fibrosis results in increases in both utrophin levels and the number of revertant myofibers in Duchenne muscular dystrophy. *Oncotarget* 6, 23249–23260. doi:10.18632/oncotarget.4021

Li, H. L., Fujimoto, N., Sasakawa, N., Shirai, S., Ohkame, T., Sakuma, T., et al. (2015). Precise correction of the dystrophin gene in duchenne muscular dystrophy patient induced pluripotent stem cells by TALEN and CRISPR-Cas9. *Stem Cell Rep.* 4, 143–154. doi:10.1016/j.stemcr.2014.10.013

Li, J., Cao, J., Li, M., Yu, Y., Yang, Y., Xiao, X., et al. (2011). Collagen triple helix repeat containing-1 inhibits transforming growth factor-b1-induced collagen type I expression in keloid. *Br. J. Dermatol* 164, 1030–1036. doi:10.1111/j.1365-2133.2011.10215.x

Li, Z. B., Kollias, H. D., and Wagner, K. R. (2008). Myostatin directly regulates skeletal muscle fibrosis. *J. Biol. Chem.* 283, 19371–19378. doi:10.1074/jbc.M802585200

Lieber, R. L., and Ward, S. R. (2013). Cellular mechanisms of tissue fibrosis. 4. Structural and functional consequences of skeletal muscle fibrosis. *Am. J. Physiol. Cell Physiol.* 305, C241–C252. doi:10.1152/ajpcell.00173.2013

Long, C., Amoasii, L., Mireault, A. A., McAnally, J. R., Li, H., Sanchez-Ortiz, E., et al. (2016). Postnatal genome editing partially restores dystrophin expression in a mouse model of muscular dystrophy. *Science* 351, 400–403. doi:10.1126/science.aad5725

Long, C., Li, H., Tiburcy, M., Rodriguez-Caycedo, C., Kyrychenko, V., Zhou, H., et al. (2018). Correction of diverse muscular dystrophy mutations in human engineered heart muscle by single-site genome editing. *Sci. Adv.* 4, eaap9004. doi:10.1126/sciadv.aap9004

Long, C., McAnally, J. R., Shelton, J. M., Mireault, A. A., Bassel-Duby, R., and Olson, E. N. (2014). Prevention of muscular dystrophy in mice by CRISPR/Cas9-mediated editing of germline DNA. *Science* 345, 1184–1188. doi:10.1126/science.1254445

Lostal, W., Kodippili, K., Yue, Y., and Duan, D. (2014). Full-length dystrophin reconstitution with adeno-associated viral vectors. *Hum. Gene Ther.* 25, 552–562. doi:10.1089/hum.2013.210

Love, D. R., Hillt, D. F., Dicksont, G., Spurr, N. K., Byth, B. C., Marsden, R. F., et al. (1989). An autosomal transcript in skeletal muscle with homology to dystrophin. *Nature* 339, 55–58. doi:10.1038/339055a0

Lozanoska-Ochser, B., Benedetti, A., Rizzo, G., Marrocco, V., di Maggio, R., Fiore, P., et al. (2018). Targeting early PKCθ-dependent T-cell infiltration of dystrophic muscle reduces disease severity in a mouse model of muscular dystrophy. *J. Pathol.* 244, 323–333. doi:10.1002/path.5016

Lu, Q. L., Mann, C. J., Lou, F., Bou-Gharios, G., Morris, G. E., Xue, S. A., et al. (2003). Functional amounts of dystrophin produced by skipping the mutated exon in the mdx dystrophic mouse. *Nat. Med.* 9, 1009–1014. doi:10.1038/nm897

Ma, N., Chen, D., Lee, J. H., Kuri, P., Hernandez, E. B., Kocan, J., et al. (2022). Piezo1 regulates the regenerative capacity of skeletal muscles via orchestration of stem cell morphological states. *Sci. Adv.* 8, eabn0485. doi:10.1126/sciadv.abn0485

Maffioletti, S. M., Noviello, M., English, K., and Tedesco, F. S. (2014). Stem cell transplantation for muscular dystrophy: The challenge of immune response. *Biomed. Res. Int.* 2014, 964010–964012. doi:10.1155/2014/964010

Maggio, I., Liu, J., Janssen, J. M., Chen, X., and Goncalves, M. A. (2016a). Adenoviral vectors encoding CRISPR/Cas9 multiplexes rescue dystrophin synthesis in unselected populations of DMD muscle cells. *Sci. Rep.* 6, 37051. doi:10.1038/srep37051

Maggio, I., Stefanucci, L., Janssen, J. M., Liu, J., Chen, X., Mouly, V., et al. (2016b). Selection-free gene repair after adenoviral vector transduction of designer nucleases: Rescue of dystrophin synthesis in DMD muscle cell populations. *Nucleic Acids Res.* 44, 1449–1470. doi:10.1093/nar/gkv1540

Maino, E., Wojtal, D., Evagelou, S. L., Farheen, A., Wong, T. W. Y., Lindsay, K., et al. (2021). Targeted genome editing *in vivo* corrects a Dmd duplication restoring wild-type dystrophin expression. *EMBO Mol. Med.* 13, e13228. doi:10.15252/emmm.202013228

Makarova, K. S., Wolf, Y. I., Iranzo, J., Shmakov, S. A., Alkhnbashi, O. S., Brouns, S. J. J., et al. (2020). Evolutionary classification of CRISPR-cas systems: A burst of class 2 and derived variants. *Nat. Rev. Microbiol.* 18, 67–83. doi:10.1038/s41579-019-0299-x

Malerba, A., Boldrin, L., and Dickson, G. (2011). Long-term systemic administration of unconjugated morpholino oligomers for therapeutic expression of dystrophin by exon skipping in skeletal muscle: Implications for cardiac muscle integrity. *Nucleic Acid. Ther.* 21, 293–298. doi:10.1089/nat.2011.0306

Mali, P., Yang, L., Esvelt, K. M., Aach, J., Guell, M., DiCarlo, J. E., et al. (2013). RNA-guided human genome engineering via Cas9. *Science* 339, 823–826. doi:10.1126/science.1232033

Malik, V., Rodino-Klapac, L. R., Viollet, L., Wall, C., King, W., Al-Dahhak, R., et al. (2010). Gentamicin-induced readthrough of stop codons in Duchenne muscular dystrophy. *Ann. Neurol.* 67, 771–780. doi:10.1002/ana.22024

Mamchaoui, K. (2018). Myoblots: Dystrophin quantification by in-cell Western assay for a streamlined development of duchenne muscular dystrophy (DMD) treatments. *Neuropathol. Appl. Neurobiol.* 44, 463–473. doi:10.1111/nan.12448

Mann, C. J., Honeyman, K., Cheng, A. J., Ly, T., Lloyd, F., Fletcher, S., et al. (2001). Antisense-induced exon skipping and synthesis of dystrophin in the mdx mouse. *Proc. Natl. Acad. Sci. U. S. A.* 98, 42–47. doi:10.1073/pnas.011408598

Mareedu, S., Million, E. D., Duan, D., and Babu, G. J. (2021). Abnormal calcium handling in duchenne muscular dystrophy: Mechanisms and potential therapies. *Front. Physiol.* 12, 647010–647019. doi:10.3389/fphys.2021.647010

Markham, B. E., Kernodle, S., Nemzek, J., Wilkinson, J. E., and Sigler, R. (2015). Chronic dosing with membrane sealant poloxamer 188 NF improves respiratory dysfunction in dystrophic mdx and mdx/utrophin-/- mice. *PLoS One* 10, e0134832. doi:10.1371/journal.pone.0134832

Mata López, S., Balog-Alvarez, C., Vitha, S., Bettis, A. K., Canessa, E. H., Kornegay, J. N., et al. (2020). Challenges associated with homologous directed repair using CRISPR-Cas9 and TALEN to edit the DMD genetic mutation in canine Duchenne muscular dystrophy. *PLoS One* 15, e0228072. doi:10.1371/journal.pone.0228072

Matre, P. R., Mu, X., Wu, J., Danila, D., Hall, M. A., Kolonin, M. G., et al. (2019). CRISPR/Cas9-Based dystrophin restoration reveals a novel role for dystrophin in bioenergetics and stress resistance of muscle progenitors. *Stem Cells* 37, 1615–1628. doi:10.1002/stem.3094

Mauro, A. (1961). Satellite cell of skeletal muscle fibers. *J. Biophys. Biochem. Cytol.* 9, 493–495. doi:10.1083/jcb.9.2.493

Mayer, U., Saher, G., Fassler, R., Bornemann, A., Echtermeyer, F., Mark, H. V. D., et al. (1997). Absence of integrin alpha 7 causes a novel form of muscular dystrophy. *Nat. Genet.* 17 (3), 318–323. doi:10.1038/ng1197-318

Mázala, D. A. G., Novak, J. S., Hogarth, M. W., Nearing, M., Adusumalli, P., Tully, C. B., et al. (2020). TGF-β–driven muscle degeneration and failed regeneration underlie disease onset in a DMD mouse model. *JCI Insight* 5, e135703. doi:10.1172/jci.insight.135703

McCourt, J. L., Rhett, K. K., Jaeger, M. A., Belanto, J. J., Talsness, D. M., and Ervasti, J. M. (2015). *In vitro* stability of therapeutically relevant, internally truncated dystrophins. *Skelet. Muscle* 5, 13. doi:10.1186/s13395-015-0040-z

McDonald, C. M., Henricson, E. K., Abresch, R. T., Duong, T., Joyce, N. C., Hu, F., et al. (2018). Long-term effects of glucocorticoids on function, quality of life, and survival in patients with duchenne muscular dystrophy: A prospective cohort study. *Lancet* 391, 451–461. doi:10.1016/S0140-6736(17)32160-8

McDonald, C. M., Marbán, E., Hendrix, S., Hogan, N., Ruckdeschel Smith, R., Eagle, M., et al. (2022). Repeated intravenous cardiosphere-derived cell therapy in late-stage duchenne muscular dystrophy (HOPE-2): A multicentre, randomised, double-blind, placebo-controlled, phase 2 trial. *Lancet* 399, 1049–1058. doi:10.1016/S0140-6736(22)00012-5

McDonald, C. M., Sajeev, G., Yao, Z., McDonnell, E., Elfring, G., Souza, M., et al. (2020). Deflazacort vs prednisone treatment for duchenne muscular dystrophy: A meta-analysis of disease progression rates in recent multicenter clinical trials. *Muscle Nerve* 61, 26–35. doi:10.1002/mus.26736

McDonald, D. G. M., Kinali, M., Gallagher, A. C., Mercuri, E., Muntoni, F., Frcpch, H. R., et al. (2002). Fracture prevalence in Duchenne muscular dystrophy. *Dev. Med. Child. Neurol.* 44, 695–698. doi:10.1017/s0012162201002778

McElroy, S. P., Nomura, T., Torrie, L. S., Warbrick, E., Gartner, U., Wood, G., et al. (2013). A lack of premature termination codon read-through efficacy of PTC124 (ataluren) in a diverse array of reporter assays. *PLoS Biol.* 11, e1001593. doi:10.1371/journal.pbio.1001593

Mcmahon, C. D., Popovic, L., Oldham, J. M., Jeanplong, F., Smith, H. K., Kambadur, R., et al. (2022). *Myostatin-deficient mice lose more skeletal muscle mass than wild-type controls during hindlimb suspension*, 82–87.

McNally, E. M., and Pytel, P. (2007). Muscle diseases: The muscular dystrophies. *Annu. Rev. Pathol.* 2, 87–109. doi:10.1146/annurev.pathol.2.010506.091936

McNally, E. M., and Wyatt, E. J. (2017). Mutation-based therapy for duchenne muscular dystrophy: Antisense treatment arrives in the clinic. *Circulation* 136, 979–981. doi:10.1161/CIRCULATIONAHA.117.028382

McNally, E. (2012). *Novel targets and approaches to treating skeletal muscle disease*. First Edit. Elsevier Inc. doi:10.1016/B978-0-12-381510-1.00081-8

Mcpherron, A. C., Lawlert, A. M., and Lee, S. (1997). Regulation of skeletal muscle mass in mice by a new TGF-beta superfamily member. *Nature* 38711, 83–90. doi:10.1038/387083a0

Mead, A. F., Petrov, M., Malik, A. S., Mitchell, M. A., Childers, M. K., Bogan, J. R., et al. (2014). Diaphragm remodeling and compensatory respiratory mechanics in a canine model of Duchenne muscular dystrophy. *J. Appl. Physiol.* 116, 807–815. doi:10.1152/japplphysiol.00833.2013

Mendell, J. R., Al-zaidy, S. A., Rodino-klapac, L. R., Goodspeed, K., Gray, S. J., Kay, C. N., et al. (2021). Current clinical applications of *in vivo* gene therapy with AAVs. *Mol. Ther.* 29, 464–488. doi:10.1016/j.ymthe.2020.12.007

Mendell, J. R., Al-Zaidy, S., Shell, R., Arnold, W. D., Rodino-Klapac, L. R., Prior, T. W., et al. (2017). Single-dose gene-replacement therapy for spinal muscular atrophy. *N. Engl. J. Med.* 377, 1713–1722. doi:10.1056/nejmoa1706198

Mendell, J. R., Campbell, K., Rodino-Klapac, L., Sahenk, Z., Shilling, C., Lewis, S., et al. (2010). Dystrophin immunity in duchenne's muscular dystrophy. *N. Engl. J. Med.* 363, 1429–1437. doi:10.1056/nejmoa1000228

Mendell, J. R., Goemans, N., Lowes, L. P., Alfano, L. N., Berry, K., Shao, J., et al. (2016). *Longitudinal effect of eteplirsen versus historical control on ambulation in Duchenne muscular dystrophy*. doi:10.1002/ana.24555

Mendell, J. R., Sahenk, Z., Lehman, K., Nease, C., Lowes, L. P., Miller, N. F., et al. (2020). Assessment of systemic delivery of rAAVrh74.MHCK7.micro-dystrophin in children with duchenne muscular dystrophy: A nonrandomized controlled trial. *JAMA Neurol.* 77, 1122–1131. doi:10.1001/jamaneurol.2020.1484

Mendell, J. R., Shilling, C., Leslie, N. D., Flanigan, K. M., Al-Dahhak, R., Gastier-Foster, J., et al. (2012). Evidence-based path to newborn screening for duchenne muscular dystrophy. *Ann. Neurol.* 71, 304–313. doi:10.1002/ana.23528

Meng, X. M., Nikolic-Paterson, D. J., and Lan, H. Y. (2016). TGF-B: The master regulator of fibrosis. *Nat. Rev. Nephrol.* 12, 325–338. doi:10.1038/nrneph.2016.48

Merchant, F. A., Holmes, W. H., Capelli-Schellpfeffer, M., Lee, R. C., and Toner, M. (1998). Poloxamer 188 enhances functional recovery of lethally heat-shocked fibroblasts. *J. Surg. Res.* 74, 131–140. doi:10.1006/jsre.1997.5252

Mercuri, E., Bönnemann, C. G., and Muntoni, F. (2019). Muscular dystrophies. *Lancet* 394, 2025–2038. doi:10.1016/S0140-6736(19)32910-1

Mercuri, E., and Muntoni, F. (2013). Muscular dystrophies. *Lancet* 381, 845–860. doi:10.1016/S0140-6736(12)61897-2

Meyer, G. A., and Lieber, R. L. (2011). Elucidation of extracellular matrix mechanics from muscle fibers and fiber bundles. *J. Biomech.* 44, 771–773. doi:10.1016/j.jbiomech.2010.10.044

Meyers, T. A., and Townsend, D. W. (2019). Cardiac pathophysiology and the future of cardiac therapies in duchenne muscular dystrophy. *Int. J. Mol. Sci.* 20, 4098. doi:10.3390/ijms20174098

Michel, R. N., Chakkalakal, J. V., Miura, P., Be, G., and Jasmin, B. J. (2008). Modulation of utrophin A mRNA stability in fast versus slow muscles via an AU-rich element and calcineurin signaling. *Nucleic Acids Res.* 36, 826–838. doi:10.1093/nar/gkm1107

Miller, J. B., Zhang, S., Kos, P., Xiong, H., Zhou, K., Perelman, S. S., et al. (2017). Non-viral CRISPR/Cas gene editing *in vitro* and *in vivo* enabled by synthetic nanoparticle Co-delivery of Cas9 mRNA and sgRNA. *Angew. Chem. Int. Ed. Engl.* 56, 1059–1063. doi:10.1002/anie.201610209

Min, Y. L., Bassel-Duby, R., and Olson, E. N. (2019a). CRISPR correction of duchenne muscular dystrophy. *Annu. Rev. Med.* 70, 239–255. doi:10.1146/annurev-med-081117-010451

Min, Y. L., Li, H., Rodriguez-Caycedo, C., Mireault, A. A., Huang, J., Shelton, J. M., et al. (2019b). CRISPR-Cas9 corrects Duchenne muscular dystrophy exon 44 deletion mutations in mice and human cells. *Sci. Adv.* 5, eaav4324. doi:10.1126/sciadv.aav4324

Mitrpant, C., Fletcher, S., Iversen, P. L., and Wilton, S. D. (2009). By-passing the nonsense mutation in the 4CV mouse model of muscular dystrophy by induced exon skipping. *J. Gene Med. A cross-disciplinary J. Res. Sci. gene Transf. its Clin. Appl.* 11, 46–56. doi:10.1002/jgm.1265

Moe, K. T., Yin, N. O., Naylynn, T. M., Khairunnisa, K., Wutyi, M. A., Gu, Y., et al. (2011). Nox2 and Nox4 mediate tumour necrosis factor-alpha-induced ventricular remodelling in mice. *J. Cell Mol. Med.* 15, 2601–2613. doi:10.1111/j.1582-4934.2011.01261.x

Mojumdar, K., Liang, F., Giordano, C., Lemaire, C., Danialou, G., Okazaki, T., et al. (2014). Inflammatory monocytes promote progression of Duchenne muscular dystrophy and can be therapeutically targeted via CCR2. *EMBO Mol. Med.* 6, 1476–1492. doi:10.15252/emmm.201403967

Mokri, B., and Engel, A. G. (1975). Duchenne dystrophy: Electron microscopic findings pointing to a basic or early abnormality in the plasma membrane of the muscle fiber. *Neurology* 25, 1111–1120. doi:10.1212/wnl.25.12.1111

Montanaro, F., Lindenbaum, M., and Carbonetto, S. (1999). alpha-Dystroglycan is a laminin receptor involved in extracellular matrix assembly on myotubes and muscle cell viability. *J. Cell Biol.* 145, 1325–1340. doi:10.1083/jcb.145.6.1325

Moore, T. M., Lin, A. J., Strumwasser, A. R., Cory, K., Whitney, K., Ho, T., et al. (2020). Mitochondrial dysfunction is an early consequence of partial or complete dystrophin loss in mdx mice. *Front. Physiol.* 11, 690. doi:10.3389/fphys.2020.00690

Moorwood, C., Lozynska, O., Suri, N., Napper, A. D., Diamond, S. L., and Khurana, T. S. (2011). Drug discovery for Duchenne muscular dystrophy via utrophin promoter activation screening. *Utrophin Promot. Act. Screen.* 6, 261699–e26211. doi:10.1371/journal.pone.0026169 via

Moretti, A., Fonteyne, L., Giesert, F., Hoppmann, P., Meier, A. B., Bozoglu, T., et al. (2020). Somatic gene editing ameliorates skeletal and cardiac muscle failure in pig and human models of Duchenne muscular dystrophy. *Nat. Med.* 26, 207–214. doi:10.1038/s41591-019-0738-2

Morgan, J., and Muntoni, F. (2021). Changes in myonuclear number during postnatal growth–implications for AAV gene therapy for muscular dystrophy. *J. Neuromuscul. Dis.* 1–8, S317–S324. doi:10.3233/JND-210683

Moss, F. P., and Leblond, C. P. (1971). Satellite cells as the source of nuclei in muscles of growing rats. *Anat. Rec.* 170, 421–435. doi:10.1002/ar.1091700405

Mulivor, A., Cannell, M., Davies, M., Sako, D., Liu, J., Bresnahan, D., et al. (2014). "ACE-083, a ligand trap for members of the TGFβ superfamily, increases muscle mass locally in a mouse model of Duchenne muscular dystrophy," in *Presented at action Duchenne int. Conf., 12th, london, nov*, 7–8.

Mullard, A. (2021a). N E W S and A N A LY S I S News in BRieF FDA outlines steps for individualized drug development. *Nat. Rev. Drug Discov.* 20 (2), 91. doi:10.1038/d41573-021-00009-7

Mullard, A. (2021b). N E W S and A N A LY S I S News in BRieF FDA outlines steps for individualized drug development. *Nat. Rev. Drug Discov.* 20, 6939926.

Muntoni, F., Tejura, B., Spinty, S., Roper, H., Hughes, I., Layton, G., et al. (2019). A phase 1b trial to assess the pharmacokinetics of Ezutromid in pediatric duchenne muscular dystrophy patients on a balanced diet. *Clin. Pharmacol. Drug Dev.* 8, 922–933. doi:10.1002/cpdd.642

Nallamilli, B. R. R., Chaubey, A., Valencia, C. A., Stansberry, L., Behlmann, A. M., Ma, Z., et al. (2021). A single NGS-based assay covering the entire genomic sequence of the DMD gene facilitates diagnostic and newborn screening confirmatory testing. *Hum. Mutat.* 42, 626–638. doi:10.1002/humu.24191

Nelson, C. E., Hakim, C. H., Ousterout, D. G., Thakore, P. I., Moreb, E. A., Castellanos Rivera, R. M., et al. (2016). *In vivo* genome editing improves muscle function in a mouse model of Duchenne muscular dystrophy. *Science* 351, 403–407. doi:10.1126/science.aad5143

Nelson, C. E., Robinson-Hamm, J. N., and Gersbach, C. A. (2017). Genome engineering: A new approach to gene therapy for neuromuscular disorders. *Nat. Rev. Neurol.* 13, 647–661. doi:10.1038/nrneurol.2017.126

Nelson, C. E., Wu, Y., Gemberling, M. P., Oliver, M. L., Waller, M. A., Bohning, J. D., et al. (2019). Long-term evaluation of AAV-CRISPR genome editing for Duchenne muscular dystrophy. *Nat. Med.* 25, 427–432. doi:10.1038/s41591-019-0344-3

Nelson, D. M., Lindsay, A., Judge, L. M., Duan, D., Chamberlain, J. S., Lowe, D. A., et al. (2018). Variable rescue of microtubule and physiological phenotypes in mdx muscle expressing different miniaturized dystrophins. *Hum. Mol. Genet.* 27, 2090–2100. doi:10.1093/hmg/ddy113

Nguyen, Q., and Yokota, T. (2019). Antisense oligonucleotides for the treatment of cardiomyopathy in duchenne muscular dystrophy. *Am. J. Transl. Res.* 11, 1202–1218.

Niks, E. H., and Aartsma-Rus, A. (2017). Exon skipping: A first in class strategy for duchenne muscular dystrophy. *Expert Opin. Biol. Ther.* 17, 225–236. doi:10.1080/14712598.2017.1271872

Nishi, M., Yasue, A., Nishimatu, S., Nohno, T., Yamaoka, T., Itakura, M., et al. (2002). A missense mutant myostatin causes hyperplasia without hypertrophy in the mouse muscle. *hypertrophy mouse muscle* 293, 247–251. doi:10.1016/S0006-291X(02)00209-7

Nishida, K., Arazoe, T., Yachie, N., Banno, S., Kakimoto, M., Tabata, M., et al. (2016). Targeted nucleotide editing using hybrid prokaryotic and vertebrate adaptive immune systems. *Science* 353, aaf8729. doi:10.1126/science.aaf8729

Novak, J. S., Hogarth, M. W., Boehler, J. F., Nearing, M., Vila, M. C., Heredia, R., et al. (2017). Myoblasts and macrophages are required for therapeutic morpholino antisense oligonucleotide delivery to dystrophic muscle. *Nat. Commun.* 8, 941. doi:10.1038/s41467-017-00924-7

Odom, G. L., Gregorevic, P., and Chamberlain, J. S. (2007). Viral-mediated gene therapy for the muscular dystrophies: Successes, limitations and recent advances. *Biochim. Biophys. Acta* 1772, 243–262. doi:10.1016/j.bbadis.2006.09.007

Olson, E. N. (2021). Toward the correction of muscular dystrophy by gene editing. *Proc. Natl. Acad. Sci. U. S. A.* 118, e2004840117. doi:10.1073/pnas.2004840117

Onopiuk, M., Brutkowski, W., Wierzbicka, K., Wojciechowska, S., Szczepanowska, J., Fronk, J., et al. (2009). Mutation in dystrophin-encoding gene affects energy metabolism in mouse myoblasts. *Biochem. Biophys. Res. Commun.* 386, 463–466. doi:10.1016/j.bbrc.2009.06.053

Ousterout, D. G., Kabadi, A. M., Thakore, P. I., Majoros, W. H., Reddy, T. E., and Gersbach, C. A. (2015). Multiplex CRISPR/Cas9-based genome editing for correction of dystrophin mutations that cause Duchenne muscular dystrophy. *Nat. Commun.* 6, 6244. doi:10.1038/ncomms7244

Pant, M., Sopariwala, D. H., Bal, N. C., Lowe, J., Delfin, D. A., Rafael-Fortney, J., et al. (2015). Metabolic dysfunction and altered mitochondrial dynamics in the utrophin-dystrophin deficient mouse model of duchenne muscular dystrophy. *PLoS One* 10, e0123875. doi:10.1371/journal.pone.0123875

Papa, S., and Skulachev, V. P. (1997). Reactive oxygen species, mitochondria, apoptosis and aging. *Mol. Cell Biochem.* 174, 305–319. doi:10.1023/A:1006873518427

Passaquin, A. C., Renard, M., Kay, L., Challet, C., Mokhtarian, A., Wallimann, T., et al. (2002). Creatine supplementation reduces skeletal muscle degeneration and enhances mitochondrial function in mdx mice. *Neuromuscul. Disord.* 12, 174–182. doi:10.1016/s0960-8966(01)00273-5

Percival, J. M., Siegel, M. P., Knowels, G., and Marcinek, D. J. (2013). Defects in mitochondrial localization and ATP synthesis in the mdx mouse model of Duchenne muscular dystrophy are not alleviated by PDE5 inhibition. *Hum. Mol. Genet.* 22, 153–167. doi:10.1093/hmg/dds415

Perez-Pinera, P., Kocak, D. D., Vockley, C. M., Adler, A. F., Kabadi, A. M., Polstein, L. R., et al. (2013). RNA-guided gene activation by CRISPR-Cas9-based transcription factors. *Nat. Methods* 10, 973–976. doi:10.1038/Nmeth.2600

Pertille, A., De Carvalho, C. L. T., Matsumura, C. Y., Neto, H. S., and Marques, M. J. (2010). Calcium-binding proteins in skeletal muscles of the mdx mice: Potential role in the pathogenesis of Duchenne muscular dystrophy. *Int. J. Exp. Pathol.* 91, 63–71. doi:10.1111/j.1365-2613.2009.00688.x

Pescatori, M., Broccolini, A., Minetti, C., Bertini, E., Bruno, C., D'amico, A., et al. (2007). Gene expression profiling in the early phases of DMD: A constant molecular signature characterizes DMD muscle from early postnatal life throughout disease progression. *FASEB J.* 21, 1210–1226. doi:10.1096/fj.06-7285com

Pestronk, A., Parhad, I., Drachman, D., and Price, D. L. (1982). Membrane myopathy: Morphological similarities to duchenne muscular dystrophy. *Muscle Nerve* 5, 209–214. doi:10.1002/mus.880050306

Petrillo, S., Pelosi, L., Piemonte, F., Travaglini, L., Forcina, L., Catteruccia, M., et al. (2017). Oxidative stress in duchenne muscular dystrophy: Focus on the NRF2 redox pathway. *Hum. Mol. Genet.* 26, 2781–2790. doi:10.1093/hmg/ddx173

Petrof, B. J., Shrager, J. B., Stedman, H. H., Kelly, A. M., and Sweeney, H. L. (1993). Dystrophin protects the sarcolemma from stresses developed during muscle contraction. *Proc. Natl. Acad. Sci. U. S. A.* 90, 3710–3714. doi:10.1073/pnas.90.8.3710

Pfizer (2014). *Pfizer initiates phase 2 study of PF-06252616 in Duchenne muscular dystrophy*. Press Release. Dec. 17 Available at: http://www.pfizer.com/news/press-release/press-release-detail/pfizer_initiates_phase_.2_study_of_pf_06252616_in_duchenne_muscular_dystrophy.

Phelps, S. F., Hauser, M. A., Cole, N. M., Rafael, J. A., Hinkle, R. T., Faulkner, J. A., et al. (1995). Expression of full-length and truncated dystrophin mini-genes in transgenic mdx mice. *Hum. Mol. Genet.* 4, 1251–1258. doi:10.1093/hmg/4.8.1251

Pickar-Oliver, A., Gough, V., Bohning, J. D., Liu, S., Robinson-Hamm, J. N., Daniels, H., et al. (2021). Full-length dystrophin restoration via targeted exon integration by AAV-CRISPR in a humanized mouse model of Duchenne muscular dystrophy. *Mol. Ther.* 29, 3243–3257. doi:10.1016/j.ymthe.2021.09.003

Pinniger, G. J., Terrill, J. R., Assan, E. B., Grounds, M. D., and Arthur, P. G. (2017). Pre-clinical evaluation of N-acetylcysteine reveals side effects in the mdx mouse model of Duchenne muscular dystrophy. *J. Physiol.* 595, 7093–7107. doi:10.1113/JP274229

Politano, L., Nigro, G., Nigro, V., Pilus, G., Papparella, S., Paciello, O., et al. (2003). Gentamicin administration in Duchenne patients with premature stop codon. Preliminary results. *Acta Myol.* 22, 15–21.

Politano, L. (2021). Read-through approach for stop mutations in Duchenne muscular dystrophy. An update. *update* 12, 43–50. doi:10.36185/2532-1900-041

Pons, F., Nicholson, L. V., Robert, A., Voit, T., and Leger, J. J. (1993). Dystrophin and dystrophin-related protein (utrophin) distribution in normal and dystrophin-deficient skeletal muscles. *Neuromuscul. Disord.* 3, 507–514. doi:10.1016/0960-8966(93)90106-t

Powers, S. K., Ji, L. L., Kavazis, A. N., and Jackson, M. J. (2011). Reactive oxygen species: Impact on skeletal muscle. *Compr. Physiol.* 1, 941–969. doi:10.1002/cphy.c100054

Prayle, A., and Smyth, A. R. (2010). Aminoglycoside use in cystic fibrosis: Therapeutic strategies and toxicity. *Curr. Opin. Pulm. Med.* 16, 604–610. doi:10.1097/MCP.0b013e32833eebfd

Qi, L. S., Larson, M. H., Gilbert, L. A., Doudna, J. A., Weissman, J. S., Arkin, A. P., et al. (2013). Repurposing CRISPR as an RNA-guided platform for sequence-specific control of gene expression. *Cell* 152, 1173–1183. doi:10.1016/j.cell.2013.02.022

Rafael, J. A., Cox, G. A., Corrado, K., Jung, D., Campbell, K. P., and Chamberlain, J. S. (1996). Forced expression of dystrophin deletion constructs reveals structure-function correlations. *J. Cell Biol.* 134, 93–102. doi:10.1083/jcb.134.1.93

Ramos, J. N., Hollinger, K., Bengtsson, N. E., Allen, J. M., Hauschka, S. D., and Chamberlain, J. S. (2019). Development of novel micro-dystrophins with enhanced functionality. *Mol. Ther.* 27, 623–635. doi:10.1016/j.ymthe.2019.01.002

Ran, F. A., Hsu, P. D., Lin, C. Y., Gootenberg, J. S., Konermann, S., Trevino, A. E., et al. (2013). Double nicking by RNA-guided CRISPR Cas9 for enhanced genome editing specificity. *Cell* 154, 1380–1389. doi:10.1016/j.cell.2013.08.021

Reid, M. B. (2001). Invited review: Redox modulation of skeletal muscle contraction: What we know and what we don't. *J. Appl. Physiol.* 90, 724–731. doi:10.1152/jappl.2001.90.2.724

Reid, M. B., Shoji, T., Moody, M. R., and Entman, M. L. (1992). Reactive oxygen in skeletal muscle. II. Extracellular release of free radicals. *J. Appl. Physiol.* 73, 1805–1809. doi:10.1152/jappl.1992.73.5.1805

Reisz-porszasz, S., Bhasin, S., Artaza, J. N., Shen, R., Sinha-hikim, I., Hogue, A., et al. (2022). *Lower skeletal muscle mass in male transgenic mice with muscle-specific overexpression of myostatin*, 876–888.

Ricotti, V., Spinty, S., Roper, H., Hughes, I., Tejura, B., Robinson, N., et al. (2016). Safety, tolerability, and pharmacokinetics of SMT C1100, a 2-arylbenzoxazole utrophin modulator, following single- and multiple- dose administration to pediatric patients with duchenne muscular dystrophy. *PLoS One.* 11, 1–16. doi:10.1371/journal.pone.0152840

Rimessi, P., Sabatelli, P., Fabris, M., Braghetta, P., Bassi, E., Spitali, P., et al. (2009). Cationic PMMA nanoparticles bind and deliver antisense oligoribonucleotides allowing restoration of dystrophin expression in the mdx mouse. *Mol. Ther.* 17, 820–827. doi:10.1038/mt.2009.8

Roberts, R. G., Coffey, A. J., Bobrow, M., and Bentley, D. R. (1993). Exon structure of the human dystrophin gene. *Genomics* 16, 536–538. doi:10.1006/geno.1993.1225

Rogers, G. L., Martino, A. T., Aslanidi, G. V., Jayandharan, G. R., Srivastava, A., and Herzog, R. W. (2011). Innate immune responses to AAV vectors. *Front. Microbiol.* 2, 194. doi:10.3389/fmicb.2011.00194

Rong, Z., Fu, X., Wang, M., and Xu, Y. (2012). A scalable approach to prevent teratoma formation of human embryonic stem cells. *J. Biol. Chem.* 287, 32338–32345. doi:10.1074/jbc.M112.383810

Rooney, J. E., Gurpur, P. B., and Burkin, D. J. (2009a). *Laminin-111 protein therapy prevents muscle disease in the mdx mouse model for Duchenne muscular dystrophy*, 106.

Rooney, J. E., Gurpur, P. B., Yablonka-reuveni, Z., and Burkin, D. J. (2009b). Laminin-111 restores regenerative capacity in a mouse model for alpha7 integrin congenital myopathy. *Am. J. Pathol.* 174, 256–264. doi:10.2353/ajpath.2009.080522

Rooney, J. E., Welser, J. V., Dechert, M. A., Flintoff-dye, N. L., Kaufman, S. J., and Burkin, D. J. (2006). *Severe muscular dystrophy in mice that lack dystrophin and 7 integrin*. doi:10.1242/jcs.02952

Rosenberg, A. S., Puig, M., Nagaraju, K., Hoffman, E. P., Villalta, S. A., Rao, V. A., et al. (2015). Immune-mediated pathology in Duchenne muscular dystrophy. *Sci. Transl. Med.* 7, 299rv4. doi:10.1126/scitranslmed.aaa7322

Rouger, K., Larcher, T., Dubreil, L., Deschamps, J.-Y., le Guiner, C., Jouvion, G., et al. (2011). Systemic delivery of allogenic muscle stem cells induces long-term muscle repair and clinical efficacy in duchenne muscular dystrophy dogs. *Am. J. Pathol.* 179, 2501–2518. doi:10.1016/j.ajpath.2011.07.022

Rybakova, I. N., Amann, K. J., and Ervasti, J. M. (1996). A new model for the interaction of dystrophin with F-actin. *J. Cell Biol.* 135, 661–672. doi:10.1083/jcb.135.3.661

Ryu, S. M., Koo, T., Kim, K., Lim, K., Baek, G., Kim, S. T., et al. (2018). Adenine base editing in mouse embryos and an adult mouse model of Duchenne muscular dystrophy. *Nat. Biotechnol.* 36, 536–539. doi:10.1038/nbt.4148

Saclier, M., ben Larbi, S., My Ly, H., Moulin, E., Mounier, R., Chazaud, B., et al. (2021). Interplay between myofibers and pro-inflammatory macrophages controls muscle damage in *mdx* mice. *J. Cell Sci.* 134, jcs258429. doi:10.1242/jcs.258429

Saleh, A. F., Arzumanov, A. A., and Gait, M. J. (2012). "Overview of alternative oligonucleotide chemistries for exon skipping," in *Exon skipping: Methods and protocols*. Editor A. Aartsma-Rus (Totowa, NJ: Humana Press), 365–378. doi:10.1007/978-1-61779-767-5_23

Salva, M. Z., Himeda, C. L., Tai, P. W., Nishiuchi, E., Gregorevic, P., Allen, J. M., et al. (2007). Design of tissue-specific regulatory cassettes for high-level rAAV-mediated expression in skeletal and cardiac muscle. *Mol. Ther.* 15, 320–329. doi:10.1038/sj.mt.6300027

Schneider, A. E., and Aartsma-Rus, A. (2021). Developments in reading frame restoring therapy approaches for Duchenne muscular dystrophy. *Expert Opin. Biol. Ther.* 21, 343–359. doi:10.1080/14712598.2021.1832462

Schnepp, B. C., Clark, K. R., Klemanski, D. L., Pacak, C. A., and Johnson, P. R. (2003). Genetic fate of recombinant adeno-associated virus vector genomes in muscle. *J. Virol.* 77, 3495–3504. doi:10.1128/jvi.77.6.3495-3504.2003

Schuh, R. A., Jackson, K. C., Khairallah, R. J., Ward, C. W., and Spangenburg, E. E. (2012). Measuring mitochondrial respiration in intact single muscle fibers. *Am. J. Physiol. Regul. Integr. Comp. Physiol.* 302, R712–R719. doi:10.1152/ajpregu.00229.2011

Sciorati, C., Rigamonti, E., Manfredi, A. A., and Rovere-Querini, P. (2016). Cell death, clearance and immunity in the skeletal muscle. *Cell Death Differ.* 23, 927–937. doi:10.1038/cdd.2015.171

Sharma, G., Sharma, A. R., Bhattacharya, M., Lee, S. S., and Chakraborty, C. (2021). CRISPR-Cas9: A preclinical and clinical perspective for the treatment of human diseases. *Mol. Ther.* 29, 571–586. doi:10.1016/j.ymthe.2020.09.028

Sheikh, O., and Yokota, T. (2021). Restoring protein expression in neuromuscular conditions: A review assessing the current state of exon skipping/inclusion and gene therapies for duchenne muscular dystrophy and spinal muscular atrophy. *BioDrugs* 35, 389–399. doi:10.1007/s40259-021-00486-7

Sinadinos, A., Young, C. N. J., Al-Khalidi, R., Teti, A., Kalinski, P., Mohamad, S., et al. (2015). P2RX7 purinoceptor: A therapeutic target for ameliorating the symptoms of duchenne muscular dystrophy. *PLoS Med.* 12, e1001888. doi:10.1371/journal.pmed.1001888

Skuk, D., Goulet, M., Roy, B., Chapdelaine, P., Bouchard, J.-P., Roy, R., et al. (2006). Dystrophin expression in muscles of duchenne muscular dystrophy patients after high-density injections of normal myogenic cells. *J. Neuropathol. Exp. Neurol.* 65, 371–386. doi:10.1097/01.jnen.0000218443.45782.81

Skuk, D., Roy, B., Goulet, M., Chapdelaine, P., Bouchard, J.-P., Roy, R., et al. (2004). Dystrophin expression in myofibers of duchenne muscular dystrophy patients following intramuscular injections of normal myogenic cells. *Mol. Ther.* 9, 475–482. doi:10.1016/j.ymthe.2003.11.023

Smythe, G. M., Hodgetts, S. I., and Grounds, M. D. (2000). Immunobiology and the future of myoblast transfer therapy. *Mol. Ther.* 1, 304–313. doi:10.1006/mthe.2000.0049

Soblechero-Martín, P., López-Martínez, A., de la Puente-Ovejero, L., Vallejo-Illarramendi, A., and Arechavala-Gomeza, V. (2021). Utrophin modulator drugs as potential therapies for Duchenne and Becker muscular dystrophies. *Neuropathol. Appl. Neurobiol.* 47, 711–723. doi:10.1111/nan.12735

Sonnemann, K. J., Heun-johnson, H., Turner, A. J., Baltgalvis, K. A., Lowe, D. A., and Ervasti, J. M. (2009). Functional substitution by TAT-utrophin in dystrophin- deficient mice. *PLoS Med.* 6, e1000083. doi:10.1371/journal.pmed.1000083

Sorichter, S., Mair, J., Koller, A., Pelsers, M. M., Puschendorf, B., and Glatz, J. F. (1998). Early assessment of exercise induced skeletal muscle injury using plasma fatty acid binding protein. *Br. J. Sports Med.* 32, 121–124. doi:10.1136/bjsm.32.2.121

Sorichter, S., Puschendorf, B., and Mair, J. (1999). Skeletal muscle injury induced by eccentric muscle action: Muscle proteins as markers of muscle fiber injury. *Exerc Immunol. Rev.* 5, 5–21.

Spencer, M. J., Montecino-Rodriguez, E., Dorshkind, K., and Tidball, J. G. (2001). Helper (CD4+) and cytotoxic (CD8+) T cells promote the pathology of dystrophin-deficient muscle. *Clin. Immunol.* 98, 235–243. doi:10.1006/clim.2000.4966

Spencer, M. J., Walsh, C. M., Dorshkind, K. A., Rodriguez, E. M., and Tidball, J. G. (1997). Myonuclear apoptosis in dystrophic mdx muscle occurs by perforin-mediated cytotoxicity. *J. Clin. Investigation* 99, 2745–2751. doi:10.1172/JCI119464

Spinazzola, J. M., and Kunkel, L. M. (2016). Pharmacological therapeutics targeting the secondary defects and downstream pathology of Duchenne muscular dystrophy. *Expert Opin. Orphan Drugs* 4, 1179–1194. doi:10.1080/21678707.2016.1240613

Spurney, C. F. (2011a). Cardiomyopathy of duchenne muscular dystrophy: Current understanding and future directions. *Muscle Nerve* 44, 8–19. doi:10.1002/mus.22097

Spurney, C. F., Guerron, A. D., Yu, Q., Sali, A., van der Meulen, J. H., Hoffman, E. P., et al. (2011b). Membrane sealant Poloxamer P188 protects against isoproterenol induced cardiomyopathy in dystrophin deficient mice. *BMC Cardiovasc Disord.* 11, 20. doi:10.1186/1471-2261-11-20

Stedman, H. H., Sweeney, H. L., Shrager, J. B., Maguire, H. C., Panettieri, R. A., Petrof, B., et al. (1991). The mdx mouse diaphragm reproduces the degenerative changes of Duchenne muscular dystrophy. *Nature* 352, 536–539. doi:10.1038/352536a0

Stephenson, A. A., and Flanigan, K. M. (2021). Gene editing and modulation for Duchenne muscular dystrophy. *Prog. Mol. Biol. Transl. Sci.* 182, 225–255. doi:10.1016/bs.pmbts.2021.01.029

Straub, V., Bittner, R. E., Leger, J. J., and Voit, T. (1992). Direct visualization of the dystrophin network on skeletal muscle fiber membrane. *J. Cell Biol.* 119, 1183–1191. doi:10.1083/jcb.119.5.1183

Straub, V., Rafael, J. A., Chamberlain, J. S., and Campbell, K. P. (1997). Animal models for muscular dystrophy show different patterns of sarcolemmal disruption. Available at: http://www.jcb.org.

Suzuki, K., Tsunekawa, Y., Hernandez-Benitez, R., Wu, J., Zhu, J., Kim, E. J., et al. (2016). *In vivo* genome editing via CRISPR/Cas9 mediated homology-independent targeted integration. *Nature* 540, 144–149. doi:10.1038/nature20565

Szabo, P. L., Ebner, J., Koenig, X., Hamza, O., Watzinger, S., Trojanek, S., et al. (2021). Cardiovascular phenotype of the Dmd^{mdx} rat - a suitable animal model for Duchenne muscular dystrophy. *Dis. Model Mech.* 14, dmm047704. doi:10.1242/dmm.047704

Tabebordbar, M., Lagerborg, K. A., Stanton, A., King, E. M., Ye, S., Tellez, L., et al. (2021). Directed evolution of a family of AAV capsid variants enabling potent muscle-directed gene delivery across species. *Cell* 184, 4919–4938 e22. doi:10.1016/j.cell.2021.08.028

Tabebordbar, M., Zhu, K., Cheng, J. K. W., Chew, W. L., Widrick, J. J., Yan, W. X., et al. (2016). *In vivo* gene editing in dystrophic mouse muscle and muscle stem cells. *Science* 351, 407–411. doi:10.1126/science.aad5177

Taglia, A., Petillo, R., D'Ambrosio, P., Picillo, E., Torella, A., Orsini, C., et al. (2015). Clinical features of patients with dystrophinopathy sharing the 45-55 exon deletion of DMD gene. *Acta Myol.* 34, 9–13.

Takeda, S., Clemens, P. R., and Hoffman, E. P. (2021). Exon-skipping in duchenne muscular dystrophy. *J. Neuromuscul. Dis.* 8, S343–S358. doi:10.3233/JND-210682

Taylor, M., Jefferies, J., Byrne, B., Lima, J., Ambale-Venkatesh, B., Ostovaneh, M. R., et al. (2019). Cardiac and skeletal muscle effects in the randomized HOPE-Duchenne trial. *Neurology* 92, e866–e878. doi:10.1212/WNL.0000000000006950

Terrill, J. R., Duong, M. N., Turner, R., Le Guiner, C., Boyatzis, A., Kettle, A. J., et al. (2016). Levels of inflammation and oxidative stress, and a role for taurine in dystropathology of the Golden Retriever Muscular Dystrophy dog model for Duchenne Muscular Dystrophy. *Redox Biol.* 9, 276–286. doi:10.1016/j.redox.2016.08.016

Terrill, J. R., Radley-Crabb, H. G., Grounds, M. D., and Arthur, P. G. (2012). N-Acetylcysteine treatment of dystrophic mdx mice results in protein thiol modifications and inhibition of exercise induced myofibre necrosis. *Neuromuscul. Disord.* 22, 427–434. doi:10.1016/j.nmd.2011.11.007

Terrill, J. R., Radley-Crabb, H. G., Iwasaki, T., Lemckert, F. A., Arthur, P. G., and Grounds, M. D. (2013). Oxidative stress and pathology in muscular dystrophies: Focus on protein thiol oxidation and dysferlinopathies. *FEBS J.* 280, 4149–4164. doi:10.1111/febs.12142

Tidball, J. G., and Villalta, S. A. (2010). Regulatory interactions between muscle and the immune system during muscle regeneration. *Am. J. Physiology-Regulatory, Integr. Comp. Physiology* 298, R1173–R1187. doi:10.1152/ajpregu.00735.2009

Tidball, J. G., Welc, S. S., and Wehling-Henricks, M. (2018). "Immunobiology of inherited muscular dystrophies," in *Comprehensive physiology* (Wiley), 1313–1356. doi:10.1002/cphy.c170052

Tinsley, J., Deconinck, N., Fisher, R., Kahn, D., Phelps, S., Gillis, J. M., et al. (1998). Expression of full-length utrophin prevents muscular dystrophy in mdx mice. *Nat. Med.* 4, 1441–1444. doi:10.1038/4033

Tobin, J. F., and Celeste, A. J. (2005). Myostatin, a negative regulator of muscle mass: Implications for muscle degenerative diseases. *Curr. Opin. Pharmacol.* 5, 328–332. doi:10.1016/j.coph.2005.01.011

Townsend, D., Blankinship, M. J., Allen, J. M., Gregorevic, P., Chamberlain, J. S., and Metzger, J. M. (2007). Systemic administration of micro-dystrophin restores cardiac geometry and prevents dobutamine-induced cardiac pump failure. *Mol. Ther.* 15, 1086–1092. doi:10.1038/sj.mt.6300144

Townsend, D., Turner, I., Yasuda, S., Martindale, J., Davis, J., Shillingford, M., et al. (2010). Chronic administration of membrane sealant prevents severe cardiac injury and ventricular dilatation in dystrophic dogs. *J. Clin. Investigation* 120, 1140–1150. doi:10.1172/JCI41329

Townsend, D. W., Yasuda, S., McNally, E., and Metzger, J. M. (2011). Distinct pathophysiological mechanisms of cardiomyopathy in hearts lacking dystrophin or the sarcoglycan complex. *FASEB J.* 25, 3106–3114. doi:10.1096/fj.10-178913

Townsend, D., Yasuda, S., Chamberlain, J., and Metzger, J. M. (2009). Cardiac consequences to skeletal muscle-centric therapeutics for Duchenne muscular dystrophy. *Trends Cardiovasc Med.* 19, 50–55. doi:10.1016/j.tcm.2009.04.006

Townsend, D., Yasuda, S., Li, S., Chamberlain, J. S., and Metzger, J. M. (2008). Emergent dilated cardiomyopathy caused by targeted repair of dystrophic skeletal muscle. *Mol. Ther.* 16, 832–835. doi:10.1038/mt.2008.52

Tsuda, T. (2018). Clinical manifestations and overall management strategies for duchenne muscular dystrophy. *Methods Mol. Biol.* 1687, 19–28. doi:10.1007/978-1-4939-7374-3_2

Tulangekar, A., and Sztal, T. E. (2021). Inflammation in duchenne muscular dystrophy-exploring the role of neutrophils in muscle damage and regeneration. *Biomedicines* 9, 1366. doi:10.3390/biomedicines9101366

Turner, P. R., Westwood, T., Regen, C. M., and Steinhardt, R. A. (1988). Increased protein degradation results from elevated free calcium levels found in muscle from mdx mice. *Nature* 335, 735–738. doi:10.1038/335735a0

Tyler, K. L. (2003). Origins and early descriptions of Duchenne muscular dystrophy. *Muscle Nerve* 28, 402–422. doi:10.1002/mus.10435

Van Deutekom, J. C. T., Bremmer-Bout, M., Janson, A. A. M., Ginjaar, I. B., Baas, F., Den Dunnen, J. T., et al. (2001). Antisense-induced exon skipping restores dystrophin expression in DMD patient derived muscle cells. *Hum. Mol. Genet.* 10, 1547–1554. doi:10.1093/hmg/10.15.1547

Verma, A. (2018). Recent advances in antisense oligonucleotide therapy in genetic neuromuscular diseases. *Ann. Indian Acad. Neurol.* 21, 3–8. doi:10.4103/aian.AIAN_298_17

Vidal, B., Serrano, A. L., Tjwa, M., Suelves, M., Ardite, E., de Mori, R., et al. (2008). Fibrinogen drives dystrophic muscle fibrosis via a TGFbeta/alternative macrophage activation pathway. *Genes Dev.* 22, 1747–1752. doi:10.1101/gad.465908

Villalta, S. A., Rosenberg, A. S., and Bluestone, J. A. (2015). The immune system in Duchenne muscular dystrophy: Friend or foe. *Rare Dis.* 3, e1010966. doi:10.1080/21675511.2015.1010966

Voisin, V., Se, C., Yu, H., Gillet, B., J, M. I., De, S., et al. (2005). L -arginine improves dystrophic phenotype in mdx mice. *Neurobiol. Dis.* 20, 123–130. doi:10.1016/j.nbd.2005.02.010

Vulin, A., Leturcq, F., and Kaplan, J. (2004). *Splicingexonskippingcorrextion-Mice* 306, 4.

Wagner, K. R., Fleckenstein, J. L., Amato, A. A., Barohn, R. J., Bushby, K., Escolar, D. M., et al. (2008). *A phase I/II trial of MYO-029 in adult subjects with muscular dystrophy*, 561–571. doi:10.1002/ana.21338

Wagner, K. R., Hamed, S., Hadley, D. W., Gropman, A. L., Burstein, A. H., Escolar, D. M., et al. (2001). Gentamicin treatment of Duchenne and Becker muscular dystrophy due to nonsense mutations. *Ann. Neurol.* 49, 706–711. doi:10.1002/ana.1023

Wallace, G. Q., Lapidos, K. A., Kenik, J. S., and McNally, E. M. (2008). Long-term survival of transplanted stem cells in immunocompetent mice with muscular dystrophy. *Am. J. Pathology* 173, 792–802. doi:10.2353/ajpath.2008.080259

Walsh, F. S., and Celeste, A. J. (2005). *Myostatin: A modulator of skeletal-muscle stem cells*, 1513–1517.

Wang, B., Li, J., and Xiao, X. (2000). Adeno-associated virus vector carrying human minidystrophin genes effectively ameliorates muscular dystrophy in mdx mouse model. *Proc. Natl. Acad. Sci. U. S. A.* 97, 13714–13719. doi:10.1073/pnas.240335297

Wang, D., Zhong, L., Nahid, M. A., and Gao, G. (2014). The potential of adeno-associated viral vectors for gene delivery to muscle tissue. *Expert Opin. Drug Deliv.* 11, 345–364. doi:10.1517/17425247.2014.871258

Wang, J. Z., Wu, P., Shi, Z. M., Xu, Y. L., and Liu, Z. J. (2017). The AAV-mediated and RNA-guided CRISPR/Cas9 system for gene therapy of DMD and BMD. *Brain Dev.* 39, 547–556. doi:10.1016/j.braindev.2017.03.024

Wang, Z., Storb, R., Halbert, C. L., Banks, G. B., Butts, T. M., Finn, E. E., et al. (2012). Successful regional delivery and long-term expression of a dystrophin gene in canine muscular dystrophy: A preclinical model for human therapies. *Mol. Ther.* 20, 1501–1507. doi:10.1038/mt.2012.111

Wang, Z., Zhu, T., Qiao, C., Zhou, L., Wang, B., Zhang, J., et al. (2005). Adeno-associated virus serotype 8 efficiently delivers genes to muscle and heart. *Nat. Biotechnol.* 23, 321–328. doi:10.1038/nbt1073

Wasala, L. P., Watkins, T., Wasala, N., Burke, M., Yue, Y., Lai, Y., et al. (2022). The implication of hinge 1 and hinge 4 in micro-dystrophin gene therapy for Duchenne muscular dystrophy. *Hum. Gene Ther.* 34, 459–470. doi:10.1089/hum.2022.180

Watchko, J., O'Day, T., Wang, B., Zhou, L., Tang, Y., Li, J., et al. (2002). Adeno-associated virus vector-mediated minidystrophin gene therapy improves dystrophic muscle contractile function in mdx mice. *Hum. Gene Ther.* 13, 1451–1460. doi:10.1089/10430340260185085

Wehling, M., Spencer, M. J., and Tidball, J. G. (2001). A nitric oxide synthase transgene ameliorates muscular dystrophy in mdx mice. *J. Cell Biol.* 155, 123–131. doi:10.1083/jcb.200105110

Wei, T., Cheng, Q., Min, Y. L., Olson, E. N., and Siegwart, D. J. (2020). Systemic nanoparticle delivery of CRISPR-Cas9 ribonucleoproteins for effective tissue specific genome editing. *Nat. Commun.* 11, 3232. doi:10.1038/s41467-020-17029-3

Weir, A. P., Burton, E. A., Harrod, G., and Davies, K. E. (2002). A- and B-utrophin have different expression patterns and are differentially up-regulated in mdx muscle. *J. Biol. Chem.* 277, 45285–45290. doi:10.1074/jbc.M205177200

Weir, A. P., Morgan, J. E., and Davies, K. E. (2004). A-utrophin up-regulation in mdx skeletal muscle is independent of regeneration. *Neuromuscul. Disord.* 14, 19–23. doi:10.1016/j.nmd.2003.09.004

Welch, E. M., Barton, E. R., Zhuo, J., Tomizawa, Y., Friesen, W. J., Trifillis, P., et al. (2007). PTC124 targets genetic disorders caused by nonsense mutations. *Nature* 447, 87–91. doi:10.1038/nature05756

Whitehead, N. P., Kim, M. J., Bible, K. L., Adams, M. E., and Froehner, S. C. (2015). A new therapeutic effect of simvastatin revealed by functional improvement in muscular dystrophy. *Proc. Natl. Acad. Sci. U. S. A.* 112, 12864–12869. doi:10.1073/pnas.1509536112

Whitehead, N. P., Pham, C., Gervasio, O. L., and Allen, D. G. (2008). N-Acetylcysteine ameliorates skeletal muscle pathophysiology in mdx mice. *J. Physiol.* 586, 2003–2014. doi:10.1113/jphysiol.2007.148338

Whitehead, N. P., Yeung, E. W., Froehner, S. C., and Allen, D. G. (2010). Skeletal muscle NADPH oxidase is increased and triggers stretch-induced damage in the mdx mouse. *PLoS One* 5, e15354. doi:10.1371/journal.pone.0015354

Williams, I. A., and Allen, D. G. (2007). The role of reactive oxygen species in the hearts of dystrophin-deficient mdx mice. *Am. J. Physiol. Heart Circ. Physiol.* 293, H1969–H1977. doi:10.1152/ajpheart.00489.2007

Wojtal, D., Kemaladewi, D. U., Malam, Z., Abdullah, S., Wong, T. W., Hyatt, E., et al. (2016). Spell checking nature: Versatility of CRISPR/Cas9 for developing treatments for inherited disorders. *Am. J. Hum. Genet.* 98, 90–101. doi:10.1016/j.ajhg.2015.11.012

Wu, B., Li, Y., Morcos, P. A., Doran, T. J., Lu, P., and Lu, Q. L. (2009). Octa-guanidine morpholino restores dystrophin expression in cardiac and skeletal muscles and ameliorates pathology in dystrophic mdx mice. *Mol. Ther.* 17, 864–871. doi:10.1038/mt.2009.38

Wu, B., Lu, P., Benrashid, E., Malik, S., Ashar, J., Doran, T. J., et al. (2010). Dose-dependent restoration of dystrophin expression in cardiac muscle of dystrophic mice by systemically delivered morpholino. *Gene Ther.* 17, 132–140. doi:10.1038/gt.2009.120

Wu, B., Moulton, H. M., Iversen, P. L., Jiang, J., Li, J., Li, J., et al. (2008). Effective rescue of dystrophin improves cardiac function in dystrophin-deficient mice by a modified morpholino oligomer. *Proc. Natl. Acad. Sci. U. S. A.* 105, 14814–14819. doi:10.1073/pnas.0805676105

Xiao, X. A., Li, J. A., and Samulski, R. J. (1996). Efficient long-term gene transfer into muscle tissue of immunocompetent mice by adeno-associated virus vector. *J. Virol.* 70, 8098–8108. doi:10.1128/Jvi.70.11.8098-8108.1996

Xu, L., Park, K. H., Zhao, L., Xu, J., El Refaey, M., Gao, Y., et al. (2016). CRISPR-Mediated genome editing restores dystrophin expression and function in mdx mice. *Mol. Ther.* 24, 564–569. doi:10.1038/mt.2015.192

Yang, J., Ratovitski, T., Brady, J. P., Solomon, M. B., Wells, K. D., and Wall, R. J. (2001). *Expression of myostatin pro domain results in muscular transgenic mice*, 361.

Yang, Y., Wang, L., Bell, P., McMenamin, D., He, Z., White, J., et al. (2016). A dual AAV system enables the Cas9-mediated correction of a metabolic liver disease in newborn mice. *Nat. Biotechnol.* 34, 334–338. doi:10.1038/nbt.3469

Yasuda, S., Townsend, D., Michele, D. E., Favre, E. G., Day, S. M., and Metzger, J. M. (2005). Dystrophic heart failure blocked by membrane sealant poloxamer. *Nature* 436, 1025–1029. doi:10.1038/nature03844

Yin, H., Saleh, A. F., Betts, C., Camelliti, P., Seow, Y., Ashraf, S., et al. (2011). Pip5 transduction peptides direct high efficiency oligonucleotide-mediated dystrophin exon skipping in heart and phenotypic correction in mdx mice. *Mol. Ther.* 19, 1295–1303. doi:10.1038/mt.2011.79

Yokota, T., Lu, Q. L., Partridge, T., Kobayashi, M., Nakamura, A., Takeda, S., et al. (2009). Efficacy of systemic morpholino exon-skipping in Duchenne dystrophy dogs. *Ann. Neurol.* 65, 667–676. doi:10.1002/ana.21627

Young, C. S., Hicks, M. R., Ermolova, N. V., Nakano, H., Jan, M., Younesi, S., et al. (2016). A single CRISPR-cas9 deletion strategy that targets the majority of DMD patients restores dystrophin function in hiPSC-derived muscle cells. *Cell Stem Cell* 18, 533–540. doi:10.1016/j.stem.2016.01.021

Young, C. S., Mokhonova, E., Quinonez, M., Pyle, A. D., and Spencer, M. J. (2017). Creation of a novel humanized dystrophic mouse model of duchenne muscular dystrophy and application of a CRISPR/Cas9 gene editing therapy. *J. Neuromuscul. Dis.* 4, 139–145. doi:10.3233/JND-170218

Yu, H. K., Liu, X., Pan, M., Chen, J. W., Liu, C., Wu, Y., et al. (2022). Performance of passive muscle stiffness in diagnosis and assessment of disease progression in duchenne muscular dystrophy. *Ultrasound Med. Biol.* 48, 414–421. doi:10.1016/j.ultrasmedbio.2021.09.003

Yuan, J., Ma, Y., Huang, T., Chen, Y., Peng, Y., Li, B., et al. (2018). Genetic modulation of RNA splicing with a CRISPR-guided cytidine deaminase. *Mol. Cell* 72, 380–394. doi:10.1016/j.molcel.2018.09.002

Yuasa, K., Miyagoe, Y., Yamamoto, K., Nabeshima, Y., Dickson, G., and Takeda, S. (1998). Effective restoration of dystrophin-associated proteins *in vivo* by adenovirus-

mediated transfer of truncated dystrophin cDNAs. *FEBS Lett.* 425, 329–336. doi:10.1016/s0014-5793(98)00251-8

Yue, Y., Ghosh, A., Long, C., Bostick, B., Smith, B. F., Kornegay, J. N., et al. (2008). A single intravenous injection of adeno-associated virus serotype-9 leads to whole body skeletal muscle transduction in dogs. *Mol. Ther.* 16, 1944–1952. doi:10.1038/mt.2008.207

Zhang, Y., Long, C., Li, H., McAnally, J. R., Baskin, K. K., Shelton, J. M., et al. (2017). CRISPR-Cpf1 correction of muscular dystrophy mutations in human cardiomyocytes and mice. *Sci. Adv.* 3, e1602814. doi:10.1126/sciadv.1602814

Zhang, Y., Nishiyama, T., Olson, E. N., and Bassel-Duby, R. (2021). CRISPR/Cas correction of muscular dystrophies. *Exp. Cell Res.* 408, 112844. doi:10.1016/j.yexcr.2021.112844

Zhao, Q. D., Viswanadhapalli, S., Williams, P., Shi, Q., Tan, C., Yi, X., et al. (2015). NADPH oxidase 4 induces cardiac fibrosis and hypertrophy through activating Akt/mTOR and NFκB signaling pathways. *Circulation* 131, 643–655. doi:10.1161/CIRCULATIONAHA.114.011079

Zhou, L., Porter, J. D., Cheng, G., Gong, B., Hatala, D. A., Merriam, A. P., et al. (2006). Temporal and spatial mRNA expression patterns of TGF-beta1, 2, 3 and TbetaRI, II, III in skeletal muscles of mdx mice. *Neuromuscul. Disord.* 16, 32–38. doi:10.1016/j.nmd.2005.09.009

Zhu, P., Wu, F., Mosenson, J., Zhang, H., He, T. C., and Wu, W. S. (2017). CRISPR/Cas9-Mediated genome editing corrects dystrophin mutation in skeletal muscle stem cells in a mouse model of muscle dystrophy. *Mol. Ther. Nucleic Acids* 7, 31–41. doi:10.1016/j.omtn.2017.02.007

Zhu, X., Hadhazy, M., Wehling, M., and Tidball, J. G. (2000). Dominant negative myostatin produces hypertrophy without hyperplasia in muscle. *FEBS Lett.* 474, 71–75. doi:10.1016/s0014-5793(00)01570-2

Zincarelli, C., Soltys, S., Rengo, G., and Rabinowitz, J. E. (2008). Analysis of AAV serotypes 1-9 mediated gene expression and tropism in mice after systemic injection. *Mol. Ther.* 16, 1073–1080. doi:10.1038/mt.2008.76

Zuris, J. A., Thompson, D. B., Shu, Y., Guilinger, J. P., Bessen, J. L., Hu, J. H., et al. (2015). Cationic lipid-mediated delivery of proteins enables efficient protein-based genome editing *in vitro* and *in vivo*. *Nat. Biotechnol.* 33, 73–80. doi:10.1038/nbt.3081

Wagner, K. R., Kuntz, N. L., Koenig, E., East, L., Upadhyay, S., and Shieh, P. B. (2021). Safety, tolerability, and pharmacokinetics of casimersen in patients with Duchenne muscular dystrophy amenable to exon dose-titration trial. *Muscle Nerve.* 64, 285–292. doi:10.1002/mus.27347

frontiers | Frontiers in Physiology

TYPE Original Research
PUBLISHED 26 June 2023
DOI 10.3389/fphys.2023.1166206

OPEN ACCESS

EDITED BY
Katsumasa Goto,
Toyohashi Sozo University, Japan

REVIEWED BY
Arnaud Ferry,
Université de Paris, France
Xin Xie,
Zhejiang University, China

*CORRESPONDENCE
R. W. Grange,
rgrange@vt.edu

RECEIVED 14 February 2023
ACCEPTED 10 May 2023
PUBLISHED 26 June 2023

CITATION
Hamm SE, Yuan C, McQueen LF, Wallace MA, Zhang H, Arora A, Garafalo AM, McMillan RP, Lawlor MW, Prom MJ, Ott EM, Yan J, Addington AK, Morris CA, Gonzalez JP and Grange RW (2023), Prolonged voluntary wheel running reveals unique adaptations in mdx mice treated with microdystrophin constructs ± the nNOS-binding site. *Front. Physiol.* 14:1166206. doi: 10.3389/fphys.2023.1166206

Prolonged voluntary wheel running reveals unique adaptations in mdx mice treated with microdystrophin constructs ± the nNOS-binding site

S. E. Hamm[1], C. Yuan[1], L. F. McQueen[1], M. A. Wallace[1], H. Zhang[1], A. Arora[1], A. M. Garafalo[1], R. P. McMillan[1], M. W. Lawlor[2], M. J. Prom[2], E. M. Ott[2], J. Yan[1], A. K. Addington[1], C. A. Morris[3], J. P. Gonzalez[3] and R. W. Grange[1]*

[1]Department of Human Nutrition, Foods and Exercise and Metabolism Core, Virginia Tech, Blacksburg, VA, United States, [2]Department of Pathology and Neuroscience Research Center, Medical College of Wisconsin and Diverge Translational Science Laboratory, Milwaukee, WI, United States, [3]Solid Biosciences, Inc., Cambridge, MA, United States

We tested the effects of prolonged voluntary wheel running on the muscle function of mdx mice treated with one of two different microdystrophin constructs. At 7 weeks of age mdx mice were injected with a single dose of AAV9-CK8-microdystrophin with (gene therapy 1, GT1) or without (gene therapy 2, GT2) the nNOS-binding domain and were assigned to one of four gene therapy treated groups: mdxRGT1 (run, GT1), mdxGT1 (no run, GT1), or mdxRGT2 (run,GT2), mdxGT2 (no run, GT2). There were two mdx untreated groups injected with excipient: mdxR (run, no gene therapy) and mdx (no run, no gene therapy). A third no treatment group, Wildtype (WT) received no injection and did not run. mdxRGT1, mdxRGT2 and mdxR performed voluntary wheel running for 52 weeks; WT and remaining mdx groups were cage active. Robust expression of microdystrophin occurred in diaphragm, quadriceps, and heart muscles of all treated mice. Dystrophic muscle pathology was high in diaphragms of non-treated mdx and mdxR mice and improved in all treated groups. Endurance capacity was rescued by both voluntary wheel running and gene therapy alone, but their combination was most beneficial. All treated groups increased *in vivo* plantarflexor torque over both mdx and mdxR mice. mdx and mdxR mice displayed ~3-fold lower diaphragm force and power compared to WT values. Treated groups demonstrated partial improvements in diaphragm force and power, with mdxRGT2 mice experiencing the greatest improvement at ~60% of WT values. Evaluation of oxidative red quadriceps fibers revealed the greatest improvements in mitochondrial respiration in mdxRGT1 mice, reaching WT levels. Interestingly, mdxGT2 mice displayed diaphragm mitochondrial respiration values similar to WT but mdxRGT2 animals showed relative decreases compared to the no run group. Collectively, these data demonstrate that either microdystrophin construct combined with voluntary wheel running increased *in vivo* maximal muscle strength, power, and endurance. However, these data also highlighted important differences between the two microdystrophin constructs. GT1, with the nNOS-binding site,

improved more markers of exercise-driven adaptations in metabolic enzyme activity of limb muscles, while GT2, without the nNOS-binding site, demonstrated greater protection of diaphragm strength after chronic voluntary endurance exercise but decreased mitochondrial respiration in the context of running.

KEYWORDS

endurance, muscle strength, AAV (adeno-associated virus), microdystrophin, longevity

Introduction

Duchenne muscular dystrophy (DMD) is a fatal, progressive, muscle wasting disease caused by mutations on the X chromosome that lead to an absence of functional dystrophin. (Yiu and Kornberg, 2015; Duan et al., 2021). Dystrophin is a large muscle protein that links ɣ-actin in the myofiber to the dystrophin-glycoprotein complex (DGC), which spans the sarcolemma. (Gao and McNally, 2015; Duan et al., 2021). The DGC thus links the inside of the muscle fiber to the extracellular matrix and provides several important signaling functions for the cell. (Gao and McNally, 2015). Absence of dystrophin leads to loss of the DGC and all of its functions. (Gao and McNally, 2015; Duan et al., 2021). Consequently, muscles are susceptible to damage and necrosis, resulting in loss of ambulation, cardiomyopathy, and respiratory failure. (Gao and McNally, 2015; Duan et al., 2021).

Treatment for patients with DMD has historically been corticosteroids, which reduce inflammation and slow disease progression. (Duan et al., 2021). Recently, gene-based therapeutics such as induction of utrophin overexpression, exon-skipping drugs, and microdystrophin gene therapy have been tested in clinical trials. (Duan et al., 2021). Microdystrophin gene therapy delivers a truncated version of dystrophin, engineered to contain the most important parts of dystrophin to retain function, but small enough to fit into the available adeno-associated viral (AAV) vectors (~5 kb). (Chamberlain and Chamberlain, 2017; Duan, 2018a). Two important microdystrophin constructs include H2μDys and μDys-5R. Versions of each are being used in clinical trials. (Duan, 2018a; Duan, 2018b; Ramos et al., 2019). The structure of each contain an actin-binding domain (ABD), Hinge domain 1 (H1) and 4 or 5 spectrin-like repeats (R). (Duan, 2018b). Both constructs also contain Hinge domain 4 (H4) and a portion of the cysteine-rich region (CR) that is critical for binding to β-dystroglycan in the DGC. (Duan, 2018b). H2μDys includes Hinge domain 2, which contains a polyproline site proposed to be detrimental to structure of the cytoskeleton and extracellular matrix when delivered to mdx mice. (Banks et al., 2010). μDys-5R is known for its unique nNOS-binding site at R16 and R17, which has been shown to restore nNOS localization to the sarcolemma and reduce functional ischemia in the limbs during exercise and, independent of exercise, lead to increased force output over other microdystrophins. (Lai et al., 2009; Lai et al., 2013; Zhang et al., 2013; Ramos et al., 2019). With potential success of clinical trials forthcoming, it is becoming increasingly important to determine the limitations of these microdystrophin constructs, especially in relation to exercise. (Harper et al., 2002; Liu et al., 2005; Bostick et al., 2011).

Voluntary wheel running is beneficial to mdx muscle, (Dupont-Versteegden et al., 1994; Landisch et al., 2008; Baltgalvis et al., 2012; Selsby et al., 2013), whereas other exercise modalities such as forced treadmill training regimens exacerbate the dystrophic condition. (Aartsma-Rus and van Putten, 2014; Schill et al., 2016; Rodgers et al., 2020). Few studies have examined the effects of exercise on mini- or microdystrophin gene therapy. (Shin et al., 2011; Zhang et al., 2013; Rodgers et al., 2020; Hamm et al., 2021). When forced treadmill running was used, studies report at least partial rescue of muscle function from exercise-induced damage. (Shin et al., 2011; Rodgers et al., 2020). mdx mice treated with microdystrophin that performed voluntary wheel running for 13 days ran farther than their untreated controls, but other aspects of skeletal muscle function were not measured. (Shin et al., 2011). In a recent study, we demonstrated that 21 weeks of voluntary wheel running was beneficial to young mdx mice treated with microdystrophin gene therapy. (Hamm et al., 2021).

The objectives of our current study were to determine if (1) prolonged (52 weeks) voluntary wheel running and (2) microdystrophin construct structure (± nNOS binding site) in mdx mice will sustain the functional benefits we reported for microdystrophin combined with short-term (21 weeks) voluntary wheel running in mdx mice (Hamm et al., 2021). To address these two objectives, we assessed the effects of 52 weeks of voluntary wheel running on whole body endurance and muscle function in young mdx mice treated with μDys-5R (with the nNOS-binding site, gene therapy 1, GT1) or H2μDys (without the nNOS-binding site, gene therapy 2, GT2) microdystrophin gene therapy constructs. Our data demonstrate that either the GT1 or the GT2 gene therapy improved several functional assessments similarly in mdx mice, with or without voluntary wheel running. Treated mice with either the GT1 or the GT2 microdystrophin construct and did not run displayed enhanced endurance capacity (i.e., time to exhaustion on a treadmill running test) and improved plantarflexor torque. Mice that were treated with either the GT1 or the GT2 microdystrophin construct and performed voluntary wheel running exhibited further improvement in endurance capacity and similar improvements in plantarflexor torque. However, improvements in *ex vivo* contractile assessments and metabolic assays were dependent on the GT1 or GT2 microdystrophin construct and activity level (i.e., run versus no run). Thus, prolonged voluntary wheel running complemented the functional improvements provided by both microdystrophin constructs but also revealed the unique benefits of each microdystrophin construct to dystrophic muscle.

Materials and methods

Animal studies

All animal experiments were approved by the Institutional Animal Care and Use Committee at Virginia Tech, and in concordance with NIH guidelines. Four-week-old male wildtype (WT; C57BL-10ScSnJ/Jax strain #000476) and male mdx (C57BL/

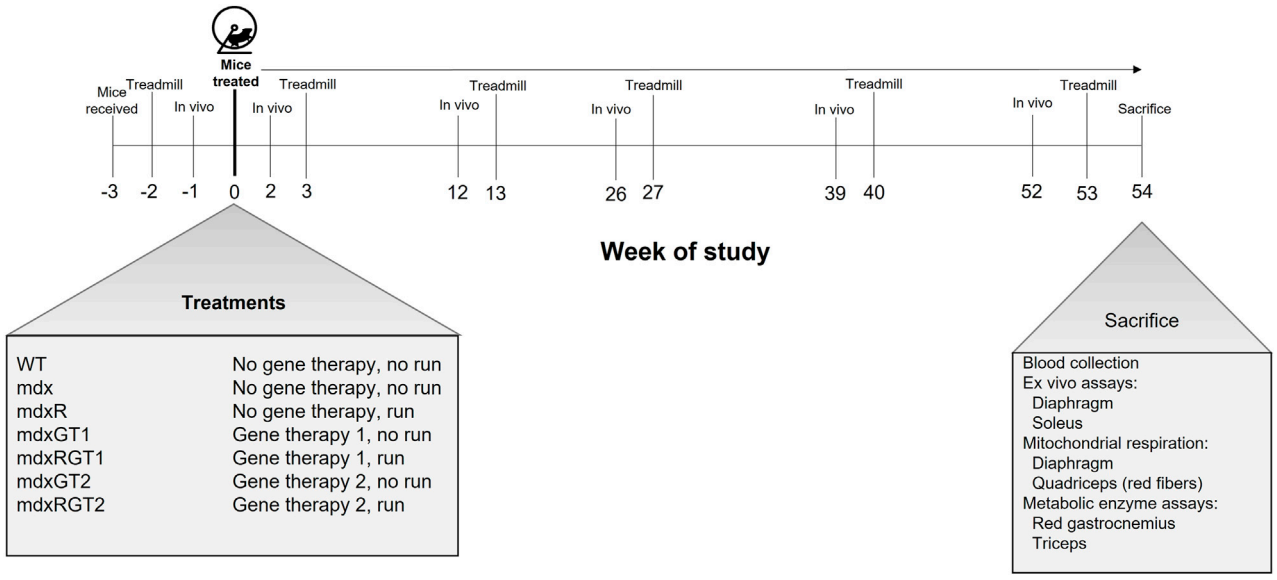

FIGURE 1
Timeline of study and mouse groups. Mice were received at age 4 weeks (Week−3) and administered treatment and housed with wheels at age 7 weeks (Week 0). mdxR, mdxRGT1, and mdxRGT2 groups had access to a running wheel from Week 0 through 54. Mice were assessed for *in vivo* plantarflexor torque at Weeks -1, 2, 12, 39 and 52. Treadmill runs to exhaustion were conducted at Weeks -2, 3, 13, 27, 40 and 53. Mice were sacrificed and various assays conducted at Age 61 weeks (Week 54). At start of study, n = 8 each group. See Materials and methods for details.

10ScSn-DMDmdx/Jax strain #001801) mice were purchased from the Jackson Laboratory (Bar Harbor, ME; WT n = 8, mdx n = 48). The total of 56 mice were purchased in four cohorts of 10 and two cohorts of 8 mice (age 4 weeks) over 6 weeks. Mice in each cohort were assigned to one of the experimental groups each week (e.g., 1-2 mice/experimental group). Mice in both WT and the various mdx groups were staggered over the 6 weeks, e.g., not all WT mice started the same week, but were distributed over the 6 weeks. The mdx groups were similarly distributed. All groups (n = 8) followed the same timeline (Figure 1). It was necessary to stagger the groups so assays post-sacrifice could also be staggered over 6 weeks at the end of the study, i.e., data could not be collected from 56 mice if they all started the study simultaneously. Mice were initially group-housed (3-4 mice/cage) in a temperature-controlled room (21.1°C) with a 12-h light/12-h dark cycle and were given access to water and chow (Harlan-Teklad 2018) *ad libitum* until 7 weeks of age. The environmental and water/food conditions were maintained throughout the study. At 7 weeks of age, mice were treated with gene therapy (treated groups; mdxGT1, mdxRGT1, mdxGT2, mdxRGT2) or excipient (non-treated groups; WT, mdx, mdxR) and housed with free-spinning wheels (running groups; mdxR, mdxRGT1, mdxRGT2) or locked wheels (cage-active groups; WT, mdx, mdxGT1, mdxGT2). N values were variable during the study due to various uncontrollable complications, primarily the unexpected illness and/or death of mice (Supplementary Table S8). Mouse masses at sacrifice are reported in Supplementary Table S9.

Voluntary wheel running

Protocol was followed as previously described. (Hamm et al., 2021). All mice were single housed starting at age 7 weeks (Week 0, Figure 1) after appropriate excipient or microdystrophin injection. Mice in mdxR, mdxRGT1, and mdxRGT2 groups were single housed in cages with running wheels. Mice in WT, mdx, mdxGT1, and mdxGT2 groups were single housed in cages with locked running wheels. All running mice ran 54 weeks. However, the mice were sacrificed on different days (i.e., Monday vs. Friday) during week 54, so mice ran until sacrifice at 54 weeks, but we reported running distance for 52 weeks to standardize the run duration between mice. Thus, our wheel running figure (Figures 5D, E) only shows distances for 0–52 weeks.

AAV construct and delivery

Two microdystrophin constructs were tested. Recombinant AAV9 was produced at the Vector Core of the University of Massachusetts Medical School. Both constructs were under the control of the creatine kinase 8 (CK8) skeletal and cardiac muscle-specific promoter. The gene-of-interest (GOI) plasmid used for production of the GT1 construct coded for a five-repeat microdystrophin sequence, μDys-5R, which contains the R16/R17 nNOS-binding specific repeats. The gene-of-interest (GOI) plasmid used for production of the GT2 construct coded for a four-repeat microdystrophin sequence, H2μDys, which does contain the R16/R17 nNOS-binding specific repeats. Animals were administered a single dose of each construct at a dose of 2×10^{14} vg/kg or an equivalent volume of excipient (phosphate buffered saline + 0.001% Pluronic F-68) via tail vein injection at age 7 weeks with a U100 28Gx1/2 insulin syringe (Becton Dickson, Franklin Lakes, *NJ*).

Assessment of microdystrophin protein by western blot and immunofluorescence

Western blot

Total protein from diaphragm, heart, and quadriceps collected at the conclusion of the study was prepared to determine the content of microdystrophin as previously described (Hamm et al., 2021). Microdystrophin protein levels were compared to a standard microdystrophin reference sample characterized as 100% of normal dystrophin and run on each blot alongside study samples to allow for blot-to-blot interpretation. Relative protein levels were evaluated using a one-way ANOVA with Prism software (GraphPad Prism 9.0).

Immunofluorescence

Isopentane-frozen diaphragm strip, heart, and quadriceps muscle specimens obtained at the conclusion of the study were sectioned at 8-µm thickness and immunostained per standard techniques for dystrophin/microdystrophin (Leica, NCL-DYSB) as previously described. (Hamm et al., 2021). Evaluation of percent dystrophin- or microdystrophin-positive fibers was performed by a neuropathologist using a standard fluorescent microscope and estimated to the nearest 5%.

Assessment of dystrophic pathology

H&E-stained sections of frozen diaphragm, quadriceps, and heart muscle tissues collected at the conclusion of the study were assessed for histological features specific to myofiber degeneration and regeneration associated with dystrophic muscle pathology as previously described. (Hamm et al., 2021). Dystrophic grade was assigned by the estimated proportion of tissue that showed evidence of active/recent dystrophic changes, including myonecrosis, inflammation, myophagocytosis, and basophilic fibers. All of these pathological findings correspond to evidence of recent muscle damage that would have occurred during the post-treatment period. More chronic dystrophic changes (internal nucleation, fibrosis, fatty replacement) are not an element of this dystrophic grading system, as it is not possible to determine whether these changes were present before treatment was started. The grading scale used for reporting is as follows: Grade 0 = normal, grade 1 = chronic regenerative changes only, grade 1.5 = very mild (<5% of muscle area with active dystrophic pathology), grade 2 = mild (6%–20% of muscle area with active dystrophic pathology), grade 2.5 = mild to moderate (21%–30% of muscle area with active dystrophic pathology), grade 3 = moderate (31%–50% of muscle area with active dystrophic pathology), grade 3.5 = moderate to severe (51%–60% of muscle area with active dystrophic pathology) and grade 4 = severe (>60% of muscle area with active dystrophic pathology).

Assessments before, during, and after the period of voluntary wheel running

Treadmill fatigue tests

A treadmill fatigue test was used to determine endurance capacity. Endurance capacity is defined as the ability of the mouse to exercise for an extended period of time as demonstrated by time to exhaustion during a treadmill running test. All mice were subjected to treadmill training and fatigue tests as previously described. (Hamm et al., 2021). Briefly, mice were subjected to a short training protocol on a 6-lane treadmill (Columbus Instruments) for 3 days and a fatigue test on the fourth day. For the fatigue test, there is a progressive increase in speed every 2 min for 5 steps starting at 0.02 to 0.1 m/s, in 0.02 m/s increments and an increase of 0.1 m/s on the sixth step to 0.2 m/s. For steps 7–11, speed is increased every 1,200 s from 0.3 to 0.5 m/s in 0.05 m/s increments. The test is over when the mouse is fatigued after three failures. Failure is defined as the inability of the mouse to keep running after aggressive physical nudges with a bottle brush (Fisher). Each mouse was allowed three failures before it was considered fatigued. The treadmill was paused using a custom pause function in the instrument software and time to fatigue was recorded. Fatigued mice were quickly removed from the treadmill and the protocol resumed promptly for the remaining mice. Fatigue tests were performed at Baseline (2 weeks pre-treatment) and subsequently following each *in vivo* contractile assessment (3, 13-, 27-, 40-, and 53-weeks post-treatment; Figure 1).

In vivo skeletal muscle contractile properties

In vivo isometric plantarflexor torque and torque-velocity were assessed 1 week prior to, and at 2-, 12-, 26-, 39-, and 52-weeks after treatment to determine plantarflexor contractile performance (Figure 1). Body mass was recorded prior to each experiment. Mice were anesthetized with isoflurane (VetOne Fluriso, Boise, Idaho) and prepared as previously described. (Hamm et al., 2021). Following the experiment, mice recovered in a clean cage on top of a heated pad. After mice were fully awake and mobile in the recovery chamber, they were placed in a clean cage with an active or locked running wheel as necessary and returned to the vivarium. *In vivo* contractile properties were determined using methods described previously. (Hamm et al., 2021).

Isometric torque-frequency experiments were performed as described. (Hamm et al., 2021). Briefly, the plantarflexors were stimulated in a series of increasing frequencies from 1–200 Hz. Data were plotted as torque normalized to mouse body mass (mN x m/g) vs. frequency.

Torque-velocity was determined by measuring torque output at set velocities. (Baltgalvis et al., 2012). In this method, the pedal moves passively to 19° dorsiflexion, then the plantarflexors are stimulated at 300 Hz while the pedal moves to 19° plantarflexion at a set velocity. Torque was measured at 1,200°/s, 1,000°/s, 800°/s, 600°/s, 400°/s, 200°/s, and 100°/s, with stimulation durations of 0.0317, 0.038, 0.0475, 0.063, 0.095, 0.190, 0.380s, respectively. Due to the high stimulation frequency, 3 min of rest were given between each stimulation. Peak torque during active stimulation was determined. Peak torque was multiplied by angular velocity to obtain power values. Values were normalized to body mass (g).

Assessments of isolated soleus and diaphragm muscle contractile properties

Ex vivo contractile properties

Soleus muscles and diaphragm strips were carefully dissected and placed in a jacketed water bath to determine contractile

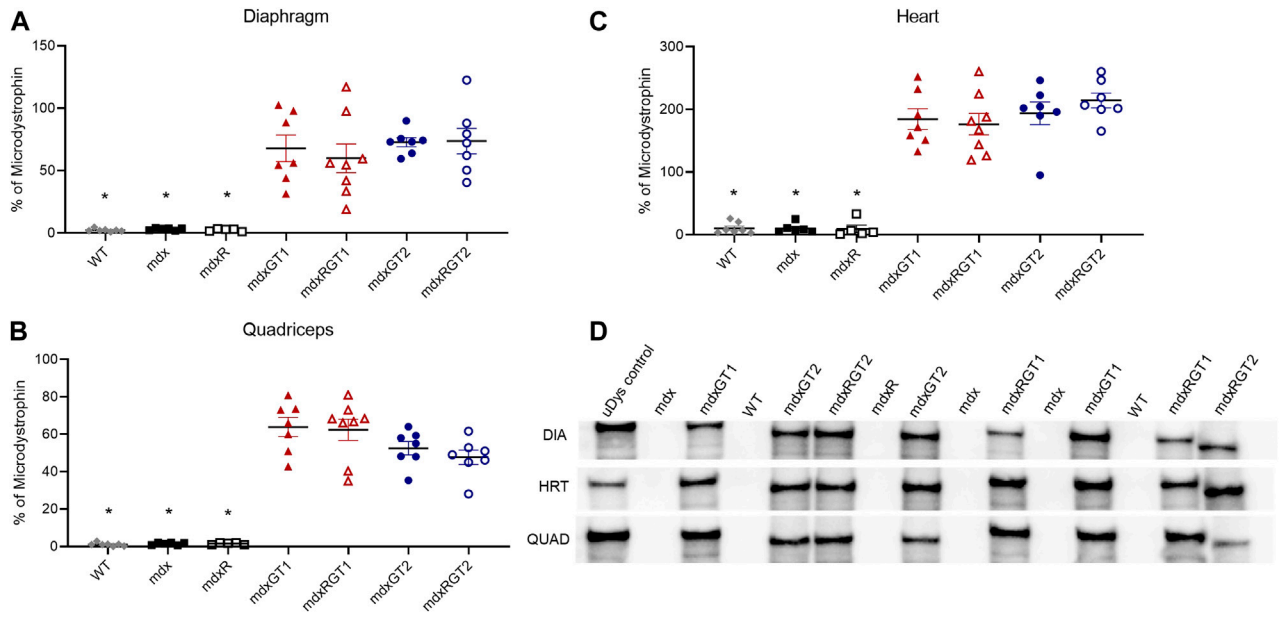

FIGURE 2
Microdystrophin protein content in diaphragm, quadriceps, and heart by quantification of volume of microdystrophin bands on western blot **(A–C)**. **(A)*** WT, mdx, mdxR < mdxGT1, mdxRGT1, mdxGT2, mdxRGT2. **(B)*** WT, mdx, mdxR < mdxGT1, mdxRGT1, mdxGT2, mdxRGT2. **(C)*** WT, mdx, mdxR < mdxGT1, mdxRGT1, mdxGT2, mdxRGT2. **(D)** Representative western blots of uDys-5R (GT1; 147 kDa) and H2μDys (GT2; 138 kDa) microdystrophin constructs. All comparisons $p < 0.05$.

properties including force, velocity, power, and responses to eccentric contractions as previously described. (Hamm et al., 2021).

Assessments of mitochondrial respiration

Permeabilized fibers of red (oxidative) quadriceps were prepared and high resolution O_2 consumption measurements were performed as previously described to determine mitochondrial respiration. (Hamm et al., 2021). Similarly, diaphragm fibers were permeabilized with a saponin treatment, and fibers were washed and placed in buffer in the chamber of an Oroboros Oxygraph-2k (Oroboros Instruments, Innsbruck, Austria) as described. O_2 consumption was measured using a series of substrate injections to elicit activity of mitochondrial enzymes of the electron transport chain similar to the procedure used for quadriceps fibers, with a few key differences. Substrate injections were as follows: 10 mM glutamate/malate, 0.5uM rotenone, 10 mM succinate, 5 mM ADP, and 0.5 mM FCCP. Fiber bundles were removed from the chamber, washed with dH_2O, and freeze dried as previously described. Freeze-dried bundles were weighed, and data were normalized to mass (mg) of the bundles.

Assessment of metabolic enzyme activities

Red and white gastrocnemius, as well as whole triceps, were prepared and assayed as previously described to determine the activities of various metabolic enzymes. (Hamm et al., 2021). Citrate Synthase (CS), Malate Dehydrogenase (MD), and Cytochrome c oxidase (COX) were assayed in red and white gastrocnemius and whole triceps. Phosphofructokinase (PFK) and β-hydroxyacyl - CoA dehydrogenase (βHAD)were assayed in red gastrocnemius and whole triceps.

Statistical analysis

GraphPad Prism 9.0 was used to perform all statistical analyses. Data were analyzed with a one-way (group) or a two-way ANOVA (e.g., group x time) as required. Treatment group was considered a single independent variable, instead of gene therapy or running each as independent variables. Thus, a one-way ANOVA was used for simple comparisons like microdystrophin content (independent variable: group, dependent variable: microdystrophin content) or treadmill time to fatigue (independent variable: group, dependent variable: time to fatigue). A two-way ANOVA was used when we tested the effects of two independent variables such as group and time on torque output (independent variable1: group, independent variable 2: time, dependent variable: torque). If a significant interaction between two factors occurred, Tukey's HSD test was used to determine differences between means. Data are presented as mean ± SEM. Statistical significance was accepted at $p < 0.05$.

Results

Study strategy

In this study, we aimed to determine if μDys-5R (GT1, with the nNOS binding site) and H2μDys (GT2, without the nNOS binding site) treatment would improve running performance and muscle function in mdx mice during prolonged voluntary wheel running for 52-weeks (Figure 1). Treated animals were separated into gene therapy (mdxGT1, n = 8; mdxGT2, n = 8) and gene therapy combined with voluntary wheel running (mdxRGT1, n = 8;

mdxRGT2, $n = 8$) groups. Each treated group was administered a single intravenous dose of AAV9-CK8-microdystrophin at approximately 7 weeks of age and followed for 54 weeks post treatment. Control groups of WT sedentary mice ($n = 8$), mdx sedentary mice ($n = 8$), and mdx mice that performed voluntary wheel running (mdxR, $n = 8$) were evaluated alongside treated groups throughout the study. *In vivo* plantarflexor contractile assessments and treadmill fatigue tests were performed to test plantarflexor and whole-body muscle function, respectively. At the end of the study, tissues were collected for analysis of microdystrophin protein expression, dystrophic muscle pathology, and mitochondrial respiration. Diaphragm strips and whole soleus muscles were isolated for *ex vivo* contractile analyses. The n values for the majority of assessments after baseline measures and during and after completion of the study were WT, 7; mdx, 6; mdxR, 5; mdxGT1, 7; mdxRGT1, 8; mdxGT2, 7; mdxRGT2, 7; specific n values for each assessment are reported in Supplementary Table S8.

Diaphragm, quadriceps, and heart muscles displayed robust expression of microdystrophin protein, demonstrated by both Western blot and quantification of immunofluorescence

Western blot

Microdystrophin protein levels were evaluated via Western blot (Figure 2; Supplementary Table S1) and immunofluorescence (Figure 3; Supplementary Table S2) to assess expression in muscles. Western blot data for each sample were normalized to a standard microdystrophin reference sample characterized as 100% of normal dystrophin that was run alongside study samples on each blot and expressed as mean % ± SEM. WT (2 ± 0), mdx (3 ± 0) and mdxR (2 ± 0) diaphragm samples were negative for microdystrophin protein bands at 147 kDa (Figure 2D) and quantified at relative % of microdystrophin levels similar to background. Microdystrophin levels were significantly increased to levels of 73 ± 4 for mdxGT2 and 74 ± 10 for mdxRGT2 mice ($p < 0.05$). mdxGT1 and mdxRGT1 mice displayed similarly strong relative expression at 68 ± 11 and 60 ± 12, respectively (**Figure 2A**; $p < 0.05$). Quadriceps from treated mice displayed increased relative expression across groups compared to the background levels in WT (1 ± 0), mdx (1 ± 0), and mdxR (2 ± 0) untreated control samples (**Figure 2B**; mdxGT1: 64 ± 5; mdxRGT1: 62 ± 6; mdxGT2: 53 ± 4; mdxRGT2: 48 ± 4; $p < 0.05$). Robust microdystrophin expression was observed in heart muscle of treated animals regardless of construct compared to background levels in WT (10 ± 3), mdx (10 ± 3), and mdxR (9 ± 6) samples (Figure 2C; mdxGT1: 184 ± 17; mdxRGT1: 176 ± 17; mdxGT2: 194 ± 18; mdxRGT2: 214 ± 12; $p < 0.05$).

Immunofluorescence

Immunofluorescence analysis was performed to evaluate the number of fibers positive for anti-dystrophin antibody (DYSB) staining to detect the presence of full-length dystrophin or microdystrophin and expressed as mean % ± SEM. Compared to the mdx or mdxR revertant positive fiber levels (0–1) in diaphragm, quadriceps, and heart, all treated groups demonstrated greater expression (Figure 3; Supplementary Table S2; $p < 0.05$). Higher microdystrophin expression was evident in GT2 treated diaphragms (mdxGT2 89 ± 3; mdxRGT2 90 ± 3) compared to GT1 (mdxGT1 56 ± 7; mdxRGT1 66 ± 8; $p < 0.05$), regardless of activity level (Figure 3A). Analysis of quadriceps showed treated mice had similar levels of microdystrophin positive fibers (Figure 3B; mdxGT1 87 ± 5; mdxRGT1 83 ± 3; mdxGT2 91 ± 4; mdxRGT2 86 ± 3). However, mdxRGT1 and mdxRGT2 showed a running-dependent decrease in microdystrophin compared to WT levels of dystrophin (100 ± 0; $p < 0.05$). Robust expression of microdystrophin was confirmed in heart muscle of all treated groups (mdxGT1 100 ± 0; mdxRGT1 100 ± 0; mdxGT2 100 ± 0; mdxRGT2 99 ± 1), which were rescued to WT levels of dystrophin (Figure 3C; 100 ± 0). Representative immunofluorescence images are shown for each treated mdx group (Figure 3).

Both microdystrophin constructs similarly improved dystrophic muscle pathology in animals performing voluntary exercise

Dystrophic muscle pathology in the diaphragm, heart, and quadriceps was assessed at the end of the study (Figure 4; Supplementary Table S3). Representative images of the diaphragm are shown for each mdx group (Supplementary Figure S1). Data are presented as mean ± SEM. Diaphragm dystrophic pathology was high in mdx (3.9 ± 0.1) and mdxR (3.6 ± 0.4) mice, but improved in mdxGT1 (2.7 ± 0.2), mdxRGT1 (2.5 ± 0.2), mdxGT2 (1.7 ± 0.2), and mdxRGT2 (1.6 ± 0.3) groups (all $p < 0.05$). Dystrophic pathology was low in heart muscle of all groups (WT 0.0 ± 0.0; mdx 1.0 ± 0.4; mdxR 1.2 ± 0.5; mdxGT1 0.0 ± 0.0; mdxRGT1 0.3 ± 0.3; mdxGT2 0.0 ± 0.0; mdxRGT2 0.0 ± 0.0). No differences in quadriceps dystrophic pathology were observed between treated and untreated mice, regardless of construct or activity level (WT 0.0 ± 0.0; mdx 2.0 ± 0.3; mdxR 1.8 ± 0.3; mdxGT1 1.4 ± 0.1; mdxRGT1 1.4 ± 0.1; mdxGT2 1.4 ± 0.1; mdxRGT2 1.6 ± 0.2).

Both microdystrophin gene constructs improved time to fatigue, but voluntary wheel running further enhanced endurance capacity

Treadmill fatigue tests were performed to assess whole-body muscle function (Figure 5; Supplementary Table S4). Time to fatigue data are presented as mean ± SEM minutes. Baseline (2 weeks before treatment) and Final (53 weeks post-treatment) treadmill fatigue tests demonstrate depressed running ability in mdx mice (Baseline 54 ± 10; Final 33 ± 7 min) by 50% compared to WT (Figures 5A–C; Baseline 91 ± 12; Final 81 ± 11 min; $p < 0.05$). In the final test of the study, running ability was rescued by both running alone (mdxR 108 ± 5 min, $p < 0.05$) and gene therapy alone (Figure 5B; mdxGT1 75 ± 8 min; mdxGT2

10.3389/fphys.2023.1166206

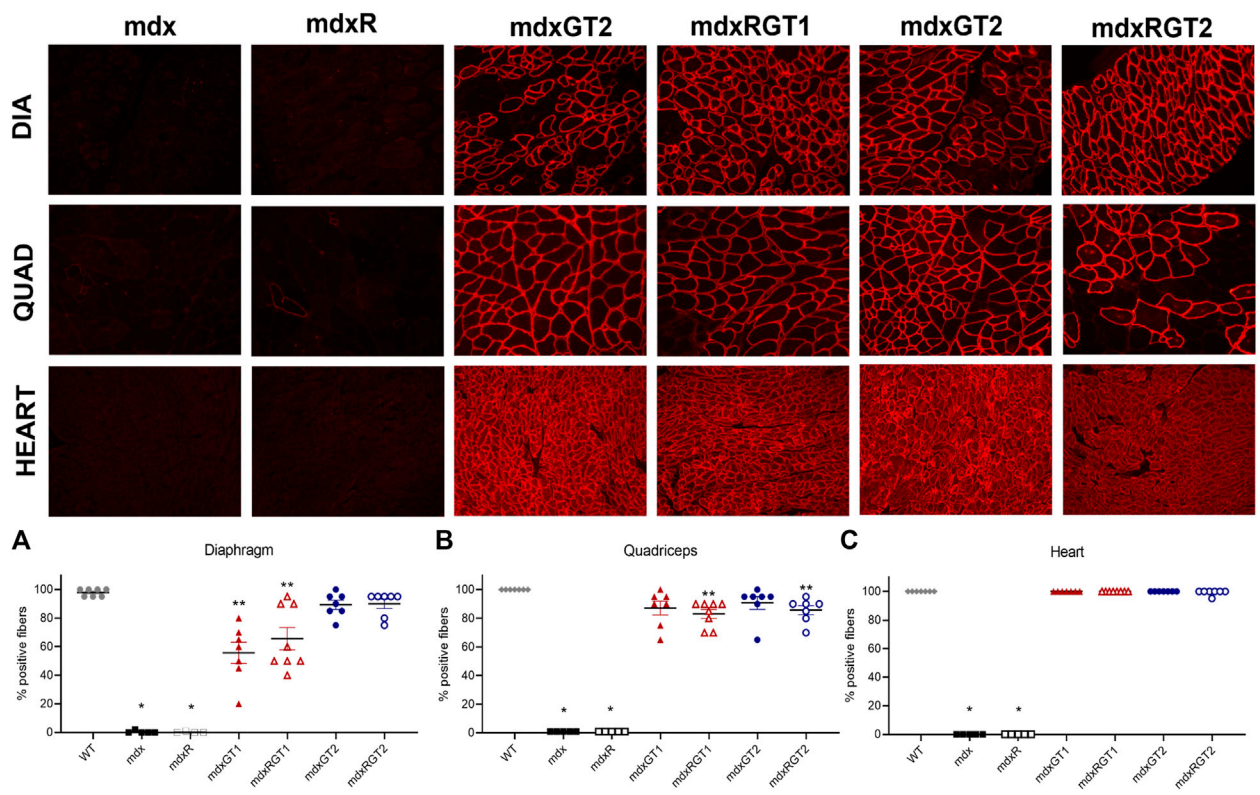

FIGURE 3
Microdystrophin protein content in diaphragm, quadriceps, and heart by quantification of immunofluorescence **(A–C)**. **(A)***mdx, mdxR < all groups. **mdxGT1, mdxRGT1 < WT, mdxGT2, mdxRGT2. **(B)*** mdx, mdxR < all groups. **mdxRGT1, mdxRGT2 < WT. **(C)*** mdx, mdxR < all groups. Representative images of diaphragm (DIA), quadriceps (QUAD), and heart from treated groups. All comparisons $p < 0.05$.

96 ± 11 min; $p < 0.05$). Mice treated with gene therapy combined with voluntary wheel running (mdxRGT1 125 ± 4 min; mdxRGT2 141 ± 7 min; $p < 0.05$) experienced the greatest benefit, regardless of gene therapy construct (Figure 5B). Interestingly, mdxR mice improved treadmill time ~46% by week 13 (81 ± 17 min) and by week 53, times were similar to mdxGT2 mice (Figures 5B,C). Voluntary wheel running distance was recorded over 52 weeks (Figures 5D,E; Supplementary Table S5). Weekly running distance is presented as mean ± SEM kilometers. Over the 52 weeks, mdxRGT2 mice (47 ± 2 km; $p < 0.05$) ran more per week than mdxR (32 ± 2 km) and mdxRGT1 mice (Figure 5D; 31 ± 2 km). This was confirmed by relative analysis comparing weekly running distance to each mouse's week 1 distance (Figure 5E). However, increased levels of voluntary wheel running in mdxRGT2 mice did not elevate their final treadmill time to fatigue over mdxRGT1 mice (Figure 5C).

Microdystrophin gene therapy improved plantarflexor torque output, independent of construct or voluntary wheel running

Contractile properties of plantar flexors were tested at baseline (1 week before treatment) and at 2-, 12-, 26-, 39-, and 52-weeks post-treatment to assess *in vivo* muscle function (Figure 6; Supplementary Table S6). Data are presented as mean ± SEM of normalized 120 Hz peak torque (mN*m/g) or 800°/s peak power (mW/g). At baseline, mdx mice (0.28 ± 0.02 mN*m/g) demonstrated low torque outputs compared to WT mice (0.34 ± 0.02 mN*m/g; $p < 0.05$) (Figure 6A). By 2 weeks, all groups treated with microdystrophin gene therapy with (mdxRGT1 0.38 ± 0.02 mN*m/g; mdxRGT2 0.41 ± 0.03 mN*m/g) and without (mdxGT1 0.41 ± 0.02 mN*m/g; mdxGT2 0.38 ± 0.01 mN*m/g) voluntary wheel running as well as untreated mice that performed voluntary wheel running (mdxR 0.35 ± 0.01 mN*m/g) improved torque output over mdx mice (0.26 ± 0.01 mN*m/g; all comparisons $p < 0.05$) (Figure 6B). By 12 weeks post-treatment, torque values of mdxR mice (0.34 ± 0.02 mN*m/g) returned to levels similar to mdx (0.32 ± 0.02 mN*m/g) (Figure 6D). At the end of the study, mice treated with both gene therapies, with (mdxRGT1 0.34 ± 0.02 mN*m/g; mdxRGT2 0.37 ± 0.02 mN*m/g) and without (mdxGT1 0.34 ± 0.02 mN*m/g; mdxGT2 0.36 ± 0.01 mN*m/g) voluntary wheel running, maintained their torque outputs similar to WT (0.33 ± 0.02 mN*m/g) and were greater than both untreated mdx groups (mdx 0.21 ± 0.02 mN*m/g; mdxR 0.23 ± 0.02 mN*m/g; $p < 0.05$). mdxRGT2 mice produced the highest torque values at the final time point (Figure 6C).

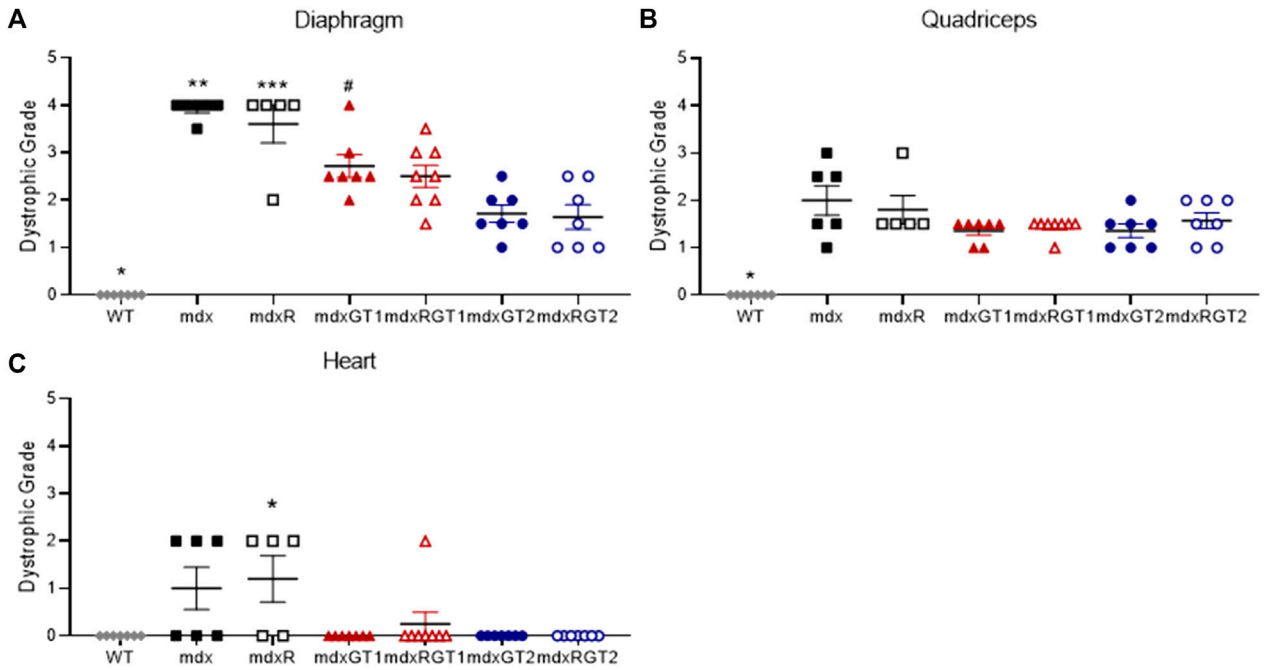

FIGURE 4
Dystrophic muscle pathology of diaphragm, quadriceps, and heart presented as dystrophic grade. **(A)** Diaphragm *WT < all groups. **mdx > all groups except mdxR. ***mdxR > WT, mdxRGT1, mdxGT2, mdxRGT2. #mdxGT1 >mdxGT2, mdxRGT2. **(B)** Quadriceps *WT < all groups. **(C)** Heart *mdxR < WT, mdxGT1, mdxGT2, mdxRGT2. All comparisons $p < 0.05$.

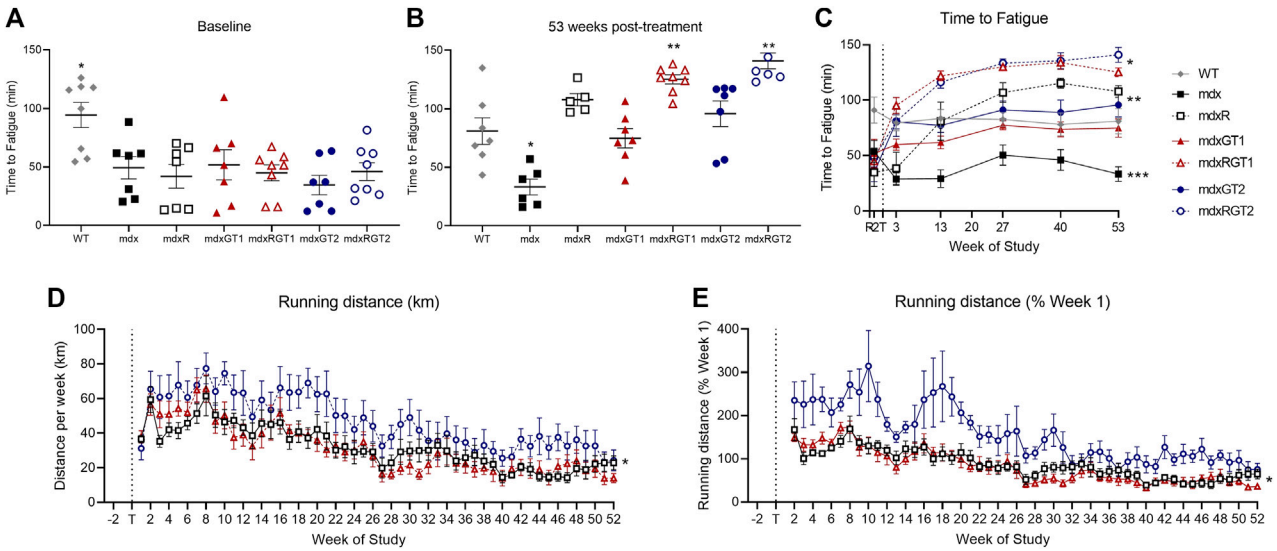

FIGURE 5
Running capacity. Treadmill fatigue test **(A–C)** and running wheel activity **(D, E)**. **(A)** Baseline treadmill time to fatigue. *WT > all groups. **(B)** 53 weeks post-treatment treadmill time to fatigue. *mdx < all groups. **mdxRGT1, mdxRGT2 > WT, mdxGT1, mdxGT2. **(C)** Treadmill time to fatigue at all timepoints. *mdxRGT1, mdxRGT2 > all groups post-treatment. *mdxR, mdxGT2 > mdxGT1 post-treatment. ***mdx < all groups post-treatment. **(D)** Running wheel distance per week. *mdxRGT2 > mdxR, mdxRGT1. **(E)** Running wheel activity as percent of week 1. *mdxRGT2 > mdxR, mdxRGT1. All comparisons $p < 0.05$.

Similarly, plantarflexor power of mdx mice (0.99 ± 0.09 mW/g) at baseline was lower than WT (1.55 ± 0.18 mW/g,; $p < 0.05$) (Figure 6E). However, by 52 weeks post-treatment, mdxGT1 (1.83 ± 0.22 mW/g), mdxGT2 (1.82 ± 0.21 mW/g), and mdxRGT2 (1.83 ± 0.21 mW/g) mice displayed higher power outputs vs. WT mice (1.44 ± 0.15 mW/g; $p < 0.05$) (Figure 6G).

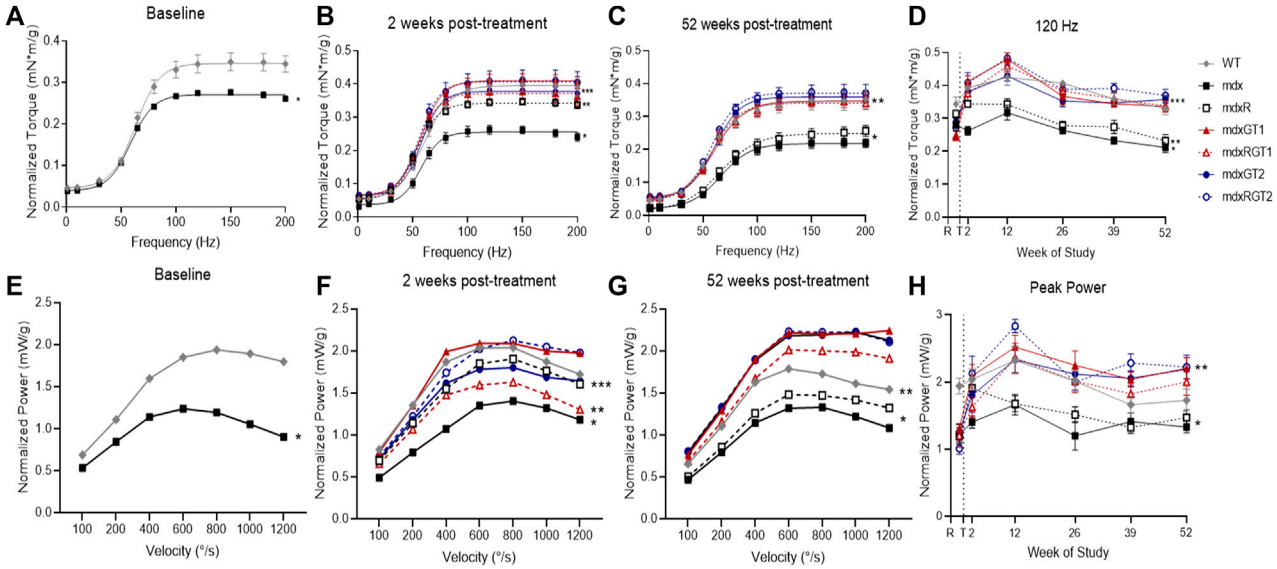

FIGURE 6
In vivo contractile properties of plantarillexors. Plantarflexor torque **(A–D)** and plantarflexor power **(E–H)**. **(A)** Baseline torque curve. *mdx < WT. **(B)** 2 weeks post-treatment. *mdx < all groups. **mdxR < mdxGT1, mdxRGT1, mdxRGT2. ***WT, mdxGT2, mdxRGT1 < mdxGT1, mdxRGT2. **(C)** 52 weeks post-treatment. *mdx, mdxR < all groups. **WT, mdxGT1, mdxRGT1<mdxRGT2. **(D)** Peak torque values (120 Hz) at all time points. *mdx < all groups. **mdxR < WT, mdxGT1, mdxRGT1, mdxGT2, mdxRGT2. ***mdxRGT2 > mdxGT2. **(E)** Baseline power curve. *mdx < WT. **(F)** 2 weeks post-treatment. *mdx < WT, mdxR, mdxGT1, mdxGT2, mdxRGT2. **mdxRGT1 < WT, mdxGT1, mdxRGT2. ***mdxGT2 < mdxGT1. **(G)** 52 weeks post-treatment. *mdx, mdxR < all other groups. **WT < mdxGT1, mdxGT2, mdxRGT2. **(H)** Peak power (800°/s) at all time points. *mdx, mdxR < all other groups. **mdxRGT2 > WT, mdxRGT1. All comparisons $p < 0.05$.

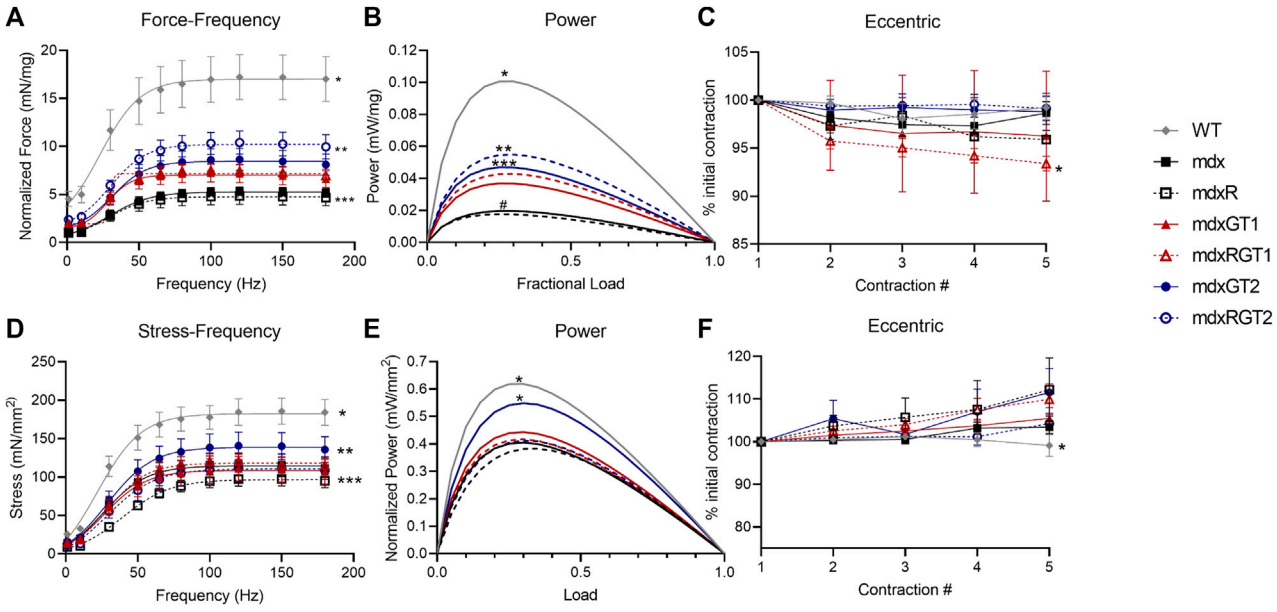

FIGURE 7
Ex vivo contractile properties. Diaphragm **(A–C)** and soleus **(D–F)**. **(A)** *WT > all other groups. **mdxRGT2 > mdxGT1, mdxRGT1, mdxGT2. ***mdx, mdxR < all other groups. **(B)** *WT > all other groups. **mdxRGT2 > mdxGT1, mdxRGT1. ***mdxGT2 > mdxGT1. #mdx, mdxR < all other groups. **(C)** *mdxRGT1 <mdxRGT2. **(D)** *WT > all groups. **mdxGT2 > mdxR, mdxGT1, mdxRGT2. ***mdxR < mdxRGT1. **(E)** *WT, mdxGT2 > all other groups. **(F)** *WT < mdxR, mdxRGT1, mdxGT2. All comparisons $p < 0.05$.

Post-treatment, mdx (1.40 ± 0.08 mW/g) and mdxR (1.58 ± 0.10 mW/g) mice produced lower power than all other groups across the course of the study (WT 1.95 ± 0.12 mW/g; mdxGT1 2.22 ± 0.08 mW/g; mdxRGT1 1.96 ± 0.12 mW/g; mdxGT2 2.10 ± 0.09 mW/g; mdxRGT2 2.29 ± 0.14 mW/g; all comparisons $p < 0.05$ (Figure 6H).

Microdystrophin gene therapy two (GT2) better preserved diaphragm function when combined with prolonged endurance exercise

At the conclusion of the study, mice were sacrificed, and *ex vivo* contractile experiments were conducted on diaphragm strips and whole soleus muscles (Figure 7; Supplementary Table S7). Absolute force and power, diaphragm strip mass, and soleus cross sectional area (CSA) are reported in Supplementary Table S7. Normalized forces and powers relative to strip mass for diaphragm and for soleus relative to CSA are described below to account for the potential bias of strip or muscle size. Diaphragm data are presented as mean ± SEM of normalized 120 Hz peak force (mN/mg) or power (mW/mg) at 40% maximum load (Figures 7A–C; Supplementary Table S7). WT mice produced the greatest diaphragm force (17.2 ± 2.3 mN/mg), while mdx (5.3 ± 0.4 mN/mg) and mdxR (4.8 ± 0.9 mN/mg) groups produced less force than all other groups (Figure 7A; $p < 0.05$). mdxRGT2 (10.1 ± 1.1 mN/mg; $p < 0.05$) produced higher force than other gene therapy-treated groups (mdxGT1 7.2 ± 1.0 mN/mg; mdxGT2 8.6 ± 1.1 mN/mg; mdxRGT1 7.7 ± 0.6 mN/mg). Similar to force, power analysis revealed that WT (0.095 ± 0.02 mW/mg) produced higher power than other groups, while mdx (0.019 ± 0.0 mW/mg) and mdxR (0.016 ± 0.0 mW/mg) values were depressed compared to all groups (Figure 7B; mdxGT1 0.035 ± 0.01 mW/mg; mdxRGT1 0.041 ± 0.01 mW/mg; mdxGT2 0.044 ± 0.01 mW/mg; mdxRGT2 0.052 ± 0.01 mW/mg; all comparisons $p < 0.05$). mdxRGT2 produced similar power to mdxGT2, and both produced higher power values than mdxGT1. mdxRGT2 also produced greater power than mdxRGT1 ($p < 0.05$). The only group that experienced minimal force loss (~7%) due to eccentric contractions was mdxRGT1 (Figure 7C; $p < 0.05$).

Soleus function demonstrated better force outputs in sedentary mice treated with microdystrophin gene therapy two (GT2)

Soleus data are presented as mean ± SEM of normalized 120 Hz peak stress (mN/mm^2) or power (mW/mm^2) at 40% maximum load (Figures 7D–F; Supplementary Table S7). The soleus stress-frequency measurements displayed a low force output in mdx groups ($p < 0.05$) compared to WT (184.8 ± 17.4 mN/mm^2). mdxGT2 (140.8 ± 17.7 mN/mm^2) mice displayed greater soleus stress over mdxR (97.4 ± 8.9 mN/mm^2), mdxGT1 (110.9 ± 16.2 mN/mm^2), mdxRGT2 (111.9 ± 18.0 mN/mm^2) (Figure 7D; $p < 0.05$). Power values in mdxGT2 (0.53 ± 0.06 mW/mm^2) mice were similar to WT (0.58 ± 0.05 mW/mm^2) and higher ($p < 0.05$) than all other groups (Figure 7E; mdx 0.39 ± 0.06 mW/mm^2; mdxR 0.38 ± 0.08 mW/mm^2; mdxGT1 0.42 ± 0.08 mW/mm^2; mdxRGT1 0.40 ± 0.04 mW/mm^2; mdxRGT2 0.40 ± 0.07 mW/mm^2). Soleus muscles did not experience force loss when subjected to the eccentric injury protocol (Figure 7F). mdxR, mdxRGT1, and mdxGT2 displayed slightly elevated force output compared to WT ($p < 0.05$).

Oxidative red quadriceps fibers of mdxRGT1 mice displayed elevated mitochondrial respiration to WT levels. Mitochondrial respiration of diaphragm fibers of mdxGT2 mice were rescued to WT levels

Mitochondrial respiration, a key measure of oxidative capacity, was evaluated in red quadriceps fibers and diaphragm strips (Figure 8). Red muscle has a higher proportion of oxidative fibers. Data are presented as mean ± SEM pmols/s*mg. mdxRGT1 improved succinate-stimulated respiration of red quadriceps fibers almost two-fold over mdx mice (Figure 8A). ADP-stimulated respiration was similarly improved over both mdx and mdxR mice. In diaphragm, both WT (11.5 ± 8.3 pmols/s*mg) and mdxGT2 (11.1 ± 8.9 pmols/s*mg) mice had ~30% greater succinate-stimulated respiration than mdx (8.8 ± 3.6 pmols/s*mg) and mdxR (5.2 ± 3.4 pmols/s*mg) groups (Figure 8B; $p < 0.05$). WT (11.4 ± 8.8 pmols/s*mg) increased ADP-stimulated respiration over mdxR (4.7 ± 3.0 pmols/s*mg), while mdxGT2 (11.0 ± 9.1 pmols/s*mg) respiration was higher than both mdx (8.7 ± 3.6 pmols/s*mg) and mdxR values; all comparisons $p < 0.05$.

mdxRGT1 mice demonstrated the highest number of positive changes in metabolic enzymes of limb muscle compared to other groups

Metabolic enzyme activities were assessed in gastrocnemius (gastroc) and triceps (Supplementary Figures S2, 3). Citrate synthase (CS), malate dehydrogenase (MD) and cytochrome C oxidase (COX) activities were measured in both red and white gastrocnemius (Supplementary Figures S2A–C), while phosphofructokinase (PFK) and β-hydroxyacyl-CoA-dehydrogenase (βHAD) were only measured in red (Supplementary Figures S2D, E). Enzyme activities were higher in red vs. white muscle (Supplementary Figures S2A–C). CS activity in red gastroc was elevated in mdxRGT1 compared to mdx and WT groups (Supplementary Figures S2A). Both mdxRGT1 and mdxRGT2 displayed increased βHAD activity compared to mdx mice in red muscle (Supplementary Figures S2E). mdxRGT2 βHAD activity was also higher than WT. White muscle showed no differences between groups Supplementary Figures S2E; all comparisons $p < 0.05$.

In triceps, both treated running groups displayed elevated CS activity compared to mdx and mdxGT1 (Supplementary Figures S3A). In addition, mdxRGT2 CS activity was greater than WT, mdxR, and mdxGT2 (Supplementary Figures S3A). Interestingly, mdxR triceps had higher MD activity than mice treated with gene therapy alone, regardless of construct. mdxR COX activity was also higher than mdxGT1. Triceps PFK activity was greater in mdxRGT1 than WT and both sedentary treated groups. No differences in βHAD activity of triceps were observed Supplementary Figures S2E; all comparisons $p < 0.05$.

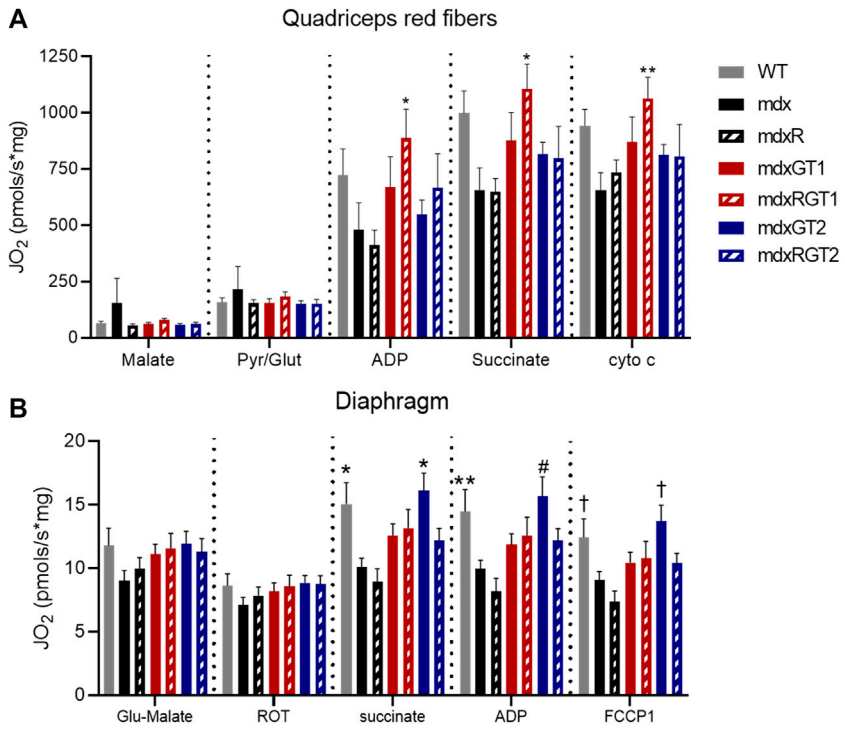

FIGURE 8
Mitochondrial respiration in red quadriceps and diaphragm fibers. **(A)** Red quadriceps. *mdxRGT1 > mdx, mdxR. **mdxRGT1 > mdx. **(B)** Diaphragm. *WT, mdxGT2 > mdx, mdxR. **WT > mdxR. #mdxGT2 > mdx, mdxR. †WT, mdxGT2 > mdxR. All comparisons $p < 0.05$.

Discussion

Study objectives

The objectives of our current study were to determine if (1) prolonged (52 weeks) voluntary wheel running and (2) microdystrophin construct structure (± nNOS binding site) in mdx mice would sustain the functional benefits we reported for microdystrophin combined with short-term (21 weeks) voluntary wheel running in mdx mice (Hamm et al., 2021). We tested two microdystrophin constructs, μDys-5R (GT1), that includes the nNOS binding site and H2μDys (GT2), that does not include the nNOS binding site. We tested these two microdystrophin constructs with and without voluntary wheel running using comprehensive whole-body endurance and muscle function assessments in mdx mice. We performed these assessments on 7 groups: mdx, mdxR, mdxGT1, mdxRGT1, mdxGT2, mdxRGT2 and WT mice.

Main findings

(1) Both microdystrophin constructs improved running capacity alone, but even moreso when combined with voluntary wheel running; (2) improvements in plantarflexor torque were comparable between all gene therapy treated groups, independent of running; (3) mdxRGT2 diaphragms performed better in *ex vivo* contractile assessments than other treated groups, with or without running; (4) mdxGT2 mice demonstrated higher force outputs in *ex vivo* soleus; (5) mdxRGT1 mice displayed the greatest adaptation to mitochondrial function in red quadriceps fibers as well as the highest number of adaptations in metabolic enzyme activity measured in limb muscles; and, (6) mdxGT2 mice produced diaphragm mitochondrial respiration rates similar to WT and higher than other mdx groups. Thus, prolonged voluntary wheel running complemented the functional improvements provided by both microdystrophin constructs but also revealed the unique benefits of each microdystrophin construct to dystrophic muscle. The experimental outcomes that distinguish the gene therapy-treated groups highlight the benefits of each construct and may help to elucidate their unique mechanisms of rescue.

Microdystrophin as treatment for dystrophic muscle

DMD causes progressive skeletal muscle weakness, respiratory deficits, and cardiomyopathy. (Duan et al., 2021). Accordingly, mdx mice display decreased muscle strength and power, which is especially progressive in the diaphragm with age. (Dupont-Versteegden and McCarter, 1992; Lynch et al., 1997). In cardiac muscle, young mdx mice display electrocardiographic abnormalities but have very mild fibrosis or overall pathology. (Chu et al., 2002; Van Erp et al., 2010). Microdystrophin gene therapy is one strategy being used to restore muscle function to dystrophic muscle. Microdystrophin construct

optimization has been a topic of interest in DMD research for some time. (Rafael et al., 1996; Chamberlain and Chamberlain, 2017; Duan, 2018a; Ramos et al., 2019). Several constructs are currently being tested in clinical trials, including constructs with and without the nNOS binding site (Chamberlain and Chamberlain, 2017; Duan, 2018a) that are similar to those used in the present study. With the potential success of clinical trials forthcoming, it is becoming increasingly important to determine the limitations of these microdystrophin constructs, especially in relation to exercise. At present, the combination of exercise and microdystrophin treatments are best assessed pre-clinically.

Outcomes of uDys-5R (GT1) ± exercise

μDys-5R (GT1) is a newer microdystrophin construct that contains spectrin-like repeats 16 and 17, which form its unique nNOS-binding site. Unlike other microdystrophins, μDys-5R (GT1) can localize nNOS to the sarcolemma, like full-length dystrophin. (Lai et al., 2013). Dystrophic limb muscles experience ischemia during exercise. (Sander et al., 2000; Zhang et al., 2013). μDys-5R (GT1) has been shown to improve muscle perfusion in mdx mice during uphill treadmill exercise, likely due to its proper localization of nNOS. Our data demonstrated that GT1 improved running capacity alone, but even moreso when combined with voluntary wheel running to support the potential influence of the nNOS binding site. GT1 has also been shown to restore diaphragm force to WT levels and was protective during an eccentric injury protocol. (Lai et al., 2009). In the current study, we observed that mdx mice treated with GT1 displayed lower diaphragm force and power than WT mice and the activity-matched mdx mice treated with GT2. Conversely, mdxRGT1 mice improved mitochondrial respiration in red quadriceps, as well as CS activity in red gastroc. CS activity is a biomarker of mitochondrial density, so this combination indicates positive mitochondrial adaptations in red muscle to improve oxidative capacity. Both mdxRGT1 and mdxRGT2 displayed elevated βHAD activity compared to mdx, perhaps indicating a shift to favoring fatty acid oxidation to support endurance exercise. In the triceps, both treated groups that performed voluntary wheel running had elevated CS. Interestingly, triceps MD, and COX activity were upregulated in mdxR mice only. mdxRGT1 also displayed elevation of PFK enzymatic activity in triceps, indicating higher levels of glycolytic activity. Although all running groups experienced some metabolic changes compared to sedentary groups, mdxRGT1 displayed the greatest benefit. One potential explanation is that the nNOS-binding site improved blood flow to exercising limb muscles and in turn drove endurance-induced adaptations in mdxRGT1 mice. This potential mechanism should be explored in future studies. (Ferry et al., 2015).

Outcomes of H2μDys (GT2) ± exercise

H2μDys (GT2) has been described as being less beneficial to muscle than variations with H3 and μDys-5R (GT1). (Lai et al., 2009; Duan, 2018b; Ramos et al., 2019). Nevertheless, we recently demonstrated that H2μDys gene therapy combined with 21 weeks of voluntary wheel running was beneficial to mdx mice. (Hamm et al., 2021). Treadmill endurance capacity of mdx mice was improved with gene therapy but improved even further with the addition of voluntary wheel running. (Hamm et al., 2021). Similarly, herein, our data demonstrated that GT2 improved running capacity alone, but similar to GT1 demonstrated increased running capacity with voluntary wheel running in mdxRGT2 mice similar to that of mdxRGT1 mice. Notably, this similar running capacity suggests the absence of the nNOS binding site in GT2 does not limit adaptation to running, and also suggests the possibility of other adaptive mechanisms to enhance endurance. A potential detriment of H2μDys (GT2) is the polyproline site that is thought to create chronic strain on the myotendinous junctions of the Achilles tendon, which anchors the soleus and gastrocnemius muscles to the calcaneus. (Banks et al., 2010). The soleus and gastrocnemius are the two main plantarflexors and are critical to the "push off" phase of gait during walking and running. Previous studies have shown improvements in plantarflexor and soleus function in mdx mice after voluntary wheel running. (Hayes and Williams, 1996; Baltgalvis et al., 2012; Selsby et al., 2013). We also reported improvements in plantarflexor torque were independent of running, but running was not detrimental. (Hamm et al., 2021). Herein, we demonstrated peak plantarflexor torque was improved with running (mdxR) over mdx mice across all time points post-treatment. Peak torque was further improved over untreated mice by both GT1 and GT2 constructs, regardless of activity level. mdxRGT2 mean peak plantarflexor torque was higher than mdxGT2 post-treatment, However, assessment of the plantarflexor soleus *ex vivo*, revealed force and power that were higher in sedentary mdxGT2 mice compared to other treated groups. These data suggest that voluntary wheel running may not be as beneficial to soleus muscle force and power of GT2 treated mice, but nevertheless the mdxRGT2 mice could run exceptionally well.

Effects of running and the GT1 and GT2 microdystrophins on the cardiorespiratory system

Diaphragm

Respiratory failure and cardiomyopathy are two primary causes of mortality in patients with DMD. Herein, we focused on the functional improvements in the diaphragm. The diaphragm is critical to respiratory function and is one of the most affected muscles, recapitulating DMD pathology moreso than other muscles in mdx mice (Stedman et al., 1991; Dupont-Versteegden and McCarter, 1992; Lynch et al., 1997). Therefore, examining diaphragm performance is key to preclinical studies in mdx mice. It is unclear whether prolonged voluntary wheel running is beneficial (Dupont-Versteegden et al., 1994) or detrimental to diaphragm function of mdx mice. (Selsby et al., 2013). In the present study, diaphragm force was similarly low in both mdxR and mdx groups. Additionally, our data suggest that voluntary wheel running differentially affected the diaphragms of mice treated with each gene therapy. mdxRGT1 and mdxRGT2 mice each performed exceptionally well in treadmill tests, indicating a robust respiratory capacity. However, mitochondrial respiration of the running groups remained

similar to mdx levels in the diaphragm, indicating that their exceptional endurance capacity is not due to diaphragm adaptations in mitochondrial respiration. Interestingly, mdxRGT2 mice demonstrated the best *ex vivo* diaphragm function of all mdx groups, while mdxRGT1 function was improved to a more moderate degree. Microdystrophin expression measured by immunofluorescence was lower in diaphragms of GT1-treated mice (mdxGT1, mdxRGT1) compared to GT2-treated mice (mdxGT2, mdxRGT2). In addition, diaphragm muscle pathology was slightly worse in mdxGT1 mice. Collectively, these data could explain the reduced diaphragm force outputs in mdx mice treated with GT1 (mdxGT1, mdxRGT1) herein. However, *ex vivo* diaphragm force was depressed in treated mice that ran compared with sedentary treated mice. (Hamm et al., 2021). In the current study, diaphragm force output was higher in mdxRGT2 mice compared with mdxGT2 mice. Based on these data, it appears that with age, voluntary wheel running can be beneficial to maintaining force output in the diaphragms of mice treated with GT2. Diaphragm force output was improved in both groups treated with GT1 (mdxGT1, mdxRGT1) but to a lesser degree compared to mdxRGT2 and WT. Therefore, running may not be as beneficial to GT1-treated diaphragms.

Cardiomyopathy

The cardiac phenotype of young mdx mice is mild. Several studies show that using a cardiac-specific AAV serotype, such as AAV9, induces robust microdystrophin expression, normalizes electrical activity, and prevents progression of pathophysiology in several mouse models of DMD. (Bostick et al., 2008; Shin et al., 2011; Howard et al., 2021). Previous studies in young, untreated mdx mice indicated that voluntary wheel running induces changes in the structure of the heart, some positive (Selsby et al., 2013) and some detrimental. (Costas et al., 2010; Hourdé et al., 2013). In our study, we did not directly assess cardiac function, but found that untreated mdx mice that performed voluntary wheel running (mdxR) showed a similarly mild cardiac dystrophic pathology compared to mdx mice. mdxR mice also performed as well as mdxGT2 mice, and even better than mdxGT1 mice in the treadmill test. Recently and herein we show that young mdx mice treated with GT2 gene therapy are not only able to tolerate exercise but thrive when performing endurance tests, especially after performing voluntary wheel running. (Hamm et al., 2021). In addition, after 52 weeks of running, at 14 months old, treated mice display low to no cardiac dystrophic pathology. Although assumptions about cardiac function cannot be fully extrapolated from these data, our findings suggest that either microdystrophin gene therapy combined with voluntary exercise is not detrimental to cardiac muscle of young mdx mice.

Summary

The purpose of this study was to determine if voluntary wheel running would be beneficial to mdx mice treated with either the GT1 or the GT2 microdystrophin construct. Among the main findings, both microdystrophin constructs improved running capacity when combined with voluntary wheel running; while improvements in plantarflexor torque were comparable between all gene therapy treated groups, independent of running. Our data also indicated that the nNOS-binding site in GT1 may promote endurance exercise-driven adaptations in metabolic enzyme activity and the mitochondria of limb muscle. Further, in the diaphragm, GT2 can result in a high degree of force production when prolonged endurance exercise is applied but the addition of running to animals treated with this construct decreases mitochondrial respiration. These findings demonstrate that prolonged (52 weeks) voluntary wheel running and a microdystrophin construct structure with or without the nNOS binding site in mdx mice will sustain the functional benefits we reported for microdystrophin combined with short-term (21 weeks) voluntary wheel running in mdx mice (Hamm et al., 2021). Our findings further demonstrate that prolonged voluntary wheel running complemented the functional improvements provided by both microdystrophin constructs but also revealed the unique benefits of each to dystrophic muscle. Our data also suggest further studies should be conducted to evaluate the hardiness of each construct in different muscles and to elucidate the mechanisms that drive these differential adaptations.

Data availability statement

The raw data supporting the conclusions of this article will be made available by the authors, without undue reservation.

Ethics statement

The animal study was reviewed and approved by Virginia Tech Institutional Animal Care and Use Committee.

Author contributions

Conceptualization, RG, SH, JG, CM, and ML. Methodology, RG, SH, RM, JG, CM, and ML. Investigation, RG, SH, CY, LM, MW, HZ, AA, AG, RM, ML, MP, EO, JY, and AA. Formal Analysis, RG, SH, CY, HZ, RM, MP, EO. Resources, SH. Writing—Original Draft, RG, SH, and ML. Writing—Review and editing, RG, SH, JG, and ML. Visualization, RG, SH, CY, ML, and MP. Supervision, RG and JG. Project Administration, RG, SH, and HZ. Funding Acquisition, RG and JG. All authors listed have made a substantial, direct, and intellectual contribution to the work and approved it for publication.

Funding

Provided by Solid Biosciences Inc.

Conflict of interest

CAM and JPG are employees of Solid Biosciences Inc. MWL is a member of the Scientific Advisory Board and receives research funding from Solid Biosciences. MWL is founder and owner of Diverge Translational Science Laboratory. MWL, MJP, and EMO

are employees of Diverge Translational Science Laboratory, which receives research funding from Solid Biosciences.

The remaining authors declare that the research was conducted in the absence of any commercial or financial relationships that could be construed as a potential conflict of interest.

Publisher's note

All claims expressed in this article are solely those of the authors and do not necessarily represent those of their affiliated organizations, or those of the publisher, the editors and the reviewers. Any product that may be evaluated in this article, or claim that may be made by its manufacturer, is not guaranteed or endorsed by the publisher.

Supplementary material

The Supplementary Material for this article can be found online at: https://www.frontiersin.org/articles/10.3389/fphys.2023.1166206/full#supplementary-material

References

Aartsma-Rus, A., and van Putten, M. (2014). Assessing functional performance in the Mdx mouse model. *J. Vis. Exp.* 85, 51303. doi:10.3791/51303

Baltgalvis, K. A., Call, J. A., Cochrane, G. D., Laker, R. C., Yan, Z., and Lowe, D. A. (2012). Exercise training improves plantarflexor muscle function in mdx mice. *Med. Sci. Sports Exerc* 44, 1671–1679. doi:10.1249/MSS.0b013e31825703f0

Banks, G. B., Judge, L. M., Allen, J. M., and Chamberlain, J. S. (2010). The polyproline site in Hinge 2 influences the functional capacity of truncated dystrophins. *PLoS Genet.* 6, e1000958. doi:10.1371/journal.pgen.1000958

Bostick, B., Shin, J. H., Yue, Y., and Duan, D. (2011). AAV-microdystrophin therapy improves cardiac performance in aged female mdx mice. *Mol. Ther.* 19, 1826–1832. doi:10.1038/mt.2011.154

Bostick, B., Yue, Y., Lai, Y., Long, C., Li, D., and Duan, D. (2008). Adeno-associated virus serotype-9 microdystrophin gene therapy ameliorates electrocardiographic abnormalities in mdx mice. *Hum. Gene Ther.* 19, 851–856. doi:10.1089/hum.2008.058

Chamberlain, J. R., and Chamberlain, J. S. (2017). Progress toward gene therapy for duchenne muscular dystrophy. *Mol. Ther.* 25, 1125–1131. doi:10.1016/j.ymthe.2017.02.019

Chu, V., Otero, J. M., Lopez, O., Sullivan, M. F., Morgan, J. P., Amende, I., et al. (2002). Electrocardiographic findings in mdx mice: A cardiac phenotype of duchenne muscular dystrophy. *Muscle Nerve* 26, 513–519. doi:10.1002/mus.10223

Costas, J. M., Nye, D. J., Henley, J. B., and Plochocki, J. H. (2010). Voluntary exercise induces structural remodeling in the hearts of dystrophin-deficient mice. *Muscle Nerve* 42, 881–885. doi:10.1002/mus.21783

Duan, D., Goemans, N., Takeda, S., Mercuri, E., and Aartsma-Rus, A. (2021). Duchenne muscular dystrophy. *Nat. Rev. Dis. Prim.* 7, 13–19. doi:10.1038/s41572-021-00248-3

Duan, D. (2018). Micro-dystrophin gene therapy goes systemic in duchenne muscular dystrophy patients. *Hum. Gene Ther.* 29, 733–736. doi:10.1089/hum.2018.012

Duan, D. (2018). Systemic AAV micro-dystrophin gene therapy for duchenne muscular dystrophy. *Mol. Ther.* 26, 2337–2356. doi:10.1016/j.ymthe.2018.07.011

Dupont-Versteegden, E. E., and McCarter, R. J. (1992). Differential expression of muscular dystrophy in diaphragm versus hindlimb muscles of mdx mice. *Muscle Nerve* 15, 1105–1110. doi:10.1002/mus.880151008

Dupont-Versteegden, E. E., McCarter, R. J., and Katz, M. S. (1994). Voluntary exercise decreases progression of muscular dystrophy in diaphragm of mdx mice. *J. Appl. Physiol.* 77, 1736–1741. doi:10.1152/jappl.1994.77.4.1736

Ferry, A., Benchaouir, R., Joanne, P., Peat, R. A., Mougenot, N., Agbulut, O., et al. (2015). Effect of voluntary physical activity initiated at age 7 months on skeletal hindlimb and cardiac muscle function in mdx mice of both genders. *Muscle and Nerve* 52, 788–794. doi:10.1002/mus.24604

Gao, Q., and McNally, E. M. (2015). The dystrophin complex: Structure, function and implications for therapy. *Compr. Physiol.* 5, 1223–1239. doi:10.1002/cphy.c140048

Hamm, S. E., Fathalikhani, D. D., Bukovec, K. E., Addington, A. K., Zhang, H., Perry, J. B., et al. (2021). Voluntary wheel running complements microdystrophin gene therapy to improve muscle function in mdx mice. *Mol. Ther. - Methods and Clin. Dev.* 21, 144–160. doi:10.1016/j.omtm.2021.02.024

Harper, S. Q., Hauser, M. A., DelloRusso, C., Duan, D., Crawford, R. W., Phelps, S. F., et al. (2002). Modular flexibility of dystrophin: Implications for gene therapy of duchenne muscular dystrophy. *Nat. Med.* 8, 253–261. doi:10.1038/nm0302-253

Hayes, A., and Williams, D. A. (1996). Beneficial effects of voluntary wheel running on the properties of dystrophic mouse muscle. *J. Appl. Physiol.* 80, 670–679. doi:10.1152/jappl.1996.80.2.670

Hourdé, C., Joanne, P., Medja, F., Mougenot, N., Jacquet, A., Mouisel, E., et al. (2013). Voluntary physical activity protects from susceptibility to skeletal muscle contraction-induced injury but worsens heart function in mdx mice. *Am. J. Pathol.* 182, 1509–1518. doi:10.1016/j.ajpath.2013.01.020

Howard, Z. M., Dorn, L. E., Lowe, J., Gertzen, M. D., Ciccone, P. C., Rastogi, N., et al. (2021). Micro-dystrophin gene therapy prevents heart failure in an improved Duchenne muscular dystrophy cardiomyopathy mouse model. *JCI Insight* 6, e146511. doi:10.1172/jci.insight.146511

Lai, Y., Thomas, G. D., Yue, Y., Yang, H. T., Li, D., Long, C., et al. (2009). Dystrophins carrying spectrin-like repeats 16 and 17 anchor nNOS to the sarcolemma and enhance exercise performance in a mouse model of muscular dystrophy. *J. Clin. Invest.* 119, 624–635. doi:10.1172/JCI36612

Lai, Y., Zhao, J., Yue, Y., and Duan, D. (2013). α2 and α3 helices of dystrophin R16 and R17 frame a microdomain in the α1 helix of dystrophin R17 for neuronal NOS binding. *Proc. Natl. Acad. Sci. U. S. A.* 110, 525–530. doi:10.1073/pnas.1211431109

Landisch, R. M., Kosir, A. M., Nelson, S. A., Baltgalvis, K. A., and Lowe, D. A. (2008). ADAPTIVE AND NONADAPTIVE RESPONSES TO VOLUNTARY WHEEL RUNNING BY mdx MICE. *Muscle Nerve* 38, 1290–1303. doi:10.1002/mus.21141

Liu, M., Yue, Y., Harper, S. Q., Grange, R. W., Chamberlain, J. S., and Duan, D. (2005). Adeno-Associated virus-mediated microdystrophin expression protects young mdx muscle from contraction-induced injury. *Mol. Ther.* 11, 245–256. doi:10.1016/j.ymthe.2004.09.013

Lynch, G. S., Rafael, J. A., Hinkle, R. T., Cole, N. M., Chamberlain, J. S., and Faulkner, J. A. (1997). Contractile properties of diaphragm muscle segments from old mdx and old transgenic mdx mice. *Am. J. Physiol.* 272, C2063–C2068. doi:10.1152/ajpcell.1997.272.6.C2063

Rafael, J. A., Cox, G. A., Corrado, K., Jung, D., Campbell, K. P., and Chamberlain, J. S. (1996). Forced expression of dystrophin deletion constructs reveals structure-function correlations. *J. Cell. Biol.* 134, 93–102. doi:10.1083/jcb.134.1.93

Ramos, J. N., Hollinger, K., Bengtsson, N. E., Allen, J. M., Hauschka, S. D., and Chamberlain, J. S. (2019). Development of novel micro-dystrophins with enhanced functionality. *Mol. Ther.* 27, 623–635. doi:10.1016/j.ymthe.2019.01.002

Rodgers, B. D., Bishaw, Y., Kagel, D., Ramos, J. N., and Maricelli, J. W. (2020). Micro-dystrophin gene therapy partially enhances exercise capacity in older adult mdx mice. *Mol. Ther. - Methods and Clin. Dev.* 17, 122–132. doi:10.1016/j.omtm.2019.11.015

Sander, M., Chavoshan, B., Harris, S. A., Iannaccone, S. T., Stull, J. T., Thomas, G. D., et al. (2000). Functional muscle ischemia in neuronal nitric oxide synthase-deficient skeletal muscle of children with Duchenne muscular dystrophy. *Proc. Natl. Acad. Sci. U. S. A.* 97, 13818–13823. doi:10.1073/pnas.250379497

Schill, K. E., Altenberger, A. R., Lowe, J., Periasamy, M., Villamena, F. A., Rafael-Fortney, J. A., et al. (2016). Muscle damage, metabolism, and oxidative stress in mdx mice: Impact of aerobic running. *Muscle Nerve* 54, 110–117. doi:10.1002/mus.25015

Selsby, J. T., Acosta, P., Sleeper, M. M., Barton, E. R., and Sweeney, H. L. (2013). Long-term wheel running compromises diaphragm function but improves cardiac and plantarflexor function in the mdx mouse. *J. Appl. Physiol. (1985)* 115, 660–666. doi:10.1152/japplphysiol.00252.2013

Shin, J. H., Nitahara-Kasahara, Y., Hayashita-Kinoh, H., Ohshima-Hosoyama, S., Kinoshita, K., Chiyo, T., et al. (2011). Improvement of cardiac fibrosis in dystrophic mice by rAAV9-mediated microdystrophin transduction. *Gene Ther.* 18, 910–919. doi:10.1038/gt.2011.36

Stedman, H. H., Sweeney, H. L., Shrager, J. B., Maguire, H. C., Panettieri, R. A., Petrof, B., et al. (1991). The mdx mouse diaphragm reproduces the degenerative changes of Duchenne muscular dystrophy. *Nature* 352, 536–539. doi:10.1038/352536a0

Van Erp, C., Loch, D., Laws, N., Trebbin, A., and Hoey, A. J. (2010). Timeline of cardiac dystrophy in 3-18-month-old MDX mice. *Muscle Nerve* 42, 504–513. doi:10.1002/mus.21716

Yiu, E. M., and Kornberg, A. J. (2015). Duchenne muscular dystrophy. *J. Paediatr. Child. Health* 51, 759–764. doi:10.1111/jpc.12868

Zhang, Y., Yue, Y., Li, L., Hakim, C. H., Zhang, K., Thomas, G. D., et al. (2013). Dual AAV therapy ameliorates exercise-induced muscle injury and functional ischemia in murine models of Duchenne muscular dystrophy. *Hum. Mol. Genet.* 22, 3720–3729. doi:10.1093/hmg/ddt224

Frontiers in Physiology

Understanding how an organism's components work together to maintain a healthy state

The second most-cited physiology journal, promoting a multidisciplinary approach to the physiology of living systems - from the subcellular and molecular domains to the intact organism and its interaction with the environment.

Discover the latest Research Topics

See more →

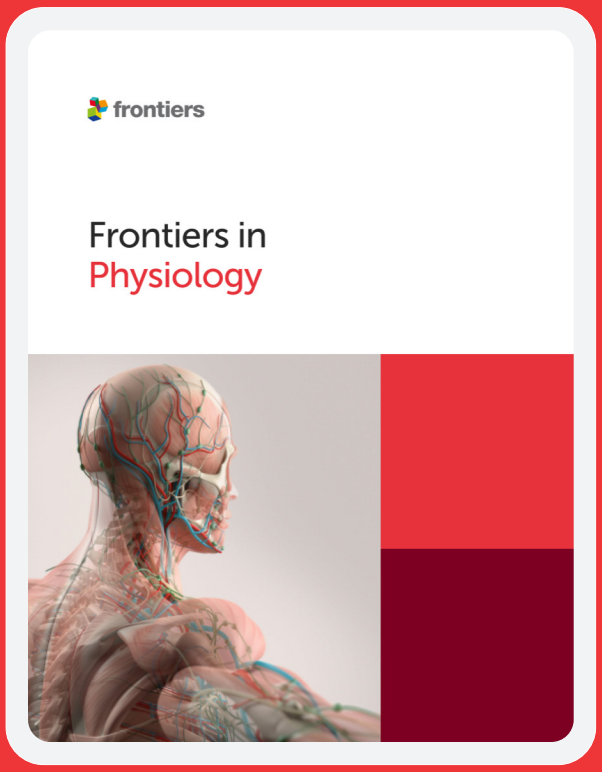

Frontiers

Avenue du Tribunal-Fédéral 34
1005 Lausanne, Switzerland
frontiersin.org

Contact us

+41 (0)21 510 17 00
frontiersin.org/about/contact